IAEA-208 VOL. 1

NEUTRON CROSS SECTIONS FOR REACTOR DOSIMETRY

VOL.I
REVIEW PAPERS

PROCEEDINGS OF A CONSULTANTS' MEETING
ON INTEGRAL CROSS-SECTION MEASUREMENTS
IN STANDARD NEUTRON FIELDS FOR REACTOR DOSIMETRY
ORGANIZED BY THE
INTERNATIONAL ATOMIC ENERGY AGENCY
AND HELD IN VIENNA, 15–19 NOVEMBER 1976

A TECHNICAL DOCUMENT ISSUED BY THE
INTERNATIONAL ATOMIC ENERGY AGENCY, VIENNA, 1978

NEUTRON CROSS SECTIONS FOR REACTOR DOSIMETRY
IAEA, VIENNA, 1978
Printed by the IAEA in Austria

PLEASE BE AWARE THAT
ALL OF THE MISSING PAGES IN THIS DOCUMENT
WERE ORIGINALLY BLANK

The IAEA does not maintain stocks of reports in this series. However, microfiche copies of these reports can be obtained from

INIS Microfiche Clearinghouse
International Atomic Energy Agency
Kärntner Ring 11
P.O. Box 590
A-1011 Vienna, Austria

on prepayment of US $0.65 or against one IAEA microfiche service coupon.

FOREWORD

The Consultants' Meeting on Integral Cross Section Measurements in Standard Neutron Fields for Reactor Dosimetry was convened by the IAEA Nuclear Data Section in Vienna, 15 - 19 November 1976, as part of the IAEA Programme on Benchmark Neutron Fields Applications for Reactor Dosimetry, described in INDC(SEC)-54/L+Dos, July 1976.

The need for the application of benchmark neutron fields, particularly for the validation and improvement of neutron data required for reactor dosimetry, was recognized by the IAEA Consultants' Meeting on Nuclear Data for Reactor Neutron Dosimetry, held in September 1973 [INDC(NDS)-56/U], and supported by the Agency's Working Group on Reactor Radiation Measurements and International Nuclear Data Committee.

The importance and usefulness of this approach was well demonstrated by the US Interlaboratory LMFBR Reaction Rate (ILRR) programme [Nuclear Technology 25, no.2, Feb. 1975] and was extensively discussed at the First ASTM-EURATOM Symposium for Reactor Dosimetry, Petten, Sept. 1975 [EUR-5667 e/f].

The present Consultants' Meeting is the first international meeting devoted to this subject; it summarizes progress in this field in laboratories of the IAEA member states.

The main results of the meeting are as follows:

- a comprehensive survey of benchmark neutron fields available at present for reactor dosimetry applications and their classification in three categories;
- review of the methods used at present for spectral characterization of neutron fields: direct spectrometry, activation, analytical calculations, and of results obtained with these methods;
- review of the present status of integral and differential neutron cross-section data for reactor dosimetry and new classification of the reactions in two categories;
- discussion of methodology for validation and adjustment of differential neutron data on the basis of integral data;
- better understanding has been reached between scientists working in the fields of integral and differential data measurements.

The proceedings of the meeting are published in two volumes. Volume I contains the review papers and Volume II the contributed papers presented at the meeting. The summary report, published as INDC(NDS)-81/L+M, is included in Volume I because of its importance for a better understanding of the results of the meeting.

M.F. Vlasov

Scientific Secretary

TABLE OF CONTENTS OF VOLUMES I AND II

C O N T E N T S , V o l u m e I : REVIEW PAPERS

I. OVERVIEW

II. SPECTRAL CHARACTERIZATION OF BENCHMARK NEUTRON FIELDS

III. INTEGRAL DATA IN BENCHMARK NEUTRON FIELDS

IV. DIFFERENTIAL CROSS-SECTION DATA FOR REACTOR DOSIMETRY

V. VALIDATION AND ADJUSTMENT OF DIFFERENTIAL CROSS SECTIONS ON THE BASIS OF INTEGRAL DATA

CONTENTS, Volume II : CONTRIBUTED PAPERS

I. SPECTRAL CHARACTERIZATION OF BENCHMARK NEUTRON FIELDS

II. INTEGRAL DATA IN BENCHMARK NEUTRON FIELDS

SUMMARY REPORT

I. INTRODUCTION AND OVERVIEW

1. Importance of Neutron Dosimetry - The importance of well-understood, firmly established and standardized neutron dosimetry methods has become more evident since the IAEA Consultants' Meeting on Nuclear Data for Reactor Neutron Dosimetry (Vienna, 10 - 12 September 1973)*. The interest in dosimetry for fast reactor applications, which was already substantial, appears to have further increased; a growing realization of the importance of dosimetry is obvious for reactor vessel surveillance and for other safety-related applications. More requirements for more accurate dosimetry come from several issues connected with the fuel cycle. Dosimetry is an essential part of the various shielding problems which are receiving general attention for all types of reactors and which have given rise to a programme of coordinated evaluation and benchmark experiments (also promoted by the I.A.E.A.)** which is parallel to, and has many interfaces with, the present dosimetry benchmark programme. Controlled thermonuclear applications call for exacting dosimetry measurements in order to investigate crucial material problems; interpretation of actual or projected damage measurements and extrapolation to fusion reactor environments rely heavily upon dosimetry to correlate effects in very different neutron spectra.

2. Status of Dosimetry Data - Some substantial improvements in neutron cross-sections and other dosimetry data have been achieved since the 1973 Consultants Meeting. However, the situation remains far from satisfactory: important gaps and discrepancies are still present, and new ones have been identified, so that a continuation of the dosimetry benchmark programme appears fully justified.

3. Consistency - The importance of arriving at a consistent cross-section set for the validation of reactor physics calculations and for spectrum unfolding is enhanced by the opportunity of putting together information derived from various sources when expensive experiments are involved, such as for instance in material irradiation programmes. This necessity was identified, among others, by the recent IAEA Specialists' Meeting on Radiation Damage Units (Harwell, 2 - 3 November 1976).

---

* further referred to as 1973 Consultants' Meeting.

** see for example Proceedings of Techn. Committee Meeting on Differential and Integral Nuclear Data Requirements for Shielding Calculations, Vienna, 10-15 October 1976, to be published as IAEA Technical Report.

4. International Cooperation - International cooperation, both on the basis of bi-lateral or multi-lateral programmes, and through international organizations, has been effective in this first period of implementation of the recommendations of the 1973 Consultants' Meeting. For instance, the Euratom Working Group on Reactor Dosimetry has entirely adopted these recommendations and worked for their implementation; the programme has been extensively reviewed at the First ASTM-Euratom Symposium on Reactor Dosimetry (Petten, September 1975). Coordinated programmes of measurements and evaluations on benchmark neutron spectra have involved the N.B.S.*, the P.T.B.**, the Imperial College***, CEN/SCK+ Mol, the Romanian ITN++ and the US laboratories involved in the ILRR+++ programme. It is important that this kind of international cooperation be continued and extended in the future, and that it involves exchange of information, data, codes, detectors, instruments and personnel so as to improve the quality and the reliability of the experiments and of their evaluation.

5. Purpose of Benchmark Experiments - Dosimetry benchmark neutron fields serve three general objectives, which had already been identified at the time of the 1973 Consultants' Meeting:

a) validation and/or calibration of experimental techniques;

b) validation and/or improvement of cross sections and other nuclear data needed for proper application of experimental techniques;

c) validation and/or improvement of analytical methods needed to extrapolate dosimetry data from a monitoring or surveillance position to the location of interest.

Although all of these objectives are important, the present programme is particularly focused on the second.

The way in which the benchmark programme may be instrumental in reaching these aims has been further investigated and will be discussed later.

---

* National Bureau of Standards, Washington
** Physikalisch-Technische Bundesanstalt, Braunschweig
*** Imperial College of London University
\+ Centre d'Etude de l'Energie Nucléaire, Mol
++ Institute for Nuclear Technology, Bucharest
+++ Interlaboratory LMFBR Reaction Rate Programme.

6. Reference Set of Cross-Sections - The ENDF/B-IV Dosimetry File has been made generally available, as recommended at the 1973 Consultants Meeting. This has proved very valuable in providing one reference set of cross sections that has made the intercomparison of results and predictions possible on a unified data basis. This library has in fact been extensively used throughout the world for the analysis of dosimetry experiments. It is hoped that this will in turn produce a valuable feedback of information to the ENDF/B evaluators in terms of data testing and indications for future improvements.

The aim of arriving at a generally accepted, internally consistent and extended dosimetry data file based on the ENDF/B specifications remains one of the fundamental objectives of this programme.

7. Cross-Section and Spectrum Processing - Even when the data base is common, some differences can be introduced by the method which is used to collapse or interpolate the data to a given group structure in order to use them in unfolding procedures or to calculate reaction rates. Although these uncertainties are less important for reaction cross sections than in other cases (particularly in the procedure of calculating the flux density spectrum itself) it is recommended that the cross-section processing method which is used be clearly specified when reporting results; in particular, if a weighting spectrum has been employed, it should be explicitly indicated.

8. Accuracies required - The target accuracies for dosimetry methods depend on the accuracies required for the integral quantities of final interest (such as radiation damage, activations, fuel burn-up etc). In most applications these last accuracies typically range from 5 to 20% (1σ)*. In some cases, required accuracies have recently been re-evaluated to more stringent specifications, partly also as a consequence of improved understanding of the damage functions. These requirements are reflected in target accuracies to be set for flux-fluence-spectral determination for the three categories of benchmark fields (see point II-1), depending on their intended use (a, b or c of point 5.). At the 1975 Petten Symposium, these accuracy requirements were stated to be in the $\pm$ 2 to 5% (1σ) range for LMFBR and somewhat less stringent for LWR and CTR applications.

(*) σ here stands for a standard deviation resulting from a combination of random and systematic uncertainties (uncertainties of corrections) assuming these have been assessed or estimated accordingly.

Present state-of-the-art accuracies are estimated to be in the range of ± 2 to 30% (1σ), depending on the particular spectral parameter and benchmark category. Although the ± 2 to 5% (1σ) goal objective may be considered ambitious for some applications, it is nevertheless reasonable. It is likely that, at least on the long term, most reactor fuels and materials development programmes will not accept an uncertainty greater than ± 5% (1σ). In order to achieve such an accuracy routinely, however, it is necessary to work towards a better level of accuracy, namely 2 to 5%.

9. Sensitivity Studies - The importance of sensitivity studies to correlate the target accuracies for the benchmark experiments with the accuracies required for the integral quantities of final interest had been identified at the 1973 Consultants' Meeting; however, very few investigations of this type have been reported since. All the theoretical and calculational tools to perform such a sensitivity analysis now appear to be available, and the importance of comprehensive and possibly intercompared sensitivity calculations for dosimetry is re-iterated. Notice has been taken of the extensive sensitivity calculations which are being carried out in the frame of the shielding benchmark programme.

10. Implementation - Important as it is to develop better dosimetry methods and to improve the accuracy of those presently available, one should bear in mind that this is of little value if it is not accompanied by a timely application of what is already available for the solution of everyday problems. It is a fact that nuclear programmes often do not make full use of already well-established and reliable dosimetry methods, but still employ or rely upon old methods and data that introduce appreciable uncertainties and consequent economic penalties. An important effort should be made towards the end of making all the interested people aware of the possibilities and advantages offered by the best dosimetry methods and data now available and by international cooperation in this non-proprietary field. Progress in this regard is being furthered by a series of ASTM-Euratom International Symposia on Reactor Dosimetry, the first one of which was held in Petten, September 22-26, 1975, and a second one is being planned for 3-7 October 1977 in the USA.

Interactions with other IAEA programmes - Both the development and the implementation of the recommended dosimetry benchmark programme would benefit from increased interactions with other IAEA programmes, in addition to those directly sponsored by the Nuclear Data Section. In particular:

a) Cooperation with the IAEA-NEA-EURATOM sponsored shielding benchmark programme. It would be desirable that the dosimetry used in that programme were based on the present recommendations, and conversely that the dosimetry programme could use the results of the shielding benchmark experiments and of the sensitivity calculations.

b) Increased cooperation with the IAEA's Research Programme on Irradiation Embrittlement of Pressure Vessel Steels is desirable. The excellent work in this programme would benefit from improved dosimetry techniques.

c) There is naturally a close connection between the Dosimetry Benchmark Programme and some of the activities sponsored by the International Working Group on Reactor Radiation Measurements, such as the recommendations on radiation damage units and the intercomparison of unfolding codes.

d) The IAEA Programme on Intercomparison of Peak Analysis for Ge(Li) Detectors is interesting for dosimetry methods.

e) Prospective users of dosimetry methods should be informed of the views expressed by this Consultants' Meeting and asked for their comments, which could help for a better orientation of future dosimetry activities. These users are represented, among others, by the International Working Group on Fast Reactors, by the International Fusion Research Council, the International Working Group on Reactor Radiation Measurements and other appropriate committees.

II. DEFINITION OF BENCHMARK NEUTRON FIELDS

1. Categories of benchmark neutron fields - The rather broad and open definition of dosimetry benchmarks given at the 1973 Consultants' Meeting has been more exactly qualified. Three types of benchmark neutron fields for reactor dosimetry have now been identified and defined as follows:

   Standard: a permanent and reproducible neutron field with neutron flux intensity, energy spectra and angular flux distributions characterized to state-of-the-art accuracy. The main characterizations must be verified by interlaboratory measurements and calculations.

   Reference: a permanent and reproducible neutron field, less well characterized than a standard but accepted as a measurement reference by a community of users.

   Controlled Environment: a neutron field, physically well-defined and with some spectrum definition, employed for a restricted set of validation experiments.

2. Standard fields -At the moment,in some of the most important standard fields, discrepancies still appear to be present in the reaction rate measurements for some of the best known dosimetry reactions. The list of standard fields has therefore been limited to those contained in Table 1. It is considered important that more fields be added to the list; in particular it is recommended that an important effort of better qualification and of reaching consistency with reaction rate measurements be done on the short term at least for the 235-U fission spectrum, the $\Sigma\Sigma$-type facilities and the ISNF.

3. Reference fields - The reference fields identified on the basis of presently available information are listed in Table 2. This list should be periodically updated as new information becomes available. In particular it is hoped that neutron fields covering the high energy region of importance for Controlled Thermonuclear Reactors (CTR) and other radiation damage work, based on harder-than-fission spectra, should qualify for this category of benchmarks.

TABLE 1. STANDARD NEUTRON FIELDS FOR REACTOR DOSIMETRY

Neutron Field	Average Energy	Energy Range for Data Testing	Status of Group-Flux Spectrum Characterization
Thermal Maxwellian	0.025 eV	< 0.4 eV	± 2-5% theory of thermal equilibrium, and spectrometry
Epithermal-1/E	0.75 MeV	0.4 eV to 0.1 MeV	
^{252}Cf spontaneous fission	2.13 MeV	0.1 to ∿ 18 MeV	± 13%, E < 0.25 MeV ± 2%, 0.25 < E < 8 MeV ± 9%, 8 < E < 12 MeV *differential spectrometry ± 10%, 12 < E < 15 MeV, multiple foils

*The NBS recommended spectrum shape based on an evaluation of differential spectrometry results reported up to 1974 is recognized as an acceptable spectrum description for practical applications. See paper by Grundl and Eisenhauer, this meeting.

TABLE 2. REFERENCE NEUTRON FIELDS FOR REACTOR DOSIMETRY

Neutron Field *	Av. Energy (MeV)	Energy Range for Data Testing and Calibration (MeV)	Status of Group Flux Spectrum Characterization
^{235}U thermal fission	1.97	0.1 to ∿ 18	± 15%, E < 0.25 MeV ± 2-5%, 0.25 < E < 8 MeV ± 5%, 8 < E < 12 MeV (differential spectrometry) ± 10%, 12 < E < 15 MeV, multiple foil
Sigma Sigma ($\Sigma\Sigma$)	0.76	0.01 to ∿ 18	± 15%, E < 0.1 keV, multiple foil ± 5%, 0.1 keV < E < 2 MeV, spectrometry and computation ± 5%, E > 2 MeV, multiple foil
ISNF	0.80	0.008 to ∿ 18	± 5%, E < ∿ 2 MeV, computation ± 2-5%, 2 < E < 12 MeV, computation and spectrometry (fission spectrum)
BIG TEN **	0.58	0.01 to ∿ 18	± 5%, 0.05 < E < 2 MeV, computation and spectrometry ± 5%, E > 2 MeV, multiple foil and computation
CFRMF **	0.76	0.01 to ∿18	± 15% (E < 0.01 MeV) Multiple foils and computations; ± 5% (0.01 MeV < E < 2) Spectrometry and computations; ± 5-10% (E > 2 MeV) Multiple foils and computations.

* References or reference information for these neutron fields are given in the various individual papers presented at this meeting. Particular reference is made to the papers by Grundl et al. and McElroy et al.

** Central core position.

TABLE 2. REFERENCE NEUTRON FIELDS FOR REACTOR DOSIMETRY
(continued)

Neutron Field	Av. Energy (Mev)	Energy Range for Data Testing and Calibration (MeV)	Status of Group Flux Spectrum Characterization
APFA-III **	1.5	0.01 to 18	± 5-20% (0.01 MeV < E < 10 MeV) Spectrometry and computations; ± 5-20% (0.01 MeV < E < 18 MeV) Multiple foils and computations
TAPIRO **	1.5	0.01 to 18	± 5-20% (0.01 MeV < E < 10 MeV) Spectrometry and computations ; ± 5-20% (0.01 MeV < E < 18 MeV) Multiple foils and computations.
YAYOI **	1.5	0.01 to 18	± 5-20% (0.01 MeV < E < 10 MeV) Spectrometry and computations; ± 5-20 (0.01 MeV < E < 18 MeV) Multiple foils and computations.
YAYOI (Lead intermediate column)	1.5	10^{-7} to 2	± 5-20%, spectrometry, multiple foils, computations
Borated Graphite with Electron Linac (1/E spectrum in keV region) Japanese Facility.		10^{-6} to 10	± 5 - 10%, time-of-flight and computations.
Fe BLOCK (shielding benchmark)		0.01 to 1	± 10% or better, Spectrometry, multiple foils, several interlaboratory calculations and measurements.
Na BLOCK (shielding benchmark)		10^{-6} to 5	± 10% or better, Spectrometry, multiple foils, several interlaboratory calculations and measurements.

** Central core position

TABLE 2. REFERENCE NEUTRON FIELDS FOR REACTOR DOSIMETRY
(continued)

Neutron Field	Av. Energy (MeV)	Energy Range for Data Testing and Calibration (MeV)	Status of Group Flux Spectrum Characterization
ANL-Tandem $^{9}Be(d,n)$ reaction		Tailored distributions with mean energies: ∿1, ∿2, ∿3, up to ∿8 MeV.	$> \pm$ 10–30% (0.1 MeV $< E <$ 18 MeV) Spectrometry and theory; $> \pm$ 10–30% (0.1 MeV $< E <$ 18 MeV) Multiple foils and theory.
UC-Davis Cyclotron $^{9}Be(d,n)^{10}B$		Tailored distributions with mean energies, as above, up to ∿15 MeV.	$> \pm$ 10–30% (0.1 MeV $< E <$ 30 MeV) Spectrometry and theory; $> \pm$ 10–30% (0.1 MeV $< E <$ 30 MeV) Multiple foils and theory.

4. Controlled environments - A preliminary and incomplete list of controlled environments can be found in Table 3. These fields can play an important role in dosimetry applications, and a better characterization and fuller documentation should be encouraged.

5. Survey of benchmark fields - An international survey has been initiated to compile information on existing and proposed neutron fields that may qualify as dosimetry benchmarks. This survey has been based on the wide distribution of an extensive questionnaire covering all the relevant characteristics of the fields. It is recommended that full answers are promptly provided to the questionnaire by all those who have not yet done so. Physical description that allows interlaboratory calculation of the benchmarks should be supplied , as well as spectra in tabular or analytical form, and a suggested interpolation procedure.

6. Compendium - The answers so far received to the questionnaire have been compiled in a first compendium that is part of Grundl's and Eisenhauer's paper, this meeting.

TABLE 3 *)CONTROLLED-ENVIRONMENT BENCHMARKS FOR DOSIMETRY DATA DEVELOPMENT AND TESTING

Benchmark	Approximate Major Data Testing Energy Range (MeV)	Status of Group Flux Spectral Characterization
Thermal Type		
a) HFIR	10^{-10} to 18	±5 to 30%, Multiple-foils and computations.
b) BSR	10^{-10} to 18	±5 to 30%, Multiple-foils and computations.
c) BR2-Cd Loops	4×10^{-7} to 18	±5 to 30%, Multiple-foils and computations.
d) HFR	10^{-10} to 18	±5 to 30%, Multiple-foils and computations.
e) KUR	10^{-10} to 18	± 5 to 30 %, Multiple foils, ^{6}Li and ^{3}He Sandwich counters, and computations.
f) Etc.		

* From the report by McElroy et al. this meeting. Some references or reference information for these neutron fields are also given in the various individual papers presented at this meeting.

TABLE 3 (Continued)

Benchmark	Approximate Major Data Testing Energy Range (MeV)	Status of Group Flux Spectral Characterization
LWR-Surveillance		
a) ILR-PV Mockup	10^{-10} to 18	±5 to 30%, Multiple-foils and computations.
b) Japanese-PV Mockup	10^{-10} to 18	±5 to 30%, Multiple-foils and computations.
c) Browns Ferry* #3 (BWR)	10^{-10} to 18	±5 to 30%, Multiple-foils and computations.
d) McQuire 1* (PWR)	10^{-10} to 18	±5 to 30%, Spectrometry and multiple-foils, computations.
e) BR3 (PWR)*	10^{-10} to 18	±5 to 30%, Multiple-foils and computations.
f) ORR-PV Mockup*	10^{-10} to 18	±5 to 30%, Spectrometry and multiple-foils, computations.
g) Etc.		

* Planned measurements, computations, and/or spectrometry.

TABLE 3 (Continued)

Benchmark	Approximate Major Data Testing Energy Range (MeV)	Status of Group Flux Spectral Characterization
FAST Reactor Type		
a) ECEL Core 14-13	$\sim 10^{-6}$ to 18	±5 to 30%, Spectrometry, computations, and multiple-foils.
b) ECEL Core 16	$\sim 10^{-6}$ to 18	±5 to 30%, Spectrometry, computations, and multiple-foils.
c) EMC-FTR	$\sim 10^{-6}$ to 18	±5 to 30%, Spectrometry, computations, and multiple-foils.
d) EBR-II 31F Run	10^{-10} to 18	±5 to 30%, Multiple-foils and computations.
e) EBR-II 50H Run	10^{-10} to 18	±5 to 30%, Multiple-foils and computations.
f) EBR-II 75D Run	10^{-10} to 18	±5 to 30%, Multiple-foils and computations.
g) FTR-IRT*	10^{-10} to 18	±5 to 10%, Spectrometry, computations, and multiple-foils.
h) VIPER	10^{-4} to 10	±5 to 15%, Spectrometry, compilations and multiple foils.
i) STEK Cores	$\sim 10^{-6}$ to 18	±5 to 30%, " " "
j) etc.		

* Planned tests in a cooled in-reactor-thimble (IRT) in the Fast Test Reactor central core region.

TABLE 3 (Continued)

Benchmark	Approximate Major Data Testing Energy Range (MeV)	Status of Group Flux Spectral Characterization
CTR Type		
a) HENRE-$^{3}H(d,n)^{4}He$	10^{-2} to 16	±5 to 30%, Spectrometry, computations, and multiple-foils.
b) RTNS $^{3}H(d,n)^{4}He$	10^{-2} to 16	±5 to 30%, Spectrometry, computations, and multiple-foils.
c) CTR BLANKET MODEL LOCATIONS (D-T Reaction)	10^{-4} to 16	$\geq \pm$ 5 to 30%, Computations and multiple-foils.
d) etc.		

III. DETERMINATION OF NEUTRON FLUX-SPECTRA

A. Summary

Comments and Conclusions:

1. A major conclusion from recent and current data testing work is that spectrum averaged cross section data for dosimetry reactions as measured in standard and reference benchmark neutron fields depart from computed ones, not only because of absolute total flux level normalization and evaluated energy-dependent cross section inadequacies, but also because the spectra of most of these benchmarks are often inaccurate in the energy ranges not covered or poorly covered by differential neutron spectrometry techniques.

2. While the most precise determination of the spectral shape for some standard and reference fields will be accomplished by spectrometry and computations, in other cases, a combination of calculations, neutron differential spectrometry, and integral measurements will be required. For the standard and reference benchmark fields identified in the papers of this conference, Tables 1 and 2 , the total flux value and broad energy group spectral shape uncertainties for the more important energy regions are currently estimated to be in the $\pm$ 2 to 5% (1σ) and $\pm$ 4 to 15% (1σ) range, respectively. For a number of important controlled environments, Table 3, the uncertainties are considerably greater, in the $\pm$ 5 to 15% (1σ) and $\pm$ 5 to 30% (1σ) and higher ranges, respectively.

3. In considering the resolution of the problems and the achievement of higher accuracies, item 1 and 2 above, the following conclusions and/or recommendations are offered.

   a) Flux-level Normalization

   In addition to the documentation and reporting of the experimenters' own absolute value of total flux, a value should be established through a flux transfer from a Cf-252 neutron source*/.

---

*/ see paper by Grundl and Eisenhauer, presented at this meeting.

This flux transfer or normalization, using the ^{239}Pu (n,f) reaction, is rather direct and its accuracy is of the order of $\pm$ 2% (1σ) or better for certain classes of benchmark fields. If a reaction other than ^{239}Pu (n,f) is used, the uncertainty will be somewhat higher.

b) Spectrum Shape Determination

No single differential spectrometry method allows the determination of the entire spectrum shape to the goal accuracy of $\pm$ 5 to 10% (1 σ), or better. The (n,p), ^{6}Li (n,α)T and ^{3}He(n,p)T spectrometers have attained a stage of development that allows spectral measurements in the range of 10 keV to $\sim$ 6 MeV, to approach the above goal accuracy. This accuracy can be obtained, however, only if the results of several experimenters and measurement techniques are combined.

Except for a few standard and reference neutron fields (such as thermal, 1/E, and the Intermediate-energy Standard Neutron Field (ISNF), no calculational method allows the determination of the spectrum shape to the goal accuracy of $\pm$ 5 to 10% (1 σ), or better.

The required level of accuracy for spectral shape determination in some benchmark fields will necessitate the combined use of data obtained from differential spectrometry, analytical calculations, and integral measurements. The development of new and/or improved unfolding codes to handle and combine simultaneously the results of these three techniques is desired. The success of such techniques, however, will depend on the availability of data and analytical methods for handling errors and their correlations, not only on the cross section data files, but also on the spectrometry and reaction rate data.

In the range above approximately 2 MeV, new spectrometry measure - ments by independent and/or new techniques are needed, such as nuclear emulsions,track recorders, ^{4}He recoil spectrometry, and organic proton recoil scintillators wherever applicable.

Recommendations: It is recommended that available codes that will handle the combined results of calculations, spectrometry, and integral measurements be applied to the simultaneous analysis of the data obtained in the best known benchmark fields.

B. Analytical Calculations

Comments and Conclusions:

1. Uncertainties in analytical computations are of two general types:
   a) Nuclear Data

      Errors related to uncertainties in the cross sections, fission spectra and angular distributions of neutrons for the materials in the system.

   b) Modeling

      Errors arising from the approximations necessary to perform the computations, including geometrical representation, multi-group energy structure and material changes due to burnup, etc.

   Uncertainties in the nuclear data can be quantified, but this has not been generally done and constitutes a major undertaking. Modeling approximations can be estimated by parametric studies.

2. One-dimensional geometries studied with fine energy group structures and high order expansions are the only ones, in practice, for which precise calculations are available. In such instances, the accuracy of the spectral determination is limited by the accuracy of the nuclear data.

3. Very often, systems with complicated geometries are analyzed with low-dimensional and/or synthesis techniques. In such cases, geometrical approximations are responsible for additional uncertainties.

4. Perturbation of nuclear data used in transport calculations to provide consistency, in a maximum likelihood sense, with reaction rate data can be identified as a potentially powerful method which can be applied in a few important cases (see McCracken's paper at this meeting).

Recommendations

1. It is recommended that sensitivity analyses be performed for dosimetry standard and reference neutron fields, and in some cases controlled environments. An effort to extend the ENDF/B cross section error file to dosimetry data and associated sensitivity codes should be undertaken.

2. For systems where modeling errors are significant, the generation of spatial importance functions should be considered in order to provide insight into ways of reducing the number of compromises made in the calculations.

3. The use of calculated flux spectra, either by themselves or in combination with experimental results, in data testing can only be recommended in cases where errors have been estimated by means of careful sensitivity studies. Such methods as ANISN-SWANLAKE are now widely available and should be generally used for calculations for the standard and reference fields.

C. Spectrometry Measurements

Comments and Conclusions:

1. Substantial progress has been made during the last few years in the characterization of the standard fission neutron spectra of ^{235}U and ^{252}Cf using differential methods.

The recent evaluation of J. Grundl et al. gave average fission neutron energies of 1.970 $\pm$ 0.014 MeV and 2.130 $\pm$ 0.027 MeV for the ^{235}U and ^{252}Cf fission neutron spectra , respectively. The average departure of the experimental spectrometry data from a reference Maxwellian is less than 5% in the energy range from 0.25 to 8 MeV. Due to necessary corrections for secondary interactions of fission neutrons in the ^{235}U target samples, the ^{235}U fission neutron spectrum appears to be somewhat harder (2.017 $\pm$ 0.015 MeV) compared to the recently evaluated value.

Whether the slopes of the spectra are better described by a Maxwellian or Watt function can finally be determined only on the basis of an evaluation which considers not only the statistical errors but also contributions due to uncertainties in backgrounds, detector efficiency, energy resolution, secondary processes in the samples, etc.

The largest uncertainties in the knowledge of the fission neutron spectra still exist in their low and high energy ends, which contain about 6% of the total neutrons. In certain cases, however, these energy tails are of importance and therefore their knowledge should be improved.

2. The neutron spectrum is one of the most important characteristics of a benchmark neutron field. Its determination should be unique, i.e. only subject to changes in the material and physical characteristics of the field. The closest approach to this ideal situation is actually given by differential neutron spectrometry where the derived spectrum characteristics, generally, depend only upon a single well-known cross section. The applicable energy range, resolution, and estimated accuracy of a number of spectroscopy methods are given in Table 4.

3. For neutron spectrometry in some fast neutron spectrum fields, a ^{3}He proportional counter and a double scintillator time-of-flight method are also applicable (see paper by SEKIGUCHI et al. at this meeting).

   a) ^{3}He proportional counter $\sim$10% 0.1 - $\sim$2 MeV

   b) double scintillator time-of-flight method: $\sim$10% 5×10^{-2} - $\sim$10MeV

Table 4: Comparison of Selected Differential Reactor Neutron Spectroscopy Methods.

Method	E_L [a]	E_u [b]	Resolution	Accuracy % (1σ) [c]
1. (n,p) Emulsions				
- Collimated Source	5×10^{-1}	20	Fair	5 - 10% 0.5 < E < 10 MeV 10 - 20% 10 < E < 20 MeV
- Non-Collimated Source	5×10^{-1}	10		10 - 15% 0.5 < E < 3 MeV 15 - 25% 3 < E < 10 MeV
2. (n,p) Proportional Counters	1×10^{-3}	2.5	Good	10 - 50% 0.001 < E < 0.02 MeV 5 - 10% 0.02 < E < 1.0 MeV 10 - 25% 1.0 < E < 2.5 MeV
3. $^{6}Li(n,t)\,^{4}He$ [d]	1×10^{-2}	6.5	Fair	5 - 10% 0.01 < E < 0.15 MeV 10 - 20% 0.15 < E < 0.3 MeV 5 - 10% 0.3 < E < 0.8 MeV 5 - 15% 0.8 < E < 4.0 MeV 15 - 25% 4.0 < E < 10.0 MeV
4. Time-of-flight (TOF)				10 - 15% 0.00001 < E < 0.001 MeV
- $^{3}H(d,n)^{4}He$ Source	5×10^{-5}	0.2	Good	15 - 20% 0.001 < E < 0.02 MeV 20 - 30% 0.02 < E < 0.2 MeV
- LINAC Source	10^{-9}	10	Good	5 % 10^{-9} < E < 10^{-3} MeV 10 - 20% 10^{-3} < E < 1 MeV 20 % 1 < E < 5 MeV

a) Approximate lower energy limit of applicability, MeV.

b) Approximate upper energy limit of applicability, MeV.

c) Typical accuracies for coarse group structures.

d) The current accuracy of $^{6}Li\,(n,t)^{4}He$ spectroscopy is mainly dominated by the uncertainty in the angular and total reaction cross sections.

4. For the establishment of clean Maxwellian standard thermal neutron fields, it is desirable to measure the thermal neutron spectrum by a chopper time-of-flight method. The superiority of using heavy water as a moderator for a thermal neutron facility compared with a crystalline material such as graphite is shown by the chopper measurements of Kanda et al., reported at this meeting

Recommendations

1. In-core neutron spectrometry is complex and expensive. Experimental planning of neutron spectrum measurements should at least consider two independent techniques.

2. The experimental spectral data, the cross sections and response functions used and the nuclear characteristics of the benchmark field in which the measurement was performed, should be available upon request.

3. Experimental differential spectral results in the benchmark fields must be intercompared and the spectrum reevaluated by taking into account the latest reliable results.

4. Differential neutron spectrometry data should be introduced into unfolding codes as are the integral data.

5. (n,p) spectrometry: Nuclear emulsions should be used in benchmark fields.

6. Techniques covering the higher MeV region ($\sim$2 to 50 MeV) must be further developed, especially keeping in mind the needs of CTR reactor development programs.

7. ^{6}Li (n,α)T spectrometry: cross section improvement is needed for
   a) σ (n,α) for En $>$5 MeV, and
   b) $\frac{d\sigma}{d\Omega}$ for En $<$100 keV.

8. In order to intercalibrate methods of neutron spectrometry, it would be helpful if IAEA would promote some international intercomparisons. (IAEA might supply some transfer instruments with established unfolding techniques, as the Bureau International des Poids et Measures (BIPM) does for the international intercalibration of fast neutron fluence).

D. Integral Measurements

Comments and conclusions:

1. Since 1973 the importance of intercomparing neutron spectrum unfolding programs has been emphasized by experts at the first ASTM-Euratom Symposium on Reactor Dosimetry and by members of the International Working Group on Reactor Radiation Measurements.

2. It is recognized that some activities in this field are initiated and supported by the IAEA. Valuable information on general unfolding techniques is now available in the Proceedings of a Seminar Workshop on Radiation Energy Spectra Unfolding, held at Oak Ridge, April 1976 (see report ORNL/RSIC-40).

3. At the present meeting further results of intercomparison studies have been reported (see contribution by Zijp). Also some new approaches on simultaneous unfolding of data from different spectrometry techniques have been communicated (see contribution by MacCracken, Najzer, Williams and Hannan.)

Recommendations

1. The merits of some promising unfolding codes like SAND-II, RFSP-JUL and CRYSTAL BALL should be studied further.
   The IAEA is requested to make these programs available to interested laboratories upon request.

2. For more specific recommendations on unfolding, reference is made to the results of a workshop on unfolding at the First ASTM-Euratom Symposium on Reactor Dosimetry at Petten, September 1975.

3. When in practical dosimetry applications, in the absence of spectrum information, the concept of equivalent fission neutron fluence is used, one should apply those values of average fission neutron cross sections which result from integral experiments in a ^{235}U fission neutron spectrum (see paper by Fabry et al., Session III).

E. Cross-Section and Spectrum Processing

Comments and Conclusions:

Even when the data base is common, some differences can be introduced by the method which is used to collapse or interpolate the data to a given group structure in order to use them in unfolding procedures or to calculate reaction rates. For measured spectral data even the adoption of a common group structure is questionable: the most adequate group widths and boundaries being dependent on such parameters as experimental resolution, bin width and on the spectrum itself.

Recommendations:

1. When spectral data are given it would be highly advisable to specify the interpolation scheme or to agree on a common one. Attention should also be paid to error propagation.

2. It is recommended that the cross-section processing method which is used be clearly specified when reporting results. In particular, if a weighting spectrum has been employed, it should be explicitly indicated.

IV. INTEGRAL MEASUREMENTS IN BENCHMARK NEUTRON FIELDS

A. Comments and Conclusions:

1. The data development and testing approach first applied to the development of the SAND-II cross section file, and subsequently recommended by the 1973 Consultants' Meeting has been further validated for establishing accepted reference sets of evaluated energy-dependent cross sections for dosimetry applications.

2. Using the above approach, some specific recommendations for further study of reactions in the ENDF/B-IV file have been delineated. (See paper by A. Fabry et al., Session III.)

3. A few sustained inconsistencies still exist and a vigorous and well-planned, coordinated international interlaboratory effort will be required to resolve them. More specific information is provided in the paper by Fabry et al., this meeting, Session III.

B. Recommendations

1. Reaction rate measurements form the backbone of reactor neutron dosimetry. Such measurements must be done with accuracies in the 2-5% (1σ) range, depending on the reaction. Past evidence suggests that systematic errors are best identified and minimized through interlaboratory comparisons, preferably involving independent techniques. It is thus recommended that such intercomparisons continue to be done on as large a basis as possible and be considered mandatory in the case of fundamental reaction rate measurements in standard and reference radiation fields; this requirement may be somewhat relaxed in the study of controlled environments. It is, however, essential that careful documentation of the measurements be provided by the experimenters.

2. Discrepancies up to 10% exist between absolute average cross section measurements in the U-235 fission neutron spectrum. In order to investigate these discrepancies, an interlaboratory experiment is being organized under the sponsorship of the IAEA; it involves the transfer of a fission spectrum assembly and of irradiated detectors*/ between Mol (Belgium), Osaka (Japan), the Seibersdorf Laboratory (Austria) and laboratories participating in the US Interlaboratory LMFBR Reaction Rate (ILRR) program. It is recommended that the scope of this experiment be enlarged so as to encompass as many as possible contributions from other interested laboratories.

3. Inconsistencies between measured and computed average cross sections in the fission neutron spectrum of U-235 have decreased significantly in the past three years but continue to be an issue of relevance in terms of international standardization of dosimetry, in particular because the high energy ($\geq$ 2.5 MeV) tails of the reactor core neutron spectra are often close to fission neutron spectra.

On the other hand, consistency is observed for the Cf^{252} spontaneous fission neutron spectrum, but very few measurements have been performed so far in this benchmark.

A critical appraisal of this situation leads to the following recommendations:

3.1. The neutron flux spectral shapes of the U-235 and Cf-252 fission neutron spectra should be compared directly

a) by spectrometry techniques **/

b) by means of double reaction rate ratio ***/ measurements, which are extremely sensitive to spectral shape differences.

---

*/ Reactions ^{235}U (n,f) F.P., ^{238}U(n,f) F.P., and ^{58}Ni(n,p) ^{58}Co.

**/ Work along such line is in progress at PTB; experts from CEN-SCK, Mol, Belgium, have volunteered to supplement this effort by performing ^{6}Li (n,α) spectrometry at the PTB facilities, if the experimental conditions are adequate.

***/ It has been suggested that such measurements could be performed at NBS.

3.2. Laboratories operating ^{252}Cf sources should be encouraged to perform detector exposures to a certified fluence and distribute the detectors to outside laboratories for reaction rate measurements.
Particular emphasis should be placed upon the $^{58}Ni(n,p)^{58}Co$ reaction.

4. Measurements of cross sections for non-threshold reactions in fast and intermediate-energy neutron fields involve self-shielding corrections that may be substantial. There is a need for additional measurements of these corrections and for confrontation with their computed values. In this context, total cross sections for non-threshold reactions should be included in dosimetry files.

5. New resonance integral measurements are necessary for the reactions $^{45}Sc\ (n,\gamma)^{46}Sc$; $^{58}Fe\ (n,\gamma)^{59}Fe$; $^{63}Cu\ (n,\gamma)^{64}Cu$; $^{6}Li\ (n,\alpha)^{3}H$; and $^{10}B\ (n,\alpha)^{7}Li$.

6. When data are reported from reaction rate measurements in standard or reference neutron fields it is essential that sufficient information be given to allow interpretation of the data according to alternative normalization schemes. To achieve this we recommend that errors be quoted separately for measured absolute reaction rates on the one hand and normalizing parameters on the other. These remarks apply especially to average cross section and spectral index data. In general it is desirable that systematic errors be identified and presented separately from each other and from random errors.

7. Reaction rate traverse measurements performed in shielding benchmark experiments, well characterized by means of spectrometry, could help to establish energy-dependent cross section trends. Results of such well documented experiments should be applied to dosimetry data testing.

8. The IAEA has already established an important programme on irradiation embrittlement of pressure vessel steels (coordinated Research Programme on Irradiation Embrittlement of Pressure Vessel Steels, IAEA-176, 1974). It is desirable to promote the study of pressure vessels in benchmark experiments (for example work at JAERI, CEN/SCK and ORNL) and in operating power reactors. The IAEA should promote international intercomparison of both experimental and theoretical results in connection with the above programme of already established work.

9. Fission rate measurements in standard and reference neutron fields are usually performed by means of absolute fission chambers. Consistently applied solid state track recorder methods can valuably supplement the fission chamber results and should be applied more systematically. ^{6}Li (n,α) and ^{10}B (n,α) reaction rate measurements techniques using nuclear emulsions and solid state track recorders need to be developed and applied in standard and reference neutron fields to provide good data for comparison with the total helium production method.

C.E.N./S.C.K. will start in MOL- $\Sigma\Sigma$ the $^{10}B/^{6}Li$ spectral index measurement, for comparison with the total helium production data, by using their ^{10}B and ^{6}LiF BCMN deposits, positionned in front of fine grain nuclear emulsions.

10. The use of fission detectors requires a knowledge of yields for selected fission products from several fissile nuclides as a function of the energy of the neutrons inducing fission. The nuclear cross section data and decay schemes for such fission products are also required.

- The fissile nuclides of main interest in dosimetry are ^{235}U, ^{239}Pu, ^{238}U, ^{237}Np.

As had already been stated at former meetings, the yields of the fission products ^{95}Zr, ^{97}Zr, ^{103}Ru, ^{131}I, ^{132}Te, ^{137}Cs, ^{140}Ba and ^{148}Nd should be known to an accuracy of $\approx$ 2% (1σ) for the fast breeder programmes, and between 2 and 10% for other reactor programmes.

- The accuracies (1σ) to which "fast reactor fission yields" are known can be assumed to be

  1.5% for ^{235}U fission
  1 to 2 % for ^{239}Pu fission
  1.5 to 3 % for ^{238}U fission
  5 to 10% for ^{237}Np fission.

  - There is still a need to evaluate the energy dependence of the fission yields for the thermal to fast reactor-neutron range, especially for those fission products for which the difference between thermal and fast reactor neutron-yields is considerable (^{103}Ru, ^{131}I, ^{132}Te, ^{140}Ba). Similarly, it seems that for CTR applications fission yields for mean energies up to about 20 MeV may be required.

11. Calibrations of detector sets in standard neutron fields (when available), reduce the relative errors in reaction rate determinations between different foil materials. The influence of the two main sources of error - the reaction rate determination and the cross section - is minimized in this way. Relative errors in reaction rate determination may be reduced to one or two percent. The results (fluence or spectra) are then relative to the standard spectrum measured so that the error then depends upon the precision to which the standard (fluence or spectrum) is known.

    It is recommended that this dosimetry approach be implemented whenever possible and that standard neutron fields be consequently made available to any interested user.

12. Materials used as neutron dosimeters must be accurately defined and contain a minimum of impurities. Enriched isotopes are sometimes required. A pool of such materials including fissionable materials should be established, possibly by the IAEA at its Seibersdorf Laboratory. The Agency should promote the establishment of a close working relationship between different centres which fabricate and provide such detector materials.

The pool of these materials should be open to Member States. This cooperative effort should establish the necessary procedures that are needed to maintain a uniform level of overall standardization of the necessary physical and chemical properties of the materials and fabrication of the detectors.

13. For the radioisotopes resulting from important dosimetry reactions a list of recommended values for decay parameters (γ-intensities, half-lives) should be prepared and distributed by the IAEA.

14. The dosimetry reactions have been classified in two categories. Category I reactions are defined as reactions,

a. whose differential-energy cross section is well known over their response range in standard neutron fields;

b. which are consistent with integral measurements in the standard neutron fields.

The following reactions belong to Category I:

$^{197}Au(n,\gamma)^{198}Au$, $^{239}Pu(n,f)$ F.P., $^{237}Np(n,f)$ F.P., $^{238}U(n,f)$ F.P., $^{56}Fe(n,p)^{56}Mn$, $^{27}Al(n,\alpha)^{24}Na$, $^{63}Cu(n,2n)^{62}Cu$(*) and $^{58}Ni(n,2n)^{57}Ni$(*).

A number of other reactions are considered Category I candidates: $^{235}U(n,f)$ F.P., $^{59}Co(n,\gamma)^{60}Co$, $^{238}U(n,\gamma)^{239}U$, $^{115}In(n,n')^{115m}In$, $^{58}Ni(n,p)^{58}Co$, $^{32}S(n,p)^{32}P$, $^{54}Fe(n,p)^{54}Mn$, $^{59}Co(n,\alpha)^{56}Mn$, $^{103}Rh(n,n')^{103}Rh^{m}$.

All other reactions used for dosimetry are Category II reactions.

It is recommended that caution be exercised when using the Category II reactions for neutron spectrum adjustment or unfolding.

(*) For the very high energy range, accuracies of the order of $\pm$ 10 % are presently acceptable.

V. DIFFERENTIAL MEASUREMENTS AND EVALUATIONS

1. The development of consistent sets of cross section data for a selected group of dosimetry reactions has not turned out to be an easy task. The current accuracy goal of better than ± 5% (1σ) has not been achieved with the possible exception of a few "Category I" reactions. It is clear that an international effort is desirable in order to achieve the stated goal and that it will have to involve investigation of decay schemes and a variety of "benchmarks" integral experiments as well as of differential (monoenergetic) measurements. A first step has been taken by adoption of the ENDF-B-IV dosimetry evaluated data file as the reference library of differential cross sections. This file represents the best available set to date. It appears that the uncertainty in the experimental data included in evaluated files cannot be expected to become less than 4 - 7% with the exception of a few special cases. The major source of uncertainties come from the neutron fluence determination.

2. For threshold reaction cross sections used in reactor dosimetry, the energy range of main interest is from threshold up to 4-6 MeV above it: the range of 20% reaction response in fission spectrum. Differential measurements are encouraged to be done especially in this energy range.

3. The problem of error files was not addressed in the ENDF/B-IV dosimetry file. In many applications such as neutron spectrum unfolding by multiple foil activation techniques, error files are important (e.g. error propagation calculations). It is recommended therefore that evaluators of energy-dependent cross section data provide confidence statements for successive energy regions specifying where possible the random and systematic contributions. It is further recommended that practical procedures are developed to account for propagation of errors in cross section data.

   The proposal to carry out a detailed analysis of the variance/covariance estimates of the ^{235}U fission cross section by the task force* and the covariance subcommittee of CSEWG should be monitored closely to determine the feasibility of use with dosimetry files.

4. In principle it is possible to intercalibrate absolute fission detectors used in some integral measurements with those used in differential measurements. It is recommended that this possibility be investigated for use.

5. The large discrepancy between integral and differential data for the ^{63}Cu (n,α) ^{60}Co reaction may be resolved by two new experiments: measurement near threshold (5 - 6 MeV, low resolution is acceptable) and a new 14 MeV measurement (where an accuracy of 5% (1σ) or better is needed).

---

*) M. Bhat NEANDC/NEACRP Specialists Meeting on Fast Neutron Fission Cross Section of ^{233}U, ^{235}U, ^{238}U and ^{239}Pu. NEANDC(US)-199/L, ERDA-NDC 5/L, ANL-76-90, Ed. Poenitz & Smith.

6. Integral data testing of the ENDF/B-IV dosimetry file suggests that for a number of threshold reactions, existing inconsistencies can be explained by flux scale normalization errors in differential-energy cross section measurements. The suggested normalization factors+ are as follows:

^{232}Th (n,f): 1.15
^{47}Ti (n,p): 0.825*
^{54}Fe (n,p): 0.967*
Ti (n,x) ^{46}Sc: 1.128
^{59}Co (n,α) ^{56}Mn: 0.98

It is recommended that evaluators of differential-energy cross sections examine whether such renormalizations are acceptable.

7. It is recommended that differential cross section measurements be undertaken for: ^{45}Sc (n,γ) in the energy region .5 eV - 1 MeV,

^{93}Nb (n,n') $^{93}Nb^{m}$
^{199}Hg (n,n')$^{199}Hg^{m}$ from threshold to 10 MeV.

8. With a view towards application of dosimetry for radiation damage studies, it is recommended that differential cross section data for helium production in reactor structural materials be performed. (See recommendations of I.A.E.A. Specialists Meeting on Radiation Damage Units, Harwell, 2-4 Nov.1976).

9. The List of reactions of interest to reactor neutron metrology** is given below.

The table is arranged as follows:

Category:

The dosimetry reactions have been classified in two categories. Category I reactions are defined as reactions:

a. for which the energy dependent cross sections are well known over their response range in standard neutron fields;

b. for which calculated reaction rates in the standard neutron fields are consistent with the measured reaction rates.

+ A. Fabry (Session III paper).

* A new evaluation by C. Philis, D. Smith and A. Smith, reported by B.A. Magurno at this meeting (preliminary results), should solve the discrepancy for Ti(n,α)^{46}Sc; however, the discrepancy for ^{47}Ti(n,p) remains.

** submitted by W.L. Zijp, Petten.

All other reactions used for neutron metrology are category II reactions. However, some of them, denoted with II*, are considered category I candidates. They will reach the status of category I after removal of some inconsistencies between integral measurements and differential evaluations, at least as concerned the 235U fission neutron spectrum, the $\Sigma\Sigma$ spectrum and the ISNF spectrum.

Reaction:

This column lists the reactions of interest in order of increasing proton number. The first part of the table contains the non-threshold reactions. The second part lists the threshold reactions.

Response remarks:

The information refers for the (n,γ) reactions to the energy E_r of the main resonance, and for the other reactions to the energy range comprising 90% response in a Watt fission neutron spectrum. For some reactions the information was not readily available.

Evaluations and compilations:

This column contains some relevant recent general literature references, described below the end of the table.

Applications:

Here indications are given of the field of applications. The code used is as follows:

a. Often used for flux density determinations (here a knowledge of integral cross sections and decay scheme data is required).

b. Often used in triple foil ("Sandwich") techniques (here a knowledge of resonance activation integral and decay scheme data is required, and also supplementary data to calculate self-shielding factors).

c. Often used for fluence determinations (here a knowledge of integral cross sections and decay scheme data is required).

d. Often used in spectrum unfolding techniques using computer codes like SAND-II and SPECTRA (here a knowledge of energy dependent cross section data is required).

e. Useful in measurements for CTR applications.

Special remarks:

Where it seemed appropriate, some special comment is given.

Non-threshold reactions:

category	reaction	response remarks	evaluations and compilation	applications	special remarks
II	$^{6}Li(n,\alpha)^{3}H$		1 6 7		total He production of particular importance
II	$^{10}B(n,\alpha)^{7}Li$		7		total He production of particular importance
II	$^{23}Na(n,\gamma)^{24}Na$	E_r = 2850 eV	2 6 7	b d	
II	$^{30}Si(n,\gamma)^{31}Si$		2 6		
II	$^{45}Sc(n,\gamma)^{46}Sc$		6 7	d	
II	$^{51}V(n,\gamma)^{52}V$	E_r = 4162 eV	2 6	b	
II	$^{55}Mn(n,\gamma)^{56}Mn$	E_r = 337 eV	2 6	b d	
	$^{58}Fe(n,\gamma)^{59}Fe$		2 6 7	c d	
	$^{58}Co^{m}(n,\gamma)^{59}Co$				Important to derive burn-up correction for nickel as fast neutron detector.
II	$^{58}Co(n,\gamma)^{59}Co$				Important to derive burn-up correction for nickel as fast neutron detector.
II*	$^{59}Co(n,\gamma)^{60}Co$	E_r = 132 eV	1 2 6 7	a b c d	σ_o, I and $\sigma(E)$ of particular importance
II	$^{63}Cu(n,\gamma)^{64}Cu$	E_r = 580 eV	2 6 7 8	a b d	
II	$^{64}Ni(n,\gamma)^{65}Ni$		2 6		
II	$^{71}Ga(n,\gamma)^{72}Ga$	E_r = 95 eV	6	b	
II	$^{75}As(n,\gamma)^{76}As$	E_r = 47 eV	6	b	
II	$^{80}Se(n,\gamma)^{81}Se$	E_r = 1965 eV	6	b	
II	$^{81}Br(n,\gamma)^{82}Br$	E_r = 101 eV	6	b	
II	$^{93}Nb(n,\gamma)^{94}Nb$		4		Suggested as possible long term fluence detector
II	$^{98}Mo(n,\gamma)^{99}Mo$	E_r = 12 and 480 eV	2 6	b	
II	$^{100}Mo(n,\gamma)^{101}Mo$	E_r = 97.3 and 364 eV	6	b	
II	$^{103}Rh(n,\gamma)^{104}Rh$	E_r = 1.257 eV	6	b	
II	$^{108}Pd(n,\gamma)^{109}Pd$	E_r = 2.96 eV	6	b	
II	$^{109}Ag(n,\gamma)^{110}Ag^{m}$		2 6	c d	Together with $^{59}Co(n,\gamma)$ important in double foil technique to determine fluence of thermal and intermediate neutrons. Long $T_{\frac{1}{2}}$ replacement for $^{197}Au(n,\gamma)^{198}Au$.
II	$^{114}Cd(n,\gamma)^{115}Cd$	E_r = 120 eV	6	b	
II	$^{115}In(n,\gamma)^{116}In^{m}$	E_r = 1.46 eV	2 6 7 8	a b d	
II	$^{121}Sb(n,\gamma)^{122}Sb$		6	b	
II	$^{133}Cs(n,\gamma)^{134}Cs$	E_r = 5.9 eV	6	b	
II	$^{139}La(n,\gamma)^{140}La$	E_r = 72.4 eV	2 6	b	
II	$^{152}Sm(n,\gamma)^{152}Sm^{m}$	E_r = 8.01 eV	6	b	
II	$^{151}Eu(n,\gamma)^{152}Eu^{m}$		2 6		
II	$^{164}Dy(n,\gamma)^{165}Dy$		2 6	a	
II	$^{175}Lu(n,\gamma)^{176}Lu$		2 6		
II	$^{176}Lu(n,\gamma)^{177}Lu$		2 6		
II	$^{181}Ta(n,\gamma)^{182}Ta$		6	d	Long $T_{\frac{1}{2}}$ replacement for $^{197}Au(n,\gamma)^{198}Au$
II	$^{186}W(n,\gamma)^{187}W$		2 6	b	
	$^{197}Au(n,\gamma)^{198}Au$	E_r = 4.90 eV	1 2 6 7 8	a b d	
	$^{232}Th(n,\gamma)^{233}Th$		6 7		
II*	$^{235}U(n,f)$**	0.19...5.1 MeV	123 5678	a c d	
II*	$^{238}U(n,\gamma)^{239}U$		1 2 6 7		Of particular importance
I	$^{239}Pu(n,f)$**	0.27...5.1 MeV	1 2 6 7 8	a c d	

* category I candidate.

** the yields for the fission products ^{95}Zr, ^{137}Cs, ^{140}Ba and ^{148}Nd belong to the second category.

Threshold reactions:

category	reaction	response remarks	evaluations and compilation	applications	special remarks
II	$^{19}F(n,2n)$		6	e	Threshold ~11.8 MeV
II	$^{23}Na(n,2n)^{22}Na$				Very high threshold = 12.5 MeV
II	$^{24}Mg(n,p)^{24}Na$	6.5...11.5 MeV	2 5 6 8	d	
II	$^{27}Al(n,p)^{27}Mg$	3.5... 9.3 MeV	1 2 3 5 6 7 8	d	Of particular importance
I	$^{27}Al(n,\alpha)^{24}Na$	6.4...11.9 MeV	2 3 4 5 6 7 8 9	a d e	
II	$^{28}Si(n,p)^{28}Al$	5.4...10.1 MeV	6		
II	$^{31}P(n,p)^{31}Si$	2.2... 7.0 MeV	2 3 4 5 6 8 9	d	
II*	$^{32}S(n,p)^{32}P$	2.5... 7.5 MeV	2 3 4 5 6 7 8 9	a d	
II	$^{34}S(n,\alpha)^{31}Si$	5.1...10.4 MeV	6		
II	$^{35}Cl(n,\alpha)^{32}P$	3.2... 8.0 MeV	6		
II	$^{46}Ti(n,p)^{46}Sc$	3.4... 9.1 MeV	2 3 4 5 6 7 8 9	a c d	Particular interest in $Ti(n,x)^{46}Sc$
II	$^{47}Ti(n,p)^{47}Sc$	2.1... 7.0 MeV	2 3 4 5 6 7 8 9	d	
II	$^{48}Ti(n,p)^{48}Sc$	6.6...12.8 MeV	2 3 4 5 6 7 8 9	d	
II	$^{55}Mn(n,2n)^{54}Mn$		2 3 4 5 7 8 9	d	Possible long term fluence monitor
II*	$^{54}Fe(n,p)^{54}Mn$	2.3... 7.8 MeV	1 2 3 5 6 7 8	a c d	Of particular importance
I	$^{56}Fe(n,p)^{56}Mn$	5.5...11.0 MeV	2 3 4 5 6 7 8	d	
II	$^{59}Co(n,p)^{59}Fe$		6		Might be of interest
II*	$^{59}Co(n,\alpha)^{56}Mn$		2 3 4 5 6 7 8 9	e	
II	$^{59}Co(n,2n)^{58}Co$		6 7		
II*	$^{58}Ni(n,p)^{58}Co$	2.1... 7.0 MeV	1 2 3 5 6 7 8	a d	Includes $^{58}Ni(n,p)^{58}Co^{m}$
II	$^{58}Ni(n,\alpha)^{55}Fe$		1 2 5 6		Of particular importance
I	$^{58}Ni(n,2n)^{57}Ni$	13.2...17.0 MeV	6 7 8 9	e	Very high threshold
II	$^{60}Ni(n,p)^{60}Co$	2.7... 9.6 MeV	6 7		
II	$^{63}Cu(n,\alpha)^{60}Co$	6.1...11.3 MeV	1 2 3 5 6 7 8 9	a c d	Of particular importance
I	$^{63}Cu(n,2n)^{62}Cu$	11.9...16.4 MeV	1 2 3 5 6 7 8 9	e	
II	$^{65}Cu(n,p)^{65}Ni$		6	d	
II	$^{65}Cu(n,2n)^{64}Cu$		2 3 5 6		
II	$^{64}Zn(n,p)^{64}Cu$	2.3... 7.8 MeV	2 3 5 6 8	d e	
II	$^{64}Zn(n,2n)^{63}Zn$		6		
II	$^{90}Zr(n,2n)^{89}Zr$	12.5...16.7 MeV	6 8 9	d	
II	$^{93}Nb(n,n')^{93}Nb^{m}$		1 2 5 6		Low threshold of particular importance
II	$^{93}Nb(n,2n)^{92}Nb$		2 3 4 5 6 8 9		
II	$^{92}Mo(n,p)^{92}Nb$		2 5 6		
II	$^{94}Mo(n,p)^{94}Nb$				Possible long term fluence monitor
II*	$^{103}Rh(n,n')^{103}Rh^{m}$		1 2 3 5 6 8		Low threshold; of particular importance
II*	$^{115}In(n,n')^{115}In^{m}$	1.2... 5.8 MeV	1 2 3 5 6 7 8	a d	Low threshold; of particular importance
II	$^{127}I(n,2n)^{126}I$	10.0...14.6 MeV	2 3 5 6 7 8	a d e	High threshold
II	$^{199}Hg(n,n')^{199}Hg^{m}$				Recently suggested
II	$^{232}Th(n,f)$	1.5... 7.2 MeV	1 2 3 5 7 8	d	Of particular interest; fission product activities contain information on irradiation history
I	$^{238}U(n,f)$**	1.5... 6.7 MeV	1 2 3 5 7 8	a c d	
I	$^{237}Np(n,f)$**	0.69...5.6 MeV	1 2 3 5 7 8	a c d	

* category I candidate

** the yields for the fission products ^{95}Zr, ^{137}Cs, ^{140}Ba and ^{148}Nd belong to the second category.

Literature references, quoted in column 4:

[1] Vlasov, M.; Dunford, C.; Schmidt, J.J.; Lemmel, H.D.: "Status of neutron cross section data for reactor radiation measurements", INDC(NDS)-47/L (IAEA, Vienna, 1972).

[2] Zijp, W.L.: "Nuclear data for neutron metrology" RCN-73-017; Proc. Symposium on Applications of Nuclear Data in Science and Technology, held in Paris, 12-16 March 1973; Vol.2, p. 271 (IAEA, Vienna, 1973).

[3] Zijp, W.L.; Voorbraak, W.P.; Nolthenius, H.J.: "Compilation of evaluated cross section data used in fast neutron metrology" RCN-196 (Reactor Centrum Nederland, Petten, 1973).

[4] Vlasov, M.F.; Fabry, A.; McElroy, W.N.: "Status of Neutron Cross Sections for Reactor Dosimetry", Proc. International Conference on the Interactions of Neutrons with Nuclei, held in Lowell, USA, 6-9 July 1976; Vol.2, p. 1187.

[5] Schett, A.; Okamoto, K.; Lesca, L.; Frühner, F.H.; Liskien, H.; Paulsen, A.: "Compilation of threshold reaction neutron cross sections for neutron dosimetry and other applications", EANDC 95 "U" (OECD, CCDN, Saclay, February 1974); with updated index to the reactions, May 1975.

[6] "Handbook of Nuclear Activation Cross Sections" IAEA Technical Reports Series No. 156 (IAEA, Vienna, 1974).

[7] Magurno, B.A. (editor): "ENDF/B-IV dosimetry file" Report BNL-NCS-50446 (NTIS, April, 1975).

[8] Fabry, A.; Ceulemans, H.; Van de Plas, P.; McElroy, W.N.; Lippincott, E.P.: "Reactor dosimetry integral reaction rate data in LMFBR benchmark and standard neutron fields: status, accuracy and implications". Paper prepared for the First ASTM-Euratom Symposium on Reactor Dosimetry, held at Petten, September 22-26, 1975.

VI. USE OF INTEGRAL EXPERIMENTS

1. High priority should be given to the establishment of important fields and reactions as Standard Fields and Category I reactions respectively; in particular discrepancies between measured and calculated reaction rates of several important reactions in the U-235 fission spectrum should be investigated.

2. The choice of reactions to be used in a given environment will be limited by practical considerations, but there may still remain a large choice. It is desirable to focus attention on a more limited number of reactions which might be of particular importance in Multiple Foil Analysis. It is recommended that the feasibility of identifying such reactions by means of a sensitivity study be investigated.

   In order to predict accurately the reaction rates and their variances in Standard Neutron Fields and Reference Neutron Fields evaluators of both should be encouraged to provide an approximate correlation function for the evaluated spectra. Where this is not possible details of the calculations and measurements (with a full list of estimated uncertainties) used to evaluate the field should be supplied.

3. For the same reason evaluators of cross-sections used in dosimetry should be encouraged to provide an estimate, however approximate, of the cross-section correlation function.

4. The establishment of more extreme Reference Neutron Fields is desirable to give knowledge of the performance of reactions important to dosimetry in the energy ranges not being considered at present.

VII. SUMMARY OF CONCLUSIONS

1. The most significant advances in the dosimetry benchmark programme since September 1973 are the following:

   - The availability of the ENDF/B-IV Dosimetry File and its wide use as a reference set,

   - an improved characterization by measurements and calculations of the benchmark neutron fields,

   - the collection and compilation of information on benchmarks,

   - a number of consistent applications of benchmark measurements to spectrum and/or cross-section validation or correction.

2. The most significant conclusions reached at this meeting are:

   - The identification of a limited number of standard neutron fields (thermal, 1/E, ^{252}Cf spontaneous fission) and of Category I dosimetry reactions (^{197}Au(n,γ)^{198}Au; ^{237}Np (n,f) F.P.; ^{238}U(n,f) F.P.; ^{56}Fe(n,p)^{56}Mn; ^{27}Al(n,α)^{24}Na; ^{63}Cu(n,2n)^{62}Cu; ^{58}Ni(n,2n)^{57}Ni). Reaction rate measurements of Category I reactions in the standard field yield results consistent with calculations using ENDF/B-IV cross-sections and the recommended representations of the standard spectra.

   - The agreement on the principles of a procedure to use measurements in benchmark fields to improve the knowledge of the reference fields and controlled environments and/or of CategoryII reaction cross-sections.

3. Some of the most important recommendations coming from the meeting are:

   - ENDF/B-IV dosimetry cross-sections and agreed representations for the standard spectra should be used, at least in parallel with other cross-sections and representations.

- Efforts should be made to remove inconsistencies between integral measurements and differential evaluations at least as concerns the ^{235}U fission spectrum, the $\sum\sum$-type facilities and the ISNF, and the cross-sections for $^{58}Ni\ (n,p)^{58}Co$; $^{235}U(n,f)$ F.P., $^{59}Co(n,\gamma)^{60}Co$; $^{115}I(n,n')^{115}In^{m}$, $^{54}Fe(n,p)^{54}Mn$; $^{103}Rh(n,n')^{103}Rh^{m}$ and some others, see page 29, so as to qualify them as standard spectra and Category I reactions, respectively.

- Some assessment of errors and of correlations should be made for the dosimetry cross-sections.

- Further efforts should be made to arrive at a better characterization of benchmark neutron fields, including interlaboratory measurements and calculations; it is important that some indications on the confidence to assign to fluxes and spectra are reached.

- Efforts to improve the knowledge of Category II reactions should be focused with first priority on a restricted number of reactions of primary interest for dosimetry applications.

- Simultaneous analysis of measurements of several reactions in different benchmark fields appears the most promising way to arrive at physically meaningful results; such analyses should be carried out in several laboratories and the results compared.

- The necessity of a limited number of new differential measurements and evaluations of dosimetry cross-sections has been identified; for all the other reactions of interest for dosimetry, the improvement of cross-sections is expected to be derived from a combination of integral and differential measurements, when available, which should yield internally consistent data.

- International cooperation is essential in reaching these goals; closer links should be established between the present programme and other programmes sponsored by the IAEA and by other international organizations, so that the full variety of available and identified benchmark fields is employed.

- Substantial efforts should be undertaken, preferably by the IAEA Seibersdorf Laboratory, to create a pool of dosimetry materials (in particular fissionable isotopes) accessible to the whole dosimetry community.

Supplement I

Consultants' Meeting

on Integral Cross-Section Measurements

in Standard Neutron Fields for Reactor Dosimetry

Vienna, 15 - 19 November 1976

AGENDA

MONDAY, 15 NOVEMBER, morning session

Opening of the meeting by Dr. J.J. Schmidt, IAEA

SESSION I. OVERVIEW

Chairman: Dr. J.A. Grundl

1.1 Review:

1.1a 'Benchmark neutron fields for reactor dosimetry' (J.A. Grundl, NBS, Washington)

1.1b 'Power reactor pressure vessel benchmarks' (F. Rahn, EPRI, Palo Alto)

1.1c 'Remarks on terminology and symbols for physical quantities in neutron metrology" (S. Wagner, PTB, Braunschweig)

1.2 Contributed papers

1.2a 'One material experiments in the frame of power reactor pressure vessel benchmarks' (G.De Leeuw-Gierts, C.E.N.-S.C.K., Mol)

1.2b 'Spectrum characterization and threshold reaction rate measurements in the neutron field of VIPER' by M.H. McTaggart (J.G. Williams, London Univ.)

MONDAY, 15 NOVEMBER, afternoon session and TUESDAY, 16 NOVEMBER morning session

SESSION II. Spectral Characterization of Benchmark Neutron Fields

Chairman: Dr. W.N. McElroy

2.1 Review:

2.1a 'Spectral characterization by combining neutron spectroscopy, analytical calculations and integral measurements' (W.N. McElroy, HEDL, Richland)

2.1b 'A review of the standard fission neutron spectra of ^{235}U and ^{252}Cf' (H.H. Knitter, Geel)

2.1c 'In-pile neutron spectroscopy: status' (G. de Leeuw, CEN-SCK, Mol)

2.2 Contributed papers

2.2a 'Standards for thermal neutrons at the PTB' (S.Wagner, PTB)

2.2b 'Fast neutron standards at the PTB' (S. Wagner, PTB, Braunschweig)

2.2c 'A Californium-252 fission spectrum irradiation facility for neutron reaction rate measurements' by J.A. Grundl, V.Spiegel, C.M. Eisenhauer, H.T. Heaton, II, D. Guliam and J. Bigelow' (J.A. Grundl, NBS)

2.2d 'The IAEA Programme on intercomparison of the computer codes for neutron spectra unfolding by activation technique', Progress report (B. Cross, IAEA)

2.2e 'Comparison of neutron spectrum unfolding codes', by W. Zijp and H.J. Nolthenius (W. Zijp, ECN, Petten)

2.2f 'Spectral characterization of the NISUS neutron field' by J.G. Williams and A.H.M.A. Hannan (J.G. Williams, London University)

2.2g 'Studies of neutron standard fields in the fast source reactor 'YAYOI', by A. Sekiguchi et al. (I. Kimura, RRI, Osaka)

2.2h 'Thermal neutron field with a heavy water facility', by K. Kanda et al. (I. Kimura, RRI, Osaka)

2.2i 'The coupled fast reactivity measurements facility (CFRMF)' by J.W. Rogers, Y.D. Harker and D.A. Millsap. (A. Fabry, CEN-SCK, Mol)

2.2j 'The IAEA Intercomparison of methods for processing Ge(Li) γ-ray spectra', Progress report (R.M. Parr, IAEA)

2.3 Discussion and Recommendations for Sessions I & II.

TUESDAY, 16 NOVEMBER, afternoon, and WEDNESDAY, 17 NOVEMBER morning session

SESSION III. Integral Data in Benchmark Neutron Fields

Chairman: Dr. A. Fabry

3.1 Review

3.1a 'Review of microscopic integral cross section data in fundamental reactor dosimetry benchmark neutron fields' Part I, by A. Fabry et al., (for Part II: see agenda item 5.1c)
(A. Fabry, CEN/SCK, Mol)

3.1b 'Ratios of measured and calculated reaction rates for some known spectra' (W. Zijp, ECN, Petten)

3.2 Contributed papers

3.2a 'General remarks on the benchmark studies'
(W. Zijp, ECN, Petten)

3.2b 'Intercomparison of the intermediate energy standard neutron field at the NISUS and Mol-ΣΣ- facilities by means of absolute fission chambers', by A. Fabry, J.G. Williams and A.H.M.A. Hannan, D. Azimi-Garakani.
(J.G. Williams, London University)

3.2c 'Activation foil data for NISUS, ΣΣ-Mol and ^{235}U fission spectrum' by A.H.M.A. Hannan and J.G. Williams
(J.G. Williams, London University)

3.2d 'Integral cross section measurements with regard to the low and high energy part of the Californium-252 neutron spectrum'
(W. Mannhart, PTB, Braunschweig)

3.2e 'Spectrum averaged cross-section measurements in the fast neutron field of a uranium fission plate'
(D.Najzer, Ljubljana, Inst.J.Stefan)

3.2f 'Fission product yield ratios for ^{235}U fission by thermal and ^{252}Cf neutrons' , by K. Debertin
(S. Wagner, PTB, Braunschweig)

3.2g 'Measurement and evaluation of threshold reaction cross sections in standard neutron fields'
(I. Kimura, RRI, Osaka)

3.2h 'Quality control and calibration of miniature fission chambers by exposure to standard neutron fields. Application to the measurement of fundamental integral cross section ratios'
(A. Fabry, CEN/SCK Mol)

3.2i 'Measuring of a few integral data in the ~~SS~~ neutron field'
(I. Gârlea, INT, Bucharest)

3.2j 'Progress report on detector cross section benchmark measurements in the Tapiro reactor', by M. Martini, P. Moioli, and F. Sirito (U. Farinelli, CNEN / CSN Casaccia)

3.2k 'Comparison of integral cross-section values of several cross section libraries in the SAND-II format'
(W.L. Zijp, Petten)

3.2l 'Comparison of DETAN-74 and ENDF/B-IV cross section data in 620 groups' (W.L. Zijp, Petten)

3.2m 'Status of fission product yields used in fast reactor dosimetry' (G. Lammer, IAEA)

3.3 Discussion and Recommendations for Session 3

WEDNESDAY, 17 NOVEMBER, morning and afternoon sessions

SESSION IV. Differential Cross-Section Data for Reactor Dosimetry

Chairman: Dr. B. Magurno

4.1 Review

4.1a 'Remarks concerning the accurate measurement of differential cross sections for threshold reactions used in fast neutron dosimetry for fission reactors', by D. Smith, ANL, Argonne
(M. Vlasov, IAEA)

4.1b 'Comments on excitation functions of threshold reactions used in reactor neutron dosimetry'
(M.Vlasov, IAEA)

4.1c 'Status of some activation cross sections for reactor neutron dosimetry in the range 13 - 15 MeV'
(H. Vonach, IRK, Vienna)

4.1d 'Status of the ENDF/B-V dosimetry file'
(B. Magurno, BNL)

4.2 Contributed papers

4.2a 'Cross-section requirements for reactor neutron flux measurements from the user's point of view' by M. Mas and R. Lloret (R. Lloret, CEN, Grenoble)

4.2b 'Evaluations of $^{27}Al\ (n,\alpha)^{24}Na$, $^{27}Al(n,p)^{27}Mg$ and $^{58}Ni(n,p)^{58}Co$ cross sections', by T. Asami (I. Kimura, RRI, Kyoto Univ. Osaka)

4.3 Discussion and Recommendations for Session IV

THURSDAY, 18 NOVEMBER, morning session

SESSION V. Validation and Adjustment of Differential Cross Sections on the Basis of Integral Data

Chairman: Prof. U. Farinelli

5.1 Review

5.1a 'General proposals of methodology for cross-section validation and adjustment' (U. Farinelli, CNEN,CSN Casaccia)

5.1b 'Foil activation detectors - some remarks on the choice of detectors, the adjustment of cross-sections and the unfolding of flux spectra' (A.K. Mac Cracken, Winfrith)

5.1c 'Review of microscopic integral cross section data in fundamental reactor dosimetry benchmark neutron fields', Part II (for Part I see 3.1a) (A. Fabry, CEN/SCK, Mol)

5.2 Contributed papers

5.2a 'On the possibility of unfolding simultaneously data from multiple foil, proton recoil and other neutron spectrometers by the SAND-II type unfolding codes' (M. Najzer, Institute J. Stefan, Ljubljana)

5.3 Discussion and Recommendations for Session V

THURSDAY, 18 NOVEMBER, afternoon

Meetings of working groups.

FRIDAY, 19 NOVEMBER

SESSION VI. Conclusions and Recommendations to the IAEA

Chairman: Dr. J. Grundl

Scientific Secretary: Dr. M. Vlasov

Review and finalization of conclusions and recommendations of the working groups.

Closing and adjournment of the meeting. (Prof. U. Farinelli, Dr. J.A. Grundl)

Supplement II

IAEA Consultants' Meeting on Integral Cross-Section Measurements in Standard Neutron Fields

Vienna, 15 - 19 November 1976

List of Participants

De Leeuw-Gierts, G.	Centre d'Etude de l'Energie Nucléaire B-2400 Mol
De Leeuw-Gierts, S.	"
Ertek, C.	Seibersdorf Laboratory I.A.E.A.
Fabry, A.	Centre d'Etude de l'Energie Nucléaire B-2400 Mol
Farinelli, U.	C.N.E.N.-R.I.T. C.S.N. Casaccia I-00060 Santa Maria di Galeria Roma
Gârlea, I.	Institute for Nuclear Technology P.O.Box 5204 Bucharest-Magurele 7000 Romania
Grundl, J.A., Chairman	U.S. Department of Commerce National Bureau of Standards Bldg. 235, Room A-157 Washington, D.C. 20234, USA
Hannan, A.H.M.A.	U.L.R.C. Silwood Park, Sunninghill Ascot, Berks., SL5 7PY, U.K.
Kimura, I.	Research Reactor Institute Kyoto University, Kumatori Sennan-Gun, Osaka-Fu, Japan
Knitter, H.H.	Bureau Central de Mesures Nucléaires Steenweg naar Retie B-2400 Geel

Lammer, G.	Nuclear Data Section I.A.E.A.
Lessler, R.*	Nuclear Data Section I.A.E.A.
Lloret, R.	C.E.N./G. Service des Piles/Dos. 85 X Centre de Tri F-38041 Grenoble Cedex
MacCracken, A.K.	U.K.A.E.A. A.E.E. Winfrith B 21 Dorset/Dorchester U.K.
Magurno, B.	N.N.C.S.C. Brookhaven National Laboratory Upton, N.Y. 11973, USA
Mannhart, W.	Physikalisch-Technische Bundesanstalt Bundesallee 100 D-3300 Braunschweig
McElroy, W.N.	Westinghouse Hanford Company P.O.Box 1970 Richland, Washington 99352 USA
Najzer, D.	Institute J. Stefan P.O.Box 199 61001 Ljubljana, Yugoslavia
Okamoto, K.*	Nuclear Data Section I.A.E.A.
Rahn, F.J.	Electric Power Research Institute 3412 Hillview Avenue Palo Alto, Ca. 94303, USA
Reijonen, H.*	Physics Section I.A.E.A.
Schmidt, J.J.	Nuclear Data Section I.A.E.A.
Vlasov, M., Scientific Secretary	"
Vonach, H.K.	Institut f. Radiumforschung u. Kernphysik Boltzmanngasse A-1090 Vienna

* Observers

Wagner, S.	Physikalisch-Technische Bundesanstalt Bundesallee 100 D-3300 Braunschweig
Williams, J.G.	U.L.R.C. Silwood Park, Sunninghill Ascot, Berks., SL5 7 PY, UK
Zijp, W.L.	Netherlands Energy Research Foundation (ECN) Petten, The Netherlands

I. OVERVIEW

I.1. BENCHMARK NEUTRON FIELDS FOR REACTOR DOSIMETRY

J. Grundl and C. Eisenhauer
National Bureau of Standards
Washington, D. C. 20234, U.S.A.

ABSTRACT

The necessity for benchmark neutron fields measurements to achieve reliable reactor dosimetry is widely recognized. An organized response to this recognition is the IAEA Program, "Benchmark Neutron Fields Applications for Reactor Dosimetry." This report presents one step in the IAEA Program: A first compendium of information on benchmark neutron fields employed for dosimetry data generation, detector calibration, and dosimetry methodology referencing. The information presented is based on results of an IAEA worldwide survey of neutron fields suitable as reactor dosimetry benchmarks. Neutron fields included cover the energy range from fission spectrum neutrons to Maxwellian thermal, and a neutron flux range from 10^7 to 10^{11} n/cm^2 s . The summary includes a physical description of each system, features of the irradiation facility, and assigned spectra based on spectrometry and calculation. Also included are measured and predicted cross section ratios for a set of representative integral detectors: threshold reactions (Np(n,f), $^{238}U(n,f)$, $^{58}Ni(n,p)$, $Al(n,\alpha)$), and full-energy-range reactions ($^{239}Pu(n,f)$, $^{235}U(n,f)$, $Au(n,\gamma)$). Simple general formulations for interpreting integral detector responses are introduced and along with them a few principles of neutron field characterization based on benchmark calibrations.

Key words: Reactor fuels; reactor materials; neutron reactions; fission.

1. INTRODUCTION

Recognition that benchmark neutron field measurements are a necessary component of neutron field characterization for reactor dosimetry has become widespread. (1,2,3,4,5) Higher confidence levels required for estimating neutron-induced fuels and materials changes in power reactors, long-term measurement maintenance, and the need to validate neutron detection methods, all establish the motivation for this recognition. The variety and complexity of power reactor radiation environments which must be investigated and monitored provide additional emphasis for the recognition.

The identification of neutron fields with proper characteristics for referencing neutron dosimetry measurement methods is underway. The varied requirements and expectations for these fields, however, do not encourage rapid progress. In 1973, the IAEA Consultants Meeting on Nuclear Data for Reactor Neutron Dosimetry laid the groundwork and stated the need for well-characterized neutron fields to provide measurement assurance for dosimetry measurement methods. (2) Substantial experience in the use of benchmark neutron fields to achieve interlaboratory measurement consistency and to provide activation detector calibrations has been gained in the Interlaboratory LMFBR Reaction Rate Program (ILRR) serving the U.S. fast breeder development effort. (1) Modest attention with international participation was focused again on the problem during the ASTM-EURATOM Symposium on Reactor Dosimetry at Petten in September 1975. A workshop session at this symposium attempted to delineate systematically the concept, and use of benchmarks for reactor dosimetry. (3)

Subsequent to the Petten symposium the IAEA initiated a program under the heading "Benchmark Neutron Fields Applications for Reactor Dosimetry." This activity begins as a two step related effort:

1. Initiate an international survey to compile information on existing and proposed neutron fields suitable for referencing reactor dosimetry measurements. (6)

2. Convene a "Consultants Meeting on Integral Cross Section Measurements in Standard Neutron Fields for Reactor Dosimetry" in order to appraise the status of, and make recommendation for, reactor dosimetry neutron data in identified and documented benchmark neutron fields.

This paper is a first-round report of the results of the international survey. It will summarize in the form of a compendium a physical description of each facility, characteristics of the neutron field, selected reaction rate ratios both measured and predicted, and availability of the facility for dosimetry referencing irradiations.

Reactor neutron dosimetry for the purpose of this compilation encompasses (1) fluence and spectrum characterizations for exposures of fuels and materials in the core of nuclear reactors, and for materials integrity problems out-of-core as far as the periphery of the primary containment vessel; and (2) determination of isotopic fission rates in reactor fuels. Special requirements for various types of power reactors, e.g. existing light water systems vs. the LMFBR, will not be much distinguished. Further, this first compilation will be restricted to standard and reference neutron fields understood within the context of the following characteristics:

1. Simple and well-defined geometry;
2. Adequate neutron fluence and stable flux density;
3. Reproducible and accurately characterized neutron spectra based on spectrum measurements and/or reliable calculations;
4. Sustained availability for measurements.

Other neutron fields which do not meet these requirements, sometimes referred to as controlled radiation environments, are important because of their relevance to specific nuclear development efforts, and also because of essential limitations in standard and reference neutron fields now available. It is planned that the IAEA survey ultimately will summarize the features of these supplementary neutron fields.

Section 2 presents some elementary considerations associated with the application of benchmark neutron fields to the standardization of reactor neutron dosimetry methods. The benchmark neutron field compendium itself is given in section 3 of this paper, followed in section 4 by a summary of selected integral detector responses for each benchmark, both observed and predicted.

2. SOME PRINCIPLES OF NEUTRON FIELD CHARACTERIZATION BASED ON BENCHMARK CALIBRATION

Characterization of neutron fields in and around fuels and materials testing and power reactors employs passive integral detectors almost exclusively. Dominant among these are activation detectors although alternative techniques, notably helium accumulation fluence monitors and track recorders, are under development. The neutron response of all such detectors is wholly described by a single microscopic reaction cross section, the energy dependence of which distinguishes two classes of detectors. Threshold detectors which respond only to neutrons above a certain energy not always well defined form the first class; full-energy-range detectors which respond to neutrons of all energies form the second class.

A reactor dosimetry benchmark is a well-characterized neutron field which will provide a fluence of neutrons adequate to obtain an accurate integral detector response and which exhibits a known spectrum that is relevant for the dosimetry environment to be monitored. Response ratios among a set of integral detectors exposed to such a benchmark field provide a test of the detector reaction cross sections over the energy range of the benchmark spectrum. If observed and predicted detector response ratios disagree, some adjustment of the cross sections may be justified, or for detectors with reliable cross sections, allowed adjustments of certain of the benchmark spectra may be required.

Similarly, if the detector technique employed in the benchmark exposure is the same as, or calibrated relative to, the technique used in the dosimeter monitoring exposure, observed and predicted ratios for the benchmark may be brought into agreement by adjusting the overall detection efficiencies. Establishing detection efficiencies in this way removes a number of systematic errors associated with the detection scheme. Examples are absolute cross section scales, activation counter calibrations, and nuclear parameters including branching ratios and fission yields. This error reduction in turn allows a wider choice of detectors and gamma detection arrangements.

2.1 Brief Formulations

Some analytic expressions for observed and derived integral detector responses are needed to move from the general assertions just given to specific applications. As noted above, dosimetry applications are the proper orientation for benchmark descriptions, and therefore, the formulations below are in terminology applicable to activation detectors. Modifications required for other types of integral detectors involve for the most part time-integrated quantities, e.g., flux-fluence, decay constants, etc., and do not affect the principles of benchmark calibration.

Spectrum and cross section definitions

$(nv)_o$, $(nvt)_o$ = total energy integrated flux and fluence, respectively.

$\psi(E)$ = neutron spectrum normalized to unity.

$\psi(>E_t)$ = fraction of spectrum above neutron energy E_t:

$\sigma(E)$ = detector reaction rate cross section vs. energy.

$\sigma(E)$ = $\sigma_o \cdot s(E)$, where σ_o is the absolute cross section scaling factor, and $s(E)$ the cross section shape normalized to unity over a relevant benchmark spectrum, $\psi_b(E)$:

$$\int_0^\infty s(E)\psi_b(E)dE = 1$$

$\bar{\sigma}$ = spectrum-averaged cross section:

$$\bar{\sigma} = \sigma_o \int_0^\infty s(E)\psi(E)dE$$

$\bar{\sigma}(>E_t)$ = spectrum-averaged cross section truncated at E_t:

$$\bar{\sigma}(>E_t) = \sigma_o \int_{E_t}^\infty s(E)\psi(E)dE / \int_{E_t}^\infty \psi(E)dE \qquad (1)$$

$\frac{[\sigma(E)\psi(E)]}{\bar{\sigma}}$ = detector response function

E_p = truncation energy for defining a detector energy response range. For percentile P, the truncation energy is defined by

$$P = \frac{1}{\bar{\sigma}} \int_{E_p}^{\infty} \sigma(E)\psi(E)dE, \qquad (2)$$

where $E_p(P=0.5)$ = median energy, and for this paper $E_p(P=0) = 20$ MeV, $E_p(P=1) = 0.4$ eV.

Observed reaction rate

$$R = \varepsilon_\gamma \cdot \mu(\lambda,\bar{N},Br,Y,I,...) \cdot D \qquad (3)$$

R = observed activation detector disintegration rate in distintegrations per second (dps) at end of irradiation.

D = observed gamma counting rate after neutron field exposure in counts per second (c/s).

ε_γ = gamma counting efficiency.

μ = composite factor for converting gamma counting rate of a detector to disintegration rate: decay constant (λ), effective number of detector atoms ($\bar{N}$), branching ratio (Br), fission yield (Y), γ-ctg losses and activation interference (I).

Derived reaction rate

$$R_e = G(\lambda,t) \cdot \bar{N} \cdot \bar{\sigma} \cdot (nvt)_o \qquad (4)$$

R_e = derived reaction rate (dps) from fluence $(nvt)_o$ at the end of an irradiation in a neutron field with spectrum $\psi(E)$.

$G(\lambda,t)$ = activation decay rate factor. At the end of an irradiation at constant flux and duration t, $G(\lambda,t) = [1 - \exp(-\lambda t)]/t$.

Uncertainty in spectrum average cross section

Spectrum and cross section errors are estimated in multigroup formats. The spectrum-average cross section as a discrete summation,

$$\bar{\sigma} = \sigma_o \sum_i s_i \psi_i \Delta E_i \qquad (5)$$

is subject to an error propagation which must account for the normalization of the neutron spectrum as well as errors in cross sections and spectrum:

$$\left(\frac{\delta\bar{\sigma}}{\bar{\sigma}}\right)^2 = \left[\frac{\delta\sigma_o}{\sigma_o}\right]^2 + \sum_i \left(\frac{\delta s_i}{s_i}\right)^2 \left(\frac{\sigma_o s_i}{\bar{\sigma}}\right)^2 \psi_i^2 (\Delta E)^2_i + \sum_i \left(1 - \frac{\bar{\sigma}_i}{\bar{\sigma}}\right)^2 \left(\frac{\delta\psi_i}{\psi_i}\right)^2 \psi_i^2 (\Delta E)^2_i \qquad (6)$$

2.2. Neutron Flux Transfer

When the total neutron flux and fluence, $(nv)_o$ and $(nvt)_o$, can be specified for the benchmark irradiation of a dosimetry detector, it is sometimes possible to perform a direct neutron flux transfer to the dosimetry field under study. This is most successful when the dosimetry detector cross section is largely energy independent over the dosimetry spectrum energy response range, or when the detector response function $[s(E)\psi(E)]$, for the benchmark and dosimetry study fields are well matched. An example of the first circumstance is the $^{239}Pu(n,f)$ detector applied to fast reactor spectra, an example of the second is $^{238}U(n,f)$ applied to dosimetry fields where the fission spectrum dominates the energy distribution above 1.5 MeV.

Observed reaction rates, eq. 3, obtained with experimental techniques matched in the benchmark and dosimetry field are set equal to the derived reaction rate, eq. 4 involving the

computed average cross section and the neutron fluence in the two fields. Using the notation of eqs. 3 and 4,

$$\text{dosimetry field:} \quad \varepsilon_\gamma \cdot \mu \cdot D_s = G \cdot \bar{N} \cdot \bar{\sigma}_s \cdot (nvt)_{os}$$

$$\text{benchmark field:} \quad \varepsilon_\gamma \cdot \mu \cdot D_b = G \cdot \bar{N} \cdot \bar{\sigma}_b \quad (nvt)_{ob}$$

Dividing, the dosimetry field fluence $(nvt)_{os}$ is obtained in terms of the benchmark field fluence,

$$(nvt)_{os} = \frac{D_s}{D_b} \cdot \frac{\bar{\sigma}_b}{\bar{\sigma}_s} \cdot (nvt)_{ob} \quad , \qquad (7)$$

and the only experimental quantities involved are the activation count rates.

The cross section ratio in eq. 7 for appropriate detectors will be near unity. The absolute cross section scale cancels and the remaining uncertainty due to cross section shape errors, $\delta s(E)$, propagates more nearly on the ratio itself. Hence, a ± 10% cross section shape error would affect a flux transfer involving a cross section ratio of 1.1 by about ± 1%. An exception to this occurs when the detector response ranges for the benchmark and dosimetry fields are very different. In this case spectrum uncertainties, presumably dominated by the dosimetry field, will propagate into the flux transfer according to the last term of eq. 6.

A brief list of truncated cross sections for the common flux transfer detectors, $^{239}Pu(n,f)$ and $^{238}U(n,f)$, are given in Table I. The benchmarks listed are described in the following section with a summary description given in Table IIA and IIB. Values in Table I show that cross section ratios for neutron fluence transfer do not exceed 1.1 in important cases. At the present time only ^{252}Cf fission neutron irradiation facilities are capable of giving absolute neutron fluences. (9) Therefore, neutron fluence transfer should be considered as a measurement procedure to be used among benchmarks as well as from benchmarks to reactor dosimetry environments.

3. COMPENDIUM OF BENCHMARK NEUTRON FIELDS

The classification of neutron fields suitable for calibrating, referencing and validating reactor dosimetry measurements was discussed at length in conjunction with the Petten Workshop on Benchmarks for Dosimetry in 1975. (3) The criteria for three categories of facilities under the basic heading "benchmarks" focused on the avilability and quality of the neutron fields. The designations and classification statements are as follows:

Benchmark neutron fields for reactor dosimetry:

Standard: A permanent and reproducible neutron field with neutron flux intensity, energy spectra, and spatial and angular flux distributions characterized to state-of-the-art accuracy. Important field quantities must be verified by interlaboratory measurements and calculations.

Reference: A permanent and reproducible neutron field less well characterized than a standard and accepted as a measurement reference by a community of users.

Controlled Environment: A neutron field physically well-defined, and with some spectrum definition, employed for a restricted set of validation experiments.

No attempt was made to classify existing benchmark fields within this framework. The categories themselves do not fully satisfy everyone, constrained as they are by a flexible use of the term benchmark. This in turn is a reflection of the common necessity to employ for dosimetry referencing what is conveniently at hand to meet a wide range of development-oriented requirements. A review of the categories and a provisional classification of dosimetry benchmarks is a task for the Consultant's Meeting for which this compendium is prepared.

The benchmarks will be grouped according to neutron field characteristics. Natural sources and distributions are taken up first: they represent primary neutron energy distributions of interest for nuclear energy, those for which flux and spectrum are best known from theoretical considerations and/or from a multiplicity of spectrometry measurements. Driven neutron fields are next: these facilities make use of reactor neutrons, fully thermalized in some

cases, to produce fast reactor-like spectra which are known from accurate computations and/or experiment. Critical assemblies from reactor physics which make up the last group are low-power reactor facilities with simple geometry and few materials so that spectra obtained from neutron transport calculations may be presumed reliable. As noted earlier controlled neutron environments will not be included in this report.

A summary list of the benchmark fields is given in the two parts of Table II. Average energy, median energy and the 90% spectrum energy range are given for each field. A cursory facility description for orientation and some indication of neutron fluxes and fluences available for irradiations also are included.

The focus of interest for all dosimetry benchmarks is the neutron spectrum. For this compendium the benchmark spectra other than fission neutrons will be assigned on the basis of the recommendation of the laboratories responsible for each facility. Where possible, the relative contribution of calculation and differential spectrometry to the recommendation will be included. Table IIIA and IIIB present the assigned benchmark spectra together in a 30-group format. Interpolation of the various group structures and analytic descriptions which were available to us, and by which the benchmark spectra are described, was carried out with the NBS DETAN code. This code interpolates an input multigroup spectrum on a logarithmic energy scale to a 620-group structure and then recombines it to an arbitrary coarse group structure as required. Group flux normalization of the input spectrum is maintained.

3.1 NATURAL SOURCES AND DISTRIBUTIONS

^{252}Cf FISSION NEUTRON FIELDS

Fluxes of pure fission neutrons in an isolated environment are most easily created with intense sources of ^{252}Cf spontaneous fission neutrons. Irradiation facilities using ^{252}Cf sources are in existence at NBS in the U.S. and at PTB in the Federal Republic of Germany, and are available for dosimetry-related measurements. (9,10) In this report the NBS Facility will be described in detail followed by summary characteristics for the PTB facility. A cooperative program is presently underway which will intercompare ^{252}Cf source strengths at NBS and PTB.

Physical description. Each californium source is a desk-shaped deposit in an aluminum pellet encapsulated in a single stainless steel cylinder. Sintered particles of $Cf_2O_2SO_4$ are dropped into the aluminum pellet cylinder and aluminum powder pressed in to fill a central tapered bore. The pellet is placed in the steel capsule and the cap welded in place for closure. Physical specifications for the source components are as follows:

	Mass	Thickness of cyl. wall (mm)
sintered beads [$Cf_2O_2SO_4$]: (localized displacement $\sim$1.4 mm^3)	$\sim$3 mg ^{252}Cf	
aluminum pellet: (6.4 mm dia. x 5.7 mm long)	0.48 g	2.16 ± 0.1
stainless steel capsule: (7.6 mm dia. x 7.6 mm long; ss type 304)	1.39 g	0.53 ± .03
capsule total:	1.87 g	2.7 mm

The position of the Cf deposit relative to capsule surfaces is known to ± 0.5 mm. This estimate is based on constraints of fabrication and is verified by means of x-ray photographs. Neutron emission due to (α,n) reactions in either oxygen or aluminum is negligible. An upper limit of $\sim 2 \times 10^{-5}$ for the ratio of (α,n) to fission neutrons is estimated for thorough mixing of californium with aluminum or oxygen.

Two Cf-252 irradiation facilities are available at NBS. An isolated, lightweight source-detector assembly in a room with an open ceiling is employed for measurements which are not selectively sensitive to low-energy neutrons (nearest room boundary is 2.2 m). For minimal boundary return of neutrons, an alternative arrangement employing an outdoor mast places the same source-detector assembly 5 meters above the earth.

Neutron flux and fluence. The near-point source of ^{252}Cf produces a flux which falls off as $1/R^2$ with a gradient of $2\ \Delta R/R$. The free-field flux is established on the basis of neutron source strength and distance alone. Gradients for typical conditions of irradiation at R=5 cm, a disk detector of thickness 0.5 mm and diameter 12 mm, are 2% across the detector thickness and a center-to-edge ratio of 1.015.

Neutron field parameters for a nominal 5 cm source-to-detector distance excluding neutron return from the environment are as follows:

Free-field fission neutron flux	1×10^7 n/cm^2 sec
Source decay rate	2.3% per month
Free-field fluence for 100 hr exposure	4×10^{12} n/cm^2
Source capsule scattering (inelastic plus net elastic inscatter)	1.1%
Gamma ray exposure (3.4 years after separation)	150 R/hr

The components of the error in the free-field flux are:

Error components for free-field fission

Neutron flux (1σ)

source strength	± 1.1%
source capsule and support structure scattering	± 0.7% (max.)
distance measurements (typical for compensated flux geometry)	± 0.6%
Total free field flux error (rms sum):	± 1.4%(1σ)

Neutron flux monitoring and normalization. The flux at a given point depends only on the strength of the Cf source and its decay rate of 2.3% per month. Hence, flux monitoring generally is not required and can, in fact, introduce unwarranted flux perturbations. The facility is generally available for active or passive irradiations and certified fission neutron fluences have been provided.

Neutron spectrum. The assigned neutron spectrum, X(E), is based on an evaluation of eight documented spectrometry measurements.(29,30) Up to 12 MeV the fission spectrum is described by a reference Maxwellian M(E) corrected by four linear and one exponential piecewise-continuous segments, $\mu(E)$. The reference Maxwellian is

$$M(E) = 0.663 \sqrt{E} \exp(-1.5\ E/2.13), \quad E \text{ in MeV},$$

and the evaluated spectrum, $X(E) = \mu(E)M(E)$. The analytic correction factors and the energy ranges over which they apply are given below:

Energy Interval (MeV)	$\mu_{Cf}(E)$
0.0 - 0.25	1 + 1.20E - 0.237
0.25 - 0.8	1 - 0.14E + 0.098
0.8 - 1.5	1 + 0.024E - 0.0332
1.5 - 6.0	1 - 0.0006E+ 0.0037
6.0 - 20	1.0 exp[-0.03(E-6.0)/1.0]

Error analysis for the evaluated spectrum was carried out in an eight-group format. The result is as follows:

Energy Boundaries (MeV)	Evaluated Spectrum		
		1σ	2σ
0.0	0.047	± 13%	± 26%
0.25	0.184	± 1.1%	±3.3%
0.8	0.220	± 1.8%	±3.6%
1.5	0.194	± 1.0%	±3.1%
2.3	0.200	± 2.0%	±3.0%
3.7	0.146	± 2.1%	±4.8%
8	0.0087	± 8.5%	±17%
12	(0.00058)		
20			

Spectrum uncertainties given at both the 67% and 95% confidence levels are based on the departure of experimental data subsets from the evaluated spectrum, $\mu(E)M(E)$.

Unique features. The unique feature of a ^{252}Cf irradiation facility is the simple dependence of the neutron flux on a measured source strength and a distance measurement. Based on international intercomparisons, source strengths are believed to be accurate to ±1.1%(1σ). Uncertainty in flux due to distance measurements is typically ±0.6% when a compensated flux measurement is performed at a source-to-detector distance of 5 cm. In this arrangement, where the source is located midway between two nearly identical detectors, the linear terms in the flux uncertainties due to the uncertainty in source position compensate, and the dominant error is the distance uncertainty between the two detectors. The latter distance is a bench measurement which can be carried out and shown to be stable to <±0.1 mm.

SPECIAL FEATURES OF THE PTB ^{252}Cf IRRADIATION FACILITY (10)

The neutron source consists of two ceramic tablets containing ^{252}Cf doubly encapsulated in zircaloy. The emission rate of the cylindrical double-source capsule (11 mm dia. x 22 mm height) was about 1×10^9 n/sec at the beginning of 1977. The absolute source strength has been established to an accuracy of ± 1.7% (1σ) by gold foil activation in a waterbath facility. Irradiation of source-detector arrangements are carried out above ground and open air on a 17 meter mast. The irradiation facility will be available generally for interlaboratory experiments after the middle of 1977.

235U CAVITY FISSION SOURCES

Cavity fission sources are in operation at several facilities including the BR-1 reactor at CEN/SCK, Belgium, the KUR reactor at Kyoto University in Japan, and the NBS reactor in the USA. The facility at CEN/SCK will be described in this report.

Physical description. Various arrangements are employed at CEN/SCK to produce thermal-neutron-induced fission neutron spectra in a one-meter spherical cavity in the vertical graphite thermal column of the BR-1 reactor. In the principal experimental set-up, the exposure zone is within a 1 mm thick co-extruded, homogeneous cadmium tube of inner diameter 3.1 cm and about 2 meter long. The tube is placed vertically along the polar axis of the spherical cavity in the BR-1 thermal column. The bottom of this tube is tightly closed by a cadmium plate while the top is open just above the reactor shielding in order to allow easy access for fission chamber traverses with the reactor operating at full power. The fission source is a 93% enriched, 0.1 mm thick and 7.7 cm long metallic uranium sheet, wrapped around the cadmium tube at the cavity center. This uranium converter is protected by a very thin (<0.02 mm) aluminum wrapping.

The experimental configuration in the spherical cavity of the BR-1 thermal columns is shown below:

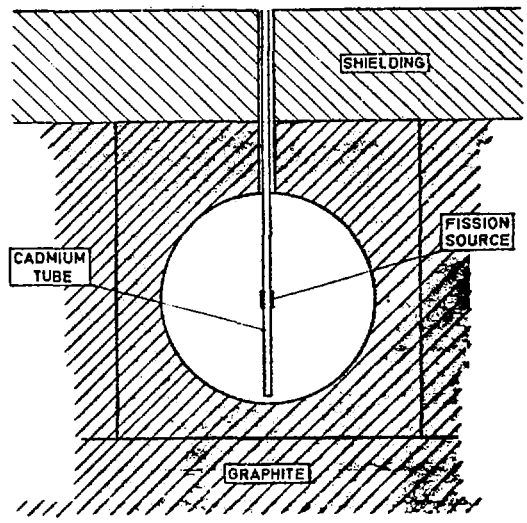

EXPERIMENTAL CONFIGURATION IN THE SPHERICA CAVITY OF THE BR-1 THERMAL COLUMN.

Neutron flux and fluence. Exact geometrical calculations of the spatial distribution of the uncollided flux per unit source strength are carried out by means of the computer code INTRAN. The background of neutrons returned from the cavity walls can be estimated very accurately from a spatial traverse along the polar axis. Such a traverse shows a background which is invariant with distance beyond about 20 cm from the center of the cavity.

Neutron flux monitoring. The cavity fission source at CEN/SCK at present is used primarily for cross section ratio measurements. Flux monitoring procedures have been developed but have not been set up on a permanent basis.

Neutron spectrum. The assigned neutron spectrum $\chi(E)$, is based on an evaluation of major documented spectrometry measurements.(29,30) Up to 12 MeV the fission spectrum is described by a reference Maxwellian M(E) corrected by piecewise-continuous functions, $\mu(E)$, four linear and one exponential. The reference Maxwellian is

$$M(E) = 0.750 \sqrt{E} \exp(-1.5\ E/1.97),\ E \text{ in MeV.}$$

and the evaluated spectrum $X(E) = \mu(E)M(E)$. The analytic correction functions and the energy ranges over which they apply are given below:

Energy Interval (MeV)	$\mu_{25}(E)$
0.0 - 0.25	1 + 0.8E - 0.153
0.25 - 0.8	1 - 0.14E + 0.082
0.8 - 1.5	1 + 0.040E - 0.062
1.5 - 6.0	1 + 0.01E - 0.017
6.0 - 20	1.043 exp[-0.06(E-6.0)/1.043]

Error analysis for the evaluated spectrum was carried out in an eight group format. The result is as follows:

Energy Boundaries (MEV)	Evaluated Spectrum	Uncertainty 1σ	Uncertainty 2σ
0.0			
0.25	.054	± 16%	± 32%
0.8	.197	± 4.1%	± 6.2%
1.5	.229	± 3.0%	± 4.8%
2.3	.195	± 3.1%	± 5.2%
3.7	.192	± 2.0%	± 3.0%
8	.127	± 4.8%	± 8.0%
12	.0056	± 5.3%	± 11%
20	(.0003)		

3.2 DRIVEN NEUTRON FIELDS

NEAR-1/E SPECTRUM (ISNF/CV)

Physical description. The ISNF/CV facility is set up in the ISNF cavity in the graphite thermal column of the NBS reactor - see ISNF description in this section. A square opening, 30 cm x 30 cm provides access to the center of the graphite column and split graphite blocks containing the ISNF cavity are inserted through the biological shield of the reactor and into the thermal column opening with the reactor at full power. The ISNF/CV arrangement is identical to that of the ISNF described later in this section except that the ^{10}B shell is replaced by a 14 cm dia. x 0.8 mm thick cadmium shell which excludes thermal neutrons from the central region of the cavity.

Fission neutrons from the fission converter disks, partially moderated in the surrounding graphite, return to the center of the cavity, creating a near-1/E spectrum from 0.4 eV to ~ 0.1 MeV. Other fission neutrons which return after a few collisions in the graphite (and also the uncollided component from the source disks) make up the spectrum in the MeV energy range.

Neutron flux and fluence. The thermal neutron flux in the cavity is ~ 1 x 10^{11} cm^{-2} sec^{-1} and each fission source disk operates at a fission power of about one watt. Eight disks are used in normal operations, giving a total neutron source strength in the thermal column cavity of about 8 x 10^{11} sec^{-1}. The resultant flux and fluence at the center of the cavity can be described as follows:

Total neutron flux intensity: ~ 1.6 x 10^{9} $n \cdot cm^{-2} \cdot s^{-1}$
Typical maximum fluence: ~ 2.5 x 10^{14} $n \cdot cm^{-2}$
Neutron field gradient: ~ 2% over 4 cm
Average and median neutron energies: 0.75 eV and 0.17 MeV respectively.
Spectrum energy range: 90% between 6 eV and 3.0 MeV
Response range of 1/v-detector: 90% between 0.9 eV and 0.67 keV

Neutron flux monitoring. Flux monitoring for routine irradiations will be accomplished by means of fission chambers and/or activation foils located inside of the cadmium shell. The ISNF/CV facility is not yet available for calibration irradiations.

Neutron spectrum. As with the ISNF, the assigned spectrum is established by means of computation. Carbon cross sections used in the calculations performed at NBS are based on ENDF/B-III data averaged in a 40-group energy structure. Calculations are made by the method of discrete ordinates in the S8, P3 approximation. The calculated flux at the center of the facility deviates from 1/E with a monotonic slope: 18% deviation from 1/E per decade over the energy range 0.4 eV and 10 keV.

INTERMEDIATE-ENERGY STANDARD NEUTRON FIELD (ISNF)

Physical description. The initial ISNF facility has been set up in the graphite thermal column of the NBS reactor. A square opening, 30 cm x 30 cm provides access to the center of the graphite column (parallelepiped 1.4 x 1.3 x 0.94 meter, density 1.71 g/cm^3). Split graphite blocks containing the ISNF cavity and cylindrical access penetrations may be inserted through the biological shield of the reactor and into the thermal column opening with the reactor at full power. A detailed schematic cross section of the ISNF arrangement within the cavity is shown below.

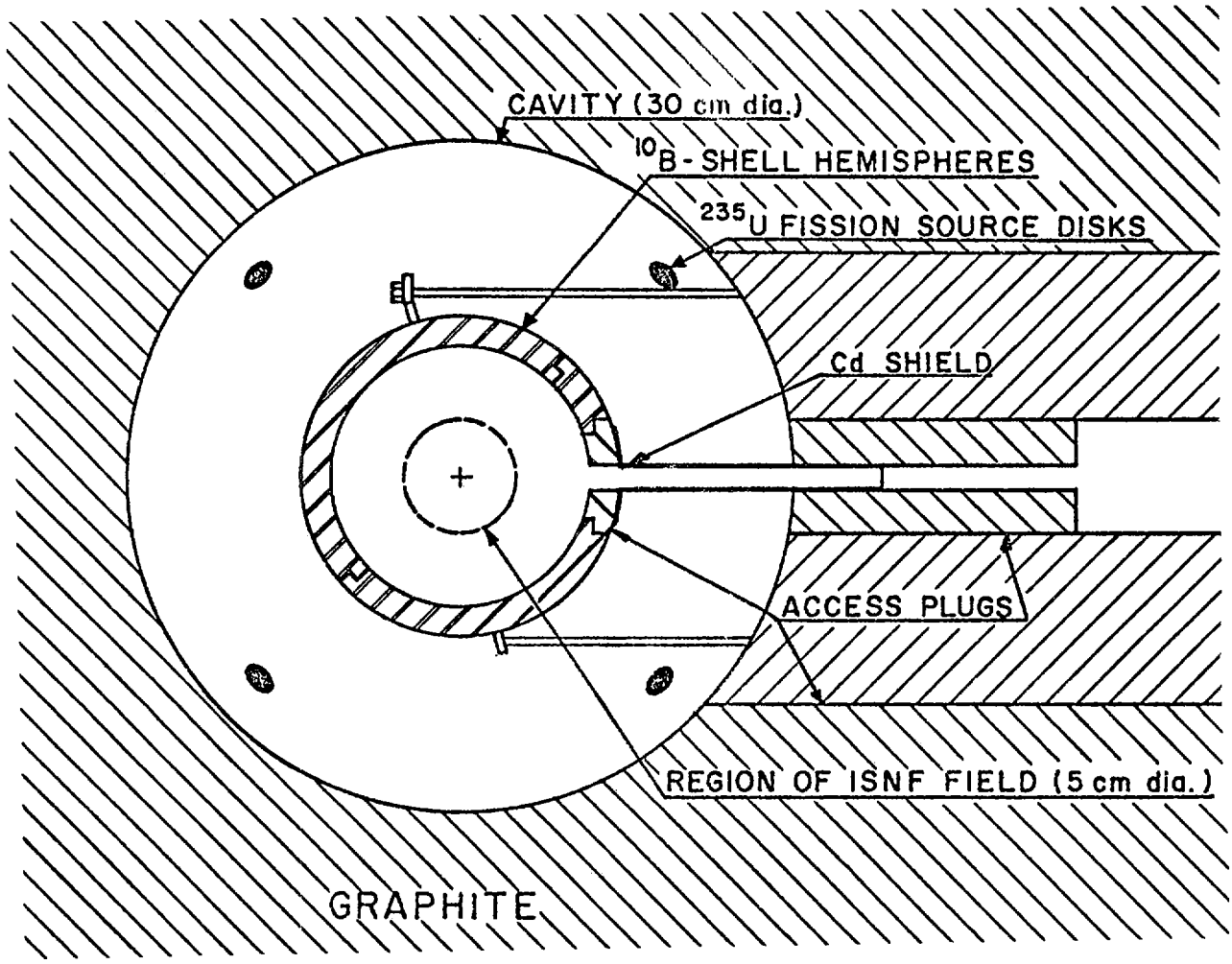

Fission neutrons from the fission converter disks are partially moderated in the surrounding graphite. Those which return to the cavity are transmitted by the boron-10 shell (along with an uncollided component from the source disks) to produce the ISNF neutron field at the center of the cavity.

Three levels of access are available: (1) instruments and/or irradiation samples may be inserted or removed through a 5 cm dia. cylindrical channel; (2) the boron-10 shell and graphite pieces to which it is attached slide in a 20 cm dia. cylindrical access; and (3) the entire 30 cm x 30 cm cavity block may be withdrawn or inserted with the reactor at full power. Four of the eight ^{235}U fission source disks are indicated in symmetric array near the surface of the cavity. The flanged cadmium shield which fits over the stems of instruments placed inside the shell, prevents thermal neutrons from streaming through the hole in the shell access plug. Shell access plugs without a hole are available for passive detector irradiations which do not involve instrument stems. Streaming through access holes, by wall-return neutrons in particular, is a characteristic problem for any driven, one-dimensional neutron fields. Careful experimental investigation is required to demonstrate that the problem is under control.

The crucial component of the ISNF is the boron-10 shell. Two shells formed as stepped hemispheres by techniques of powder metallurgy are now available: thick and thin shells have thicknesses of 1.29 cm and 0.638 cm and an O.D. of 14.36 cm. The powder required for the shell fabrication was a mixture of 95% enriched boron-10 metal and aluminum in an atom density fraction of 0.27 aluminum. The absolute absorption thickness of the shells is determined by means of neutron transmission measurements in the 25 keV filtered beam at the NBS reactor. This measurement provides a basis for spectrum calculations which includes only the shape of the ^{10}B absorption cross section.

The fission source disks are 93% enriched uranium metal 16 mm dia. x 0.15 mm thick placed 1 cm from the surface of the 30 cm dia. cavity.

An inventory of ISNF components and their physical properties is given below. Included are some characteristic nuclear parameters appropriate for the neutron transport problem.

INVENTORY AND PHYSICAL PROPERTIES OF ISNF COMPONENTS
(thick shell only)

1. Graphite Thermal Column

—dimensions: 1.4 x 1.3 x 0.94 m
—graphite density: 1.71 g/cm^3
—cavity diameter: 29.8 cm

2. Boron-10 Shells

—dimensions:	outside diameter:	14.26 cm
	surface area at mean diameter:	523 cm^2
	thickness	1.26 g/cm^2
—mass:	total	1.389 kg
	boron-10	0.663 kg
	boron-11	0.032 kg
	aluminum	0.674 kg
	other (C,Si,Fe,Pb,U238)	0.7%
—density:	boron-10	0.975 g/cm^3
	boron	1.025 "
	aluminum	0.992 "
—thickness	boron-10	0.0764 atom/barn
	aluminum	0.0287 "

—fraction of a mean free path for neutrons

	1 MeV	0.1 MeV	25 keV	2.7 KeV
absorption	.025	.145	.29	.88
scattering	.30	.33	.20	.23

3. Fission Source Disks

—dimensions: 16 mm dia. x 0.15 mm thick
—thickness: 0.22 gm/cm^2 ^{235}U metal (93.5% enriched) each;
—fission source strength: 4 x 10^{10} fiss/sec per disk
—total fission neutron source strength (8 disks, reactor 10 MW)
$\sim$8 x 10^{11} neut/sec

4. Aluminum structures inside of cavity

—protective shell enclosure for boron-10 shell:
0.70 mm thick, 121 g

Neutron flux and fluence. The thermal neutron flux in the cavity is $\sim 1 \times 10^{11}$ $cm^{-2}sec^{-1}$ and each disk operates at a fission power of about one watt. Eight disks are used in normal operations so that the total neutron source strength in the thermal column cavity is about 6×10^{11} sec^{-1}. The resultant flux and fluence at the center of the cavity are as follows:

Total neutron flux intensity: 0.8×10^{9} $n \cdot cm^{-2} \cdot s^{-1}$

Typical maximum fluence: $\sim 1.5 \times 10^{14}$ $n \cdot cm^{-2}$

Neutron field gradient: ~2% over 4 cm

Average and median neutron energies: 1.0 MeV and 0.56 MeV respectively

Spectrum energy range: 90% between 8 keV and 3.5 MeV

Response range of a 1/v-detector: 90% between 0.5 keV and 1.5 MeV

Specific neutron flux intensities are established by flux transfer (see section 2.2) from the NBS ^{252}Cf source using $^{239}Pu(n,f)$ as the transfer reaction.

Neutron flux monitoring. Flux monitoring for routine irradiations will be accomplished by means of fission chambers and/or activation foils located inside of the boron-10 shell. The ISNF facility is not yet available for routine service irradiations.

Neutron spectrum. Assignment of the ISNF spectrum is based solely on neutron transport calculations which are subject to sensitivity studies. The cross sections used in calculations carried out at NBS through 1976 are based on ENDF/B-III spectrum averaged in a 40-group energy structure. The spectrum at the center of the ISNF was calculated with the discrete ordinates code ANISN (S8, P3 approx.). A linear diagram showing the radial coordinates of ISNF-1 is given below.

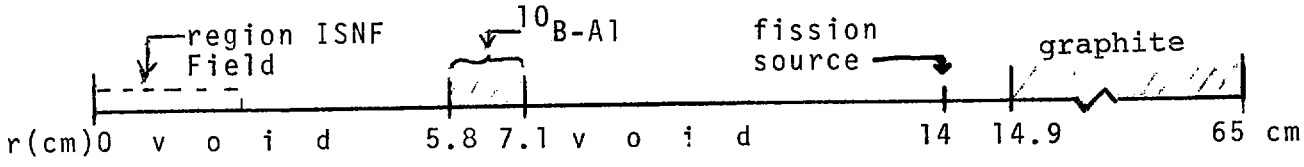

The sensitivity of the calculated spectrum to variations in several parameters has been investigated. For example, a 1% increase in graphite density increases the flux around 10 keV by about 1%. An uncertainty of about 7% in source position produces only 1% uncertainty in the flux below 200 keV. Effects of uncertainties in the angular distribution of scatter in graphite and perturbations due to aluminum in the system have also been investigated. Uncertainties due to cross section data and energy-group structure are currently under investigation by means of new 240-group calculations. These latest calculations make use of ENDF/B-IV cross sections.

Unique features. The ISNF was designed so that the spectrum at the center is determined largely by the kinematics of elastic scattering and 1/v neutron absorption, and could be calculated to an accuracy limited only by the uncertainty of the input nuclear data. This was accomplished by designing the system as a one-dimensional spherically symmetric configuration and choosing boron-10 and carbon as the main material constituents. Cross sections for these materials are among the best known of all elements. A compromise of fabrication in the current realization of the ISNF introduces aluminum into the ^{10}B shell. The effect of the aluminum is to modulate the spectrum slightly near scattering resonances.

SECONDARY INTERMEDIATE-ENERGY STANDARD NEUTRON FIELD

Physical descriptions. The generic name Sigma Sigma (ΣΣ) will be used for these fission-neutron-driven, spherical shell arrangements which are in operation at three laboratories in Europe. The facility description here will be specifically for the Sigma Sigma at CEN/SCK, Mol, Belgium which has been in operation since 1970. Departures of other Sigma Sigma systems from this, the original facility will be described separately. The CEN/SCK facility is well described both physically and neutronically in reference 15.

Sigma Sigma is a thermal-fast coupled spherical source assembly located within a conventional graphite thermal column. A spherical source shell of natural uranium metal 24.5 cm o.d. x 5.0 cm thick, is mounted at the center of a 50 cm diameter spherical cavity in the graphite. An inner shell of aluminum-clad vibrocompacted natural boron carbide 17.5 mm thick defines a central fast flux exposure void, 11 cm in diameter. The one-dimensional configuration of materials is as follows:

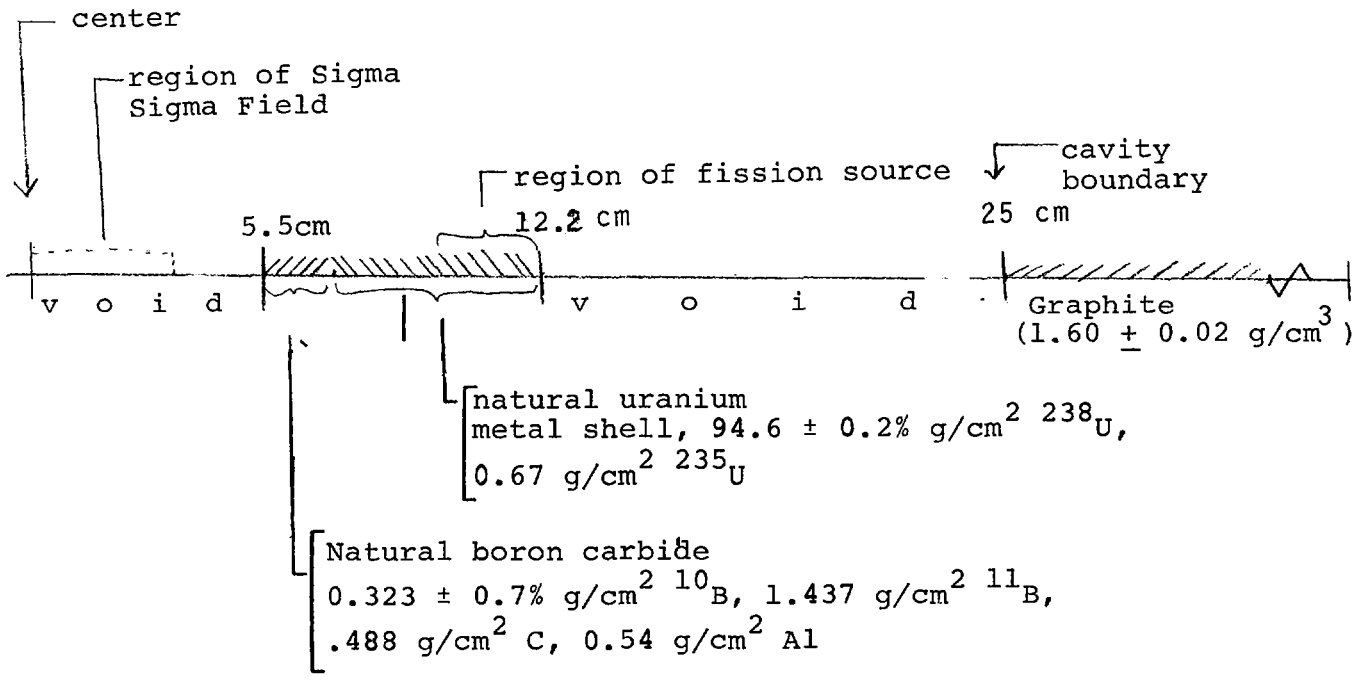

A schematic view of the cavity arrangement in the thermal column of the BR-1 reactor is as shown below:

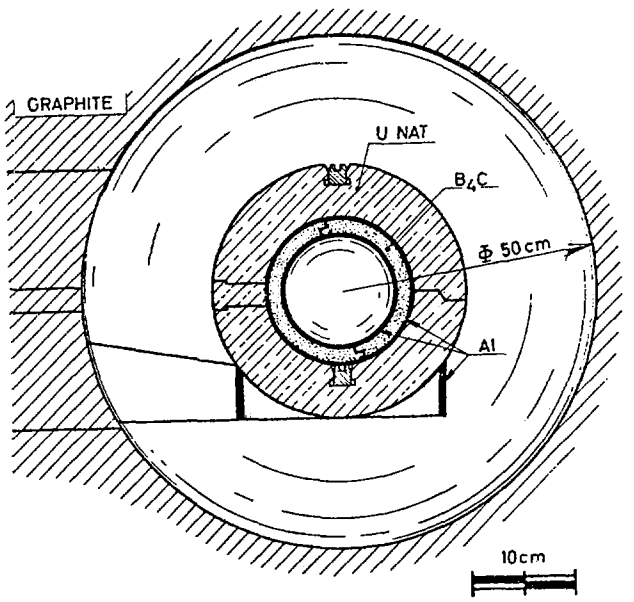

The natural uranium shell converts the thermal column neutrons into fission neutrons with most coming from the first one centimeter of the outer portion of the uranium shell. The fission neutrons arrive at the center of the system degraded in energy primarily due to elastic scattering in the graphite and inelastic scattering in the uranium. The inner boron carbide shell preferentially absorbs low-energy neutrons shaping this portion of the spectrum to make the Sigma Sigma energy distribution relevant for fast reactor applications. An extensive effort was undertaken to obtain shell components with well-understood and verified physical characteristics.

The shell system is mounted at the cavity center by means of an aluminum ring and bracket. The entire shell assembly can be removed from the thermal column and transferred to a hot cell for assembly-disassembly operations. Both passive and active detectors are operated in the system; for the latter, the issue of perturbations of the field due to access holes must be understood. These effects have been studied intensively, both by experiment and by computation.

Neutron flux and fluence. The total neutron flux available for normal scheduled irradiations is 7×10^8 n/cm^2 sec, and fluences of up to 5×10^{14} can be provided. The gradient of the total neutron flux over the central region is symmetric about the center; the flux increase is not more than 4% at + 3 cm from the center in the worst case of a direction along the thermal column axis. Both computation and measurement indicate that there is no energy dependence of the anisotropy in the central region. The uranium shell also is a good gamma-ray absorber and the resulting gamma-to-neutron ratio for Sigma Sigma is of the order 6×10^{-7} (rad/h)/(cm^{-2}sec^{-1}).

Neutron flux monitoring. Central reaction rate measurements in Sigma Sigma are monitored by means of fission chambers and by foil activation at a maximum of three positions, two near the pole of the uranium shell and one within the central exposure zone. The reactions ^{115}In(n,n') and ^{197}Au(n,γ) are the commonly used monitors. The principle fission chamber monitor is placed in a horizontal channel of the thermal column; an auxillary monitor is fixed in the Sigma Sigma. Routine irradiation monitoring is accurate to better than ± 0.5% over a flux level range that reaches down to ∿3% of maximum. The Sigma Sigma irradiation facility at CEN/SCK has been used for a wide variety of interlaboratory measurements in the past and continues as a facility for scheduled interlaboratory experiments.

Neutron spectrum. The base neutron spectrum calculation for Sigma Sigma is a 100-group, $S_{16}P_3$ ANISN transport calculation using ENDF/B-III cross sections. (12) More detailed 208 group computations in the S_8 diagonal transport approximation and based on two versions of the German KEDAK file were carried out in order to investigate the sensitivity to the input nuclear data. The convergence of the discrete-ordinates solution with respect to the spatial and angular meshes and to the order of the down-scattering matrix was also studied. Between 6 keV and 5.6 MeV the computational base is considered reliable. The low-energy tail below 6 keV is not so reliable because of the difficulties of preparing proper self-shielded cross sections for ^{238}U. The neutron spectrum in Sigma

Sigma has been measured by three laboratories, GfK (Karlsruhe), RCN (Petten), and CEN/SCK itself. Proton-recoil spectra were measured by all three laboratories with spherical proportional counters; in addition, $^{3}He(n,p)t$ and $^{6}Li(n,\alpha)t$ spectrometer measurements have been performed by GfK and CEN/SCK respectively. General agreement among the observed spectra is ±5% between 20 keV and 4 MeV. The departures between spectrometry and the base ENDF/B-III calculation are below ± 15%.

The assigned spectrum for Sigma Sigma at the present is that given in Table A.1. of Reference 15. It was obtained from a combination of spectrometry measurements and discrete-ordinates calculations.

Unique features. The ΣΣ facility has been used extensively for interlaboratory comparisons of fission rate measurements. Central fission rate scales are established to an accuracy of ± 1.5-2% for the fissionable isotope ^{233}U, ^{235}U, ^{238}U, ^{239}Pu and ^{241}Pu. The facility is currently applied for the calibration of activation fission foils and miniature fission chambers for reactor physics and neutron dosimetry applications.

CFRMF NEUTRON FIELD

Physical description. The coupled Fast Reactivity Measurements Facility (CFRMF) is a zoned core critical assembly with a fast-neutron spectrum zone in the center of an enriched ^{235}U water-moderated thermal "driver" zone. (18) The thermal driver zone fuel elements are convential plate-type elements of fully enriched uranium clad in aluminum. The fast zone along the central axis of the fuel element array is constructed of materials for keeping the zone water-free and to tailor a neutron energy spectrum characteristic of an LMFBR. The diagram below shows a midplane cross section of the filter unit which is 61 cm long and extends through most of the CFRMF core in a vertical direction.

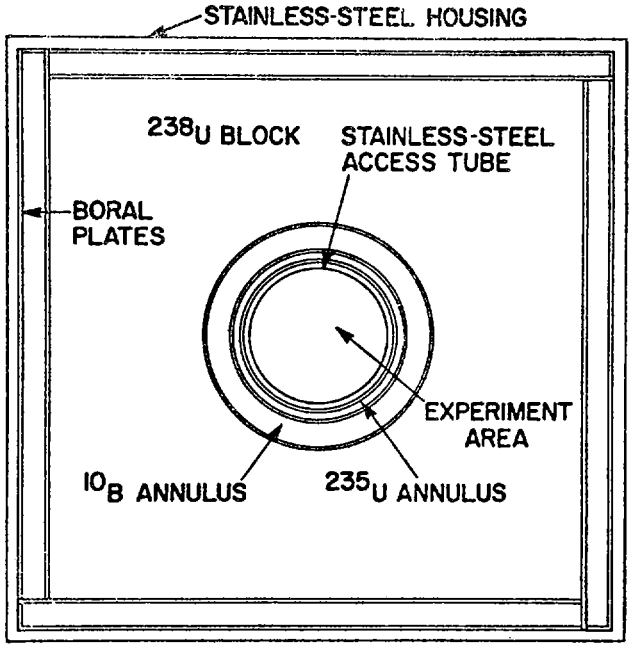

The thermal driver zone spectrum incident on the filter unit is tailored in the following general manner. The outer boral plates attenuate neutrons below 1 keV by absorption. The ^{238}U block (14.5 cm square) degrades the spectrum by inelastic scattering. The ^{10}B annulus (0.635 cm thick) attenuates the neutrons below 1 keV further and insures that no thermal neutrons reach the experimental region. The ^{235}U annulus (0.89 mm thick) has no significant effect on the spectrum other than a small enhancement of the fission spectrum component.

Neutron flux and fluence. All experimental tests for dosimetry are performed at the core center line with vertical access. Irradiation packages and support arrangements up to 3.8 cm in diameter may be introduced into the central fast zone where neutron fluxes of up to 10^{11} are established with the reactor operating at 10 KW. Maximum neutron fluences are largely a matter of scheduling for long irradiations. For ILRR irradiations fluences of 0.2 to 1 x 10^{16} were provided during pre-planned experiments at intervals of a few months.

Spatial gradients in CFRMF have been examined extensively with activation detectors (^{235}U, Au(n,γ), $^{63}Cu(n,\gamma)$) and fission chambers (^{235}U, ^{238}U, ^{239}Pu, and ^{237}Np). The axial distribution is observed to have a proper cosine dependence out to 20 cm above and below core center. The central 2.5 cm along the vertical axis, the primary location for dosimetry tests, and the horizontal plane 3.8 cm above the centerline, the location of flux normalization monitors, were examined in much greater detail. The Au capture reaction establishes the flux as 0.3% lower at 2.5 cm above core center. Because the CFRMF filter unit does not preserve cylindrical symmetry the possibility of azimuthal gradients in the central irradiation position is not ruled out. Azimuthal profiles obtained for the threshold reaction $^{115}In(n,n')$ show no significant gradient; for Au capture a gradient of up to $\sim$4% has been identified.

The gamma-to-neutron ratio for CFRMF is estimated to be $\sim 3 \times 10^{-6}$ (R/hr)/cm^{2}sec).

Neutron flux monitoring. At constant power level the reactor instrumentation provides the basic flux monitoring capability for irradiation experiments. The reliability of this routine monitoring scheme has been checked against high resolution fission chambers placed in the central test region. Short term reproducibility of the fission chamber, run-to-run at the same power level, relative to the reactor instrumentation is better than $\pm$0.2%. Long term reproducibility tests over a period of two years indicate drifts of up to (1.6 $\pm$ 0.3)%. Linearity of the reactor instrumentation against the fission chamber for power level changes of up to a factor of 17

show discrepancies of up to (3.5 ± 0.3)%. Activation monitors (Au(n,γ) and In(n,n')) also have been employed for flux monitoring during ILRR dosimetry test irradiations.

The conclusion of these extensive tests of flux monitoring methods is that for chain reacting systems, redundant monitoring including the placement of monitor detectors at the dosimetry test position are mandatory if run-to-run normalization is involved in the measurement, and precision requirements are <1%.

Neutron Spectrum. There is a continuing effort to improve knowledge of the CFRMF spectrum both by calculation and by spectrometry measurement. Three different computer codes have been employed for calculations: (a) SCAMP, a one-dimensional S_n transport code covering the energy range 10 MeV to thermal (S_8, P1 approx.); (b) RABBLE, a multiregion resonance absorption cross section code to calculate the spectrum from 53-keV down to 0.88 eV; and (c) RAFFLE , a monte carlo routine. A basic 69-group energy structure was employed with group average cross sections prepared with ENDF/B III and IV as input. Various parameters of the system and the calculation were investigated including the interaction of the filter unit with the equilibrium thermal driver spectrum.

Measurements of the CFRMF spectrum have been carried out with proton-recoil and $^6Li(n,\alpha)$ spectrometers. Gas proportional counters of the cylindrical Bennett type and spherical Benjamin type provided proton-recoil results from ∿2.5 MeV down to ∿3 keV; a $^6Li(n,\alpha)$ sandwich-type spectrometer has been employed for measurements between ∿3 keV and ∿6 MeV. (18, 31)

The assigned spectrum for CFRMF is based on calculations with ENDF/B-IV cross sections and is reported in the paper by J.W. Rogers. (31)

LEAD PILE AT YAYOI

YAYOI is a fast neutron source reactor of flexible design operated by the Faculty of Engineering of the University of Tokyo. (24) The aim of the reactor facility is fundamental research and training in fast and intermediate energy neutron research. The enriched uranium metal core, movable in a long horizontal channel, furnishes several kinds of neutron fields depending upon the environment into which the core is placed. Two such benchmark fields will be described in this compendium.

The neutron field at the center of a large block driven by the YAYOI core placed near the edge will be described briefly here. (19) The fast neutron field at the center of the YAYOI core when placed inside of a depleted uranium blanket and an outer lead reflector is described under Reactor Physics Criticals, section 3.3.

Physical description. The lead pile driven by YAYOI is a [parallelpiped] of octagonal shape (2.5 m face-to-face separation and 2.5 m high). The YAYOI core and uranium blanket configuration (see section 3.3) is placed inside of the lead pile close to one of the eight faces. The benchmark neutron field is at the center of the lead block about 1.0 m from the center of the YAYOI core. A horizontal penetration of square cross section (20 cm x 20 cm) reaches to the central region of the lead block and is left open; thus it becomes part of the benchmark configuration. The lead pile is fabricated as a 160 ton casting of 99.99% pure lead. A significant amount of iron is included in the system as structural supports and more importantly within the central channel of the lead pile. The latter channel provides the option of placing the YAYOI core anywhere along the center-line of the pile.

Neutron flux and fluence. The spatial distribution of the neutron flux along the open channel in the lead pile has been measured by means of gold foil activation and compared with the results of two-dimensional discrete ordinates calculations (TWOTRAN II). The gold foil mapping, sensitive primarily to the flux between 2 eV and 8 eV, does not agree well with calculations indicating that extraneous neutrons from steel structures and from outside of the

pile contribute significantly to the flux. Extensive TWOTRAN II calculations have been performed in order to map various components of the spectrum throughout the lead block.

The total flux was obtained by means of TWOTRAN calculations normalized to a fission rate density in the YAYOI core measured with small ^{235}U fission chambers.

Neutron spectrum. Spectrum calculations for the lead pile driven by YAYOI have been carried out by discrete ordinate methods using ANISN and TWOTRAN II. The ANISN code with an angular guadrature of S-8, provided neutron flux distributions in a one-dimensional spherical model of the driven pile. Fundamental aspects of neutron spectra also were obtained with the one-dimensional calculations in spite of the imperfect representation of the geometrical buckling. In addition, two-dimensional flux distributions were obtained from TWOTRAN II calculations using the r-z geometry option and S-6 angular quadrature. All of these calculations employed the ABBN cross section library (26 neutron groups) and included resonance self-shielding factors for ^{238}U, ^{235}U, Pb and Fe.

These spectrum calculations were checked in the low energy range by means of resonance activation detectors employing the sandwich foil technique. The energy range from a few eV to a few keV was covered with Au, In, W, Co, and Mn capture detectors. Spectrometry measurements have been performed with a spherical proton recoil counter (energy range: 40 keV to 300 keV), and also with a ^{3}He spectrometer (energy range: 0.15 MeV to 5 MeV) which was checked with monoenergetic neutrons in the energy range 0.25 keV to 0.57 keV.

The spectrum is dominated by an approximate 1/E dependence from epithermal up to a few tenths of an MeV. At higher energies inelastic scattering is important. An analytic representation of the spectrum in terms of elastic and inelastic scattering modes has been derived. The result is:

$$\phi(u) = 6.10 \times 10^{4} \left[E^{0.109} \exp(-0.00376E - 0.0316/\sqrt{E})\right] + 7.00 \times 10^{3} \left[E^{0.450} \exp(-1.00 \times 10^{-6} E^{2})\right].$$

Good agreement is stated to exist between calculation and experiment at the pile center, and the accuracy of the spectrum is estimated to be ± 10% above 0.2 MeV and ± 20% below 0.2 MeV.

3.3 REACTOR PHYSICS CRITICALS

BIG-TEN CRITICAL ASSEMBLY

Physical description. This critical assembly operated at Los Alamos Scientific Laboratory is an all uranium metal system constructed in exact cylindrical geometry. (23) As the name implies, BIG-TEN is a 10% enriched uranium critical assembly which in the central region (25 cm dia. x 25 cm long) is made up of homogeneous metal. Around the central region the 10% enrichment is made up of alternating annular metal plates (53 cm O.D. x 56 cm long total) consisting of 93% enriched uranium and natural uranium of proper relative thickness. These two regions make up the BIG-TEN enriched core (10.1% ^{235}U); surrounding the core is a 15 cm thick reflector of depleted uranium metal which provides channels for control and safety rods. The complete assembly, 84 cm in diameter and 97 cm in length is supported in two main sections on a split table assembly machine. Access to the central region is through a conventional axial glory hole of 7.6 cm maximum diameter.

Neutron flux and fluence. The BIG-TEN, critical assembly, designed as a zero-power reactor physics facility, operates routinely with central fluxes of $\sim 10^{9}$ to 10^{10} n/cm^2 sec. By special arrangement flux levels up to 10^{11} may be provided and fluences of $\sim 10^{16}$ have been given for a limited number of dosimetry calibrations.

Neutron flux monitoring. BIG-TEN is designed for reactor physics applications and as such it is not normally instrumented for reproducing power levels precisely or guaranteeing linearity between power level readings. Hence, for calibration irradiations flux monitoring detectors must be set up for the purpose. For ILRR integral detector irradiations carried out over a period of some months, special external fission chambers were installed along with a double fission chamber operated in the central glory hole position along with the activation detectors. Gold capture and In(n,n') monitor foils were also in the central location. Quite unanticipated and unique experimental problems with the central double fission chamber for these ILRR irradiations proved the essential validity of requiring redundant flux level monitoring for high-investment experiments.

The BIG-TEN critical assembly is not available as a routine calibration facility. Recognized interlaboratory agreements may be arranged in order to schedule irradiations.

Neutron spectrum. Calculation of the BIG-TEN spectrum was performed using the TWO-TRAN two-dimensional transport code with S_4 angular segmentation. Transport corrected P_0 cross sections were prepared in 88 groups from ENDF/B-IV using the IDX processing code. Spectrum measurements over the energy range from 23 keV to 2.6 MeV with cylindrical proton-recoil proportional counters have been reported. (23) A special feature of these measurements was the determination of response functions for the detectors with monoenergetic neutrons and the incorporation of these results into the detector response matrix used to unfold the BIG-TEN spectrum. Differential spectrometry with a $^6Li(n,\alpha)$ sandwich spectrometer have also been performed at core center and cover the energy range from $\sim$3 keV to $\sim$6 MeV.

The assigned spectrum for BIG-TEN, as presented in Table III is based on computation alone using ENDF/B-IV cross sections.

YAYOI CENTRAL NEUTRON FIELD

YAYOI is a fast neutron source reactor of flexible design operated by the Faculty of Engineering of the University of Tokyo. (24) The aim of this reactor facility is fundamental research and training in fast and intermediate-energy neutron research. The enriched uranium metal core, movable in a long horizontal channel, furnishes several kinds of neutron fields depending upon the environment into which the core is placed. Two such fields are labeled benchmarks and will be described in this compendium.

The field at the YAYOI core center when the core is surrounded by a blanket of depleted uranium and an outer reflector of lead is described in this section under Reactor Physics Criticals. The neutron field at the center of a large block of lead driven by the YAYOI core is described under Driven Neutron Fields, section 3.2.

Physical description. The YAYOI core is a right circular cylinder (12.5 cm dia. x 15.5 cm long) of 93% enriched uranium metal. The core is surrounded by an annular blanket of depleted uranium. The core and the blanket are inside of a large lead reflector. A vertical glory hole (2.3 cm dia.) provides a penetration through the reflector and core near the core center line. Another cylindrical penetration (5.7 cm dia.) runs vertically along one planar surface of the cylinder core. Four safety and shim rods (4 to 6 cm dia.) operate in channels near the core. A cross section of the core and the uranium blanket is shown below:

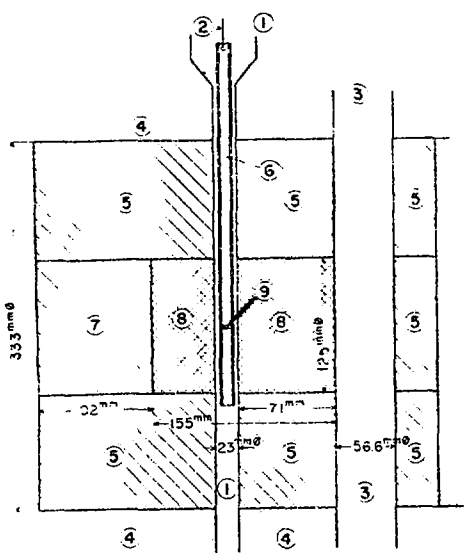

(1) Glory hole
(3) Grazing channel
(4) Lead reflector
(5) Depleted uranium blanket
(8) ^{235}U cylindrical core
(9) Region of benchmark field

YAYOI Core Configuration

Neutron flux and fluence. The reactor operates normally with air cooling at 2 KW and provides a flux at the core center of 7.5 x 10^{11} n/cm^2 sec. In order to maintain access to the core, the reactor is limited to 3 kwh of operation per week. This corresponds to a fluence of 4 x 10^{15} n/cm^2 for core center irradiations. Spatial distributions of flux in the glory hole have been measured with activation foils: $^{235}U(n,f)$, $^{238}U(n,f)$, $^{115}In(n,n')$, $^{197}Au(n,\gamma)$, and $^{58}Ni(n,p)$. The fission spectrum component based on these measurements relative to 1.00 at the center, is about 0.92 and 0.7 at radii of 2 cm and 4 cm respectively. Similarly, the spectrum component comprising the energy range of inelastically scattered neutrons falls to about 0.98 and 0.95 at 2 cm and 4 cm respectively. Glory hole traverses with $^{197}Au(n,\gamma)$ detectors indicates that there is some leakage of thermal and epithermal neutrons into the core region from the outer shield region.

The gamma-to-neutron ratio for YAYOI core center is 1.6 x 10^{-6} (R/hr)/(n/cm^2 sec). The gamma field measurement was made with low neutron sensitivity TLD detectors (Mg_2 SiO4:Tb).

Neutron flux monitoring. For routine irradiations the conventional reactor power level monitoring systems are employed. The detectors for these systems are two fission chambers for start-up and compensated ion chambers for full power operation. The precision for run-to-run normalizations is estimated to be less than a few percent.

The YAYOI core irradiation facility has been employed for Japanese interlaboratory measurements.

Neutron spectrum. Calculation of the YAYOI core has been carried out with the ANISN transport code in the P-5,S-8 approximation. Cross sections for the calculation are from the ENDF/B-III file reduced to 39-groups with 1/E, and fission spectrum weighting. Spectrometry at the core center has been carried out with a specially prepared ^6Li sandwich counter. The assigned spectra appearing in Table III is from the ANISN calculations.

Unique features. Pulsed operation of YAYOI is expected in the near future making it possible to do time-of-flight spectrometry. As part of the analysis of space and energy dependence of the neutron flux in YAYOI a simple expression consisting of two spectrum modes has been proposed: A fission-spectrum component and an inelastic-scattering component. A final spectrum representation has been obtained based on integral detector responses including $^{232}Th(n,f)$ and $^{237}Np(n,f)$ in addition to the reactions listed above.

TAPIRO FAST SOURCE REACTOR

Physical description. This small compact reactor with a ^{235}U metal core and copper reflector is operated by the CNEN Laboratory at Cassaccia, Italy. (25,28) The cylindrical core (12.6 cm dia. x 10.9 cm high) is enriched uranium metal alloy (98.5% uranium enriched to 93.5% ^{235}U, 1.5% molybdenum) with 0.5 mm thick stainless steel cladding. The cylindrical copper reflector surrounding the core is 80 cm in diameter and 72 cm in height. Access to core center is by means of a horizontal glory hole 0.8 cm in diameter.

Neutron flux and fluence. The reactor, is operated normally at 5 kW with helium cooling and provides a central flux of the order of 1×10^{13} n/cm^2 sec. Measured axial distributions of the neutron flux have been reported for one full energy range detector, $^{235}U(n,f)$, and three high-energy detectors, $^{115}In(n,n')$, $^{58}Ni(n,p)$, and $^{27}Al(n,d)$. Agreement with calculation is good.

Neutron flux monitoring. Accuracy and reproducibility of power level measurements by standard reactor control instrumentation generally are not satisfactory for neutron dosimetry measurements. Run-to-run monitoring including different power levels is normally done by means of gold foil activation in the same positions. The estimated accuracies attained by this technique are $\sim$ 5% for individual power levels and $\sim$ 1% for run-to-run normalization.

Cooperation with other laboratories for neutron dosimetry measurements in the TAPIRO facility or for detector intercomparisons is encouraged.

Neutron spectrum. For purpose of calculation, the reactor was represented in both one-dimensional and two-dimensional geometry. The equivalent radius of the core for the one-dimensional calculations was chosen so as to preserve the value of k-eff given by the two-dimensional calculations (which in turn will reproduce the experimental value). The one-dimensional calculations were performed by means of the ANISN code in the S-8 approximation with isotropic scattering. The cross sections were derived from the ENDF/B-III files and collapsed to 27 or 35 groups by means of the MC^2 code.

4. DETECTOR RESPONSE SUMMARY

A rather extensive array of measured integral detector reaction rates already exists for the benchmark fields listed in Table IIA and IIB. Much of this experimental information has been evaluated by Fabry in reference 32. Laboratories included in the IAEA survey will be requested to furnish results of all documented reaction rate measurements for their benchmark fields. A representative set of benchmark measurement results are included in this report. They will summarize the existing situation regarding consistency of dosimetry-related, reaction rates in benchmarks. The detector reactions chosen for the summary,

full-energy range: $^{239}Pu(n,f)$, $^{235}U(n,f)$, $Au(n,\gamma)$,
threshold: $Np(n,f)$, $^{238}U(n,f)$, $^{58}Ni(n,p)$,

exemplfy the entire range of detector responses available for fission reactor dosimetry with the exception of single resonance type detectors.

Energy response features of an integral detector may be described by a 90% energy response range (5% excluded above an upper energy limit and 5% below a lower energy limit), and a median response energy which divides the energy range into regions of equal response. In terms of eq. 2 the median energy is E(P=0.5) and the response range extends from a lower limit $E_p(P=0.95)$ to an upper limit $E_p(P=0.5)$. Response ranges for some of the detectors listed above are shown in Table IV. The response ranges shown for threshold detectors are little changed for all reactor dosimetry benchmarks. The fission spectrum dominates the benchmarks above about 2 MeV, and there is little evidence to indicate that this situation is greatly different in and around materials test and power reactors. The extent to which this latter statement is correct is important for the orientation of reactor dosimetry calibrations and requires further investigation.

The median energies indicated in Table IV show some of the useful response distinctions that are possible. The invariance of the $^{239}Pu(n,f)$ median energy for all but the near-1/E field is a mark of its energy independence and consequently its usefulness as a total flux monitor.

4.1 Observed Detector Responses

Measurements of recent vintage for most of the detectors listed above are available for important benchmarks: fission spectra, the one-dimensional driven systems, the clean reactor physics critical BIG-TEN, and the high-power driven system CFRMF. The data for the most part come from the ILRR program efforts and are given in Table V.

Absolute integral cross sections have been determined only for ^{252}Cf fission neutrons and of these the $^{239}Pu(n,f)$ detector is chosen as the normalizing reaction because of the energy independence of its cross section over the fast-neutron energy range. The measured value 1804 ± 45 mb is reported in reference 33. The $^{239}Pu(n,f)$ cross sections for other spectra in Table III, given in brackets, are derived from this value on the basis of calculated ratios of spectrum-average cross sections. The values in bracket do not depart greatly from the ^{252}Cf value (maximum of 10% for BIG-TEN) so that spectrum uncertainties are not important. In the rest of the Table, measured cross section ratios or spectral indexes for the other reactions are given relative to $^{239}Pu(n,f)$. (14,33,34,35)

Error assignments in Table V are of quite different quality. For fission spectra the measurements are mostly single laboratory results although in some cases detection methods have been subject to interlaboratory checks. (36) At present the ISNF measurements entered in parenthesis are preliminary. For the three remaining benchmarks, organized interlaboratory-measurement results obtained within the framework of the ILRR Program are reported. Uncertainties for the latter are consensus estimates based on a critical review by participating laboratories. (34)

4.2 Computed Detector Responses

According to eq. 4 and the definitions preceding it, a detector response derived or expected for a benchmark is based on the microscopic reaction cross section:

$$\overline{\sigma} = \sigma_0 \int_0 s(E)\psi(E)dE. \qquad (14)$$

Because the spectrum for many benchmarks is specified in a multigroup format, a proper and consistent spectrum interpolation scheme is required to calculate spectrum-averaged quantities. The computed cross sections for this paper make use of the DETAN code which performs a simple linear interpolation of multigroup spectra on a logarithmic energy scale with a final adjustment to preserve each group flux. The latter step is essential because of neutron balance generally involved in the multigroup transport computations which generate the spectra.

A brief summary of computed reaction rate cross section ratios or spectral indexes for the dosimetry benchmarks covered in this report is given in Table VI. They are based on multigroup spectra recommended by respondents to the IAEA benchmark survey and listed here in Table IIIA, B, and on the ENDF/B-IV dosimetry file of energy-dependent cross section in a 620-group structure. The fission spectra employed are from a published evaluation of sixteen best-documented differential spectrometry measurements. (29,30) Spectrum uncertainties were included in this evaluation so that it is possible to establish errors for the computed fission-spectrum cross sections using the last term of eq. 6. The resulting errors for fission spectra appear in Table VI.

Ratios of observed-to-predicted spectral indexes have been formed with the computed values of Table VI. They are presented in Table IV below the observed spectral index. These double ratios provide a glimpse of the experimental situation surrounding dosimetry benchmark data.

Fission detectors have long been the center of integral detector testing in benchmark neutron fields. In the fission spectrum fields agreement between observation and prediction is within 3% for the spectral indexes, Np/^{239}Pu and ^{238}U/^{239}Pu. This agreement is obscured, however, by the nearly 5% discrepancy for the non-spectrum-dependent fission cross section ratio ^{235}U/^{239}Pu. Using ^{235}U as a basis for spectral index formation as is commonly done would indicate more serious spectral index discrepancies.

The discrepancy between these two fissile materials is important, not only for dosimetry and fission rates in fuels, but for the differential fission cross sections which are in the ENDF/B-IV evaluation. For the most part, the fission cross section of ^{239}Pu has been established relative to ^{235}U, and therefore, the disagreement indicated by the fission spectrum measurements is a good example of a strong confrontation between integral measurements and differential data.

REFERENCES

1. W. N. McElroy, "Data Development and Testing for Fast Reactor Dosimetry," Nuclear Technology 25, 177 (1975).

2. C. L. Dunford, M. F. Vlasov, "Proceedings of a Consultants' Meeting on Nuclear Data for Reactor Neutron Dosimetry," Vienna, 10-12 September 1973, Report INDC (NDS)-56/U, IAEA (1973).

3. A. Fabry, J. Grundl, "Report of Workshop Session on Reactor Dosimetry Benchmarks," First ASTM-EURATOM Symposium on Reactor Dosimetry, Proc. to be published, Petten, Netherlands (1975).

4. R. Odette, N. Dudey, W. McElroy, R. Wullaert, A. Fabry, "Application of Advanced Irradiation Analysis Methods to Light Water Reactor Pressure Vessel Test and Surveillance Programs," ASTM Int. Symp. on the Effects of Radiation on Structural Materials, St. Louis, (1976).

5. H. Farrar, IV, E. Lippincott, W. McElroy, "Dosimetry for Fluence Applications," Petten Symposium, ibid. 3.

6. M. Vlasov, "LAEA Programme on Benchmark Neutron Fields Applications for Reactor Dosimetry," INDC (SEC)-54/L+Dos. (July, 1976).

7. E. P. Lippincott, Private communication (1975).

8. C. Z. Serpan, Jr., B. H. Menke, "Nuclear Reactor Neutron Energy Spectra," ASTM Data Series Publication DS 52, 05-05200-35, Philadelphia (1974).

9. J. A. Grundl, V. Spiegel, C. Eisenhauer, H. Heaton, D. Gilliam, J. Bigelow, "A Californium-252 Fission Spectrum Irradiation Facility for Neutron Reaction Rate Measurements," Nuclear Technology, (March, 1977).

10. W. G. Alberts, J. Bortfeldt, E. Gunther, K. Knauf, M. Matzke, G. Rassl, V. Spiegel, K. F. Walz, "Measurement of Cross Sections for Threshold Reactions Induced by Californium-252 Spontaneous Fission Neutrons," NBS Spec. Publ. 425, Vol. I, p. 273 (1975).

11. A. Fabry, J. A. Grundl, C. Eisenhauer, "Fundamental Integral Cross Section Ratio Measurements in the Thermal-Neutron-Induced Uranium-235 Fission Neutron Spectrum," NBS Spec. Publ. 425, Vol. I, p. 254 (1975).

12. A. Fabry, J. D. Jenkins, "Wall Return Neutron Fluxes for High and Intermediate-Energy Cavity Neutron Sources," Trans. Am. Nucl. Soc. 15, 2 (1972).

13. I. Kimura, K. Kobayashi, "Intercomparison of Reactor Dosimetry Cross Sections Measured in a Thermal Reactor in a Fast Reactor and with an Enriched Uranium Fission Plate," ibid., 3. Also, J. Nuel. Sci. Tech. 8 [2], 59 (1971).

14. Documentation available on request from U. S. National Bureau of Standards, Center for Radiation Research.

15. A. Fabry, G. DeLeeuw, S. DeLeeuw, "The Secondary Intermediate-Energy Standard Neutron Field at the Mol-ΣΣ Facility," Nucl. Tech. 25, 2, 349 (1975).

16. A. C. Besant, J. Emmett, C. Campbell, M. Kerridge, T. Jones, Nucl. Eng. Intern., 425, (May, 1973).

17. I. Girlea, C. Miron, A. Fabry, CEN/SCK Report BLG 512 (1976).

18. J. W. Rogers, D. A. Millsap, Y. D. Harker, "CFRMF Neutron Field Flux Spectral Characterization," Nucl. Tech. 25, 2,330 (1975).

19. T. Kosako, M. Nakazaua, H. Wakaboyashi, A. Sekiguchi, "Applications of a Lead Pile Coupled with Fast Reactor Core of YAYOI as an Intermediate Energy Neutron Standard Field," Report UTWL-R, Nucl. Eng. Res. Lab., Univ. of Tokyo, (October, 1976).

20. L. Greenwood, R. Heinrich, N. Dudey, "A Detailed Comparison of Differential and Integral Cross Section Measurements," ibid., 3.

21. R. Peterson, G. Newby, "An Unreflected ^{235}U Critical Assembly," Nucl. Sci. and Eng. 1, 112 (1956).

22. J. Grundl, "Fission-Neutron Spectra: Macroscopic and Integral Results," Proc. of Symp. on Neutron Standards and Flux Normalization, CONF-701002, ANL (August, 1971). See also CSEWG benchmark listings.

23. E. J. Dowdy, E. J. Lozito, and E. A. Plassman, "The Central Neutron Spectrum of the Fast Critical Assembly Big-Ten," Nucl. Tech. 25, 2,381 (1975).

24. K. Kobayashi, I. Kimura, M. Hakazawa, M. Akiyama, "Fission Spectrum Averaged Cross Sections of Some Threshold Reactions Measured with Fast Reactor YAYOI," J. Nucl. Sci. and Tech. 13, No. 10, 531 (October 1976). Also S. Tamura et al., "Physics of Fast Reactors," Proc. Int. Symp., Tokyo, 1973, Vol. I, 152 (1973), IAEA, Vienna.

25. A. D'Angelo, M. Martini, M. Salvatores, "The TAPIRO Fast Source Reactor as a Benchmark for Nuclear Data Testing," Energia Nucleare (Milan), 20, 11, 612 (1973).

26. A. D'Angelo, M. Martini, M. Salvatores, "^{235}U Compact Cu-Reflected TAPIRO Reactor Integral Experiments Results and a Check of Some High-Energy ENDF/B-III Data," Trans. Am. Nucl. Soc., 17, 498 (1973).

27. M. Martini, M. Belli, M. F. Sirito, "The TAPIRO Fast Source Reactor as a Benchmark to Test Activation Detector Cross Sections," ibid. 3.

28. M. Martini, P. Mocoli, F. Sirito, "Progress Report on Detector Cross Section Benchmark Measurements in the TAPIRO Reactor, This Proceedings (1977).

29. J. A. Grundl, C. M. Eisenhauer, "Fission Spectrum Neutrons for Cross Section Validation and Neutron Flux Transfer," Conf. on Nucl. Cross Sections and Technology, Washington, D. C. (1975).

30. J. Grundl, C. Eisenhauer, "Fission Rate Measurements for Materials Neutron Dosimetry in Reactor Environments," ibid. 3.

31. J. W. Rogers, Y. D. Harker, D. A. Millsap, "The Coupled Fast Reactivity Measurement Facility (CFRMF)", This Proceedings (1977).

32. A. Fabry, H. Ceulemans, P. Van de Plas, W. McElroy, E. Lippincott, "Reactor Dosimetry Integral Reaction Rate Data in LMFBR Benchmark and Standard Neutron Fields: Status, Accuracy Implications," ibid. 3.

33. D. M. Gilliam, C. Eisenhauer, H. T. Heaton, II, J. A. Grundl, "Fission Cross Section Ratios in the ^{252}Cf Neutron Spectrum (^{235}U: ^{238}U: ^{239}Pu: ^{237}Np)," Conf. on Nucl. Cross Sections and Technology, Washington, D. C. (1975).

34. W. N. McElroy, ed., ILRR Progress Reports, Nos. 1 through 10, HEDL-TME 75-130 (1970-1975).

35. J. Grundl, D. M. Gilliam, N. D. Dudey, R. J. Popek, "Measurement of Absolute Fission Rates," Nucl. Tech., 25, 237 (1975).

36. H. Pinter, W. Scholtyssek, P. Fehsenfeld, H. A. J. Van Der Camp, W. H. J. Quaadvliet, A. Fabry, G. and S. DeLeeuw, F. Cops, J. Grundl, D. Gilliam, C. Eisenhauer, "Interlaboratory Comparison of Absolute Fission Rate and Uranium-238 Capture Rate Measurements in the MOL-ΣΣ Secondary Intermediate-Energy Standard Neutron Field," Conf. on Nucl. Cross Sections and Technology, Washington, D. C. (March 1975).

TABLE I. TRUNCATED SPECTRUM AVERAGE CROSS SECTIONS FOR NEUTRON FLUX TRANSFER

SPECTRUM	Pu239 fission			U238 fission		
	*90% response range, E(P)		+truncated cross section	*90% response range		+truncated cross section
	P=0.95 (keV)	P=0.05 (MeV)	$\bar{\sigma}$(>E(P=0.95)) (mb)	P=0.95 (keV)	P=0.05 (MeV)	$\bar{\sigma}$(>E(P=0.95)) (mb)
Benchmark neutron fields						
^{252}Cf fission	290	5.2	1810	1520	7.2	550
^{235}U fission	240	5.1	1790	1510	6.7	540
Sigma Sigma	1.1	2.9	1746	1410	6.4	510
BIG TEN	44	2.5	1608	1400	6.7	512
Reactor dosimetry neutron fields						
FTR Core (7)	2×10^{-1}	2.2	2004	1390	6.5	510
EBR-II (7)	47.6	2.9	1640	1180	6.0	500
LWR Core (8)	2×10^{-3}	0.8	11100	1490	6.8	540
LWR Pressure Vessel (8)	1×10^{-3}	1.1	10720	1560	7.9	560

*Fraction of detector response below E(P=0.95) is 5%; fraction above E(P=0.05) is 5%. (See Section 2.1, eq. 2)

+Spectrum average cross section truncated at E(P=0.95). (See Section 2.1, eq. 1)

TABLE II-A

SUMMARY LIST OF STANDARD AND REFERENCE NEUTRON FIELDS FOR REACTOR DOSIMETRY

Neutron Field	Designation	Location	Neutron Energy Spectrum Distribution E(P)* Av. Energy	median energy P=0.95	P=0.5	P=0.05	DESCRIPTION	AVAILABILITY
			(MeV)	(keV)	(keV)	(MeV)		
NATURAL SOURCES AND DISTRIBUTIONS								
fission spectra								
^{252}Cf	XCF-5-1	NBS(USA) PTB (Germany) U.London (England) IEP (Hungary)	2.13	260	1680	5.5	Low-scatter, near-point, sources in isolated geometry. Spontaneous fission neutron source strength by total absorption, internationally compared. Fundamental fast neutron flux standard. (9,10)	Fission neutron fluxes up to $\sim 1 \times 10^7$ available on request. Free field fluences of $\gtrsim 10^{13}$ certified to $\lesssim \pm 2\frac{1}{2}\%$ (1σ). (9)
^{235}U	XU-5-1	NBS(USA) CEN/SCK (Belgium) Kyoto U. (Japan)	1.94	240	1570	5.1	Thermal-neutron fission converters in thermal column cavities; also isolated converters. Source-detector geometries and cavity return background established by computation and experiment. (11,12,13)	Fission neutron fluxes up to $\sim 3 \times 10^{11}$ available for planned experiments.
thermal Maxwellian	Th20-1	NBS(USA) PTB (Germany) Kyoto (Japan) Others	(0.025 ev)				Beams or isotropic fluxes of well-moderated neutrons at a nominal temperature of 20° C. Source driven piles or reactor thermal columns are employed. Flux established by gold activation or fission counting. Flux perturbations by detectors are a common limit on accuracy.	Beams of $\gtrsim 5 \times 10^6$; isotropic fluxes of up to $\sim 10^{11}$ in thermal column cavities where flux perturbations are minimized.

*Fraction of spectrum below E(P=0.95) is 5%, fraction above E(P=0.05) is 5%. (See Sec. 2.1, eq. 2.)

TABLE II-B

SUMMARY LIST OF STANDARD AND REFERENCE NEUTRON FIELDS FOR REACTOR DOSIMETRY

Neutron Field	Designation	Location	Neutron Energy Spectrum Distribution E(P)* Av. Energy (MeV)	P=0.95 (keV)	median energy P=0.5 (keV)	P=.05 (MeV)	DESCRIPTION	AVAILABILITY
DRIVEN NEUTRON FIELDS								
ISNF	ISNF-1	NBS(USA)	0.8	8.0	565	3.5	Fission-source-driven isotropic flux at center of 30 cm dia. spherical cavity in graphite thermal column. Low-energy cut-off with boron-10 shell. Primary intermediate-energy flux standard with spectrum established by exact neutron transport computations. (14)	Facility operational in 1976 with verified central flux of 1×10^9. Not yet available for routine certified fluences
Sigma Sigma	SS-5-1	CEN/SCK (Belgium) U. London (England) ITN (Romania)	0.76	20	400	2.9	Fission-source-driven isotropic flux at center of spherical cavity in graphite thermal column. Natural uranium and boron shells form breeder-reactor-like spectrum which is specified on the basis of calculation and experiment. (15,16,17)	Facilities well-established and available for scheduled irradiations. Fluxes of 7×10^8 and fluences $\sim 5 \times 10^{14}$.
CFRMF	CFRMF -5-1	ANC(USA)	0.76	16	363	2.8	Zoned-core critical assembly with partial cylinder symmetry. Conventional thermal-driver spectrum filtered to a fast spectrum along a central axis by means of U238, U235, and ^{10}B. Spectrum specified on the basis of calculation and experiment. (18,31)	Fluxes of up to $\sim 10^{11}$ available for planned experiments. Fluences up to $\sim 10^{16}$ have been furnished for dosimetry calibration.
near 1/E	ISNF/CV	NBS(USA)	0.75	0.0061	166	3.0	Fission-source-driven isotropic flux at cavity center in a graphite thermal column. Cadmium enclosure cuts spectrum at 0.41 ev; unmoderated fission neutrons become important above 0.3 MeV. Spectrum established by computation. (14)	Facility in place but not routinely operational. Near-1/E flux (0.4 ev < E < 0.3 MeV) of 1.6×10^9 estimated.
Lead Pile	YOPP-7-1	U.Japan (Japan)	0.084	7×10^{-3}	8.4	0.477	Large lead block driven by YAYOI reactor near the outside surface. Central spectrum obtained by 2-D discrete ordinates and spectrometry. (19)	
Accelerator Spectra		ANL(USA)					Tandem accelerator with $B_e{}^9(d,n)$ reaction at E_d = 14-16 MeV. Neutron spectrum in forward direction measured by time-of-flight extends to ~ 20 MeV maximum. (20)	
REACTOR PHYSICS CRITICALS								
GODIVA	LGODV -5-1	LASL(USA)	1.51	143	1020	4.5	Isolated spherical critical assembly of 93.5% enriched uranium metal. Critical mass and spectrum a basic reactor physics benchmark. (21,22)	No longer available.
BIG TEN	BIG10 -5-1	LASL(USA)	0.58	48	315	2.18	All-uranium critical assembly with a homogeneous central region of 10% enriched uranium metal. Spectrum at core center established on the basis of calculation primarily and some spectrometry. (23)	Fluxes up to 8×10^{10} available for planned experiments. Fluences limited to $\sim 10^{16}$.
YAYOI	YAY-7-1	U.Japan (Japan)	1.38	113	889	4.22	Cylindrical critical assembly of 93% enriched uranium metal with a depleted uranium blanket and surrounded by a thick reflector of lead Spectrum at core center based on calculation and experiment. (24)	Flux ϕ of 7.5×10^{11} available for detector irradiations. Fluences limited to 4×10^{15}.
TAPIRO	TAP-7-1	CNEN (Italy)	1.44	122	0.9	4.4	Fast source reactor with a U-235 metal core and thick copper reflector. Spectrum at core center based on calculation (25,26,27)	Fluxes up to $\sim 3 \times 10^{12}$ available at core center.

*Fraction of spectrum below E(P=0.95) is 5%, fraction above E(P=0.05) is 5%. (See Sec. 2.1, eq. 2.)

TABLE III-A BENCHMARK SPECTRA IN 30-GROUP FORMAT

			NATURAL SOURCES AND DISTRIBUTIONS		DRIVEN NEUTRON FIELDS		
GROUP	EHIGH	DELTA-U	CF-252 FISSION	U-235 FISSION	ISNF-1	SIGMA-SIGMA	CFRMF
1	1.800+01	4.055-01	5.839-04	2.619-04	7.380-05	5.146-05	6.623-05
2	1.200+01	4.055-01	8.749-03	5.569-03	1.570-03	1.244-03	1.478-03
3	8.000+00	2.769-01	2.507-02	1.944-02	5.456-03	4.290-03	4.513-03
4	6.065+00	1.931-01	3.455-02	2.944-02	9.383-03	5.617-03	6.428-03
5	5.000+00	3.011-01	8.656-02	7.804-02	2.554-02	1.566-02	1.662-02
6	3.700+00	2.097-01	8.137-02	7.665-02	2.902-02	1.840-02	1.731-02
7	3.000+00	2.657-01	1.184-01	1.152-01	5.788-02	3.147-02	2.932-02
8	2.300+00	4.274-01	1.938-01	1.953-01	1.153-01	6.548-02	5.684-02
9	1.500+00	6.286-01	2.202-01	2.292-01	1.710-01	1.359-01	1.279-01
10	8.000-01	6.931-01	1.361-01	1.454-01	1.571-01	2.212-01	2.200-01
11	4.000-01	6.931-01	6.154-02	6.704-02	1.233-01	1.951-01	1.999-01
12	2.000-01	5.880-01	1.986-02	2.259-02	7.661-02	1.120-01	1.130-01
13	1.111-01	5.000-01	7.108-03	8.379-03	5.055-02	6.447-02	6.681-02
14	6.738-02	5.000-01	3.274-03	3.941-03	4.099-02	4.266-02	4.318-02
15	4.087-02	5.000-01	1.522-03	1.857-03	3.171-02	2.755-02	2.880-02
16	2.479-02	5.000-01	7.124-04	8.762-04	2.740-02	2.034-02	1.789-02
17	1.503-02	5.000-01	3.336-04	4.125-04	2.163-02	1.338-02	1.250-02
18	9.119-03	5.000-01	1.570-04	1.948-04	1.663-02	7.414-03	8.255-03
19	5.531-03	5.000-01	7.395-05	9.192-05	1.300-02	5.524-03	7.596-03
20	3.355-03	5.000-01	3.491-05	4.344-05	9.599-03	3.569-03	6.044-03
21	2.035-03	5.000-01	1.647-05	2.051-05	6.749-03	2.315-03	5.394-03
22	1.234-03	5.000-01	7.783-06	9.697-06	4.452-03	1.971-03	3.617-03
23	7.485-04	5.000-01	3.673-06	4.578-06	2.684-03	1.596-03	2.760-03
24	4.540-04	5.000-01	1.734-06	2.162-06	1.441-03	1.374-03	1.642-03
25	2.754-04	5.000-01	8.185-07	1.020-06	6.635-04	4.956-04	1.062-03
26	1.670-04	5.000-01	3.871-07	4.826-07	2.493-04	2.269-04	6.085-04
27	1.013-04	5.000-01	1.827-07	2.278-07	7.143-05	3.283-04	3.234-04
28	6.144-05	5.000-01	8.632-08	1.076-07	1.391-05	2.521-04	1.522-04
29	3.727-05	1.500+00	6.915-08	8.621-08	1.033-06	8.564-05	7.596-05
30	8.315-06	3.000+00	8.053-09	1.004-08	1.682-08	1.505-06	3.705-07
	4.140-07						

Group fluxes obtained from assigned spectra and the DETAN interpolation code - see section 3.

TABLE III-B BENCHMARK SPECTRA IN 30-GROUP FORMAT

		DRIVEN NEUTRON FIELDS			REACTOR PHYSICS CRITICALS			
GROUP	EHIGH	DELTA-U	ISNF/CV	YOPP	GODIVA	BIG TEN	YAYOI	TAPIRO
1	1.800+01	4.055-01	5.188-05	0.000	1.743-04	6.797-05	1.859-04	0.000
2	1.200+01	4.055-01	1.103-03	3.173-08	3.706-03	1.055-03	3.661-03	2.740-03
3	8.000+00	2.769-01	3.834-03	9.125-08	1.291-02	3.046-03	9.771-03	1.106-02
4	6.065+00	1.931-01	6.521-03	3.204-07	1.911-02	4.301-03	1.537-02	1.679-02
5	5.000+00	3.011-01	1.786-02	1.270-06	4.791-02	1.161-02	4.278-02	4.267-02
6	3.700+00	2.097-01	2.049-02	5.481-06	5.089-02	1.190-02	4.415-02	4.535-02
7	3.000+00	2.657-01	4.056-02	1.630-05	7.850-02	1.915-02	7.147-02	7.047-02
8	2.300+00	4.274-01	7.874-02	2.348-04	1.496-01	3.859-02	1.364-01	1.362-01
9	1.500+00	6.286-01	1.148-01	1.795-03	2.236-01	9.680-02	2.091-01	2.139-01
10	8.000-01	6.931-01	1.091-01	5.753-02	2.056-01	2.233-01	2.112-01	2.219-01
11	4.000-01	6.931-01	8.676-02	8.383-02	1.256-01	2.479-01	1.445-01	1.377-01
12	2.000-01	5.880-01	5.763-02	5.996-02	4.898-02	1.494-01	6.238-02	5.814-02
13	1.111-01	5.000-01	4.049-02	5.014-02	1.911-02	9.277-02	2.670-02	2.401-02
14	6.738-02	5.000-01	3.487-02	5.559-02	8.618-03	5.785-02	1.243-02	1.124-02
15	4.087-02	5.000-01	3.077-02	6.281-02	3.508-03	2.797-02	5.663-03	4.534-03
16	2.479-02	5.000-01	2.767-02	6.112-02	1.363-03	9.806-03	2.279-03	1.947-03
17	1.503-02	5.000-01	2.525-02	5.613-02	5.014-04	3.144-03	9.039-04	7.885-04
18	9.119-03	5.000-01	2.320-02	5.081-02	1.819-04	9.738-04	2.391-04	4.068-04
19	5.531-03	5.000-01	2.166-02	4.820-02	6.457-05	2.937-04	2.776-04	1.076-04
20	3.355-03	5.000-01	2.033-02	4.594-02	2.429-05	9.534-05	4.488-04	3.017-05
21	2.035-03	5.000-01	1.918-02	4.283-02	8.581-06	3.298-05	2.357-05	1.199-05
22	1.234-03	5.000-01	1.817-02	3.826-02	2.953-06	8.721-06	2.778-06	4.194-06
23	7.485-04	5.000-01	1.725-02	3.389-02	1.007-06	2.710-06	1.369-06	2.544-07
24	4.540-04	5.000-01	1.643-02	3.094-02	4.172-07	1.117-06	5.384-07	4.146-08
25	2.754-04	5.000-01	1.569-02	2.866-02	1.270-07	3.457-07	1.468-07	1.144-08
26	1.670-04	5.000-01	1.501-02	2.682-02	5.162-08	1.360-07	6.523-08	4.167-09
27	1.013-04	5.000-01	1.439-02	2.493-02	2.370-08	3.499-08	2.921-08	1.424-08
28	6.144-05	5.000-01	1.381-02	2.308-02	6.041-09	2.657-08	7.982-09	1.287-08
29	3.727-05	1.500+00	3.863-02	5.813-02	2.140-09	2.939-08	5.778-09	5.047-09
30	8.315-06	3.000+00	6.945-02	5.833-02	0.000	0.000	1.038-09	5.516-09
	4.140-07							

TABLE IV RESPONSE RANGE OF REPRESENTATIVE ACTIVATION DETECTORS IN REACTOR DOSIMETRY BENCHMARKS

Neutron Field	Spectrum, E(P)[a]			^{239}Pu (n,f)			Au(n,γ)			^{237}Np(n,f)			^{58}Ni(n,p)		
	Median Energy (P=0.5)	90% range P=0.95	P=0.05	Median Energy (P=0.5)	90% range P=0.95	P=0.05	Median Energy (P=0.5)	90% range P=0.95	P=0.05	Median Energy (P=0.5)	90% range P=0.95	P=0.05	Median Energy (P=0.5)	90% range P=0.95	P=0.05
	MeV	keV	MeV	MeV	keV	MeV	MeV	keV	MeV	MeV	keV	MeV	MeV	kev	MeV
^{235}U Fission Spectrum	1.57	237	5.14	1.66	260	5.24	0.71	58	2.92	1.96	670	5.65	4.10	2090	7.63
ISNF	0.56	7.9	3.46	0.55	1.33	3.44	6×10^{-3}	0.33	0.93	1.54	540	4.53	3.74	1853	7.27
Sigma Sigma	0.40	20.4	2.87	0.39	1.13	2.93	0.026	0.076	0.80	1.17	447	4.26	3.82	1850	7.57
Big Ten	0.32	47.5	2.18	0.33	46.8	2.39	0.169	23.9	0.79	0.94	382	4.20	4.03	1940	7.71
Near-1/E	0.166	6×10^{-3}	3.00	1.3×10^{-5}	1.1×10^{-3}	0.79	5×10^{-6}	8×10^{-4}	7×10^{-5}	1.53	493	4.54	3.74	1870	7.28

a) Fraction of spectrum below E(P=0.95) is 5%, fraction above E(P=0.05) is 5%. (See Sec. 2.1, eq. 2.)

TABLE V
SELECTED MEASURED REACTION RATE CROSS SECTIONS FOR REACTOR DOSIMETRY BENCHMARKS

Detector		Fission Spectra		Driven Systems		Reactor Physics Criticals	
Reaction	Median Response Energy E(P=0.5) (MeV)	^{252}Cf	^{235}U	ISNF	Sigma Sigma	Big Ten	CFRMF
Normalizing Cross Section, X							
$\sigma_f(^{239}Pu)$		1804 ± 45 mb	[1796]	[1835]	[1761]	[1611]	[1781]
obs./calc.	-	1.008 ± .025	-	-	-	-	-
Cross Section Ratios -- Threshold Reactions							
Np(n,f)/X	0.9 - 2.1	0.737 ± 2.2%	0.734 ± 3.0%	-	0.338 ± 2.8%	0.265 ± 2.2%	0.309 ± 2.3%
obs./pred.		0.976 ± 2.2%	0.990 ± 3.0%		0.972	0.928	0.950
$^{238}U(n,f)/X$	2.6 - 2.8	0.177_3 ± 1.7%	0.168_6 ± 2.2%	(0.0803)[a] ± 1.8%	0.0466 ± 2.5%	0.0311 ± 1.9%	0.0424 ± 1.9%
obs./pred.		1.006 ± 1.7%	1.015 ± 2.2%	1.060	1.002	0.958	0.983
$^{58}Ni(n,p)/X$	4.1	0.0654 ± 3.5%	0.0604 ± 5.0%	-	0.0154 ± 4%		0.0135 ± 4.0%
obs./pred.		1.017 ± 3.5%	1.059 ± 5.1%		1.153		1.019
$Al(n,\alpha)/X$	8.5	5.58×10^{-4} ± 3.3%	3.93×10^{-4} ± 5.7%	-	0.971×10^{-4} ± 4.5%		0.905×10^{-4} ± 3.8%
obs./pred.		0.943 ± 3.5%	1.010 ± 5.9%		1.104		0.914
Cross Section Ratios -- Non-threshold Reactions							
$^{235}U(n,f)/X$	-	0.667 ± 1.6%	0.664 ± 2.2%	(0.867)[a] ± 1.8%	0.847 ± 2.1%	0.835 ± 1.5%	0.873 ± 1.6%
obs./pred.		0.961 ± 1.6%	0.953 ± 2.2%	0.967	0.976	0.979	0.975
$Au(n,\gamma)/X$	-	0.0529 ± 3.5%	0.0465 ± 6.5%	-	0.236 ± 3.5%		0.238 ± 4.0%
obs./pred.		1.18 ± 3.5%	0.979 ± 6.5%		1.191		1.021

[a](Preliminary values)

TABLE VI

BRIEF COMPENDIUM OF COMPUTED REACTION RATE CROSS SECTIONS FOR REACTOR DOSIMETRY BENCHMARKS

Neutron Field	Spectrum, E(P)[a] Median energy P=0.5 (MeV)	90% range P=0.95 (keV)	90% range P=0.05 (MeV)	Normalization Reaction σ_f(Pu 239) (mb)	Cross Section Ratio [X/Pu 239] Threshold Reactions Np(n,f)	^{238}U(n,f)	^{58}Ni(n,p)	^{46}Ti(n,p) (x10^{-3})	Non-threshold Reactions ^{235}U(n,f)	^{45}Sc(n,γ)	Au(n,γ)	^{59}Co(n,γ)
Natural Sources and Distribution												
Fission Spectra[b]												
^{252}Cf	1.68	260	5.5	1789 (2)	0.755 (5)	0.176 (2)	0.0643 (8)	7.0 (1)	0.694 (1)		0.0447 (8)	
^{235}U	1.57	240	5.1	1781 (3)	0.741 (7)	0.166 (2)	0.057 (1)	5.6 (2)	0.697 (2)		0.048 (1)	
thermal Maxwellian[c]	.04 eV	.01 eV	.12 eV	(741x10^3)					(0.779)	(.034)	(.133)	(.050)
Driven Neutron Fields												
ISNF	0.56	8.0	3.5	1822	0.431	0.0757	0.02069	1.678	0.898	0.01216	0.2327	0.02574
Sigma Sigma	0.40	20	2.9	1746	0.348	0.0467	0.01335	1.186	0.868	0.01080	0.1982	0.02440
CFRMF	0.38	15	2.9	1781	0.325	0.0431	0.01325	1.280	0.896	0.01123	0.2330	0.0503
Near-1/E (ISNF/CV)	0.166	0.0061	3.0	10540	0.0518	0.00907	0.00250	0.203	0.820	0.0295	3.55	0.213
Reactor Physics Criticals												
Godiva	1.02	143	4.5	1730	0.632	0.1199	0.0387	3.72	0.724	0.00460	0.0651	0.00458
Big Ten	0.32	44	2.33	1611	0.2855	0.0325	0.01001	0.973	0.853	0.00994	0.2576	0.00782
YAYOI	.89	113	4.22	1715	0.590	0.108	0.0337	3.16	0.739	0.00522	0.0743	0.0050
Tapiro	0.90	122	4.3	1716	0.598	0.1083	0.0343	3.21	0.734	0.00508	0.713	0.00489

[a] Fraction of spectrum below E(P=0.95) is 5%, fraction above E(P=0.05) is 5%. (See Sec. 2.1, eq 2)

[b] Error due to evaluated spectrum uncertainties given in parenthesis as std. dev. of last significant figure.

[c] (Experimental Values)

I.2. POWER REACTOR PRESSURE VESSEL BENCHMARKS AN OVERVIEW

Frank J. Rahn
Electric Power Research Institute
Palo Alto, California 94303

ABSTRACT

A review is given of the current status of experimental and calculational benchmarks for use in understanding the radiation embrittlement effects in the pressure vessels of operating light water power reactors. The requirements of such benchmarks for application to pressure vessel dosimetry are stated. Recent developments in active and passive neutron detectors sensitive in the ranges of importance to embrittlement studies are summarized and recommendations for improvements in the benchmark are made.

INTRODUCTION

The continued assurance of the safety and integrity of nuclear reactor components requires an understanding of the changes in material properties that such components sustain as a function of irradiation and the radiation flux and spectrum to which these components are exposed over the lifetime of the system. For current generation power reactors, interest is focused on radiation induced changes to the mechanical characterization of the pressure vessel, in particular the embrittlement and fracture toughness properties.[1] Light water reactor (LWR) pressure vessels are fabricated of low carbon steel, with a ferritic body centered cubic microstructure.[2] The IAEA has already established an important program studying the irradiation embrittlement of pressure vessel steels. In part, the purpose of the IAEA's program on benchmark neutron fields and reactor dosimetry is to support the requirements of the pressure vessel program.[3]

Service requirements for nuclear pressure vessels include design operating temperatures up to 325°C and pressures up to 70 bars for boiling water reactors (BWR) and up to 155 bars for pressurized water reactors (PWR). Of prime concern is the ability to heat up and cool down the reactor system during normal and unrestrictive operations over the 40-year design life of the plant. Neutron irradiation of the pressure vessel changes the transition temperature and results in transition from ductile to brittle fracture as measured by the Charpy test. The operating

envelope, required to maintain operation of the plant within the ductile regime of the pressure vessel, severely constricts as the pressure vessel accumulates neutron fluence.[4,5] Therefore, the demonstration of the safety of power reactors and of their conformance to the various codes and regulation guides, mandates a reasonably precise knowledge of the neutron radiation field in which the pressure vessel resides.

CHARACTERIZATION OF THE NEUTRON ENVIRONMENT AT THE PRESSURE VESSEL OF OPERATING POWER REACTORS

The majority of LWR's are designed to operate at powers of between 30 and 105 kw/liter. The number of neutrons arriving at the pressure vessel, however, is not particularly related to these numbers or the size of the core itself. Rather it is the power in the assemblies on the periphery and the relationship of these peripheral assemblies to the inner edge of the pressure vessel that are important. In terms of constructing viable benchmarks characteristic of an LWR the following comments are applicable:

A. Water Region

The region between the edge of the core and the pressure vessel is filled with coolant, as shown in Figure 1, for a typical PWR. This water gap ranges between 30 and 60 cm in width. This is a wide enough region so that an equilibrium spectrum of neutrons is established and, as a consequence, the spectrum of neutrons impinging on the pressure vessel wall is nearly independent of the type and all other parameters of the reactor. The magnitude of the flux at the pressure vessel is determined by the leakage of neutrons out of the edge of the core and the size of the water region.

B. Azimuthal Variation

Again referring to Figure 1, there is a very apparent geometrical effect around the edge of the core where the corners are closer to the pressure vessel than the flats. This gives rise to a very pronounced azimuthal effect in the magnitude of the flux around the inside edge of the pressure vessel. A plot of this variation for a PWR is shown in Figure 2. Calculations typically predict a ratio of about 3:1 peak to average in the fast flux incident on the wall of pressure vessel.

C. Axial Flux Profile

Axially the variation in the fluence is dependent on the equilibrium cycle burnup profile in the core. This tends to maximize the fluence around the core mid-plane area. Above and below the beltline region, the flux is falling off so rapidly that such potentially troublesome areas as the reactor nozzles are not expected to see enough fluence over a plant lifetime that material property changes due to irradiation are a problem. Because of the axial and azimuthal variations in the flux magnitude, one might properly think of the pressure vessel as having embrittlement sensitized "zones", rather than the whole pressure vessel as being "burned out". These zones do not necessarily extend completely through the pressure vessel in the radial direction.

D. Spectrum

As outlined in A. above, the water region in LWR's is sufficiently wide to establish an equilibrium spectrum. The effect of the water region is to strongly decouple, in the neutronic sense, the details of the core and other components from what happens in the pressure vessel. The spectrum impinging of the pressure vessel is very close to 1/E for $0.414\ eV \leq E \leq 2.5\ MeV$, and has a high energy tail, due mainly to uncollided fission neutrons from the core, above 2.5 MeV. Figure 3 shows the results of a calculation of the spectral effects in a PWR. In the pressure vessel, the spectrum starts changing very rapidly. The iron inelastic cross section very quickly attenuates the high energy neutrons relative to those at lower energies. In the keV energy range, the neutron transmission is quite high due to the minima in the iron cross section, which shows up quite prominently around 25 keV. At the 1/4t position in the pressure vessel, the neutron spectrum is quite different from that entering the pressure vessel, and is shifted downward in energy. This spectral shift is important because there are good theoretical reasons to believe that lower energy neutrons produce fewer lattice dislocations and other effects on the microstructure level which relate to the mechanical macro-properties of steel.

E. Flux Gradient

Figure 4 shows the radial behavior of the neutron flux for various energy groups. Away from the core, the fast flux drops off quite dramatically, approximately one decade every 16 to 18 cm. This gives rise to the pronounced azimuthal and axial effects described above. The magnitude of the flux gradient complicates the interpretation of data obtained at accelerated surveillance positions and the extrapolation of these effects to the pressure vessel. When interpreting experimental data, relatively small positioning errors can have large effects in the experimental uncertainties.

F. Thickness of Pressure Vessel

The thickness of the pressure vessel ranges between 15 and 30 cm. The material is low carbon steel. The thinner vessels are found in BWR's, the thicker in PWR's. The neutron spectrum and the magnitude of the flux at the 1/4t position of the pressure vessel and in the reactor cavity are determined by this thickness. Such quantities are essentially characterized by the transmission properties of thick sections of iron.

References 6-8 give additional information concerning the above remarks.

OPERATIONAL BENCHMARK REQUIREMENTS

The experimental benchmark neutron fields are divided into three distinct types: standard field, reference field and controlled environment. The reference experimental measurements planned on operating light water reactors fall into the latter type. An integral part of an experimental program is the comparison of the data with results from computer codes so as to produce a validated analytic method of estimating the flux and spectrum in the vicinity of the pressure vessel. In addition, there are a series of computational benchmarks available which are intended to check the methodology, data and adequacy of the models used to calculate quantities of interest.

The purpose of the experimental program is to obtain high accuracy and precision quantities which can be related to the materials effects occurring in the pressure vessel under irradiation and which can be used to validate the calculational methodology.[9] This mandates that the neutron flux and spectrum be determined as the intermediary between the radiation exiting the core and the various changes in macroscopic properties of the pressure vessel.[10,11]

The salient features required by operational benchmarks are the following:

(a) A relatively complete flux and spectrum mapping starting at the edge of the core through the outside edge of the pressure vessel. This should include detectors in the water gap radially outward from the core, and in a sufficient number of axial and azimuthal positions within the water region in order to assure complete knowledge of the neutron field impinging on the pressure vessel. In addition, detectors should be positioned on both sides of the pressure vessel to measure the transmission and the change in spectrum in the steel. Such complete knowledge is required to validate the computational methods and to establish a self-consistent set of experimental points.

(b) The principal energy range of interest for dosimetry purposes is the range $0.1 \leq E \leq 5$ MeV. It is the neutrons in this energy range which are the greatest contributors to radiation embrittlement in steels. However, information on the spectra in the energy region $1 \leq E \leq 100$ keV is important for shielding problems due to the high transmission of neutrons through steel for these energies. The most important location for spectral measurements in this energy range is at the exit surface of the pressure vessel. At this point the usual calculational approach is to interface the 2D finite difference transport calculations used inside the pressure vessel with the 3D Monte Carlo and albedo scattering techniques used in

the reactor cavity region. Flux and spectral measurements, then, in the 1 to 100 keV range are necessary to verify the deep penetration predictions and establish the source for the Monte Carlo simulations. Thermal flux measurements are usually required for activation considerations, and for corrections of the various detector responses to the fast flux. For fast neutrons, an LWR water gap is approximately 7 mean free paths (mfp) wide. For neutrons much below 1 MeV, the concept of spatial distances in terms of mean free paths is somewhat misleading, because the neutron density at these energies is due to high energy neutrons, undergoing collision and rapidly thermalizing. The pressure vessel is about 1.5 mfp wide for BWR's and 2.0 mfp wide for PWR's. At the inside edge of the pressure vessel, the expected flux (< 0.1 MeV) is approximately 3.6×10^{9} n/cm^2/sec for a BWR and 1.4×10^{10} n/cm^2/sec for a PWR, for plants producing 3400 MWth and 3600 MWth, respectively.

(c) There are special considerations which determine the proper balance between desired accuracy and what is obtainable on commercial operating reactors. On such plants, operational considerations, accessibility and instrument locatability require very precise planning to bring off a successful experimental program. These various considerations, and especially the problem of equipment installation, almost in themselves require that the experiment be performed during a reactor start up. It is essential that a set of precalculations exist to bracket the fluxes and fluences expected.

(d) The detectors should be chosen with some care, and should have overlapping energy ranges. Redundancy is important in achieving a self-consistent set of measurements. There are several different classes of detectors, each of which has particular virtues and disadvantages for use in operating benchmarks. They are:

(1) Activation Foils - provide good coverage of the thermal range and energies between 0.5 and 8.0 MeV. Since these are passive detectors and have a long history of use they are ideally suited to in-vessel measurements. When using such detectors care must be given to the quality assurance of the foil materials, and multi-laboratory intercomparison of the activation counting is recommended.[12,13,14]

(2) Proton Recoil Detectors - give good resolution spectra from a few keV to a few MeV and are capable of covering the range from 0.1 to 1 MeV where activation foils have difficulties. The proton recoil detectors are usually H_2 or CH_4 filled at various pressures. Experimental devices are being tested using ^4He. Proton recoil detectors are not operable in neutron fluxes higher than about 10^6 $n/cm^2/sec$. When used in an operating reactor environment, they are not suitable for use inside the pressure vessel and can be used outside the pressure vessel only during low or zero power operation. At low power, the fission distribution within the core may be appreciably different and influence the axial total flux results in the cavity.

(3) Special and Experimental Detectors[15] - In pressure vessel surveillance (PVS) applications, highly specialized miniature proportional counters will be required. Consequently, accurate treatment of proportional counter finite size effects will be mandatory.

A proton recoil method which introduces less perturbation and possesses considerably reduced finite size effects is emulsion-photographic track plate proton recoil spectrometry. The emulsion technique possesses the advantages of passive monitoring; however, just as for active

spectrometry, low power clean environments are mandatory. Hence, it is appropriate to combine the emulsion method with active neutron spectrometry techniques wherever possible.

For actual PVS experiments in operating reactors, it is only possible to utilize passive multiple foil flux-fluence spectrometry. In such PVS irradiations it is highly advantageous to use time integrative passive monitors. While the passive multiple foil spectrometry has utilized radiometric dosimeters in the main, in PVS applications the length of irradiation is often ill-defined and the power-time history of the reactor can also introduce considerable uncertainty. Hence, for more accurate data from PVS surveillance experiments, it will be necessary to exploit time integrative passive monitors, such as long-lived radiometric dosimeters (encapsulated fission foils providing long half-life fission products such as ^{137}Cs), and in particular, solid state track recorders (SSTR), and helium accumulation fluence monitors (HAFM). It is noted that the latter two passive methods possess higher sensitivity than radiometric dosimeters. Moreover, these two methods compliment each other in terms of the neutron sensitivity provided for the broad energy range of interest, 0.01 to 6.0 MeV, in PVS applications. HAFM utilizing ^{6}Li or ^{10}B will provide good sensitivity in the low energy region, whereas SSTR incorporating fission threshold nuclides such as ^{232}Th, ^{238}U, or ^{237}Np, will provide good complimentary sensitivity at higher energy.

For longer term PVS irradiation where the fast fluence exceeds 10^{18} neutrons/cm^2, another time integrative passive neutron dosimeter that can be used is crystalline

quartz. Physical changes in the crystalline quartz can be examined such as changes in density and in the refractive index of the medium. These properties can provide sensitive indicators of fast fluence that accrues during PVS irradiations.

THE CURRENT OPERATING REACTOR BENCHMARK STATUS

There are currently several experiments which could qualify as either reference neutron field or controlled neutron environment benchmarks. The experimental facilities are located in the United States, Europe and Japan.

A. Research Reactors

(1) Japan JRR-4 Reactor. A series of experiments were made with the JRR-4 reactor mocked up with various iron water configuration arranged to simulate the core structure, thermal shield and pressure vessel of a LWR.[16] Some of the results are shown in Figures 5 to 7. The experiments were analyzed using the 2-D transport code PALLAS.[17] Emphasis was on the energy region 1 to 10 MeV. The dosimeters used in the experiment are given in Table 1.

(2) Belgium - CEN/SCK - BR 1 Reactor. Multishell systems made of an outer natural Uranium driver and of inner iron shells are being studied.[18] The iron laminations are set up at the center of a 1 meter spherical cavity in the graphite thermal column of the BR 1 reactor. Neutron spatial, angular and spectral distributions will be measured using ^{6}Li, proton recoil and foil detectors. The system is essentially one-dimensional, with homogeneous material zones and the source has a reasonably well-known spectrum. The system will be used

for spectral dependent transmission measurements of hollow iron spheres with 2 to 14 cm wall thickness. As such, experiments of this nature will provide clean experimental and calculational benchmarks of relevance to LWR pressure vessel dosimetry programs. Such a facility will also provide a secondary calibration for dosimetry instrumentation in a well-characterized field whose spectrum can be modified to match a realistic LWR environment.

(3) United States ORR Reactor at Oak Ridge National Lab. The Oak Ridge Research Reactor (ORR) is a 30 MW test reactor used for irradiation experiments[19]. Figure 8 shows a plan view of the core and experimental regions. Currently, a series of 4T-CT (4 thickness, compact tension) specimens of pressure vessel materials are being irradiated.[20] Under consideration is the use of the ORR as an irradiation facility to do simulated pressure vessel experiments. Simulated pressure vessel plates 122x122x30 cm (made up to twelve 122x122x2.5 cm slabs) can be inserted into the poolside facility. A water gap of 30 cm between the reactor face the specimens will reduce the fast flux (> 1 MeV) from 1×10^{14} to 1×10^{12} n/cm^2/sec and produce a spectrum characteristic of LWR reactors. Simultaneous irradiation of dosimetry and metallurgical specimens for the surveillance and HSST program can be handled. Complete instrumentation of the pressure vessel specimens for dosimetry and temperature control can be accomplished.

B. Commercial Operating Reactors

A set of experimental measurements on two operating power reactors is being sponsored by the Electric Power Research Institute. Included in the program is a set of pre- and post-experiment calculations using two-dimensional DOT calculations and three-dimensional MORSE calculations.

This set of experiments is believed to be the only completely characterized measurements made on operating reactors for pressure vessel dosimetry purposes which could qualify as an industry-wide benchmark. For other recent measurements, see References 21 and 22.

(1) BWR - Browns Ferry 3 (BFS) - Tennessee Valley Authority. This is a 1075 MWe reactor with 8x8 fuel assemblies. Commercial operation is expected about 12/76. There are two parts to the neutron measurements at BF3. The first is the in-vessel dosimetry at 18 positions between the core and the pressure vessel. This includes measurements at 3 radial, 2 axial and 2 azimuthal positions. A plan view of these positions is given in Figure 9. Table 2 gives a listing of the activation foils used. These foils will be irradiated during the first operating cycle of the reactor. The second part of the BF3 project consists of activation foil measurements in the reactor cavity between the pressure vessel and the shield wall. The dosimeters will be strung axially in the cavity from the feedwater nozzle to the head access area, at four azimuthal positions. Table 3 gives the activation foils which will be placed in the reactor cavity during the first refueling. The combination of the in-vessel and in-cavity measurements will provide a complete neutron and spectral mapping for $0.5 \leq E \leq 5.0$ MeV and will provide a sensitive test of the calculational methods now used.

(2) Westinghouse PWR McGuire 1 - Duke Power Company. This is a 1180 MWe reactor scheduled for commercial operation 12/77. The reactor cavity is of the narrow gap design, which is about 17 cm across of which 12 cm is filled with thermal insulation. Such a design cuts down considerable the neutron streaming in this area. Figure 10 shows the details of the McGuire 1 reactor. The planned measurements consist of activation foil

detectors placed in the reactor cavity gap and proton recoil detectors in the ex-core detector positions. The proton recoil measurements will be conducted during zero power start-up operations. Table 4 gives the details of the foil detectors and Table 5 the proton recoil monitors to be used at the McGuire 1 unit.

A primary objective of the experimental program at these reactors is to apply and validate use of the LFMBR dosimetry techniques for LWR pressure vessel irradiation and dosimetry programs. Such validation would lead to improved ASTM procedures for damage analysis practices. This effort will be interlaboratory in scope and involve a major cooperative effort supported by the U.S. Nuclear Regulatory Commission (NRC) and involving the National Bureau of Standards (NBS). The NRC will support work at HEDL in the following areas:

- Design, acquisition and development of Solid State Track Recorders
- EPRI, NBS and CEN/SCK passive and active sensor calibrations and cross validations
- Selection of simulated pressure vessel fields and the establishment of an experimental program for neutron penetration studies
- Study of damage mechanisms for selection of applicable irradiation effects for data correlation
- Updating the American Society for Testing and Materials (ASTM) procedures and interaction with Committees E10.05 on Dosimetry, E10.08 on Procedures for Neutron Radiation Damage Simulation and E10.02 on Radiation Induced Changes in Metals.

(3) Belgium - BR 3 Reactor CEN/SCK. BR 3 is a PWR power plant, operated at a power of 11 MWe, which is also used to irradiate experimental fuels to extreme exposure conditions.[23] At present, one third of the core loading is mixed oxide fuel. The pressure vessel material is A302-B steel. At the end of the present cycle, the fast fluence (> 1 MeV) at the inner wall of the vessel will be 5.6×10^{19} n/cm^2. In the frame of the surveillance program, tensile and impact specimens are irradiated at two locations inside the vessel, one in the radial reflector at the reactor mid-plane level and the other above the core. At these locations, the fast flux level is respectively about 40 and 2 times higher than at the inner side of the vessel wall. The irradiation temperature is 295 ± 20°C. The neutron dose at these locations is based on the ^{54}Fe (n, p) ^{54}Mn reaction.

The DTF-IV transport code is being compared with the SABINE diffusion code used for design. This work includes sensitivity calculations with respect to cross section changes. Thermal and fast flux measurements are being made in the reactor core, and outside the pressure vessel in the neutron shield tank. Track recorders associated with ^{238}U thin deposits are used to determine fast fluences at low fluxes. The use of quartz dosimeters is being considered.

C. Calculational Benchmarks

There are two calculational benchmark efforts applicable to LWR's now underway. The first was produced by the OECD Nuclear Energy Agency's Committee on Reactor Physics and the second by the American Nuclear Society Shielding Standards Subcommittee 6.2.

(1) The OECD Nuclear Energy Agency - Reactor Shielding Benchmark No. 2 - is a 2-dimensional model of a 1300 MW standard power reactor of the PWR type. A one-dimensional solution is also desired. Figure 11 shows the calculational geometry. The specifications[24] were produced by G. Hehn (IKE) and J. Koban (KWU), and published in 3/76.

(2) The ANS 6.2 Committee has produced a series of three interrelated calculational benchmark problems. They consist of a radial one-dimensional, a two-dimensional core problem and a three-dimensional cavity streaming problem for a PWR reactor. Figures 12 and 13 show the geometrical arrangement being considered for calculation. Final publication of the benchmark set is expected this year.[25]

NEUTRON FIELD REQUIREMENTS FOR LWR EXPERIMENTAL CALIBRATION

Radiation fields are required for use as permanent reference field for calibration purposes that are available to all users. Such fields would serve as standards for benchmark experiments, as well as provide quality assurance on pressure vessel surveillance dosimeters, etc. The following radiation fields would be appropriate for LWR dosimetry work:

	Type	Energy Range (MeV)	Possible Facility
1.	Thermal Spectrum	$< 0.4 \times 10^{-6}$	various reactor beams of known flux, gradient and thermalized spectrum
2.	Epithermal - 1/E	0.4×10^{-6} - 1.0	no facility currently exists which maintains a standard 1/E field at the higher energy range; however, near 1/E fields exist to about 0.1 MeV
3.	Fission Spectrum (^{252}Cf,^{235}U)	0.1 - 10	NBS (USA), MOL (Belgium) PTB (Germany), Kyoto (Japan)
4.	Secondary Standard	10^{-4} - 1.0	$\Sigma\Sigma$ type

These fields would be classified as either standard neutron fields or reference neutron fields according to the terminology of the Petten Symposium in 1975.

The accuracy required of the above neutron fields is shown in Table 6. This table differentiates between what is currently available and the accuracy ultimately required. For the controlled radiation environment accuracy requirements, there is a wide and somewhat arbitrary band on the accuracy achievable. This reflects the realization that the accuracy expected on experimental measurements in operating commercial LWR's versus those in research facilities are quite different.

CONCLUSIONS AND RECOMMENDATIONS

There is currently either under way or in the planning stage a series of remarkable programs which are directly applicable to reactor dosimetry problems in light water reactors. In this brief paper it is not possible to completely summarize all of them in a thorough manner. However, in an overview of the field there are several areas in which further research is called for. I will limit my remarks to what I perceive should be done in the intermediate term (5-year time span). Five areas in particular could benefit by expanded programs, they are:

(1) Further international cooperation is called for, especially in obtaining good experimental and calculational benchmarks, for the exchange of ideas in dosimetry and dosimetry techniques, and in reporting and disseminating the results obtained. The IAEA should promote the multiple foil technique, and the development of spectra unfolding techniques. Reference spectra (thermal, 1/E, $\Sigma\Sigma$, fission) should be well documented and used to check unfolding techniques.

(2) Special emphasis should be placed on obtaining reliable data on operating reactors and prototypes. The need is for in-vessel flux and spectra measurements between the core and the pressure vessel. Such measurements should concentrate around the edge of the core and the wall of the pressure vessel. There is a further need for information axially above and below the core in the support plate, baffle and flow straightener regions. Consideration should also be given to the area outside the pressure vessel, around the coolant nozzles and around major penetrations.

(3) The development of sensitivity studies and importance function studies is required. The spatial importance of neutrons in various energy groups in reaching the pressure vessel and other components of interest, the sensitivity of various macroscopic changes in materials to uncertainties in the neutron flux and spectra, and the sensitivity of deep penetration neutrons and activation detectors to cross section uncertainties should be studied.

(4) From the materials side, the need exists for better correlation of the material properties with changes in spectra, and in obtaining well-characterized data bases on material properties where all significant factors in the irradiations, especially the spectrum, are recorded. The work on the irradiation of thick section steel samples, and steels behind iron filters, characteristic of dosimetry at various places interior to the pressure vessel are extremely useful and should be expanded. Increased cooperation with the IAEA's research coordination program on Irradiation Embrittlement of Pressure Vessel Steels is desirable. The excellent work in this IAEA program would benefit from improved dosimetry techniques.

(5) Adherence to what is known as the Inter-Laboratory Reaction Rate (ILRR) principle, namely that the dosimeters used in benchmark experiments should be exposed to known, well-characterized and permanent neutron fields, should be encouraged. Good examples of such fields are the ΣΣ facilities and the NBS fission spectrum field. It is important that this methodology be used so that detectors can be properly referenced and, if needed, can be recalibrated at a later time.

The application of the above recommendations will improve the situation with regards to LWR power reactor benchmarks, and significantly contribute to our knowledge of radiation effects to pressure vessels.

Acknowledgements

The author wishes to thank the many individuals who have contributed ideas and information for inclusion in this paper. They include A. Fabry and J. Debrue of MOL, R. Gold and W. McElroy of HEDL, J. Grundl of NBS, and Frank Kam of ORNL.

References

1. S. H. Bush, "Radiation Damage in Pressure Vessel Steels for Commercial LWRs," Conf. American Society for Engineering Education, June 16-19, 1975, Colorado State University, Ft. Collin, Co.

2. Symposium, "Effects of Radiation on Structural and Mechanical Properties of Metals and Alloys," ASTM Special Technical Publication 529, Sept. 1973.

3. "Coordinated Research Programme on Irradiation Embrittlement of Pressure Vessel Steels," IAEA-176, Report of the Research Coordination Meeting held by the IAEA in Vienna, Oct. 23-25, 1974.

4. R. A. Wullaert, et al., "Fracture Toughness Data for Ferritic Nuclear Pressure Vessel Materials," EPRI Report NP-121, April 1976.

5. H. S. Palme, "Radiation Embrittlement Sensitivity of Reactor Pressure Vessel Steels," Babcock & Wilcox Topical Report BAW-10056, March 1973.

6. A. L. Lowe, et al., "Analysis of Capsule Data, Reactor Vessel Materials Surveillance Program," Babcock & Wilcox Report BAW-1421, Rev. 1, Sept. 1975.

7. L. B. Miller, et al., "Study of Radiation Dosage to Structural Components in Nuclear Reactors," EPRI Report NP-152, January 1976.

8. S. L. Anderson and M. A. Capo, "Comparison of Measurements and Calculations of Neutron Streaming in a PWR Primary Shield Annulus," Transactions of the American Nuclear Society, 23, p. 617, June 1976.

9. G. Hehn and P. Stiller, "Prediction of Radiation Damage in Structural Materials Outside the Reactor Core," Paper 32, Proc. of 1st ASTM-EURATOM Symposium, Petten, The Netherlands, Sept. 22-25, 1975.

10. C. Z. Serpan, Jr., "Reliability of Fluence-Embrittlement Projections for Pressure Vessel Surveillance Analyses," Nuclear Technology, 12, p. 108, (1971).

11. R. Odette, et al., "Application of Advanced Irradiation Methods to Light Water Reactor Pressure Vessel Test and Surveillance Programs," Symposium on the Effects of Radiation on Structural Materials, St. Louis, U.S.A., May 1976.

12. Nuclear Technology, 25, 1975.

13. Proc. of a Consultants' Meeting on Nuclear Data for Reactor Neutron Dosimetry, IAEA, Vienna, September 10-12, 1973.

14. Proc. of the ASTM-EURATOM Symposium on Reactor Dosimetry, Petten, The Netherlands, September 1975.

15. Private Communication, W. McElroy and R. Gold.

16. K. Takeuchi, et al., "Neutron Energy Spectrum Determination for Irradiation Damage Study of Reactor Structural Materials," Proc. of the ASTM-EURATOM Symposium on Reactor Dosimetry, Petten, The Netherlands, September 1975.

17. K. Takeuchi and A. Yamaji, J. Nucl. Sci. Technol., 11, p. 49 (1974).

18. G. De Leeuw and S. De Leeuw, contributed paper, this conference.

19. T. M. Sims and J. H. Swanks, "Oak Ridge Research Reactor (ORR) Experimental Facilities." Internal ORNL Report, unpublished.

20. R. G. Berggren, "Description of Second 4T-CT Irradiation Experiment," Internal ORNL Report, unpublished.

21. L. E. Steel and C. Z. Serpan, Jr., "Analysis of Reactor Vessel Radiation Effects Surveillance Programs," ASTM Special Technical Publication 481, Dec. 1970.

22. S. L. Anderson and M. A. Capo, Trans, Am. Nucl. Society, 23, 617 (1976).

23. Private Communication, J. Debrue.

24. G. Hehn and J. Koban, OECD Nuclear Energy Agency Committee on Reactor Physics, NEACRP-L-151, March 1976.

25. G. L. Simmons, private communication.

Figure Captions

1. Plan view of a typical PWR showing material zones and power density in the core. Taken from ANS 6.2 Benchmark Problem #2.

2. Typical PWR Azimuthal Neutron Flux Distribution for One Octant. Taken from Ref. 7.

3. Calculated neutron spectrum for a PWR at various radial positions moving radially outward from the core. Refer to Figure 1 for the geometrical model.

4. Calculated spatial dependence of the neutron flux for various energy groups, as given by the one-dimensional code ANISN. Refer to Figures 1 and 3 for geometry and spectra.

5. Comparison of the results from the Computer Code PALLAS and the measured neutron energy spectra in a water configuration of the JRR-4 reactor.

6. Comparison of PALLAS and the measured neutron energy spectra in an iron-water configuration of JRR-4.

7. PALLAS calculated neutron energy spectra at several positions of a simulated power reactor geometry in JRR-4. Figures 5 through 7 taken from Ref. 16.

8. Plan view of the ORR reactor and experimental positions. Taken from Ref. 19.

9. Plan view of the in-vessel experimental dosimeter positions for flux and spectral measurements in the Browns Ferry III BWR.

10. Plan and elevation views of the core and reactor cavity areas in the McGuire I PWR. Taken from Ref. 8.

11. PWR geometry used for 2D benchmark calculations for the Reactor Shielding Benchmark No. 2 issued by the OECD Nuclear Energy Agency.

12. PWR geometry under consideration for use in 2D benchmark calculations around the pressure vessel from the ANS 6.2 Shielding Computations Subcommittee.

13. PWR geometry under consideration for use in 3D benchmark calculations in the reactor cavity area, from ANS 6.2.

Table 1

Neutron dosimeters used in the JRR-4 reactor for spectral determination in irradiation damage studies of reactor structural materials:

$^{27}Al(n, \alpha)^{24}Na$	$^{54}Fe(n, p)^{54}Mn$
$^{56}Fe(n, p)^{56}Mn$	$^{64}Zn(n, p)^{64}Cu$
$^{24}Mg(n, p)^{24}Na$	$^{58}Ni(n, p)^{58}Co$
$^{27}Al(n, p)^{27}Mg$	$^{115}In(n, n')^{115\ m}In$

Table 2

In-Vessel Dosimeters in Browns Ferry III

The dosimeter capsules are small carbon steel cylinders containing special neutron fluence monitors. Two capsules will be placed in each of four capsule holders. The holders will be located in two azimuthal positions near the core mid-plane and two positions near the core top edge. The dosimeters will remain in the reactor about one year.

The activation monitor materials will be:

^{235}U	Fe	Ti
^{238}U	Al	Ni
^{237}Np	Co	Ag
^{232}Th	Cu	Sc

and Cu CdO thermal neutron shields.

Table 3

In-Cavity Dosimeters in Browns Ferry III

The dosimeters will be placed in-cavity supported by Ni wire. The wire itself will be used as a monitor. The dosimeter capsules will contain:

^{235}U	1-5 mg	Ti	200 mg
^{238}U	200 mg	Cu	800 mg
^{237}Np	30 mg	Al + 1/2% Co	100 mg
^{232}Th	500 mg	Ag	250 μg
Ni	50 mg	Sc	0.5 mg
Fe	200 mg		

Table 4

Dosimeters for Use in McGuire I

The dosimeters will be the same as in Table 3 for the BWR Browns Ferry III, with the possible exception of Sc and Al + 1/2% Co. The final quantities of each material have not yet been decided.

Table 5

Proton Recoil Monitors to be Used at McGuire I

Present plans call for the use of proton recoil detectors in the ex-core instrument positions of the McGuire I PWR to make spectral measurements at about 1% (or less) of full power. Geometry of the detectors will be cylindrical with about a 5 cm diameter. The following two detectors will be used:

Type	Pressure
10% methane - 90% argon	2 bar
10% hydrogen - 90% argon	4 bar

Table 6

	Accuracy Required* (2σ)		
Energy Range	Standard** Radiation Field	Reference** Neutron Fields	Controlled Radiation Environment
thermal	<4% (4%)	≤10% (6%)	≤10% (10%)
0.414 eV - 1.0 keV	<10% (10%)	≤10% (_20%)	≤20% (30%)
1.0 keV - 100 keV	↓	↓	≤10% (20%)
0.1 MeV - 1.0 MeV	↓	≤6% (≤20%)	≤6% (20%)
1.0 MeV - 4.5 MeV	↓	↓	≤6% (20%)
4.5 MeV - 10 MeV	↓	≤10% (≤20%)	≤10% (30%)

*the first number is what is ultimately needed, the second is what is believed to be currently achievable with state-of-the-art techniques for measuring integral flux over the energy interval.

**for standard and reference fields, the accuracy is specified for LWR, LFMBR and CTR requirements, reflecting the overall requirements for all of these systems.

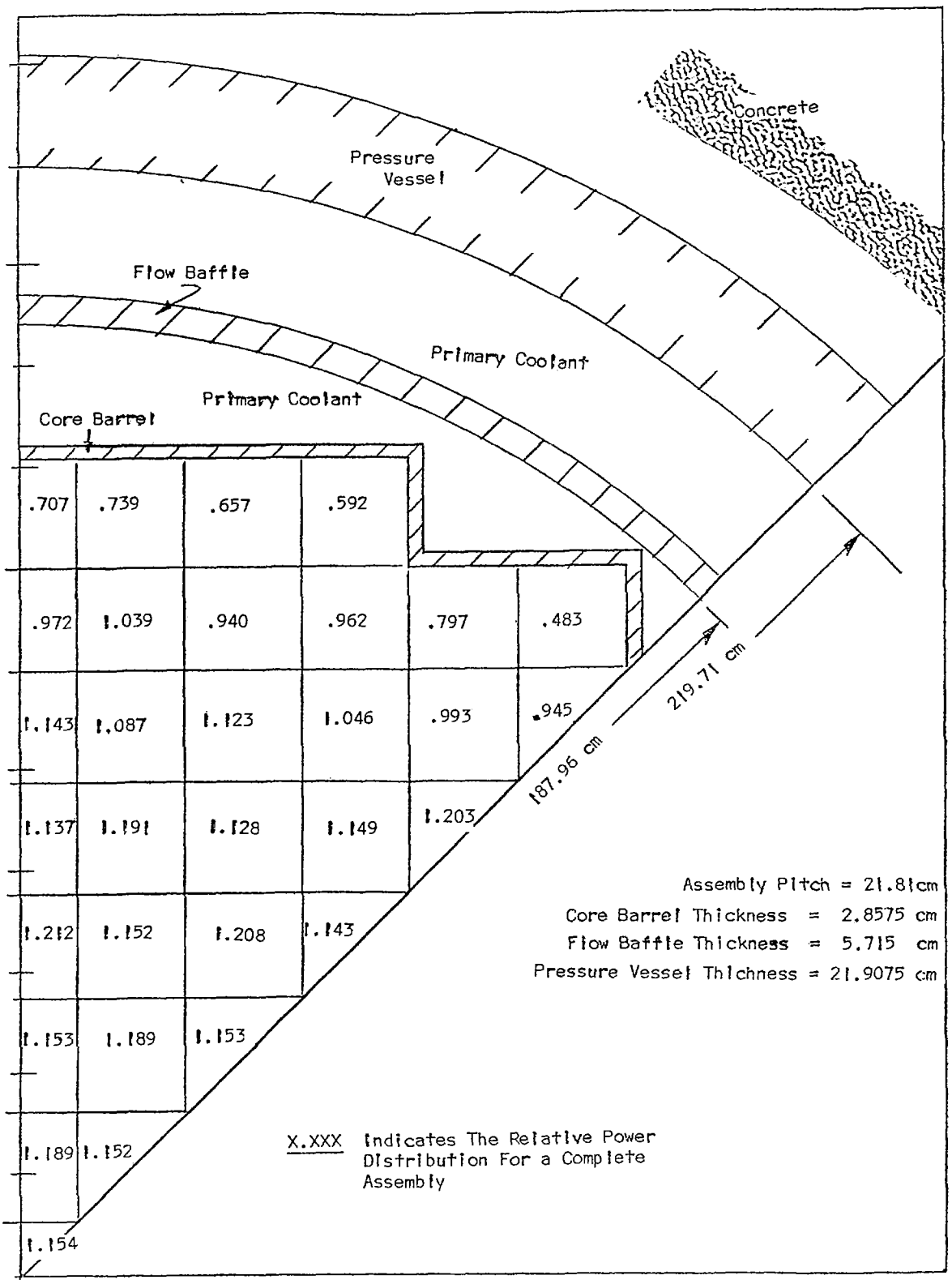
Concrete
Pressure Vessel
Flow Baffle
Primary Coolant
Primary Coolant
Core Barrel
.707 .739 .657 .592
.972 1.039 .940 .962 .797 .483
1.143 1.087 1.123 1.046 .993 .945
1.137 1.191 1.128 1.149 1.203
1.212 1.152 1.208 1.143
1.153 1.189 1.153
1.189 1.152
1.154
219.71 cm
187.96 cm
Assembly Pitch = 21.81cm
Core Barrel Thickness = 2.8575 cm
Flow Baffle Thickness = 5.715 cm
Pressure Vessel Thichness = 21.9075 cm
X.XXX Indicates The Relative Power Distribution For a Complete Assembly

Fig. 1

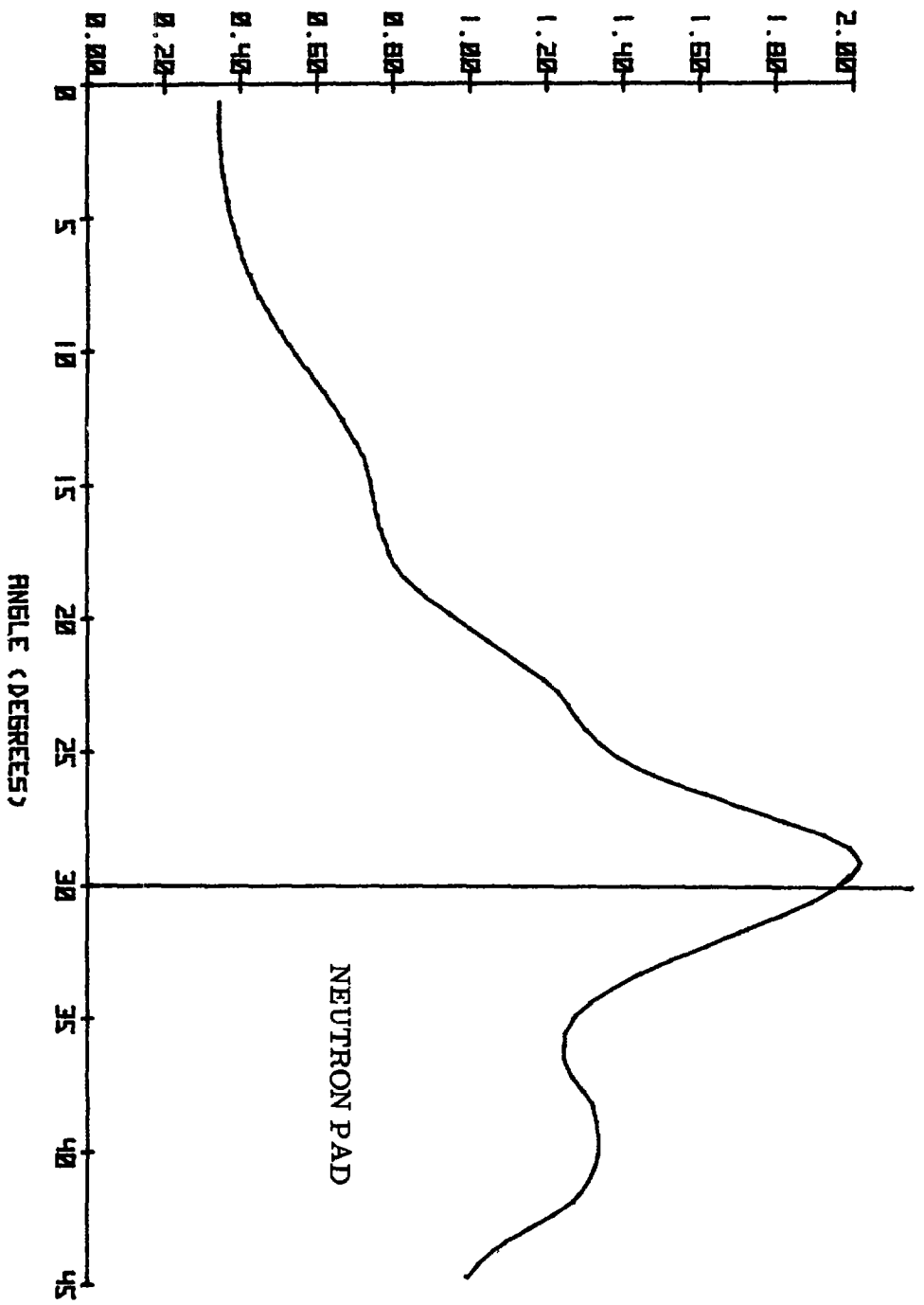
NEUTRON FLUX (NORMALIZED)
0.00
0.20
0.40
0.60
0.80
1.00
1.20
1.40
1.60
1.80
2.00
0
5
10
15
20
25
30
35
40
45
ANGLE (DEGREES)
NEUTRON PAD

Fig. 2

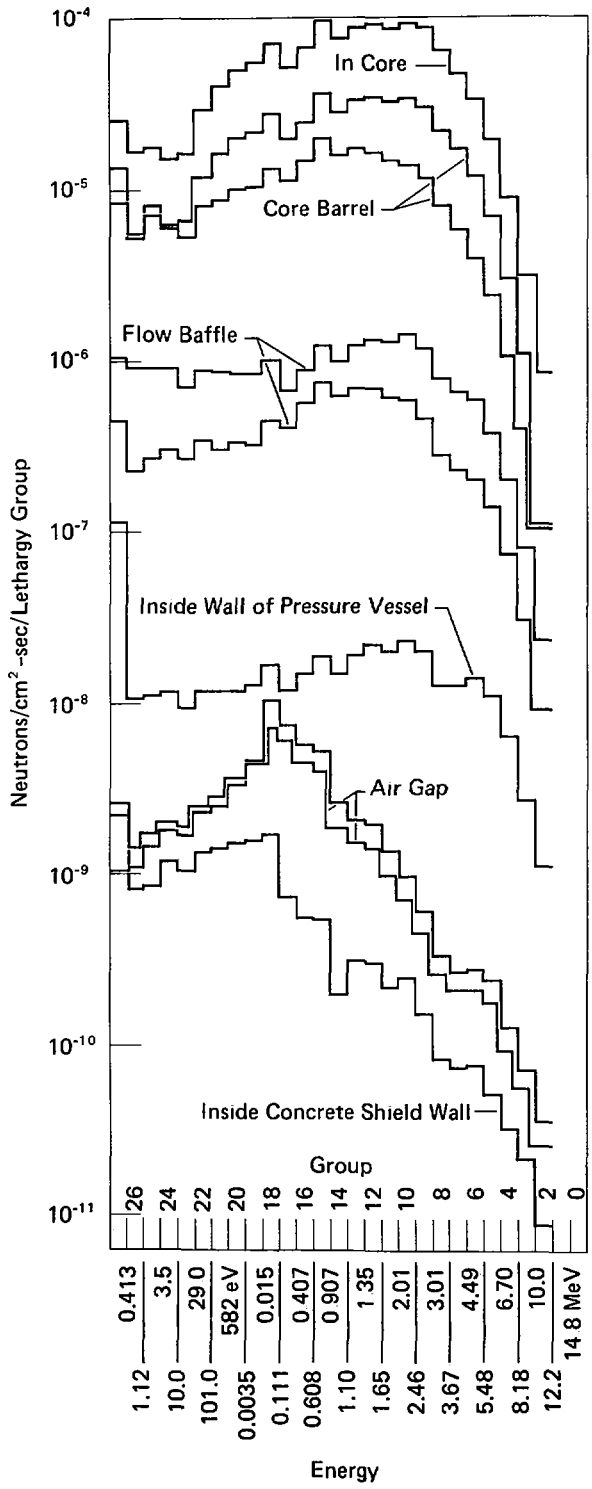
Neutrons/cm²-sec/Lethargy Group
10⁻⁴
10⁻⁵
10⁻⁶
10⁻⁷
10⁻⁸
10⁻⁹
10⁻¹⁰
10⁻¹¹
In Core
Core Barrel
Flow Baffle
Inside Wall of Pressure Vessel
Air Gap
Inside Concrete Shield Wall
Group
26 24 22 20 18 16 14 12 10 8 6 4 2 0
0.413 3.5 29.0 582 eV 0.015 0.407 0.907 1.35 2.01 3.01 4.49 6.70 10.0 14.8 MeV
1.12 10.0 101.0 0.0035 0.111 0.608 1.10 1.65 2.46 3.67 5.48 8.18 12.2
Energy

Fig. 3

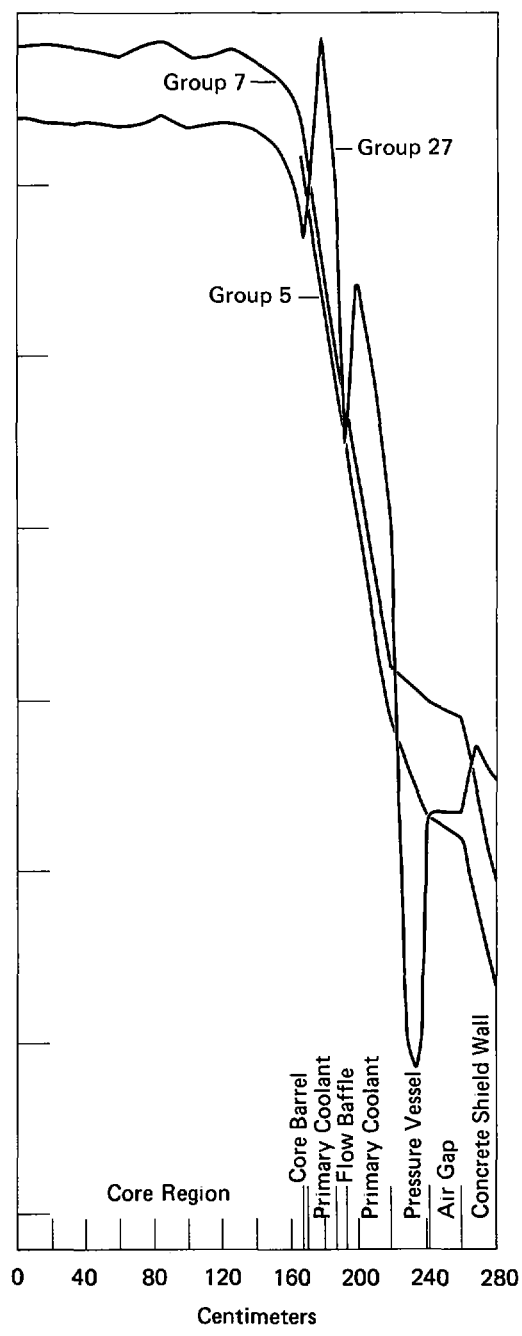
Group 7
Group 27
Group 5
Core Region
Core Barrel
Primary Coolant
Flow Baffle
Primary Coolant
Pressure Vessel
Air Gap
Concrete Shield Wall
0 40 80 120 160 200 240 280
Centimeters

Fig. 4

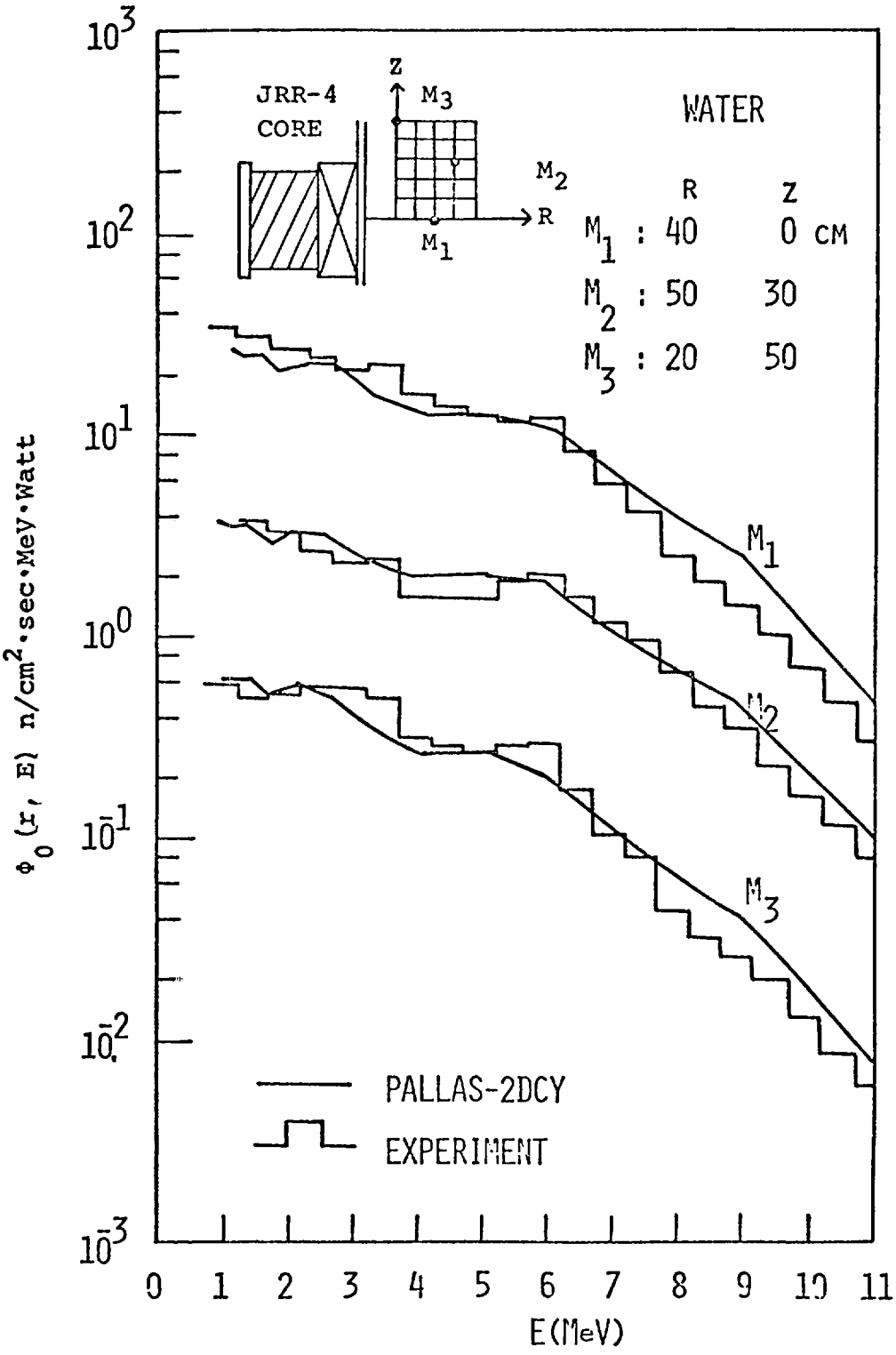
JRR-4
CORE
Z
R
M1
M2
M3
WATER
R Z
M1 : 40 0 cm
M2 : 50 30
M3 : 20 50
PALLAS-2DCY
EXPERIMENT
E(MeV)
φ0(r, E) n/cm2·sec·MeV·Watt

Fig. 5

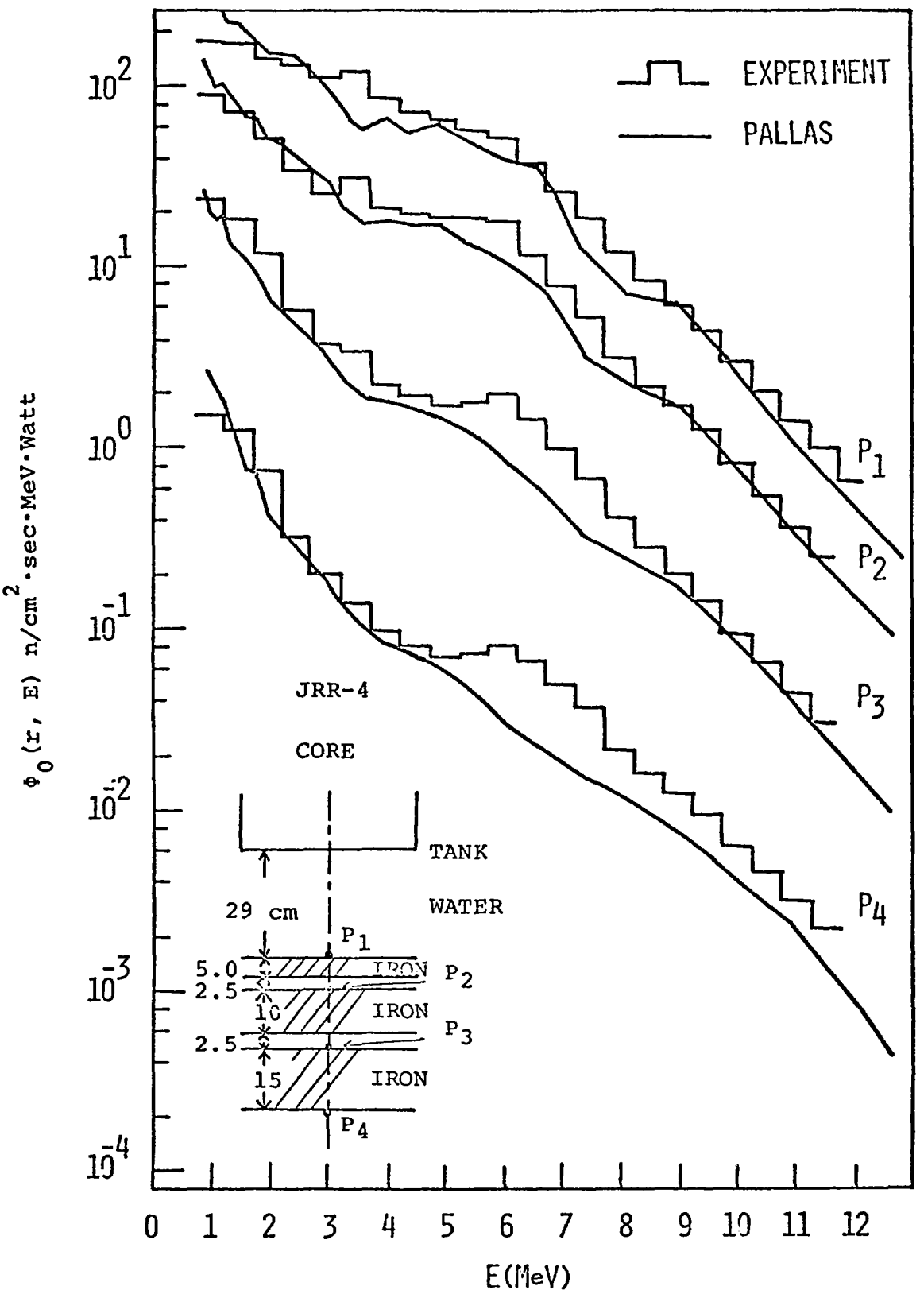
EXPERIMENT
PALLAS
10^2
10^1
10^0
10^{-1}
10^{-2}
10^{-3}
10^{-4}
$\phi_0(r, E)$ n/cm^2·sec·MeV·Watt
P1
P2
P3
P4
JRR-4
CORE
TANK
WATER
29 cm
5.0
2.5
10
2.5
15
IRON
IRON
IRON
0 1 2 3 4 5 6 7 8 9 10 11 12
E(MeV)

Fig. 6

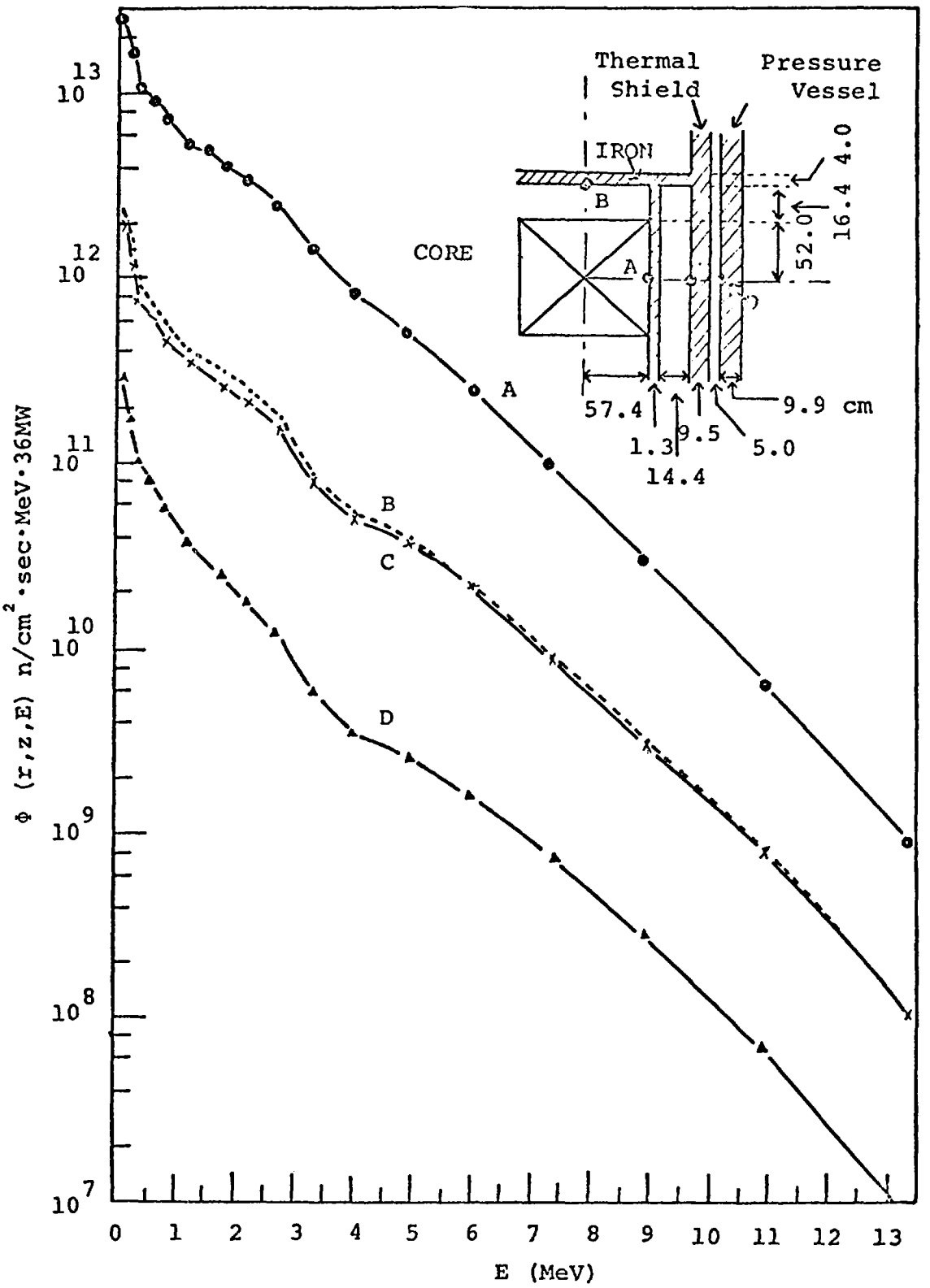
Thermal Shield
Pressure Vessel
IRON
B
A
CORE
4.0
16.4
52.0
57.4
1.3
9.5
14.4
5.0
9.9 cm
A
B
C
D
10^{13}
10^{12}
10^{11}
10^{10}
10^{9}
10^{8}
10^{7}
Φ (r,z,E) n/cm^2·sec·MeV·36MW
0 1 2 3 4 5 6 7 8 9 10 11 12 13
E (MeV)

Fig. 7

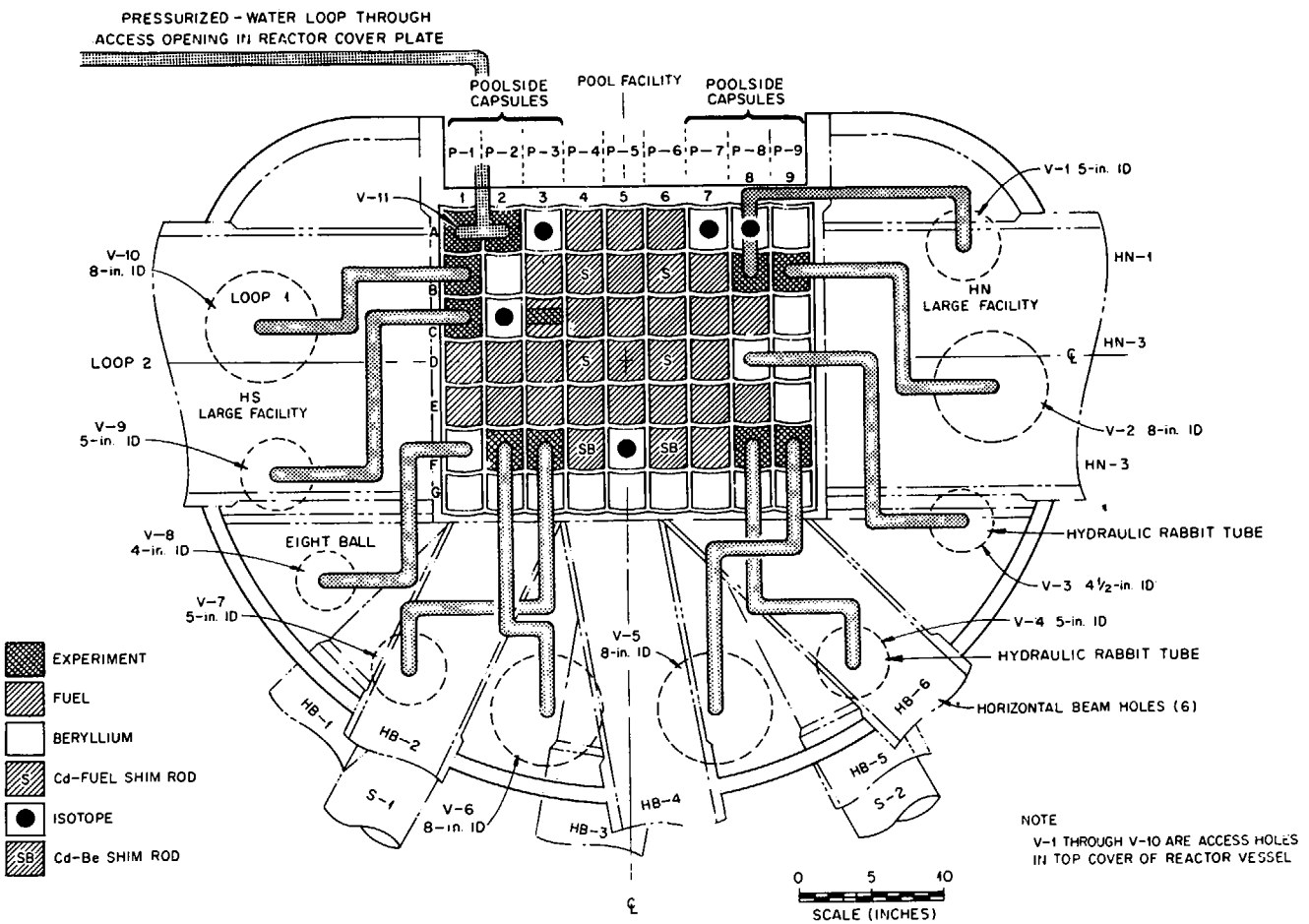
PRESSURIZED - WATER LOOP THROUGH ACCESS OPENING IN REACTOR COVER PLATE
POOLSIDE CAPSULES
POOL FACILITY
POOLSIDE CAPSULES
P-1 P-2 P-3 P-4 P-5 P-6 P-7 P-8 P-9
1 2 3 4 5 6 7 8 9
A B C D E F G
V-11
V-10 8-in. ID
LOOP 1
LOOP 2
HS LARGE FACILITY
V-9 5-in. ID
V-8 4-in. ID
EIGHT BALL
V-7 5-in. ID
V-5 8-in. ID
V-6 8-in. ID
V-1 5-in. ID
HN-1
HN LARGE FACILITY
HN-3
V-2 8-in. ID
HN-3
HYDRAULIC RABBIT TUBE
V-3 4½-in. ID
V-4 5-in. ID
HYDRAULIC RABBIT TUBE
HORIZONTAL BEAM HOLES (6)
HB-1
HB-2
HB-3
HB-4
HB-5
HB-6
S-1
S-2
S
SB
EXPERIMENT
FUEL
BERYLLIUM
Cd-FUEL SHIM ROD
ISOTOPE
Cd-Be SHIM ROD
NOTE
V-1 THROUGH V-10 ARE ACCESS HOLES IN TOP COVER OF REACTOR VESSEL
0 5 10
SCALE (INCHES)

Fig. 8

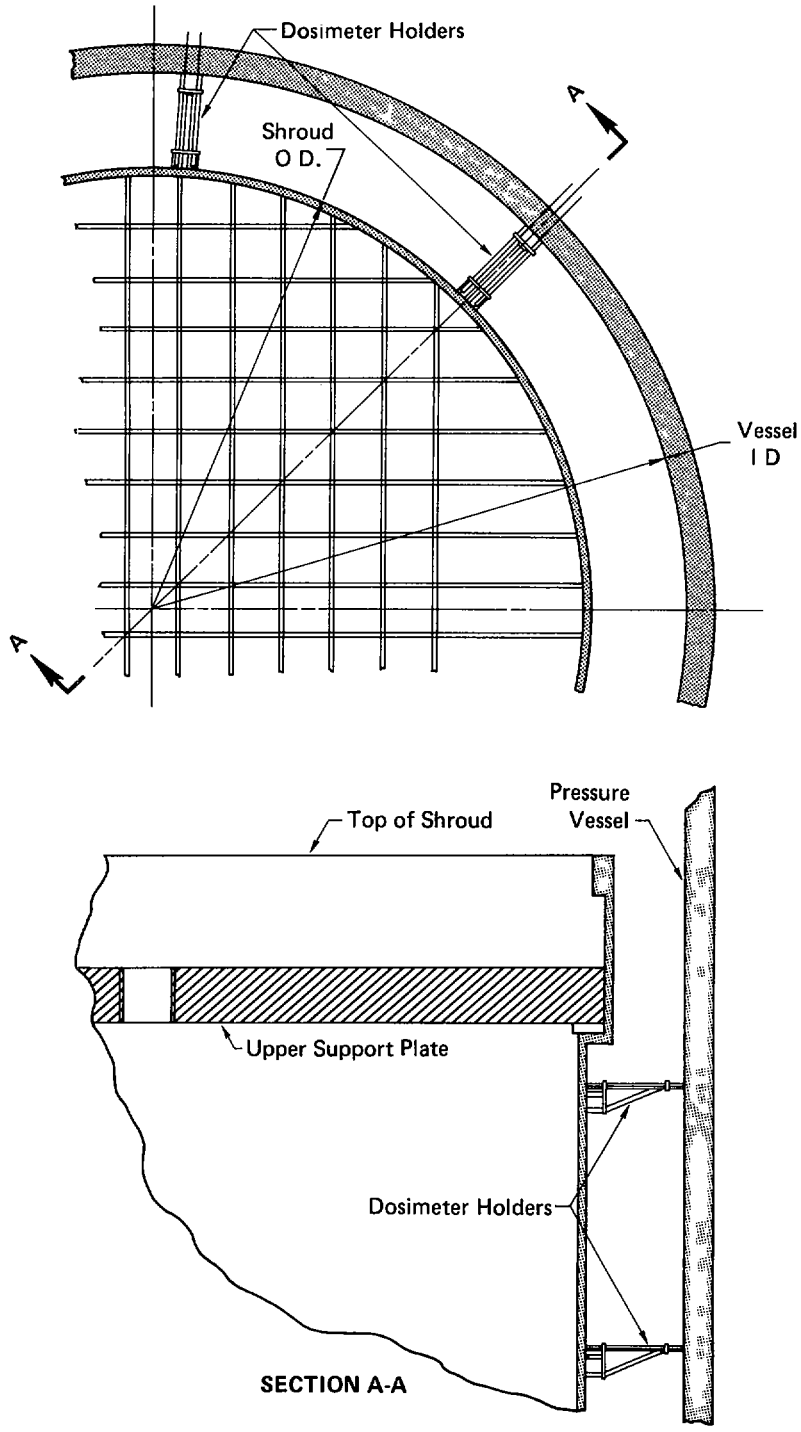
Dosimeter Holders
Shroud
O D.
A
Vessel
I D
A
Top of Shroud
Pressure
Vessel
Upper Support Plate
Dosimeter Holders
SECTION A-A

Fig. 9

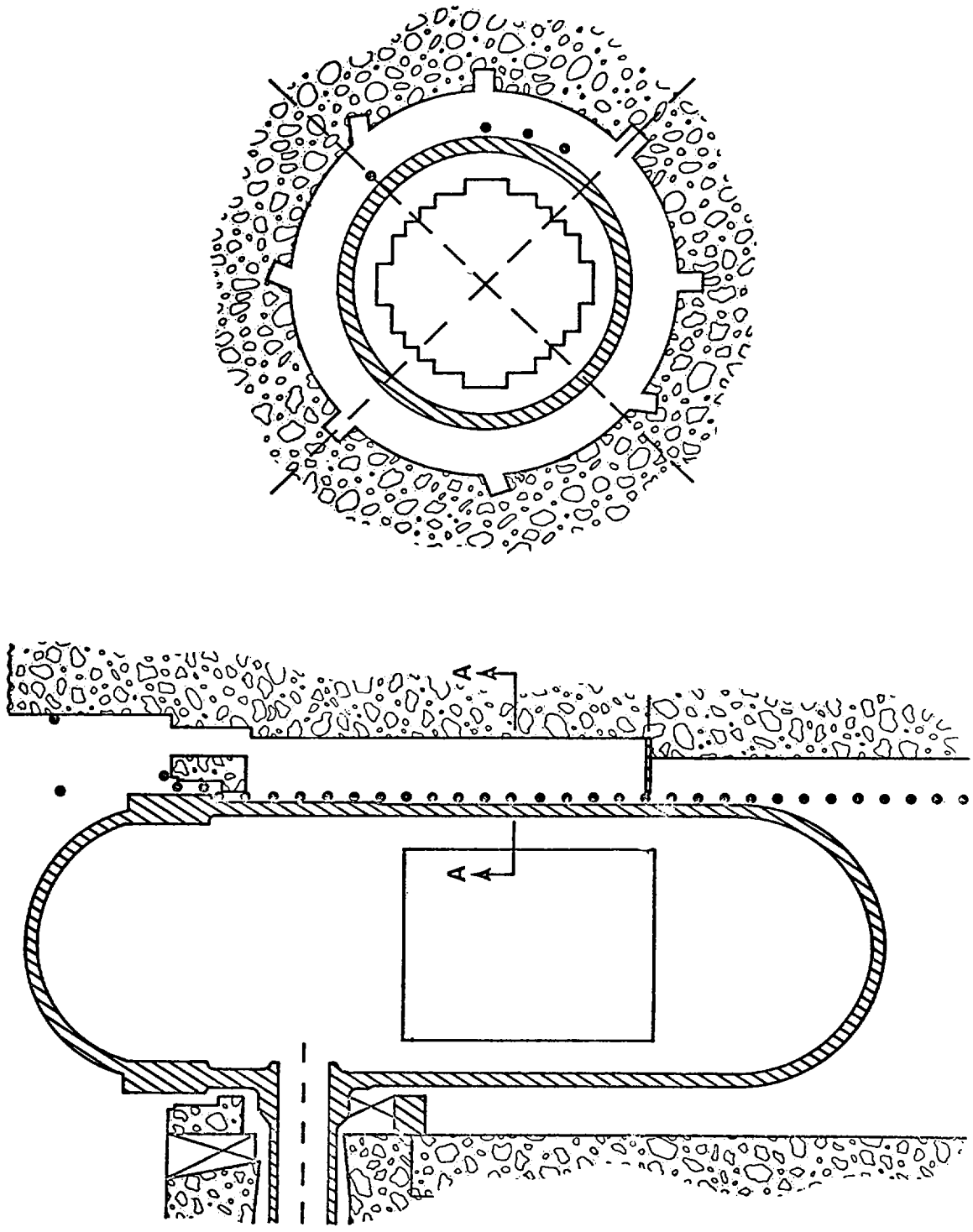

Fig. 10

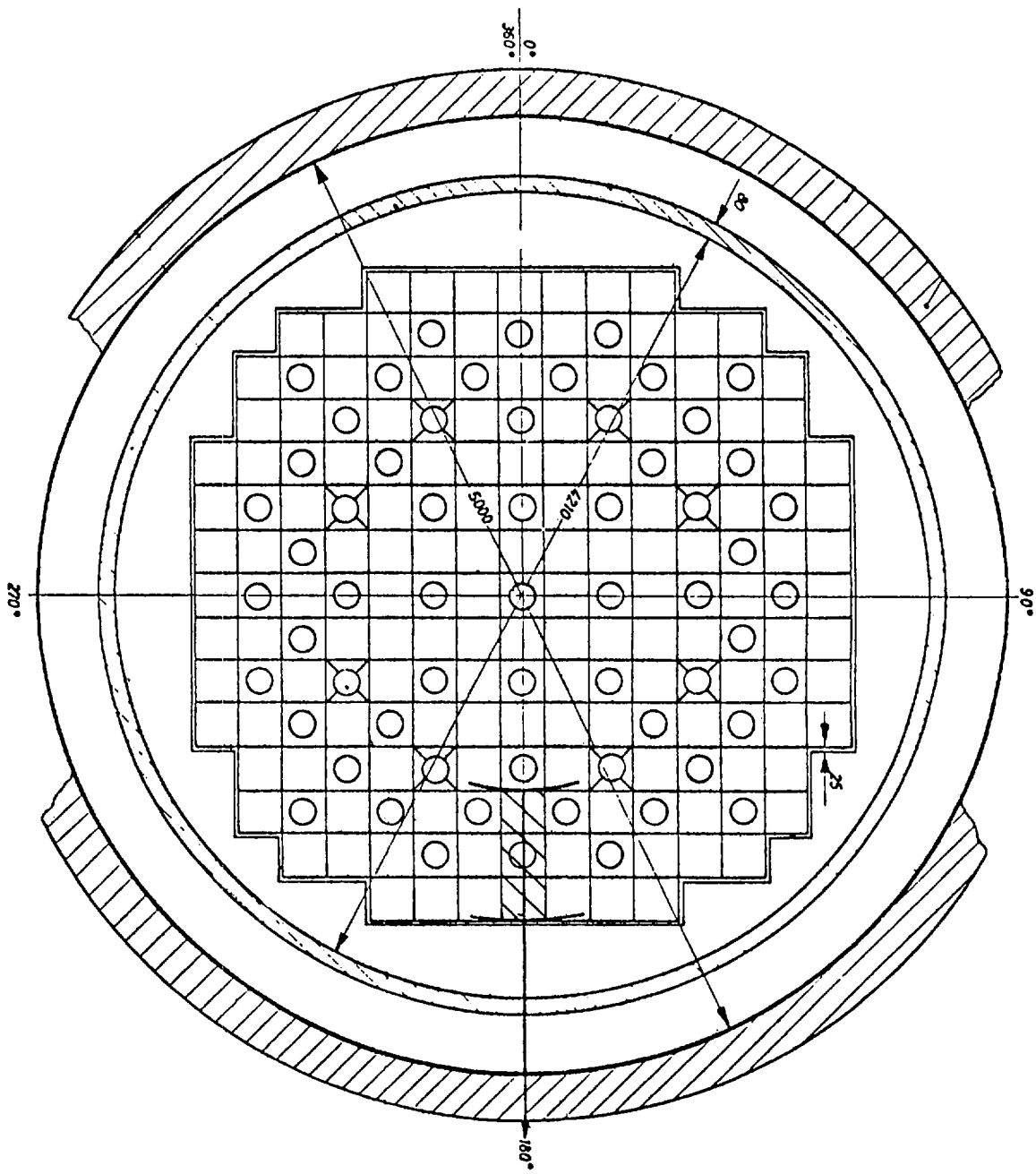

Fig. 11

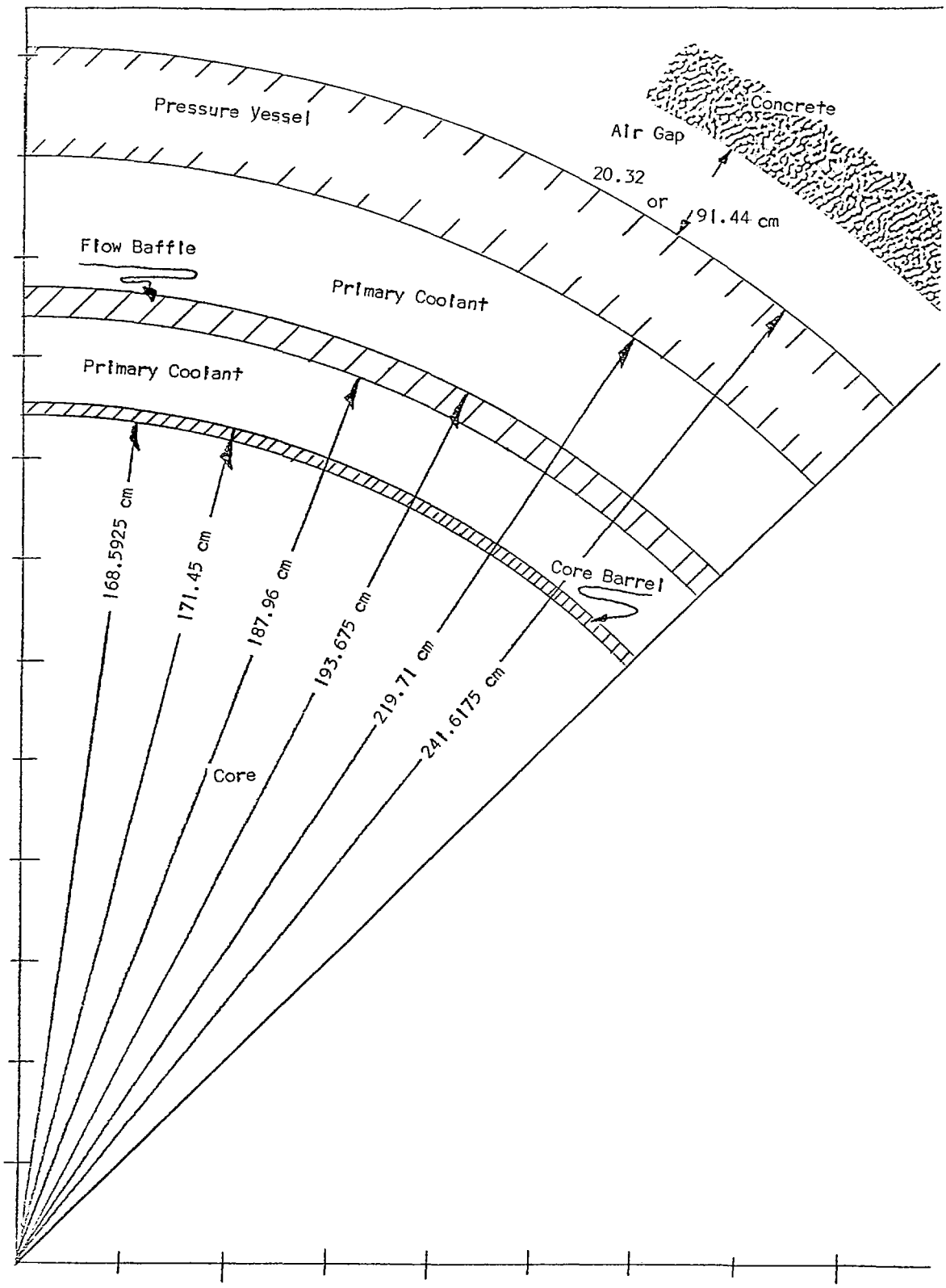
Pressure Vessel
Concrete
Air Gap
20.32
or
91.44 cm
Flow Baffle
Primary Coolant
Primary Coolant
168.5925 cm
171.45 cm
187.96 cm
193.675 cm
219.71 cm
241.6175 cm
Core Barrel
Core

Fig. 12

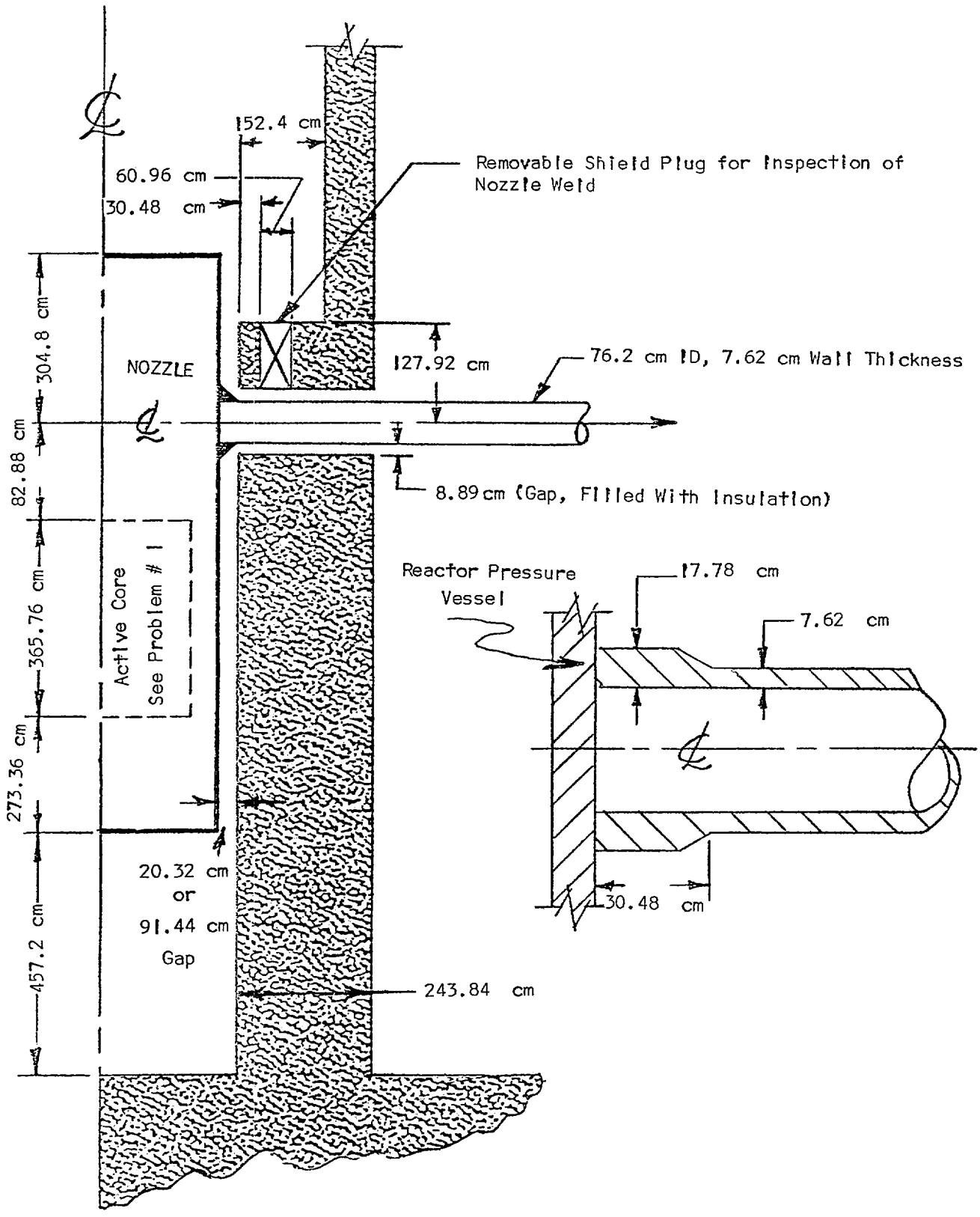
152.4 cm
60.96 cm
30.48 cm
Removable Shield Plug for Inspection of Nozzle Weld
304.8 cm
NOZZLE
127.92 cm
76.2 cm ID, 7.62 cm Wall Thickness
82.88 cm
8.89 cm (Gap, Filled With Insulation)
Reactor Pressure Vessel
17.78 cm
7.62 cm
365.76 cm
Active Core
See Problem # 1
273.36 cm
20.32 cm
or
91.44 cm
Gap
457.2 cm
243.84 cm
30.48 cm

Fig. 13

I.3. Remarks on Terminology and Symbols for Physical Quantities in Neutron Metrology

S. R. Wagner
Physikalisch-Technische Bundesanstalt (PTB), Braunschweig
Federal Republic of Germany

Abstract:
Terms and symbols for some physical quantities commonly used in neutron metrology are given according to ISO recommendations.

The terminology used hitherto by many people for certain physical quantities in neutron metrology is not unequivocal and uniform, sometimes it can even be misleading. Often the terms and symbols used are in contradiction to the recommendations of the International Organization for Standardization (ISO).

One reason for the unsatisfactory situation is the sloppy use of the words "differential" and "integral". In the following the correct terms and symbols for some quantities of interest will be given according to ISO recommendations /1/.

The cross section $\sigma = \sigma(E)$ is generally a function of the energy E of the incident particle or photon.

The total cross section σ_{tot} or σ_T is the sum of all cross sections corresponding to the various reactions or processes between incident particle or photon and target particle.

The angular cross section $\sigma_\Omega = \frac{d\sigma}{d\Omega}$ is the cross section for ejecting or scattering a particle or photon into an element of solid angle $d\Omega = \sin\vartheta d\vartheta d\alpha$ divided by this element. It is generally a function of the energy E of the incident particle or photon and of ϑ and α.

The spectral cross section $\sigma_{E'} = \frac{d\sigma}{dE'}$ is the cross section for a process in which the energy E' of the ejected or scattered particle or photon is in an element of energy divided by this element. It is generally a function of the energy E of the incident particle or photon and of the energy E' of the ejected or scattered particle or photon.

The spectral angular cross section $\sigma_{\Omega,E} = \frac{d^2\sigma}{d\Omega dE}$ is the cross section for ejecting or scattering a particle or photon into an element of solid angle with energy in an element of energy divided by the product of these two elements. It is generally a function of E, E', ϑ and α.

The macroscopic cross section or cross section density Σ is the sum of the cross sections for a reaction or process of specified type over all atoms in a given volume divided by that volume. $\Sigma = n_1\sigma_1 + \ldots + n_i\sigma_i + \ldots$, where n_i is the number density and σ_i is the cross section for atoms of type i.

The total macroscopic cross section or total cross section density Σ_{tot} or Σ_T is the sum of total cross sections for all atoms in a given volume divided by that volume.

The mean cross sections $\bar{\sigma} = \frac{\int \sigma(E)\varphi_E(E)\,dE}{\varphi}$ is the cross section averaged over the spectral flux density $\varphi_E(E)$ of particles.

Remarks:
The quantities $\sigma(E)$, σ_E and Σ are of different dimension.

Symbols for differential quantities should be marked as such by writing the independent variable of the derivative as an index.

Flux density φ of particles or photons

The angular flux density $\varphi_\Omega = \frac{d\varphi}{d\Omega}$ of particles or photons is the flux density of all particles or photons all the directions of movement of which point into an element of solid angle $d\Omega$, divided by this element.

Spectral flux density $\varphi_E = \frac{d\varphi}{dE}$ of particles or photons

(E energy of particles or photons)

Spectral angular flux density $\varphi_{\Omega,E} = \frac{d^2\varphi}{d\Omega dE}$ of particles or photons

The flux density $\varphi(E)$ then is

$$(E) = \int_0^E \varphi_E(E')dE'$$

$\varphi(E)$ and φ_E are quantities of different dimension.

The fluence Φ of particles is the time integral of the flux density

$$\Phi(T) = \int_0^T \varphi(t)dt$$

Time integrals of other quantities may be formed accordingly; "fluence" then, replaces "flux density" in the corresponding terms.

Correspondingly:

Energy flux density ψ of particles or photons.

Spectral energy flux density $\psi_E = \frac{d\psi}{dE}$ of particles or photons.

Angular energy flux density $\psi_\Omega = \frac{d\psi}{d\Omega}$ of particles or photons.

Spectral angular energy flux density $\psi_{\Omega,E} = \frac{d\psi}{d\Omega dE}$ of particles or photons.

Energy fluence Ψ of particles or photons.

$$\Psi(T) = \int_0^T \psi(t)dt$$

Time integrals of other quantities may be formed accordingly; "energy fluence" then, replaces "energy flux density" in the corresponding terms.

References:

/1/ International Standard ISO 31/X: Quantities and units of nuclear reactions and ionizing radiations. First edition - 1973-07-01; Ref. No. ISO 31/X-1973(E)

II. SPECTRAL CHARACTERIZATION OF BENCHMARK NEUTRON FIELDS

II.1. Spectral Characterization by Combining Neutron Spectroscopy, Analytical Calculations, and Integral Measurements

W.N. McElroy, R. Gold and E.P. Lippincott
Hanford Engineering Development Laboratory, Richland, Wash.

A. Fabry, Centre d'Etude de l'Energie Nucléaire
Mol, Belgium.

J.H. Roberts, Macalester College, St.Paul, Minnesota.

Abstract:

Status and trends of differential spectrometry, calculations, and integral measurements for characterizing neutron spectra are assessed. Emphasis is placed upon the state-of-the-art accuracy that has actually been attained in standard, reference, and controlled-environment benchmark neutron fields. The utility of SAND-II unfolding is stressed for the comparison of differential spectrometry, integral measurements and calculations. Selective adjustments of both spectra and cross sections are still necessary, even for the most advanced benchmark fields and best known cross sections.

I. INTRODUCTION

The role and importance of benchmark neutron fields for dosimetry for reactor design, fuels and materials development programs, reactor operations, and reactor surveillance programs is well established as a result of: the IAEA Consultants' Meeting on Nuclear Data for Reactor Neutron Dosimetry;[1] the First ASTM-Euratom International Symposium on Reactor Dosimetry;[2] the U. S. Interlaboratory LMFBR Reaction Rate (ILRR) program;[3] and other international activities.

This paper, as well as others such as that by G. and S. DeLeeuw[4], presents an appraisal of the status and/or future direction of neutron spectral characterization work associated with the three categories of dosimetry benchmark neutron fields:

1) Standard fields; 2) Reference fields; and 3) Controlled-environment neutron fields.[5,6]

Dosimetry benchmark neutron fields serve three general objectives:[5]

a) Validation and/or calibration of experimental techniques;
b) validation and/or improvement of cross section and other nuclear data (e.g., fission yields) needed for proper application of experimental techniques; and
c) validation and/or improvement of analytical methods needed to extrapolate dosimetry data from a monitoring or surveillance position to the location of interest.

The accuracy requirements for neutron flux-fluence-spectral determination for the three categories of benchmark fields is dependent on their intended use, a, b, or c above. Currently, these accuracy requirements are tending towards the 2 to 5% (1σ) range by approximately 1980,[7]

depending on the particular spectral parameter; i.e., total absolute and relative integral flux, flux fraction above some specified neutron energy E, time integrated fluxes (fluences), spectrum mean energy, and absolute and relative spectral shapes. Present state-of-the-art accuracies are estimated to be in the range of 2 to 30% (1σ), depending on the particular parameter and benchmark field category.

The most precise and accurate spectral characterization for many of the benchmark neutron fields will be achieved by combining data obtained from "Neutron Spectroscopy", "Analytical Calculations", and "Integral Measurements".[1,2,3,4,8,9] In the following sections of this paper, these three approaches are discussed separately and accuracies that are achievable by the individual and combined application of the methods are reviewed. This is done concurrently with a brief discussion and summary of the status of spectral characterization for a number of selected benchmark neutron fields of current interest to the participants of this consultants' meeting.

II. DIFFERENTIAL NEUTRON SPECTROSCOPY

A "state-of-the-art" comparison of differential reactor neutron spectroscopy that is available for benchmark field measurements is presented in Table I. This comparison is not exhaustive, but has been confined to those selected techniques which have generally found world-wide acceptance.[2,3,4,10] This table does not deal with what limiting accuracies may or may not be achievable. Rather, the accuracy levels assigned in Table I are estimates of the best work that has actually been attained to date. All of these techniques possess limitations, in that no single spectroscopy method provides an ideal solution, i.e., possesses good sensitivity, accuracy, and resolution over the entire neutron energy region of interest in reactor applications, namely from 4×10^{-7} MeV up to 15 MeV for fission and higher for fusion reactors. In this regard, Table I contains the approximate lower and upper energy limits of applicability, E_L and E_u, for each of these selected methods. Consequently, many different methods of differential spectroscopy must often be used to cover the energy region of interest for a given benchmark neutron field.

Perhaps an even more unfortunate shortcoming of all current differential spectroscopy methods is the general inability to conduct measurements in high power reactor benchmark environs. The inapplicability of differential reactor neutron spectroscopy techniques in high power environments can be traced to inherent limitations, such as:

1) count rate limitations,
2) radiation damage (of detectors and/or electronic components),

TABLE I. COMPARISON OF SELECTED DIFFERENTIAL REACTOR NEUTRON SPECTROSCOPY METHODS

	Method	E_L [a]	E_u [b]	Resolution	Accuracy % (1σ)	
1.	(n,p) Emulsions					
	• Collimated Source	3×10^{-1}	15		15%	0.3<E<0.4 MeV
					5-10%	0.4<E<7 MeV
					10-50%	7<E<15 MeV[c]
				Fair		
	• Non-Collimated Source	3×10^{-1}	3		5-10%	0.3<E<1 MeV
					10-50%	1<E<3 MeV[d]
2.	(n,p) Proportional Counters	1×10^{-3}	2.5	Good	10-50%	0.001<E<0.03 MeV
					5-10%	0.03<E<1.0 MeV
					10-25%	1.0<E<2.5 MeV
3.	$^6Li(n,t)^4He$	1×10^{-2}	6.5	Fair	10-25%	0.01<E<0.5 MeV[e]
					10-15%	0.5<E<2.0 MeV[e]
					15-30%	2.0<E<6.5 MeV[e]
4.	Time-of-Flight (TOF)					
	• $^3H(d,n)^4He$ Source	5×10^{-5}	0.2		10-15%	10^{-5}<E<0.001 MeV
					15-20%	0.001<E<0.02 MeV
					20-30%	0.02<E<0.2 MeV
				Good		
	• LINAC Source	5×10^{-5}	5		10-15%	10^{-5}<E<0.001 MeV
					15-20%	0.001<E<0.02 MeV
					10%	0.02<E<0.5 MeV
					15%	0.5<E<1.0 MeV
					20%	1.0<E<5.0 MeV

a) Approximate lower energy limit of demonstrated applicability, MeV.

b) Approximate upper energy limit of demonstrated applicability, MeV.

c) The large errors at ∿15 MeV are dominated by statistics for a typical fission neutron spectrum.

d) The large errors at ∿3 MeV are dominated by statistics for degraded fission neutron spectra such as typically found in fast reactors. For sufficiently hard neutron spectra it should be possible to extend work up to ∿20 MeV with an accuracy similar to that attained in the 0.3<E<1 MeV region.

e) The current accuracy of $^6Li(n,t)^4He$ spectroscopy is mainly dominated by the uncertainty in the angular and total reaction cross sections.

3) sensitivity to background radiation components (principally the gamma-ray component), and
4) temperature sensitivity (of detectors and/or electronic components).

Although limitations frequently arise which are uniquely associated with a specific technique, different spectroscopy methods often share common shortcomings. As had been stressed in a recent review,[10] one such shortcoming is the need for unfolding which is apparently a universal necessity in all differential reactor neutron spectrometry methods. This universal requirement may well stem from one of the chief intrinsic characteristics of the neutron, namely neutral charge. In neutral particle detection, one customarily uses interactions that produce charged particle reaction products which are, in turn, readily detected. Hence the response of such a detector need not generally be in one-to-one correspondence with the energy of the incident neutrons. Any departure from this one-to-one correspondence automatically necessitates unfolding.

The discovery and validation of a differential neutron spectroscopy method which could be applied in high power reactor benchmark environments must necessarily be classified as a major breakthrough in research reactor technology. However, in assessing possible future directions and developments in differential reactor neutron spectroscopy less ambitious goals are obviously more prudent and realistic. Perhaps the major emphasis will occur in the higher region extending to 15 MeV and above, where impetus will be provided by Controlled Thermonuclear Reactor (CTR) research.[7] Here one can anticipate a re-emergence of the proton-recoil photographic emulsion technique, which possesses fundamental advantages for the high energy range for both fission and fusion reactor applications, such as small inexpensive passive detector packages of good energy sensitivity and negligible spectral perturbation.

In these higher energy neutron environments, increasing emphasis will also be placed on reactions which produce helium, i.e., alpha particles. The helium yield of many relevant reactions is vastly increased in more energetic CTR neutron spectra. Mass spectrometry techniques have already been perfected for measuring helium production in high power irradiations.[11] ^{4}He-recoil proportional counter spectroscopy has also been advanced[10] as a means of extending the current energy domain of applicability of

proportional counter techniques (see Table I). Perhaps the most appealing aspect of this technique is the adaptation of already existing hardware and instrumentation. By simply filling with helium instead of hydrogen or methane, proportional counters (already employed in the proton-recoil method) can be directly applied for α-recoil spectrometry. Estimates of $E_u \approx 15$ MeV have been forcasted, provided that proportional counters of high quality and helium of very high purity are employed. This estimate implies that just as with proton-recoil spectroscopy, accurate unfolding of finite-size effects in α-recoil proportional counters must be performed.

Two particularly important spectral characteristics, which have generally been neglected in differential reactor neutron spectroscopy, namely absolute flux measurements and observation of angular flux anisotropy, will quite likely be singled out for emphasis in future work. Only very limited absolute spectral measurements have been carried out using proton recoil emulsions[12] and proportional counters.[13] On the other hand, additional information that can be obtained by means of nuclear emulsions is knowledge of the anisotropy of the neutron flux.[14] If, in the emulsion measurements of the proton spectrum[15,16] (which can be unfolded to give the neutron spectrum), the direction of the proton track is recorded,* anisotropies in the neutron flux can be detected. Any deviation of the proton-recoil spectrum from isotrophy automatically implies a deviation from isotrophy for the angular neutron flux.

For neutrons of energy ∿ 250 keV, nuclear emulsions loaded with glass specks[17] containing ^{6}Li can provide some knowledge of the anisotropy in neutron flux. For example, in the ^{6}Li(n,α) t reaction the sum of the ranges of the alpha particle and triton is significantly longer if the triton goes in a forward instead of a backward cone. Thus, there will be a strong correlation between the direction of the long tracks and the neutron direction. The ^{6}Li(n,α) t cross section resonance at ∿ 250 keV significantly increases the number of triton-alpha pairs and thereby provides improved statistical accuracies of angular observations in the vicinity of the resonance.

---

* For protons >2 MeV, the direction of the proton velocity can be determined with close to 100% certainty. This confidence factor decreases as proton tracks get shorter.

In hazarding one final projection for possible future directions of differential reactor neutron spectroscopy, one cannot ignore the virtual explosion of activity and developments which have occurred in the field of Solid State Track Recorders (SSTR) over the last decade or so.[18] In particular, the ability to extract relevant physical data such as mass, charge and energy from the shape of tracks formed in SSTR is a striking advance. This recent development, which is commonly referred to as track profile analysis, can only be considered to be in the very formative stages. This ability coupled with the vast improvements of α-particle sensitive SSTR, such as Makrofol E and cellulose nitrate, augurs for the evolution of SSTR differential neutron spectroscopy methods. Advanced SSTR techniques for observing angular flux anisotropy should also become possible. Such methods would, of course, be direct descendants of emulsion techniques and thereby automatically possess many advantages. However, in contrast with emulsions, the insensitivity of SSTR to electrons would provide an enormous advantage for reactor applications. Moreover, the reduced α-particle range also implies improved high energy sensitivity with less attendant stress on the need for finite-size corrections.

III. ANALYTICAL CALCULATIONS

In this section, a brief discussion is presented of the status and future trends in neutron flux-spectral characterization of benchmark neutron fields by analytical calculations. Uncertainties in such computations are of two general types:

a) Nuclear Data - Errors related to uncertainties in the nuclear data for the materials in the system including the various cross sections, fission neutron spectra, and spectra and angular distributions of other emitted or scattered neutrons.

b) Modeling - Errors arising from the approximations necessary to perform the computation including the geometrical representation of the system, the multi-group representation of neutron cross sections and spectra, and time steps taken between changes in composition due to burnup, fission product production, control rod movement, etc.

Uncertainties of the first type can be quantified, but this has not been done generally and constitutes a major undertaking. In this regard, some sensitivity studies have been done to investigate the effects of nuclear data uncertainties on important reactor parameters, such as fission ratios.

Uncertainties of the second type are systematic in nature: to quantify them for a given physical system amounts to establishing the deviation between an approximate and exact solution. This can be managed to some extent by comparison of a set of converging approximations or by comparing independent codes and approaches.

Indeed, the stationary space, angle and energy distribution of neutrons in any macroscopic medium is governed by the analytic linear integro-differential Boltzmann neutron transport equation, which expreses the conservation of the angular neutron flux. If that law is written for a finite phase space cell, the analytic equation is replaced by an equivalent difference equation amenable to Monte Carlo or discrete-ordinates solution. In such discretizations, the absolute errors introduced by the choice of a finite spatial, angular and energy mesh can be assessed by comparison with the solutions obtained for finer mesh selections.

In practice, only for one-dimensional geometries can sufficiently fine energy group structures and high enough order expansions of the elastic scattering kernel be adopted to insure a numerically precise approximation to the exact solution; in such conditions, the accuracy of the spectral determination is only limited by the accuracy with which the nuclear data are known for all the materials constituting the medium considered, including the neutron source; e.g., usually, the uranium-235 and/or plutonium-239 fission neutron spectra.

If nuclear data uncertainties are small enough in the energy ranges where neutronic interactions in any given material are significant, the neutron spectrum may be calculated to a degree satisfactory enough for the system to deserve the label of standard.* This is the case for:

---

* Two standard neutron fields are not discussed in this section for obvious reasons: the thermal neutron induced uranium-235 fission neutron spectrum and the californium-252 spontaneous fission neutron spectrum.

- Some carefully established thermal neutron beams or thermal neutron distributions in bulk graphite.
  Some carefully established 1/E neutron spectra in the energy range below ∿ 10 keV.
- The ISNF, Intermediate-Energy Standard Neutron Field, in the energy range below ∿ 1 MeV: in this system, the dominating interactions are scattering in carbon and absorption in boron-10, two processes for which the differential-energy cross sections in the energy range affecting the central flux spectrum are known to the degree of accuracy of primary standards.

The neutron flux spectrum in a standard field is usually amenable to an analytical characterization better than ±5% (1σ) and the total flux to better than ±2% (1σ). It is to be noted that accurate analytical computability is not the only nor an indispensable criterion for a system to be considered a standard neutron field; in general, the accuracy of the neutron flux characterization is the main criterion, be it analytically or experimentally based.[6] For example, the secondary intermediate-energy standard neutron field ΣΣ, a one-dimensional spherical assembly like the ISNF, involves a thick natural uranium source shell, where uncertainties in the uranium-238 elastic and inelastic scattering cross sections hamper an accurate analytical characterization of the neutron spectrum; hence this is considered a secondary rather than a primary field, but still a standard field.

Very often, systems with higher order geometries are handled by one- or two-dimensional approaches; e.g., a two-dimensional reference neutron field like BIG-10 or TAPIRO is idealized into a one-dimensional cylindrical or spherical representation, a three-dimensional system like CFRMF is treated in a one-dimensional cylindrical approximation or in a two-dimensional model (see Table III references). In such cases, in addition to the basic nuclear data, approximations of the true geometry are responsible for uncertainties in the final solution.

Controlled environments are the most complex of all benchmarks in terms of analytical characterization. An example is given by EBR-II dosimetry measurements[19-30] in a large array of structural pin subassemblies distributed throughout the reactor core and first reflector rows. In spite of rather detailed geometric and compositional representations and

a marriage of XY and RZ transport theory solutions, accurate predictions of the neutron spectra and spatial distributions cannot necessarily be achieved at all reactor locations.[19,20] Further, the greater the distance one moves away from the core center, the more severe are the uncertainties. There is a transition in fact between locations in which the calculations serve as a potential guide in evaluating the experimental techniques (in particular for the data testing of dosimetry and gas production cross section files) and more remote positions where the experiment provides the needed reference to evaluate computational models.[2,27,31-42] At the pressure vessel of an LWR or a LMFBR reactor, clearly, measurements must be used to validate the calculations.

Most current applications of analytical methods provide neutron flux-spectra solutions without assigned uncertainties. For most benchmarks, computational errors are dominated by inadequate knowledge of all the necessary cross sections. A major effort to improve this situation is that associated with the development of the ENDF/B cross section error file and the associated sensitivity codes, the FORSS package, at ORNL.[43-46] This is a powerful analytical tool which can be used to study the relationship between cross sections and their uncertainties and integral experiments and their uncertainties. It has been applied to the analysis of fast reactor benchmarks and is recommended for analysis of dosimetry standard and reference neutron fields and, depending on the specific case, to some controlled environments.

IV. INTEGRAL MEASUREMENTS

The reader is referred elsewhere for detailed discussions of the relative merit and application of different methods of multiple-foil-integral flux-spectral determination.[1,2,47,48] The present discussion will be limited to a brief review and up-dating of results that have been obtained with the SAND-II method, primarily, for a number of standard and reference benchmark fields.[3,8,9,49]

The newest version of the SAND-II Monte Carlo error analysis code was utilized for this study. This code uses a weighting procedure based on the use of the square root of the sum of the variances of the individual foil reaction rate and evaluated energy-dependent cross section error assignments. Detailed information on the code's algorithm, test results

using different weighting procedures, a listing, and instructions for its use are provided elsewhere.*[47,50]

In addition to the dependence of the flux-spectral solution on uncertainties in measured and evaluated sets of reaction rates and energy dependent cross sections, there is a dependence on the input form of the spectrum, $\phi^{\circ}(E)$, and the selected set of reactions, i = 1,2,...n, in equation (1), Section V. Factors controlling the accuracy of any integrally derived benchmark flux-spectrum are therefore:

1) Reaction set selection;
2) Measured reaction rates;
3) Evaluated reaction cross sections;
4) Input spectral shapes;
5) Solution uniqueness; and
6) Unfolding code.

This is illustrated schematically in Figure 1 which is a flow diagram showing current ranges of estimated accuracy of input and output information associated with the SAND-II multiple foil technique of flux-spectra determination for fast reactor fission neutron fields. Given an input set of 1) measured reaction rates, 2) associated evaluated energy dependent cross sections, and 3) an evaluated spectral shape (based on calculations and/or differential neutron spectroscopy), calculated reaction rates are compared with measured reaction rates and the input spectrum is adjusted iteratively to secure the best fit between calculated and measured reaction rate values.

The relative importance of uncertainties and/or exactness in each of the factors (1 to 6, above) for standard, reference, and controlled-environment field flux-spectral characterization must be individually assessed. For example, the current accuracies of the determination of the absolute values of total flux from multiple-foil integral measurements for standard, reference, and controlled benchmark fields are approximately 2-3% (1σ), 3-5% (1σ), and 5-15% (1σ), respectively. The corresponding broad group spectral shape characterization accuracies for the energy regions of major concern are $\sim$ 4-6% (1σ), $\sim$ 5-15% (1σ), and $\sim$ 5-30% (1σ), respectively. Specific examples of the accuracy of the determination of multiple-foil adjusted

---

* The code is available through the Radiation Shielding Information Center, Oak Ridge, Tennessee.

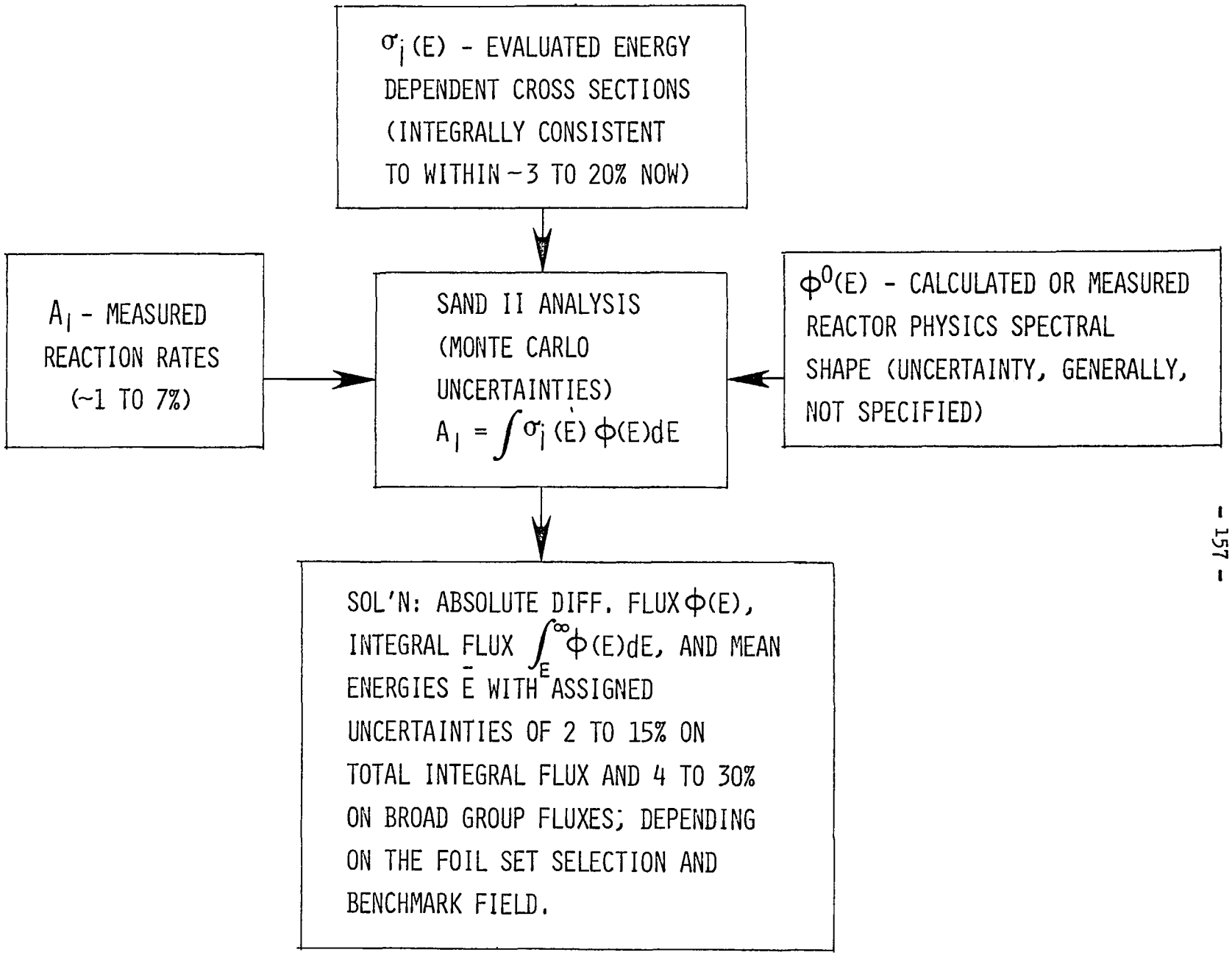

FIGURE 1. FLOW CHART - NEUTRON FLUX-SPECTRA DETERMINATION FOR FAST REACTORS

flux-spectra for several benchmark fields is considered next.

In a companion paper,[9] a selection is presented of the reactions that can be considered as belonging to category I as defined previously;[1] in addition, for a number of category II threshold reactions also defined in Reference (1),bias factors are given by which the cross sections are to be rescaled in order to provide consistent results; also the ^{59}Co capture reaction is suggested as a category I candidate for some applications. Using both category I reactions and those category II reactions which have been validated in Reference (9), an improved spectral characterization has been derived for two standards and two reference neutron fields. Except for BIG-10, the input spectral shapes are the ones recommended to CSEWG[51] in 1975. For BIG-10, the input spectral shape is based on a transport theory computation by Hansen et al using ENDF/B-III nuclear data.

1. Standard - χ_{82} and χ_{25}

Figures 2 and 3 show the present results for the spontaneous californium-252 and the thermal neutron induced uranium-235 fission neutron spectra, respectively. The spectral data on these figures are expressed as ratios to the reference Maxwellian shapes and the dashed lines represent the NBS evaluations. The data are presented in the 15 group format used for SAND-II error propagation: the numerator is the adjusted or evaluated total flux in group g, χ_g, while the denominator is the integrated reference Maxwellian flux $\int_g \chi_M(E)\,dE$; the exact expressions accepted for the Maxwellian shapes $\chi_M(E)$ in the two fields are explicitly written on the ordinate of each figure.

The SAND-II uncertainties associated with the adjusted spectra are shown as error bars, while for the NBS evaluations, they are displayed as shaded areas corresponding to the original NBS evaluated group segmentation.[52]

At neutron energies above 13 MeV, differential spectroscopy data for χ_{25} and χ_{82} are extremely inaccurate. Consequently, previous integral measurements for the (n,2n) reactions for ^{63}Cu and ^{58}Ni have been used in the present study for adjustment of the high-energy tails.

It is seen from the figures that:

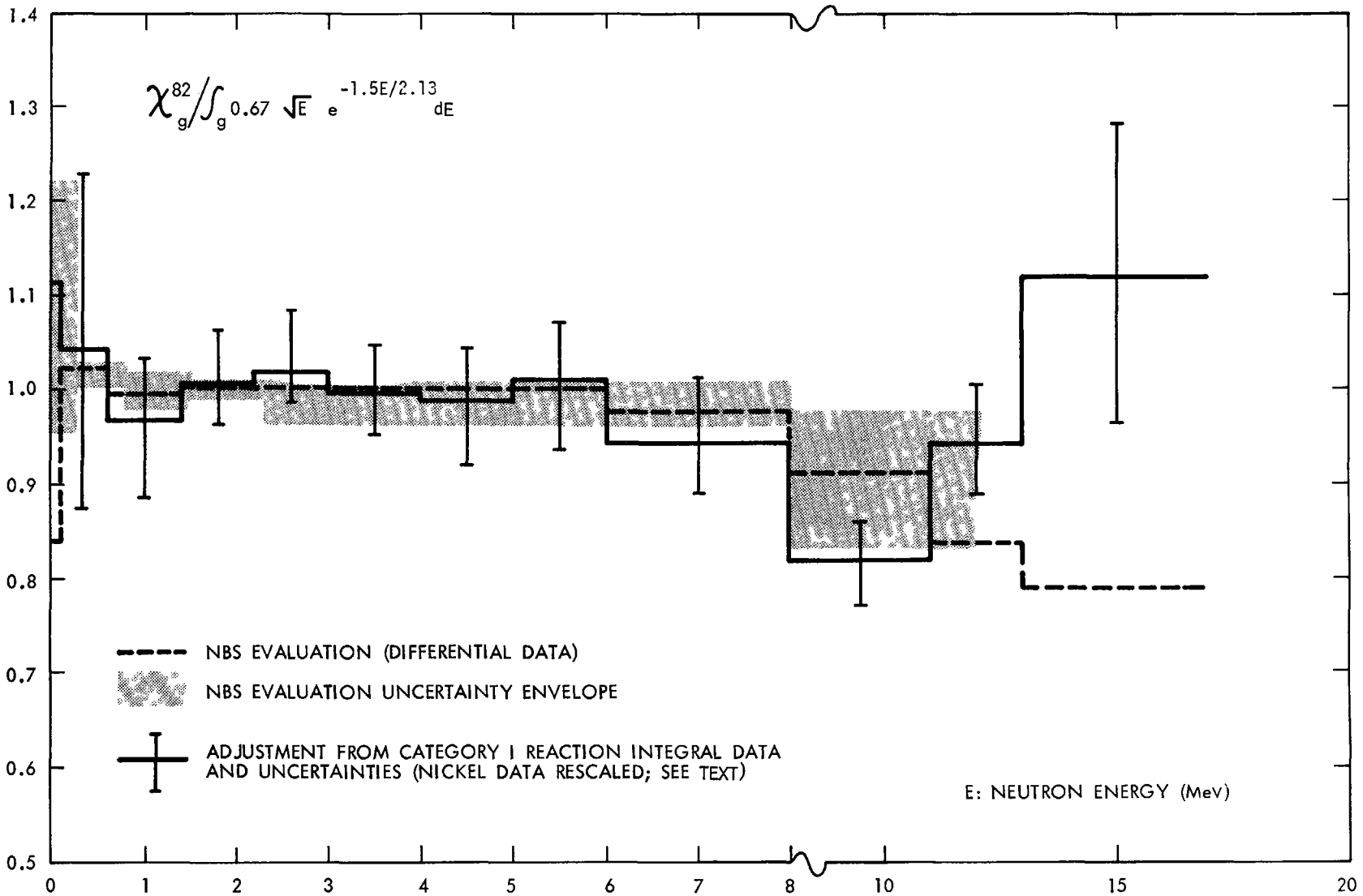

FIGURE 2. DEVIATION OF THE ^{252}Cf SPONTANEOUS FISSION SPECTRUM NEUTRON DISTRIBUTION FROM A REFERENCE MAXWELLIAN SHAPE

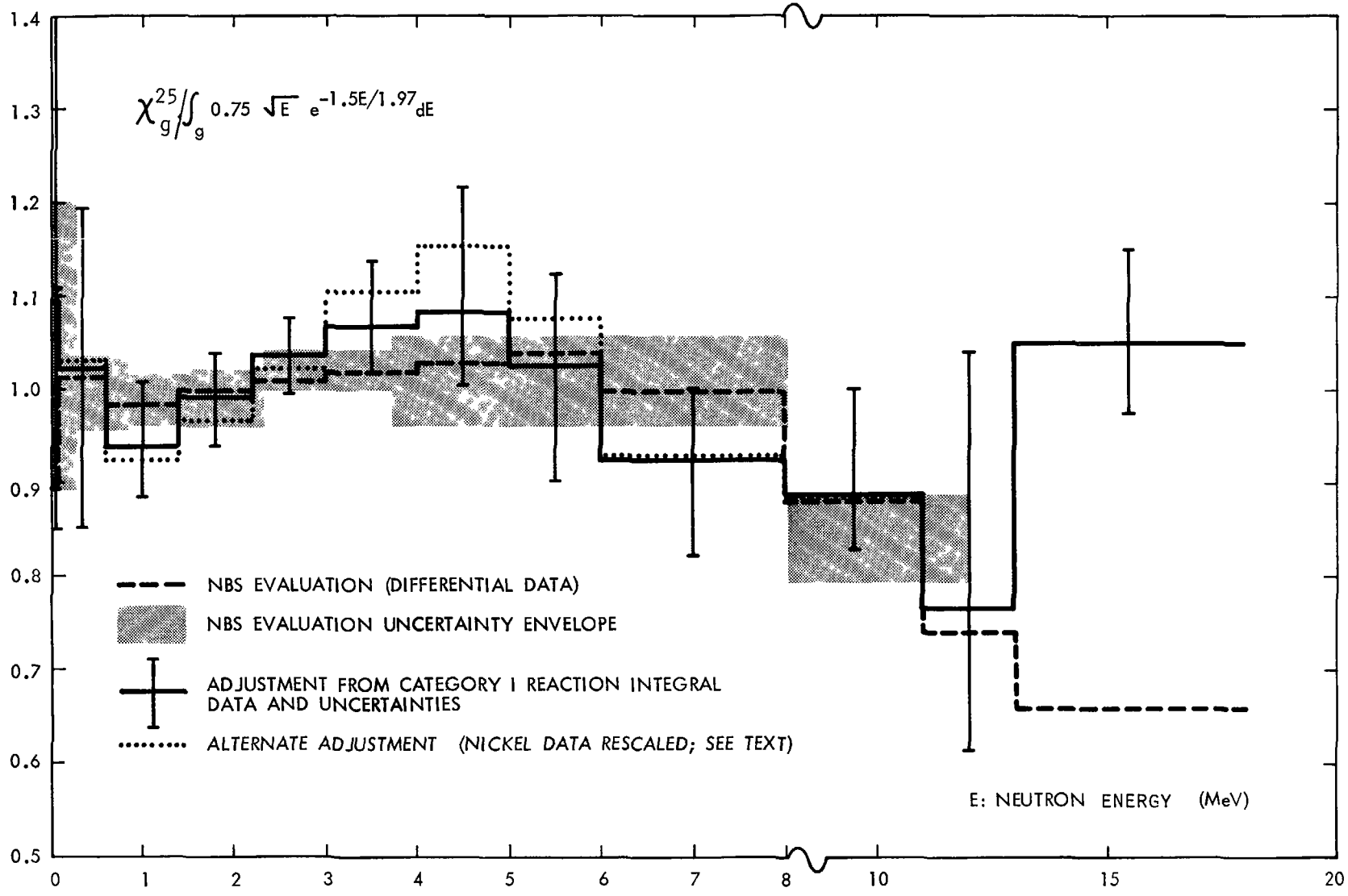

FIGURE 3. DEVIATION OF THE ^{235}U FISSION SPECTRUM NEUTRON DISTRIBUTION FROM A REFERENCE MAXWELLIAN SHAPE

a) For both fission spectra, the integrally derived high energy tails above 10 MeV are significantly harder than according to the NBS evaluations; within uncertainties, they are also closer to the Maxwellian representations and the deviations from the Maxwellian as displayed by the NBS evaluations, in this energy range, are not confirmed.

b) Below 10 MeV, the californium-252 spectrum from the NBS evaluation is well reproduced by unfolding from integral measurements.

c) For the uranium-235 fission neutron spectrum, integral data exhibit significantly higher fluxes in the 3-6 MeV range than according to the NBS evaluation. This trend is consistent with the most recent time-of-flight measurements[52,53] and with the suggestion by Knitter[53] of the need for finite fission source corrections in previous work on this spectrum.

2. Reference - CFRMF and BIG-10

In Figures 4 and 5, the SAND-II adjusted spectra for two reference neutron fields, CFRMF[3,47,51,54-56] and BIG-10[3,57-59] are compared to analytical, transport theory computations based on the ENDF/B-III cross section file. Within uncertainties, the multiple foil results generally agree well with the computations except above ~1-2 MeV where harder spectra are measured. Studies by Harker, et al, indicate that this is due to inadequate uranium-238 inelastic scattering data in ENDF/B-III.* It is also associated to some degree with the representation of χ_{25} in the calculations. Considerable improvement is obtained if ENDF/B-IV nuclear data are preferred, as shown by Figure 6 for CFRMF. The calculated results are due to Harker, et al, using ENDF/B-IV data. This example illustrates strikingly the previously published statements[3,9] that multiple foil measurements are necessary to properly characterize the high (>1-2 MeV) and low (<10 KeV) energy tails of some standard and reference benchmark neutron spectra. This is obviously more true for controlled environments, which inherently require modeling assumptions that can invoke significantly higher errors.

---

* The existence of this type of inadequacy had been considered in an earlier study based on comparisons of T-O-F, multiple-foils, and calculational results for the APFA-III (Godiva). (60)

FIGURE 4 COMPARISON OF SAND-II AND CALCULATED SPECTRUM FOR CFRMF
(CALCULATIONS BASED ON ENDF/B-III DATA)

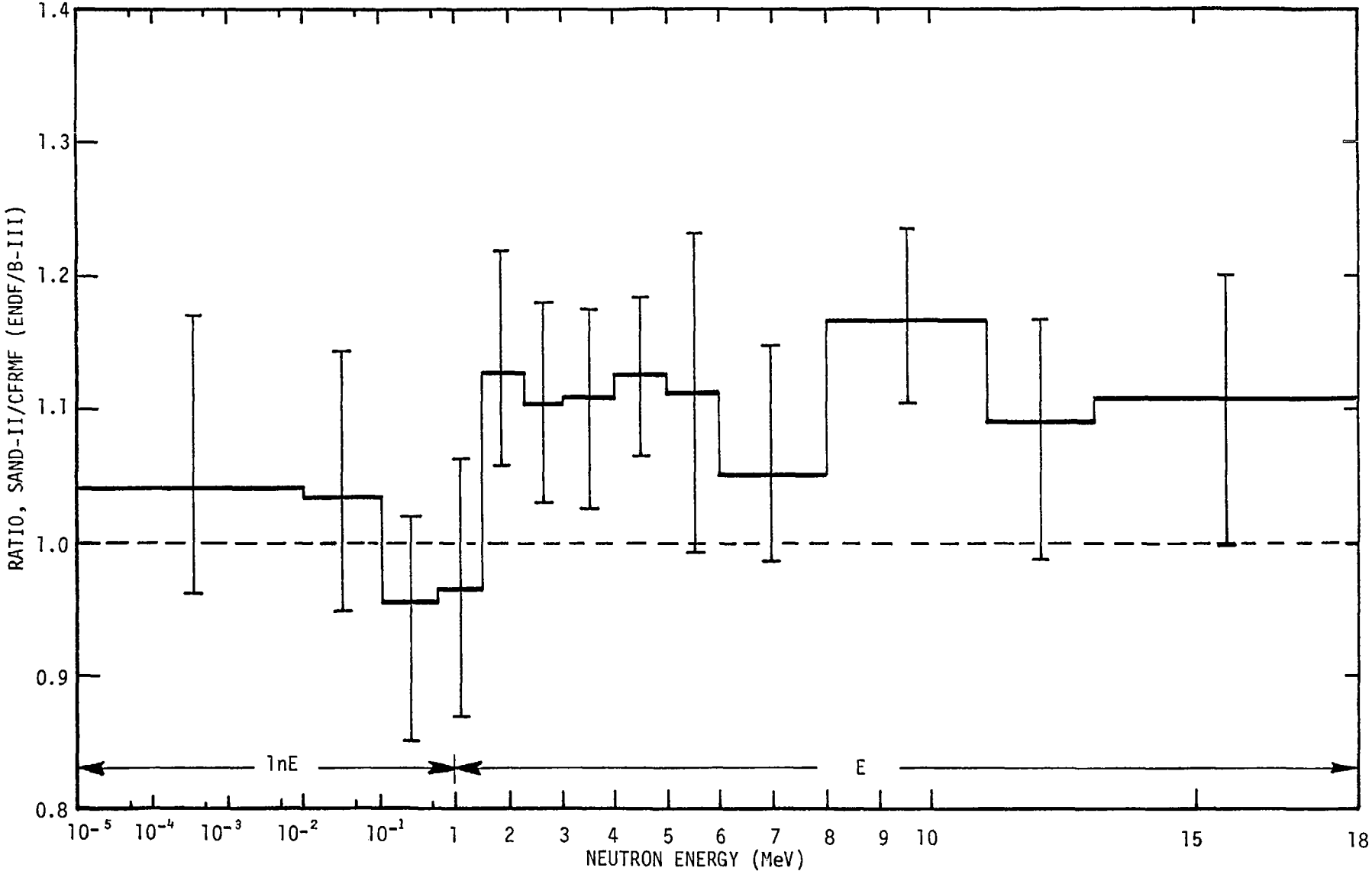

FIGURE 5 COMPARISON OF SAND-II AND CALCULATED SPECTRUM FOR BIG-10
(CALCULATIONS BASED ON ENDF/B-III DATA)

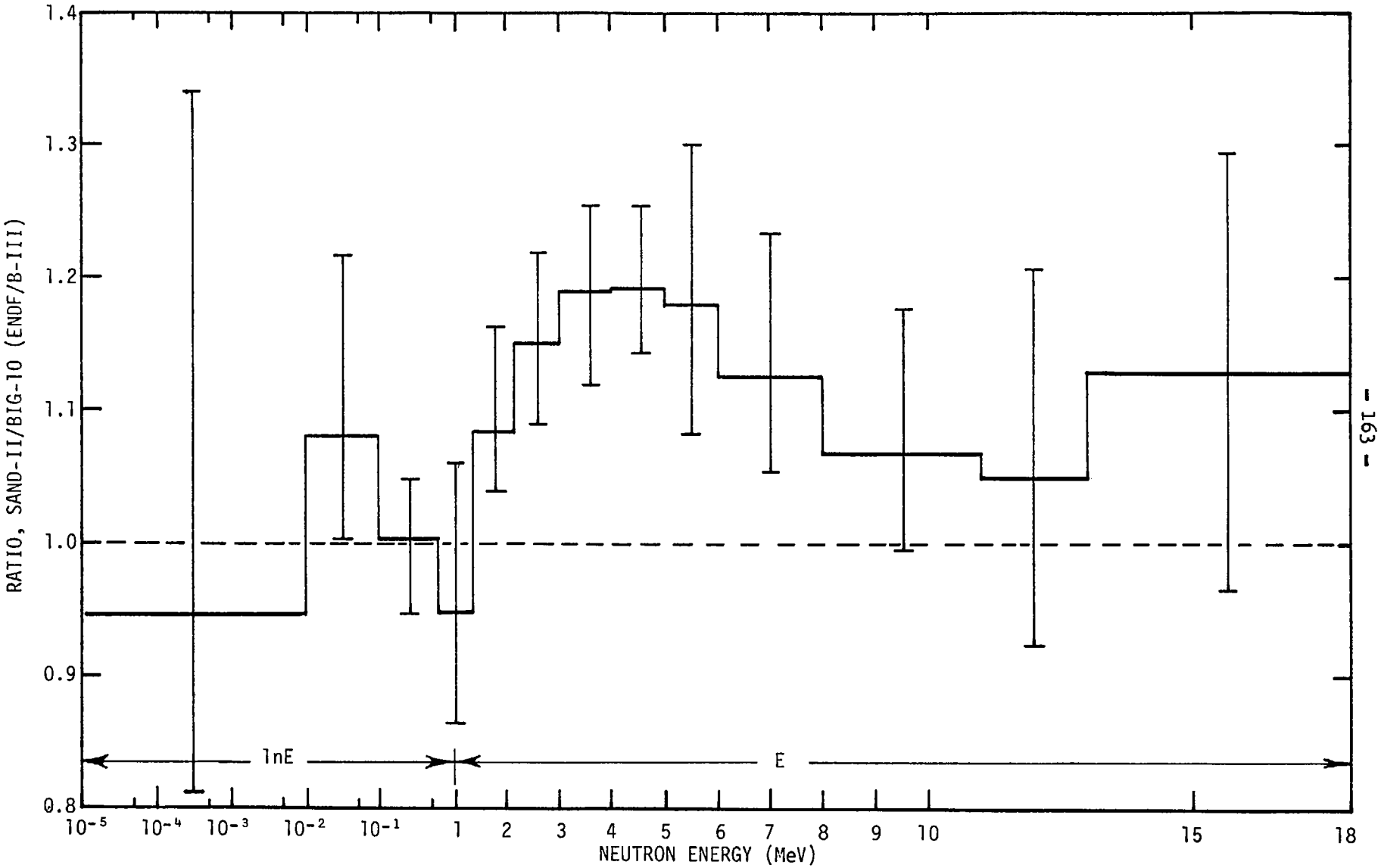

FIGURE 6 COMPARISON OF SAND-II AND CALCULATED SPECTRUM FOR CFRMF
(CALCULATIONS BASED ON ENDF/V-IV DATA)

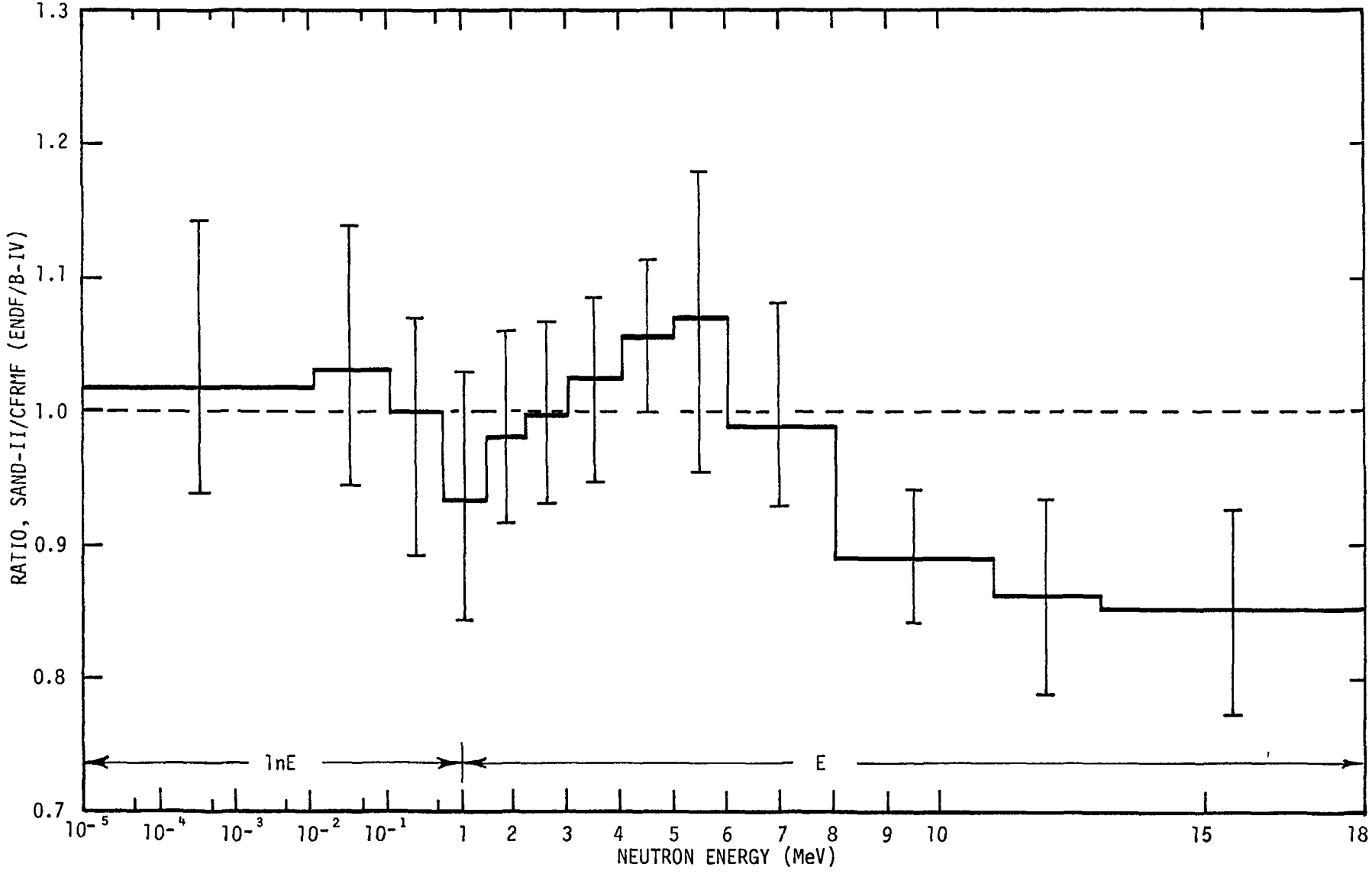

3. Controlled - EBR-II

Finally, for several controlled environment fields in the Experimental Breeder Reactor-II (EBR-II), Figure 7 shows typical differences between the input reactor physics and SAND-II multiple foil adjusted values of group fluxes for four different axial locations in row 2. Large bias differences, up to ∿ 40% or more, are seen between the calculated and multiple foil adjusted group flux values. Generally, the individual SAND-II group flux errors are estimated to be in the range of ±5 to 30% (1σ) for these EBR-II measurements.[27-31]

In conclusion, the multiple foil technique is an essential part of any systematic effort to accurately characterize the neutron flux-fluence spectra in benchmark fields and other reactor environments. It provides an effective marriage of analytical methods, differential spectrometry, and integral measurements producing insights such as those demonstrated above and thereby leads to a reduction of overall errors. Furthermore, it is at present, the only approach that provides reliable estimates of both relative and absolute errors of neutron flux-fluence spectra for all benchmark fields.

V. STATUS OF FLUX-SPECTRAL CHARACTERIZATION FOR SELECTED BENCHMARK NEUTRON FIELDS

Depending on the energy region and the benchmark neutron field, significant differences exist between differential neutron spectrometry, multiple-foil-derived integral measurements, and calculated flux-spectra.[2,3,8,9,31,47,48,51,62] For standard and reference benchmark fields, the total flux value and broad energy group spectral shape uncertainties for the more important energy regions are currently estimated to be in the ∿ 2 to 5% (1σ) and ∿ 4 to 15% (1σ) range, respectively. For a number of important controlled benchmark fields identified in this paper, the uncertainties are considerably greater, in the ∿ 5 to 15% and ∿ 5 to 30% (1σ) and higher ranges, respectively. As such, integral data testing of evaulated dosimetry and gas production cross sections, particularly for broad spectrum monitors, is now limited to the ∿ 5 to 10% (1σ) and above range. Based on goal accuracy objectives of ∿ 2 to 5% (1σ) for most environmental characterization parameters used for fission reactor design,

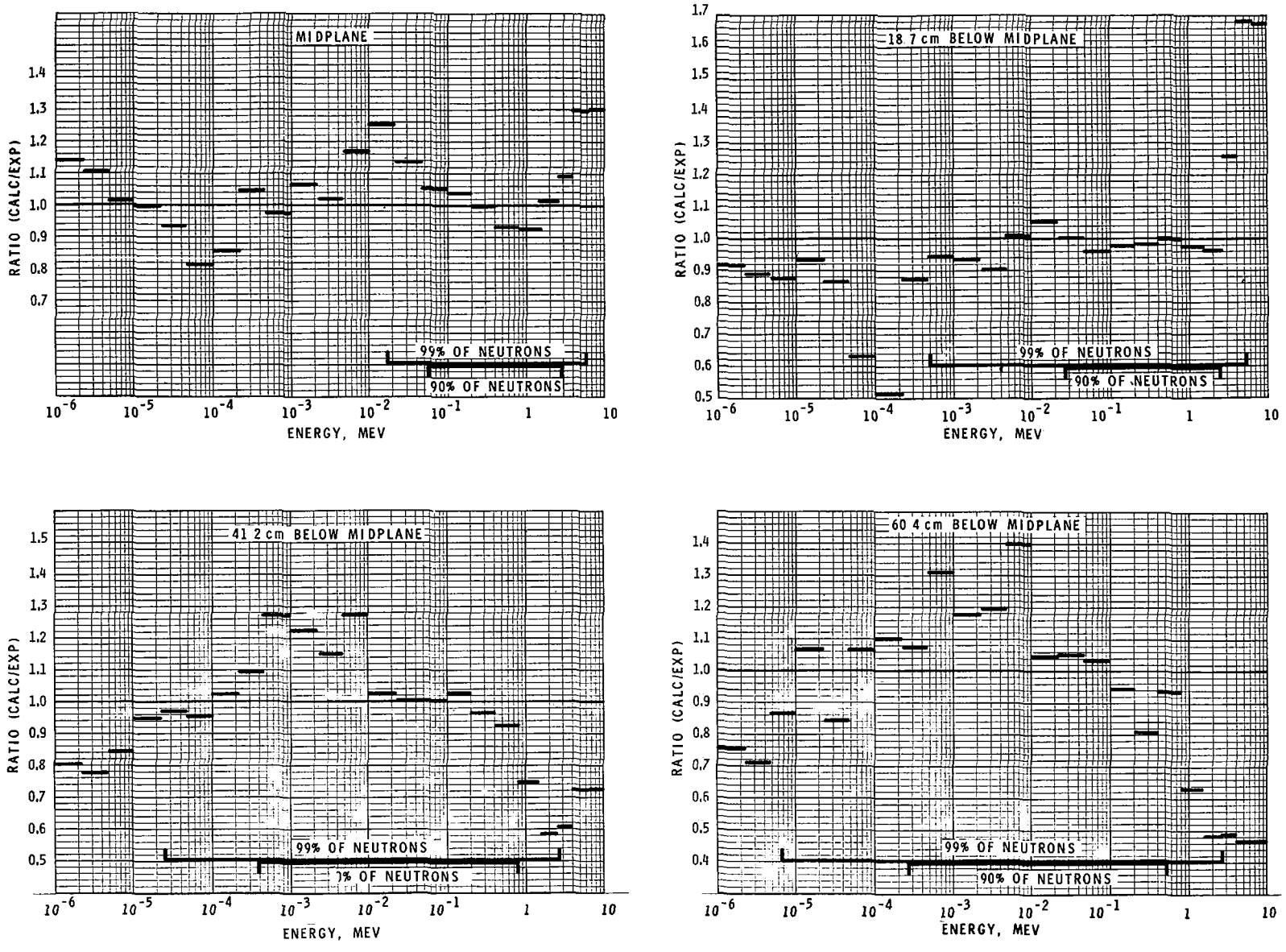

FIGURE 7 MEASURED TO CALCULATED SPECTRAL COMPARISON AT FOUR AXIAL LOCATIONS IN ROW 2 - EBR-II RUN 50H

development, and surveillance programs,[7] broad energy group flux spectral characterization requirements for benchmark neutron fields have been placed in the ∿ 5 to 10% (1σ) range or better. To achieve and validate this level of accuracy for most standard, reference, and a few controlled benchmark fields will require the combined use of data obtained from differential neutron spectrometry, analytical calculations, and integral measurements.

For instance, and as already inferred in previous sections, studies of the measured ^{252}Cf and ^{235}U and calculated ΣΣ, CFRMF, and BIG-10 benchmark spectral shapes indicate that (1) integral measurements must be relied upon to define and validate the highest energy (∿ greater than 1-2 MeV) and lowest (less than ∿ 10 keV) parts of the spectrum for many of the fields, and (2) that differential neutron spectrometry must be relied upon to define and validate the spectrum for the intermediate energy region between ∿ 0.01 to 2 MeV. These studies also indicate that future flux-spectral benchmark characterization work will involve the use of more complex computer codes that solve the system of equations by appropriate types of minimization procedures,[47,63,64,65]

$$A_i \pm \delta A_i = \int [\sigma_i(E) \pm \delta\sigma_i] \cdot [\phi(E) \pm \delta\phi]\, dE \qquad i=1,\ldots n, \quad (1)$$

where A_i is a measured reaction rate for the i sensor, $\sigma_i(E)$ is the corresponding energy dependent cross section, $\phi(E)$ is the benchmark neutron field energy dependent spectrum, and δA_i, $\delta\sigma_i$, and $\delta\phi$ are the associated input errors.

The solution of equation (1) will result in an adjusted "best" set of input values of A_i, $\sigma_i(E)$, and $\phi(E)$ which are all consistent within assigned uncertainties. It is anticipated that the use of such an approach will be essential since the "δ" errors for A_i, $\sigma_i(E)$, and $\phi(E)$ will all be tending towards the ±2-5% (1σ) range and, therefore, none of the error contributions can be ignored.

In a few instances, such as for thermal, 1/E, and the intermediate-energy standard neutron fields (ISNF), the spectral shapes will be well enough established (at the ±5% or better level by computations), that neither integral or differential spectrometry measurements can be expected to significantly improve the shape.

For the purposes of this meeting and to serve as a focal point for continuing the discussion of required international work in the area of benchmark field flux-spectral characterization, summary tabulations are provided in Tables II through IV for a number of selected standard, reference, and controlled benchmark fields that have been identified and for which data are or could be made available for reactor dosimetry data development and testing. Where known, estimates are given of the current benchmark field uncertainties associated with neutron spectrometry, analytical calculations, and/or integral measurements. This list was reviewed, modified, and updated as a part of the work of this consultants' meeting.*

VI. CONCLUSIONS

The status has been reviewed of flux-spectral characterization for the three categories of benchmark fields: Standard, Reference, and Controlled-Environment. While the most precise determination of the spectral shape for some standard and reference fields will be accomplished by spectrometry and/or computations, in other cases, a combination of calculations, neutron differential spectrometry, and integral measurements will be required. Present state-of-the-art accuracies for establishing values of flux and broad energy group spectral shapes are estimated to be in the range of 2 to 30% (1σ), depending on the particular parameter and benchmark field category. To satisfy goal accuracy objectives of $\sim$ 2 to 5% (1σ) by $\sim$ 1980 for the routine determination of important reactor environmental characterization parameters (such as total flux-fluence, flux-fluence > 0.1 or > 1 MeV, etc.), the above quoted 2 to 30% (1σ) uncertainties need to be reduced to the 2 to 10% (1σ) range for most dosimetry benchmark fields.

---

* As a result of the recommendations of this meeting, some standard neutron fields identified in this paper are listed as reference neutron fields in Table III.

TABLE II. STANDARD NEUTRON FIELDS FOR REACTOR DOSIMETRY

Neutron Field	Average Energy	Energy Range for Data Development, Testing, and Calibration	Status of Group-Flux Spectrum Characterization
Thermal Maxwellian	0.025 eV	<0.4 eV	±2-5%* Theory of thermal equilibrium, and spectrometry. [5,6]
Epithermal-1/E	0.75 MeV	0.4 eV to 0.1 MeV	±5% Computations and/or chopper measurements. [5,6]
^{252}Cf spontaneous fission (χ_{82})	2.13 MeV	0.1 to ∿18 MeV	±13% (E<0.25 MeV) ± 2% (0.25<E<8 MeV) ± 9% (8<E<12 MeV)] Differential spectrometry** ±10% (12<E<18 MeV), Multiple foils. [2,5,6,8,9, and this meeting]

* Estimated 1σ errors, this and subsequent tables.

** The NBS recommended spectrum shape based on an evaluation of differential spectrometry results reported up to 1974 is recognized as an acceptable spectrum description for practical applications. See paper by Grundl and Eisenhauer, this meeting. The multiple foil results are unnecessary and unjustified for the energy range of major interest for this standard field.

TABLE III. REFERENCE NEUTRON FIELDS FOR REACTOR DOSIMETRY

Neutron Field	Average Energy (MeV)	Energy Range for Data Development, Testing, and Calibration (MeV)	Status of Group Flux Spectrum Characterization
^{235}U thermal fission (χ_{25})	1.97	0.1 to ∿18	±15% (E < 0.25 MeV) ±2-5% (0.25 < E < 8 MeV) ± 5% (8 < E < 12 MeV) Differential spectrometry; ±10% (12 < E < 15 MeV) Multiple foil. (2,5,6,8,9, and this meeting)
Sigma Sigma ($\Sigma\Sigma$)	0.76	0.01 to ∿18	±15% (E < 0.1 keV) Multiple foil; ± 5% (0.1 keV < E < 2 MeV) Spectrometry and computation; ± 5% (E > 2 MeV) Multiple foil. (2-6,8,9, and this meeting)
ISNF	0.80	0.008 to ∿18	± 5% (E < ∿ 2 MeV) Computation; ±2-5% (2 < E < 12 MeV) Computation and spectrometry (fission spectrum). (5,6,9)
BIG TEN	0.58	0.01 to ∿18	± 5% (0.05 < E < 2 MeV) Computation and spectrometry; ± 5% (E > 2 MeV) Multiple foil and computation. (2-6,9, and this meeting)
CFRMF	0.76	0.01 to ∿18	±15% (E < 0.01) Multiple foils and computations; ± 5% (0.01 < E < 2) Spectrometry and computations; ± 5-10% (E > 2) Multiple foils and computations. (2-6,9, and this meeting)

TABLE III. REFERENCE NEUTRON FIELDS FOR REACTOR DOSIMETRY
(continued)

Neutron Field	Average Energy (MeV)	Energy Range for Data Development, Testing, and Calibration (MeV)	Status of Group Flux Spectrum Characterization
APFA-III*	≲1.5	0.01 to 18	±5-20% (0.01 < E < 10) Spectrometry and computations; ±5-20% (0.01 < E < 18) Multiple foils and computations. (3,48,60)
TAPIRO*	≲1.5	0.01 to 18	±5-20% (0.01 < E < 10) Spectrometry and computations; ±5-20% (0.01 < E < 18) Multiple foils and computations.(2,5,and this meeting
YAYOI*	≲1.5	0.01 to 18	±5-20% (0.01 < E < 10) Spectrometry and computations; ±5-20% (0.01 < E < 18) Multiple foils and computations.(2,5,and this meeting)
YAYOI (Lead Intermediate column)		10^{-7} to 2	±5-20%, Spectrometry, multiple foils, computations.(2,5,and this meeting)
Borated Graphite with Electron Linac (1/E Spectrum in KeV region)		10^{-6} to 10	±5-10% Time-of-flight and computations. (68)
Fe BLOCK (shielding benchmark)		0.01 to 1	±10% or better. Spectrometry, multiple foils, several interlaboratory calculations and measurements. (61)
Na BLOCK (shielding benchmark)		10^{-6} to 5	±10% or better. Spectrometry, multiple foils, several interlaboratory calculations and measurements. (61)

*Central core position, Godiva and Flattop type ∿93% enriched ^{235}U bare and reflected cores.

TABLE III. REFERENCE NEUTRON FIELDS FOR REACTOR DOSIMETRY
(continued)

Neutron Field	Average Energy (MeV)	Energy Range for Data Development, Testing, and Calibration (MeV)	Status of Group Flux Spectrum Characterization
Accelerator $^{9}Be(d,n)^{10}B$ reaction		Tailored distributions with mean energies: ∿2, ∿3, etc. up to ∿8 MeV.	>±10-30% (0.1 < E < 30) Spectrometry and theory; >±10-30% (0.1 < E < 30) Multiple foils and theory. (5,6,66,67)
Cyclotron $^{9}Be(d,n)^{10}B$ reaction		Tailored distributions with mean energies, as above, up to ∿15 MeV.	>±10-30% (0.1 < E < 30) Spectrometry and theory; >±10-30% (0.1 < E < 30) Multiple foils and theory. (67)
Etc.			

TABLE IV. CONTROLLED-ENVIRONMENT BENCHMARKS FOR REACTOR DOSIMETRY

Benchmark	Approximate Major Energy Range for Data Development, Testing, and Calibration (MeV)	Status of Group Flux Spectral Characterization
Thermal Type		
a) HFIR	10^{-10} to 18	±5 to 30%, Multiple-foils and computations. (33)
b) BSR	10^{-10} to 18	±5 to 30%, Multiple-foils and computations. (33)
c) BR2-Cd Loops	4×10^{-7} to 18	±5 to 30%, Multiple-foils and computations. (35)
d) HFR	10^{-10} to 18	±5 to 30%, Multiple-foils and computations. (69)
e) KUR	10^{-10} to 18	±5 to 30%, Multiple-foils, ^{6}Li and ^{3}He sandwich counters and computations. (68)
f) etc.		

TABLE IV. CONTROLLED-ENVIRONMENT BENCHMARKS FOR REACTOR DOSIMETRY
(Continued)

Benchmark	Approximate Major Energy Range for Data Development, Testing, and Calibration (MeV)	Status of Group Flux Spectral Characterization
LWR-Surveillance		
a) ILR-PV Mockup	10^{-10} to 18	±5 to 30%, Multiple-foils and computations. (32)
b) Japanese-PV Mockup	10^{-10} to 18	±5 to 30%, Multiple-foils and computations. (41)
c) Browns Ferry* #3 (BWR)	10^{-10} to 18	±5 to 30%, Multiple-foils and computations. (37)
d) McGuire 1* (PWR)	10^{-10} to 18	±5 to 30%, Spectrometry, multiple-foils, and computations. (37)
e) BR3 (PWR)*	10^{-10} to 18	±5 to 30%, Multiple-foils and computations. (70)
f) ORR-PV Mockup*	10^{-10} to 18	±5 to 30%, Spectrometry, multiple-foils, and computations. (71)
g) etc.		

*Planned measurements, computations, and/or spectrometry.

TABLE IV. CONTROLLED-ENVIRONMENT BENCHMARKS FOR REACTOR DOSIMETRY
(Continued)

Benchmark	Approximate Major Energy Range for Data Development, Testing, and Calibration (MeV)	Status of Group Flux Spectral Characterization
Fast Reactor Type		
a) ECEL Core 14-13	$\sim 10^{-6}$ to 18	±5 to 30%, Spectrometry, computations, and multiple-foils. (72)
b) ECEL Core 16	$\sim 10^{-6}$ to 18	±5 to 30%, Spectrometry, computations, and multiple-foils. (48)
c) EMC-FTR	$\sim 10^{-6}$ to 18	±5 to 30%, Spectrometry, computations, and multiple-foils. (39)
d) EBR-II 31F Run	10^{-10} to 18	±5 to 30%, Multiple-foils and computations. (26)
e) EBR-II 50H Run	10^{-10} to 18	±5 to 30%, Multiple-foils and computations. (19,20,27,28,29)
f) EBR-II 75D Run	10^{-10} to 18	±5 to 30%, Multiple-foils and computations. (30)
g) FTR-IRT*	10^{-10} to 18	±5 to 10%, Spectrometry, computations, and multiple-foils.
h) VIPER	10^{-4} to 10	±5 to 15%, Spectrometry, computations, and multiple-foils. (73)
i) STEK CORES	$\sim 10^{-6}$ to 18	±5 to 30%, Spectrometry, computations, and multiple-foils. (74)
j) etc.		

*Planned tests in a cooled in-reactor-thimble (IRT) in the Fast Test Reactor central core region.

TABLE IV. CONTROLLED-ENVIRONMENT BENCHMARKS FOR REACTOR DOSIMETRY
(Continued)

Benchmark	Approximate Major Energy Range for Data Development, Testing, and Calibration (MeV)	Status of Group Flux Spectral Characterization
CTR Type		
a) HENRL- $^{3}H(d,n)^{4}He$	10^{-2} to 16	±5 to 30%, Spectrometry, computations, and multiple-foils. (75,76,77)
b) RTNS $^{3}H(d,n)^{4}He$	10^{-2} to 16	±5 to 30%, Spectrometry, computations, and multiple-foils. (78,79)
c) CTR BLANKET MODEL LOCATIONS (D-T Reaction)	10^{-4} to 16	≥±5 to 30%, Computations and multiple-foils. (80)
d) etc.		

REFERENCES

1. M. F. Vlasov and C. L. Dunford, "Proceedings of a Consultants' Meeting on Nuclear Data for Reactor Neutron Dosimetry", Vienna, 10-12 September 1973, Report INDC(NDS)-56/U, IAEA (1973).

2. Proceedings of the First International ASTM-EURATOM Symposium on Reactor Dosimetry, Petten, Netherlands, September 22-26, (1975).

3. W. N. McElroy, et al., Special Series, Nucl. Techn. 25, 177-422 (1975).

4. G. and S. DeLeeuw, "In-Pile Neutron Spectroscopy: Status:, CEN/SCK Report (1976), Proceedings this meeting.

5. M. F. Vlasov (editor), "IAEA Programme on Benchmark Neutron Fields Applications for Reactor Dosimetry", INDC (SEC)-54/L+Dos., (1976).

6. J. A. Grundl and C. Eisenhauer, "Benchmark Neutron Fields for Reactor Dosimetry", NBS Report (1976), Proceedings this meeting.

7. W. N. McElroy, R. A. Bennett, D. L. Johnson, and N. D. Dudey, "Neutron Environmental Characterization Requirements for Reactor Fuels and Materials Development and Surveillance Programs", HEDL-SA 911, Hanford Engr. Develop. Lab., (1975) and in Ref. 2.

8. M. F. Vlasov, A. Fabry, and W. N. McElroy, "Status of Neutron Cross Sections for Reactor Dosimetry", HEDL-SA 890, Special Contributed Paper to 1976 International Conference on the Interactions of Neutrons with Nuclei, July 6-9, 1976, Lowell, Mass. (1976).

9. A. Fabry, W. N. McElroy, L. S. Kellogg, E. P. Lippincott, J. A. Grundl, D. M. Gilliam, and G. E. Hansen, "Review of Microscopic Integral Cross Section Data in Fundamental Reactor Dosimetry Benchmark Neutron Fields", HEDL-SA 1148 (1976), Proceedings this meeting.

10. R. Gold, "Neutron Spectrometry for Reactor Applications: Status, Limitations and Future Directions", HEDL-SA 901 (1975), and in Ref. 2.

11. H. Farrar, E. P. Lippincott, and W. N. McElroy, "Dosimetry for Fluence Applications", HEDL-SA 939 (1975), and in Ref. 2.

12. J. H. Roberts, "Absolute Flux Measurements of Anisotropic Neutron Spectra with Proton Recoil Tracks in Nuclear Emulsions", Rev. Sci. Instr. 28, 677 (1957).

13. R. Gold, "Energy Spectrum of Fast Cosmic Ray Neutrons Near Sea Level", Phys. Rev. 165, 1406 (1968).

14. T. Iijima and S. Momoto, "Measurements of Anisotropic Fast Neutron Spectrum with Nuclear Emulsions", Nucl. Sci. and Eng. 22, 102 (1965).

15. L. Rosen, "Nuclear Emulsion Techniques for the Measurements of Neutron Energy Spectra", Nucleonics 11, 7, 32 (1953) and L. Cranberg, G. Frye, N. Nereson, and L. Rosen, "Fission Neutron Spectrum of ^{235}U", Phys. Rev. 103, 662 (1956).

16. J. H. Roberts and A. N. Behkami, "Measurement of Anisotropic Fast-Neutron Spectra with Nuclear Emulsion Techniques", Nuclear Applications 4, 182 (1967).

17. J. H. Roberts and F. E. Kinney, "Measurement of Neutron Spectra by Use of Nuclear Emulsions Loaded with ^{6}Li Glass Specks", Rev. Scien. Instr. 28, 610 (1957).

18. R. L. Fleischer, P. B. Price, and R. M. Walker, Nuclear Tracks in Solids, University of California Press, Berkeley, California (1975).

19. B. R. Sehgal and D. Meneghetti, "Analyses of Dosimetry Spectrometry in EBR-II Systems", ANS Mtg. Irradiation Experimentation in Fast Reactors, Jackson, Wyoming, Sept. 10-12, 355 (1973).

20. B. R. Sehgal and R. H. Rempert, Nucl. Technol. 25, 390 (1975).

21. D. Meneghetti, E. R. Ebersole, and P. Walker, Nucl. Technol. 25, 406 (1975).

22. B. R. Sehgal and F. S. Kirn, Trans. Am. Nucl. So. 14, 778 (1971).

23. D. Meneghetti and K. E. Phillips, Trans. Am. Nucl. Soc., 15, 538 (1972).

24. N. D. Dudey and R. R. Heinrich, "Flux Characterization and Neutron-Cross-Section Studies in EBR-II", ANL-7629, Argonne National Laboratory (1970).

25. N. D. Dudey, R. R. Heinrich, R. J. Popek, R. P. Larsen, and R. D. Oldham, "Activation-Rate Measurements in the ZPR-3 Mockup Critical Experiments. Part 1, Measurements of Foil-Activation Rates and Fission Yields in Assembly 60 of ZPR-3 Mockup of EBR-II with a Uranium Blanket", ANL-7781, Argonne National Laboratory (1971).

26. W. N. McElroy, J. L. Jackson, J. A. Ulseth, and R. L. Simons, "EBR-II Dosimetry Test Data Analysis (Reactor Runs 31E and 31F)", BNWL-1402, Battelle-Pacific Northwest Laboratories (1970).

27. W. N. McElroy, "Fast Reactor Flux-Spectral Characterization", ANS Mtg. Irradiation Experimentation in Fast Reactors, Jackson, Wyoming, Sept. 10-12, 333 (1973).

28. J. L. Jackson, W. N. McElroy, J. A. Ulseth, and L. S. Kellogg, "EBR-II Dosimetry Tests", ANS Mtg. Irradiation Experimentation in Fast Reactors, Jackson, Wyoming, Sept. 10-12, 383 (1973), and HEDL-TME 73-62, Hanford Engng. Develop. Lab. (1975).

29. W. N. McElroy, J. A. Ulseth, E. P. Lippincott, W. Y. Matsumoto, and L. S. Kellogg, "Fission Rates, Burnup, and Neutron Flux-Fluence-Spectra Characterization for Mixed Oxide Fuel Experiments in the EBR-II", HEDL-TME 75-74, Hanford Engng. Develop. Lab. (1975).

30. E. P. Lippincott, J. A. Ulseth, L. S. Kellogg, A. I. Davis, and W. N. McElroy, "EBR-II 75D High Power Dosimetry Test - Preliminary Report", HEDL-TME 75-86, Hanford Engng. Develop. Lab. (1975).

31. W. N. McElroy and R. E. Dahl, "Neutron Dosimetry for Fast Reactor Applications", Irradiation Effects on Structural Alloys for Nuclear Reactor Applications, ASTM STP-484, 375-399, American Society for Testing and Materials (1970).

32. C. Z. Serpan, Jr., "Reliability of Fluence-Embrittlement Projections for Pressure Vessel Surveillance Analyses", Nucl. Techn. 12, 108 (1971).

33. F. B. K. Kam and J. H. Swanks, "Neutron Flux Spectrum in the HFIR Target Region", ORNL-TM-3322, Oak Ridge National Lab. (1971); J. D. Jenkins, "Determination of the Fast Neutron Flux and Spectrum in the Oak Ridge Bulk Shielding Reactor With Application to Radiation Damage Experiments", ORNL-TM-3542, Oak Ridge National Lab. (1971).

34. E. W. Etherington, "The Calculation of Atomic Displacement Dose in Fast Reactors", (1975), in Ref. 2.

35. J. Debrue, Ch. DeRaedt, L. Leenders, N. Maene, and R. Menil, "Dosimetry Work in Connection with Irradiation in the High Flux Materials Testing Reactor BR-2", (1975), in Ref. 2; and M. H. Ceulemans, J. Debrue, A. Demildt, A. Fabry, J. Planquart, M. Soenen, and G. Van Massenhove, "Description of Experimental Facilities for Fast Reactor Research and Development at SCK/CEN", Brochure, Mol, Belgium (1975).

36. G. Minsart and C. Van Bosstraeten, "Contribution to the Study of the Reactor Shielding Benchmark n°2 (PWR) Proposed by the NEA", Proceedings Joint Technical Meeting on "Differential and Integral Data Requirements for Shielding Calculations", Vienna, October 12-15 (1976).

37. F. Rahn, "Power Reactor Pressure Vessel Benchmarks, An Overview", EPRI Report, (1976), Proceedings this meeting.

38. E. T. Boulette, D. R. Marr, and W. L. Bunch, "Analysis of the FTR/EMC Neutron Shielding Experiment", HEDL-TME 73-27, Hanford Engng. Develop. Lab. (1973).

39. J. V. Nelson, E. P. Lippincott, R. A. Bennett, W. N. McElroy, and J. W. Daughtry, "Measurement and Calculation of Neutron Spectra in the FTR Engineering Mockup Critical", HEDL-TME 76-88 (1976).

40. L. B. Miller, R. E. Jarka, and D. C. Kaul, "Study of Radiation Dosage to Structural Components in Nuclear Reactors", SAI Report (1976).

41. K. Takenchi, T. Miura, and A. Yamaji, "Neutron Energy Spectrum Determination for Irradiation Damage Study of Reactor Structural Materials", (1975), in Ref. 2.

42. M. Galliani, N. Benatti, and A. Puliandri, "Garigliano Nuclear Power Plant Vessel's Material Surveillance Program Fast Neutron (E>1 MeV) Flux Measurement", (1975), in Ref. 2.

43. R. C. Weisbin, J. H. Marable, J. L. Lucius, E. M. Oblow, F. R. Mynatt, R. W. Peelle, and F. G. Perey, "Application of FORSS Sensitivity and Uncertainty Methodology to Fast Reactor Benchmark Analysis", ORNL/TM-5563 (1976).

44. C. R. Weisbin, E. M. Oblow, J. Ching, J. E. White, R. Q. Wright, and J. D. Drischler, "Cross Section and Method Uncertainties: The Application of Sensitivity Analysis to Study Their Relationship in Radiation Transport Benchmark Problems", ORNL-TM-4847 (ENDF-218), August 1975; see also, RSIC Code Collection PSR-93.

45. F. C. Difilippo, "SUR, A Program to Generate Error Covariance Files", ORNL/TM-5223 (March 1976).

46. F. G. Perey, G. DeSanssure, and R. B. Perez, "Estimated Data Covariance Files of Evaluated Cross Sections - Examples for ^{235}U and ^{238}U", Advanced Reactors: Physics, Design, and Economics, edited by Kalfelz and Karan, Pergamon Press, p. 578 (1975).

47. D. K. Trubey, Compiler, "A Review of Radiation Energy Spectra Unfolding", Proceedings of a Seminar-Workshop, April 12-13, 1976, ORNL/RSIC-40 (1976).

48. A. Fisher, "International Intercomparison of Neutron Spectra Evaluating Methods Using Activation Detectors", Jul-1196, Kernforschungsanlage Jülich, Germany (1975).

49. A. Fabry, H. Ceulemans, P. Vandeplas, W. N. McElroy, and E. P. Lippincott, "Reactor Dosimetry Integral Reaction Rate Data in LMFBR Benchmark and Standard Neutron Fields: Status, Accuracy and Implications", (1975), in Ref. 2.

50. C. A. Oster, W. N. McElroy, R. L. Simons, E. P. Lippincott, and G. R. Odette, "A Modified Monte Carlo Program for SAND-II With Solution Weighting and Error Analysis", Report HEDL-TME 76-60 (1976).

51. E. M. Bohn, et al., editors, "Benchmark Testing of ENDF/B-IV", report ENDF-230 Vol. I (1976).

52. J. A. Grundl and C. Eisenhauer, "Fission Rate Measurements for Materials Neutron Dosimetry in Reactor Environments", in Ref. 2.

53. N. M. Islani, H. Knitter, Nucl. Sci. Eng. 50, 108 (1973); P. I. Johansson, B. Holmquist, T. Wiedling, L. Jeki, "Precision Measurement of Prompt Fission Neutron Spectra of ^{235}U, ^{238}U, and ^{239}Pu"; and H. Knitter in Proceed. Specialist Meeting on Fission Neutron Spectra and Inelastic Scattering, Harwell (April 1975).

54. J. W. Rogers, D. A. Millsap, and Y. D. Harker, "Fast Neutron Spectrum and Dosimetry Studies in the Coupled Fast Reactivity Measurements Facility", (1975), in Ref. 2.

55. J. W. Rogers, Y. D. Harker, and D. A. Millsap, "The Coupled Fast Reactivity Measurements Facility (CFRMF)", EG&G Report 1976, Proceedings this meeting.

56. G. DeLeeuw-Gierts, S. DeLeeuw, H. H. Gelmick, and J. W. Rogers, "Neutron Spectrometry Data in LMFBR Benchmark and Standard Neutron Fields", (1975), in Ref. 2.

57. E. J. Dowdy, E. J. Lozito, and E. A. Plassmann, Nucl. Techn. 25, 381 (1975).

58. E. J. Lozito, "Measurement of the Neutron Spectrum of a Fast Critical Assembly (BIG-Ten) Using Proton Recoil Proportional Counting", Texas Agric. and Mech. Univ. Thesis (Ph.D.); University Microfilms Order No. 75-15,041 (1975).

59. G. DeLeeuw-Gierts, S. DeLeeuw, G. H. Hansen, and H. H. Helmick, "Neutron Spectrum of BIG-Ten by Lithium-6 Spectrometry", CEN/SCK Report (1976).

60. W. N. McElroy, R. J. Armani, and E. Tochilin, Nucl. Sci. Engr. 48, 51-71 (1972).

61. Proceedings of the Joint IAEA-OECD(NEA) Technical Committee Meeting on Differrential and Integral Nuclear Data Requirements for Shielding Calculations, Vienna 12-15 October 1976, being published by the IAEA; Proceedings of the Specialists' Meeting on Sensitivity Studies and Shielding Benchmarks, Paris 7-10 October 1975, published by OECD-NEA, Paris 1976.

62. W. N. McElroy, Proc. Nuclear Cross Sections and Technology Conference, NBS Special Publication 425, Vol. I, 189 (1975).

63. A. K. McCracken, M. J. Grimstone, "The Experimental Data Processing Program Radak", (1975), in Ref. 2.

64. A. K. McCracken and A. Packwood, "Foil Activation Detectors - Some Remarks on the Choice of Detectors, The Adjustment of Cross Sections, and the Unfolding of Flux Spectra", UKAEA Report (1976), Proceedings this meeting.

65. J. G. Williams and A. H. M. A. Hannan, "Spectral Characterization of the NISUS Neutron Field", ULRC Report (1976), Proceedings this meeting.

66. W. N. McElroy, Compiler, "LMFBR Reaction Rate and Dosimetry 4th Quarterly Progress Report", HEDL-TME 72-90, ANL-11 (1972).

67. R. R. Heinrich and L. R. Greenwood, in "CTR Quarterly Progress Report", ANL/CTR-76-2 (1976); D. R. Nethaway, R. A. Van Konynenberg, and T. M. Adams, "Measurement of the Neutron Spectrum from the Reaction of 30-MeV Deutrons on Thick Beryllium Target", UCRL-52024, Lawrence Livermore Lab. (1976).

68. I. Kimura, et al, "Measurements and Evaluation of Threshold Reaction Cross Sections in Standard Neutron Fields", RRI Report (1976), Proceedings this meeting.

69. A. Tas, C. A. Verspuy, and W. L. Zijp, "Characteristics of H. F. R. Facilities", R. M. G. Note 75/21, Reactor Centrum Nederland (1975).

70. R. Billiau, K. Bobin, G. Michiels, and J. Proost, "Annual Scientific Report", BLG-495, CEN/SCK (1973). Background information is provided in this report on the BR-3 LWR power reactor which has been considered for some specialized in- and ex-vessel dosimetry data development and testing work.

71. T. M. Sims and J. H. Swanks, "Oak Ridge Research Reactor (ORR) Experiment Facilities and Capabilities", ORNL Brochure (1976). A simulated pressure vessel mockup (4'x4'x12", of twelve 1" slabs) irradiation facility has been considered for insertion in the ORR.

72. W. N. McElroy, S. Berg, T. B. Corcket, and R. J. Tuttle, Nucl. Sci. Engr. 36, 15-27 (1969).

73. M. H. McTaggart, "Spectrum characterization and Threshold Reaction Rate Measurements in the Neutron Field of VIPER", UKAEA Report (1976), Proceedings this meeting.

74. W. L. Zijp, H. J. Nolthenius, and J. H. Baard, "Neutron Spectra in the STEK Facility Determined with the SAND-II Activation Technique", RCN-232, Reactor Centrum Nederland, Sept. 1975; and A. Fischer, H. J. Noltenius, and W. L. Zijp, "Comparison of SAND-II and RFSP-JUL Spectrum Unfolding Codes for Several Neutron Spectra in the STEK Facility", RCN-75-115, Reactor Centrum Nederland, September 1975.

75. A. A. O'Dell, "Monte Carlo Characterization of the Near-Field Energy and Angular Distribution for the HENRE D-T Neutron Generator", EGG 1183-2298 (1972).

76. R. C. Barrall, J. A. Holmes, and M. Silbergeld, "High Energy Neutron Cross Section Validation and Neutron Flux Spectrum Using the HENRE Source", AFWL-TR-68-134, Air Force Weapons Laboratory (1969).

77. R. C. Barrall, M. Silbergeld, and D. G. Gardner, "A Method for Estimating Neutron Flux Density, Fluence, and Average Energy of Neutrons from the $T(d,n)^4He$ Reaction:, SUHP-69-2, Stanford University (1969).

78. E. Goldberg, R. Griffith, and C. Logan, "Peak Flux Measurements of the LLL High-Intensity 14 MeV Neutron Source", UCRL-51317, Lawrence Livermore Lab. (1972).

79. R. A. Van Konynenburg, "Neutron Dosimetry (14 MeV) for Foil Samples Irradiated with the LLL Rotating Target Neutron Source", UCRL-51393, Rev. 1 (1974).

80. L. J. M. Kuijpers, "Experimental Model Studies for a Fusion Reactor Blanket", Thesis, Institut fur Reaktor-Entwicklung (IRE) of the Kernforschungsanlage, Julich GmbH, Federal Republic of Germany, November 1976.

II.2. A REVIEW ON STANDARD FISSION NEUTRON SPECTRA OF ^{235}U AND ^{252}Cf

H. -H. KNITTER
Central Bureau for Nuclear Measurements
EURATOM
Geel, Belgium

ABSTRACT

The usefulness of the two fission neutron spectra of ^{235}U and ^{252}Cf as standard neutron fields are discussed. A summary of the spectrum measurements is presented. The present knowledge of the spectra obtained from the experiments is given.

I. INTRODUCTION

Several years ago it was recommended by the IAEA Consultants' Meeting on Prompt Fission Neutron Spectra (1) that the spectra of ^{235}U and ^{252}Cf should be determined such, that they can be used as standard neutron fields. The advantages to use the ^{235}U fission neutron spectrum induced by thermal neutrons as a standard neutron field are :

- ^{235}U is widely available in quantities, sufficient for fission spectrum measurements.
- The main impurity ^{238}U does not fission at incident neutron energies from thermal to some 100 keV.
- The specific activity of ^{235}U is comparatively low.
- It shows fission with thermal neutrons and is therefore applicable in measurements at reactors and also with low-energy neutrons from accelerators.

The most important advanges of the ^{252}Cf fission neutron spectrum as standard neutron field are :

- ^{252}Cf is widely available also.

- It shows spontaneous fission.
- One can determine the source strength
- ^{252}Cf has a high specific neutron yield of 2.2. 10^6 n/sμg and therefore low mass neutron sources can be fabricated.
- The ratio of spontaneous fission to α decay is 0.03. The α-decay rate is low enough to permit an incorporation of a source with useful strength in a detector like a ionization chamber or a gas scintillation counter.

During the last two to three decades many fission neutron spectrum measurements were done, employing different experimental techniques. A summary is made in table 1 and table 2 for ^{235}U and ^{252}Cf respectively.

2. MATHEMATICAL REPRESENTATION OF THE FISSION NEUTRON SPECTRA

In the literature one finds several mathematical expressions to represent the shape of the fission neutron spectrum. The most important representations are :

$$N(E) \simeq \sqrt{E}\, e^{-E/T} \qquad (1)$$

Maxwell distribution

$$N(E) \simeq e^{-AE} \sinh \sqrt{BE} \qquad (2)$$

Watt distribution

$$N(E) \simeq \sum_k \nu_k \frac{e^{-\frac{E_f^k}{T_k}}}{\sqrt{T_k E_f^k}}\, e^{-\frac{E}{T_k}} \sinh \frac{2}{T_k}\sqrt{E_f^k E}$$

k : L. H

$$+ \nu_c \frac{E}{T_c^2}\, e^{-\frac{E}{T_c}} \qquad (3)$$

In expression (3) the two terms in the sum represent Watt distributions for the neutrons emitted by the light and heavy fission fragment group respectively, the third term gives the distribution for the scission or "central" neutrons as proposed by Bohr and Wheeler (35)

The common base of these representations is the neutron evaporation process. In applications the simplest form, namely the Maxwell distribution, has been mainly used.

3. THE ^{235}U FISSION NEUTRON SPECTRUM

The shape of the fission neutron spectrum of ^{235}U has been measured in many experiments as displayed in table 1. A large energy range of the fission neutrons is covered from hundred keV up to 20 MeV. In this energy range the neutron fluence per unit energy interval varies by as much as 6 orders of magnitude. This makes it evident that it is a difficult task to determine the whole fission neutron spectrum with a high degree of accuracy in a single measurement.

Prior to 1967 a Maxwellian distribution with an average fission neutron energy $\bar{E}$ = 1.935 MeV was used in many calculations for the fission neutron spectrum of ^{235}U.

In the work of Grundl (7) a high average fission neutron energy of 2.20 MeV was reported, and this gave the impact to study again the fission neutron spectrum of ^{235}U. Since then, several measurements were done, employing different neutron detection systems like time-of-flight detectors, ^{6}Li spectrometers, proton recoil counters, fission neutron age-measurements, activation detectors, etc.. The recent results summarized in table I show clearly a higher value than 1.935 MeV for the average energy of the fission neutrons. For the ^{235}U fission neutron spectrum the most recent evaluations (36) and (37) yield also the higher average energies of (1.978 $\pm$ 0.046) MeV and (1.970 $\pm$ 0.014) MeV respectively.

At the Specialists' Meeting on Fission Neutron Spectra and Inelastic Scattering at Harwell in April 1975 Dr. J.M. Adams took the responsibility to compare the latest fission neutron spectrum measurements of ^{235}U and ^{239}Pu available from Cadarache, Geel, Harwell and Studsvik. It became evident, that these spectra could only be compared with each other, if all the measurements were corrected in the same way, that means also for the secondary processes of the fission neutrons in the sample. This correction has so far been applied only to the ^{235}U and

^{239}Pu spectra measured in Geel (16,38). It was shown that this correction was not negligible. The spectra of the other laboratories were corrected using the same program and procedure as described in ref. (16). Adams (39) gives for a Watt representation the following weighted mean parameters of the accordingly corrected measurements of the ^{235}U fission neutron spectrum :

$$A = (1.012 \pm 0.0011)\ MeV^{-1} \qquad B = (2.189 \pm 0.155)\ MeV^{-1}$$

$$\overline{E} : 2.016\ MeV$$

Although this is not a value coming from an evaluation, there is now an encouraging agreement with the average fission neutron energy obtained by integral methods. For example McElroy's Sand II mean neutron energy for the presently adjusted ^{235}U fission neutron spectrum is (2.043 $\pm$ 0.025)MeV (40).

3. THE ^{252}Cf FISSION NEUTRON SPECTRUM

Most of the measurements of the fission neutron spectrum of ^{252}Cf are summarized in table 2. Compared to the ^{235}U measurements the problem due to secondary effects of fission neutrons in the sample is less severe. A recent evaluation of the ^{252}Cf fission neutron spectrum (37) showed good agreement in shape with a Maxwell distribution and gave an average fission neutron energy of (2.130 $\pm$ 0.027) MeV. The average departure of the experimental data from the reference Maxwellian function is less than 5 % in the energy range 0.25 to 8 MeV , a range which contains 94 % of the spectrum. Above and below this range the measurements become uncertain as one can see from fig.1 (41). At low and high neutron energies the experiments suffer from the low count rate. Moreover, at the high energy of the spectrum the energy determination becomes difficult. Also the relative detector efficiency has shaping influence on the spectrum and has to be determined in careful measurements.

A fine structure has been observed (29,42) in spectra with high statistical accuracy which were obtained by the time-of-flight method. However the authors of ref. (43) show, that Nitrogen along the flight path is the reason for the structure. Fig. 2 (43) may illustrate this effect.

4. CONCLUSIONS

From the facts mentioned in section 3, it seems that the average energy of the ^{235}U fission neutron spectrum is slightly larger than 2.00 MeV. For the energy range 0.25 to 8 MeV the evaluation of Grundl et al. (37) concludes that the average departure of the experimental data form the reference Maxwellian is less than 5 %. However, wether the shape of the ^{235}U fission neutron spectrum is better described by a Maxwellian, Watt or any other function can finally be said only on the base of an evaluation which considers not only the statistical errors, but also contributions due to uncertainties in backgrounds, detector efficiency, energy resolution, secondary processes in the sample etc.. These uncertainties should be reflected in the weights given to the experimental points in least squares fit procedures.

For the ^{252}Cf fission neutron spectrum Grundl et al. (37) evaluated an average fission neutron energy of (2.130 $\pm$ 0.027) MeV. The average departure of the experimental data from the reference Maxwellian is less than 5 % in the energy range 0.25 to 8.0 MeV.

The largest uncertainties in the knowledge of the ^{235}U and ^{252}Cf fission neutron spectra still exist on their low and high energy ends, which contain about 6 % of the spectrum. In certain cases, however, these energy regions can be of importance. Therefore the knowledge of the spectra also in these regions should be improved.

REFERENCES

(1) Proc. of Consultants' Meeting on Prompt Fission Neutron Spectra, held by I.A.E.A., Vienna (1971).

(2) WATT, B.E., Phys. Rev. 87 (1952) 1037.

(3) CANBERG, L, FRYE, G., NERESON, N., ROSEN, L., Phys. Rev. 103 (1956) 662.

(4) BONNER, T.W., Nucl. Phys. 23 (1961) 116.

(5) CONDE, H., DURING, G., Arkiv Physik 29 (1965) 313.

(6) BARNARD, E., FERGUSON, A.T.G., Mc MURRAY, W.R., VAN HEERDEN, I.J., Nucl. Phys. 71 (1965) 228.

(7) GRUNDL, J.A., Nucl. Sci. Eng. 31 (1968) 191.

(8) BRESESTI, A.M., BRESESTI, M., ROTA, A., RYDIN, R.A., Nucl. Sci. Eng. 40 (1970) 331.

(9) FABRY, A., DE COSTER, M., G. MINSART, G., SCHEPERS, J.C., VANDEPLAS, P., Proc. of Sec. Int. Conf. on Nucl. Data for Reactors, Helsinki (1970), IAEA Vienna, II 535.

(10) STORY, J.S., Proc. of Sec. Int. Conf. on Nucl. Data for Reactors, Helsinki (1970), IAEA Vienna, II 721.

(11) SMITH, A.B., Nucl. Sci. Eng. 44 (1971) 439.

(12) ALMEN, E., HOLMQVIST, B., WIEDLING, T., Report AE-429, Akticbolaget Atomenergi, Studsvik, Sweden (1971).

(13) RICKARD, I.C., "The Measurement of Fast Neutron Spectra with Semiconductor Detectors", PhD thesis submitted to the University of London, March 71, as reported in ref.

(14) CAMPBELL, C.G., ROWLANDS, J.L., Proc. of the 14th EACRP Meeting, Stockholm, Sweden (1971).

(15) WERLE, H., BLUHM, H., "Prompt Fission Spectra" IAEA Vienna (1972), 65.

(16) ISLAM, M.M., KNITTER, H.-H., Nucl. Sci. Eng. 50 (1973) 108.

(17) JOHANSSON, P.I., HOLMQVIST, B., WIEDLING, T., JEKI, I., Proc. of Conference on Neutron Data and Technology, Washington, March 1975.

(18) HJALMAR, E. HILDINGSLATIS, THOMPSON, St.G., Ark. Fys. 10 (1955) 357.

(19) SMITH, A.B., FIELDS, P.R., ROBERTS, J.H., Phys. Rev. 108 (1957) 441.

(20) BONNER, T.W., Nucl. Phys. 23 (1961) 116.

(21) BOWMAN, H.R. . THOMPSON, St.G., MILTON, J.C.D., SWIATECKI, W.J., Phys. Rev. 126 (1962) 2120.

(22) CONDE H., DURING, G.
Proc. of Symposium on Physics and Chemistry of Fission, Salzburg 2 (1965) 93, Editor IAEA Vienna.

(23) MEADOWS, J.W.
Phys. Rev. 157 (1967) 1076.

(24) GREEN,L., Nucl. Sci. Eng. 37 (1969) 232.

(25) ZAMYATNIN, Yu.S., Proc. of Conf. on Nuclear Data for Reactors, Helsinki , 2 (1970) 183, Editor IAEA Vienna.

(26) WERLE, H., BLUHM. H., Prompt Fission Neutron Spectra, IAEA Vienna 1971, 65.

(27) JEKI, L., KLUGE, Gy. LAJTAI, A., DYACHENKO, P.P., KUZMINOV, B.D., Proc. Consultants' Meeting on Prompt Fission Neutron Spectra, IAEA Vienna (1971) 81.

(28) KNITTER, H.-H., PAULSEN, A., LISKIEN, H., ISLAM, M.M., ATKE 22 (1973) 81.

(29) GREEN, L., MITCHEL, J.A., STEEN, N.M., Nucl. Sci. Eng. 50 (1973) 257.

(30) SPIEGEL, V., Nucl. Sci. Eng. 54 (1974) 28.

(31) BLINOV, M.W., WITENKO, B.A., KASARINOV, N.M., KRISJUK, I.T., TUS, B.T., Proc. of Second All Union Conf. on Neutron Physics, 4, 138, Kiev, June (1973).

(32) ALEKSANDROVA, Z.A., BOLSHOV, V.I., KUZNETSOV, V.F., SMIRENKIN, G.N., TARASKO, M.Z. ,Atomnaya Energiya 36 (1974) 282.

(33) KOGELNIKOVA, G.W.n KUSMINOV, B.P., LOWTSHIKOVA, G.H., SALNIKOV, O.A., SEMENOVA, N.N., NESTERENKO, W.S., TRUFANOV, A.M., FETIKOV,N.I., (1975), Report FEI-575.

(34) R.H. JOHNSON, WEHRING, B.W., DORNING, J.J., INGORSOLL, D.T., Transactions ANS 22 (1975)727.

(35) BOHR, N., WHEELER, J.A., Phys. Rev. 56 (1939) 426.

(36) KOSTER, A., Proc. of Consultants'Meeting on Prompt Fission Neutron Spectra, IAEA Vienna 1971,19.

(37) GRUNDL, J.A., EISENHAUER, C.M., Proc. Conf. on Neutron Cross Sections and Technology, Washington 1975, 1 (1975) 250.

(38) KNITTER H.-H., ATKE 24 (1975) 76.

(39) ADAMS, J.M., U.K. Nuclear Data Progress Report for the Period April 1975 to March 1976, NEANDC(E) 172-U 8 (1976) 14.

(40) FABRY, A., CEULEMANS, H., VANDEPLAS, P., McELROY, W.N., LIPPINCOTT, E.P., Reactor Dosimetry Integral Reaction Rate Data in LMFBR Benchmark and Standard Neutron Fields : Status, Accuracy and Implications, First ASTM-Euratom Symposium on Reactor Dosimetry, Petten Ndl (September 1975).

(41) LISKIEN,H., Neutron Standards and Their Applications, Int Conf. on Interactions of Neutrons with Nuclei, Lowell Mass., July 1976.

(42) NEFEDOV, V.N. MELNIKOV, A.K., STAROSTOV, B.I., Proc. of Constultants' Meeting on Prompt Fission Neutron Spectra, IAEA Vienna 1971, 89.

(43) GUENTHER, P., HAVEL, D., SJOBLOM, R., SMITH, A., ANL/NDM-19 (1976).

(44) HILL, D , Phys. Rev 87 (1952) 1034.

TABLE I · Summary of the Results of Fission Neutron Spectra Measurement Reported for Incident Neutron Energy Below 1 MeV

Reference	Year	Incident neutron energy (MeV)	Secondary neutron energy range (MeV)	Type of Measurement	Form of fit	Average Energy E (MeV)
Watt[2]	1952	Thermal	3.3 -17	Proton recoil	Watt	2.0[b]
Cranberg et al.[3]	1956	0.005-0 080	0.18 - 2.7	T-O-F	Watt	1 981[a]
		Thermal	0 35 -12	Emulsion	Maxwellian	1.935[a]
Bonner[4]	1961	Thermal	< 4	Sphere moderated	Maxwellian	1 998 ± 0.045
Condé and During[5]	1965	0.04	~0 3 - 7.5	T-O-F	Maxwellian	1.86 ± 0 06
Barnard et al.[6]	1965	0.1	0.3 - 4	T-O-F	Maxwellian	1.946 ± 0.045
Grundl[7]	1968	Thermal	0 8 -16	Activation detector	5 groups	2.20
Bresesti et al.[8]	1970	Thermal	~0.4 -20	Activation detector	Watt	2.0
Fabry et al.[9]	1970	Thermal		Activation detector	Watt and other forms	1.984 to 2.024
Story[10]	1970	Thermal		Age measurements	Maxwellian	2.025 ± 0.03
Smith[11]	1971	0.035 & 0 40	0 3 - 1 6	T-O-F	Maxwellian	2 11 ± 0.21
Almén et al[12]	1971	0.95	0 95 - 9.5	T-O-F	Maxwellian	1 905 ± 0 015
Rickard[13]	1971	Thermal		^{6}Li spectrometer	Maxwellian	2.01 ± 0.06
Campbell and Rowlands[14]	1971	Thermal		Reactor measurement	Maxwellian	2.10 ± 0 10
Werle and Bluhm[15]	1972	Thermal	0 1 -10	Proton recoil	Maxwellian	1.956 ± 0.12[c]
				^{3}He-spectrom	Maxwellian	2.020 ± 0.025[d]
Islam and Knitter[16]	1972	0.40	0.55 - 7.0	T-O-F	Watt and Maxwellian	2.06 ± 0.05
Johansson et al[17]	1975	0.10, 0.18, 0,53 2.07	0.16 -15	T-O-F	Maxwellian	1.977 ± 0.045
					Watt	1.992

[a] From the combined results of the two measurements covering the energy range between 0.18 and 12 MeV
[b] Combined with the data of D. Hill[44] from 0.4 to 6.4 MeV to cover the energy range of 0.4 to 17 MeV
[c] Estimated total error
[d] Statistical error only

TABLE II : SUMMARY OF RESULTS OF FISSION NEUTRON SPECTRUM MEASUREMENTS OF ^{252}Cf

References	Year	Fission neutron energy range (MeV)	Type of measurement	Form of fit	Average Energy (MeV)
Hjalmar[18]	1955	> 2	Photogr. plate	Maxwell	2.10 ± 0.13
Smith and Fieldes[19]	1957	0.2 - 7.0	T-O-F	Watt	2.36
Bonner[20]	1961	> 4	Phtotgr. plate mod. spheres		2.050 ± 0.045
Bowman et al.[21]	1962	0.5 - 6	T-O-F	Evap. Spectrum	2.34 ± 0.05
Condé and Dury[22]	1965	0.7 - 7.5	T-O-F	Maxwell	2.085 ± 0.075
Meadows[23]	1967	0.003 - 15	T-O-F	Maxwell	2.348
		0.5 - 15			2.283
Green[24]	1969		Manganese bath		2.10
Zamyatnin[25]	1970	0.04 - 6	T-O-F		2.22 ± 0.045
Werle and Bluhm[26]	1971	0.1 - 9.5	Prop. counter	Num. integr.	2.13 ± 0.12
				Maxwell	2.00
Jéky et al.[27]	1971	0.021 - 1.07	T-O-F		
Knitter et al.[28]	1973	0.15 - 15	T-O-F	Maxwell	2.13 ± 0.08
Green et al.[29]	1973	0.5 - 13	T-O-F	Maxwell	2.105 ± 0.014
Spiegel[30]	1974		Age-measurements		2.21 ± 0.05
Blinov et al.[31]	1973	0.02 - 0.20	T-O-F	$\sqrt{\text{Energy}}$	
Aleksandrova et al.[32]	1974	2.04 - 13.2	Scintillation det.	Maxwell	2.13 ± 0.045
Kogelnikova et al.[3]	1975	0.25 - 12.57	T-O-F	Maxwell	2.19 ± 0.03
Johnson et al.[34]	1975	2.6 - 15	Scintillation det.	Maxwell	2.13 ± 0.030

FIGURE CAPTIONS

Fig. 1

Point data from spectrum determinations of spontaneous fission neutrons from ^{252}Cf. The different sets were normalized at 2 MeV neutron energy (41).

Fig. 2

Observed neutron-velocity spectra and the air-correction factor (43). The unfiltered spectrum and that filtered through 10 cm of liquid nitrogen are indicated by crosses the vertical magnitude of which denote statistical uncertainty. The solid curve indicates the air-attenuation correction factor on the same time scale. Dashed lines correlate structure in the spectra and correction factor at the indicated energies in keV. "N" and "G" respectively denote the position of similar structure reported in refs. 42 and 29.

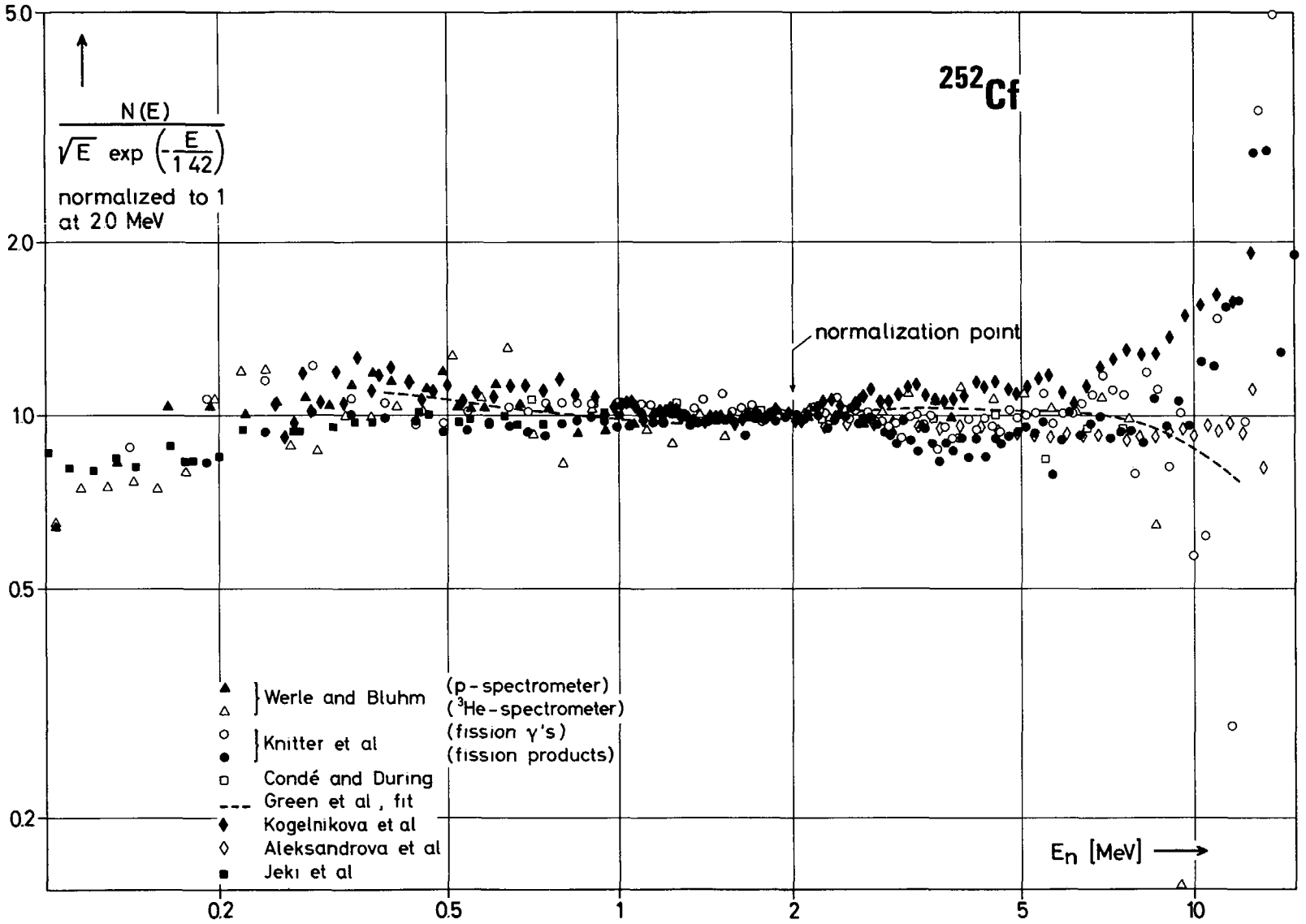
5.0
2.0
1.0
0.5
0.2
$\frac{N(E)}{\sqrt{E}\ \exp\left(-\frac{E}{1.42}\right)}$
normalized to 1
at 2.0 MeV
^{252}Cf
normalization point
Werle and Bluhm
Knitter et al
Condé and During
Green et al , fit
Kogelnikova et al
Aleksandrova et al
Jeki et al
(p-spectrometer)
(^{3}He-spectrometer)
(fission γ's)
(fission products)
E_n [MeV]
0.2
0.5
1
2
5
10

Fig. 1

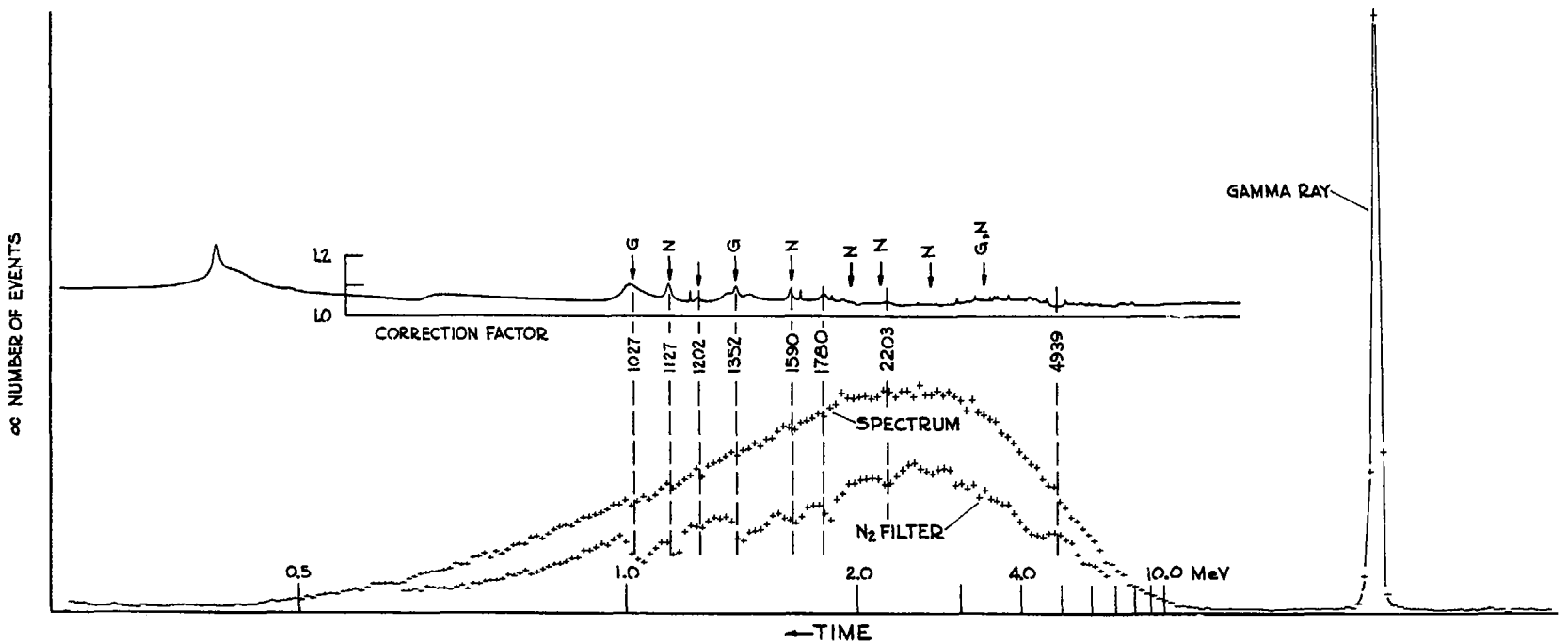
∝ NUMBER OF EVENTS
1.2
1.0
CORRECTION FACTOR
G
N
G
N
N
N
N
G,N
1027
1127
1202
1352
1590
1780
2203
4939
SPECTRUM
N2 FILTER
GAMMA RAY
0.5
1.0
2.0
4.0
10.0 MeV
TIME

Fig. 2

II.3. IN-PILE NEUTRON SPECTROMETRY: STATUS

G. De Leeuw-Gierts and S. De Leeuw,
Reactor Physics Dept.
C.E.N.-S.C.K., Mol, Belgium

Abstract:

The well assessed in-pile neutron spectrometry techniques are briefly reviewed and their status, advantages and drawbacks given. It is illustrated how systematic errors can arise and explain unexpected discrepancies between methods.

Those characteristics of the techniques that are mostly affected if optimal experimental conditions are not present, and the parameters that lead generally to inaccuracies, are put forward.

I. INTRODUCTION

It becomes more and more evident that an accurate knowledge of the neutron spectra at several locations in a reactor is necessary to be able to calculate its basic physical characteristics.
The reliability of the calculated spectra is directly related to the accuracy on the group cross sections of all the fuel and structural materials as well as to the computational methods and codes themselves; it can only be verified by comparison with experimental spectral data.

High accuracy is required over an energy range of 8 decades; ~ 100 eV → 10 MeV, to be able to predict with the required accuracy parameters as important as keff, breeding ratio.
Spectrum knowledge is also necessary for the determination of the Doppler effect, the calculation of the biological shields, damage, swelling ...

No single experimental method allows to obtain the required data from 100 eV up to 10 MeV with the target accuracy of 5 to 10 %. This accuracy can only be reached by comparison of the results of several experimenters and measurement techniques. The energy interval can be covered by the use of several methods. The in-pile differential methods cover only 3 to 4 energy decades and apply only in low power assemblies. The out of pile time of flight technique, sandwich foil and integral techniques cover the lower energy part of the spectrum and partially also the high energy range but in different experimental and nuclear conditions.

It is obvious that to reach the goal with the available experimental material a rigorous planning of the spectrum determination is necessary and that it is of the greatest importance to combine adequately several methods and to determine their design particularities so as to be able to relate accurately the partial results of each measurement.
The present paper will only deal with the status of in-pile differential neutron spectrometry techniques, a detailed description of the techniques being available in the literature.

II. SPECTRAL MEASUREMENTS

Spectrum measurements have been performed by several laboratories in critical or sub-critical facilities, in multiplying or non multiplying media.
Many measurements and intercomparisons of spectrometry methods are found for assemblies such as Vera, Zebra, Sneak, Suak, Stark, for ZPR and STSF facilities, for uranium slabs, iron or other structural materials.
In all these experiments it is assumed that the measurements were performed by specialists, having a full understanding of the technique and being familiar with all details and with all the parameters to survey all along the measurement.
Nevertheless important discrepancies, inconsistent with the accuracy claimed are observed in certain assemblies, while in other experimental facilities the same methods agree quite well.
The conclusions one may draw from it are that

1. performing a good measurement is a difficult task, systematic errors and/or non adequate or failing spectrometer or analysing devices playing an important role in it
2. the physical, neutronic and nuclear characteristics of the assembly should be much more taken into account in the planning of the measurements.

The importance of the design particularities of the assembly appears principally in the determination of the correction factors to apply, and in their evaluation because the physical and nuclear data of the reaction used for the measurement as well as the characteristics of the assembly have a strong impact on the measured spectrum.
The most important parameters for spectrum determination in a given assembly are :

the geometry and construction characteristics
angular differential neutron flux
leakages, γ-dose, power level, temperature
thermal or slow neutron component
mean energy of the neutron spectrum.

They will directly influence the choice of the detection modes and spectrometer characteristics, the most important ones being :

the design of the spectrometer in function of the measuring location
the detection efficiency and detection geometry
the approach of background measurement.

The energy range covered and the accuracy reached will depend on the adopted approach.

The energy validity limits and the reliability of the results over the energy range covered will finally be deduced not only from a careful analysis and interpretation of the measurement but also from a careful check of the adequacy of the correction factors in function of the design particularities of assembly and spectrometer. It is obvious, given the complexity of the techniques and their interaction with the characteristics of the assembly, that one may not rely upon one technique, nor upon one experimenter.

To estimate the ultimate accuracy that can really be reached in any assembly, one has to analyse the measurements done and to be done in following optics :

- In one assembly the use of several techniques allows to put forward the drawbacks, limitations and errors associated with the methods.
- The measurements with one or better several techniques in several facilities, very alike or completely different, allows the study of the errors related to the experimental conditions.

The creation of benchmarks seems to be a necessary step to quantify the relative role of the physical, neutronic and nuclear characteristics of the assembly itself in the interpretation of the measurement.

III. GENERAL REVIEW OF IN-PILE DIFFERENTIAL NEUTRON SPECTROMETRY TECHNIQUES

The experimental determination of in-pile neutron spectra is a hard job to do primarily because the severe requirement that the perturbation of the neutron population by the insertion of the spectrometer should be minimised and computable. This introduces an important restriction on the volume and the materials used for the detector head.

Practical methods allowing the determination of neutron energy spectra with high resolution are scarce and generally very sensitive to the previously mentioned characteristics of the assembly. The relative importance of the slow and fast neutron population plays a major role, the first group degrading the performance of the techniques, the second for its damage effects particularly if solid state detectors are used.
The volume restriction limits the viable spectrometers to a small number up to now : nuclear emulsions, small proportional counters, solid state detectors and a combination of both. The reactions allowing a highly accurate energy determination are limited to : (n,p) collision, $^{6}Li(n,\alpha)t$ and $^{3}He(n,p)t$ reactions.

A résumé of the acceptable experimental conditions for the measurement of neutron spectra with these methods is given in Table I together with the neutron energy range covered.
Measurements can be done in worse conditions but lead than to additional corrections and less accuracy. In addition each of these techniques has some peculiarities worthwhile to mention before attending their status :

(n,p) method : the spectrum is determined in several steps ;

^{6}Li method : although the cross section is a "Primary standard cross section" according to ENDF/B, the accuracy is still locally insufficient ;

^{3}He method : the insertion of a proton recoil counter between two solid state detectors makes the technique less straightforward ;

Nuclear emulsions : the method is time consuming or important investments for automatic scanning are necessary.

IV. STATUS OF THE (n,p), $^{6}Li(n,\alpha)t$ AND $^{3}He(n,p)t$ SPECTROMETRY TECHNIQUES

A. (n,p) spectrometry

The proton recoil neutron spectrometry has been applied for a long time. The most suited and perfected proton recoil detectors for in-pile measurements are the nuclear emulsions and small proportional counters. Presently the last one is mostly used.

Technique	ΔE_n	ϕ_S/ϕ_F	$d\phi/d$	nv	(nvt)	$\gamma_{accept.}$	$T_{accept.}$
Nucl. emuls (n,p)	400 keV - 10 MeV	Contamination $^{14}N(n,p)^{14}C$	-		(10^{10})	50 R	40°
^6Li	100 keV - 10 MeV	Epithermal peak	-		(10^{10})	100 R	
Prop.Counter (n,p)	10 keV - 2 MeV	Contamination N(n,p)C or $^3He(n,p)t$	Spherical Cylindrical: isotropic or known	10^5		$10^{-6}(Rh^{-1})/(ncm^{-2}s^{-1})$	
Solid state+PC(n,p) [1]	600 keV - 10 MeV	-	Cylindrical: isotropic	10^7	(5.10^{12})	$10^{-6}(Rh^{-1})/(ncm^{-2}s^{-1})$	25°
Solid state ^6Li	10 keV - 10 MeV	Epithermal peak	4π Collimated : isotropic or known	10^7	(5.10^{12})	$10^{-6}(Rh^{-1})/(ncm^{-2}s^{-1})$	25°
Solid state+PC^{3}He [2]	100 keV - 10 MeV	Epithermal peak	isotropic or known	5.10^6	(5.10^{12})	$10^{-6}(Rh^{-1})(ncm^{-2}s^{-1})$	25°

Table I - ACCEPTABLE EXPERIMENTAL CONDITIONS

The in-pile energy range covered by the small proportional counters, cylindrical or spherical, goes from ~ 5 to 10 keV up to 1.5 MeV. The fillings generally used to cover this energy range are 1 at, 2 at and 4 at H_2 , 2 and 4 at CH_4.
The partial energy ranges covered with these fillings and the accuracy reached will depend on the nuclear characteristics of the assembly, γ-dose, hardness of the spectrum, power ... and on the characteristics of the counter related to its design : wall and end-effects, effects due to electric field non-uniformity, energy dependence of W , general nuclear perturbations ...
In good experimental condtions 4 to 5 partial spectra lead to the final spectral shape.
To cover the part of the spectrum above 1.5 MeV, either counters filled with a gaz at higher pressure or with a gas mixture with higher stopping power, scintillator or solid state counters can be used. The assessment of these counters having not yet reached the same accuracy level as the previous ones mentioned, and because of their drawbacks (non linearity of the energy response, important neutron perturbation, sophistication) there is still a need for further research on them.

Although limiting us to measurements with well assessed techniques, important discrepancies between different experimenters or between successive measurements can be found in literature f.i.

- In [3] systematic errors related to erroneous normalisations of 20 % are reported to explain the differences between the Aldermaston and Harwell (n,p) measurements on Vera 7A. Systematic differences in hardness of the spectra are also mentioned between the Karlsruhe data on the nearly equivalent UHC assembly and the corrected Altermaston data.

- Large differences are also observed between two (n,p) spectral measurements in the CFRMF, performed by the same expert [4] ; the only differences between the two measurements being the intensity of the γ-dose, no modification of the neutronic field being cited.

- Differences between partial spectra in a common energy range, covered once with a H_2 filled counter, once with a CH_4 filled one are also mentioned [5].

- In the specialist meeting on Sensitivity Studies and Shielding Benchmarks (Paris 1975) differences in the overlapping regions of 25 % were quoted between results deduced from proportional counters operating at various pressures.

Reasons for these discrepancies are not evident and should be investigated to increase the accuracies on further measurements. It is not the aim here to make an analysis of the systematic studies performed on these counters [6,7,8] nor to compile the counter parameters subject to systematic errors, but it is intended to draw the attention, in few points, on how unexpected unaccuracies can result from the intimate relation between the assembly characteristics and the spectrometer response and from the shortcomings of the spectrometer itself, partly compensated by the introduction of correction factors.

- A fast neutron measurement must be preceded by a calibration measurement in a thermal neutron beam to determine the zero of the energy scale, the energy width of a channel and the resolution function. Either the $^{14}N(n,p)^{14}C$ or the $^{3}He(n,p)t$ reaction can be used for this purpose, by including a small amount of these gases in the counter, together with a pulser calibration.

Having in the (n,p) spectral shape no checkpoint opportunity to interprete the fast neutron measurement one has to rely fully on these data. The possibility of systematic errors resulting from this procedure is illustrated in following figures. In these examples, the adequacy and stability of the equipment are ensured by performing the measurements at the same place once with a thermal neutron source, once with a fast neutron source, and by the use of a continuous pulser measurement in the thermal and fast data recording. The importance of the only count rate parameter is put forward. Two power levels in the ratio 1 to 5 were used for the thermal calibration, using the N(n,p)C reaction. The dependency of the three parameters : zero, energy calibration and resolution function is evident (fig. 1).

Fig. 2 compares proton recoil spectra together with a check pulser peak, at 3 power levels in ratio's 1, 5 and 10. Zero, energy calibration and resolution function modifications are evident from the shape of the pulser peaks. Moreover, in the present set-up the apparently lowest validity limit is reached with the highest count rate, what for sure is impossible. Before starting a measurement, one should ensure in a preliminary experiment that the count rate at which this phenomenon would appear with the measuring system to be used is never reached.
The presence of fine structures, found in almost any neutron spectrum and generally due to reactor structural materials as O, Fe, Al furnishes a guarantee for adequate energy calibration and stated resolution function (fig. 3 [8]). The distortions in the neutron spectra one may expect from measurements performed in bad conditions are illustrated in fig. 4. Although statistics are low, the distortion of the spectra is evident, as well as the usefulness of the structures (here Fe) to display anomalies.

- Because of the absolute impossibility to detect erroneous results due to differential neutron flux anisotropies, as well as pile-up effects, it is of the greatest importance to consider the characteristics of the assembly before planning a measurement.

- The presence of a slow energy neutron component can also lead to systematic errors. In fig. 5 a proton recoil spectrum is reported, recorded in a neutron field where this component was sufficiently important to make it apparent.

- Errors can also be expected from the normalisation of the partial spectra. Accuracy on the energy calibration, stability of power level, dead times in the analysing system, accuracy of the filling, are all parameters important for the normalisation.
If normalisation is done by overlapping, count rates should be hold critically in mind, distortions appearing mostly at the end parts of the spectra.

- For CH_4 filled counters, the carbon correction, highly approximated, should be taken into account, together with the hardness of the spectrum, to determine the lower energy validity limit. Specific problems for CH_4

filled counters related to energy calibration have also been reported in literature [7] .

From these few remarks it is obvious that sufficient reasons can exist to have discrepancies, or systematic errors, decreasing the accuracy up to ~ 25 %. On the other hand, the mentioned counters, well assessed, can lead in favourable experimental conditions to spectra in much better agreement.

B. $^{6}Li(n,\alpha)t$

The $^{6}Li(n,\alpha)t$ reaction was also used from the first attempts to determine neutron spectra. At the earliest stage of development the lithium was mostly used loaded in nuclear emulsions and when solid state detectors became available, as a target sandwiched between two of them. In the beginning the neutron energy was deduced from the sum of the energies of the emitted α and triton particles : with nuclear emulsions by measuring the length of both tracks [9], with solid state detectors by summing the energy deposited in each detector [10] .

The spectrum is also deducible from the triton energy distribution and with important advantages as is seen from the theoretical analysis of the reaction.

From the laws of conservation of energy and momentum, following relations are deduced :

$$(1)\quad E_\alpha + E_t = Q + E_n$$

$$(2)\quad E_t = \left[\frac{\sqrt{M_n M_t E_n}}{M_\alpha + M_t} \cos\theta + \sqrt{\frac{M_n M_t E_n}{(M_\alpha + M_t)^2} \cos^2\theta + \frac{M_\alpha Q + E_n (M_\alpha - M_n)}{M_\alpha + M_t}} \right]^2$$

with E_α : energy of the α particle

E_t : energy of the triton

E_n : neutron energy

Q : 4.787 MeV energy released

M_n, M_α and M_t : masses respectively of the neutron, alpha and triton

θ, θ^* : angle between the neutron and triton respectively in laboratory and CM coordinates.

Figure 6 shows E_t and E_α as function of E_n for $\theta^* = \theta°$, 90° and 180° . For the application of the E_t method it is important to note that :

1) for low neutron energies, the energy of the triton, emitted forward, increases by a larger amount than the neutron energy itself, e.g. : for E_n = 25 and 50 keV, the increase in triton energy at $\theta^* = 0°$ equals 144 and 212 keV.
2) the minimum triton energy is 2.382 MeV, corresponding to E_n= 810 keV, θ^*= 180° ; the minimum α energy is 1.595 MeV corresponding to E_n = 1.695 MeV, $\theta^* = 0°$.

The $E_\alpha + E_t$ is a direct parameter, E_t is an indirect parameter : to one neutron energy corresponds a distribution of triton energies as in the (n,p) case. As a consequence : to interprete the $E_\alpha + E_t$ distribution only the (n,α) cross section must be well known, while for E_t the mono-energetic responses ($\frac{d\sigma}{d\Omega}$ data) are needed for the interpretation.
In figure 7 a few monoenergetic triton distributions $S(E_t/E_n)$ are drawn. The fact that the angular triton distributions are forward peaked, is very favourable to the use of E_t for neutron spectrometry purposes.
A review of the ^{6}Li technique was presented at the First ASTM-EURATOM Meeting held at Petten (September 1975) [11]. It is described how by the simultaneous analysis of the two solid state detector responses (E_t distributions) and of the sum response ($E_\alpha + E_t$ distribution) one can determine the neutron spectrum from a few keV up to several MeV without unaccuracies related to normalisations of partial spectra. The neutron spectrum deduced from the triton distributions goes from ~ 5 keV up to ~ 700 keV, from the sum from ~ 600 keV → several MeV [12] .

In their common energy region, the (n,p) and the ^{6}Li(n,α)t methods are in a certain way complementary. Indeed, several characteristics of the assembly that may lead to systematic errors in the (n,p) method can be displayed with the Li-6 technique and consequently avoided, on the other hand the Li-6 method is more susceptible to systematic errors related to the analysing system itself if not carefully applied.

Few examples of both statements will be illustrated.

- The impact of the assembly on the measured spectra is displayed in following figures.

- E_t spectra recorded in a too high γ field are drawn in fig. 8. The differences between both spectra, respectively measured at a power level of 5 kW and 10 kW illustrate very well that the distortion due to pile-up cannot be ignored.

- With the Li-6 method the anisotropy of the neutron field can be displayed. In an isotropic neutron flux, the triton responses of both detectors are identical, in a collimated or 2π detection mode (fig. 9).
  For a 2π detection mode forward-backward differences in spectra induce two different triton energy responses (fig. 10). In a collimated detection mode still more distorted responses are recorded if the neutron field is not isotropic. In this case the deduced neutron spectra are only approximate if the angular neutron distribution is not introduced in the unfolding code. Fig. 11 shows the spectra deduced from the two E_t distributions recorded in a highly anisotropic field.

- The importance of the temperature of the assembly is illustrated in fig. 12. Both spectra were recorded at the same place but at different temperatures. It is very important to take this characteristic into account if the thermal neutron calibration and the fast neutron measurement are not performed at the same temperature.

- As for the (n,p) measurements, fine structures furnish here too a complementary guarantee on the reliability of the results.
  The high resolution measurement drawn in fig. 13 displays very well structures compatible with the cross section of the Al present in the assembly.

- The presence of a slow neutron energy component is reflected in the triton spectrum by the presence of a peak similar to the thermal calibration peak. Here the neutron spectrum is not perturbed but the lower energy validity limit is raised.

- Systematic errors due to parameters related to the complexity of the method, the damaging of the detectors by the fast neutrons, to intermittent

failures of the electronic equipment, are possible as is with any technique, but become readily apparent during the analysis of the data.
To survey and follow damaging of the detector f.i. measurements are done in sequence. This allows also to adjust the polarisation of the detectors when the inverse current increases, so as to keep the depletion depth constant.

- Errors in the energy calibration are displayed when the 4 ADC responses are compared [11] .
  The use of 4 ADC's also allows to avoid errors such as the one encountered in the older MOL-ΣΣ measurement, where a failure occurred in the two parameter analyser; singles were lost when above the upper-edge of the region of interest.

- A striking example of a systematic error that may be made if the technique is only partially exploited is given in fig. 14. Here (curve 2) the lower level of the CFTD of the coincidence circuit was set too high, so as to cut part of the backward emitted α-particles.

- The analysis of two parameter distributions (E_t, $E_\alpha + E_t$) showed that the higher energy validity limit of the triton distribution is related to the importance of the α-response, generally negligible below 650 to 700 keV neutron energy for fast reactor type spectra.

- Supplementary errors could also come from unaccurate background substraction. Indeed as for the (n,p) measurements there are no checkpoints allowing to assume that no shifts appeared and energy calibration must rely on pulser peaks. By the insertion of an α-source, or by the two deposit techniques, these errors can be avoided.

- When comparing the $^6Li(n,\alpha)t$ and the (n,p) results, a systematic underestimation of the Li-data at 250 keV is evident (fig. 15). This can be explained by the fact that the resolution function is not perfectly unfolded and because of cross section uncertainties. This underestimation is of the order of 10 to 20 % between 200 and 300 keV. The part due to partial unfolding can be reduced to below 5 % if an approximate knowledge of the shape of the spectrum in this region is assumed.
  The angular differential cross sections are presently well known above

100 keV [14] . The improvement in the data, as compared to an unfolding performed with the theoretical R Matrix fitting the Martin's data [14] is shown in fig. 16, together with the comparison of the monoenergetic responses at 700 keV used for both interpretations. More experimental $\frac{d\sigma}{d\Omega}$ results below 100 keV are desirable.

As for the (n,p) spectrometry it is evident that systematic errors are possible, but, if the experiment is carefully made, they can be avoided, except of course for what concerns cross section unaccuracies.

With the present status of the (n,p) and $^{6}Li(n,\alpha)t$ techniques and if the experiment is well planned in function of the assembly characteristics, it is possible to determine a neutron spectrum, with errors of $\pm$ 10 % in energy intervals compatible with the resolution function of the spectrometer. By collapsing the energy intervals this error can be reduced.

C. $^{3}He(n,p)t$ semi-conductor spectrometer

Most of the remarks on the $^{6}Li(n,\alpha)t$ semi-conductor spectrometer apply also for ^{3}He spectrometer but with less cross check opportunities.
The neutron energy is here deduced only from the sum of the energies of the simultaneously emitted proton and triton particules. Because of the low Q value and high sensitivity to γ-rays, only a ^{3}He spectrometer, composed by two solid state detectors within between a miniaturized proportional counter, is well suited for in-pile measurements [2] . The proportional counter allows to discriminate the γ-background and to correct for the energy losses of the protons and tritons in the ^{3}He-gas.
In favourable conditions good agreement is obtained between (n,p) and $^{3}He(n,p)t$ results [15] .
If there was not the high degree of sophistication, ^{3}He spectrometers would probably give the most accurate results between 100 keV and 1 MeV, due to the high reaction cross-section.
Unfortunately because of the unfavourable reaction characteristics i.e. $E_t \rightarrow 0$ if $E_n \rightarrow \infty$ and $\theta + \phi \rightarrow 90°$ if $E_n \rightarrow \infty$ with $\theta + \phi = f(\theta)$, except for isotropic energy independent neutron distributions or for beam geometry,

the calculation of the geometrical efficiency is easily subject to systematic errors. The exact angular neutron distribution should be known as a function of energy.

V. CONCLUSION

The (n,p), $^{6}Li(n,\alpha)t$ and $^{3}He(n,p)t$ spectrometers attained a stage of development that allows to approach the spectral requirements between 10 keV and ~ 6 MeV, if at least two of the techniques are applied in experimental conditions close to those specified.

Because of the complexity, different but as important for each of these techniques, systematic errors can arise if not carefully applied. Moreover, to ensure the reliability of a measurement one has to critically consider the possible impacts of the assembly characteristics on the measurement and more especially on the correction factors. A universal solution does not exist, so that the planning and operational set up of the experiment is almost as important as the measurement itself.

REFERENCES

[1] DE LEEUW-GIERTS G., DE LEEUW S.
BLG 481 (1972) Annual Scientific Report 4 - 67
BLG 454 (1971).

[2] BLUHM H.
KFK 1798 (1973).

[3] KEMSHALL C.D. et al.
IAEA Specialist's Meeting
Fast Reactor Spectrum Measurements and their Interpretation
ANL 10-13 Nov. 1970.

[4] ROGERS JW
- Nuclear Technology Vol. 25 n° 2 (1975) 330-348
- First ASTM-EURATOM Symposium on Reactor Dosimetry
Petten Sept. 1975.

[5] BLUHM H. et al.
KFK 1658 RCN 172 BLG 471.

[6] - BENNETT E.F.
Nucl. Sci. Eng., 27, 16 (1967)

- BENNETT E.F., GOLD R. and OLSON J.K.
ANL - 7394 (1968).

- BENJAMIN P.W. et al.
AWRE N° 09/68 (1968).

[7] KEMSHALL C.D.
AWRE N° 031/73 (1973).

[8] VERBINSKI V.V. and GIOVANNI R.
Nucl. Instr. and Methods 114 (1974) 205-231.

[9] ROBERTS J.H., KINNEY F.E.
Rev. Sc. Instr. 28, 610 (1957).

[10] LOVE T.A., MURRAY R.B.
IRE Trans. Nucl. Science NS-8(1) : 91 (1961).

[11] DE LEEUW-GIERTS G., DE LEEUW S.
First ASTM-EURATOM Symposium on Reactor Dosimetry
Petten Sept. 22-26, 1975.

[12] DE LEEUW-GIERTS G., DE LEEUW S.
to be published in Nuclear Science and Engineering.

[13] OVERLEY J.C. et al.
Nucl. Phys. A 221 (1974) 573-592.

[14] BLUET J.C. et al.
1964, Internal Report "Centre d'Etudes Nucléaires de Cadarache"
1965, Proc. Int. Conf. on the study of Nuclear Structure with neutrons, Antwerp.

[15] WERLE H., BLUHM H., FIEG G.
First ASTM-EURATOM Symposium on Reactor Dosimetry
Petten Sept. 22-26, 1975.

[16] DE LEEUW-GIERTS G. et al.
Neutron Spectrum of Bigten by lithium-6 spectrometry. To be published.

[17] POENITZ W.P.
- Physik 268, 359-364 (1974)
- Private communication.

[18] SCHRODER IG et al.
- Conference on Nuclear Cross sections and Technology
Washington D.C. March 1975.
- Private communication.

FIGURES

Fig. 1. Thermal neutron calibration of a proton recoil proportional counter at two power levels.

Fig. 2. Proton recoil spectra recorded at three power levels with a simultaneously recorded pulser peak.

Fig. 3. Spectrum with fine structures from [8].

Fig. 4. Neutron spectra deduced from the proton recoil spectra of Fig. 2 by means of the Spec 4 code.

Fig. 5. Proton recoil spectrum with a slow $^{14}N(n,p)^{14}C$ component.

Fig. 6. Cinematics of the $^{6}Li(n,\alpha)t$ reaction.

Fig. 7. Theoretical monoenergetic triton responses for E_n = 20, 100, 200, 500 and 1000 keV.

Fig. 8. Distorted E_t spectra recorded in a high γ-field at two power levels.

Fig. 9. Comparison of the neutron spectra deduced from both E_t solid state detector responses in an isotropic neutron field [16].

Fig. 10. Comparison of the neutron spectra deduced from the two E_t solid state detector responses recorded in a 2 π detection mode, displaying a forward-backward energy dependent anisotropy.

Fig. 11. Neutron spectra deduced from the two E_t distributions recorded in an highly anisotropic neutron distribution.

Fig. 12. Shifts due to temperature variations.

Fig. 13. High resolution $E_\alpha + E_t$ measurement displaying structures compatible with the Al total cross section.

Fig. 14. Influence of the CFTD trigger level on the triton distribution [12].

Fig. 15. Comparison of the neutron spectra in MOL-ΣΣ deduced respectively from the ^{6}Li and (n,p) spectrometry techniques.

Fig. 16. Comparison of neutron spectra deduced from an E_t distribution with the Mol and [14] cross section set and the Poenitz-Overley-Schröder set [17, 18].

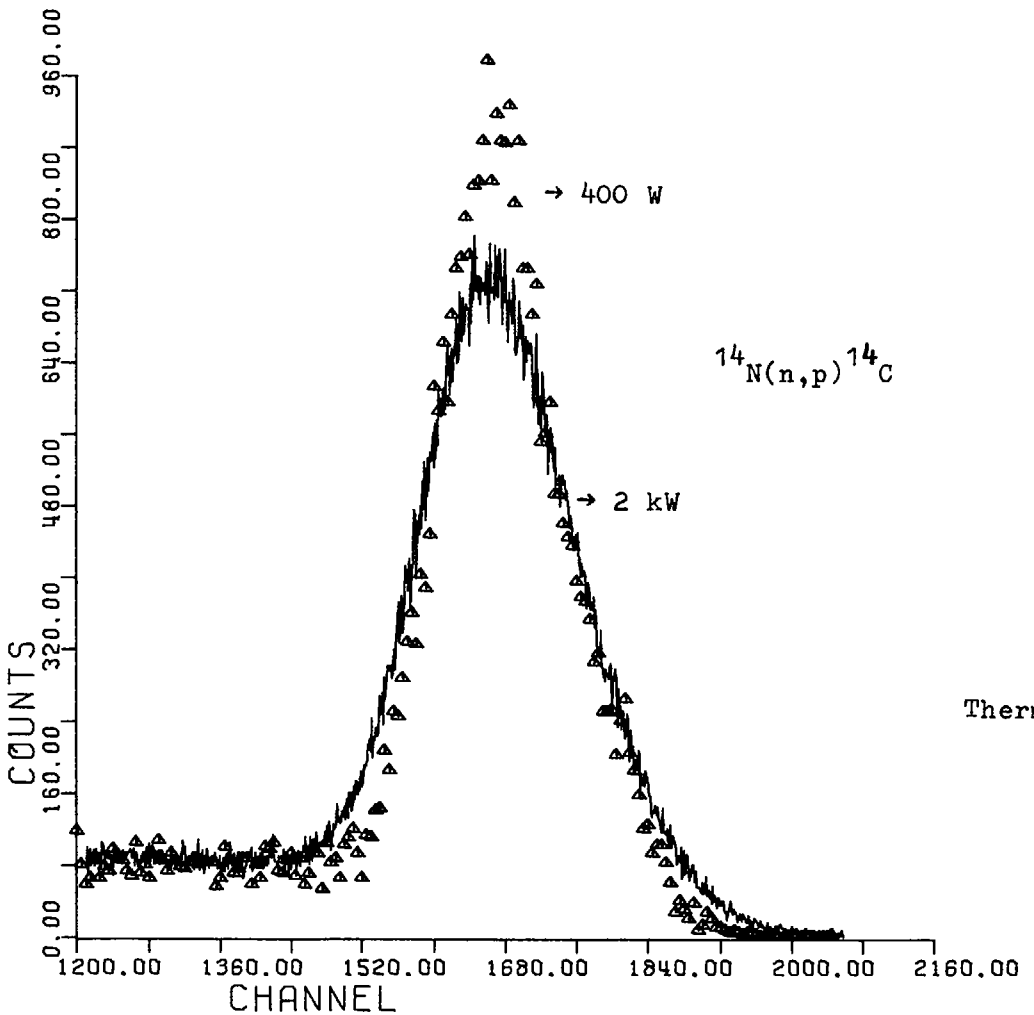

Thermal calibration

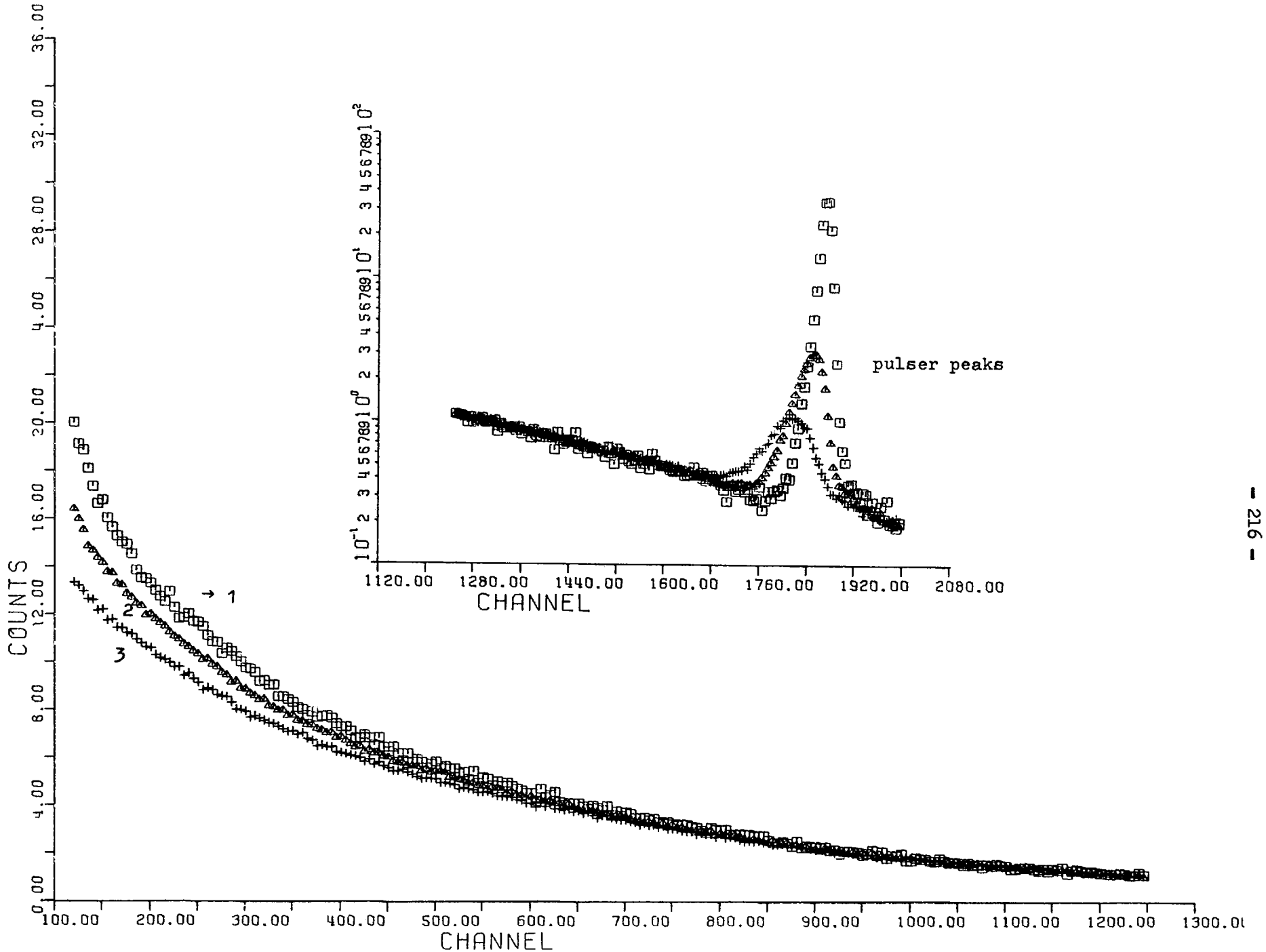
COUNTS
CHANNEL
pulser peaks
1
2
3

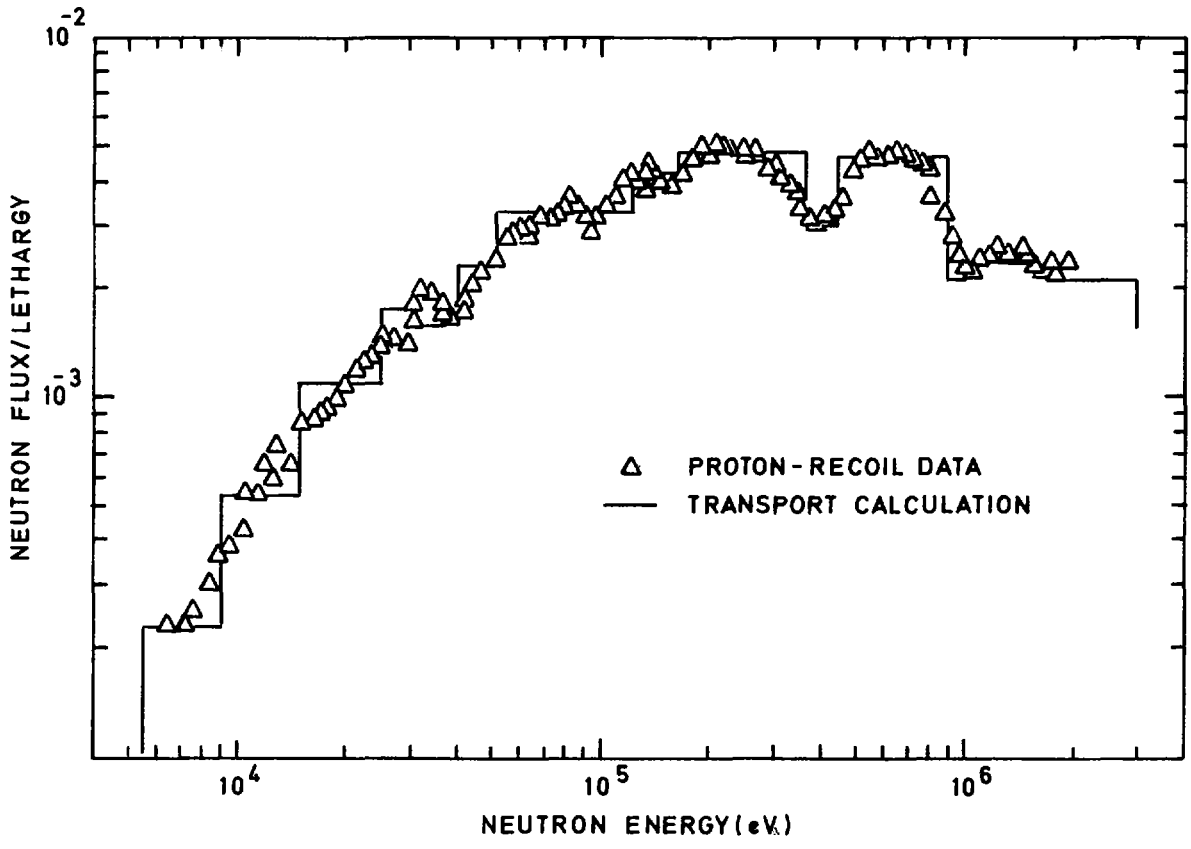
10^{-2}
10^{-3}
NEUTRON FLUX/LETHARGY
PROTON-RECOIL DATA
TRANSPORT CALCULATION
10^4
10^5
10^6
NEUTRON ENERGY(eV)

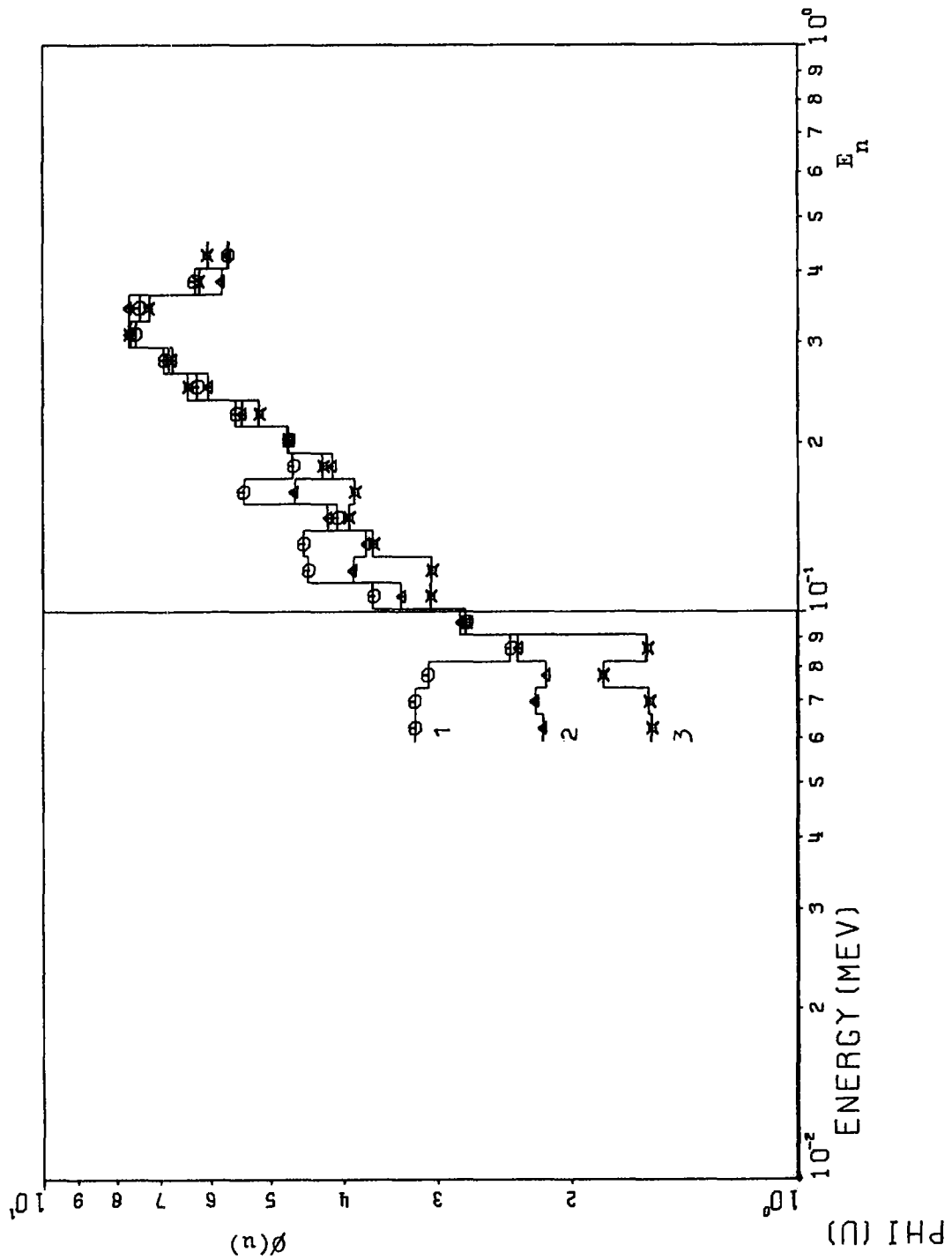
PHI (U)
ENERGY (MEV)
E_n
$\phi(u)$
1
2
3

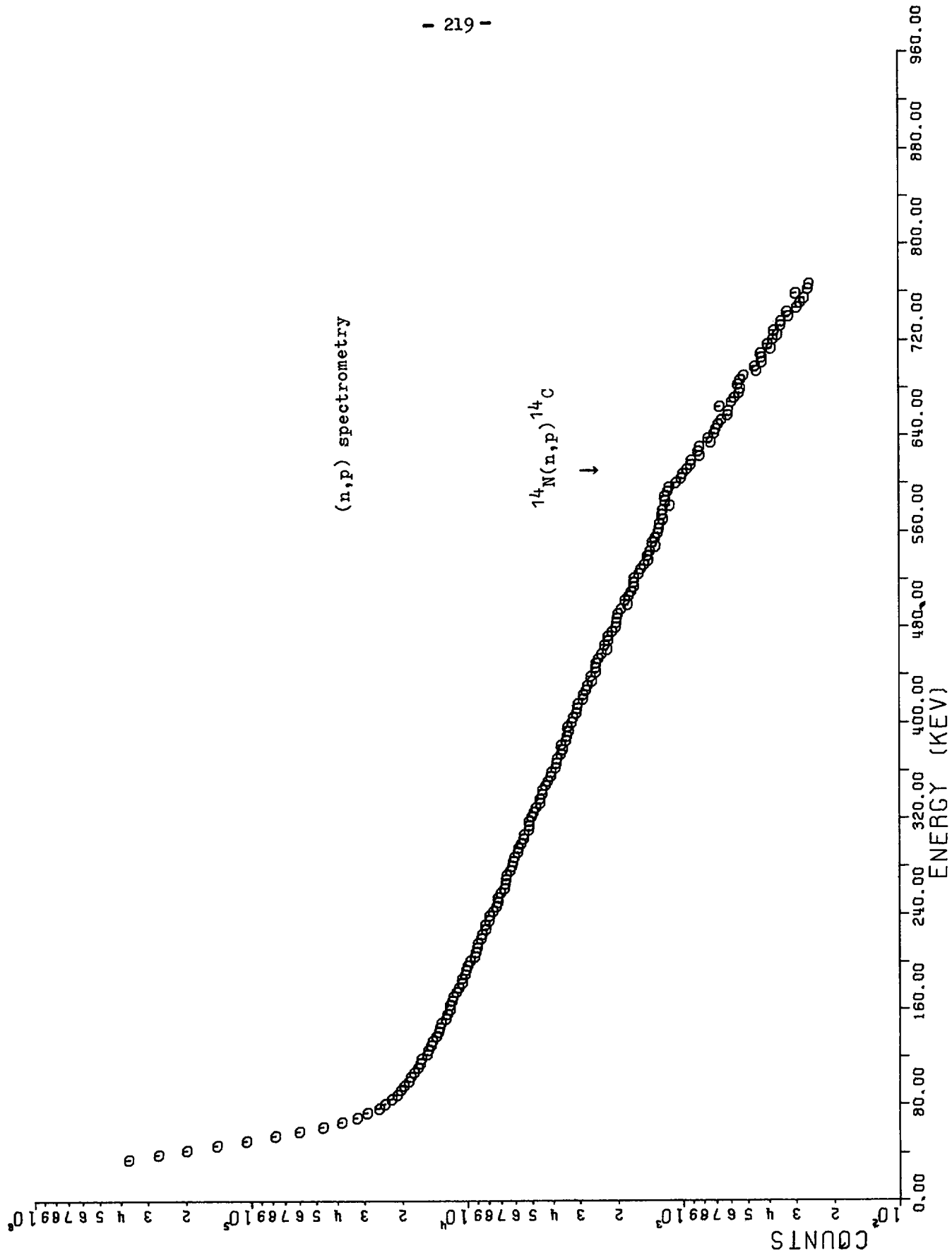
(n,p) spectrometry
$^{14}N(n,p)^{14}C$
COUNTS
ENERGY (KEV)
0.00
80.00
160.00
240.00
320.00
400.00
480.00
560.00
640.00
720.00
800.00
880.00
960.00

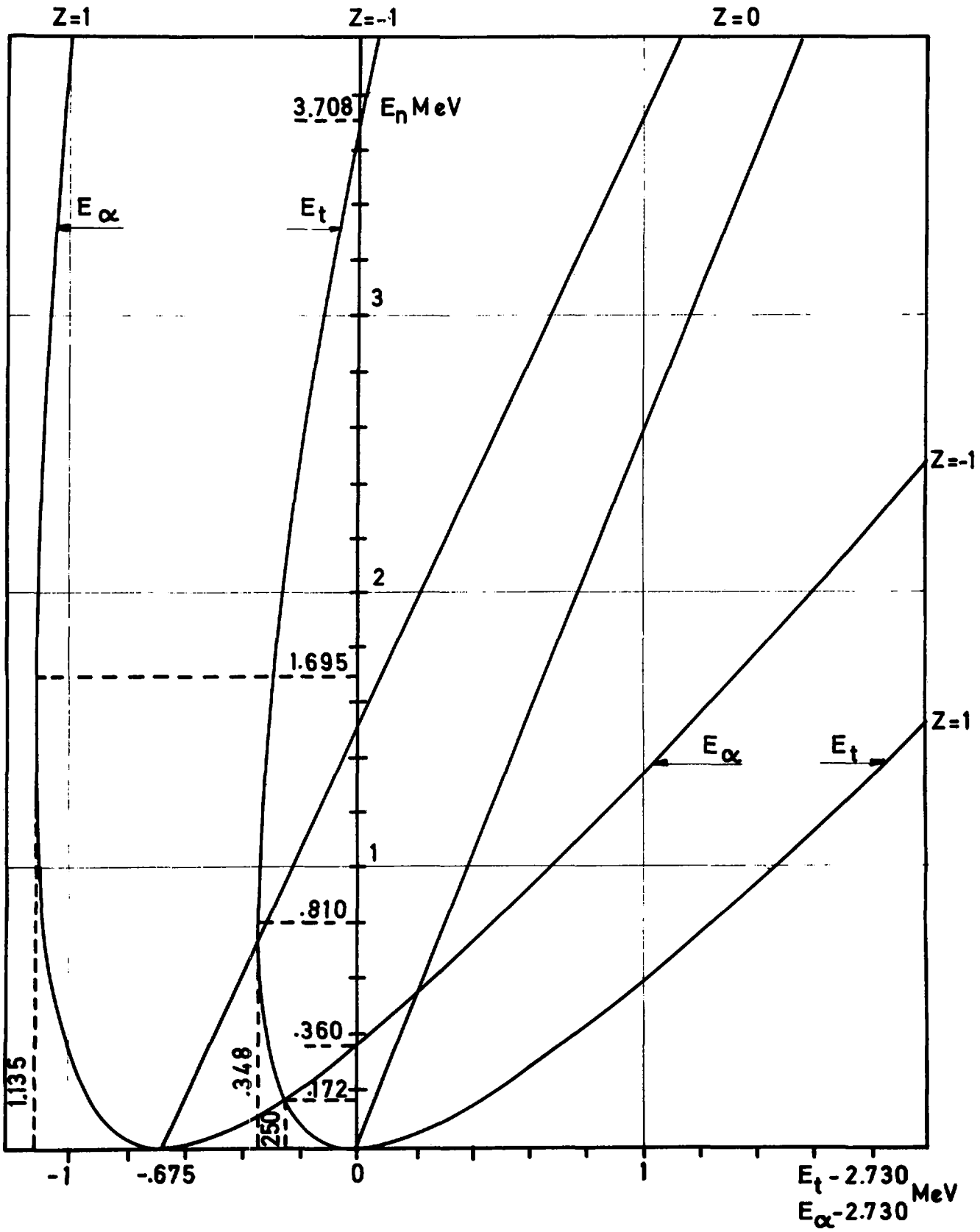
Z=1
Z=-1
Z=0
3.708
E_n MeV
E_α
E_t
3
2
1.695
1
.810
.360
.172
.348
.250
1.135
Z=-1
Z=1
E_α
E_t
-1
-.675
0
1
E_t - 2.730
E_α-2.730
MeV

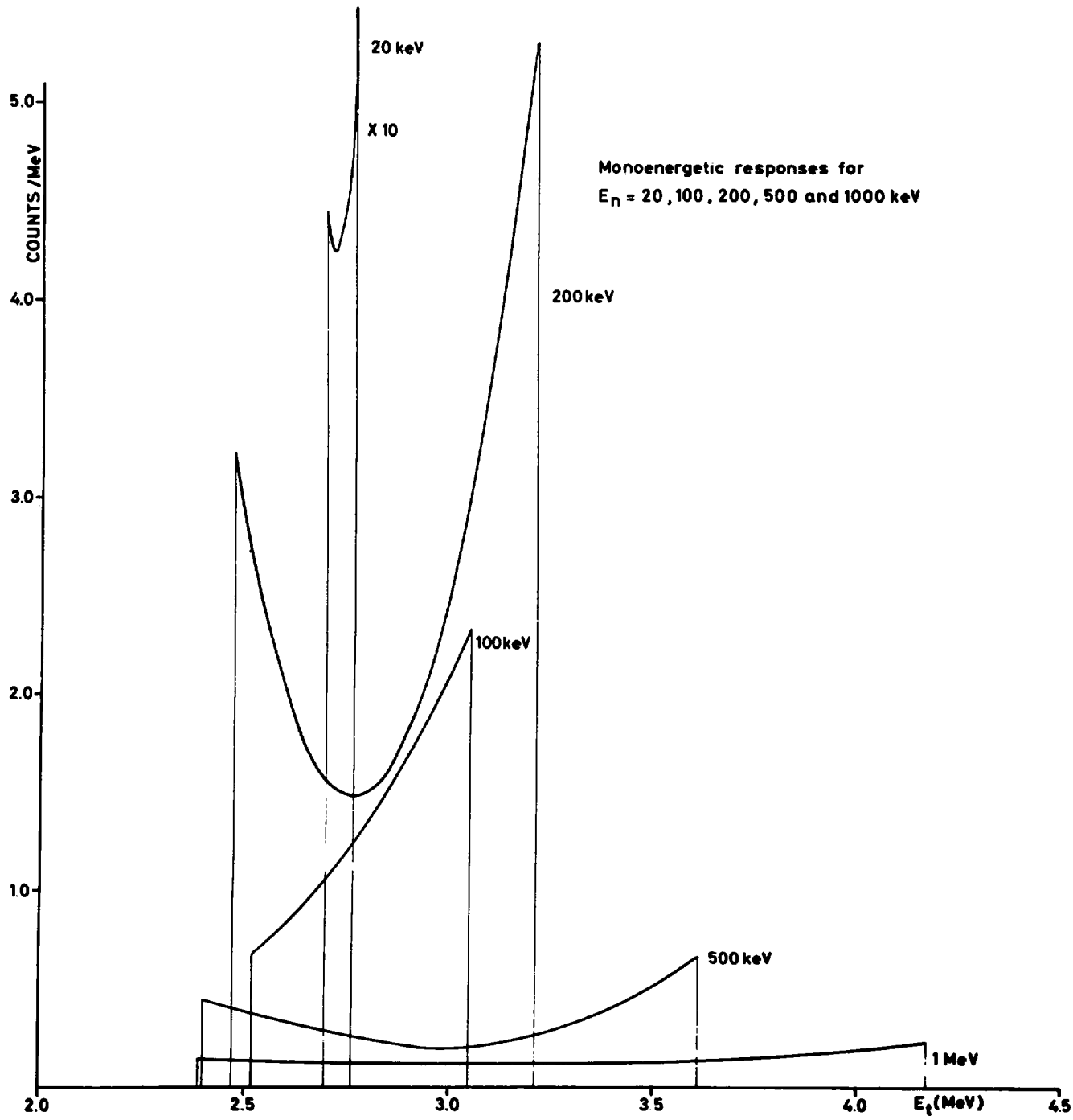
20 keV
X 10
Monoenergetic responses for
E_n = 20, 100, 200, 500 and 1000 keV
200 keV
100 keV
500 keV
1 MeV
COUNTS/MeV
5.0
4.0
3.0
2.0
1.0
2.0
2.5
3.0
3.5
4.0
4.5
E_t(MeV)

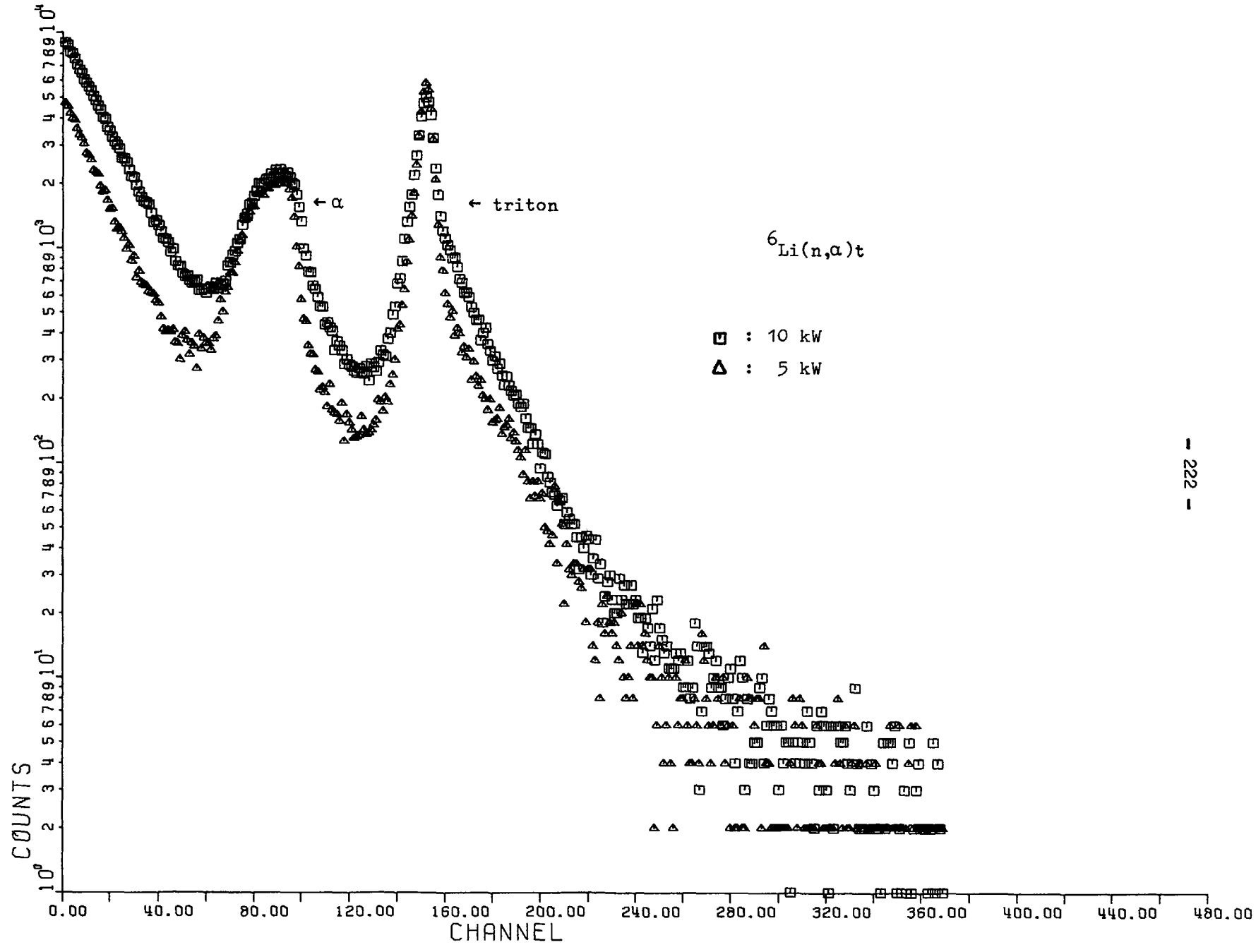
← α
← triton
^{6}Li(n,α)t
□ : 10 kW
△ : 5 kW
COUNTS
CHANNEL
0.00
40.00
80.00
120.00
160.00
200.00
240.00
280.00
320.00
360.00
400.00
440.00
480.00

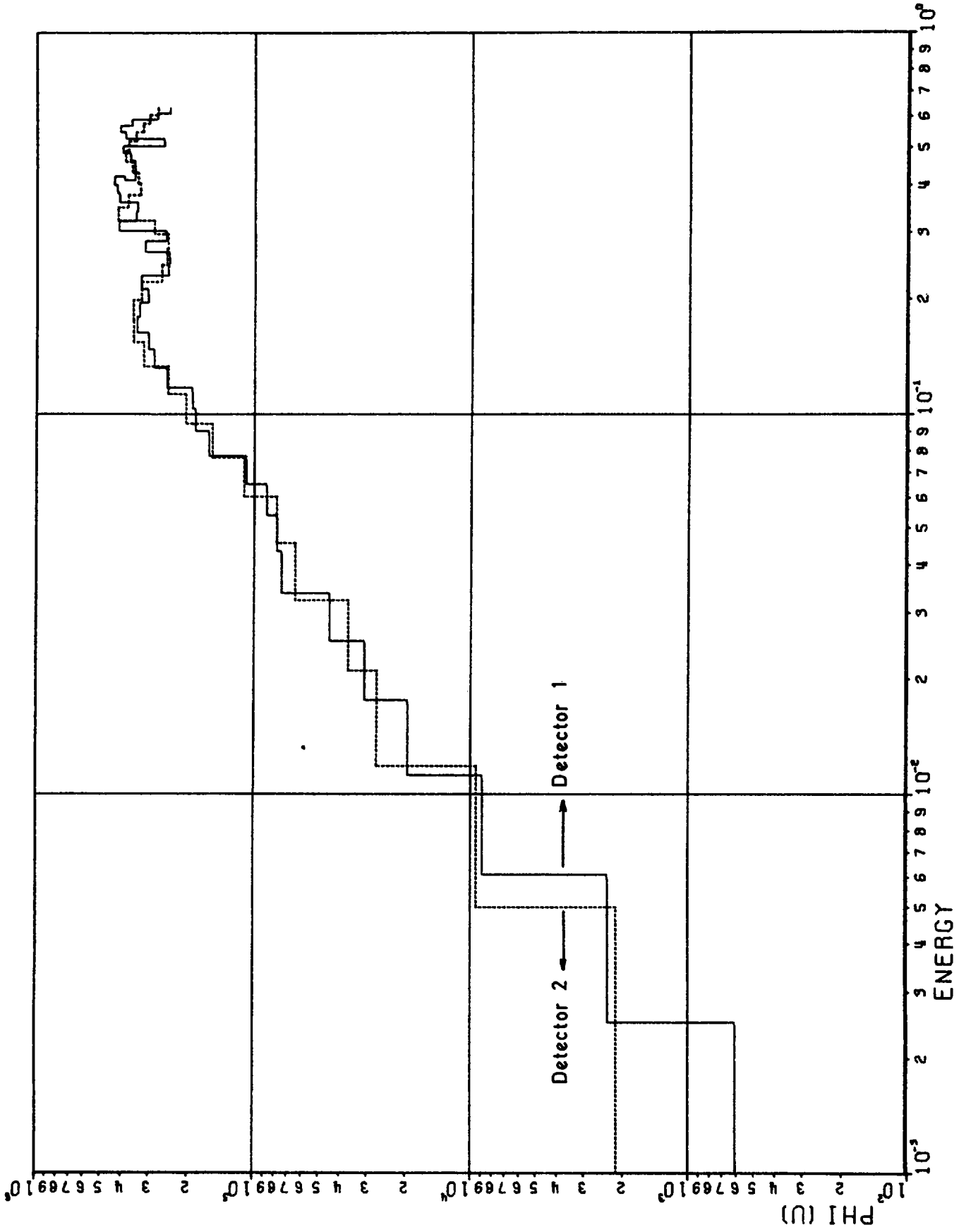
Detector 1
Detector 2
ENERGY
PHI (U)

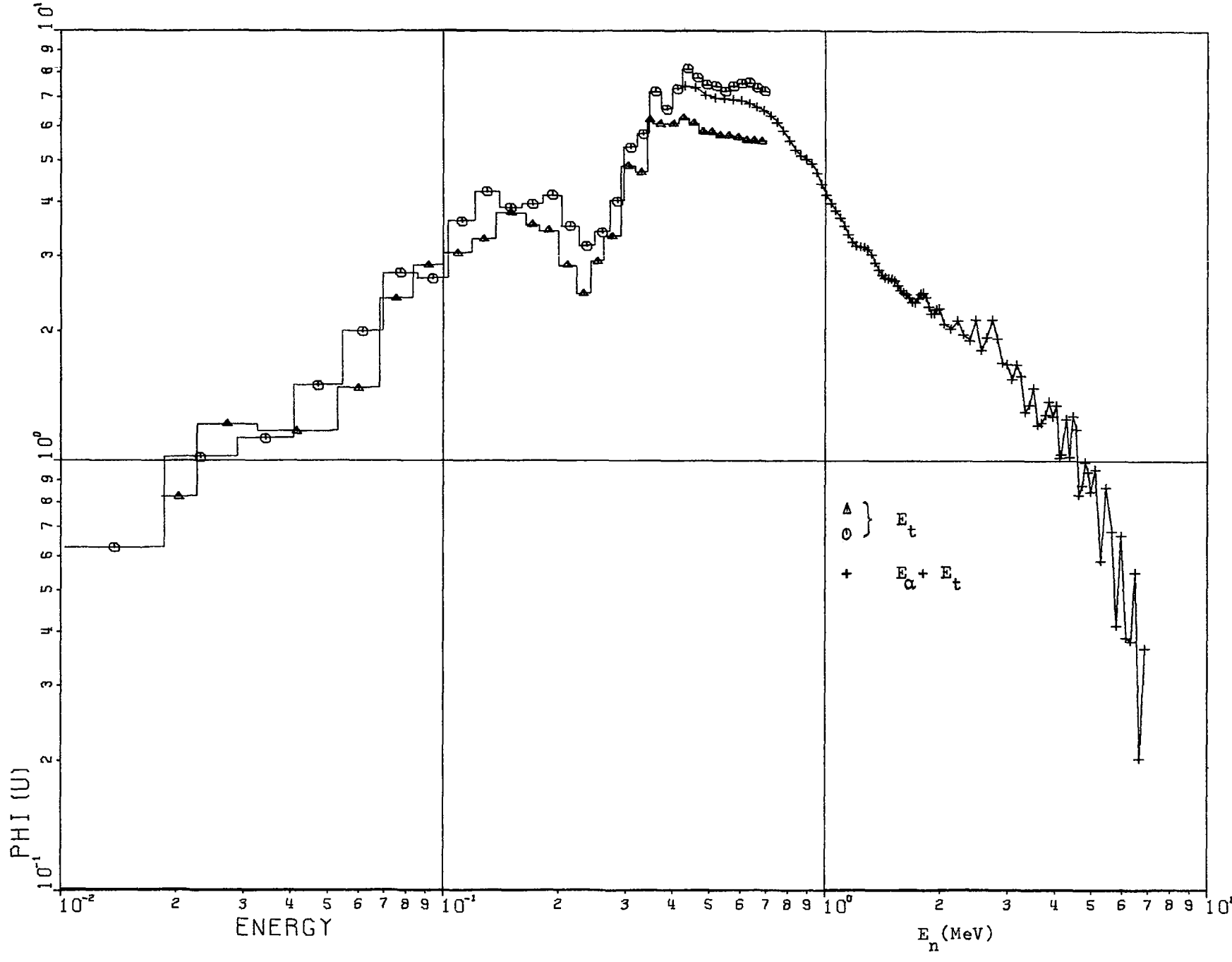
PHI (U)
ENERGY
E_n (MeV)
E_t
$E_a + E_t$

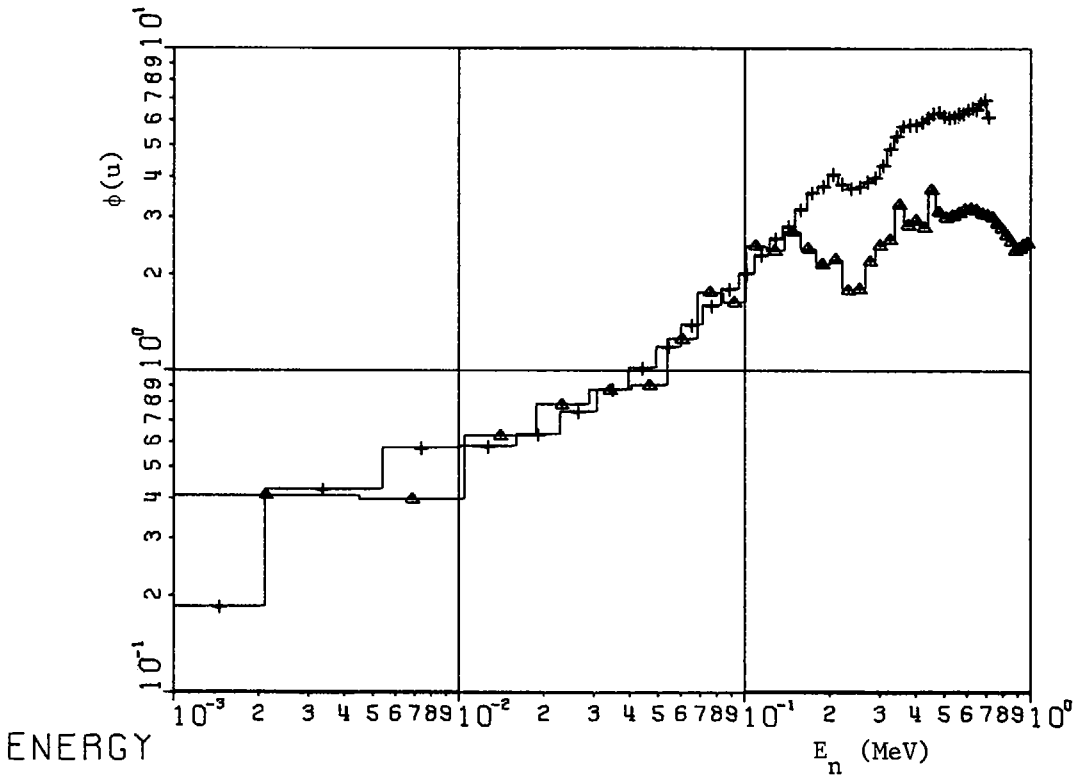
ENERGY
$\phi(u)$
10^{-1} 2 3 4 5 6 7 8 9 10^{0} 2 3 4 5 6 7 8 9 10^{1}
10^{-3} 2 3 4 5 6 7 8 9 10^{-2} 2 3 4 5 6 7 8 9 10^{-1} 2 3 4 5 6 7 8 9 10^{0}
E_n (MeV)

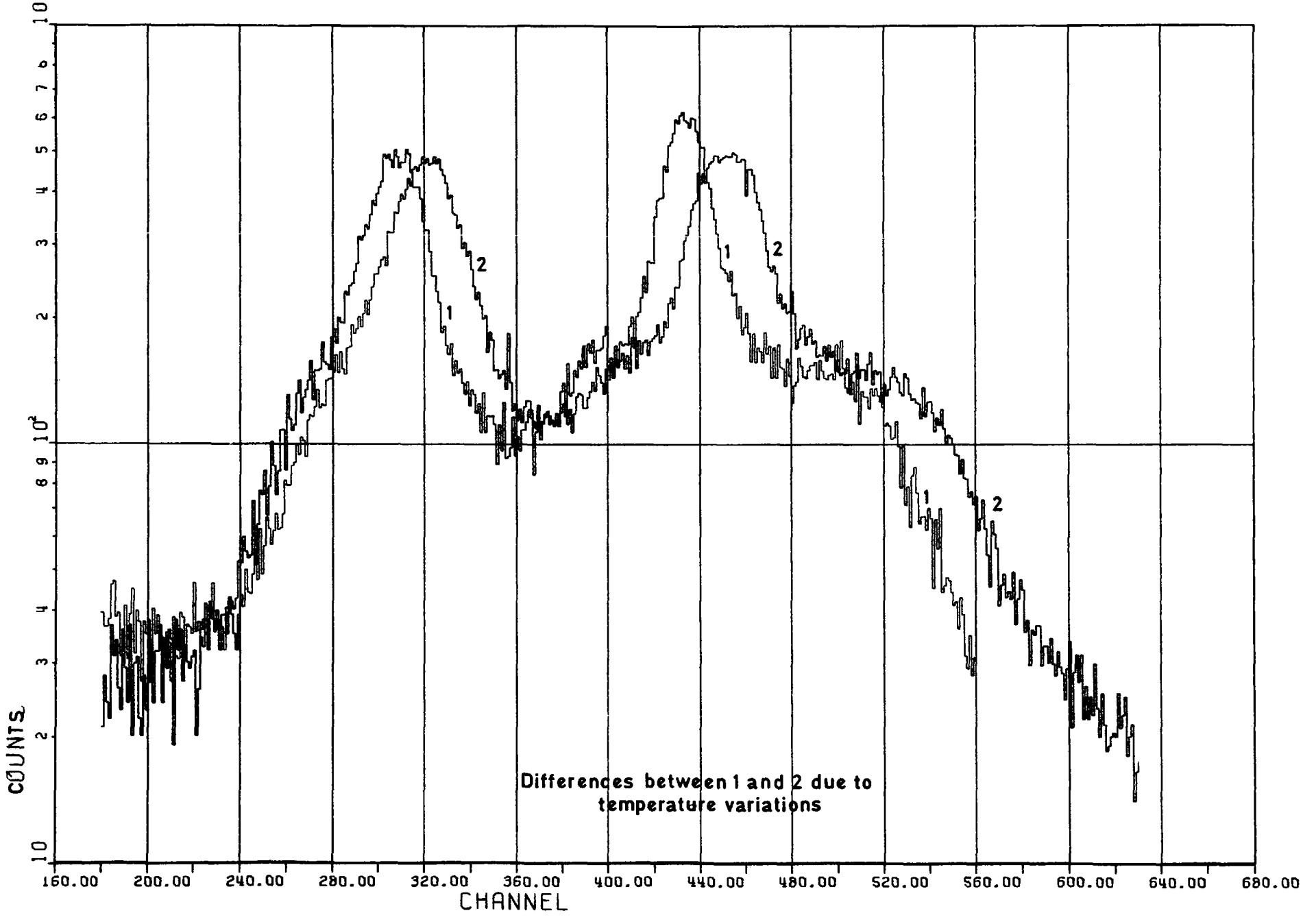
COUNTS
CHANNEL
160.00
200.00
240.00
280.00
320.00
360.00
400.00
440.00
480.00
520.00
560.00
600.00
640.00
680.00
1
2
Differences between 1 and 2 due to
temperature variations

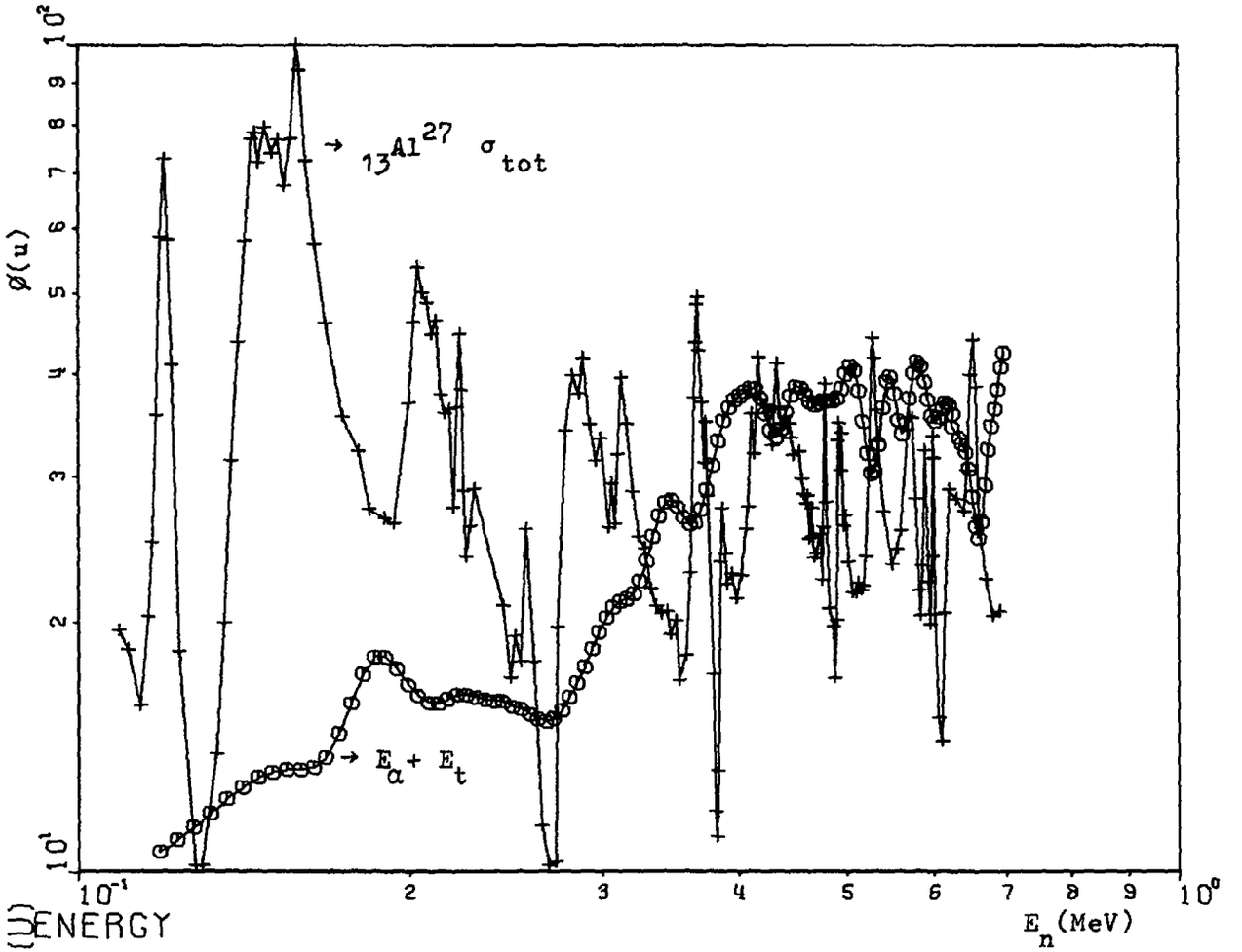

E ALPHA +E(T) DISTR. +SIGMA TOTAL VON AL 27

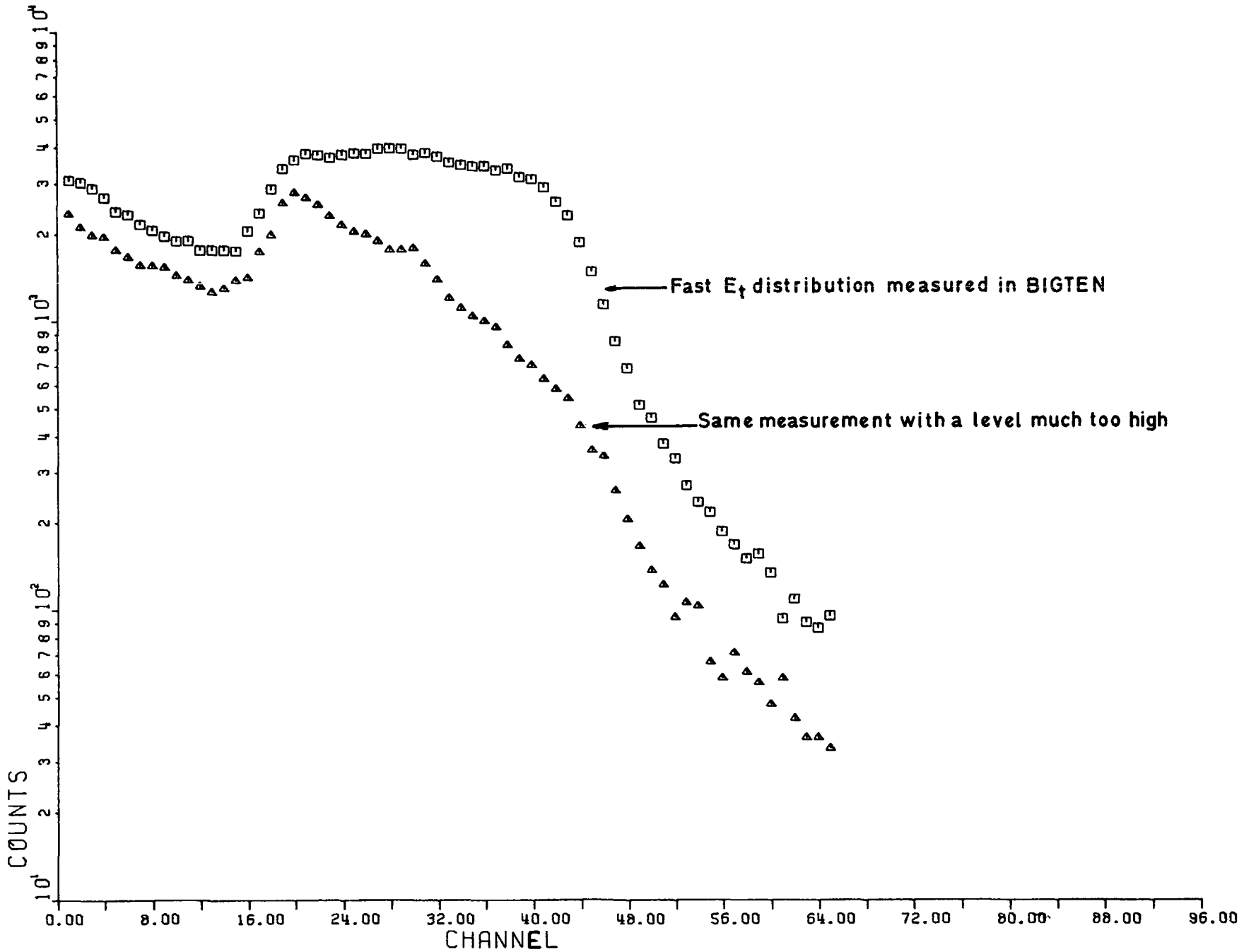
Fast E_t distribution measured in BIGTEN
Same measurement with a level much too high
COUNTS
CHANNEL
0.00
8.00
16.00
24.00
32.00
40.00
48.00
56.00
64.00
72.00
80.00
88.00
96.00

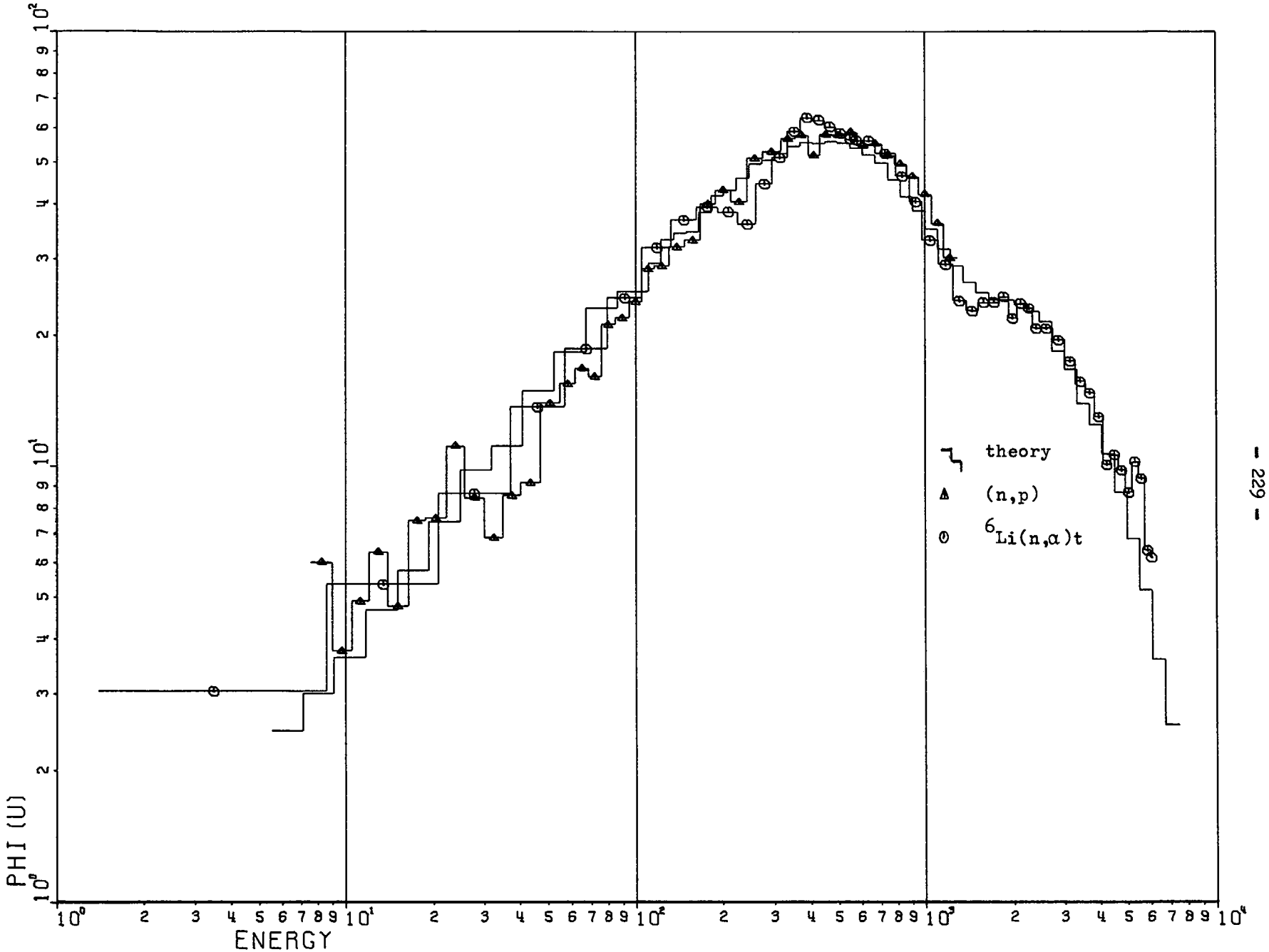
PHI (U)
ENERGY
theory
(n,p)
^{6}Li(n,α)t

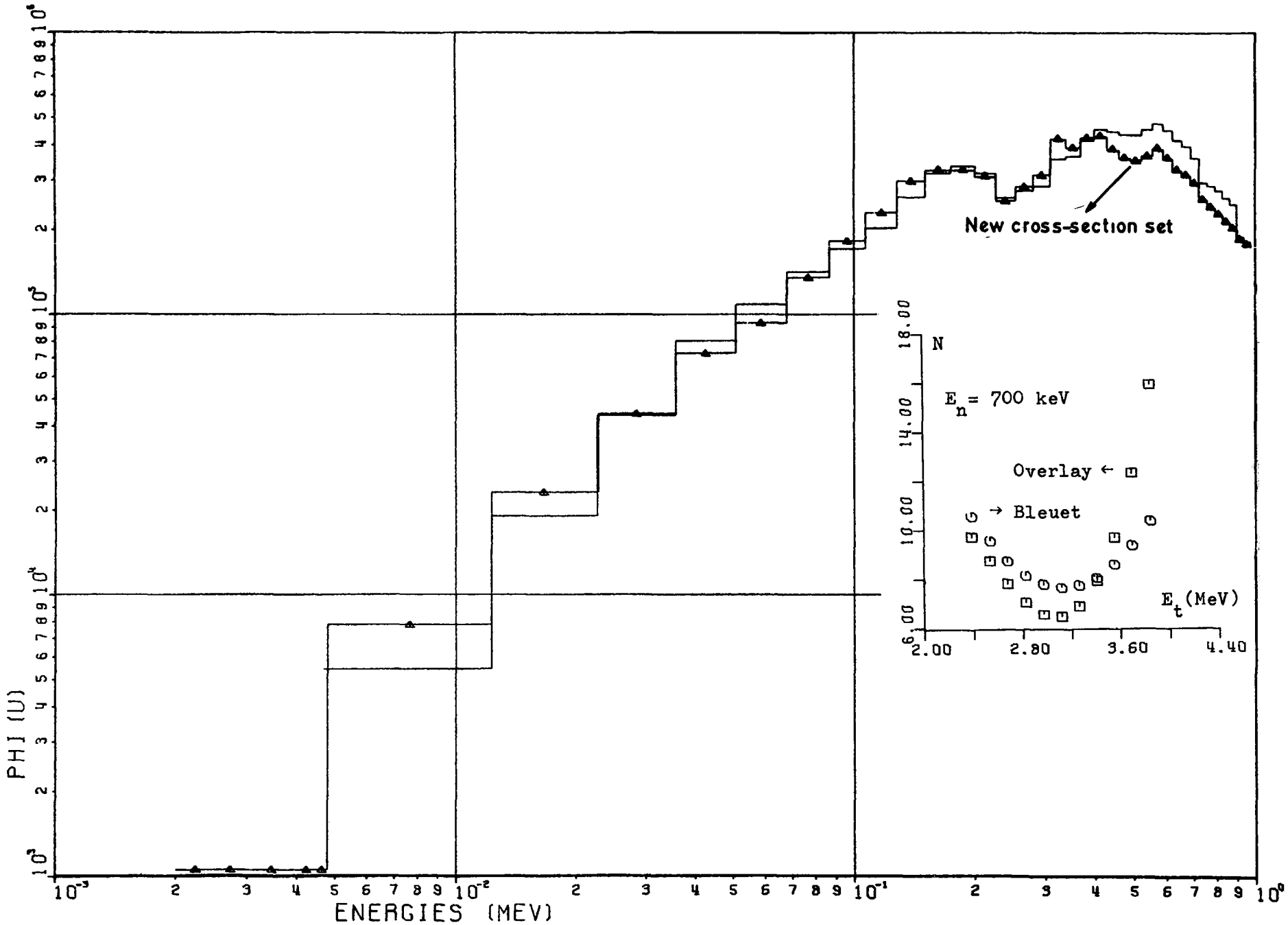
New cross-section set
N
E_n = 700 keV
Overlay ←
→ Bleuet
E_t (MeV)
18.00
14.00
10.00
6.00
2.00
2.80
3.60
4.40
PHI (U)
ENERGIES (MEV)
10^{-3}
10^{-2}
10^{-1}
10^{0}

III. INTEGRAL DATA IN BENCHMARK NEUTRON FIELDS

III.1. REVIEW OF MICROSCOPIC INTEGRAL CROSS SECTION DATA IN FUNDAMENTAL REACTOR DOSIMETRY BENCHMARK NEUTRON FIELDS

by A. Fabry, Centre d'Etude de l'Energie Nucléaire, Mol, Belgium;

W.N. McElroy, L.S. Kellogg, E.P. Lippincott, Hanford Engineering Development Laboratory, Richland, Washington;

J.A. Grundl, D.M. Gilliam, National Bureau of Standards, Washington, DC;

and G.E. Hansen, Los Alamos Scientific Laboratory, Los Alamos, New Mexico.

ABSTRACT

The accuracy of the most widely used reactor dosimetry cross section file ENDF/B-IV, is assessed in this review. This assessment is based on the comparison of spectrum-average cross sections derived from the file with microscopic integral cross sections measured in fundamental standard or reference reactor dosimetry benchmark neutron fields. International cooperation and recommendations form a base for the approach adopted for this study.

1. INTRODUCTION AND SCOPE

This paper is intended to review and critically discuss microscopic integral cross section measurement and calculation data for fundamental reactor dosimetry benchmark neutron fields.[1,2] The wording "fundamental" is used to indicate that, from the three categories[3] of benchmark neutron fields: (1) standard, (2) reference, and (3) controlled-environment, only the first two will be considered here. Specifically the review covers the following fundamental benchmarks:

- χ_{82}; the spontaneous californium-252 fission neutron spectrum standard field.[4,5,6,7]
- χ_{25}; the thermal-neutron induced uranium-235 fission neutron spectrum standard field.[8,9]
- ΣΣ; the (secondary)[10] intermediate-energy standard neutron field at the center of the Mol-ΣΣ,[11] NISUS,[12] and ITN-ΣΣ[13] facilities.
- CFRMF; the reference neutron field at the center of the Coupled Fast Reactor Measurement Facility.[14]
- BIG-10; the reference neutron field at the center of the 10% enriched uranium metal, cylindrical, fast critical.[15]
- ISNF; the (primary) Intermediate-Energy Standard Neutron Field.[16]

The restriction to standard and reference fields in the selection of data to be reviewed here does not mean that the work done in numerous controlled environments is deemed unuseful. It is believed, however, that controlled-environment data should, with some exceptions, generally serve to confirm nuclear data trends rather than to assess them; partly because of the poorer quality of integral results and neutron spectral characterization for these fields; partly also because controlled environment fields are not usually built with the primary purpose to validate and improve nuclear data, while this is one of the primary objectives for fundamental benchmarks. One of the main exceptions to the above is for data development and testing where

high flux-fluence exposures are required for stable and long half-life reaction products in controlled environment facilities such as EBR-II.

The present paper is a follow-on study of three recent publications[17,18,19] dealing with the same subject. Some redundancy in the subject material is unavoidable, but it is kept to a minimum. First, an updating of experimental results is presented; these results are compared with calculated values using the ENDF/B-IV dosimetry cross section file;[20] and finally a review is presented of the current accuracy and consistency of differential-energy cross sections and neutron spectral distributions in terms of integral reaction rate predictions. The steps involved in this review are:

(1) All measured integral reaction rates are transformed into spectral average cross sections by normalizing them with total fluxes derived through a flux transfer from a calibrated californium-252 fission neutron flux.

(2) The neutron spectra for all benchmark fields, except ^{252}Cf, are subject to an ad hoc adjustment which best matches measured spectral average cross sections for a selected set of category I* reactions. The latter have been chosen generally from among reactions with differential cross sections known to better than average accuracy and for which observed integral responses in a Cf spectrum agree well with an evaluated ^{252}Cf spectrum shape from spectrometry.

(3) On the basis of these adjusted spectral shapes, bias factors (measured to computed average cross section ratios) are defined for non-category I reactions (category II)* for each benchmark. If available studies of the evaluated differential-energy cross section of a given category II reaction suggest that the cross section shape is well defined and within uncertainties, an average bias factor is derived for each reaction. This bias factor is treated as a cross section scale normalization correction for that reaction.

In McElroy's et al companion paper to this meeting, category I reactions, supplemented by the category II reactions that can be normalized as explained above, are used to infer improved adjusted spectral shapes in

---

* Category I and II reactions are defined in Reference [1].

all benchmarks. It is recognized that the procedure followed in the two papers disregards assigned benchmark spectra based on spectrometry and/or calculation in energy ranges where these are deemed less reliable. The results of the investigation in this and McElroy el al paper are provisional and will have to be compounded with similar results obtained using assigned benchmark spectra when a number of them will have been updated by accounting for the most recent data, for instance ENDF/B-IV reactor physics computations. In this iterative way only is it possible to achieve final consistent cross sections for reactions in both categories I and II.

2. DATA DEVELOPMENT - PRESENTATION AND BRIEF DISCUSSION OF MEASURED INTEGRAL CROSS SECTIONS

2.1 NORMALIZATION OF INTEGRAL DATA

In general, integral measurements in benchmark neutron fields do not yield integral cross sections, but absolute reaction rates per nucleus per sec $\int_0^\infty \sigma_r^i(E)\ \phi_k(E)\ dE$, where $\sigma_r^i(E)$ is the evaluated differential-energy cross section for the r^{th} type reaction and i^{th} isotope, and $\phi_k(E)$ is the energy-dependent neutron flux spectrum of the benchmark field, ϕ_k.

The integral, or average, microscopic cross section is equal to the absolute reaction rate divided by the total absolute flux:

$$\bar{\sigma}_r(i,\phi_k) = \int_0^\infty \sigma_r^i(E)\ \phi_k(E)\ dE \Big/ \int_0^\infty \phi_k(E)\ dE. \qquad (1)$$

As the total flux is most often unknown, the results of such measurements are quoted as reaction rates or reaction rate ratios, e.g., integral cross section ratios. If the integral cross section however is independently known for one (or a few) reaction(s), normalization of all data is straightforward.

Another easy normalization, as done for instance by use of the SAND-II Code[21], consists of defining the total flux as the weighted mean ratio of the measured to the computed quantities, right-hand side of relation (1). The accuracy of such normalization depends on the accuracy with which the benchmark spectral shape and category I and II cross sections are known[17] and is subject to the errors involved in absolute reaction rate

determinations.

The normalization adopted for this paper (and a previous one[18]*) involves a flux transfer, using the $^{239}Pu(n,f)$ reaction and the NBS californium-252 source, along lines outlined by Grundl et al.[22,29] In this technique, all of the errors listed above either disappear or are substantially reduced. The californium source was chosen for this purpose because its strength has been established to ±1.1% (1σ)[23] in the NBS Manganous Sulfate Bath Facility relative to the internationally compared standard Ra-Be photoneutron source, NBS-1. The absolute flux at the NBS californium-252 facility is derived directly from the source strength and a distance measurement; the uncertainty of the total free-field flux is estimated to be ±1.4% (1σ). The $^{239}Pu(n,f)$ reaction was used for the transfer because the reaction cross section is among the better known reactions and because of its relatively flat shape in the energy range of interest. The $^{239}Pu(n,f)$ reaction displays almost a constant average cross section in the benchmark neutron fields: the computed values are 1789, 1781, 1754 and 1735 mb for the χ_{82}, χ_{25}, CFRMF and ΣΣ benchmarks, respectively; this is, in the worst case, a difference of only 3%. Interrelated NBS fissionable deposits of plutonium-239 have been exposed in all these neutron fields in the NBS double absolute ionization fission chamber;[24] therefore, the flux transfer is rather direct and its accuracy is of the order of ±0.8% or better.

Not surprisingly, this absolute flux normalization departs by as much as 6% for two of the benchmarks, CFRMF and ΣΣ, from the ones initially derived[2,25] by means of the SAND-II approach using both category I and II reaction cross sections, but agrees better with more recent application of this approach using just the category I type reactions; i.e., using an improved selection of the most reliable detector reactions.[17] The use of the NBS flux transfer method is the reason why the absolute values of integral data tabulated in this paper are significantly different from the ones in previous compilations.**[18,25]

2.2 SURVEY OF INTEGRAL DATA

In this section, a survey and brief discussion is provided of

---

* Tables VI and VII of this reference.

** For ΣΣ and CFRMF, see Tables IV and V of Reference [18].

the status of the development of microscopic integral cross sections in the fundamental benchmark neutron fields identified in Section 1. The emphasis here is on new data made available since - or data not covered at - the first ASTM-EURATOM 1975 symposium.[18]

χ_{82}

A large array of new integral activation cross sections has been reported recently[7] by a Hungarian group. This work seems extensive and generally agrees with earlier data, but it is poorly documented and the quoted uncertainties are large, of the order of 10%; many investigated reactions are not part of the ENDF/B-IV file and are therefore not considered for the present study. Only a few new measurements performed by this group are listed in the revised tabulation, Table I.

The capture cross section of gold recently measured by Green[6] using a californium source similar to the NBS one[4] is now preferred to previous data, which are much higher. It is wondered if the higher integral values do not bear some relationship to the materials and design of the individual sources. It is noted that the higher data are consistent with the proton recoil spectrometry observation[28] of a large excess of neutrons in χ_{82} below 1 MeV.

In conclusion, Table I gathers the experimental data presently considered as recommended for χ_{82}, and compares them with calculated values using the NBS χ_{82} spectral evaluation[29] and the ENDF/B-IV cross section file.[20]

χ_{25}

New measurements of integral fission cross sections for ^{235}U, ^{239}Pu, ^{238}U, ^{237}Np, and ^{232}Th* have been performed in the Mol Cavity Fission Neutron Spectrum Standard Field. They are reported in a contributed paper[30] to this meeting and agree very well with the revised evaluated χ_{25} data.[18]

---

* For the first time, fission cross sections for ^{233}U and ^{241}Pu have been obtained; they are $\bar{\sigma}_f(^{233}U,\chi_{25}) = (1881 \pm 64)$mb and $\bar{\sigma}_f(^{241}Pu,\chi_{25}) = (1614 \pm 60)$mb.

TABLE I. MICROSCOPIC INTEGRAL CROSS SECTIONS IN THE ^{252}Cf SPONTANEOUS FISSION NEUTRON SPECTRUM

REACTION	INTEGRAL CROSS SECTION (mb)		
	MEASURED $\bar{\sigma}_r(i,x_{82})$	CALCULATED[a] $\int_0^\infty \sigma_r^i(E)x_{82}(E)dE$	
		$\sigma_r^i(E)$: ENDF/B-IV	$\sigma_r^i(E)$: SAND II
$^{115}In(n,\gamma)^{116m}In$	125.3 ± 4.3 [26]	130.3	141.4
$^{197}Au(n,\gamma)^{198}Au$	79.9 ± 2.9 [6]	79.9	82.2
$^{235}U(n,f)$	1203 ± 30 [4]	1241	1239
$^{239}Pu(n,f)$	1804 ± 45 [27]	1789	1819
$^{237}Np(n,f)$	1332 ± 37 [27]	1351	1305
$^{103}Rh(n,n')^{103m}Rh$	757 ± 53 [7]	--	--
$^{115}In(n,n')^{115m}In$[b]	198 ± 5 [5]	191.1	190.7
$^{238}U(n,f)$	320 ± 9 [27]	315.4	313.7
$^{47}Ti(n,p)^{47}Sc$	18.9 ± 0.4 [5]	23.84	18.58
$^{58}Ni(n,p)^{58}Co$	118 ± 3 [5]	115.0	114.2
$^{54}Fe(n,p)^{54}Mn$	84.6 ± 2 [5]	89.1	87.1
$Ti(n,x)^{46}Sc$	13.8 ± 0.3 [5]	12.52	13.69
$^{27}Al(n,p)^{27}Mg$	5.1 ± 0.5 [7]	5.14	4.80
$^{56}Fe(n,p)^{56}Mn$	1.45 ± 0.035 [5]	1.475	1.549
$^{27}Al(n,\alpha)^{24}Na$	1.006 ± 0.022 [5]	1.059	1.024
$^{48}Ti(n,p)^{48}Sc$	0.42 ± 0.01 [5]	0.265	0.383
$^{55}Mn(n,2n)^{54}Mn$	0.58 ± 0.06 [7]	0.528	--
$^{59}Co(n,2n)^{58}Co$	0.57 ± 0.06 [7]	0.379	--
$^{63}Cu(n,2n)^{62}Cu$	0.30 ± 0.03 [7]	--	0.214

(a) $x_{82}(E)$: NBS evaluation[29] $\int_0^\infty x_{82}(E)dE = 1.$

(b) For ^{115m}In γ ray branching ratio of 45.9%.

(c) A value of 205 ± 9 mb. is reported in [26].

In the same facility, Williams and Hannan from the University of London Reactor Center (ULRC) have recently remeasured the fission spectrum average cross sections for the reactions $^{115}In(n,n')^{115m}In$, $^{58}Ni(n,p)^{58}Co$, $^{64}Zn(n,p)^{64}Cu$, $^{56}Fe(n,p)^{56}Mn$, $^{24}Mg(n,p)^{24}Na$ and $^{27}Al(n,\alpha)^{24}Na$. The preliminary results of this work support the χ_{25} evaluated data,[18] except for the zinc reaction.

In conclusion, recent interlaboratory work in χ_{25} provides added confidence in the previous evaluation[18] of microscopic integral cross sections for this benchmark. The results of this evaluation are compared in Table II with the values computed using different sets of available differential data.

ΣΣ

NBS-type absolute fission chambers have been used as probes to validate the spectral integrity and effective identity of the central neutron field at the Mol-ΣΣ facility[34], at the ITN-ΣΣ facility[13] (Bucharest, Rumania) and at the NISUS facility[35] (ULRC, London, Great Britain). The observed integral fission cross section ratios are displayed in Table III.

Further intercomparison of NISUS and Mol-ΣΣ has been done by the ULRC experts for 8 activation reactions.

The conclusion is that the three neutron fields are indeed neutronically equivalent in terms of integral reaction rate measurements.

In Table IV are compared ΣΣ average activation cross sections* as independently measured by the CEN-SCK, Mol experts[18] and by the ULRC, London experts. Except for the $^{27}Al(n,\alpha)^{24}Na$ reaction, the agreement is very gratifying. The ∿12% discrepancy for aluminum is difficult to understand (in χ_{25}, the Mol and ULRC data agree with each other) and requires additional work. At this stage, the ULRC datum is preferred to the CEN-SCK because it better matches the systematical trends observed when comparing the results of the different benchmarks with each other.

Table V gathers ΣΣ experimental integral cross section data as presently

---

* Data normalization as outlined in Section 2.1.

TABLE II. MICROSCOPIC INTEGRAL CROSS SECTIONS IN THE URANIUM-235 THERMAL NEUTRON INDUCED FISSION NEUTRON SPECTRUM

REACTION	EFFECTIVE THRESHOLD (MeV)	INTEGRAL CROSS SECTION (mb)						
		MEASURED	COMPUTED $\int_0^\infty \sigma_r^j(E)\, \chi_{25}(E)\, dE$					
			$\sigma_r^j(E)$: ENDF/B-IV			$\sigma_r^j(E)$: SAND-II (c)	$\sigma_r^j(E)$: RECENT LITERATURE	
			$\chi(E)$:			$\chi(E)$:	$\chi(E)$:	
		$\bar{\sigma}_r(i,\chi_{25})$	MAXWELLIAN $\bar{E}$ = 1.97 MeV	NBS EVAL.(b) $\bar{E}$=1.98 MeV	WATT $\bar{E}$ = 2.00 MeV	WATT $\bar{E}$=2.00 MeV	MAXWELLIAN $\bar{E}$ = 1.97 MeV	
							[31]	[32]
$^{115}In(n,\gamma)^{116m}In$		134.5 ± 6	137.1	135.9	135.0	146.4	--	--
$^{197}Au(n,\gamma)^{198}Au$		83.5 ± 5	85.5	84.6	83.0	85.5	--	--
$^{63}Cu(n,\gamma)^{64}Cu$		9.30 ± 1.4	11.07	10.99	10.82	10.87	--	--
$^{235}U(n,f)$		1203 ± 30	1243	1241	1241	1241	--	--
$^{239}Pu(n,f)$		1811 ± 60	1782	1781	1785	1817	--	--
$^{237}Np(n,f)$	0.6	1312 ± 50	1320	1320	1337	1293	1320	--
$^{103}Rh(n,n')^{103m}Rh$ (a)	0.8	733 ± 38	--	--	--	--	720	--
$^{115}In(n,n')^{115m}In$	1.2	189 ± 8	180.9	182.2	185.7	185.3	170	173[33]
$^{232}Th(n,f)$	1.4	81 ± 5.4	68.6	69.0	70.2	71.3	70.8	--
$^{238}U(n,f)$	1.5	305 ± 10	294.0	295.8	301.6	300.4	276	293
$^{47}Ti(n,p)^{47}Sc$	2.2	19.0 ± 1.4	21.2	21.4	21.7	17.2	--	21.0
$^{31}P(n,p)^{31}Si$	2.4	35.5 ± 2.7	--	--	--	33.0	--	--
$^{58}Ni(n,p)^{58}Co$	2.8	108.5 ± 5.4	100.5	101.6	102.8	102.2	98.1	99.4
$^{64}Zn(n,p)^{64}Cu$	2.8	29.9 ± 1.6	--	--	--	--	42.9	32.8
$^{32}S(n,p)^{32}P$	2.9	66.8 ± 3.7	63.3	64.1	65.0	60.9	64.8	--
$^{54}Fe(n,p)^{54}Mn$	3.1	79.7 ± 4.9	76.9	77.7	78.4	76.3	--	74.3
$Ti(n,x)^{46}Sc$	3.9	11.8 ± 0.75	10.08	9.99	9.92	11.28	--	--
$^{27}Al(n,p)^{27}Mg$	4.4	3.86 ± 0.25	4.16	4.12	4.10	3.84	--	3.72
$^{56}Fe(n,p)^{56}Mn$	6.0	1.035 ± 0.075	1.119	1.053	1.035	1.085	--	--
$^{59}Co(n,\alpha)^{56}Mn$	6.8	0.143 ± 0.010	0.163	0.148	0.146	--	--	--
$^{63}Cu(n,\alpha)^{60}Co$	6.8	0.500 ± 0.056	0.386	0.352	0.347	0.473	--	--
$^{24}Mg(n,p)^{24}Na$	6.8	1.48 ± 0.082	--	--	--	1.498	--	--
$^{27}Al(n,\alpha)^{24}Na$	7.2	0.705 ± 0.040	0.780	0.693	0.684	0.663	--	--
$^{48}Ti(n,p)^{48}Sc$	7.6	0.300 ± 0.018	0.195	0.173	0.169	0.236	--	--
$^{93}Nb(n,2n)^{92m}Nb$	10.2	0.475 ± 0.032	--	--	--	--	--	0.38 --
$^{127}I(n,2n)^{126}I$	10.5	1.05 ± 0.065	1.574	1.186	1.149	0.686	--	--
$^{55}Mn(n,2n)^{54}Mn$	11.6	0.244 ± 0.015	0.348	0.245	0.232	--	--	--
$^{63}Cu(n,2n)^{62}Cu$	12.4	0.122 ± 0.012	--	--	--	0.0846	--	--
$^{90}Zr(n,2n)^{89}Zr$	∿13	0.247 ± 0.017	--	--	--	0.0795	--	--
$^{58}Ni(n,2n)^{57}Ni$	∿13.5	0.00577 ± 0.00031	0.00448	0.00282	0.00254	0.00239	--	--

(a) Measured and calculated results rescaled to be consistent with a branching ratio of 45.9% for the ^{115m}In 336.2 KeV gamma ray.
(b) Segment-adjusted spectrum.
(c) SAND-II edited tape associated to NBS DETAN code.

TABLE III. INTEGRAL FISSION CROSS SECTION RATIOS MEASURED BY MEANS OF NBS-TYPE ABSOLUTE FISSION CHAMBERS[a] IN THE ΣΣ NEUTRON FIELD AT THE CENTER OF THE MOL-ΣΣ, ITN-ΣΣ AND NISUS FACILITIES

CROSS SECTION RATIO	FACILITY		
	MOL-ΣΣ	ITN-ΣΣ	NISUS
$\frac{\bar{\sigma}_f(^{239}Pu,\Sigma\Sigma)}{\bar{\sigma}_f(^{235}U,\Sigma\Sigma)}$	1.173(±2.1%)	1.169(±2.3%)	1.175(±2.3%)
$\frac{\bar{\sigma}_f(^{238}U,\Sigma\Sigma)}{\bar{\sigma}_f(^{235}U,\Sigma\Sigma)}$	0.0564(±2.5%)	0.0566(±2.5%)	0.0568(±2.7%)
$\frac{\bar{\sigma}_f(^{237}Np,\Sigma\Sigma)}{\bar{\sigma}_f(^{235}U,\Sigma\Sigma)}$	0.381(±2.8%)	0.380(±3.0%)	0.383(±3.0%)

(a) Interlaboratory results[34] in Mol-ΣΣ are 1.000: 1.167(±2%): 0.0561(±1.5%): 0.388(±2.5%) for ^{235}U: ^{239}Pu: ^{238}U: ^{237}Np, respectively.

TABLE IV. COMPARISON OF INDEPENDENT MICROSCOPIC INTEGRAL CROSS SECTION MEASUREMENTS AT THE CENTER OF THE MOL-ΣΣ FACILITY

REACTION	$\bar{\sigma}_r(i,\Sigma\Sigma)$ mb CEN-SCK	ULRC	DIFFERENCE
$^{197}Au(n,\gamma)^{198}Au$	401±10	404±13	+0.7%
$^{115}In(n,\gamma)^{116m}In$	237± 9	243± 8	+2.5%
$^{115}In(n,n')^{115m}In$	56.0±1.4	56.0±1.4	0
$^{58}Ni(n,p)^{58}Co$	26.5±0.8	26.2±0.9	-1.1%
$^{56}Fe(n,p)^{56}Mn$	0.260±0.008	0.261±0.010	+0.4%
$^{27}Al(n,\alpha)^{24}Na$	0.173±0.005	0.153±0.005	-12.3%

TABLE V. MICROSCOPIC INTEGRAL CROSS SECTIONS IN BENCHMARK NEUTRON FIELD ΣΣ

Reaction	$\bar{\sigma}_r(i,\phi)$ Measured (mb.)	$\int_0^\infty \sigma_r^i(E)\ \phi(E)dE$ [a] Calculated (mb.)	Measured/ Calculated
$^{59}Co(n,\gamma)^{60}Co$	--	41.5	--
$^{58}Fe(n,\gamma)^{59}Fe$	--	5.44	--
$^{55}Mn(n,\gamma)^{56}Mn$	36.0 ± 2.0	--	--
$^{63}Cu(n,\gamma)^{64}Cu$	36.2 ± 2.0	38.9	0.932
$^{197}Au(n,\gamma)^{198}Au$	402 ± 10	373.5	1.076
$^{238}U(n,\gamma)^{239}U$	[174 ± 7 [b]]	222	(0.784)
$^{10}B(n,\alpha)^{7}Li$	--	1518	--
$^{45}Sc(n,\gamma)^{46}Sc$	--	19.0	--
$^{115}In(n,\gamma)^{116m}In$	240 ± 9	285	0.842
$^{6}Li(n,\alpha)^{3}H$	--	923.5	--
$^{235}U(n,f)$	1512 ± 55	1525	0.991
$^{239}Pu(n,f)$	1764 ± 65	1735	1.017
$^{237}Np(n,f)$	586.5 ± 20	607	0.966
$^{103}Rh(n,n')^{103m}Rh$	281 ± 8.5	--	--
$^{115}In(n,n')^{115m}In$	56.0 ± 1.4 [c]	55.2	1.014
$^{238}U(n,f)$	84.8 ± 2.5	81.2	1.044
$^{47}Ti(n,p)^{47}Sc$	--	5.15	--
$^{58}Ni(n,p)^{58}Co$	26.5 ± 0.8	23.3	1.139
$^{54}Fe(n,p)^{54}Mn$	--	17.2	--
$Ti(n,x)^{46}Sc$	--	2.07	--
$^{27}Al(n,p)^{27}Mg$	0.983 ± 0.10	0.869	1.131
$^{56}Fe(n,p)^{56}Mn$	0.260 ± 0.008	0.230	1.130
$^{27}Al(n,\alpha)^{24}Na$	0.153 ± 0.005	0.152	1.007
$^{48}Ti(n,p)^{48}Sc$	--	0.0370	--

(a) $\sigma_r^i(E)$: ENDF/B-IV dosimetry file[20]; $\phi(E)$: as recommended in [11], normalized $\int_0^\infty \phi(E)dE=1$.

(b) Uncorrected for spectral shielding effect (~20%) in reactor constituents.

(c) For ^{115m}In γ branching ratio of 45.9%.

recommended* and compares them with predictions based on the spectral shape published earlier[11] and the ENDF/B-IV dosimetry file.[20]

CFRMF

Previous preliminary $^{10}B(n,\alpha)^{7}Li$ and $^{6}Li(n,\alpha)^{3}He$ reaction rate data** in CFRMF[36] have been updated. New measurements have been completed by Farrar and the initial results of his analysis are used here.

The uranium-238 capture rate data for CFRMF have been corrected by Harker for neutron spectrum shielding effects in the natural uranium block constituting the central zone of the reactor. To this end, Rabble,[37] a multiregion resonance absorption cross section cell code, with space-and-energy-dependent slowing-down sources and ultra-fine energy group structure ($\Delta u = 0.001$), has been used to prepare properly shielded coarse group-averaged cross sections for CFRMF. Corrections to observed uranium-238 capture rates determined in this way are of the order of 20%.***

Except for these three reaction rates, the CFRMF data remain unchanged and are compared**** in Table VI with the values computed from differential data.

BIG-10

Big-10 reaction rate data were not previously available; the data,***** quoted for the first time in this paper, Table VII, are still of a preliminary nature and do not represent a concensus of the Interlaboratory LMFBR Reaction

---

* Data normalization as outlined in Section 2.1.

** More specifically the measurements are for the total helium production, but the difference between the n, total helium and n,α reaction production of helium is negligibly small.

*** A similar correction should be applied to measured uranium-238 capture rates in $\Sigma\Sigma$, but has not yet been computed.

**** Experimental data normalized as outlined in Section 2.1.

*****Analytical flux depression corrections by Hansen have been applied to relate the response of a real detector in its real environment to the response of the corresponding infinitesimal detector at the center of a cavity-free Big-10. Such corrections never exceed 3.5%.

TABLE VI. MICROSCOPIC INTEGRAL CROSS SECTIONS IN BENCHMARK NEUTRON FIELD CFRMF

Reaction	$\bar{\sigma}_r(i,\phi)$ Measured (mb.)	$\int_0^\infty \sigma_r^i(E)\ \phi(E)dE$ [a] Calculated (mb)	Measured/ Calculated
$^{59}Co(n,\gamma)^{60}Co$	91.6 ± 3.6	85.3	1.074
$^{58}Fe(n,\gamma)^{59}Fe$	6.12 ± 0.22	6.11	1.002
$^{55}Mn(n,\gamma)^{56}Mn$	-	-	-
$^{63}Cu(n,\gamma)^{64}Cu$	45.4 ± 2.6	47.5	0.956
$^{197}Au(n,\gamma)^{198}Au$	424 ± 14	416	1.019
$^{238}U(n,\gamma)^{239}U$	223 ± 11 [b]	232	0.961
$^{10}B(n,\alpha)^{7}Li$	1814 ± 60 [c]	1694	1.071
$^{45}Sc(n,\gamma)^{46}Sc$	23.5 ± 0.9	20.1	1.166
$^{115}In(n,\gamma)^{116m}In$	281.5 ± 11	303	0.929
$^{6}Li(n,\alpha)^{3}H$	948 ± 39 [c]	988.5	0.959
$^{235}U(n,f)$	1557 ± 53	1590	0.979
$^{239}Pu(n,f)$	1783 ± 60	1754	1.016
$^{237}Np(n,f)$	551 ± 21	547	1.007
$^{115}In(n,n')^{115m}In$	51.0 ± 3.0 [d]	47.5 [d]	1.074
$^{238}U(n,f)$	75.6 ± 3.0	69.4	1.089
$^{47}Ti(n,p)^{47}Sc$	4.18 ± 0.2	4.70	0.889
$^{58}Ni(n,p)^{58}Co$	24.0 ± 0.8	21.9	1.093
$^{54}Fe(n,p)^{54}Mn$	17.5 ± 0.6	16.5	1.061
$Ti(n,x)^{46}Sc$	2.61 ± 0.10	2.15	1.214
$^{27}Al(n,p)^{27}Mg$	0.874 ± 0.033	0.887	0.985
$^{56}Fe(n,p)^{56}Mn$	-	0.238	-
$^{27}Al(n,\alpha)^{24}Na$	0.161 ± 0.005	0.162	0.994
$^{48}Ti(n,p)^{48}Sc$	0.0688 ± 0.003	0.0385	1.787

(a) $\sigma_r^i(E)$: ENDF/B-IV dosimetry file[20]; $\phi(E)$: ENDF/B-III S_N computation[14], normalized $\int_0^\infty \phi(E)\ dE = 1$.
(b) Corrected for spectral shielding effect (21%) in reactor constituents.
(c) New measurements.
(d) For ^{115m}In γ branching ratio of 45.9%.

TABLE VII. MICROSCOPIC INTEGRAL CROSS SECTIONS IN BENCHMARK NEUTRON FIELD BIG-10: PRELIMINARY [a]

Reaction	$\bar{\sigma}_r(i,\phi)$ Measured (mb.)	$\int_0^\infty \sigma_r^i(E)\ \phi(E)dE$ [b] Calculated (mb)	Measured/ Calculated
$^{59}Co(n,\gamma)^{60}Co$	12.94 ± 0.4	12.59	1.028
$^{58}Fe(n,\gamma)^{59}Fe$	4.27 ± 0.21	3.09	1.382
$^{55}Mn(n,\gamma)^{56}Mn$	-	-	-
$^{63}Cu(n,\gamma)^{64}Cu$	23.1 ± 0.9	24.8	0.932
$^{197}Au(n,\gamma)^{198}Au$	228 ± 6	219	1.041
$^{238}U(n,\gamma)^{239}U$	149.5 ± 4.5	149.2	1.002
$^{10}B(n,\alpha)^{7}Li$	1378 ± 28	1208	1.141
$^{45}Sc(n,\gamma)^{46}Sc$	17.86 ± 0.55	15.87	1.125
$^{115}In(n,\gamma)^{116m}In$	-	232.5	-
$^{6}Li(n,\alpha)^{3}H$	967 ± 19	966	1.001
$^{235}U(n,f)$	1361 ± 18 [39]	1368	0.995
$^{239}Pu(n,f)$	1632 ± 33 [39]	1605	1.017
$^{237}Np(n,f)$	433.5 ± 11 [39]	440	0.985
$^{115}In(n,n')^{115m}In$	35.65 ± 1.1 [c]	32.64 [c]	1.092
$^{238}U(n,f)$	50.9 ± 1.1 [39]	46.00	1.107
$^{47}Ti(n,p)^{47}Sc$	2.96 ± 0.13	3.13	0.945
$^{58}Ni(n,p)^{58}Co$	16.87 ± 0.34	14.56	1.159
$^{54}Fe(n,p)^{54}Mn$	12.26 ± 0.31	10.95	1.120
$Ti(n,x)^{46}Sc$	1.81 ± 0.06	1.40	1.290
$^{27}Al(n,p)^{27}Mg$	-	0.580	-
$^{56}Fe(n,p)^{56}Mn$	-	0.151	-
$^{27}Al(n,\alpha)^{24}Na$	0.110 ± 0.007	0.102	1.078
$^{48}Ti(n,p)^{48}Sc$	0.0487 ± 0.0020	0.0244	1.993

(a) Based only on HEDL, NBS and AI measurements.

(b) $\sigma_r^i(E)$: ENDF/B-IV dosimetry file[20]; $\phi(E)$: ENDF/B-III S_N computation, normalized $\int_0^\infty \phi(E)\ dE = 1$.

(c) For ^{115m}In γ branching ratio of 45.9%.

Rate (ILRR) program[2], currently responsible for the work performed in the U. S. dosimetry benchmarks.

The experimental average cross sections listed in Table VII have been normalized as outlined in Section 2.1. The fission cross sections are based on measurements[38] by means of NBS double absolute fission chambers[24] by Gilliam, Grundl et al. The $^{10}B(n,\alpha)$ and $^{6}Li(n,\alpha)$ cross sections result from helium production rate measurements by Farrar. All other cross sections have been obtained by radiometric high resolution Ge(Li) counting performed at the Hanford Engineering Development Laboratory (HEDL) and they do not include the results obtained by the other independent laboratories; the HEDL data however depart by less than ±2% from the weighted mean of all results, except in the case of the $^{27}Al(n,\alpha)^{24}Na$ reaction for which HEDL is high by approximately 4%.

ISNF

The Intermediate-Energy Standard Neutron Field (ISNF)[16], developed jointly by NBS and CEN-SCK, and in operation at NBS since 1975, is the most recent of the benchmark fields in the ILRR "family". Therefore, only two fission cross section ratios have yet been measured in this environment and the results are preliminary. They are briefly discussed in the Section 3.2.

3. DATA TESTING

3.1 PITFALLS AND PROBLEMS IN CONVENTIONAL DATA TESTING

A major conclusion from recent[17,18] and current work[19] is that integral cross section measurements for dosimetry reactions in standard and reference benchmark neutron fields show unsatisfactory departures from those computed, not only because of differential-energy cross section inadequacies, but also because the spectral shapes characteristic of these benchmarks are usually inaccurate in the energy ranges not covered or poorly covered by differential neutron spectrometry techniques;

for example - below ∿250 KeV and above ∿10 MeV for χ_{82} and χ_{25}
- below ∿10 KeV and above ∿2 MeV for ΣΣ, CFRMF and Big-10.

Even in the well covered energy ranges, the reliability sometimes remains

questionable, as is presently the case for χ_{25} between 3 and 6 MeV,[18,19] and for CFRMF between 100 and 400 KeV.[39]

Computed neutron spectra for ΣΣ, CFRMF and Big-10 are affected to a large degree by uncertainties in the uranium-238 nuclear data, most noticeably inelastic and elastic cross sections, depending on the energy range.

Consequently a direct confrontation, Table VIII, of measured integral cross sections for the various benchmarks and their computed values using spectra based only on neutron spectrometry and transport theory does not allow the dosimetry file to be unambiguously tested and adjusted. Instead, the overall approach recommended in 1973[1] must be followed; e.g., adjust the benchmark spectra on the basis of integral microscopic cross sections for a selected category I reaction set and use this improved spectral characterization to adjust differential-energy cross sections for the other reactions, labelled category II.

The impact of spectral adjustment is illustrated for fundamental fission cross sections by Tables IX and X, which present measured, computed and measured-to-computed cross section ratios before and after adjustment. It is seen that the changes in the ratios due to the adjustment are very significant; they generally remain, however, within the uncertainties of the spectral shape characterization. A striking example is the uranium-235 to uranium-238 measured-to-computed ratio in CFRMF: before spectral adjustment, this ratio is 0.899 while it becomes 0.970 with adjustment; a new computation of the CFRMF spectrum by Harker et al., using ENDF/B-IV data, provides a new ratio of 0.983, in agreement with the adjustment.

TABLE VIII RATIO OF MEASURED[a] TO COMPUTED[b] INTEGRAL CROSS SECTIONS IN DOSIMETRY BENCHMARK NEUTRON FIELDS

REACTION	NEUTRON FIELD				
	X_{82}	X_{25}	ΣΣ	CFRMF	BIG-10
$^{59}Co(n,\gamma)^{60}Co$	-	-	-	1.074	1.028
$^{58}Fe(n,\gamma)^{59}Fe$	-	-	-	1.002	1.382
$^{63}Cu(n,\gamma)^{64}Cu$	-	0.846	0.932	0.956	0.932
$^{197}Au(n,\gamma)^{198}Au$	1.000	0.987	1.076	1.019	1.041
$^{238}U(n,\gamma)^{239}U$	-	-	(~0.95[c])	0.961	1.002
$^{10}B(n,\alpha)^{7}Li$	-	-	-	1.071	1.141
$^{45}Sc(n,\gamma)^{46}Sc$	-	-	-	1.166	1.125
$^{115}In(n,\gamma)^{116m}In$	0.962	0.990	0.842	0.929	-
$^{6}Li(n,\alpha)^{3}H$	-	-	-	0.959	1.001
$^{235}U(n,f)$	0.969	0.969	0.991	0.979	0.995
$^{239}Pu(n,f)$	1.008	1.017	1.017	1.016	1.017
$^{237}Np(n,f)$	0.986	0.994	0.966	1.007	0.985
$^{115}In(n,n')^{115m}In$	1.036	1.037	1.014	1.074	1.092
$^{238}U(n,f)$	1.015	1.031	1.044	1.089	1.107
$^{47}Ti(n,p)^{47}Sc$	0.793	0.888	-	0.889	0.945
$^{58}Ni(n,p)^{58}Co$	1.026	1.068	1.139	1.093	1.159
$^{54}Fe(n,p)^{54}Mn$	0.949	1.026	-	1.061	1.120
$Ti(n,x)^{46}Sc$	1.102	1.181	-	1.214	1.290
$^{27}Al(n,p)^{27}Mg$	0.992	0.937	1.131	0.985	-
$^{56}Fe(n,p)^{56}Mn$	0.983	0.983	1.130	-	-
$^{27}Al(n,\alpha)^{24}Na$	0.950	1.017	1.007	0.994	1.078
$^{48}Ti(n,p)^{48}Sc$	1.585	1.734	-	1.787	1.993

(a) Normalized by $^{239}Pu(n,f)$ transfer from californium, text Section 2.1.

(b) $\int_0^\infty \sigma_r^i(E)\ \phi(E)\ dE$; $\sigma_r^i(E)$:ENDF/B-IV file; $\phi(E)$: as recommended, 1975, normalized $\int_0^\infty \phi(E)\ dE = 1$.

(c) Applying the spectral shielding correction computed for CFRMF.

TABLE IX. FUNDAMENTAL FISSION CROSS SECTION RATIOS
IN DOSIMETRY BENCHMARK NEUTRON FIELDS

Neutron Field	$\frac{^{235}U(n,f)}{^{238}U(n,f)}$			$\frac{^{239}Pu(n,f)}{^{235}U(n,f)}$			$\frac{^{239}Pu(n,f)}{^{238}U(n,f)}$
	Measured	Computed*	Ratio	Measured	Computed*	Ratio	Ratio
χ_{82} (a)	3.76(±1.7%)	3.935	0.955	1.500(±1.6%)	1.442	1.040	0.993
χ_{25} (a)	3.94(±2.0%)	4.195	0.939	1.505(±2.2%)	1.435	1.049	0.985
$\Sigma\Sigma$ (b)	17.8(±1.5%)	18.78	0.948	1.167(±2.0%)	1.138	1.025	0.972
CFRMF (c)	20.6(±1.4%)	22.91	0.899	1.145(±1.5%)	1.103	1.038	0.933
Big-10 (c)	26.8(±1.7%)	29.65	0.904	1.198(±1.5%)	1.173	1.021	0.923
ISNF (c)	10.8(±<3%)	11.85	0.911	1.15(±<3%)	1.114	1.033	0.941

(a) $\phi(E)$ for computation : NBS evaluation.[29]

(b) $\phi(E)$: reference.[11]

(c) $\phi(E)$: discrete-ordinates transport theory calculation based on ENDF/B-III.

(*) $\sigma_f(E)$: ENDF/B-IV.

TABLE X. RATIO OF MEASURED-TO-COMPUTED INTEGRAL FISSION CROSS SECTIONS IN DOSIMETRY BENCHMARK NEUTRON FIELDS BEFORE (b) AND AFTER (a) ADJUSTMENT OF THE SPECTRAL SHAPES

NEUTRON FIELD	$\left[\frac{^{235}U(n,f)}{^{238}U(n,f)}\right]$ Meas. / $\left[\frac{^{235}U(n,f)}{^{238}U(n,f)}\right]$ Calc.		$\left[\frac{^{239}Pu(n,f)}{^{235}U(n,f)}\right]$ Meas. / $\left[\frac{^{239}Pu(n,f)}{^{235}U(n,f)}\right]$ Calc.		$\left[\frac{^{239}Pu(n,f)}{^{238}U(n,f)}\right]$ Meas. / $\left[\frac{^{239}Pu(n,f)}{^{238}U(n,f)}\right]$ Calc.	
	b	a*	b	a*	b	a
χ_{82}	0.955	0.955**	1.040	1.040**	0.993	0.993**
χ_{25}	0.939	0.958	1.049	1.051	0.985	1.007
$\Sigma\Sigma$	0.948	0.980	1.025	1.028	0.972	1.007
CFRMF	0.899	0.970	1.038	1.030	0.933	0.999
BIG-10	0.904	0.970	1.021	1.030	0.923	0.999

* A decrease of the order of at least 5% in the U^{235} $\sigma(E)$ in the 0.01 to 1 MeV range would establish ratios much closer to unity.

** As indicated in the text, no adjustment was necessary for Cf^{252}.

3.2 SELECTION OF A CATEGORY I REACTION SET

The selection of a category I reaction set is in itself a challenging task. Reactions which are considered as standards by differential cross section measurers seem to fall naturally into such a category, yet there are notable exceptions: for fast neutron spectra, the principal information given by $^{235}U(n,f)$ and $^{239}Pu(n,f)$ reactions is on total fluence and one selects $^{239}Pu(n,f)$ for category I as the better fluence monitor and not on the basis of uncertainties in the differential cross section data. Again, the information given by either $^{234}U(n,f)$ or $^{237}Np(n,f)$ reactions is essentially equivalent and one selects $^{237}Np(n,f)$ for category I merely because more integral data are available.

Except for the addition of $^{197}Au(n,\gamma)^{198}Au$, the category I reactions selected for this study coincide with those of Vlasov et al[19], namely: $^{197}Au(n,\gamma)^{198}Au$, $^{239}Pu(n,f)$, $^{237}Np(n,f)$, $^{238}U(n,f)$, $^{58}Ni(n,p)^{58}Co$, $^{56}Fe(n,p)^{56}Mn$, $^{27}Al(n,\alpha)^{24}Na$, $^{63}Cu(n,2n)^{62}Cu$, and $^{58}Ni(n,2n)^{57}Ni$.*

---

* Uncertainties of the order of 10% are currently acceptable in the very high energy range of response of the last two reactions.

3.3 ACCURACY OF THE ENDF/B-IV DOSIMETRY FILE

This brief discussion of the accuracy of selected reactions on the ENDF/B-IV dosimetry file will be based primarily on Table XI data, in which measured-to-calculated integral cross section ratios are quoted for SAND-II adjusted benchmark spectral shapes for all fields, except for the use of the unadjusted NBS evaluated spectrum for californium-252 (see Sections 3.1 and 3.2).

The table is divided by a horizontal line that separates threshold and non-threshold reactions; the reactions are arranged, approximately, in order of increasing ΣΣ field energy response.

Also factored into the discussion is a careful outlook at the status of differential-energy cross sections.[19,20]

Non-threshold reactions*

$^{59}Co(n,\gamma)^{60}Co$: The CFRMF result suggests improper spectral characterization in the 0.1 - 1 keV range; indeed, the measured resonance integral, which accounts for more than 50% of the reaction rate in CFRMF, is reasonably well known and agrees with the calculated ENDF/B-IV value.[20] The BIG-10 results support the current file evaluation at higher energies; therefore this reaction can be used for characterizing some benchmark spectra rather than the reverse: it is a future category I candidate.

$^{58}Fe(n,\gamma)^{59}Fe$: In view of the above comments on cobalt and since the file evaluated cross section relies on a Hauser-Feshbach calculation which was lowered by 10% to establish better agreement with CFRMF integral datum,[20] the CFRMF iron result is inconclusive while the BIG-10 result suggests a serious inconsistency at higher energy; further, the measured resonance integral value is ∿33% lower

---

* Recommendations for new integral measurements for the non-threshold reactions in the ISNF fields are not re-stated here because they have already been made as a part of planned ILRR program work.

TABLE XI RATIO OF MEASURED[a] TO COMPUTED[b] INTEGRAL CROSS SECTIONS IN DOSIMETRY BENCHMARK NEUTRON FIELDS: SAND II ADJUSTED SPECTRAL SHAPES[c]

REACTION	NEUTRON FIELD				
	χ_{82}	χ_{25}	ΣΣ	CFRMF	BIG-10
$^{59}Co(n,\gamma)^{60}Co$	-	-	-	1.205	1.013
$^{58}Fe(n,\gamma)^{59}Fe$	-	-	-	1.000	1.364
$^{63}Cu(n,\gamma)^{64}Cu$	-	0.834	0.874	0.937	0.915
$^{197}Au(n,\gamma)^{198}Au$	1.000	0.972	1.002	1.000	1.019
$^{238}U(n,\gamma)^{239}U$	-	-	(0.907)[d]	0.956	0.988
$^{10}B(n,\alpha)^{7}Li$	-	-	-	1.053	1.108
$^{45}Sc(n,\gamma)^{46}Sc$	-	-	-	1.158	1.102
$^{115}In(n,\gamma)^{116m}In$	0.962	0.996	0.807	0.929	-
$^{6}Li(n,\alpha)^{3}H$	-	-	-	0.949	0.980
$^{235}U(n,f)$	0.969	0.968	0.975	0.974	0.987
$^{239}Pu(n,f)$	1.008	1.017	1.002	1.003	1.017
$^{237}Np(n,f)$	0.986	1.000	1.003	0.999	1.015
$^{115}In(n,n')^{115m}In$	1.036	1.019	0.988	1.007	1.034
$^{238}U(n,f)$	1.015	1.010	0.995	1.004	1.018
$^{47}Ti(n,p)^{47}Sc$	0.793	0.852	-	0.810	0.840
$^{58}Ni(n,p)^{58}Co$	1.026	1.020	1.008	0.999	1.017
$^{54}Fe(n,p)^{54}Mn$	0.949	0.977	-	0.967	0.975
$Ti(n,x)^{46}Sc$	1.102	1.155	-	1.125	1.129
$^{27}Al(n,p)^{27}Mg$	0.992	0.917	0.991	0.914	-
$^{56}Fe(n,p)^{56}Mn$	0.983	1.004	1.050	-	-
$^{27}Al(n,\alpha)^{24}Na$	0.950	1.022	1.000	0.999	1.014
$^{48}Ti(n,p)^{48}Sc$	1.585	1.714	-	1.686	1.859

(a) Normalized by $^{239}Pu(n,f)$ transfer from californium, text Section 2.1.

(b) $\int_0^\infty \sigma_r^i(E)\ \phi^*(E)\ dE$; $\sigma_r^i(E)$: ENDF/B-IV file; $\phi^*(E)$: SAND-II adjusted spectra[c], normalized $\int_0^\infty \phi^*(E)\ dE = 1$.

(c) Except for χ_{82}: NBS evaluation[29]

(d) Applying the spectral shielding correction computed for CFRMF.

that the calculated value[20]; a χ_{25} (or χ_{82}) and a new resonance integral measurement are recommended for this reaction.

$^{63}Cu(n,\gamma)^{64}Cu$: The $\Sigma\Sigma$ datum might be slightly inaccurate due to uncertainties in the spectrum or in self-shielding corrections; the measured resonance integral is ∿13% below the ENDF/B-IV calculated value; further, the increasing discrepancy from CFRMF through BIG-10 to χ_{25} seems to indicate a non-surprising cross section shape inadequacy above 1 keV; here, a more thorough evaluation effort of differential data is needed as well as a new resonance integral measurement.

$^{197}Au(n,\gamma)^{198}Au$: Category I, satisfactory.

$^{238}U(n,\gamma)^{239}U$: Satisfactory in terms of dosimetry applications but difficult to apply reliably in systems containing large amounts of uranium-238.

$^{10}B(n,\alpha)^{7}Li$: The integral versus differential data discrepancies are sizeable for such a supposedly standard cross section; they decrease slightly from Table VIII to Table XI; e.g., the spectral adjustments have a positive influence; the measured and calculated resonance integral values are in agreement.[20] In view of the importance of this reaction and the fact that only one integral experimental approach has been used, further independent integral measurements are recommended.

$^{45}Sc(n,\gamma)^{46}Sc$: The measured versus computed discrepancies are important but not surprising; the measured and calculated resonance integrals agree but the measured value has a ∿10% uncertainty;[20] in the energy range of relevance for BIG-10, differential measurements are very sparse, while the CFRMF datum is influenced by the complex resonance structure above

2 keV; additional differential and integral measurements are needed in this case.

$^{115}In(n,\gamma)^{116m}In$: The differential-energy cross section seems more or less acceptable if it is assumed that the ΣΣ datum is in error; the measured and calculated resonance integrals are in agreement;[20] the ΣΣ measurement should be further validated by independent group(s).

$^{6}Li(n,\alpha)^{3}H$: The BIG-10 datum supports the evaluated file very well, but the discrepancy in CFRMF is significant and puzzling as it is for $^{10}B(n,\alpha)$; there is no measured resonance integral value reported in Reference [20]; further independent integral measurements are recommended; it is most relevant to indicate here that $^{6}Li(n,\alpha)$ spectrometry[39] in CFRMF suggests a spectral depletion in the 100-400 keV range: if such an effect were real, it would help to explain and resolve the inconsistencies in present integral observations.

$^{235}U(n,f)$: Further differential measurements and evaluations are required to establish this as a category I reaction; see discussion in Section 3.2.

$^{239}Pu(n,f)$: Category I, seems satisfactory but further differential measurements below 100 keV may be necessary; in view of the $^{235}U(n,f)$ problem, a reevaluation is needed for confirmation.

Threshold reactions

The threshold reactions are not discussed individually here, but bias factors as defined in Section 1 of this paper and in Reference [19] are tentatively recommended, wherever applicable. This is done on the basis of a review of the data in Table XI as well as that in column 4, Table 1, of Reference [19].

For some reactions, such as $^{63}Cu(n,\alpha)^{60}Co$ and $^{48}Ti(n,p)^{48}Sc$, the

evidence of differential-energy cross section shape inadequacies precludes the definition of a bias factor.

For the other reactions investigated in this work, the bias factors are as follows:

$^{237}Np(n,f)$	:	Category I
$^{115}In(n,n')^{115m}In$	:	1.017 ± 0.025
$^{232}Th(n,f)$	:	1.15
$^{238}U(n,f)$	:	Category I
$^{47}Ti(n,p)^{47}Sc$	:	0.825 ± 0.03
$^{58}Ni(n,p)^{58}Co$	:	Category I
$^{32}S(n,p)^{32}P$	:	0.987
$^{54}Fe(n,p)^{54}Mn$	:	0.967 ± 0.018
$Ti(n,x)^{46}Sc$	:	1.128 ± 0.026
$^{56}Fe(n,p)^{56}Mn$	:	Category I
$^{59}Co(n,\alpha)^{56}Mn$	:	0.973
$^{27}Al(n,\alpha)^{24}Na$	:	Category I
$^{127}I(n,2n)^{126}I$	:	0.778
$^{55}Mn(n,2n)^{54}Mn$	:	0.803
$^{63}Cu(n,2n)^{62}Cu$	:	Category I (0.90)*
$^{90}Zr(n,2n)^{89}Zr$	:	1.715
$^{58}Ni(n,2n)^{57}Ni$	:	Category I (1.12)*.

It is recommended that these bias factors be considered for use in the definition of an adjusted and improved ENDF/B dosimetry cross section file. It is believed that such an improved file would have an integral consistency to better than ±5% for the designated reactions as a result of the application of the data testing approach undertaken in this paper. It is also important to note that if a bias factor for a key fluence monitor such as

---

* For the very high energy range, accuracies of the order of ±10% are presently acceptable for category I reactions.

$Ti(n,x)^{46}Sc$ had been defined by more conventional, direct data testing procedures, its value would have varied between 1.10 and 1.29; e.g., ±8%, depending on the benchmark field considered; with SAND-II adjustments, this ±8% spread is reduced to ±2-3%, which is a very significant improvement.

It must be recalled that this forced consistency ignores possible inadequacies of Category I reaction cross sections and also possible systematic errors in the integral measurements. Discrepancies between observed and expected integral results in the benchmarks are interpreted as spectrum errors alone. Thus, to be complete, this approach to spectrum characterization for neutron dosimetry must take into account as an additional error component the departures of the SAND-II adjusted spectra from the assigned spectra based on spectrometry and calculation. Alternatively a compromise spectrum may be first defined followed by the derivation of bias factors for both categories of reactions.

4. CONCLUSIONS AND RECOMMENDATIONS

The principal conclusions related to dosimetry cross section data development and testing based on this study and those presented at the Petten symposium[18] may be stated as follows:

- For category I and the best known category II ENDF/B-IV threshold reactions, integral and differential cross section data are generally consistent to within ±5% (1σ). When this is not the case, the deviations can be interpreted in an ad hoc procedure as errors in benchmark neutron field flux spectra.
- Adjustment of the benchmark neutron spectra by multiple foil unfolding on the basis of category I reactions significantly improves the overall integral versus differential data consistency, as is to be expected. These adjustments are often within the bounds of experimental uncertainties for the benchmark spectra. When this is not the case, the results suggest the existence of real biases.
- The spectral components of current benchmark neutron fields are not sufficiently well known and distinguishable to allow energy dependent adjustment of non-threshold category II cross sections. Present results do provide a good basis, however, for the future direction of evaluation work and measurements.

- When integral-differential discrepancies for category II threshold reactions are expressed as cross section rescaling or normalization factors, such bias factors can be established with uncertainties smaller than 2-3% when category I multiple foil unfolded spectral shapes are employed in place of assigned spectra based on spectrometry and calculation. Without this ad hoc adjustment biases of up to 10% or more for key fluence monitors are observed. The consequent improvement of spectrum characterization for dosimetry will depend upon the extent and reliability of the departures between unfolded and assigned spectra.

In summary, the data development and testing approach, first applied to the development of the SAND-II cross section file,[40] and subsequently recommended by the IAEA 1973 panel[1] has been further investigated and rescaled energy-dependent cross sections have been derived for category II threshold reactions. For the first time, some specific recommendations for further study of non-threshold reactions in the ENDF/B-IV file have been delineated. A few sustained problems still exist and a vigorous and well planned and coordinated international interlaboratory effort will be required to resolve them. These are:

- Uncertainties in the evaluated ENDF/B-IV differential-energy cross sections for key standard reactions such as $^{235}U(n,f)$, $^{10}B(n,\alpha)$, $^{6}Li(n,\alpha)$, $^{239}Pu(n,f)$, $^{197}Au(n,\gamma)$, and $^{58}Ni(n,p)$.
- Uncertainties in the low-energy spectrum tails (<10 keV) for all current reactor dosimetry benchmarks. More analytical work and sensitivity studies will be needed, as well as dedicated integral measurement comparisons with the Intermediate-Energy Standard Neutron Field (ISNF), to define the spectral shapes.
- Lack of a sufficient set of high-accuracy, redundant, interlaboratory microscopic integral cross section measurements; particularly for the californium-252 fission spectrum and in the intermediate-energy standard neutron fields ISNF and ΣΣ.
- Suggested uncertainties[19] regarding the shape of the ^{235}U thermal neutron induced fission neutron spectrum in the energy ranges of <250 keV, above 8 MeV and possibly also $\sim$ 2-6 MeV.

REFERENCES

[1] VLASOV, M. F., DUNFORD, C. L., "Proceedings of a Consultants' Meeting on Nuclear Data for Reactor Neutron Dosimetry", Vienna, 10-12 September 1973, Report INDC(NDS)-56/U, IAEA (1973).

[2] McELROY, W. N., et al, Special Series, Nucl. Techn. 25, 177-422 (1975).

[3] Proceedings of the First International ASTM-EURATOM Symposium on Reactor Dosimetry, Petten, September 22-26 (1975).

[4] HEATON II, H. T., GRUNDL, J. A., SPIEGEL Jr., V., GILLIAM, D. M., EISENHAUER, C., Proc. Nuclear Cross Sections and Technology Conference, NBS Special Publication 425, Vol. I, 266 (1975).

[5] ALBERTS, W. G., BORTFELDT, J., GÜNTHER, E., KNAUF, K., MATZKE, M., RASSL, G., SIEGEL, V., and WALZ, K. F., Ibid, Vol. I, 273 (1975). See also Reference [3].

[6] GREEN, L., Nucl. Sci. Eng. 58, 361-370 (1975).

[7] BUCZKÓ, M., BÖDY, Z. T., CSIKAI, J., DEZSŐ, Z., JUHÁSZ, S., AL-MUNDHERI, H. M., PETŐ, G., VARNAGY, M., "Average Cross Sections for ^{252}Cf Neutron Spectrum", International Symposium on Californium-252 Utilization, April 26-28, Paris, France (1976).

[8] FABRY, A., GRUNDL, J. A., EISENHAUER, C., Proc. Nuclear Cross Sections and Technology Conference, NBS Special Publication 425, Vol. I, 254 (1975).

[9] KIMURA, I., KOBAYASHI, K., SHIBATA, T., J. Nucl. Sci. Tech. 10, 574 (1973). KIMURA I., KOBAYASHI, K., See Reference [3].

[10] FABRY, A., VANDEPLAS, P., Fast Reactor Physics Vol. I, 389, IAEA (1968).

[11] FABRY, A., DeLEEUW, G., DeLEEUW, S., Nucl. Techn. 25, 349 (1975).

[12] BESANT, C. B., EMMETT, J., CAMPBELL, C. G., KERRIDGE, M., JONES, T., Nucl. Eng. Intern. 425, May (1973).

[13] GIRLEA, I., MIRON, C., FABRY, A., Report BLG 512 (1976).

[14] ROGERS J W, MILLSAP, D. A., HARKER, Y. D., Nucl. Techn. 25, 330 (1975).

[15] DOWDY, E. J., LOZITO, E. J., PLASSMANN, E. A., Nucl. Techn. 25, 381 (1975).

[16] GRUNDL, J. A., EISENHAUER, C., See Reference [3].

[17] McELROY, W. N., Proc. Nuclear Cross Sections and Technology Conference, NBS Special Publication 425, Vol. I, 189 (1975).

[18] FABRY, A., CEULEMANS, H., VANDEPLAS, P., McELROY, W. N., and LIPPINCOTT, E. P., See Reference [3].

[19] VLASOV, M. F., FABRY, A., McELROY, W. N., "Status of Neutron Cross Sections for Reactor Dosimetry"Special Contributed Paper to 1976 International Conference on the Interactions of Neutrons with Nuclei, July 6-9, 1976, Lowell, Mass.

[20] MAGURNO, B. A., editor, "ENDF/B-IV Dosimetry File", Report BNL-NCS-50446/ NEACRP-L-145/ENDF-216 (1975).

[21] OSTER, C. A., McELROY, W. N., MARR, J. M., "A Monte-Carlo Program for SAND-II Error Analysis", Report HEDL-TME 73-20 (1973).
OSTER, C. A., McELROY, W. N., SIMONS, R. L., LIPPINCOTT, E. P., ODETTE, G. R., "A Modified Monte Carlo Program for SAND-II With Solution Weighting and Error Analysis", Report HEDL-TME 76-60 (1976).

[22] GRUNDL, J. A., EISENHAUER, C., See Reference [3].

[23] GRUNDL, J. A., SPIEGEL, V., EISENHAUER, C. M., HEATON II, M. T., GILLIAM, D. M., BIGELOW, J., "The Californium-252 Fission Spectrum for Neutron Reaction Rate Measurements", submitted for publication in Nucl. Techn. (1976).

[24] GRUNDL, J. A., GILLIAM, D. M., DUDEY, N. D., POPEK, R. J., Nucl. Techn. 25, 237 (1975).

[25] BOHN, E. M., et al., editors, "Benchmark Testing of ENDF/B-IV", report ENDF-230 Vol. I, March (1976).

[26] PAUW, H., ATEN, A. H. W., Jr., J. Nucl. En. 25, 457 (1971).

[27] GILLIAM, D. M., EISENHAUER, C., HEATON II, H. T., GRUNDL, J. A., Proc. Nuclear Cross Sections and Technology Conference, NBS Special Publication 425, Vol. I, 270 (1975).

[28] WERLE, H., Internal Gesellshaft fur Kernforschungszentrum report, Karlsruhe, to be published (1976).

[29] GRUNDL, J. A., EISENHAUER, C. M., Proc. Nuclear Cross Sections and Technology Conference, NBS Special Publication 425, Vol. I, 250 (1975).

[30] FABRY, A., GIRLEA, I., "Quality Control and Calibration of Miniature Fission Chambers by Exposure to Standard Neutron Fields. Application to the Measurement of Fundamental Integral Cross Section Ratios", this conference.

[31] CROSS, W. G., ING, H., "Analytical Representation of Some Fast Neutron Cross Sections Useful in Dosimetry", Nucl. Sci. Eng. 58, 378 (1975).

[32] SMITH, D. L., MEADOWS, J. W., Report ANL/NDM - 13 (1975).

[33] SMITH, D. L., MEADOWS, J. W., Report ANL/NDM - 14 (1975).

[34] PINTER, M., SCHOLTYSSEK, W., FEHSENFELD, P., VAN DER KAMP, H. A. J., QUAADVLIET, H. J., FABRY, A., DeLEEUW, G. and S., COPS, F., GRUNDL, J. A., GILLIAM, D. M., EISENHAUER, C., Proc. Nuclear Cross Sections and Technology Conference, NBS Special Publication 425, Vol. I, 258 (1975).

[35] FABRY, A., WILLIAMS, J. G., HANNAN, A. H. M. A., AZIMI-GARAKANI, D., "Intercomparison of the Intermediate-Energy Standard Neutron Fields at the NISUS and Mol-ΣΣ Facilities by Means of Absolute Fission Chambers", this conference.

[36] FARRAR IV, H., McELROY, W. N., LIPPINCOTT, E. P., Nucl. Techn. 25, 305 (1975) and Reference [3].

[37] KIER, P. H., ROBBA, A. A., Report ANL-7326 (1967).

[38] GILLIAM, D. M., GRUNDL, J. A., HANSEN, G. E., HELMIK, H. H., Report HEDL-TME 75-130, p NBS-1 to NBS-31 (1975).

[39] DeLEEUW G., DeLEEUW S., See Reference [3].

[40] SIMONS, R. L., McELROY, W. N., Report BNWL-1312 (1970).

III.2. Ratios of Measured and Calculated Reaction Rates for some known Spectra

Willem L. Zijp
Henk J. Nolthenius
Jan H. Baard
(Physics Department)

Abstract:

For selected reactor neutron spectra, in which reaction rates of activation and fission detectors have been determined experimentally, also calculated values for these reaction rates were obtained, using the ENDF/B-IV and the DETAN-74 cross section libraries with a 620 group structure.
A comparison was made between experimental and calculated (integral) reaction rate values to study the performance of differential data in the reference cross section libraries.
The spectra considered are the fission neutron spectra of ^{235}U and ^{252}Cf, the spectra of the CFRMF and the ΣΣ facility (which are recognized benchmark spectra), supplemented with the neutron spectra of LFR, STEK-4000, STEK-2000, STEK-500.
The best consistency was obtained for the recognized benchmark spectra. There is some influence of the procedure for extrapolating the spectra at both ends. The method chosen indicates that neither sufficiently accurate spectrum data, nor enough experimental activities are available to make firm conclusions.
The cross section data for $^{48}Ti(n,p)$ give inconsistent results. Also the ENDF/B-IV data for $^{46}Ti(n,p)$ often tend to be inconsistent.

1. INTRODUCTION

This report presents ratios of measured and calculated activities for a few selected well known neutron spectra.
The ratios were calculated with aid of the available data for the neutron spectra and the experimentally determined saturation activities. The calculations were performed with the computer program SAND-II.
The task of this program in these calculations was to supply the spectrum data in 620 energy groups, to normalize the spectrum data with aid of the experimentally obtained activity values, and to calculate the ratio of measured (i.e. experimental) and calculated activities.
So no energy dependent spectrum modifications were performed during these calculations. In the calculations two cross section libraries have been used. Both libraries are available in the 620 groups SAND-II format.
These libraries are named DETAN-74 which is an updated SAND-II library and the ENDF/B-IV dosimetry file.
The cross section data in these libraries may show some reaction and energy dependent uncertainties.
In reference |1| a division of the activation reactions in a category I and a category II is given.
Category I reactions serve as reference: they have been selected as a set according to the following criteria:

- the set should provide a reasonable coverage of the energy range of interest in reactor technology;
- the set should contain reactions for which the differential nuclear data are the best known ones;
- the set should show consistency with respect to results of integral measurements.

Improvement of quality (i.e. precision and accuracy) or quantity (amount of experiments) of experimental data (differential or integral) should not lead to adjustment of cross section data, but only to reevaluation of the cross section data for these category I reactions.
Category II reactions include most other useful reactions for reactor radiation measurements.
The energy dependent cross data required for these reactions should be adjusted with respect to category I cross sections by a correlation scheme involving precise (and preferably interlaboratory) integral measurements in a limited set of benchmark spectra.

The data for the neutron spectra were available in various forms:
- analytical formulae;
- broad group calculations;
- point values with interpolation procedure.

In a number of cases extrapolation procedures were required at low and high energy values, because a non-negligible response contribution can be expected at these energy ranges for particular reactions.
Furthermore the broad group values were transferred to point values and with aid of SAND-II to a smooth spectrum distribution. This smooth distribution is considered as a better input spectrum for unfolding.
The smooth overall distribution gives a more reliable indication of irragularities in the unfolding than the coarse group structure.
The differences between the smooth distribution and the broad group values are also considered.
In some cases it was possible to modify the point values obtained from data with a broad group structure in such a way that the smooth distribution when condensed to the original groups yielded the same values as the original data.
The effect of this modification is also presented.

2. THE CROSS SECTION LIBRARIES

In the calculations two libraries in the SAND-II 620 group structure have been applied. Both libraries were kindly supplied by Dr A. Fabry from SCK/CEN at Mol in Belgium.
The DETAN-74 library |2| comprises the SAND-II library, supplemented and updated with 6 cross section data sets from the ENDF/B-III. Furthermore this library contains data described in |3|, while also older data are present.
The ENDF/B-IV dosimetry file is a library which contains evaluated data for dosimetry purposes |4|.
A small problem in these series of calculations was the absence of some reactions in the cross section libraries, e.g. $^{55}Mn(n,\gamma)$ in the ENDF/B-IV file and $^{59}Co(n,\alpha)$ in the DETAN-74 file.

3. SPECTRUM DATA

The spectrum data which could be used in these calculations were available in different forms.
Some spectra are described with an analytical formula (e.g. the fission neutron spectra for ^{235}U and ^{252}Cf). Other spectra are available in the form of group flux densities in a relatively broad energy structure.
For this reason a description of the origin and form of the different reference spectra is given in this section.

3.1. The fission neutron spectra

The spectra which may be described with an analytical function are the Maxwellian fission neutron spectra and the modified Maxwellian spectra. These spectra are given in |5| for ^{252}Cf and for ^{235}U.
The fission spectrum for ^{252}Cf is defined as:

$$\chi_{252} = 0.6672\ \sqrt{E}.\exp(-1.5E/2.13)$$

and for ^{235}U as:

$$\chi_{235} = 0.7501\ \sqrt{E}.\exp(-1.5E/1.97)$$

For both spectra a continuous line segment correction function is given which establishes a final fit with 16 documented differential spectromety measurements of ^{235}U thermal neutron induced and ^{252}Cf spontaneous fission neutron spectra |6|.
The line segment correction is given for 5 energy regions. Below 6 MeV the correction is a linear function of the energy. Above this value the correction function is exponential |5|.
In figure 1 plots are presented for the ^{252}Cf and ^{235}U fission neutron spectra.
The same plots for the modified neutron spectra show no clear differences on the applied scale. For this reason the ratio of the modified and the original Maxwellian are also presented in fig. 1. These plots show that the modification is rather small (<10%) in the energy region from 10^{-1} to 10 MeV. Outside this interval the minimum ratio is 0.7 for ^{252}Cf and 0.5 for ^{235}U.

3.2. The ΣΣ spectrum

The spectrum data have been obtained from |7|. These recommended data are given in a table with 145 energy values between 0.4×10^{-6} and 14.9 MeV. In that table the cumulative flux density and its second derivative are listed.

With these two values and an also published subroutine the 620 group spectrum data can be calculated for each selected energy group. This procedure was applied to calculate an input suitable for SAND-II.

The results showed some negative group flux values (e.i. from 2.7×10^{-5} to 3.6×10^{-5} MeV). These values were replaced by the last positive value at the low energy side. This can be seen in figure 2 where in order to demonstrate this effect also the $\phi_E(E)$ is plotted as function of the energy.

Some reactions may have response outside the energy interval in which spectrum information is available. For this reason an extrapolation procedure was applied.

At the low energy side a $\phi_E(E) = k.E$ distribution is used and at the high energy side a Leachman fission spectrum with the following shape is used for the extrapolation:

$$\chi_1 = k\sqrt{E}.\exp(-0.776\times E)$$

The extrapolated spectra are also shown in figure 2.

3.3. The CFRMF spectrum

The spectrum data were obtained from |8|. This information is given as group flux density values in a 69 groups structure from 0 to 10 MeV. The input of the SAND-II program requires however point values for $\phi_E(E)$. The available data can be transformed in differend ways, leading for example to:

- group values with ϕ_E is constant;
- group values with ϕ_u is constant;
- a smooth distribution.

The smooth distribution was obtained by using the group flux density as point flux density value at the energy $\Delta E/\Delta u$ (ΔE and Δu is the group widths in units of energy and lethargy respectively).

The smooth distribution between the energy point values is calculated with a log-log interpolation in the program SAND-II. If a smooth distribution has to be calculated also extrapolation in the low and the upper energy regions is performed.

The applied extrapolation method is the same as described for the ΣΣ facility. The plots of the three spectra are shown in figures 3 and 4.

3.4. The LFR spectrum

The spectrum data were available in 25 groups from 2.1×10^{-7} to 10 MeV.
The calculation data for a one slab core were taken from |9|.
The broad energy groups have not been used for the calculation of activities, since the data for the thermal group, which gives an important contribution to the reaction rate, were not given in the report.
For the further calculations the same procedure was used as applied for the STEK spectra.
The plots are shown in figure 5.

3.5. The STEK spectra

For the STEK facility, described in detail in |10|, broad group flux density data in a 26 group structure were used. These data comprise recent adjustments of previously reported data (see |11|).
The spectra were applied as broad group spectra with ϕ_u = constant.
These spectra are shown in figure 6.
The smooth spectra were obtained with another procedure as the one described for the CFRMF facility.
The start of the conversion was the same; the resulting spectrum was then condensed to the original group structure to check the procedure.
Due to the interpolation some small deviations were observed in the obtained new group values. This procedure was repeated with slightly modified input values for SAND-II.
The iteration procedure was ended if the condensed output values agreed within 0.3% with the original input data.
The smooth spectra are shown in figure 7. This figure shows also the difference between the corrected point values (as described above) and the uncorrected point values. From this figure it follows that the procedure to make a smooth distribution results in differences if the smooth distribution is condensed again. These differences are in this example at some energies in the order of 20%.

4. THE CALCULATIONS

The activities and fission rates used in the calculations are presented in table 1. In this table the uncertainty of the values is also supplied if this value was available.
The literature references serving as data sources are also listed in the table.
The spectrum data described previously and the activity values were applied in the input of SAND-II.
With aid of small programs the format of the original data was changed so that the output of these programs could be used as input for SAND-II.
One of these small programs calculated the energy points and the accompanying ϕ_E values in cases where a smooth spectrum was required.
The ITERATION mode of SAND-II was applied and the maximum number of iterations was made zero. This gives a normalized output spectrum without energy dependent modifications of the input spectrum data. The output of the program SAND-II comprises among others the ratios of measured and calculated activities.
The calculations are performed with the spectrum in a 620 groups structure and a cross section library in the same group structure.
The calculations are performed both for the category I reactions and for the combination of category I and II reactions.
The results showed that sometimes the ratio of measured and calculated activities showed large deviations from 1. In these cases new calculations were performed without the reaction giving the largest deviations. This proces was repeated until the maximum deviation from 1 was smaller than 10% for the category I reactions and smaller than 25% for the category I and II.
The results are presented for the original activity set and for a set from which all reactions with too large deviations were removed. These data are indicated in the tables with brackets.
These calculations have been performed for the two cross section libraries of interest.
For each spectrum the total standard deviation expressed in percent (s) as well as the number of input activities (n) applied are also listed.

The average energy ($\bar{E}$) in MeV and the average lethargy ($\bar{u}$) are also presented. These values are calculated with aid of artificial cross section sets |12|.
As a consequence of the normalization procedure the results presented in the table have always an average ratio of A_m/A_c equal to 1.

5. THE RESULTS

5.1.1. The fission spectra and category I reactions

The results for the ratio of measured and calculated activities is presented in table 2. From this table it follows that the A_m/A_c ratio for the reaction $^{197}Au(n,\gamma)$ is too high for all ^{252}Cf spectra.
This is probably due to an incorrect value for the ^{197}Au activity and not due to cross section uncertainties. The argument is that the results for the ^{235}U spectrum show no anomaly for ^{197}Au.
Furthermore the reaction $^{46}Ti(n,p)$ in the ^{235}U spectrum calculated with the ENDF/B-IV library gives a large value for this ratio. This effect is less pronounced for the ^{252}Cf spectrum.
The reaction $^{27}Al(n,\alpha)$ in the ^{252}Cf and the ENDF/B-IV library shows also a clear deviation. This deviation diminishes if the corrected ^{252}Cf fission spectrum is considered. This reaction is very sensitive to high energy neutrons and this part of the spectrum is appreciably changed (see figure 1).
In most cases after deletion of reactions with large ratios the standard deviations obtained with both libraries are somewhat smaller.

5.1.2. The fission spectra and categories I and II reactions

The results for the ratios are presented in table 3.
Here the same method was applied as described in 5.1.1., but in this case the category I reactions were not considered for consistency.
In the case that a category reaction was deleted in table 1, it was also not used in table 2.
The category II reactions were observed for consistency. If deviations larger than 10% occurred, these reactions were deleted and new ratios were calculated and listed in the table (between brackets).

The ratios calculated for category II reactions with the DETAN-74 library were all within a deviation of 25%. The ratios calculated with the ENDF/B-IV yielded several too large values.
In all spectra the reaction $^{48}Ti(n,p)$ gives a too high ratio for A_m/A_c. This indicates a too low cross section.
In the corrected ^{235}U fission neutron spectrum the reaction $^{63}Cu(n,\alpha)$ gives a too high value. For the normal Maxwellian this value is also rather high.
The reactions $^{55}Mn(n,2n)$ and $^{127}I(n,2n)$ give both too low results for the ^{235}U fission spectrum but the results are acceptable for the corrected fission neutron spectrum. This indicates that these reactions are also sensitive in the part of the spectrum where the correction function is important.
In this case also the standard deviations are in general somewhat smaller for the DETAN-74 library than for the ENDF/B-IV file.
Furthermore more reactions reamin in the set when the DETAN-74 library is used.

5.2.1. The ΣΣ spectrum and category I reactions

The results are presented in table 4. In all spectra and for both cross section libraries the reaction $^{58}Ni(n,p)$ gives a too large ratio. This may be due to a too high measured activity value.
The ratio for the reaction $^{197}Au(n,\gamma)$ is too large in the ENDF/B-IV library for a non-extrapolated spectrum. This is probably due to a relative important contribution to the activity of low energy neutrons.
In the spectrum with extrapolation and the DETAN-74 library a too high ratio for the reaction $^{27}Al(n,\alpha)$ was found after the deletion of the $^{58}Ni(n,p)$ reaction. The spectrum without extrapolation shows a value just below the rejection limit.
If one compares the results of both cross section libraries then one can observe that theirresuls are more or less the same. The same holds for the two forms of the spectrum except the reaction mentioned above.

5.2.2. The ΣΣ spectrum and categories I and II reactions

No extra reactions had to be removed from the category II data. The results for the two spectra and the two cross section libraries are more or less the same.

The s-values are somewhat better for the ENDF/B-IV but for these s-values the results for the reaction $^{55}Mn(n,\gamma)$ could not be used.
No clear difference is present between the results for the two forms of the spectrum.

5.3.1. The CFRMF and category I reactions

In all spectra and for both cross section libraries the ratios for the reaction $^{6}Li(n,\alpha)$ are too low (see table 4). The cross section data in both libraries are about the same (ENDF/B-III and ENDF/B-IV) so that either the experimental value is too low or the cross section too large.
The $^{46}Ti(n,p)$ reaction of the ENDF/B-IV cross section library gives a too large value. The difference between the ϕ_E and ϕ_E = constant representation of the spectrum data is rather small. The ϕ_E constant gives slightly better results.
The results for the smooth spectra are not so good as for the original data. Both libraries give comparable results if the large ratios are excluded.
The ENDF/B-IV library has in this case one reaction less ($^{46}Ti(n,p)$).

5.3.2. The CFRMF and categories I and II reactions

From the category II reactions a too large ratio is obtained for $^{48}Ti(n,p)$ with both libraries and in all spectra except the smooth spectrum with the DETAN-74 library (see table 5).
The ENDF/B-IV library gives a 20% higher ratio than the DETAN-74.
The smooth spectrum gives 20% lower ratio than the original spectrum data. This is probably due to the extrapolation.
The same effect of decrease of the ratio can also bee seen for the reaction $^{27}Al(n,\alpha)$ for this reaction the smooth spectrum gives a 10% lower ratio.
In the two original spectra the reaction $^{59}Co(n,\gamma)$ gives a too large ratio for the ENDF/B-IV results. This is improved in the smooth spectrum and thus probably also due to the extrapolation procedure.
The general results are more or less the same for the original spectra in the $\phi_E(E)$ and $\phi_u(u)$ is constant representation.
The results for the smooth spectrum seem to be better for the original set as well as the set where the largest ratios were removed. In the latter set of the smooth spectrum one more reaction was applied compared with the diminished sets of the original spectra.

The two libraries gave about the same results for all spectra.
If the too large ratios are deleted the DETAN-74 keeps the most reactions for the analysis.

5.4.1. The STEK-2000 and category I reactions

The results for three spectrum representations are presented in table 6. The results for the three spectrum forms are nearly equal, but the corrected point values (e.i. the values which give the same flux densities as the original when they are transferred to this group structure) are better than the uncorrected point values.
The rather high s-values compared with the s-values for previous described spectra might indicate a less realistic input data set. In general one may conclude that here either the input activities or the input spectrum data are not fully correct.
In this case the deleted reactions will not give much information and also the number of reactions which remain.
For the total set the ENDF/B-IV library gives a higher standard deviation than the DETAN-74.

5.4.2. The STEK-2000 and categories I and II reactions

The results presented in table 7 are similar to those described in 5.4.1. No clear difference can be seen between the three spectra and libraries due to the inconsistent input data.
In this case the DETAN-74 gives also somewhat better results but they remain rather poor.

5.5.1. Other spectra and category I reactions

The results for these spectra are given in table 8 and 10. The data for the smooth spectra are listed in table 8. Table 10 gives a comparison between the total S-values for smooth spectra and histogram data.
The results for the two STEK spectra show the same properties as the spectra described in 5.4.1.
The data for the STEK-500 are more consistent than the data for STEK-4000 and STEK-2000, but still not enough to make statements on the cross section behaviour.

The set which is obtained in the LFR shows a better performance.
For both libraries the reaction ^{235}U is deleted from the input set. This is probably due to spectrum uncertainties in the thermal and intermediate region and an inconsistency with the reaction $^{197}Au(n,\gamma)$.
The data from table 10 show that the differences in s-values for the smooth spectra and for histogram spectra are rather small for these spectra.

5.5.2. Other spectra and categories I and II reactions

These data are presented in table 9 and 11. The same comment holds as for 5.5.1. In these data the STEK-500 results are also somewhat better.
In the LFR spectrum the reaction $^{45}Sc(n,\gamma)$ is deleted for the DETAN-74 library and due to the ratio of 1.2499 for the ENDF/B-IV library it remains in the set.
But this reaction gives rather high ratios compared with other reactions.
The $^{48}Ti(n,p)$ reaction in the ENDF/B-IV library results is too large.
The results for the reaction $^{115}In(n,\gamma)$ are too low for both libraries.
This is probably due to a too low activity caused by an incorrect neutron selfshielding correction applied for the activity value.
The results in table 11 show that the differences between s-values and number of reaction are rather small for the smooth and histogram spectrum representations.

6. DISCUSSION

The applied procedures may give clear results if the spectrum data and the activity values are good enough but one has to conclude from these results that also sometimes activity values do not fit and that spectrum data are not accurate enough. This can be illustrated with the STEK data sets and e.g. the $^{197}Au(n,\gamma)$ in the ^{252}Cf spectrum.
Rather high values for the reaction $^{46}Ti(n,p)$ are found in ^{235}U fission neutron spectrum, the CFRMF spectrum and the ENDF/B-IV library.
In these spectra ratios of $A_m/A_C=1.15$ is found.
The reaction $^{27}Al(n,\alpha)$ gives a rather low value in the ^{252}Cf spectrum but the spectrum data of ^{235}U fission, $\Sigma\Sigma$ and CFRMF yield rather normal results.

The $^{48}Ti(n,p)$ reaction gives A_m/A_c ratios larger than ±25% when the ENDF/B-IV file is applied to the fission spectra, the CFRMF spectrum and the STEK spectra (ratio from 1.4-1.9).
In other cases the ^{235}U spectrum and modified ^{235}U fission spectrum have a large effect on the results, so that a reaction which is acceptable in one spectrum representation is deleted in the other spectrum representation (e.g. $^{55}Mn(n,2n)$ and $^{127}I(n,2n)$ in the ^{235}U fission spectrum and the ENDF/B-IV library.
In this case a choice of the spectrum representation is necessary to make a judgement.
In the LFRMF a low ratio for the reaction $^{6}Li(n,\alpha)$ is obtained for both libraries. The reaction $^{59}Co(n,\gamma)$ gives in the CFRMF and the ENDF/B-IV library in the CFRMF spectra without extrapolation a too large ratio, while this is not the case for the extrapolated spectrum.
This indicates that the method of interpolation is important. The method of translating broad group flux densities to input data of SAND-II seems to be not so important.
The ϕ_u = constant and the ϕ_E = constant per group did not give clear differences. The smooth spectrum gave in most cases a somewhat worser fit.
The iteration method to keep the group values of the transfered smooth spectrum equal with the original data gave no clearly better results, probably due to the quality of the data applied in these calculations.
The quality of the DETAN-74 library seems to be better taking into account the smaller s-values and the larger number of reactions kept in the analysis (the latter on the basis of our rather arbitrary criterium for deletion).

7. CONCLUSION

With the data considered not so many sharp conclusions can be obtained.
From the applied data the fission spectra, the ΣΣ and the CFRMF seem to be the only spectra with accurate experimental activities as well as reasonably fitting spectrum data.
But the spectrum data need in most cases some extrapolation which can be done rather arbitrarily, so that the results can vary dependent on the chosen method.

For the ^{252}Cf and the ΣΣ the list of available activities is rather short. This method of comparing library data indicates that neither sufficiently accurate spectrum data nor enough experimental activities are available to make firm conclusions.

8. REFERENCES

|1| Proceedings of a Consultants Meeting on Nuclear Data for Reactor Neutron Dosimetry, Vienna, 10-12 September 1973. Report INDC(NDS)-56/U (IAEA, Vienna,1974).

|2| Private communication from Dr A. Fabry coded: Eisenhauer, C.; Fabry, A.: "DETAN-74 computer code for calculating detector responses in reactor neutron spectra" (October 1974).

|3| Simons, R.L.; McElroy, W.N.: "Evaluated reference cross section library" BNWL-1312 (May, 1970).

|4| Magurno, B.A.: "ENDF/B-IV dosimetry file" BNL-NCS-50446 (National Neutron Cross Section Center, Brookhaven National Laboratory, April, 1975).

|5| Grundl, J.; Eisenhauer, C.: "Fission rate measurements for materials neutron dosimetry in reactor environments" Paper presented at 1st ASTM-Euratom Symposium on Reactor Dosimetry Petten, Netherlands, September 22-25, 1975 (National Bureau of Standards, Washington).

|6| Grundl, J.A.; Eisenhauer, C.M,: "Fission spectrum neutrons for cross section validation and neutron flux transfer" Conf. on Nucl. Cross section and Technology, Washington DC, March, 1975.

|7| Fabry, A.; Leeuw, G. de; Leeuw, S. de: "MOL ΣΣ neutron field" Nucl. Technology 25 (1975), 349, 375.

|8| McElroy, W.N., editor: "LMFBR reaction rate and dosimetry 8th progress report for the period March-September 1973"
HEDL-TME-73-54 (Hanford Engineering Development Laboratory, February, 1974).

|9| Baas, F.; Zijp, W.L.: "Neutron Metrology in the LFR. TEDDI-M spectrum calculations"
RCN-72-137 (Reactor Centrum Nederland, Petten, November 24, 1972).

|10| Klippel, H.Th.; Smit, J.: "The coupled fast-thermal critical facility STEK"
Report RCN-209 (Reactor Centrum Nederland, Petten, 1974).

|11| Zijp, W.L.; Nolthenius, H.J.; Baard, J.H.: "Neutron spectra in the STEK facility, determined with the SAND-II activation technique"
Report RCN-232 (Reactor Centrum Nederland, Petten, September 1975).

|12| Nolthenius, H.J.; Rieffe, H.Ch.: "Damage cross section library (SANDAMAGE)"
RCN-75-066 (Reactor Centrum Nederland, Petten, May 1975).

|13| Fabry, A. et al.: "Reactor dosimetry integral reaction rate data in LMFBR benchmark and standard neutron fields: status, accuracy and implications"
Report prepared for the 1st ASTM-Euratom Symposium on Reactor Dosimetry (Petten, September 22-26, 1975).

|14| McElroy, W.N.; Kellog, L.S.: "Data development and testing"
Nucl. Technology 25 (1975), 203.

|15| Zijp, W.L.; Appelman, K.H.; Nolthenius, H.J.: "Neutron Metrology in the HFR. Neutron spectra in C3, E5 and H3 as determined in FLUX-75 experiment"
RCN-75-090 (Reactor Centrum Nederland, Petten, Juyly 1975).

|16| Beyaart, L.: "Neutron Metrology in the LFR. Determination of the neutron spectrum in the VC plug"
RCN-74-015 (Reactor Centrum Nederland, Petten, January 16, 1974).

Table 1: Measured activities with their coefficients of variation (in per cent)

reaction	^{252}Cf fission |13|		^{235}U fission |14|		ΣΣ |14|		CFRMF |14|		STEK-500 |11|		HFR (E5-100) |15|		STEK-2000 |11|		STEK-4000 |11|		LFR |16|	
	A_m	ε	A_m	ε	A_m	ε	A_m	ε	A_m	ε	A_m	ε	A_m	ε	A_m	ε	A_m	ε	A_m	ε
$^{197}Au(n,\gamma)^{198}Au$	95.5	2.4	0.0704	5.1	0.278	3.5	0.273	1.7	0.132E-15	2.1	5.60E-8	5.4	0.648E-15	2.9	0.207E-14	2.2	0.105E-10	3.0
$^{197}Au(n,\gamma)^{198}Au$ Cd											4.56E-8	2.1					0.394E-11	3.0
$^{6}Li(n,\alpha)^{3}H$							0.542	3.5										
$^{10}B(n,\alpha)^{7}Li$							1.170	2.1										
$^{27}Al(n,\alpha)^{24}Na$	1.006	2.2	0.000580	2.8	0.000114	4.5	0.0001038	1.8	0.392E-19	3.7					0.337E-19	4.4		
$^{27}Al(n,\alpha)^{24}Na$ Cd											1.399E-13	4.0					0.179E-17	4.0
$^{46}Ti(n,p)^{46}Sc$	13.8	2.2	0.00984	4.1			0.001675	2.4	0.775E-18	6.9			0.970E-18	3.9	0.109E-17	13.7		
$^{46}Ti(n,p)^{46}Sc$ Cd											2.702E-12	2.1						
$^{58}Ni(n,p)^{58}Co$	118	2.5	0.0904	2.2	0.0181	4	0.01544	1.7	0.785E-17	2.3			0.101E-16	3.7	0.109E-16	2.2	0.306E-15	3.0
$^{58}Ni(n,p)^{58}Co$ Cd											2.746E-11	2.1					0.307E-15	3.0
$^{235}U(n,f)$	1203	2.5	1.0 ref.	5.6	1.0 ref.	3.5	1.000 ref.		0.399E-15	1.9	6.20E-8	6.2	0.113E-14	1.7	0.211E-14	2.9		
$^{235}U(n,f)$ Cd											8.083E-9	3.7					0.850E-12	7.0
$^{238}U(n,f)$	320	2.8	0.262	3.0	0.0530	3.5	0.0485	1.4	0.256E-16	3.0			0.349E-16	4.1	0.389E-16	8.7		
$^{238}U(n,f)$ Cd																	0.130E-14	9.0
$^{237}Np(n,f)$	1332	2.8	1.096	5.5	0.399	4	0.354	2.3										
$^{239}Pu(n,f)$	1804	2.5	1.487	3.2	1.18	3.5	1.145	1.5										
$^{23}Na(n,\gamma)^{24}Na$									0.449E-18	3.1			0.142E-17	3.5	0.282E-17	2.6		
$^{23}Na(n,\gamma)^{24}Na$ Cd											8.727E-12	3.0					0.822E-15	3.0
$^{45}Sc(n,\gamma)^{46}Sc$							0.01507	2.3	0.831E-17	2.2			0.244E-16	3.5	0.518E-16	2.2		
$^{45}Sc(n,\gamma)^{46}Sc$ Cd											3.470E-10	4.0					0.367E-13	4.0
$^{55}Mn(n,\gamma)^{56}Mn$					0.0250	4.5			0.986E-17	2.4	1.82E-9	5.5	0.689E-16	2.2	0.153E-15	2.3	0.995E-12	5.5
$^{55}Mn(n,\gamma)^{56}Mn$ Cd											3.840E-10	2+1						
$^{58}Fe(n,\gamma)^{59}Fe$							0.00393	2.1					0.950E-17	7.5	0.166E-16	3.6		
$^{58}Fe(n,\gamma)^{59}Fe$ Cd											3.282E-11	3.1						
$^{59}Co(n,\gamma)^{60}Co$							0.0588	2.7	0.770E-17	5.4	5.41E-9	5.4	0.119E-15	2.5	0.392E-15	2.1	0.269E-11	5.4
$^{59}Co(n,\gamma)^{60}Co$ Cd											1.484E-9	2.1					0.210E-12	2.5
$^{63}Cu(n,\gamma)^{64}Cu$			0.00808	15	0.0252	6	0.0292	4.7	0.117E-16	3.6	7.25E-10	7.0	0.365E-16	2.7	0.715E-16	2.4		
$^{63}Cu(n,\gamma)^{64}Cu$ Cd											1.429E-10	5.0						
$^{115}In(n,\gamma)^{116}In^{m}$	125.3	3.4	0.117	3.4	0.164	5	0.181	2.9	0.872E-16	2.1	3.57E-8	5.0	0.295E-15	2.6	0.995E-15	2.1		
$^{115}In(n,\gamma)^{116}In^{m}$ Cd											1.759E-8	2.3					0.184E-11	3.0
$^{232}Th(n,\gamma)^{233}Th$													0.473E-15	5.4				
$^{232}Th(n,\gamma)^{233}Th$ Cd																	0.256E-12	10.0
$^{238}U(n,\gamma)^{239}U$					0.122	5	0.118	2.8	0.687E-16	2.5			0.273E-15	5.5	0.675E-15	2.1		
$^{24}Mg(n,p)^{24}Na$			0.00122	2.0														
$^{27}Al(n,p)^{27}Mg$			0.0032	10	0.00065	10	0.000561	2.4										
$^{31}P(n,p)^{31}Si$			0.0288	5.6														
$^{32}S(n,p)^{32}P$			0.0552	2.9														
$^{47}Ti(n,p)^{47}Sc$	18.9	2.1	0.016	10			0.00268	4.2	0.149E-17	2.5			0.207E-17	3.5	0.197E-17	2.2		
$^{47}Ti(n,p)^{47}Sc$ Cd											4.649E-12	3.0						
$^{48}Ti(n,p)^{48}Sc$	0.42	2.4	0.000252	6.3			0.0000442	2.4	0.169E-19	2.6			0.227E-19	3.7	0.227E-19	2.6	0.577E-16	3.0
$^{48}Ti(n,p)^{48}Sc$ Cd											6.501E-14	2.1						
$^{54}Fe(n,p)^{54}Mn$	84.6	2.4	0.0660	2.4			0.01120	1.7	0.579E-17	3.4			0.716E-17	3.8	0.814E-17	2.6	0.810E-18	3.0
$^{54}Fe(n,p)^{54}Mn$ Cd											2.009E-11	2.1						
$^{56}Fe(n,p)^{56}Mn$	1.45	2.4							0.643E-19	2.8			0.798E-19	2.8	0.868E-19	2.8	0.184E-15	2.5
$^{56}Fe(n,p)^{56}Mn$ Cd											2.390E-13	3.0						
$^{55}Mn(n,2n)^{54}Mn$			0.000202	4.0														
$^{59}Co(n,\alpha)^{56}Mn$			0.000125	3.8									0.106E-18	3.9	0.115E-19	4.3		
$^{63}Cu(n,\alpha)^{60}Co$			0.00040	10														
$^{115}In(n,n')^{115}In^{m}$	198	2.5	0.150	2.1	0.0369	3.5	0.03194	4.6	0.192E-16	3.2			0.249E-16	3.1	0.263E-16	2.3		
$^{115}In(n,n')^{115}In^{m}$ Cd											5.973E-11	4.0					0.790E-15	6.0
$^{127}I(n,2n)^{126}I$			0.000872	4.6													0.820E-15	4.0
$^{232}Th(n,f)$			0.0664	4.2	0.0132	6							0.107E-16	7.4				
$^{232}Th(n,f)$ Cd																	0.310E-15	10.0

Table 2: Ratio of measured and calculated activities

Case of fission neutron spectra and category I reactions.

DETAN-74

reaction	spectrum			
	^{252}Cf Maxwellian	^{252}Cf modified Maxwellian	^{235}U modified Maxwellian	^{235}U Maxwellian
^{27}Al(n,α)^{24}Na	0.893 (0.911)	0.958 (0.976)	1.014	0.915
^{46}Ti(n,p)^{46}Sc	0.980 (1.000)	0.983 (1.002)	1.024	1.037
^{58}Ni(n,p)^{58}Co	1.018 (1.039)	1.007 (1.026)	1.051	1.077
^{197}Au(n,γ)^{198}Au	1.141	1.132	0.948	0.951
^{235}U(n,f)	0.962 (0.982)	0.947 (0.965)	0.947	0.957
^{238}U(n,f)	1.010 (1.031)	0.995 (1.014)	1.044	1.065
^{237}Np(n,f)	1.012 (1.033)	0.996 (1.015)	1.009	1.022
^{239}Pu(n,f)	0.984 (1.004)	0.982 (1.001)	0.964	0.976
n	8 (7)	8 (7)	8	8
s (in %)	6.97 (4.42)	5.71 (2.20)	4.17	5.87

ENDF/B-IV

reaction	spectrum			
	^{252}Cf Maxwellian	^{252}Cf modified Maxwellian	^{235}U modified Maxwellian	^{235}U Maxwellian
^{27}Al(n,α)^{24}Na	0.857	0.921 (0.943)	0.970 (0.990)	0.886 (0.893)
^{46}Ti(n,p)^{46}Sc	1.057 (1.060)	1.067 (1.092)	1.142	1.164
^{58}Ni(n,p)^{58}Co	1.005 (1.008)	0.995 (1.018)	1.032 (1.053)	1.072 (1.080)
^{197}Au(n,γ)^{198}Au	1.167	1.158	0.966 (0.986)	0.982 (0.990)
^{235}U(n,f)	0.955 (0.958)	0.940 (0.962)	0.934 (0.953)	0.959 (0.966)
^{238}U(n,f)	0.998 (1.001)	0.983 (1.006)	1.027 (1.048)	1.062 (1.070)
^{237}Np(n,f)	0.972 (0.975)	0.955 (0.977)	0.963 (0.983)	0.990 (0.998)
^{239}Pu(n,f)	0.994 (0.997)	0.978 (1.001)	0.968 (0.988)	0.995 (1.003)
n	8 (6)	8 (7)	8 (7)	8 (7)
s (in %)	8.83 (3.48)	7.77 (4.84)	6.61 (3.67)	8.83 (6.33)
$\bar{E}_u$ (in MeV)	2.13	2.12	1.98	1.97
	1.92	1.91	1.99	1.99

Table 3: Ratio of measured and calculated activities

Case of fission neutron spectra and categories I and II reactions.

DETAN-74

reaction	spectrum			
	^{252}Cf modified Maxwellian	^{252}Cf Maxwellian	^{235}U modified Maxwellian	^{235}U Maxwellian
$^{197}Au(n,\gamma)^{198}Au$	1.149	1.164	0.917 (0.935)	0.941
$^{27}Al(n,\alpha)^{24}Na$	0.972 (0.983)	0.911 (0.923)	0.980 (0.999)	0.905
$^{46}Ti(n,p)^{46}Sc$	0.997 (1.009)	1.000 (1.013)	0.991 (1.011)	1.027
$^{58}Ni(n,p)^{58}Co$	1.022 (1.034)	1.039 (1.053)	1.016 (1.036)	1.066
$^{235}U(n,f)$	0.961 (0.972)	0.982 (0.994)	0.916 (0.934)	0.948
$^{238}((n,f)$	1.009 (1.021)	1.031 (1.044)	1.010 (1.030)	1.054
$^{237}Np(n,f)$	1.011 (1.022)	1.033 (1.046)	0.976 (0.995)	1.012
$^{239}Pu(n,f)$	0.997 (1.008)	1.004 (1.017)	0.932 (0.951)	0.966
$^{63}Cu(n,\gamma)^{64}Cu$			0.837 (0.854)	0.857
$^{115}In(n,\gamma)^{116}In^{m}$	0.877 (0.887)	0.893 (0.905)	0.905 (0.923)	0.930
$^{24}Mg(n,p)^{24}Na$			0.913 (0.931)	0.857
$^{27}Al(n,p)^{27}Mg$			0.942 (0.961)	0.970
$^{31}P(n,p)^{31}Si$			1.008 (1.028)	1.059
$^{32}S(n,p)^{32}P$			1.043 (1.064)	1.095
$^{47}Ti(n,p)^{47}Sc$	1.006 (1.018)	1.026 (1.039)	1.076 (1.097)	1.129
$^{48}Ti(n,p)^{48}Sc$	1.084 (1.096)	0.997 (1.010)	1.192 (1.216)	1.067
$^{54}Fe(n,p)^{54}Mn$	0.961 (0.972)	0.975 (0.988)	0.991 (1.011)	1.039
$^{56}Fe(n,p)^{56}Mn$	0.927 (0.937)	0.893 (0.904)		
$^{55}Mn(n,2n)^{54}Mn$				
$^{59}Co(n,\alpha)^{56}Mn$				
$^{63}Cu(n,\alpha)^{60}Co$			0.950 (0.969)	0.910
$^{115}In(n,n')^{115}In^{m}$	1.027 (1.039)	1.051 (1.065)	0.938 (0.957)	0.980
$^{127}I(n,2n)^{126}I$			1.390	1.066
$^{232}Th(n,f)$			1.077 (1.098)	1.123
n	14 (13)	14 (13)	21 (20)	21
s (in %)	7.1 (5.15)	6.5 (5.59)	11.8 (7.96)	8.2
$\bar{E}$ (in MeV)	2.13	2.12	1.98	1.97
u	1.92	1.91	1.99	1.99

Table 3 (continued):

ENDF/B-IV

reaction	spectrum			
	^{252}Cf Maxwellian	^{252}Cf modified Maxwellian	^{235}U modified Maxwellian	^{235}U Maxwellian
^{197}Au(n,γ)^{198}Au	1.159	1.142	0.941 (0.999)	0.975 (0.977)
^{27}Al(n,α)^{24}Na	0.851	0.908 (0.961)	0.945 (1.003)	0.880 (0.882)
^{46}Ti(n,p)^{46}Sc	1.050 (1.091)	1.052 (1.113)	1.112	1.156
^{58}Ni(n,p)^{58}Co	0.998 (1.037)	0.981 (1.038)	1.005 (1.067)	1.064 (1.066)
^{235}U(n,f)	0.948 (0.985)	0.927 (0.981)	0.910 (0.966)	0.952 (0.954)
^{238}U(n,f)	0.991 (1.030)	0.969 (1.025)	1.000 (1.062)	1.055 (1.057)
^{237}Np(n,f)	0.965 (1.003)	0.942 (0.996)	0.938 (0.996)	0.983 (0.985)
^{239}Pu(n,f)	0.987 (1.026)	0.964 (1.020)	0.943 (1.001)	0.988 (0.990)
^{63}Cu(n,γ)^{64}Cu			0.831 (0.882)	0.864 (0.866)
^{115}In(n,γ)^{116}In^{m}	0.938 (0.975)	0.919 (0.972)	0.973 (1.033)	1.011 (1.013)
^{24}Mg(n,p)^{24}Na				
^{27}Al(n,p)^{27}Mg			0.877 (0.931)	0.911 (0.913)
^{31}P(n,p)^{31}Si				
^{32}S(n,p)^{32}P			0.973 (1.033)	1.032 (1.034)
^{47}Ti(n,p)^{47}Sc	0.771 (0.801)	0.758 (0.802)	0.844 (0.896)	0.892 (0.894)
^{48}Ti(n,p)^{48}Sc	1.410	1.514	1.650	1.531
^{54}Fe(n,p)^{54}Mn	0.922 (0.958)	0.907 (0.959)	0.959 (1.018)	1.016 (1.018)
^{56}Fe(n,p)^{56}Mn	0.907 (0.943)	0.939 (0.993)		
^{55}Mn(n,2n)^{54}Mn			0.932 (0.989)	0.686
^{59}Co(n,α)^{56}Mn			0.955 (1.014)	0.906 (0.908)
^{63}Cu(n,α)^{60}Co			1.283	1.225 (1.227)
^{115}In(n,n')^{115}In^{m}	1.105 (1.149)	1.078 (1.140)	1.013 (1.075)	1.070 (1.072)
^{127}I(n,2n)^{126}I			0.830 (0.881)	0.655
^{232}Th(n,f)			1.087 (1.154)	1.146 (1.148)
n	14 (11)	14 (12)	21 (18)	21 (17)
s (in %)	15.3 (8.88)	17.3 (8.45)	18.0 (7.09)	18.3 (9.98)
$\bar{E}$ (in MeV)	2.13	2.12	1.98	1.97
u	1.92	1.91	1.99	1.99

Table 4: Ratio of measured and calculated activities

Case of CFRMF and ΣΣ spectra and category I reactions.

ENDF/B-IV

reaction	spectrum			
	ΣΣ	CFRMF constant $\phi_E(E)$	CFRMF constant $\phi_u(u)$	ΣΣ with extrapolation	CFRMF smooth
$^{197}Au(n,\gamma)^{198}Au$	1.120	1.005 (1.003)	0.999 (0.998)	1.060 (1.079)	1.004 (1.000)
$^{6}Li(n,\alpha)^{3}H$		0.839	0.834		0.835
$^{10}B(n,\alpha)^{7}Li$		1.059 (1.057)	1.051 (1.050)		1.051 (1.047)
$^{27}Al(n,\alpha)^{24}Na$	1.043 (1.089)	0.988 (0.986)	1.010 (1.009)	1.050 (1.068)	0.896 (0.893)
$^{46}Ti(n,p)^{46}Sc$		1.148	1.158		1.168
$^{58}Ni(n,p)^{58}Co$	1.090	1.044 (1.042)	1.045 (1.044)	1.103	1.068 (1.064)
$^{235}U(n,f)$	0.927 (0.968)	0.956 (0.954)	0.950 (0.949)	0.937 (0.953)	0.958 (0.954)
$^{238}U(n,f)$	0.948 (0.990)	1.034 (1.032)	1.033 (1.032)	0.958 (0.975)	1.057 (1.053)
$^{237}Np(n,f)$	0.924 (0.965)	0.950 (0.948)	0.948 (0.947)	0.934 (0.950)	1.013 (1.009)
$^{239}Pu(n,f)$	0.948 (0.990)	0.977 (0.975)	0.972 (0.971)	0.958 (0.975)	0.984 (0.980)
n	7 (5)	10 (8)	10 (8)	7 (6)	10 (8)
s (in %)	8.26 (5.10)	8.15 (4.08)	8.45 (4.10)	6.89 (5.79)	9.38 (5.76)

DETAN-74

reaction	spectrum				
	ΣΣ	CFRMF	CFRMF	ΣΣ with extrapolation	CFRMF smooth
$^{197}Au(n,\gamma)^{198}Au$	1.055 (1.074)	0.956 (0.942)	0.950 (0.936)	0.999 (1.041)	0.955 (0.941)
$^{6}Li(n,\alpha)^{3}H$		0.873	0.868		0.870
$^{10}B(n,\alpha)^{7}Li$		1.039 (1.024)	1.031 (1.016)		1.033 (1.018)
$^{27}Al(n,\alpha)^{24}Na$	1.077 (1.097)	1.033 (1.018)	1.056 (1.041)	1.084	0.937 (0.924)
$^{46}Ti(n,p)^{46}Sc$		1.052 (1.037)	1.059 (1.044)		1.066 (1.051)
$^{58}Ni(n,p)^{58}Co$	1.108	1.070 (1.055)	1.070 (1.055)	1.119	1.092 (1.076)
$^{235}U(n,f)$	0.909 (0.926)	0.947 (0.934)	0.941 (0.927)	0.917 (0.956)	0.950 (0.936)
$^{238}U(n,f)$	0.948 (0.965)	1.047 (1.032)	1.046 (1.031)	0.957 (0.998)	1.071 (1.056)
$^{237}Np(n,f)$	0.969 (0.987)	1.010 (0.996)	1.008 (0.994)	0.979 (1.021)	1.044 (1.029)
$^{239}Pu(n,f)$	0.935 (0.952)	0.975 (0.961)	0.970 (0.956)	0.944 (0.984)	0.983 (0.969)
n	7 (6)	10 (9)	10 (9)	7 (5)	10 (9)
s (in %)	7.83 (6.94)	6.15 (4.42)	6.58 (4.91)	7.47 (3.29)	7.19 (5.81)
$\bar{E}_u$ (in MeV)	0.761	0,717	0.716	0.762	0.706
	3.42	3.50	3.51	3.42	3.53

Table 5: Ratio of measured and calculated activities

Case of CFRMF and ΣΣ spectra and category I reactions.

DETAN-74

reaction	spectrum				
	ΣΣ	CFRMF ϕ_E=constant	CFRMF ϕ_{i} =constant	ΣΣ with extrapolation	CFRMF smooth
$^{6}Li(n,\alpha)^{3}H$		0.871	0.864		0.880
$^{10}B(n,\alpha)^{6}Li$		1.037 (1.048)	1.027 (1.039)		1.045 (1.034)
$^{27}Al(n,\alpha)^{24}Na$	1.120 (1.133)	1.031 (1.042)	1.052 (1.065)	1.124	0.947 (0.937)
$^{46}Ti(n,p)^{46}Sc$		1.050 (1.061)	1.054 (1.067)		1.078 (1.066)
$^{58}Ni(n,p)^{58}Co$	1.153	1.068 (1.080)	1.065 (1.078)	1.161	1.105 (1.093)
$^{197}Au(n,\gamma)^{198}Au$	1.097 (1.110)	0.954 (0.964)	0.946 (0.957)	1.037 (1.062)	0.966 (0.956)
$^{235}U(n,f)$	0.945 (0.956)	0.945 (0.955)	0.937 (0.948)	0.952 (0.975)	0.961 (0.951)
$^{238}U(n,f)$	0.986 (0.998)	1.045 (1.056)	1.042 (1.055)	0.993 (1.017)	1.083 (1.071)
$^{237}Np(n,f)$	1.008 (1.020)	1.008 (1.019)	1.004 (1.016)	1.015 (1.040)	1.056 (1.045)
$^{239}Pu(n,f)$	0.973 (0.985)	0.973 (0.984)	0.966 (0.978)	0.979 (1.003)	0.994 (0.983)
$^{27}Al(n,p)^{27}Mg$	1.168 (1.182)	0.992 (1.003)	1.001 (1.013)	1.176 (1.205)	1.038 (1.027)
$^{45}Sc(n,\gamma)^{46}Sc$		1.046 (1.057)	1.035 (1.048)		1.054 (1.043)
$^{47}Ti(n,p)^{47}Sc$		1.095 (1.107)	1.093 (1.106)		1.134 (1.122)
$^{48}Ti(n,p)^{48}Sc$		1.332	1.365		1.094 (1.082)
$^{54}Fe(n,p)^{54}Mn$		1.037 (1.048)	1.037 (1.050)		1.078 (1.066)
$^{55}Mn(n,\gamma)^{56}Mn$	0.994 (1.006)			1.001 (1.026)	
$^{58}Fe(n,\gamma)^{59}Fe$		0.792 (0.801)	0.797 (0.807)		0.805 (0.796)
$^{59}Co(n,\gamma)^{60}Co$		1.141 (1.153)	1.145 (1.159)		1.103 (1.091)
$^{63}Cu(n,\gamma)^{64}Cu$	0.864 (0.874)	0.859 (0.868)	0.868 (0.879)	0.871 (0.892)	0.888 (0.878)
$^{115}In(n,\gamma)^{116}In$	0.856 (0.866)	0.938 (0.948)	0.928 (0.939)	0.849 (0.870)	0.951 (0.941)
$^{115}In(n,n')^{115}In^{m}$	0.978 (0.990)	0.997 (1.008)	0.994 (1.006)	0.985 (1.009)	1.041 (1.030)
$^{232}Th(n,f)$	1.023 (1.035)			1.030 (1.055)	
$^{238}U(n,\gamma)^{239}U$	0.835 (0.845)	0.789 (0.798)	0.781 (0.790)	0.825 (0.845)	0.796 (0.787)
n	14 (13)	21 (19)	21 (19)	14 (12)	21 (20)
(in %)	10.6 (10.2)	12.0 (9.50)	12.6 (9.59)	10.7 (9.75)	9.77 (9.54)
$\bar{E}$ (in MeV)	0.761	0.717	0.716	0.762	0.706
	3.42	3.50	3.51	3.42	3.53

Table 5 (continued): Case of CFRMF and ΣΣ spectra and categories I and II reactions.

ENDF/B-IV

reaction	spectrum			
	ΣΣ	CFRMF ϕ_E=constant	CFRMF ϕ_u=constant	ΣΣ with extrapolation	CFRMF smooth
$^{6}Li(n,\alpha)^{3}H$		0.808	0.800		0.821
$^{10}B(n,\alpha)^{6}Li$		1.021 (1.089)	1.009 (1.077)		1.034 (1.062)
$^{27}Al(n,\alpha)^{24}Na$	1.073 (1.100)	0.952 (1.016)	0.969 (1.034)	1.078 (1.090)	0.882 (0.906)
$^{46}Ti(n,p)^{46}Sc$		1.106	1.112		1.149
$^{58}Ni(n,p)^{58}Co$	1.122	1.006 (1.073)	1.003 (1.071)	1.132	1.051 (1.080)
$^{197}Au(n,\gamma)^{198}Au$	1.152	0.968 (1.033)	0.959 (1.024)	1.088 (1.100)	0.988 (1.015)
$^{235}U(n,f)$	0.954 (0.978)	0.921 (0.983)	0.912 (0.973)	0.962 (0.972)	0.943 (0.969)
$^{238}U(n,f)$	0.975 (1.000)	0.967 (1.032)	0.992 (1.059)	0.984 (0.995)	1.040 (1.069)
$^{237}Np(n,f)$	0.950 (0.974)	0.916 (0.977)	0.910 (0.971)	0.959 (0.969)	0.965 (0.991)
$^{239}Pu(n,f)$	0.975 (1.000)	0.942 (1.005)	0.934 (0.997)	0.983 (0.994)	0.968 (0.995)
$^{27}Al(n,p)^{27}Mg$	1.081 (1.109)	0.889 (0.949)	0.895 (0.955)	1.090 (1.102)	0.933 (0.948)
$^{45}Sc(n,\gamma)^{46}Sc$		1.112 (1.186)	1.109 (1.184)		1.124 (1.155)
$^{47}Ti(n,p)^{47}Sc$		0.812 (0.866)	0.810 (0.865)		0.847 (0.870)
$^{48}Ti(n,p)^{48}Sc$		1.824	1.857		1.513 (
$^{54}Fe(n,p)^{54}Mn$		0.966 (1.031)	0.965 (1.030)		1.013 (1.041)
$^{55}Mn(n,\gamma)^{56}Mn$					
$^{58}Fe(n,\gamma)^{59}Fe$		0.928 (0.990)	0.923 (0.985)		0.944 (0.970)
$^{59}Co(n,\gamma)^{60}Co$		1.298	1.306		1.122 (1.153)
$^{63}Cu(n,\gamma)^{64}Cu$	0.943 (0.967)	0.874 (0.933)	0.898 (0.958)	0.951 (0.961)	0.919 (0.944)
$^{115}In(n,\gamma)^{116}In$	0.852 (0.874)	0.884 (0.943)	0.873 (0.932)	0.844 (0.853)	0.901 (0.926)
$^{115}In(n,n')^{115}In^{m}$	1.051 (1.078)	1.038 (1.108)	1.033 (1.103)	1.060 (1.072)	1.091 (1.121)
$^{232}Th(n,f)$	1.032 (1.058)			1.041 (1.052)	
$^{238}U(n,\gamma)^{239}U$	0.840 (0.861)	0.737 (0.786)	0.733 (0.782)	0.831 (0.840)	0.754 (0.775)
n	13 (11)	21 (17)	21 (17)	13 (12)	21 (18)
s (in %)	9.58 (8.28)	22.4 (9.28)	23.1 (9.26)	9.29 (8.89)	15.6 (9.96)
$\bar{E}$ (in MeV)	0.761	0.717	0.716	0.762	0.706
u	3.42	3.50	3.51	3.42	3.53

Table 6: Ratio of measured and calculated activities

Case of STEK-2000 spectrum and category I reactions

DETAN-74

reaction	STEK-2000		
	original histogram ϕ_u=C	point values	corrected point values
$^{197}Au(n,\gamma)^{198}Au$	0.894	0.865	0.841
$^{27}Al(n,\alpha)^{24}Na$	0.789	0.831	0.964 (1.012)
$^{46}Ti(n,p)^{46}Sc$	1.102 (1.049)	1.144	1.146
$^{58}Ni(n,p)^{58}Co$	1.165	1.179	1.153
$^{235}U(n,f)$	0.961 (0.915)	0.902 (0.893)	0.870 (0.913)
$^{238}U(n,f)$	1.089 (1.036)	1.080 (1.069)	1.025 (1.075)
n	6 (3)	6 (2)	6 (3)
s (in %)	14.4 (7.39)	15.2 (12.3)	13.3 (8.19)

ENDF/B-IV

reaction	STEK-2000		
	original histogram ϕ_u=C	point values	corrected point values
$^{197}Au(n,\gamma)^{198}$	0.914 (0.935)	0.878 (0.992)	0.852 (0.946)
$^{27}Al(n,\alpha)^{24}Na$	0.739	0.778	0.902 (1.001)
$^{46}Ti(n,p)^{46}Sc$	1.211	1.280	1.297
$^{58}Ni(n,p)^{58}Co$	1.115	1.127	1.100
$^{235}U(n,f)$	0.958 (0.979)	0.892 (1.008)	0.859 (0.954)
$^{238}U(n,f)$	1.063 (1.086)	1.046	0.991 (1.100)
n	6 (3)	6 (2)	6 (4)
s (in %)	16.7 (7.98)	18.6 (1.15)	17.3 (7.08)
$\bar{E}_u$ (in MeV)			

Table 7: Ratio of measured and calculated activities

Case of STEK-2000 spectrum and categories I and II reactions

DETAN-74

reaction	STEK-2000		
	original histogram ϕ_u=C	point values	corrected point values
$^{197}Au(n,\gamma)^{198}Au$	0.903	0.888	0.868
$^{27}Al(n,\alpha)^{24}Na$	0.797	0.854	0.995 (0.981)
$^{46}Ti(n,p)^{46}Sc$	1.113 (1.045)	1.175	1.182
$^{58}Ni(n,p)^{58}Co$	1.177	1.211	1.190
$^{235}U(n,f)$	0.971 (0.911)	0.926 (0.878)	0.898 (0.886)
$^{238}U(n,f)$	1.099 (1.032)	1.109 (1.051)	1.057 (1.043)
$^{23}Na(n,\gamma)^{24}Na$	0.780	0.756	0.734
$^{45}Sc(n,\gamma)^{46}Sc$	1.251 (1.175)	1.181	1.149 (1.133)
$^{55}Mn(n,\gamma)^{56}Mn$	0.752	0.710	0.690
$^{58}Fe(n,\gamma)^{59}Fe$	1.036 (0.973)	0.956 (0.906)	0.930 (0.917)
$^{59}Co(n,\gamma)^{60}Co$	0.452	0.471	0.454
$^{63}Cu(n,\gamma)^{64}Cu$	0.539	0.513	0.497
$^{115}In(n,\gamma)^{116}In$	0.890 (0.835)	0.845 (0.800)	0.806 (0.795)
$^{238}U(n,\gamma)^{239}U$	0.937 (0.880)	0.856 (0.811)	0.834 (0.822)
$^{47}Ti(n,p)^{47}Sc$	1.348	1.394	1.362
$^{48}Ti(n,p)^{48}Sc$	1.213 (1.139)	1.252 (1.186)	1.473
$^{54}Fe(n,p)^{54}Mn$	1.148 (1.078)	1.192 (1.130)	1.175 (1.159)
$^{56}Fe(n,p)^{56}Mn$	0.919 (0.863)	1.033 (0.979)	1.145 (1.129)
$^{59}Co(n,\alpha)^{56}Mn$			
$^{115}In(n,n')^{115}In^{m}$	1.204 (1.130)	1.205 (1.141)	1.151 (1.135)
$^{232}Th(n,f)$	1.471	1.474	1.412
n	20 (11)	20 (10)	20 (10)
s (in %)	25.8 (12.6)	27.0 (14.5)	28.2 (13.9)
E_u (in MeV)			

Table 7 (continued): Case of STEK-2000 spectrum and categories I and II reactions$_{ENDF/B-IV}$

reaction	STEK-2000		
	original histogram ϕ_U=C	point values	corrected point values
$^{197}Au(n,\gamma)^{198}Au$	0.933 (0.980)	0.905 (0.974)	0.880 (0.855)
$^{27}Al(n,\alpha)^{24}Na$	0.754	0.802	0.932 (0.905)
$^{46}Ti(n,p)^{46}Sc$	1.236	1.319	1.340
$^{58}Ni(n,p)^{58}Co$	1.138	1.162	1.137
$^{235}U(n,f)$	0.978 (1.026)	0.920 (0.989)	0.888 (0.862)
$^{238}U(n,f)$	1.085 (1.139)	1.078	1.024 (0.994)
$^{23}Na(n,\gamma)^{24}Na$	0.502	0.479	0.464
$^{45}Sc(n,\gamma)^{46}Sc$	1.351	1.239	1.200 (1.165)
$^{55}Mn(n,\gamma)^{56}Mn$			
$^{58}Fe(n,\gamma)^{59}Fe$	0.918 (0.964)	0.914 (0.983)	0.884 (0.858)
$^{59}Co(n,\gamma)^{60}Co$	0.467	0.486	0.466
$^{63}Cu(n,\gamma)^{64}Cu$	0.559	0.550	0.528
$^{115}In(n,\gamma)^{116}In$	0.783 (0.822)	0.733 (0.789)	0.696
$^{238}U(n,\gamma)^{239}U$	0.794 (0.834)	0.731 (0.787)	0.708
$^{47}Ti(n,p)^{47}Sc$	1.026 (1.078)	1.050 (1.129)	1.018 (0.988)
$^{48}Ti(n,p)^{48}Sc$	1.661	1.728	1.968
$^{54}Fe(n,p)^{54}Mn$	1.104 (1.159)	1.133 (1.219)	1.117 (1.085)
$^{56}Fe(n,p)^{56}Mn$	0.951 (0.999)	1.050 (1.130)	1.156 (1.123)
$^{69}Co(n,\alpha)^{56}Mn$			
$^{115}In(n,n')^{115}In^{m}$	1.282	1.262	1.200 (1.161)
$^{232}Th(n,f)$	1.479	1.461	1.394
n	19 (9)	19 (8)	19 (10)
s (in %)	32.1 (11.3)	33.1 (17.3)	36.2 (12.7)
$\bar{E}_u$ (in MeV)			

Table 8: Ratio of measured and calculated activities

Case of other spectra and category I reactions (smooth spectra)

DETAN-74

reaction	spectrum		
	LFR	STEK-500	STEK-4000
$^{197}Au(n,\gamma)^{198}Au$	0.984 (1.008)*	0.920 (1.018)	0.666
$^{197}Au(n,\gamma)^{198}Au$ *	0.933* (0.955)*		
$^{27}Al(n,\alpha)^{24}Na$	0.927* (0.949)*	1.103	0.778
$^{46}Ti(n,p)^{46}Sc$		1.096	1.308
$^{58}Ni(n,p)^{58}Co$	0.982 (1.005)*	1.091	1.249 (1.049)
$^{58}Ni(n,p)^{58}Co$ *	1.002* (1.026)*		
$^{235}U(n,f)$	1.141*	0.828 (0.916)	0.867
$^{238}U(n,f)$	1.032* (1.057)*	0.963 (1.066)	1.133 (0.952)
n	7 (6)	6 (3)	6 (2)
s (in %)	7.22 (4.15)	11.5 (6.90)	26.6 (6.86)

ENDF/B-IV

reaction	spectrum		
	LFR	STEK-500	STEK-4000
$^{197}Au(n,\gamma)^{198}Au$	0.995 (1.019)*	0.957 (0.970)	0.661
$^{197}Au(n,\gamma)^{198}Au$ *	0.956* (0.980)*		
$^{27}Al(n,\alpha)^{24}Na$	0.901* (0.923)*	1.026 (1.040)	0.727
$^{46}Ti(n,p)^{46}Sc$		1.237	1.479
$^{58}Ni(n,p)^{58}Co$	0.973 (0.997)*	1.037 (1.052)	1.191 (1.042)
$^{58}Ni(n,p)^{58}Co$ *	0.994* (1.018)*		
$^{235}U(n,f)$	1.143*	0.818	0.847
$^{238}U(n,f)$	1.039* (1.064)*	0.925 (0.938)	1.096 (0.958)
n	7 (6)	6 (4)	6 (2)
s (in %)	7.58 (4.72)	14.1 (5.50)	31.2 (5.88)
$\bar{E}$ (in MeV)	0.0897	0.810	0.544
u	15.6	3.74	5.24

*Cd cover.

Table 9: Ratio of measured and calculated activities

Case of other spectra and categories I and II reactions (smooth spectra having 620 energy groups)

DETAN-74

reaction	spectrum		
	LFR	STEK-500	STEK-4000
$^{197}Au(n,\gamma)^{198}Au$	0.975 (0.959)	0.994 (0.944)	0.706
$^{197}Au(n,\gamma)^{198}Au$	0.924* (0.908)		
$^{27}Al(n,\alpha)^{24}Na$	0.918* (0.903)	0.983	0.710
$^{46}Ti(n,p)^{46}Sc$		1.143	1.375
$^{58}Ni(n,p)^{58}Co$	0.972 (0.956)	1.168	1.346 (1.057)
$^{58}Ni(n,p)^{58}Co$	0.993* (0.976)		
$^{235}U(n,f)$	1.130*	0.895 (0.849)	0.946
$^{238}U(n,f)$	1.022* (1.005)	1.055 (1.001)	1.263 (0.991)
$^{23}Na(n,\gamma)^{24}Na$	1.038* (1.020)	0.855 (0.812)	0.987 (0.775)
$^{45}Sc(n,\gamma)^{46}Sc$	1.324*	1.091 (1.036)	1.332 (1.046)
$^{55}Mn(n,\gamma)^{56}Mn$	1.105* (1.086)	0.999 (0.948)	0.734
$^{58}Fe(n,\gamma)^{59}Fe$			0.842
$^{59}Co(n,\gamma)^{60}Co$	1.042 (1.025)	0.459	0.518
$^{59}Co(n,\gamma)^{60}Co$	1.074* (1.056)		
$^{63}Cu(n,\gamma)^{64}Cu$		0.555	0.703
$^{115}In(n,\gamma)^{116}In$	0.258	0.937 (0.890)	0.398
$^{238}U(n,\gamma)^{239}U$		1.029 (0.977)	0.605
$^{47}Ti(n,p)^{47}Sc$	1.090* (1.072)	1.262 (1.198)	1.368 (1.074)
$^{48}Ti(n,p)^{48}Sc$	1.137* (1.118)	1.152 (1.094)	1.295 (1.017)
$^{54}Fe(n,p)^{54}Mn$	0.808* (0.795)	1.191 (1.131)	1.406 (1.104)
$^{56}Fe(n,p)^{56}Mn$		1.020 (0.969)	1.167 (0.916)
$^{115}In(n,n')^{115}In^{m}$	0.941 (0.925)	1.213 (1.152)	1.301 (1.021)
$^{115}In(n,n')^{115}In^{m}$	1.001* (0.984)		
$^{232}Th(n,\gamma)^{233}Th$	1.185* (1.166)		
$^{232}Th(n,\gamma)^{233}Th$	1.065* (1.047)		
n	20 (17)	18 (13)	19 (9)
s (in %)	20.7 (9.03)	21.2 (11.8)	33.8 (10.0)
$\bar{E}$ (in MeV)	0.0897	0.810	0.544
u	15.6	3.74	5.24

*Cd cover.

Table 9 (continued): Case of other spectra and categories I and II reactions (smooth spectra, having 620 energy groups)
ENDF/B-IV

reaction	spectrum		
	LFR	STEK-500	STEK-4000
$^{197}Au(n,\gamma)^{198}Au$	0.992 (0.990)	1.025 (0.995)	0.706
$^{197}Au(n,\gamma)^{198}Au$	0.953* (0.951)		
$^{27}Al(n,\alpha)^{24}Na$	0.898* (0.896)	0.904 (0.879)	0.668
$^{46}Ti(n,p)^{46}Sc$		1.259	1.549
$^{58}Ni(n,p)^{58}Co$	0.970 (0.968)	1.099 (1.068)	1.294 (1.045)
$^{58}Ni(n,p)^{58}Co$	0.991* (0.988)		
$^{235}U(n,f)$	1.140*	0.877	0.932
$^{238}U(n,f)$	1.036* (1.033)	1.004 (0.975)	1.230 (0.994)
$^{23}Na(n,\gamma)^{24}Na$	0.909* (0.906)	0.548	0.642
$^{45}Sc(n,\gamma)^{46}Sc$	1.253* (1.250)	1.109 (1.078)	1.363 (1.102)
$^{58}Fe(n,\gamma)^{59}Fe$			0.751
$^{59}Co(n,\gamma)^{60}Co$	1.039 (1.036)	0.711	0.503
$^{59}Co(n,\gamma)^{60}Co$	1.039* (1.036)		
$^{63}Cu(n,\gamma)^{64}Cu$		0.730	0.677
$^{115}In(n,\gamma)^{116}In$	0.229*	0.905 (0.879)	0.333
$^{238}U(n,\gamma)^{239}U$		0.971 (0.943)	0.543
$^{47}Ti(n,p)^{47}Sc$	0.809* (0.807)	0.936 (0.909)	1.032 (0.834)
$^{48}Ti(n,p)^{48}Sc$	1.591*	1.554	1.794
$^{54}Fe(n,p)^{54}Mn$	0.829* (0.827)	1.107 (1.075)	1.340 (1.083)
$^{56}Fe(n,p)^{56}Mn$		1.016 (0.987)	1.189 (0.961)
$^{59}Co(n,\alpha)^{56}Mn$			1.089 (0.880)
$^{115}In(n,n')^{115}In^{m}$	1.018 (1.015)	1.247 (1.212)	1.365 (1.103)
$^{115}In(n,n')^{115}In^{m}$	1.083* (1.080)		
$^{232}Th(n,\gamma)^{233}Th$	1.121* (1.118)		
$^{232}Th(n,\gamma)^{233}Th$	1.101* (1.099)		
n	19 (16)	17 (11)	19 (8)
s (in %)	25.3 (11.2)	23.29 (10.1)	40.1 (10.3)
$\bar{E}$ (in MeV)	0.0897	0.810	0.544
u	15.6	3.74	5.24

*Cd cover.

Table 10: Comparison of results for different spectrum representations

Case of other spectra and category I reactions

The representations refer to histogram spectra (having a coarse group structure) and to smooth spectra (having 620 point values).

	spectrum					
	LFR		STEK-500		STEK-4000	
library:	DETAN-74	ENDF/B-IV	DETAN-74	ENDF/B-IV	DETAN-74	ENDF/B-IV
n smooth	7 (6)	7 (6)	6 (3)	6 (4)	6 (2)	6 (2)
n histogram			6 (4)	6 (4)	6 (3)	6 (2)
s smooth	7.22 (4.15)	7.58 (4.72)	11.5 (6.90)	14.1 (5.50)	26.6 (6.86)	31.2 (5.88)
s histogram			8.33 (4.29)	11.5 (6.93)	28.7 (2.58)	31.3 (1.77)
$\bar{E}$	0.0897		0.810		0.544	
u	15.6		3.74		5.24	

Table 11: Comparison of results for different spectrum representations

Case of other spectra and categories I and II reactions

The representations refer to histogram spectra (having a coarse group structure) and to smooth spectra (having 620 point values).

	spectrum					
	LFR		STEK-500		STEK-4000	
library:	DETAN-74	ENDF/B-IV	DETAN-74	ENDF/B-IV	DETAN-74	ENDF/B-IV
n smooth	20 (17)	19 (16)	18 (13)	17 (11)	19 (9)	19 (8)
n histogram			18 (14)	17 (11)	19 (8)	19 (5)
s smooth	20.7 (9.03)	25.3 (11.2)	21.2 (11.8)	23.3 (10.1)	33.8 (10.0)	40.1 (10.3)
s histogram			20.2 (10.2)	22.9 (11.1)	31.5 (13.6)	37.9 (9.56)

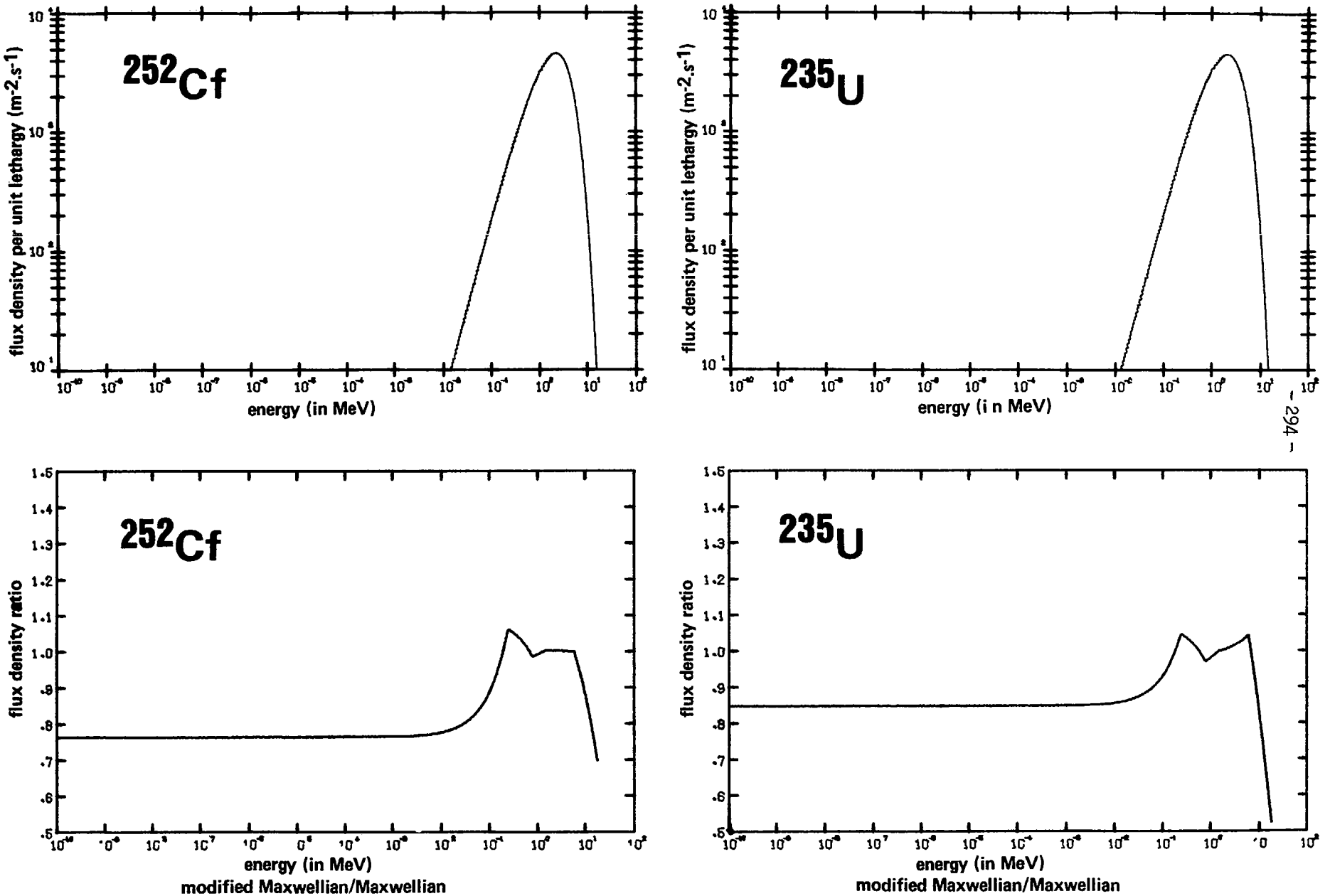

Fig. 1. THE FISSION NEUTRON SPECTRA AND RATIOS OF PURE MAXWELLIAN AND MODIFIED SPECTRA.

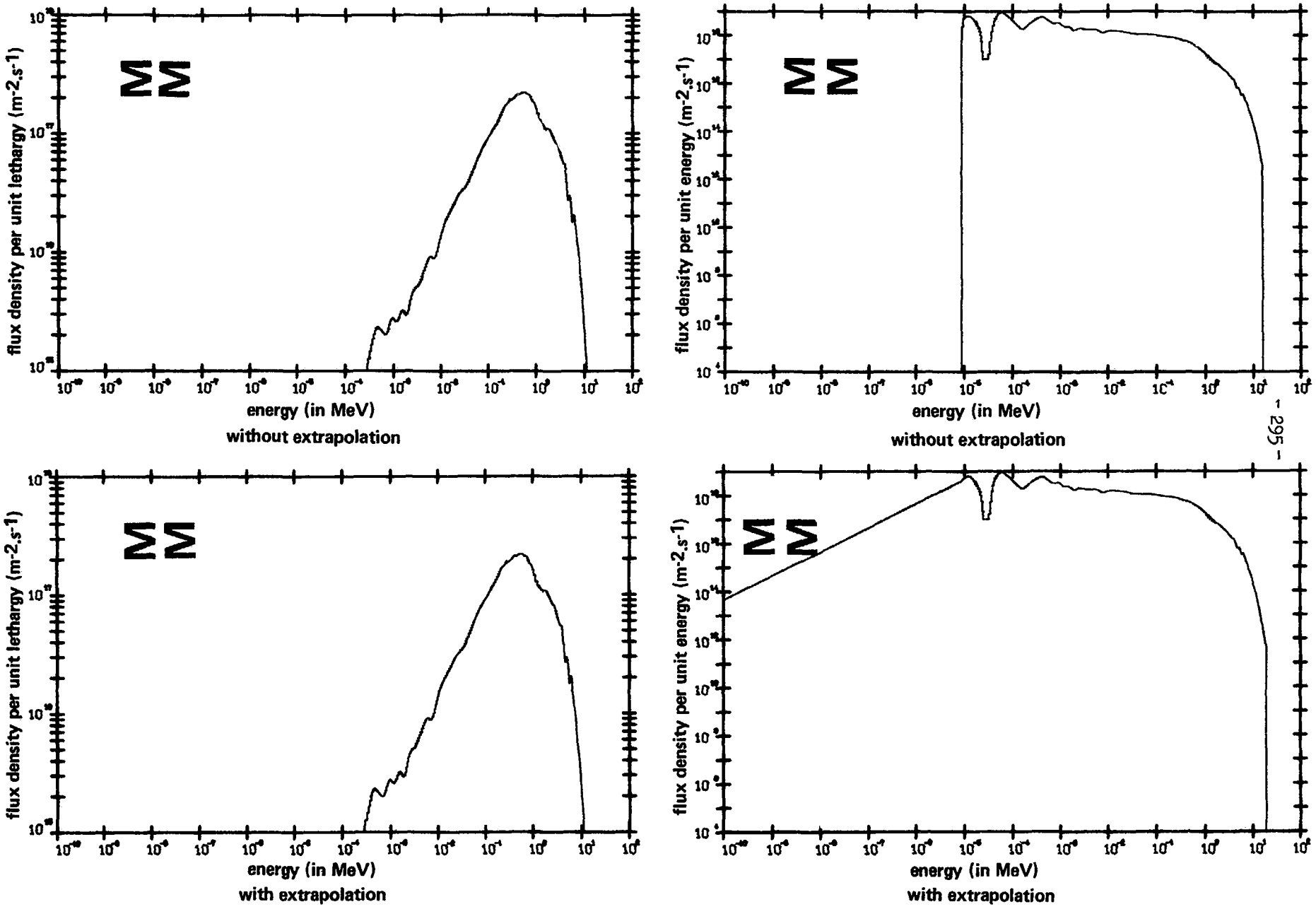

Fig. 2. DIFFERENT PRESENTATION OF THE SIGMA-SIGMA NEUTRON SPECTRUM

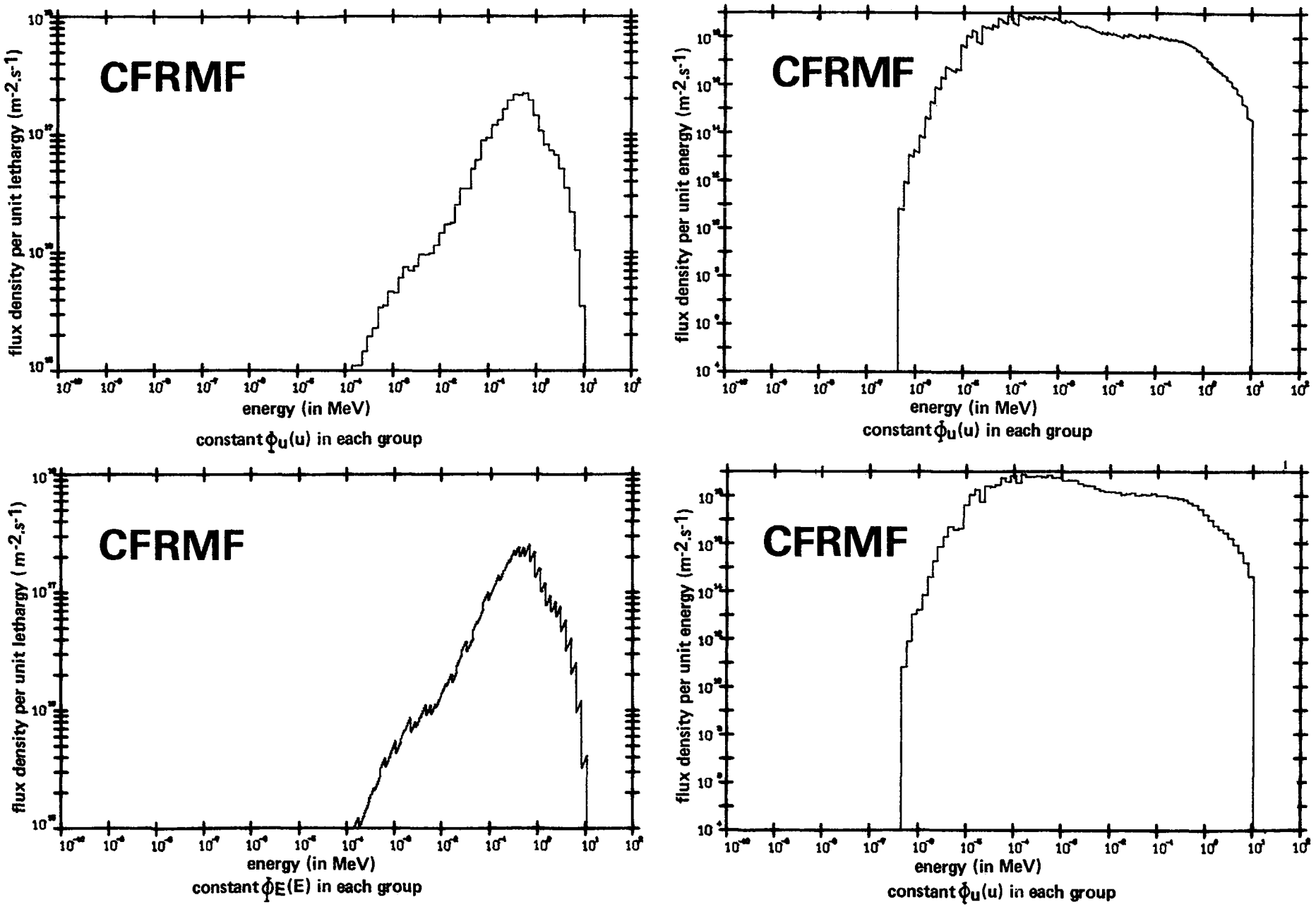

Fig 3 DIFFERENT PRESENTATIONS OF THE CFRMF NEUTRON SPECTRUM

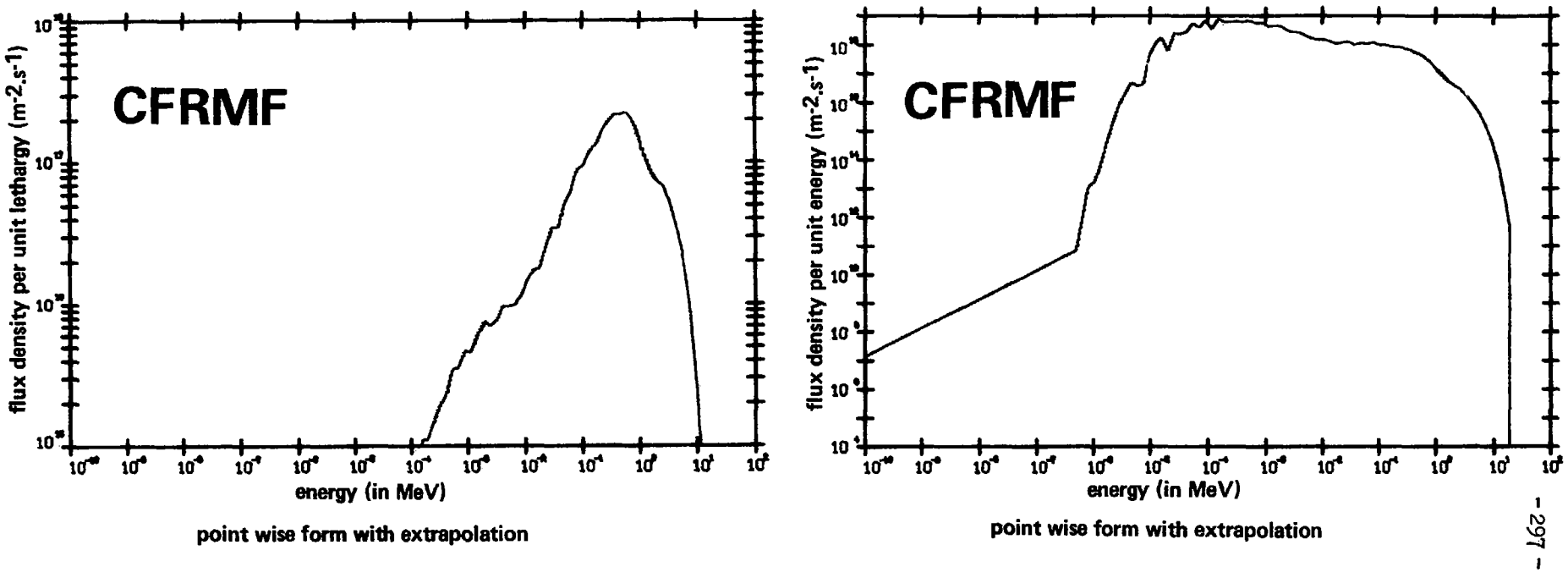

Fig. 4. SMOOTHENED PRESENTATION OF THE CFRMF NEUTRON SPECTRA

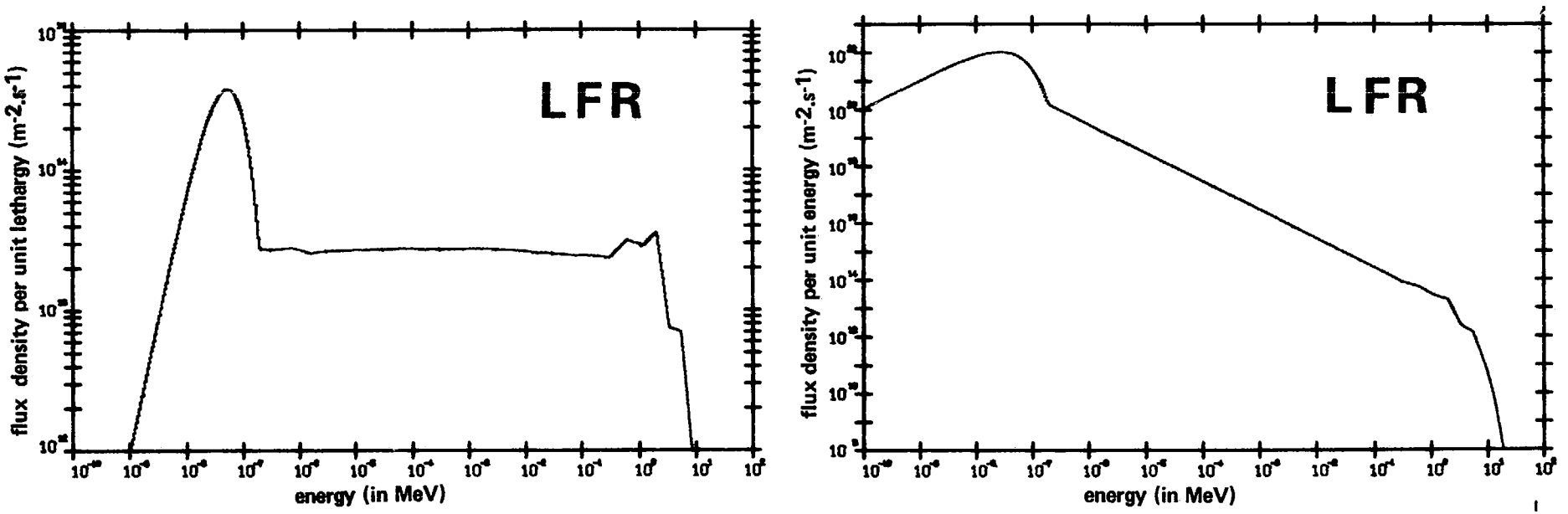

Fig. 5. THE LFR NEUTRON SPECTRUM (VC plug in a one slab core)

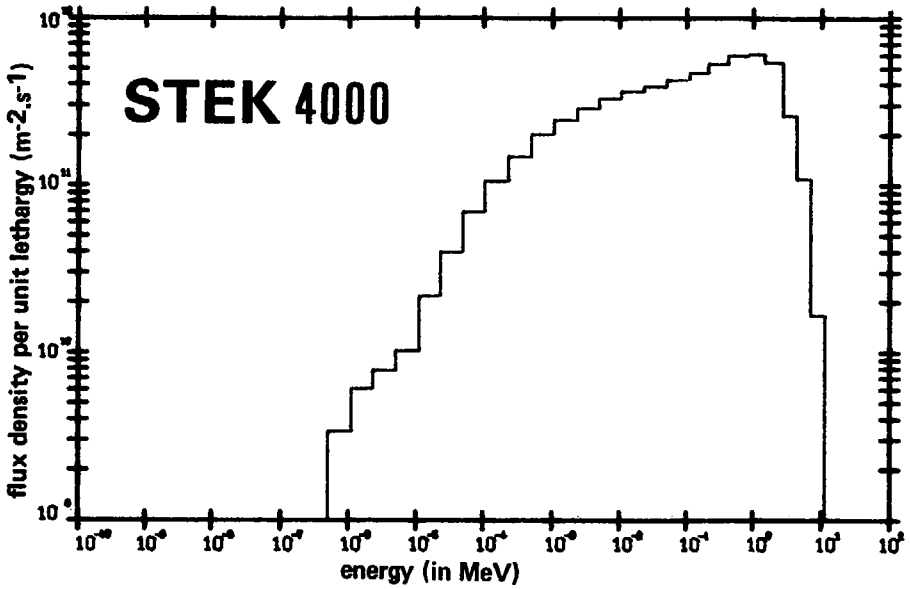

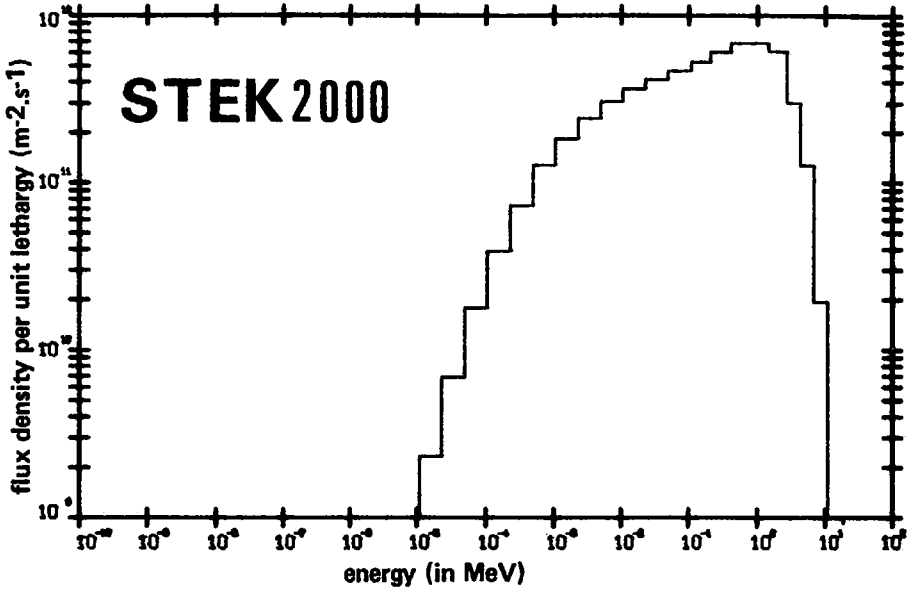

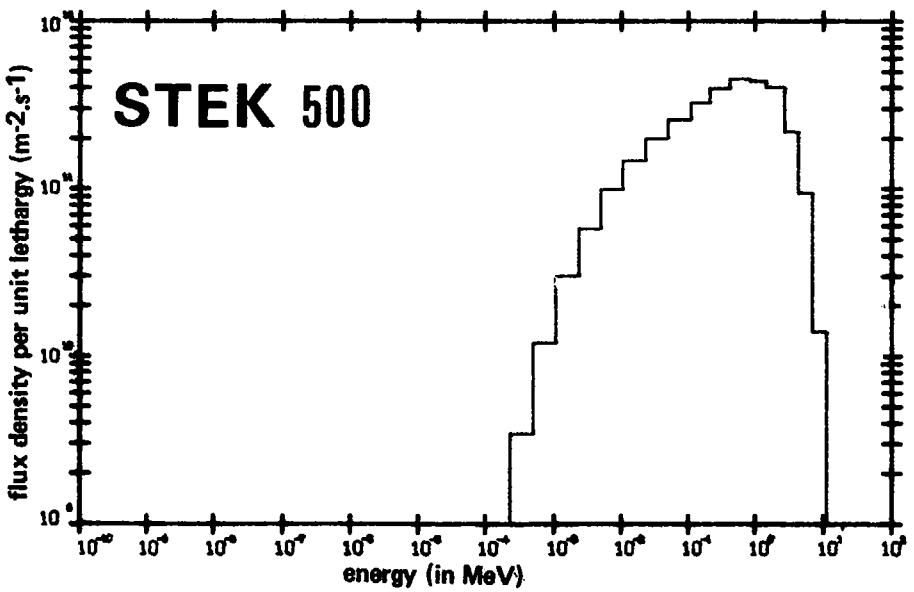

Fig. 6. NEUTRON SPECTRA FOR THREE STEK CORES

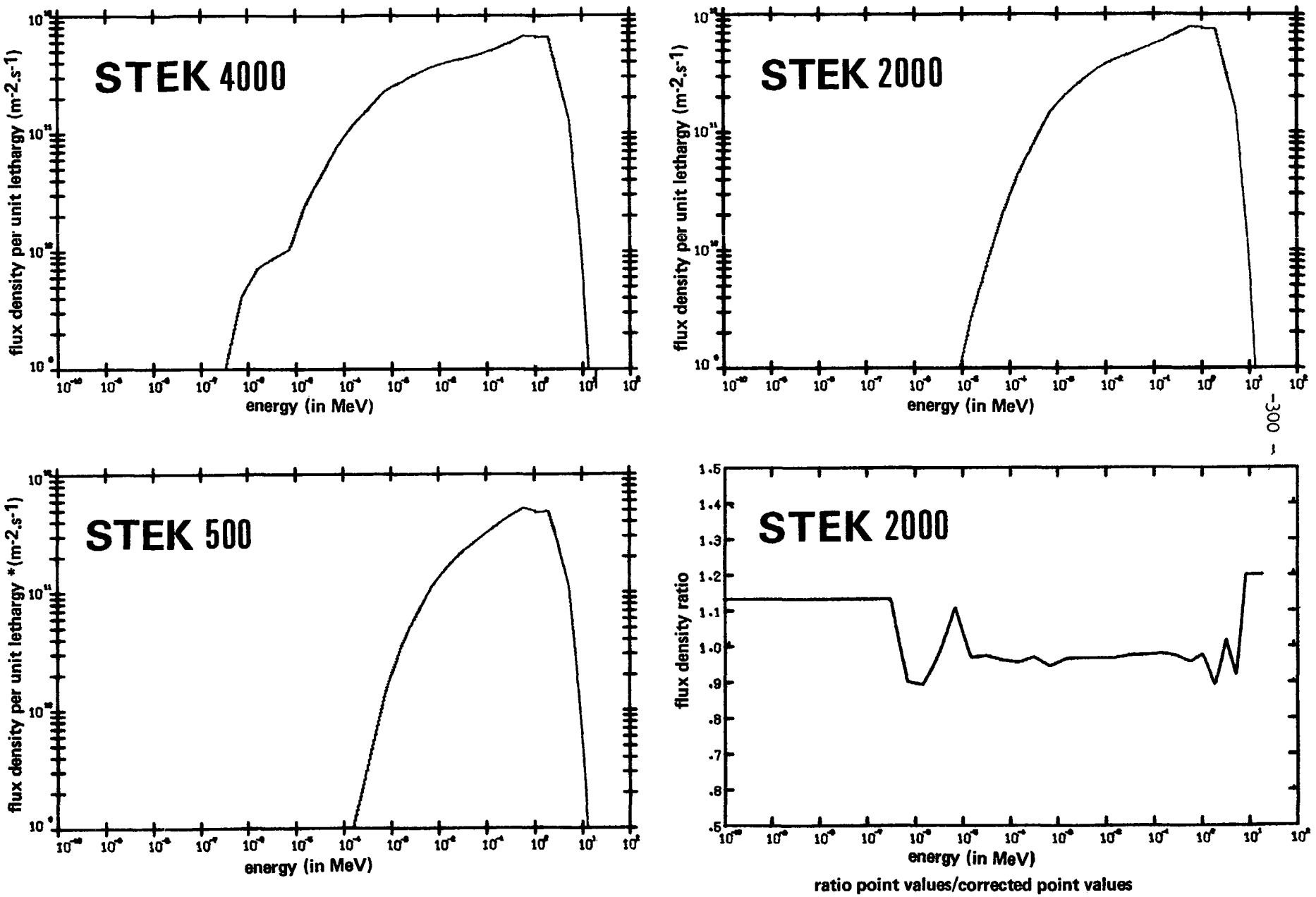

Fig. 7. SMOOTHENED PRESENTATION OF THE STEK NEUTRON SPECTRA

III.3. Status of Fission Product Yields Required for Fast Reactor Dosimetry

G. Lammer and M. Lammer

ABSTRACT

The results of recent fast fission yield measurements of Br-95, Zr-97, Ru-103, I-131, Te-132, Cs-137, Ba-140 and Nd-148 from fissions of U-235, U-238, Pu-239 and Np-237 are compared. The dependence of these yields on the flux shape in fast reactors is investigated by associating the measured values with the median neutron energy of the spectrum.

From this comparison, no evidence is found for an energy dependence of the yields, within the energy range of fast reactor neutrons. This allows to combine different yield data taken in fast reactor spectra to give evaluated "fast reactor yields". For the fission products considered, such evaluated data are given at the end of this paper.

1. Introduction

In high power FBRs, the determination of absolute fission rates is most suitably carried out by the fission foil activation technique /1/. This method, which can also be used for flux-monitoring, involves the irradiation of foils of fissionable material and subsequent gamma-activity analysis of the fission products. The fission rate is then obtained from: $F_i = R_j / Y_{ij}$.

F_i fission rate of the fissionable isotope i

R_j production rate of fission product j

Y_{ij} spectrum averaged yield of isotope j from fissions of isotope i.

For the analysis of the measured data, the knowledge of the values and accuracies of the yields of the measured fission products from the fissionable isotopes under consideration is essential. The most commonly used fission products - because of suitable lifetimes and prominent gamma-rays - are: Zr-95, Zr-97, Ru-103, I-131, Te-132, Cs-137, Ba-140 /2/. In addition, the stable isotope Nd-148 is very often used as burnup monitor. The fissionable isotopes which are most important in neutron dosimetry are: U-235, U-238, Pu-239 and Np-237.

The currently available large fission yield data files (/3/,/4/,/5/) in general only discern between thermal and "fast" neutron fission yields. These recommended "fast" yields are obtained from averaging over results from measurements performed in a variety of fast reactor spectra as well as different fission neutron spectra.

For higher accuracy requirements (for dosimetry purposes in FBRs they are typically about 2%), such an averaging procedure may, however, - for some fission products - no more be adequate. Furthermore, the fact that differences in neutron energies have not been taken into account, may be one of the reasons for observed discrepancies among evaluated data /6/ (e.g., the yields of I-131 and Cs-137 from Pu-239 show discrepancies of about 5%). Therefore, it has been recommended at the FPND Panel /6/ that experimenters associate their neutron spectrum with some kind of spectral parameter, and that the energy dependence of yield data be evaluated. All information on fast yields available up to 1973 has been compiled by J.G. Cuninghame for this Panel /7/.

In this paper, an attempt is made to associate the available fast yield data for the above-mentioned fission products with a spectral parameter, so as to find out whether there exists a significant variation of yields with shapes of fast reactor spectra.

2. Spectral parameters

The following parameters are currently in use to characterize the fast neutron spectra:

Mean energy $\bar{E}$: $\bar{E} = \dfrac{\int_0^{10\ \mathrm{MeV}} E \cdot \phi_E(E)\, dE}{\phi_{tot}}$; $\phi_E(E)$... differential neutron flux (n/cm^2 sec MeV)

ϕ_{tot}...total neutron flux (n/cm^2 sec)

Median energy E_m: $\int_0^{Em} \phi_E(E)\, dE = \int_{Em}^{10\ \mathrm{MeV}} \phi_E(E)\, dE$

Median fission energy, e.g. for U-235, E_{m5}:

$$\int_0^{E_{m5}} \sigma_{f5}\, \phi_E(E)\, dE = \int_{E_{m5}}^{10\ \mathrm{MeV}} \sigma_{f5}\, \phi_E(E)\, dE$$

Ratio of capture to fission reaction rate, e.g. for U-238, $\bar{\alpha}_8$:

$$\bar{\alpha}_8 = \overline{\sigma_{\gamma 8}} \,/\, \overline{\sigma_{f8}}$$

"Spectral index" s:

$$s = \overline{\sigma_{f8}} \,/\, \overline{\sigma_{f5}}$$

From a comparison of these parameters in different reactor spectra, it appears that the spectral index s is the parameter which is most sensitive to changes in flux shapes. It can be interpreted as an indicator of the ratio of the part of flux above about 1.3 MeV to the part below this energy. The median energy is less sensitive to changes in the flux spectrum, but has the advantage of being approximately equal to the median U-235 fission energy, and of being easily determined from a given flux spectrum. Still less sensitive are the mean energy and also $\bar{\alpha}$ (e.g. for U-238) as defined above.

3. Fast fission yields as a function of neutron energy

For a study of the dependence of fission yields on neutron energy in the range of fast reactor neutrons, it would be necessary to relate all the published yield data to one single parameter. Unfortunately, in some publications no information about the neutron spectrum in which the measurements were made is given; in some, the spectrum is shown in a figure - from which the median energy may be roughly derived; or in others any, but in general only one, of the parameters defined in Sect.2 is used. Different parameters can however only be reliably converted into each other if the shape of the neutron spectrum is known.

For the present comparison, the median (U-235-fission) energy $E_{m(5)}$ (E_m and E_{m5} were assumed to be equal) was used as energy coordinate, as this was the parameter which could be obtained from the majority of publications. In those cases where only other parameters were available, they had to be converted to E_m, assuming an approximately linear relationship between spectral parameters.

In order to avoid systematic differences arising from normalization procedures, the comparison was in most cases carried out for relative fission yield data. Ratios of yields to a chosen "standard" yield were calculated from measurements wherever this was possible without loss of information. The criteria for the selection of the "standard" nuclide were:

- that the yield of this nuclide had been determined in most of the experiments considered;
- that the measured absolute values did not change considerably with the median energy.

Table 1 shows a list of experiments considered for this review.

Table 1

Author, year, ref.	facility	spectral param. in original publication	$E_{m(5)}$ (MeV)
Maeck 75, /8/	EBR-II	E_m=0.12-0.16 MeV	0.12-0.16
Davies 69, /9/	DFR		0.15 /12/
Cuninghame 72,/10/	DFR	ϕ (u)	~0.15, ~0.25
Rajagopalan 75,/11/	PROTEUS	E_m=0.18 MeV	0.18
Scholtyssek 72,/12/	SNEAK-7b	s=0.021,0.033	0.17, 0.23 /2/
Dudey 75, /1/	EMC CFRMF		0.19 /2/ 0.34 /2/
Dudey 75, /13/	BIG-TEN	ϕ(u) /14/	~0.28
Larsen 74, /15/	ZPR-3	E_m=0.29-0.44 MeV	0.29-0.44
Zimmer 75,/16/	EBR-II	$\overline{E}$= 0.83-0.96 MeV	0.38-0.45 /2/
Cottone 75,/17/	Rapsodie	α(U5)= 0.213 s = 0.073 /18/	~0.45
Robin 71,/18/	Osiris	s = 0.089	~0.54
Lisman 70,/19/	EBR-I	E_m= 0.5 MeV	~0.7 /2/

The results of the comparison are shown in figures 1 to 25. Also included in these figures are the thermal yield-values or ratios and fast yields as evaluated by M.E. Meek and B.F. Rider /4/.

a) U-235 fast fission

Absolute yields of Zr-95 and Ba-140 are shown in figs. 1 and 2. As can be seen, the data for Zr-95 agree much better, and therefore, with the exception of Cs-137 and Nd-148, published yield data were normalized to the Zr-95 yields. For Cs-137 and Nd-148, the absolute yields are compared, as in many experiments the Zr-95 yields had not been measured together with these data.

For none of these fission products a consistent variation of the yield with the median energy can be observed. With, perhaps, the exception of Ba-140, the fast yield data shown here agree within 1-2%. As expected, the weighted average of all experiments considered is less than the thermal yield value for Zr-95, Zr-97, Cs-137 (by ≈1%) and Ba-140 (by 3.5 %), i.e. fission products which are in the peaks of the mass-curve, and higher than the thermal values for Ru-103 (by 3%) and for I-131 and Te-132 (by 8-10%). These differences between thermal and fast values are too small to make any variation with fast reactor spectra apparent.

The need for investigating the energy dependence of the yield of Nd-148, which is a very important burnup monitor, has been particularly emphasized /6/. An interesting contribution to this question was provided by W.J. Maeck, /8/, /20/, who calculated the yield ratios of stable Nd isotopes, 150/143, 150/145 and 148/143, of all available fast yield values that were related to a spectral index of the neutron spectrum. As a result, he found a clear variation of all these ratios with the spectral parameter. In the present comparison however, neither the absolute Nd-148 yields (fig. 9) nor the ratios Nd-148/Cs-137 (fig. 10) indicate any consistent energy dependence within the energy range considered. This means that the yields of the Nd-143, 145 and 150 isotopes vary with fast reactor spectra rather than the Nd-148 yield.

b) Pu-239

For Pu-239, Ba-140 was chosen as standard. From figs. 11 to 19, the following can be deduced:

Within the experimental errors, the yields of those nuclides which are in the peaks of the mass yield curve, namely Ba-140, Zr-95, Zr-97, and Cs-137, do not vary within the energy range of fast reactor spectra. For Ru-103, I-131, and Nd-148, however, a slight increase of the yield with energy is observed, whereas relative and absolute yields of mass 132 do not show this tendency.

In view of the fact that the relative variation of these yields with energy is, within the energy range investigated, comparable to the experimental errors of individual values, no definite conclusion should be drawn. In order to get a more reliable answer to the question of energy dependence, new measurements should be performed in different reactor spectra, under similar conditions, preferably in a single experiment.

c) U-238

Only neutrons with energies above the U-238 fission threshold ($\sim$ 1.3 MeV) contribute to the measured integral yields. It is therefore to be expected that the effect of varying the neutron spectrum is still less distinct for U-238 than for U-235 and Pu-239.

Relative or absolute yield values versus median energy are shown for those nuclides for which more than three different experimental data were available (figs. 20 to 24). Indeed, no consistent variation with energy is apparent. - It should also be noted that the individual experimental errors, as given by the authors, are about twice as high as those for U-235 and Pu-239.

d) Np-237

Data for the fission product yields of Np-237 are so scarce, that no attempt was made to relate them to a spectral parameter. Table 2 shows the more recent yield data that could be found for the fission products under consideration. For those fission products with more than one yield value, no real discrepancies exist, but the experimental errors are partly rather high.

Table 2

Measured yields from fast neutron fission of Np-237

Zr-95	Ru-103	I-131	Te-132
6.05±0.23 /1/	5.75±0.24 /1/	3.25±0.16 /17/	4.86±0.24 /17/
5.64±0.21 /2/	5.77±0.28 /13/	3.63±0.18 /21/	
5.98±0.26 /13/			

Cs-137	Ba-140	Nd-148
6.67±0.22 /2/	5.79±0.12 /1/	1.69±0.14 /2/
6.38±0.32 /17/	5.41±0.20 /22/	1.84±0.09 /17/
	5.53±0.22 /13/	

Conclusions

Within the uncertainties of existing experimental data, a dependence of the integral fission yields of Zr-95, Zr-97, Ru-103, I-131, Te-132, Cs-137, Ba-140, and Nd-148 from fissions of U-235, 238, Pu-239 and Np-237, on the median energy of fast reactor spectra, is either not observed or doubtful.

Therefore, it was considered to be justified to average all the available yield data measured in fast reactor spectra (not the fission spectrum or epithermal data!) in order to give a recommended "fast fission product yield".

The following averaging procedure was applied:

- The weighted averages (w.a.) of the absolute yield-values and - where applicable - of the yield ratios as described above, were calculated. In general the experimental errors as given in the publications were taken as uncertainties; only in some cases higher uncertainties were assigned in order to account for discrepancies between experimental data.

- The w.a. of absolute yields and the values resulting from the w.a. of ratios were compared. In all but one (Te-132 from Pu-239) cases the difference between these two values was less than 1.5%.

- For U-235 and Pu-239, the yields resulting from ratios were adopted. In the case of U-238, either the w.a. of absolute yields or the yield ratios were used, depending on the agreement among data.

- "Recommended" Np-237 yields were obtained from absolute data.

The adopted yields are given in Table 3. Values which were derived from only 3 or less experimental data, are shown in brackets. For comparison, the recommended yields of Meek and Rider (/4/) are included in the table.

The uncertainties of the w.a. and the agreement between the present evaluated data and those from Meek and Rider, indicate that, for the fission products of interest in fast reactor dosimetry, the following precisions in fast yields can be assumed:

- $\leq 2\%$ for U-235;
- 1.5% to 3% for Pu-239;
- 2 to 4% for U-238; and
- 5 to 10% for Np-237.

Table 3: Status of fast yield data

	U-235, fast				Pu-239, fast			
	this review		ref. /4/		this review		ref./4/	
Zr-95	6.39 ± .06	(1 %)	6.39	(1.4-2%)	4.74 ± .07	(1.5 %)	4.73	(2-2.8%)
Zr-97	5.89 ± .09	(1.6%)	5.86	(1.4-2%)	5.28 ± .06	(1.1 %)	5.11	(2-2.8%)
Ru-103	3.25 ± .05	(1.5%)	3.29	(1.4-2%)	6.94 ± .15	(2 %)	6.74	(1.4-2%)
I-131	3.16 ± .04	(1.2%)	3.24	(1.4-2%)	4.02 ± .08	(2 %)	4.08	(2-2.8%)
Te-132	4.58 ± .05	(1.1%)	4.61	(2-2.8%)	5.30 ± .09*	(1.8%)	5.23	(2-2.8%)
Cs-137	6.19 ± .07	(1.1%)	6.17	(0.7-1%)	6.59 ± .07	(1 %)	6.29	(1.4-2%)
Ba-140	6.07 ± .08	(1.3%)	6.020	(1.4-2%)	5.37 ± .06	(1 %)	5.24	(1.4-2%)
Nd-148	1.69 ± .02	(1.1%)	1.68	(0.5-0.7%)	1.68 ± .02	(1.2 %)	1.64	(1.0-1.4%)

* for the present review, the Te-132 yield was assumed to be equal to the mass yield, whereas Meek and Rider /4/ obtain a difference of ≈4% between the Te- and the mass-yield for Pu-239.

Table 3: (continued)

	U - 238				Np - 237		
	this review		ref. /4/		this review		Cuninghame /7/
Zr-95	5.13 ± .10	(2 %)	5.30	(2-2.8%)	(5.87 ± .15)	(3 %)	5.83
Zr-97	5.45 ± .07	(1.3%)	5.40	(2-2.8%)	-		5.96
Ru-103	6.36 ± .15	(2.4%)	6.35	(2-2.8%)	(5.76 ± .24)	(5 %)	5.48
I-131	3.20 ± .05	(1.6%)	3.29	(2-2.8%)	(3.42 ± .13)	(4 %)	3.33
Te-132	(5.16 ± .15)	(3 %)	5.09	(2-2.8%)	(4.86 ± .24)	(5 %)	5.97
Cs-137	(6.00 ± .10)	(1.7 %)	6.28	(2.8-4%)	(6.58 ± .18)	(3 %)	6.4
Ba-140	5.96 ± .09	(1.5 %)	6.02	(1.4-2%)	(5.66 ± .17)	(3 %)	5.93
Nd-148	(2.10 ± .05)	(2.4 %)	2.18	(2.8-4%)	(1.80 ± .07)	(4 %)	1.9

References

/1/ Dudey, N.D., et al., Nucl. Tech. 25, 294 (1975)

/2/ McElroy, W.N., Kellogg, L.S., Nucl. Tech. 25, 180 (1975)

/3/ Crouch, W.A.C., AERE-R-8152 (1976), supersedes AERE-R-7785 (1975)

/4/ Meek, M.E., Rider, B.F., NEDO-12154-1.

/5/ ENDF/B-IV, Material No. 3, 1261, 1264.

/6/ FPND Panel 1973, Bologna, Conclusions and Recommendations, IAEA-169, Vol. II, p. 201.

/7/ Cuninghame, J.G., ibid., Vol. I, p. 353

/8/ Maeck, W.J., Wash. Conf. 1975, NBS Special Publication 425, p. 378.

/9/ Davies, W., Radiochimica Acta 12, 173 (1969).

/10/ Cuninghame, J.G., et al., AERE-R-6862 (Rev.) (1972).

/11/ Rajagopalan, M., et al., Nucl. Sci. Engg. 58, 414 (1972).

/12/ Scholtyssek, W., KFK-1272/1, p. 121-14 (1972).

/13/ Dudey, N.D., Heinrich, R.R., 1st ASTM-Euratom Symposium on Reactor Dosimetry, Petten (Netherlands) 22-25 Sept. 1975; CONF-750935-12.

/14/ Dowdy, E.J., Nucl. Tech. 25, 381 (1975).

/15/ Larsen, R.P., et al., Nucl. Sci. Engg. 54, 263 (1974).

/16/ Zimmer, W.H., et al., Nucl. Tech. 25, 289 (1975).

/17/ Cottone, G., et al., NEANDC(E)-162 U/V, p. 42 (1975).

/18/ Robin, M., et al., Int. Conf. on Chem. Nucl. Data, BNES, Univ. of Kent, Canterbury, U.K. (1971), Session 1A, paper 4.

/19/ Lisman, F.L., et al., Nucl. Sci. Engg. 42, 191 (1970).

/20/ Maeck, W.J., FPND Panel 1973, Bologna, Vol. I, p. 163.

/21/ Tracy, B.L., et al., J. Inerg. Nucl. Chem. 35, 2639 (1973).

/22/ Larsen, R.P., et al., ANL-7879 (1972).

I ... experimental data from references in Table 1

x ... recommended fast yield /4/

o ... recommended thermal yield /4/

—·—·—·— weighted average (see Table 3)

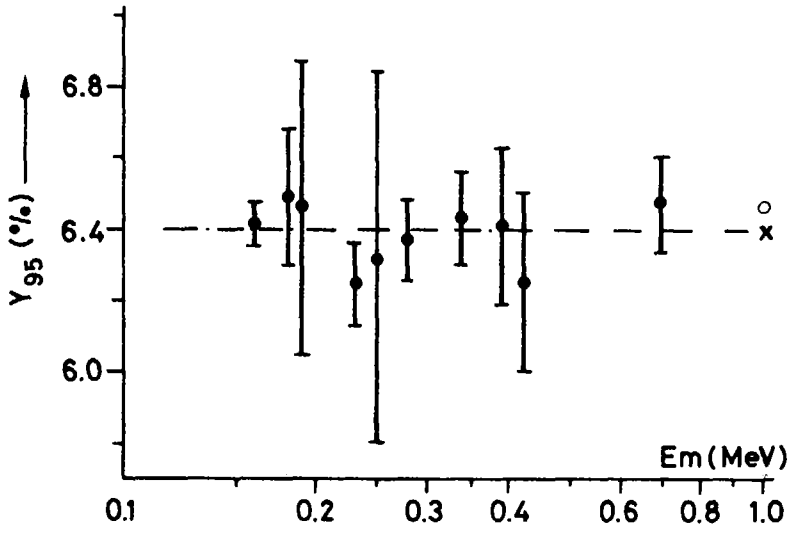

Fig. 1: Zr-95 absolute yields (="standard")

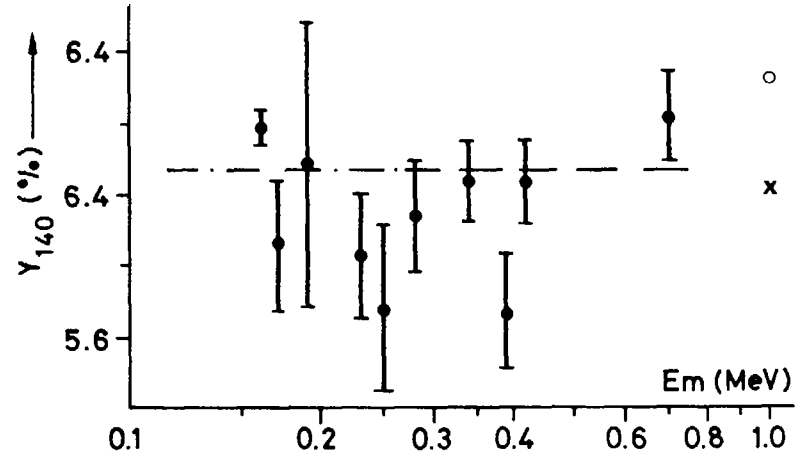

Fig. 2: Ba-140 absolute yields

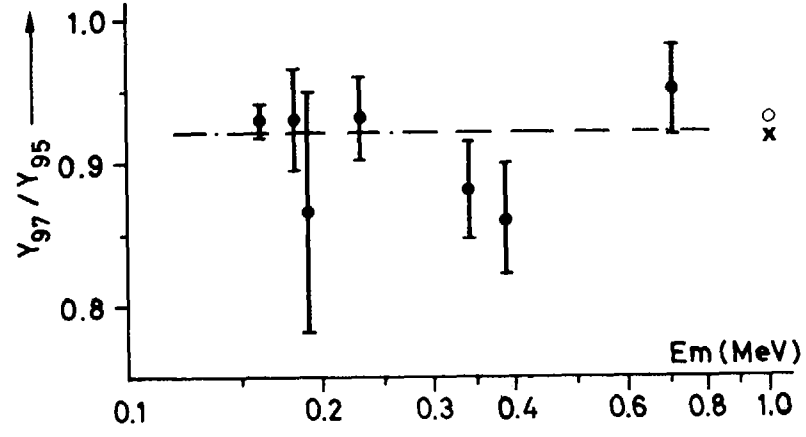

Fig. 3: Zr-97 yield relative Zr-95

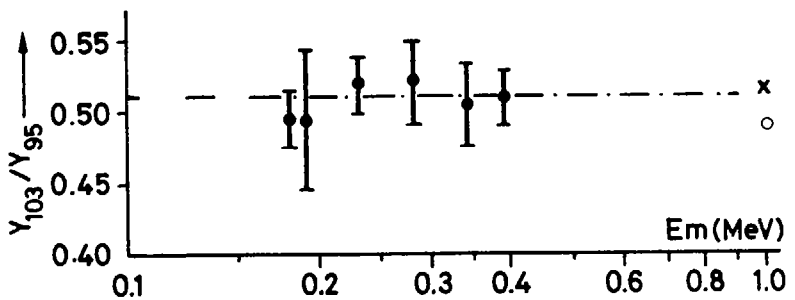

Fig. 4: Ru-103, rel Zr-95

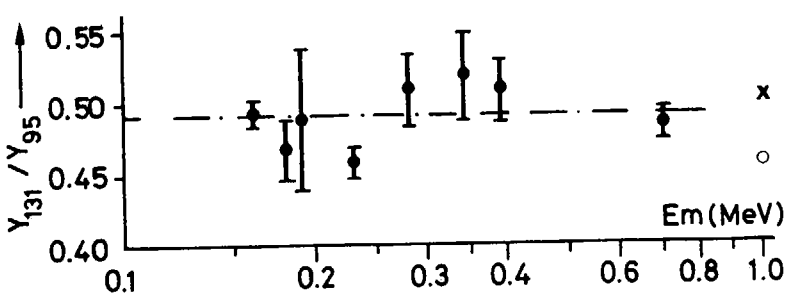

Fig. 5: I-131, rel Zr-95

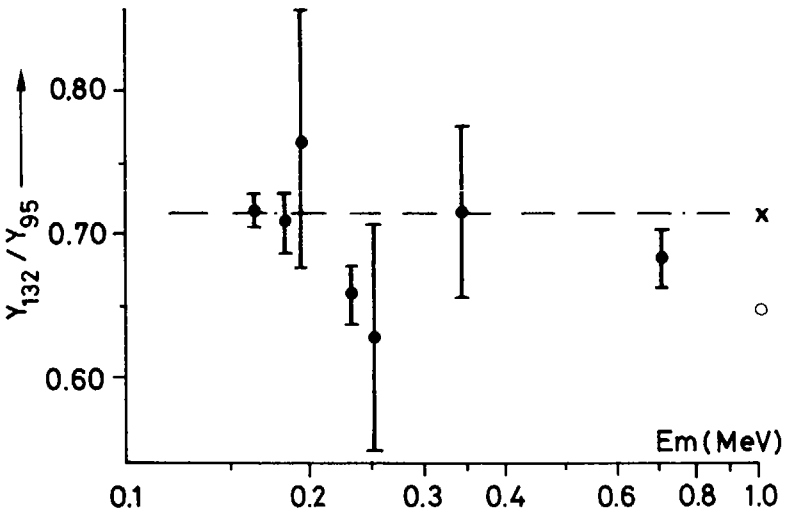

Fig. 6: Te-132, rel Zr-95

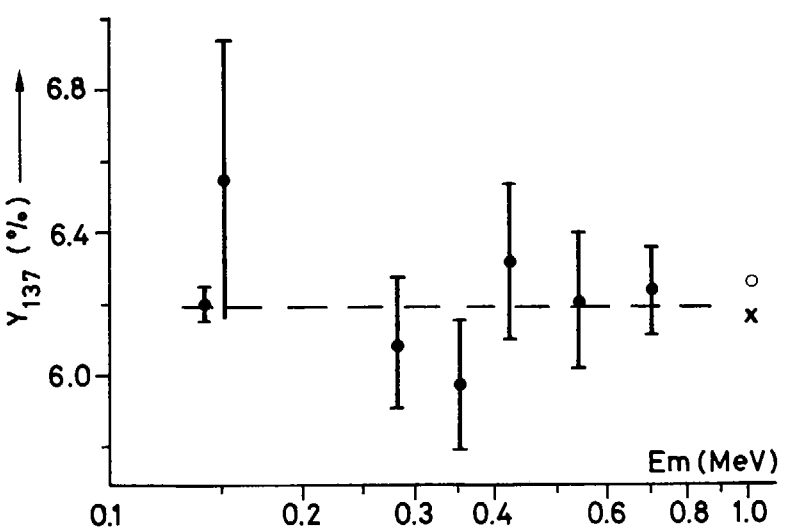

Fig. 7: Cs-137, absolute yields

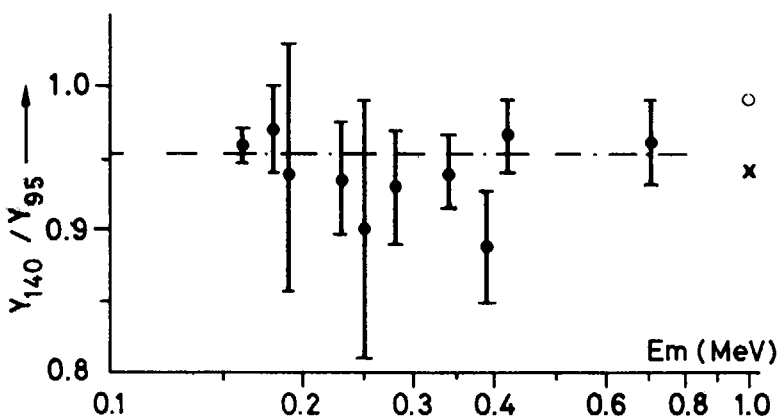

Fig. 8: Ba-140, rel Zr-95

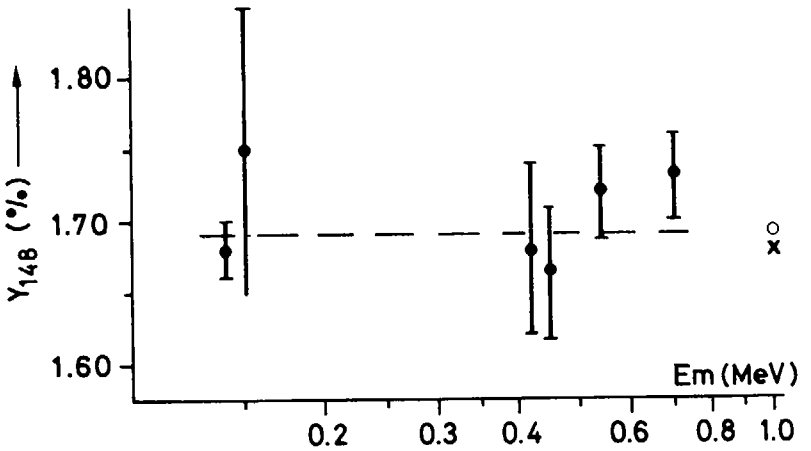

Fig. 9: Nd-148, absolute

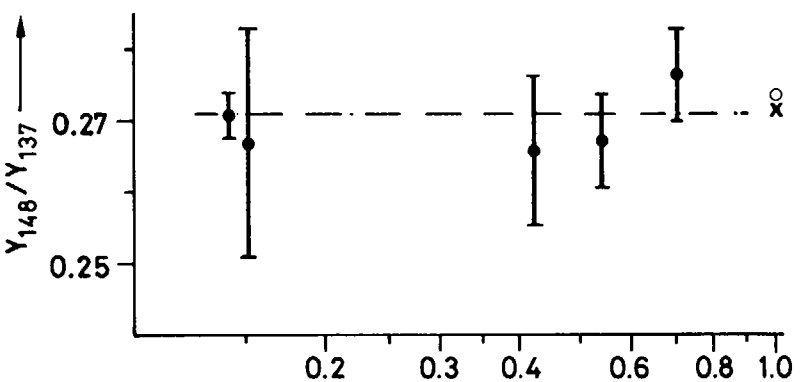

Fig. 10: Nd-148, rel Cs-137

I ... experimental data from reference in Table 1

x ... recommended fast yield /4/

o ... recommended thermal yield /4/

-.-.-.- weighted average (see Table 3)

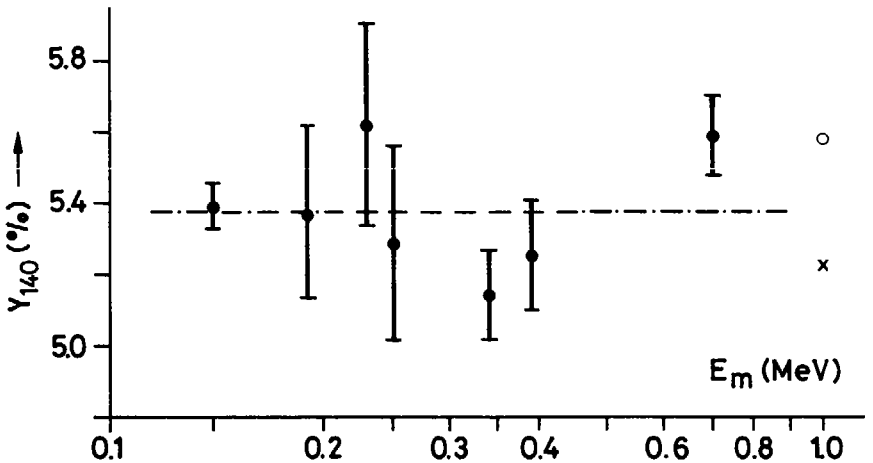

Fig. 11: Ba-140, absolute (="standard")

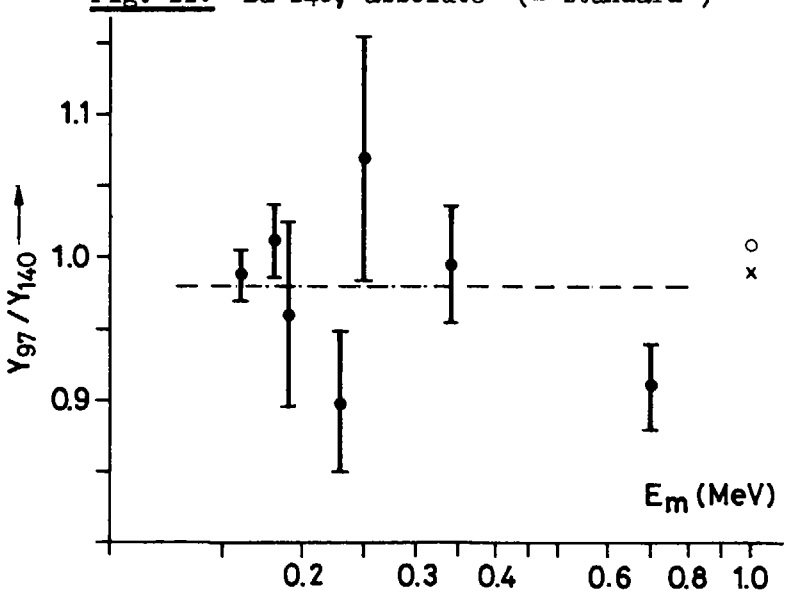

Fig. 13: Zr-97, rel Ba-140

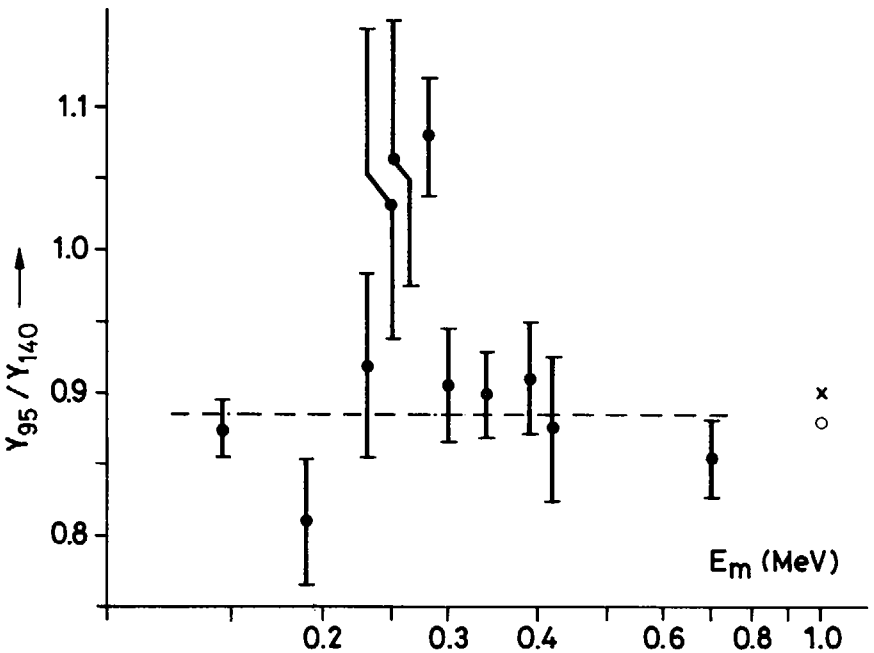

Fig. 12: Zr-95, rel Ba-140

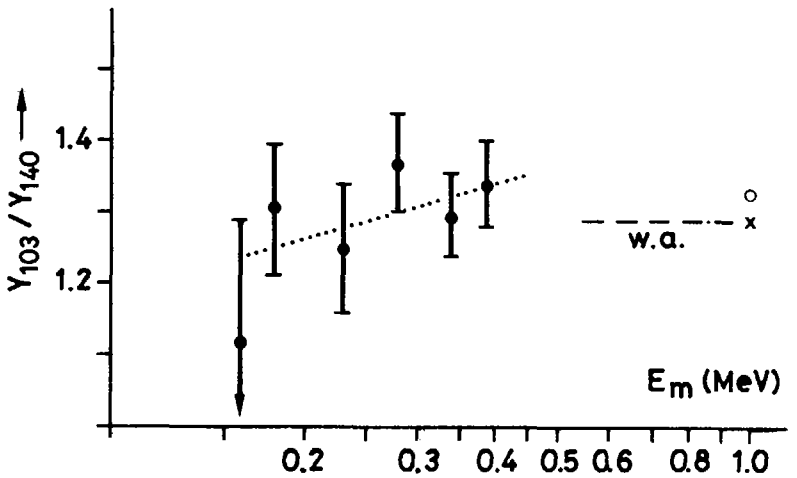

Fig. 14: Ru-103, rel Ba-140; ... eyeguide through points

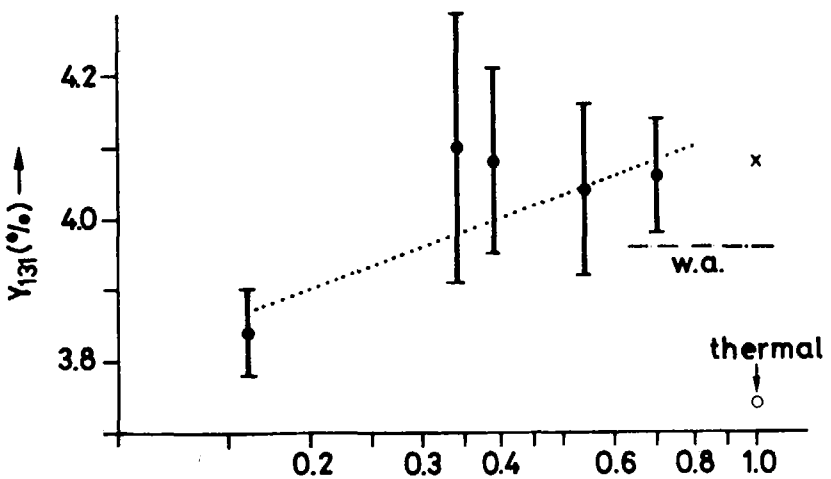

Fig. 15: I-131, absolute;
... eyeguide through points

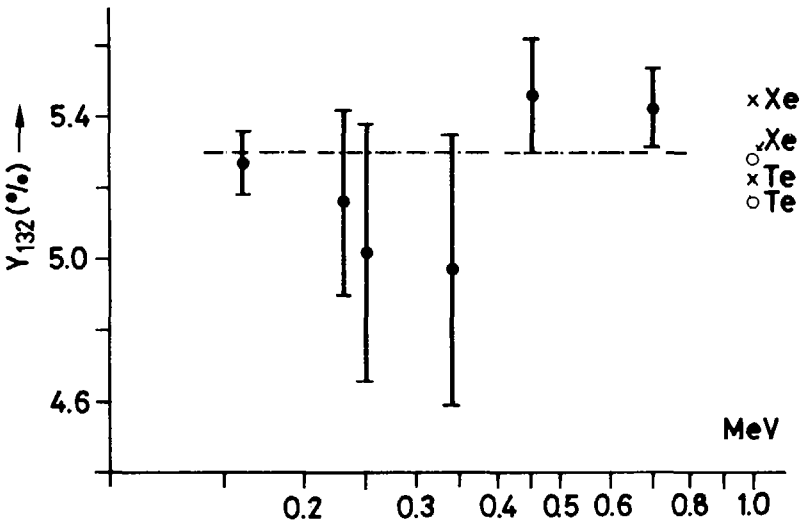

Fig. 16: Te(Xe)-132, absolute

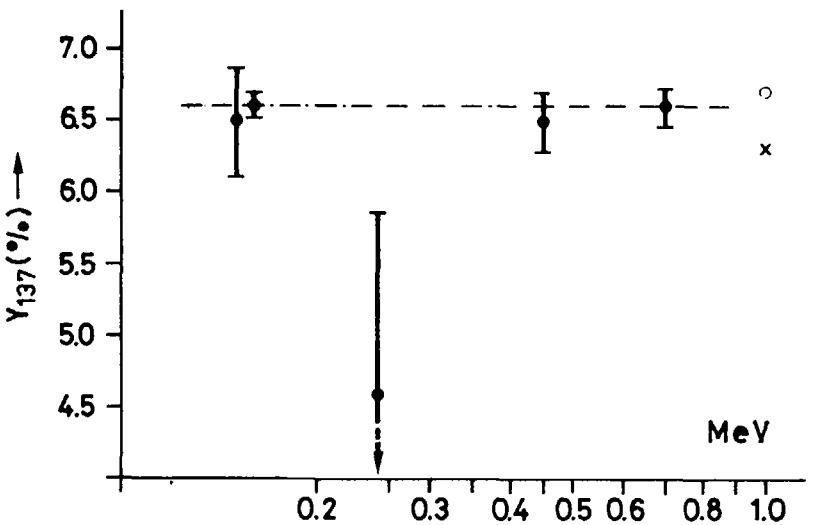

Fig. 17: Cs-137, absolute yields

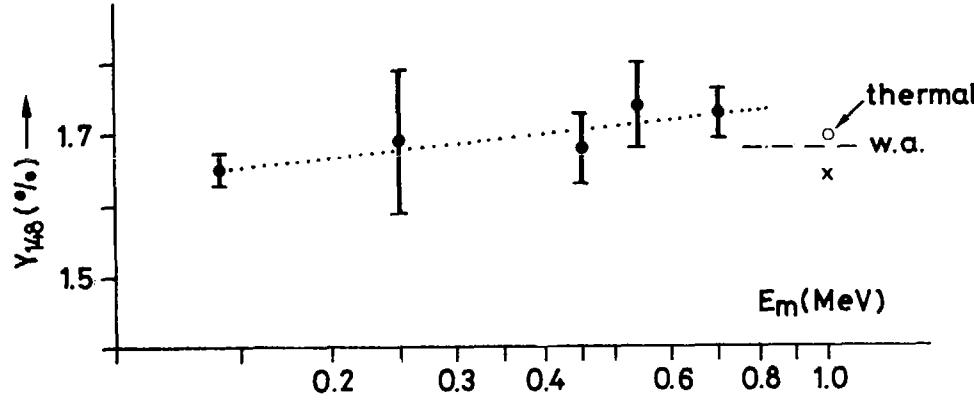

Fig. 18: Nd-148, absolute yields
... eyeguide through points

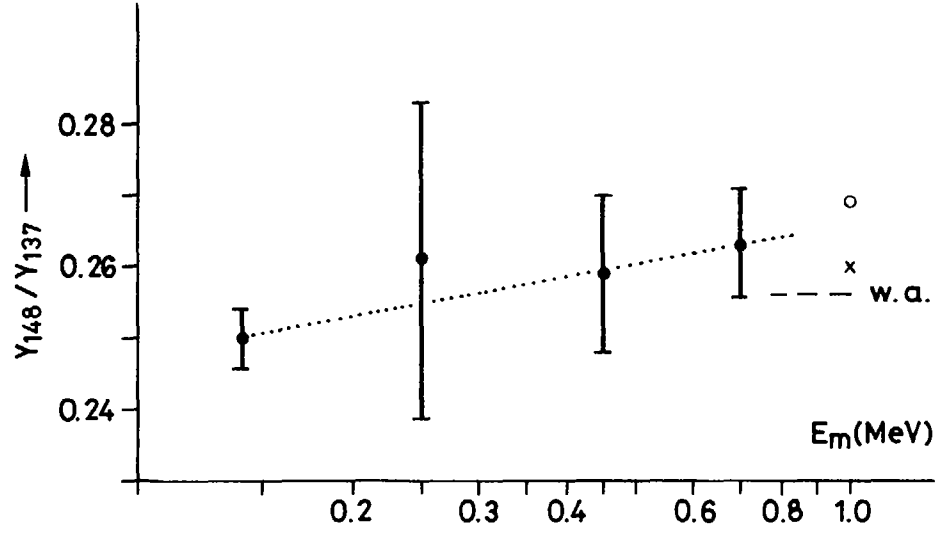

Fig. 19: Nd-148, rel Cs-137
... eyeguide through points

I ... experimental data from references in Table 1

x ... recommended fast yield /4/

-·-·-·- weighted average (See Table 3)

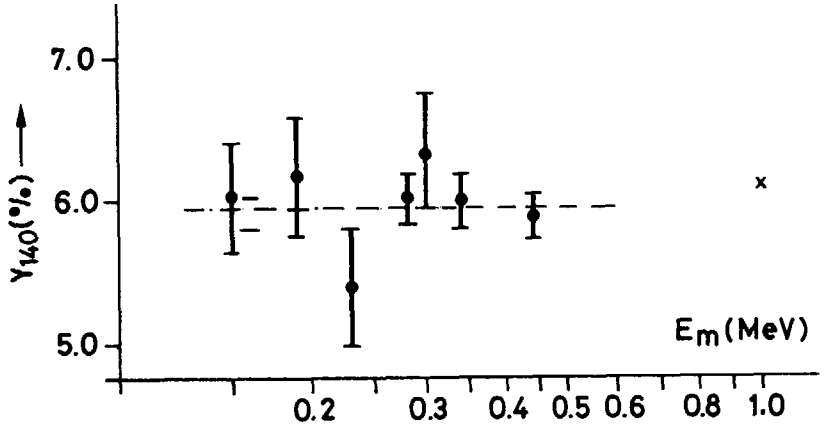

Fig. 20: Ba-140 absolute yield (= "standard")

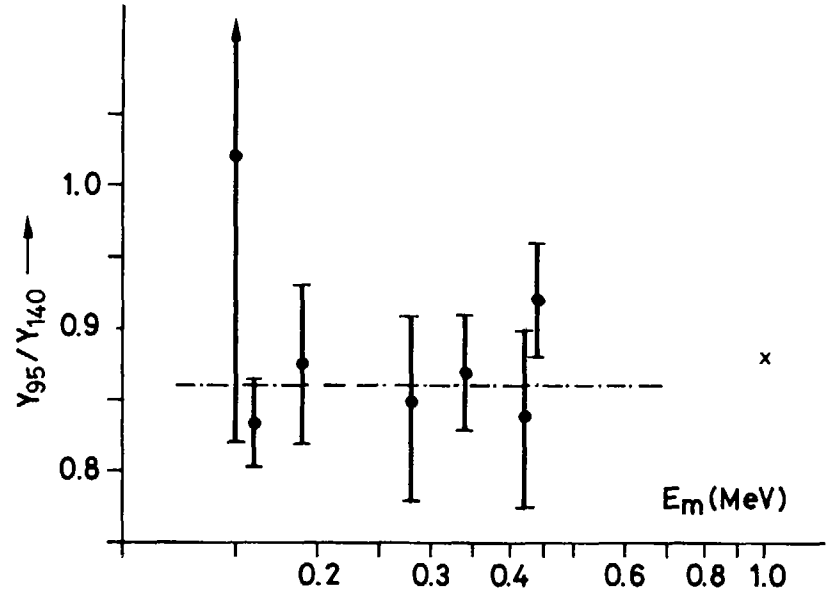

Fig. 21: Zr-95, relative Ba-140

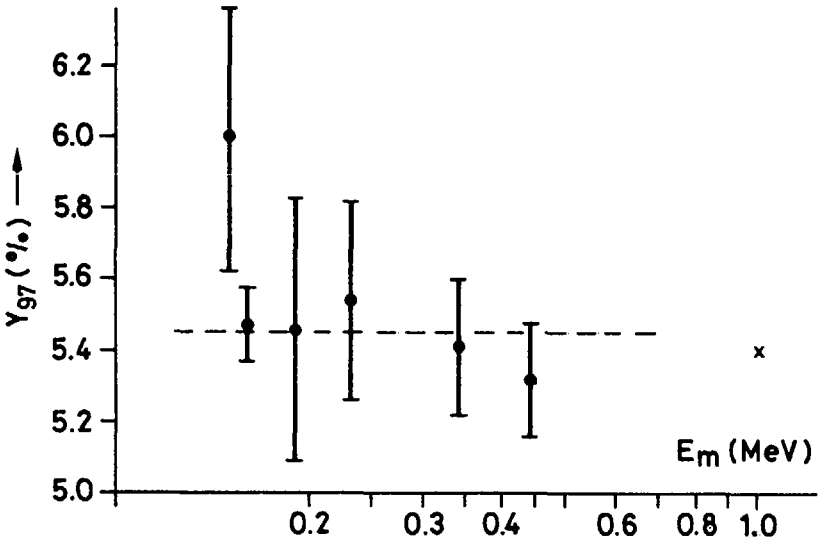

Fig. 22: Zr-97, absolute yields

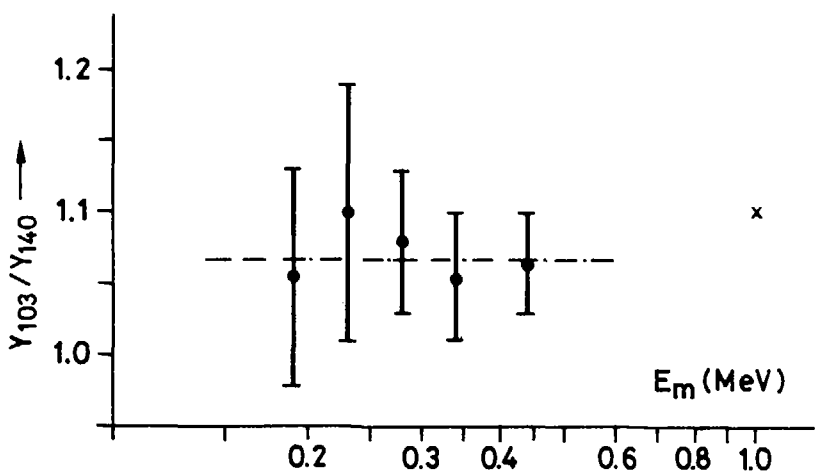

Fig. 23: Ru-103, relative Ba-140

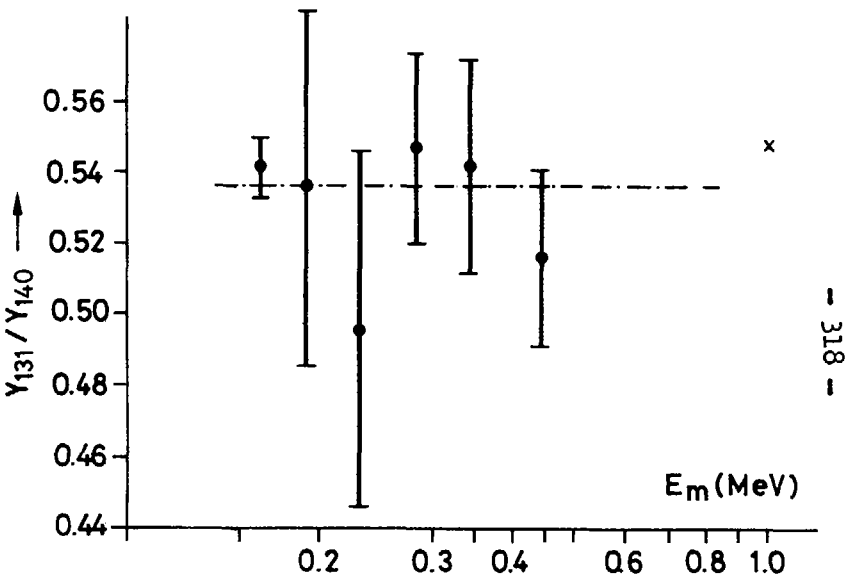

Fig. 24: I-131, relative Ba-140

IV. DIFFERENTIAL CROSS-SECTION DATA FOR REACTOR DOSIMETRY

IV.1. REMARKS CONCERNING THE ACCURATE MEASUREMENT OF DIFFERENTIAL CROSS SECTIONS FOR THRESHOLD REACTIONS USED IN FAST-NEUTRON DOSIMETRY FOR FISSION REACTORS*

Donald L. Smith

Applied Physics Division
Argonne National Laboratory
Argonne, Illinois 60439
U.S.A.

ABSTRACT

Some remarks are submitted concerning the measurement of differential cross sections for threshold reactions which are used in fast-neutron dosimetry for fission reactors. The objective is to familiarize the reader with some of the problems associated with these measurements and, in the process, to explain why the existence of large discrepancies in the data sets for many of these reactions is not surprising. Limits to the accuracy which can be expected for these cross sections in the near future--using current technology and available resources--are examined in a general way and recommendations for improving the accuracy of the differential data base for dosimetry reactions are presented.

I. Introduction

Apparently the only reliable way to quantitatively predict macroscopic phenomena (such as radiation damage) which will be observed for commercial power reactors--on the basis of test results from low-power critical facilities or from high-fluence materials test reactors--is to possess a knowledge of the neutron spectra and relative power or fluence levels of these facilities as well as an understanding of the neutron-energy dependence of the phenomena of interest. Neutron dosimetry is the term applied to that technology which is used for the purpose of defining the intensities and spectral properties of neutron fields in nuclear reactors. Detailed quantitative knowledge about a variety of selected nuclear reactions is basic to the application of current neutron dosimetry techniques.

The development of consistent sets of cross section data for a selected group of favorable dosimetry reactions has not turned out to be an

---

* This work has been supported by the U.S. Energy Research and Development Administration.

easy task. The current accuracy goal of better than 5% (1 σ) has not been achieved with the possible exception of a few so-called "Category I" reactions. At an early stage, it became clear that an international effort would be desirable in order to achieve the stated goal and that it would have to involve investigation of decay schemes and a variety of "benchmark" integral measurements as well as differential (monoenergetic) measurements.

Considerable progress has been made in recent years towards improving the knowledge of decay data for the radioactive products from fast-neutron reactions for dosimetry monitors. The development of the Ge(Li) detector for gamma-ray spectrometry is largely responsible for this progress since most dosimetry reactions produce gamma-ray active daughters which can be investigated using this method. However, the importance of some careful evaluations [e.g. Ref. 1] should not be depreciated.

Similarly, a great deal of effort has been expended in the development of benchmark and standard neutron fields for integral testing of differential cross sections for dosimetry reactions [e.g. Ref. 2]. There has been a generally well considered effort to measure the integral cross sections for selected dosimetry reactions using the available facilities. While the agreement of various integral data is generally not within the stated accuracy goal, the situation is steadily improving [e.g. Ref. 2].

Sophisticated numerical procedures for unfolding reactor-neutron spectra from the results of integral measurements have evolved in the last few years [e.g. Ref. 3]. However, these procedures do not yield unique results. Therefore, the need for accurate, direct measurement of differential cross sections remains undiminished [e.g. Ref. 4].

The accuracies to which differential cross section data for most dosimetry reactions are known are far short of the requirements. In fact, this area is currently a weak aspect of neutron dosimetry. There are both historical and technical reasons why this condition exists.

Differential cross section data is obtained from measurements performed at "monoenergetic" accelerator facilities. Although there are notable exceptions, the main emphasis at the majority of these laboratories has been on basic-nuclear-structure research rather than on development of a data base for nuclear applications. The accumulation of detailed, accurate data for quantitative applications requires redundancy of measurements and an attention to numerous details which are unnecessary for the realization of many basic research objectives. Traditionally, this sort of quantitative activity has been generally considered unappealing by members of the basic-research community. Finally, most basic nuclear research has centered on charged-particle reactions rather than neutron reactions.

The neutron energy region from 8 - 14 MeV has traditionally been a difficult one for monoenergetic measurements, and will probably continue to be a source of problems, because of the lack of a good monoenergetic neutron-source reaction to cover it. The scarcity and uncertainty of data in this region reflects this problem [5]. It will be seen in Section IV.F that this handicap will most probably be overcome by brute force. That is, that the characteristics of secondary reactions associated with proton bombardment

of triton and deuteron bombardment of deuterium will have to be studied in sufficient detail to permit accurate corrections to the data to be determined for measurements made in this region. Progress in this energy region will be strongly dependent upon the availability of large accelerators with the requisite beam energy and intensity capabilities.

Most monoenergetic measurements are ratio measurements, and there has been little consistency in the selection of standards. Many of the available data sets are reported only as cross sections with no published ratios. Thus, without knowledge of the exact values used for the standard cross sections, it is difficult to renormalize old results to account for revisions of the standard cross sections. The alternative is probably to reject them.

With the exception of certain fission cross sections and some other standards such as the $^{6}Li(n,\alpha)^{3}H$, $^{3}He(n,p)^{3}H$ and $^{10}B(n,\alpha)^{7}Li$ reactions, there has been little coordinated effort to improve the accuracy of differential cross sections for reactions relevant to dosimetry applications. Until just recently, the major contribution to improving the knowledge of these cross sections has come from compilation and evaluation efforts [e.g. Refs. 4-6]. Careful evaluation of the existing data base [6] has led to the rejection of some data sets which are greatly discrepant with respect to other corresponding sets. However, the uncertainties in many of the evaluated cross sections are still large-especially in energy intervals where the available data are sparse [4]. Evaluation cannot generate a reliable set of cross sections from a poor data base.

The remainder of this paper is concerned with a description of some details associated with differential cross section measurements. The objective is to indicate several potential sources of random and systematic error associated with these measurements. Estimates of reasonable accuracy goals are made on the basis of current technology and available resources for the measurements. Although the treatment is general, details from specific reactions are presented as examples. The experimental techniques used in differential measurements are diverse. No attempt is made to treat all of these thoroughly. As the title of the paper suggests, only threshold reactions of interest for fast-neutron dosimetry are considered. Measurement of reactions with no clearly defined thresholds-such as the (n,γ) reaction-involves different techniques than those to be discussed here. Furthermore, emphasis is placed on measurement of cross sections for reactions producing gamma-ray active daughters and for which detection of the gamma radiation forms a part of the measurement. In recent years, beta-particle detection techniques have declined in importance for dosimetry applications. This subject is not treated in this paper. Measurement of fission cross sections by detection of the fragments with an ion chamber or track recorder is described elsewhere [e.g. Refs. 7 and 8]. Detection of fission fragments is an attractive method since the fragment energies are large and their range in matter is short. The quantity of sample material used is generally about two-orders-of-magnitude smaller than is the case for gamma-ray measurements; however, the detection efficiency is commensurately larger so the sensitivities of differential measurements are similar for both techniques. In principle, (n,p) and (n,α) cross sections could be

measured by charged-particle detection. Presently, these cross sections can be measured with greater accuracy by the activation method whenever that is applicable. It must be kept in mind that comments made concerning various experimental techniques relate only to their application in differential dosimetry measurements. The capabilities and limitations of these techniques may very well be quite different in other contexts.

II. Concept of Differential Cross Section Measurements

In a broad sense, there are similarities between integral and differential cross section measurements for dosimetry reactions. Both involve determination of the neutron dose received over a specified time interval, characterization of the neutron spectrum, measurement of the induced activity in the sample, conversion of the observed activity to a reaction rate based on a knowledge of the decay properties of the daughter, and finally, computation of a cross section after the application of relevant corrections. The major differences are:

i) Geometry: In differential measurements, most of the neutrons incident upon the sample originate from a small region of space (the target). This is also usually the case in ^{252}Cf irradiations. However in reactors, the neutrons impinge on the sample from all directions in space with less spatial bias.

ii) Neutron spectrum: In differential measurements one strives to obtain a neutron source which is nearly monoenergetic. In integral measurements, the neutrons are continuously distributed over wide energy ranges.

iii) Neutron intensity: The intensity of accelerator neutron sources is generally much lower than for integral facilities (often by orders of magnitude). This leads to poorer statistics in the measurement of small cross sections. The necessity for larger samples leads to additional uncertainties caused by absorption and scattering of radiation as well as geometrical effects.

iv) Fluence stability: Standard and reference neutron fields utilized for integral measurements are generally quite stable and reproducible (usually to within $\sim$ 1%), whereas accelerator sources can be quite unstable and are not easy to reproduce with high accuracy.

To a large extent, these differences are responsible for the generally poorer accuracy of differential data in comparison with integral data. However, there are procedures for dealing with these problems, and it appears possible to obtain differential data which are nearly as accurate as integral data except at energies for which the cross sections are very small (microbarns) or for reaction products with long half lives (years).

The general relationship between the differential cross section, the reaction rate and the observed detector counts for a simple irradiation with a steady source of monoenergetic neutrons is given by the formulas

$$R = F\ N\ G_n\ \eta_n\ \sigma \tag{1}$$

$$C = b\ \varepsilon\ G_r\ \eta_r\ R\ (1-e^{-\lambda t_E}) \cdot \cdot e^{-\lambda(t_W + t)} \tag{2}$$

where

R = reaction rate,

F = neutron fluence,

N = total number of sample atoms,

G_n = geometric factor for neutron irradiation,

η_n = neutron absorption and scattering factor,

σ = differential cross section,

C = detector count rate (detection of daughter gamma-ray activity) at time t after the start of a count,

b = factor to account for mass yields (of fission products), decay branching, isotopic abundance, etc.

ε = gamma-ray detection efficiency,

G_r = geometric factor for measurement of decay radiation,

η_r = decay radiation absorption and scattering factor,

λ = decay time constant,

t_E = irradiation time (assumed constant fluence level),

t_W = wait time between end of irradiation and start of daughter activity measurement.

III. Sensitivity of Differential Cross Section Measurements

There are limits to the sensitivity of differential cross section measurements which are imposed by various experimental considerations. These limits are important because they define minimum values for measurable cross sections. Measurements attempted below these limits are not likely to yield very accurate results. Experimental factors to consider in estimating the sensitivity of conventional differential measurements are:

i) Neutron intensity: Neutron generators which are designed to yield 14-MeV neutrons are generally capable of producing as many as two-orders-of-magnitude higher intensity neutron fluences than are

accelerators used to produce neutrons over a wider range of lower energies. The present discussion excludes neutron generators since neutrons with energies < 14 MeV are the main concern for fission reactors. Considering such factors as target stability, neutron yield from conventional source reactions, resolution and geometry, the neutron fluence available for differential-cross-section measurements cannot be expected to exceed $F \sim 10^9$ neutrons /sec/sr on a sample using presently available accelerators.

ii) Sample size: The size of samples to be used for differential measurements is limited by consideration of geometry and the absorption and scattering of radiation. In the present discussion it is assumed that gamma-ray activity is measured. A practical limit for the size of a sample (all atoms) is $N < 2 \times 10^{23}$ atoms. This limit must be lowered if the gamma-ray energy is relatively low or if the atomic number is large so that gamma-ray absorption effects are significant.

iii) Detector count rate: If the full-energy-peak yield of a particular gamma ray emitted from an irradiated sample is less than $C \sim 1$ count/sec, experience has shown that the effects of background are troublesome and it is difficult to make yield measurements with the accuracy desired.

iv) Detector efficiency: Unless the decay gamma-ray spectrum is quite simple, accurate measurement of decay yields has to be made using a Ge(Li) detector. The absolute gamma-ray detection efficiency ε in standard counting geometries ultimately depends upon gamma-ray energy and detector size, but $\varepsilon \sim 0.05$ is a reasonable upper limit for gamma rays with $E_\gamma \gtrsim 1$ MeV detected by a Ge(Li) detector.

v) Irradiation time: Because of the inherent tendency of accelerator beam intensities to drift with time, neutron fluence is rarely constant. It is feasible to make a correction for this effect by recording the neutron fluence level as a function of time. When possible, it is desirable to limit irradiation times so that $\lambda t_E < 0.1$. Under these conditions, the measurement of reaction rates will not be severely influenced by the stability of the neutron fluence. Experience with accelerator operation has shown that $t_E \sim 10^5$ sec is a practical upper limit for the irradiation time.

vi) Wait time: It is possible to adhere to the requirement $\lambda t_W << 1$ for all useful dosimetry reactions. This avoids waste of activity acquired from the irradiation.

vii) Count time: There is little to be gained from counting samples for much longer than the half life of the daughter activity ($t_C \gtrsim t_{\frac{1}{2}}$). However achievement of the desired accuracies for measured differential cross sections requires that the statistical uncertainties in the detector counts be kept as small as possible. The uncertainty due to statistics should certainly not exceed $\sim 3\%$ which requires

that $C\ t_C > 10^3$.

These considerations provide constraints on Eqs. (1) and (2). It is possible to derive an order-of-magnitude formula based on Eqs. (1) and (2), as well as other considerations mentioned above, which is useful in estimating the smallest cross section values which can be measured with reasonable accuracy using available facilities and experimental techniques which are discussed in later sections of this paper.

The formula is

$$\sigma_{min} = 10^{-7}\ b\ f_C\ (t_{1/2}/t_E) \qquad (3)$$

where b and t_E are defined in Section II and

$t_{1/2}$ = half life for daughter activity,

$$f_C = \begin{cases} 1 \text{ if } C\ t_{1/2} \geq 10^3 \text{ sec} \\ (10^3/t_{1/2}) \quad \text{otherwise.} \end{cases}$$

The factor f_C is included to permit consideration of counting limitations expressed in Item (vii) above ($f_C > 1$ implies that counting limitations reduce the sensitivity).

Table I provides examples of the application of this formula over a wide range of half lives. It is interesting to compare the estimated limits with the current minimum cross section values reported in the literature. In general, it is the region from threshold up to $\sim$ 6-8 MeV excitation (the approximate nucleon binding energy) which is of greatest importance for dosimetry monitor reactions.

It would require a separate study to ascertain whether these limitations to differential measurements will present any significant problems with regard to the establishment of a data base for dosimetry reactions which is adequate to meet the needs for reactor applications. Clearly, such a study should be made so that necessary and sufficient accuracy levels can be established for specific reactions. Otherwise, the risk exists that important measurements will not be undertaken, or that resources will be wasted on achieving high accuracy where it is not required.

IV. Characteristics of Monoenergetic Accelerator Neutron Sources

Neutrons are produced at "monoenergetic" accelerator facilities by means of nuclear reactions induced by the bombardment of targets with charged-particle beams. If the neutrons produced were truly monoenergetic, with precisely known energies, and emanated isotropically from an idealized point source, then the only tasks facing the experimenter would be to measure the fluence and correct for minor geometric effects. However, since the neutron sources are not ideal in this regard, it is necessary for the experimenter to correct cross section data for the effects of the departure from ideality. Factors which have to be considered are:

i) Neutron energy resolution: Even if the neutrons are produced entirely by a single reaction process with a well-defined Q value, the energies of neutrons incident on the sample will be spread somewhat owing to finite target thickness, kinematics and finite charged-particle-beam-energy resolution. The consequences are important.

ii) Neutron-energy definition: Methods utilized in definition of neutron energy are subject to uncertainty.

iii) Angular-distribution effects: Neutron emission is not isotropic. This can lead to uncertainties in determination of the neutron fluence at the sample.

iv) Secondary-neutron reactions in the target: There are often several neutron-producing reaction channels open for a given incident charged-particle energy.

v) Background from target assemblies: At higher energies, all target assemblies produce background neutrons. The background can be variable if it is due to build up of contaminants in the vacuum system or to variations in the beam optics during an irradiation.

These particular factors will be examined to determine how they can influence the measurement of accurate differential cross sections and the generation of recommended cross section values by means of evaluation of the existing data base. Following this, the characteristics of the most commonly used "monoenergetic" neutron-producing reactions will be reviewed briefly.

A. Neutron-Energy Resolution

At low energies, neutron-energy resolution is dominated by charged-particle energy loss in the targets. Here yield considerations establish a lower practical limit for target thickness. However, at higher energies, particularly for neutron-producing reactions involving deuterium and tritium targets, the resolution is dominated by kinematic effects. At all energies, the energy resolution of the charged particle beam-normally a few kilovolts-contributes to the neutron-energy resolution. All factors considered, the practical limit of neutron-energy resolution is $\sim$ 20 - 100 keV for E_n < 5 MeV, $\sim$ 100 - 200 keV for E_n < 10 MeV and > 200 keV for E_n > 10 MeV in the measurement of differential cross sections.

There are two important consequences of finite resolution in differential cross section measurements. One is that significant uncertainties can exist in determination of the effective reaction thresholds and of the magnitudes of cross section values for energies just above these thresholds. Evaluators are familiar with situations where cross section data sets for some reactions are in disagreement by factors of two or more near threshold. Faced with data bases such as these, it is unrealistic to expect evaluators to produce sets of numbers which are reliable. Threshold uncertainties can be very significant if the threshold falls in a region of a reactor spectrum where the neutron intensity changes rapidly with energy. A second

consequence of finite resolution is experienced in reactions where the cross section fluctuates considerably with energy. Examples are the $^{27}Al(n,p)^{27}Mg$ and $^{32}S(n,p)^{32}P$ reactions. Data sets measured with different resolutions are practically incomparable for such reactions unless the energy scales and resolutions are precisely determined. Historically, this requirement has rarely been met and evaluators have had to deal with conditions which discouraged the production of reliable evaluated numbers.

With present technology, it is possible to determine the energy resolution of specific measurements to within a few kilovolts for targets less than 100-keV thick. By utilizing available range-energy data for analyzing the passage of heavy charged particles in matter, and by including detailed analysis of the effects of kinematics in computation of cross sections from raw data, measurers of differential data could progress a long way towards elimination of the deleterious effects of resolution uncertainty in their experimental data. It is impossible to select a universal number which will represent a lower limit to the uncertainty which is likely to persist in differential data due to resolution uncertainties. The effects depend too critically on reaction details. However, a comparison has been made of the results of two recent measurements of the neutron inleastic-scattering cross section for iron-a reaction which is notoriously susceptible to resolution uncertainties. The agreement of the coarse ($\sim$ 50 keV) resolution data with the fine ($\sim$ 1-2 keV) resolution data is excellent (within a few percent over a 1-MeV neutron-energy range) when the latter data set is energy-averaged to $\sim$ 50 keV resolution [10].

Both measurers and evaluators must share in the responsibility of minimizing resolution uncertainties so as to improve the differential data base for dosimetry reactions. Measurers need to accurately determine the resolution of their measurements and report and properly document their values. Evaluators need to energy-average all data for individual reactions to equivalent resolution, and reject data sets which do not report experimental resolutions or which are poorly documented, prior to performing their evaluations. While such a procedure may seem harsh and undemocratic, it appears to be the only practical way to establish the standards of quality in the data base for dosimetry reactions which will be required to meet the stated objectives.

B. Neutron-Energy Definition

Much of what was said in the preceding section about the effects of resolution uncertainty applies to energy definition. By utilizing recent Q-value and nuclear mass data, carefully calibrated electro-magnetic beam analysis and, in certain instances, time-of-flight techniques, it now appears possible to determine fast-neutron energies to better than $\sim$ 5 keV as long as the resolution is $<$ 100 keV. This accuracy should be sufficient for dosimetry applications.

However, complications arise when several samples are irradiated simultaneously by placing them at several angles relative to the incident charged-particle beam. Accurate definition of the neutron energy then involves careful determination of the geometry as well as the calibration

procedures mentioned previously. Although this procedure has been utilized by competent researchers who very carefully attended to the requisite details, it is apparent that the method has a large potential for systematic error and should be avoided when possible. Unfortunately, this is about the only way researchers at small accelerator facilities can enlarge their range of accessible neutron energies. The problem is one of economics as well as technology. However, achievement of the goal of a better-than-5-keV accuracy for routine neutron energy definition is predicated on the assumption that irradiations will be performed with neutrons emitted near zero degrees.

C. Angular Distribution Effects

Neutron emission from charged-particle-induced reactions is not isotropic. Neutron yield at back angles can be an order-of-magnitude smaller than at zero degrees for some of these reactions. While some very careful experiments which took this effect into consideration have been performed, it is evident from some other data sets in compilations of differential dosimetry data that large systematic errors exist because samples were exposed at angles other than near zero degrees, while the neutron fluence was measured in the forward direction, and incorrect angular-distribution data for the neutron source reactions were used in analysis of the experimental results.

Even if care is taken to correct the activation data from multiple-sample exposures for the source-reaction angular distribution, it is likely that the uncertainty in the final results will be at least $\sim$ 5% due to this effect alone since the angular distributions are usually not known any more accurately than this. Therefore, it is recommended that multiple-angle measurements be avoided if the uncertainties in the differential data base are to be reduced below the present level. Measurements of neutron fluence and sample irradiations should both be performed in the vicinity of zero degrees. Then, small corrections for neutron-emission anisotropy can be made with considerable reliability.

D. Secondary-Neutron Reactions

The principal neutron-source reactions used for monoenergetic measurements on reactions of interest for fast-reactor dosimetry are the $^{7}Li(p,n)^{7}Be$, $T(p,n)^{3}He$, $D(d,n)^{3}He$ and $T(d,n)^{4}He$ reactions. The latter reaction is primarily a source of neutrons with energies above 14 MeV, however it has been used for measurements at energies as low as $\sim$ 12 MeV by means of back-angle irradiations. Each of these reactions yields a single neutron-energy group over a limited range of proton or deuteron energy. However, these reactions are commonly used at higher energies where other neutron-producing-reaction channels are open. Under these conditions, the neutron sources can no longer be considered monoenergetic. These secondary reactions will be discussed in Section IV.F. In practice, for lithium, deuterium and tritium targets, the secondary reactions yield lower-intensity and lower-energy neutrons by comparison with the primary reactions. For some reactions which have been used in activation measurements, the yield of lower-energy neutrons exceeds that of the highest-energy neutrons [e.g. Ref. 11].

The effect of secondary neutrons on measurement of differential cross sections depends upon two major factors:

i) The intensity of these neutrons relative to the primary neutrons and the magnitude of the energy gap between primary and secondary neutrons.

ii) The relative shapes of the excitation functions for the standard and "unknown" reactions in a particular measurement.

If the secondary neutrons form a significant fraction (say > 30%) of the total fluence, if the standard or "unknown" cross section is changing rapidly in energy, or if the thresholds for the standard and "unknown" reaction are quite different, then the presence of secondary neutrons can produce a significant error in the measured "unknown" cross section unless accurate corrections are made. For example, in a measurement of the differential cross section for the $^{27}A\ell(n,p)^{27}Mg$ reaction at $\sim$ 10 MeV, relative to ^{238}U fission, failure to correct for neutrons from the D(d;n,p)D reaction would lead to an error of $\sim$ 13% [12]. There is need for improved knowledge of the neutron spectra from secondary reactions. There should be no fundamental problems encountered in doing this, and the contribution to the overall uncertainty in measurements of dosimetry cross sections resulting from secondary neutrons can probably be limited to < 1% for primary neutron energies below $\sim$ 10 MeV. The relative yield of secondary neutrons at higher energies is presently not well-enough known to permit any quantitative predictions to be made; however, the situation is certain to be less favorable than at lower energies.

E. Background Neutrons

Background neutrons are produced when charged particle beams collide with components of the flight tube and target assemblies. Background usually varies with time and can be a significant problem at higher bombarding energies. Use of high -Z materials in fabrication of the flight tube and target assemblies is essential, especially for slits, collimators and target beam stops. The use of clean components and well-trapped high vacuum systems is desirable. In any event, the effects of background neutrons can be measured directly with good accuracy. If this is done carefully, the uncertainty in the measured cross sections due to this effect will generally be negligible. An example of the relative importance of background is seen from the results of a measurement of the cross section for $^{58}Ni(n,p)^{58}Co$ relative to ^{238}U fission using the $^{7}Li(n,p)^{7}Be$ reaction as a neutron source. For 7.5-MeV protons and a 50-keV lithium target, $\sim$ 7% of all fissions and 4% of all sample activations were produced by background neutrons-predominantly from (p,n) reactions with the tantalum beam stop. If no correction for this background were made, the measured ratio would be in error $\sim$ 3% [13].

F. Details of Specific Neutron Source Reactions

It is unfortunate that there are very few satisfactory neutron-source reactions which can be used for routine monoenergetic measurements at neutron energies up to $\sim$ 20 MeV. The requirements for a useful source reaction

are [11]:

i) Relatively-intense neutron yield with a dominant fraction-preferably all-of the neutrons belonging to the discrete group with the highest energy.

ii) It must be possible to fabricate targets which will survive extended charged-particle bombardment without severe reduction in yield.

iii) The targets should be relatively convenient to use and not excessively expensive or hazardous to laboratory personnel.

iv) The source reaction should be useful over a significant range of neutron energies.

The $^{7}Li(p,n)^{7}Be$, $D(d,n)^{3}He$, $T(p,n)^{3}He$ and $T(d,n)^{4}He$ reactions generally satisfy these requirements to varying degrees and they are the most widely used source reactions. Other less common reactions have been used from time-to-time for special applications.

F.1 The $^{7}Li(p,n)^{7}Be$ Reaction

This reaction has been a popular neutron source at accelerator laboratories for many years. Target preparation is simple, inexpensive and not hazardous. The targets are generally fabricated by vacuum evaporation of lithium metal on high-Z backings. With proper cooling, these targets can dissipate several hundred watts/cm^2 of beam power and provide relatively stable yield for more than 100 hours continuous operation. The neutron reactions produced by proton bombardment of natural lithium are listed in Table II. This neutron source is monoenergetic over a relatively narrow energy range (Fig. 1). However, the $^{7}Li(p,n)^{7}Be$ reaction remains dominant over a larger energy range and this source has been used for precision cross-section measurements at neutron energies up to $\sim$ 6 MeV at the Argonne National Laboratory Fast-Neutron Generator [13,14]. The characteristics of the 2nd neutron group are well known in this energy range [14-16]. There is some information available on the continuous group of neutrons from the $^{7}Li(p,n^{3}He)^{4}He$ breakup reaction which yields significant numbers of neutrons for $E_p > 6$ MeV [14]. As a result of this breakup reaction, the useful range of the lithium neutron source is $E_n < 7$ MeV.

F.2 The $T(p,n)^{3}He$ Reaction

This reaction has been adopted at many laboratories as a substitute for the $^{7}Li(p,n)^{7}Be$ reaction. It has been evaluated for proton energies below $\sim$ 10 MeV [17]. It is a monoenergetic source over a much wider energy range (Table II and Fig. 1) and, if a gas target is used, it is a more intense source of neutrons above $\sim$ 1 MeV than the $^{7}Li(p,n)^{7}Be$ reaction (Table III and Fig. 2). The main drawback to this reaction is that it is inherently hazardous to laboratory personnel. Extensive precautions are required to insure that tritium is not released in the laboratory environment. Metal tritium (predominantly Ti-T) targets are safer to use, but they offer lower yield and are subject to background problems at higher energies

(Table III).

Breakup neutrons are produced at proton energies above ∿ 8.5 MeV from the T(p,np)D reaction (Table II). There is little quantitative information on this reaction. The T(p,d)D reaction competes strongly with the $T(p,n)^3He$ reaction at proton energies above ∿ 10 MeV [18] and this is reflected in the steady decrease with energy of the $T(p,n)^3He$ reaction at higher energies (Fig. 2). More measurements are needed to determine the detailed characteristics of secondary neutron production from protons or tritium. However, because of the anticipated increase of this secondary production with energy and the apparent decline of the $T(p,n)^3He$ reaction cross section, this neutron source appears to be relatively unfavorable for the production of high-energy neutrons. A practical limit of ∿ 10-11 MeV is estimated, though this is speculation based on limited information (Fig. 1).

F.3 The $D(d,n)^3He$ Reaction

This reaction appears to satisfy most requirements for a desirable source of neutrons with energies above ∿ 4 MeV (Table II and Figs. 1 and 2). Metal deuterium targets are impractical-except for low-energy measurements-because of (d,n)-reaction background. Gas targets can be fabricated readily and are safe (though sometimes troublesome) to use [12]. The $D(d,n)^3He$ reaction has been evaluated for deuteron energies below ∿ 10 MeV [17]. Breakup neutrons from the D(d,np)D reaction are produced for deuteron energies above ∿ 5 MeV (Table II). There is a fair amount of quantitative information available about the breakup neutrons [12,19]. While the breakup cross section increases rapidly with energy above threshold, the $D(d,n)^3He$ reaction also increases with energy so that the relative yields change much less rapidly. For deuteron energies of ∿ 7 MeV, the breakup neutrons constitute ∿ 25% of all zero-degree neutrons [12]. At ∿ 10-MeV deuteron energy, the corresponding figure is ∿ 35-40%. There is a large energy gap between the $D(d,n)^3He$ and D(d,np)D neutrons.

It was previously mentioned that the neutron-energy range 8-14 MeV is a difficult region for measurements because of the lack of a suitable monoenergetic neutron source reaction (Fig. 1). A case can be made for using the $D(d,n)^3He$ reaction to cover this entire energy region, and this has been done by Santry and Butler using the Chalk River Tandem Van de Graaff accelerator [e.g. Ref. 20]. Unfortunately, 10-11 MeV deuteron beams are not available at most of the laboratories currently involved in activation cross section measurements. Also, if this reaction is to be used for accurate cross section measurements up to ∿ 14 MeV, it appears necessary to obtain more accurate and detailed information on the D(d,np)D reaction than is currently available.

F.4 The $T(d,n)^4He$ Reaction

This reaction is predominantly a source of high-energy neutrons (> 14 MeV) and is of less importance for fission-reactor applications (Table II and Figs. 1 and 2). It will not be treated in this paper.

F.5 Other Reactions

There are a number of neutron-source reactions, other than those mentioned above, which are used from time-to-time in fast-neutron differential measurements. Invariably, these suffer from one or more defects such as low relative yield of the high-energy group, overall low-intensity neutron production, target fabrication difficulties, limited useful range, high cost, etc. For example, the $^{14}C(d,n)^{15}N$, $^{15}N(d,n)^{16}O$ and the $^{9}Be(d,n)^{12}C$ reactions have been used with considerable success by researchers at Geel in some selected activation cross section measurements over the neutron-energy range 6-12 MeV using a small Van de Graaff accelerator [11, 21]. The common feature of these measurements was that they were made for reactions with high thresholds so that only the highest-energy neutron group produced the observed reactions.

V. Treatment of the Effects of Non-Ideal Neutron Sources in Determination of Differential Cross Sections

Eqs. (1) and (2) assume that an ideal monoenergetic neutron source is utilized for a cross section measurement. The properties of realistic sources were reviewed in Section IV. Detailed knowledge of the characteristic of the source is of little value unless it is integrated into the data processing procedures.

Symbolically, this is accomplished by substituting the equation

$$R = F_1 \, N \, G_{n1} \eta_{n1} \sigma_1 \left(1 + \sum_{i=2}^{m} \frac{F_i \, G_{ni} \eta_{ni} \, \sigma_i}{F_1 \, G_{n1} \eta_{n1} \, \sigma_1} \right) \qquad (4)$$

for the reaction rate R in the place of Eq. (1). The sum is over the groups of secondary neutrons from the target. In fact, individual groups corresponding to a particular reaction can be further subdivided if they are broad in energy owing to resolution or breakup effects.

The fluence ratios (F_i/F_1) can be computed if the detailed properties of the source reaction are known. Computation of the factors G_n and η_n is often tedious but usually straightforward. If the factors (F_i/F_1) are not too large, then the determination of the ratios (σ_i/σ_1) is not critical. The ratios (σ_i/σ_1) can generally be estimated with sufficient accuracy from systematics or previously available data. If need be, an iterative process can be used to improve the accuracy. This method is exhibited in detail in available reports [12,13].

Practical integration of these detailed corrections into routine data processing requires utilization of digital computers. Fortunately, adequate computational capability exists at most of the laboratories where such measurements are being made.

VI. Determination of Neutron Fluence

Determination of neutron fluence F and the gamma-ray detection efficiency ε are the dominant elements of a cross section measurement. The former is usually the most difficult task and is one of the most controversial areas of fast-neutron physics.

There are two general methods for deducing neutron fluence. One involves a direct count of the incident neutrons passing through the sample. The second involves measurement of the ratio of the unknown cross section to some standard cross section. In the latter case, the absolute fluence need not be known, but the accuracy to which the unknown cross section can be determined is limited by the accuracy of the standard cross section as well as by the precision of the ratio measurement. Two rather precise ratio measurements can lead to discrepant cross sections if the standard cross sections are inconsistent. This is an important point which should always be taken into consideration by evaluators.

A. Measurements Involving Absolute Fluence Determination

Some neutron cross section measurements at neutron energies up to a few MeV have been made using "black" neutron detectors with very high efficiencies (nearly 100%) for detection of incident neutrons (e.g. Ref. 22). This method requires extensive shielding in order to form well-collimated neutron beams and pulsed-beam time-of-flight techniques to reduce background. Furthermore, there is a limitation on fluence levels which can be measured due to electronic considerations. Generally, these conditions can be met in practice. Although this method has been utilized extensively for measurement of fast-neutron capture cross sections (e.g. Ref. 23), it has not been used often in threshold-dosimetry-reaction measurements. Although limited in energy range, this method appears capable of yielding good accuracy (< 3%) in the measurement of neutron fluence up to a few MeV.

Calibrated flat-response detectors-predominantly long counters-have been used extensively in activation measurements for neutron energies up to several MeV (e.g. Ref. 20). The efficiency of these detectors is flat to within $\sim$ 10% from $\sim$ 0.1 - 5 MeV [24]. They are generally calibrated using a standardized radioactive neutron source. It is essential that care be taken to determine the response of a long counter to scattered neutrons for each new experimental configuration. While these detectors possess the advantage of high stability of response when laboratory conditions are constant, the possibilities for systematic error are many owing to the sensitivity of the response to changes in these laboratory conditions. Here it is to be understood that laboratory conditions comprise not only the physical layout of the target area but also the characteristics of the neutron-source reaction used for the measurements. If great care is taken in measurements using a long counter, it appears that the neutron fluence can be determined to within 3-5% [25].

Associated-particle detection is a method of absolute neutron fluence determination which has been used in fast-neutron studies [e.g. Refs. 26 and 27]. In this method, recoil ^{4}He particles from the T(d,n)^{4}He reaction or

^{3}He particles from the $T(p,n)^{3}He$ or $D(d,n)^{3}He$ reaction are detected. There is a one-to-one relationship between the charged-particle emission and neutron emission. This method suffers from two serious defects. First, due to kinematic considerations there are limited ranges of neutron energies for which the method can be applied. Secondly, there are numerous technical problems-associated mainly with electronic and geometric considerations-which can lead to serious errors in fluence determination. While the method can probably be used to measure neutron fluence to $\sim$ 3% accuracy [26], great care has to be taken to avoid systematic errors.

A fundamental problem associated with measurement of absolute neutron fluence by all the methods described above is that generally what is being determined is the absolute fluence within a particular solid angle which is strongly correlated with the monitor detector, but not necessarily with the sample being irradiated. In short, there is room for additional systematic error in determination of the true fluence at the sample. Furthermore, absolute fluence measurements have to be made each time a cross section is measured. This requires extensive duplication of effort which can be partially avoided if the ratio method is used.

B. Ratio Measurements

In ratio measurements the absolute neutron fluence is not measured each time which results in an economy of effort. However, one has to either make an absolute fluence determination at some point in the program, or transfer the responsibility to others by relying solely on the use of "standards". The ratio method is the most widely used approach in fast-neutron measurements and should be fully discussed. All of the problems related to this method can be grouped into two categories which are described by the following questions:

i) "How accurately are the "standard" cross sections known?"

ii) "What are the experimental limitations which govern the extent to which accuracy in the knowledge of a standard cross section can be fully utilized in measurements of the cross section ratio for an unknown relative to that standard?"

It is apparent that a crucial issue is the selection of a practical standard for use in differential dosimetry reaction measurements by the ratio method. It is suggested that the choice of this standard is not a foregone conclusion at this time, but one which should be carefully examined.

B.1 Use of Several Dosimetry Threshold Reactions as Standards

Unfortunately, there has been rather indiscriminate use of several threshold reactions-the more common of which are the $^{27}Al(n,p)^{27}Mg$, $^{27}Al(n,\alpha)^{24}Na$, $^{32}S(n,p)^{32}P$, $^{56}Fe(n,p)^{56}Mn$ and $^{58}Ni(n,p)^{58}Co$ reactions-as "standards" for measurement of less-well-known cross sections. This is unacceptable practice in development of a consistent data base for dosimetry. Not one of these reactions is well enough known at present to be used as a standard in a program with a goal of 5% or better over all accuracy.

Furthermore, the excitation functions for some of these reactions exhibit fine structure which guarantees that they will remain unsuitable for use as standards.

Much of the data resulting from measurements of this sort should be rejected in critical evaluations of dosimetry reactions. Otherwise, there will remain many hidden, convoluted normalization factors in the evaluated cross sections and progress toward development of a consistent set of dosimetry reaction cross section values will be severely hampered.

B.2 Use of The Hydrogen Standard

It has generally been contended with axiomatic certainty that the H(n,n)p reaction is the ultimate standard for differential measurements on dosimetry reactions. There is a good basis in fact for this contention. This reaction possesses almost all the desired features for a standard. The cross section is large and varies smoothly with energy. Cross-section values can actually be computed theoretically with an accuracy which may exceed experimental capabilities. The reaction can be used over a wide range of neutron energies. Furthermore, the cross section appears to be very well known ($\sim$ 1-2%) for neutron energies of interest for fast-neutron dosimetry. For a number of years, there were no changes in the accepted cross section values for this reaction. A few years ago, there were some minor revisions which altered the accepted values by $\sim$ 1-2% at certain energies [28,29].

However, the problem with the hydrogen standard is not that the cross section itself is uncertain, but rather that it is very difficult experimentally to achieve accuracies approaching the cross section accuracy in routine measurements which in one way or another are based on this standard. There is considerable potential for systematic error in measurements with hydrogeneous proportional counters, hydrogeneous scintillators or proton recoil counters. Errors can result from uncertainties in determining the hydrogen content of detectors and stabilizing this content. Spectra from hydrogeneous detectors are often difficult to analyze and there is always unwanted background which must be subtracted. Because of the large energy loss generally experienced by neutrons which scatter from hydrogen, recoil proton spectra are broad and overlap the background spectra. Proportional counters and scintillators are also gamma-ray sensitive which increases the background. Each type of hydrogeneous detector has its own characteristic features. These are worthwhile reviewing briefly.

Gas proportional counters have low efficiency, require extensive geometric corrections and suffer from wall effects at higher energies [30]. The proton recoil spectra extend to zero pulse height and suffer from noise and background interference. Efficiency calibration is critically dependent upon gas pressure. Gamma-ray interference is a problem. If care is taken, fluence can be measured with an accuracy of $\sim$ 3% at energies up to $\sim$ 1 MeV [26,30].

Organic scintillators offer the advantages of well-defined geometry and hydrogen content, large efficiency and a wider energy range for applications when compared with a gas proportional counter. However, the proton-recoil pulse-height spectra also extend to zero, there is a strong gamma-ray

sensitivity, and the pulse-height response is nonlinear [31,32]. The accuracies claimed for the calibration of these detectors are rarely better than $\sim$ 5%.

Proton recoil detectors, which detect protons emitted in the forward direction by means of surface barrier detectors, have low efficiency, but offer the desirable features of gamma-ray insensitivity and improved capability for discrimination of proton events from the background [33]. Accurate calibration of these detectors entails careful determinations of the geometry and of hydrogen content in the thin radiators. The latter is by no means trivial. The thin radiators in these detectors are known to be vulnerable to changes in hydrogen content with time. Furthermore, it is very difficult to monitor these radiators for such effects. However, these detectors can probably be routinely calibrated to an accuracy of $\sim$ 5% or better [33].

So, the attractiveness of the hydrogen standard is somewhat diminished by the difficulties involved in trying to use it in cross section measurements for dosimetry reactions. This does not imply that it should be abandoned. On the contrary, the technology for utilizing the hydrogen standard will probably develop in due time to the point where most of the current problems associated with its use are satisfactorily overcome.

B.3 Use of Fission Standards

There has been extensive experimental and evaluative effort devoted to improving the accuracy of fast-neutron fission cross sections which are considered important for fission-reactor applications [34]. As a result of this effort, the cross sections for some of these reactions, especially $^{235}U(n,f)$, are known with sufficient accuracy to merit consideration as standards. Recent estimates of the uncertainty in ^{235}U, ^{238}U and ^{237}Np fast-neutron fission are reproduced in Table IV. Most of the data on ^{238}U and ^{237}Np has been obtained from ratio measurements relative to ^{235}U fission. Therefore the accuracy of these cross sections is tied to ^{235}U. The uncertainties in the ^{238}U and ^{237}Np fission cross sections near threshold appear to be largely due to discrepancies in energy scales for various measurements. When these are resolved, the accuracy will undoubtedly improve. Progress in improving the accuracy of the ^{237}Np fission cross section has been limited since this reaction does not play a major role in current fission reactor technology. However, this reaction has merits for use as a standard and effort should be made to improve the accuracy of its cross section.

^{235}U fission is sensitive to low-energy neutrons. At higher bombarding energies, where lower-energy neutron groups and background neutrons are present, threshold reactions such as ^{238}U and ^{237}Np fission are more practical standards than ^{235}U. As indicated in Table IV, ^{235}U and ^{238}U fission can be used as standards in differential dosimetry measurements below 15 MeV with the expectation that the uncertainty in the results attributable to the standard cross section will not exceed 5-6%. Furthermore, the accuracy of the ^{235}U and ^{238}U cross section is likely to continue to improve as the result of sustained research effort in support of fission-reactor technology.

Although the cross sections for standard fission reactions are presently not known as accurately as the hydrogen standard, it is much easier to perform accurate measurements relative to the fission standards than it is to use the hydrogen standard. At present, it seems that measurements relative to the fission standards are likely to produce differential cross section values which are as accurate as the corresponding measurements relative to the hydrogen standard. Improvement of the accuracy of measurements relative to the hydrogen standard will require perfection of measurement techniques, whereas in the case of the fission standards it is an improvement in cross section accuracies which is required. At present, it does not seem likely that accuracies of much better than $\sim$ 5% in fluence determination can be achieved routinely regardless of which method is selected.

It is worthwhile to review briefly some of the desirable features of measurements relative to fission standards. There are two ways in which fission can be utilized as a standard. One involves measurement of induced gamma-ray activity from irradiated samples of fissionable material. This is the less desirable method since the uncertainties in the mass ratios and decay characteristics must be added to the cross section uncertainty. Direct detection of fission-fragments with an ionization chamber is preferable. Low-mass chambers (Fig. 3) can be constructed to minimize scattering [e.g. Ref. 13]. The unknown sample and fissionable deposit can be placed back-to-back to minimize systematic errors in fluence determination. The background pulses from noise and alpha activity are easily distinguished from the larger fission fragment pulses. The calibration of fission detectors is almost entirely governed by the mass and isotopic abundances of the fissionable material used. A well-developed technology exists for determining these parameters for fissionable deposits to $\sim$ 1% accuracy [8.35]. Furthermore, the calibrated fissionable deposits can be accurately and conveniently monitored thereafter using alpha counting techniques. In principle, it would be possible to calibrate a set of standard fissionable deposits for use in some integral measurements [7] as well as differential measurements. This procedure would be very desirable in development of an accurate cross-section data base for dosimetry applications.

B.4 Other Standards

Other reactions which are widely used as standards in other types of fast-neutron measurements are $^{197}Au(n,\gamma)^{198}Au$, $^{6}Li(n,\alpha)^{3}H$, $^{3}He(n,p)^{3}H$ and $^{10}B(n,\alpha)^{7}Li$. These standards are not particularly useful for differential dosimetry reaction measurements, so they will not be treated in this paper.

VII. Calibration of Gamma-Ray Detectors

This paper is concerned with the measurement of differential cross sections for threshold dosimetry reactions which produce gamma-ray active daughters. Careful calibration of the gamma-ray detectors used in these measurements is essential if high accuracy is to be achieved. The techniques used in calibration of gamma-ray detectors are widely known and present no special problems. They will be mentioned briefly in this paper.

There are few differences, in this regard, between integral and differ-

ential measurements. Activity measurements in differential studies are likely to be less accurate than their integral counter parts (excluding ^{252}Cf measurements). The reasons are:

i) The activity in samples irradiated at accelerator facilities is distributed less uniformly than for reactor irradiations because of the differences in the neutron environments.

ii) The activity in samples irradiated at accelerator facilities is often considerably lower than is obtained in integral measurements. Statistics can limit accuracy.

iii) Generally, larger samples are used in differential measurements than in integral measurements, so absorption corrections are larger.

iv) The lower activities of samples irradiated at accelerator facilities, by comparison with integral measurements, necessitates the placement of samples close to the detector and introduces uncertainties due to geometric and coincidence summing effects.

It seems likely that Ge(Li) detectors will eventually replace all other types of detectors for gamma-counting applications. Furthermore, mixed calibration standards are now available from centers such as the National Bureau of Standards (U.S.A.), the IAEA (Vienna, Austria) and the National Physical Laboratory (U.K.) which facilitate the task of calibrating these detectors. Assuming an accuracy of $\sim$ 1-2% in the standard reference materials used for calibration of gamma-ray detectors, it appears that a practical limit of attainable accuracy in calibration is $\sim$ 2-3% for differential measurements.

VIII. The Role of Radioactivity Data in Differential Cross Section Measurements

Here, there are no differences between the requirements for integral and differential measurements. The status of the decay data for several radioactive species has been evaluated by Helmer and Greenwood [1]. Similar compilation and evaluation effort is also in progress elsewhere, e.g. the Nuclear Data Group at Oak Ridge National Laboratory and the Table of the Isotopes Project at Lawrence Radiation Laboratory (Berkeley) in the U.S.A.

The effects of uncertainty in radioactive-decay data vary from one reaction to another and must be analyzed in each separate case. This is beyond the scope of the present paper. However, it does not appear that this aspect will be a limiting factor in development of a dosimetry cross section data set which is accurate to $\sim$ 5%.

IX. Corrections for Geometric Effects and the Absorption and Scattering of Radiation

It is difficult to make any quantitative statements concerning the uncertainties in differential data which result from the application of corrections for geometric effects and the absorption and scattering of radiation.

So much depends on the particular experimental details. What is clear is that these corrections need to be made carefully in order to avoid significant systematic errors which are very difficult to trace. This involves the application of adequate techniques (e.g. Monte Carlo analysis) and utilization of consistent supplementary nuclear data (e.g. neutron total and scattering cross sections). There is a great need for improved standards in reporting of quantitative data so that evaluators can honestly compare various data sets during the process of selecting the best possible values for reaction cross sections. There should be available a detailed description of the data analysis procedures and documentation of the origins of all supplementary nuclear data used in the analysis. Magnitudes of various estimated sources of error in the measurements and the method used to calculate the overall error should be reported. It would be useful if researchers could agree upon sets of supplementary nuclear data, which are readily available from data centers or widely circulated compilations, to use in analysis of their results.

If the corrections are properly treated, the uncertainties due to geometrical considerations can be negligible. It is possible to limit neutron absorption and scattering effects to $\sim$ 10%. These can be calculated with an accuracy of $\sim$ 10% which leads to an uncertainty of $\sim$1% in the cross section. Similarly, uncertainties in gamma-ray absorption can be minimized so that the net uncertainty in the cross section from this effect can be limited to $< 1\%$.

X. Conclusions

At this point it is possible to draw some conclusions concerning the best accuracy which can be expected in the measurement of differential cross sections for threshold dosimetry reactions within the framework of present technology. Optimistically, it appears that the uncertainty cannot be expected to fall much below the 4-7% range (Table V) for measurements within the limits which can be computed using Eq. (3). The major source of uncertainty comes from neutron fluence determination. At present, certain standard fission cross sections appear to be more convenient to use in practice than the hydrogen standard for routine measurements. The cross sections obtained from measurements using fission standards appear to be as reliable as those measured using the hydrogen standard.

The prognosis is that some improvements in experimental techniques and in the knowledge of standard cross sections will be required to meet the 5% accuracy goal; however, the requirements are not excessively stringent measured against present capabilities and the 5% accuracy goal is not unrealistic in this context.

ACKNOWLEDGEMENTS

The author is indebted to W. P. Poenitz and J. W. Meadows for offering both information and insight which were valuable in the preparation of this paper.

REFERENCES

1. R. G. Helmer and R. C. Greenwood, Nuclear Technology 25, 258 (1975).
2. A. Fabry, H. Ceulemans, P. Vandeplas, W. N. McElroy and E. P. Lippincott, "Reactor Dosimetry Integral Reaction Rate Data in LMFBR Benchmark and Standard Neutron Fields: Status, Accuracy and Implications", Proc. First ASTM-EURATOM Symposium on Reactor Dosimetry, Petten, September 22-26 (1975).
3. W. N. McElroy and L. S. Kellogg, Nuclear Technology 25, 180 (1975).
4. M. F. Vlasov, A. Fabry and W. N. McElroy, Proc. of the International Conference on the Interaction of Neutrons with Nuclei, Lowell, July 6-9 (1976).
5. A. Schett, K. Okamoto, L. Lesca, F. H. Fröhner, H. Liskien and A. Paulsen, "Compilation of Threshold Reaction Cross-Sections for Neutron Dosimetry and Other Applications", Report EANDC 95 "U", Neutron Data Compilation Centre, Saclay, France (1974).
6. "ENDF/B-IV Dosimetry File, ed. B. A. Magurno, Report BNL-NCS-50446, Brookhaven National Laboratory (1975).
7. J. A. Grundl, D. M. Gilliam, N. D. Dudey and R. J. Popek, Nuclear Technology 25, 237 (1975).
8. J. W. Meadows, Nucl. Sci. Eng. 49, 310 (1972).
9. Donald L. Smith and James W. Meadows, Nucl. Sci. Eng. 58, 314 (1975).
10. Donald L. Smith, "Fast-Neutron Gamma-Ray Production from Elemental Iron", Report ANL/NDM-20, Argonne National Laboratory (1976).
11. M. Coppola and H. H. Knitter, "$^{14}C(d,n)^{15}N$ and $^{15}N(d,n)^{16}O$ Reactions", Report EUR 3492.e, Central Bureau for Nuclear Measurements, Geel, Belgium (1967).
12. D. L. Smith and J. W. Meadows, "Method of Neutron Activation Cross Section Measurement for E_n 5.5 - 10 MeV Using the $D(d,n)^3He$ Reaction as a Neutron Source", Report ANL/NDM-9, Argonne National Laboratory (1974).
13. Donald L. Smith and James W. Meadows, "Measurement of $^{58}Ni(n,p)^{58}Co$ Reaction Cross Sections for E_n = 0.44 - 5.87 MeV", Report ANL-7989, Argonne National Laboratory (1973).
14. J. W. Meadows and D. L. Smith, "Neutrons from Proton Bombardment of Natural Lithium", Report ANL-7938, Argonne National Laboratory (1972).
15. S. A. Elbakr, I, J. van Heerden, W. J. McDonald and G. C. Neilson, "Measurements of Neutron Angular Distributions from the $^7Li(p,n)^7Be$ Reaction", Report UAE-NPL-1041, Nuclear Research Centre, University of Alberta, Edmonton, Alberta, Canada (1972).
16. H. Liskien and A. Paulsen, "An Evaluation for Cross Sections of the Reactions $^7Li(p,n)^7Be$ and $^7Be^*$", Report EANDC(E)-159 "L", Central Bureau for Nuclear Measurements, Geel, Belgium (1973).
17. Horst Liskien and Arno Paulsen, Nuclear Data Tables 11, 569 (1973).
18. L. Rosen and J. E. Brolley, Jr., Phys. Rev. Letters 2, 98 (1959).
19. H. W. Lefevre, R. R. Borchers and C. H. Poppe, Phys. Rev. 128, 1328 (1962).
20. D. C. Santry and J. P. Butler, Can. J. Phys. 54, 757 (1976).
21. H. Liskien and A. Paulsen, Nukleonik 8, 315 (1966) and A. Paulsen (Priv. Communication).

22. W. P. Poenitz, "The Black Neutron Detector", Report ANL-7915, Argonne National Laboratory (1974).
23. W. P. Poenitz, "Fast-Neutron Capture and Activation Cross Sections of Niobium Isotopes", Report ANL/NDM-8, Argonne National Laboratory (1974).
24. W. D. Allen, "Flat Response Counters", in Fast Neutron Physics I, ed. J. B. Marion and J. L. Fowler, Interscience, New York (1960), p. 361.
25. D. C. Santry and J. P. Butler, Can. J. Phys. 50, 2536 (1972).
26. H. Liskien and A. Paulsen, Nucl. Instr. Meth. 69, 70 (1969).
27. A. H. Werkheiser, J. R. Genser, R. G. Polk and T. G. Miller, "Neutron Detection Efficiency of an Organic Scintillator", Report RR-TR-71-16, U.S. Army Missile Command, Redstone Arsenal, Alabama (1971).
28. J. C. Hopkins and G. Breit, Nucl. Data Tables A9, 137 (1971).
29. L. Stewart, R. J. LaBauve and P. G. Young, Report LA-4574, Los Alamos Scientific Laboratory (1971).
30. E. F. Bennett, Nucl. Sci. Eng. 27, 16 (1967).
31. D. L. Smith, R. G. Polk and T. G. Miller, Nucl. Instr. Meth. 64, 157 (1968).
32. V. V. Verbinski, W. R. Burrus, T. A. Love, W. Zobel and N. W. Hill, Nucl. Instr. Meth. 65, 8 (1968).
33. F. Kaeppeler and F. H. Froehner, IAEA Proc. Conf. on Nucl. Data for Reactors I, 221, Helsinki (1970).
34. Proc. of NEANDC/NEACRP Specialists Meeting on Fast-Fission Cross Sections of U-233, U-235, U-238 and Pu-239, Argonne National Laboratory (1976).
35. Donald L. Smith and James W. Meadows, "Response of Several Threshold Reactions in Reference Fission Neutron Fields", Report ANL/NDM-13 (1975).

Table I

Approximate Sensitivity Limits in the Measurement of Differential Cross Sections for Several Dosimetry Reactions

Reaction	$t_{1/2}$	t_E	b	f_C	σ_{min} [a]	Current Status
$^{27}Al(n,p)^{27}Mg$	9.5 m	1-2 m	1	∿2	∿2μb	∿ 0.1 mb [b]
$^{56}Fe(n,p)^{56}Mn$	2.58 h	∿20 m	1	1	∿1μb	∿ 5μb [c]
$^{27}Al(n,\alpha)^{24}Na$	15 h	∿2 h	1	1	∿1μb	∿ 0.1 mb [b]
$^{48}Ti(n,p)^{48}Sc$	44 h	∿7 h	∿1.5	1	∿1μb	∿ 30 μb [c]
$^{58}Ni(n,p)^{58}Co$	71 d	∿1 d	∿1.5	1	∿10μb	∿ 3 μb [c]
$^{54}Fe(n,p)^{54}Mn$	312 d	∿1 d	∿20	1	∿0.5 mb	∿ 10 mb [b]
$^{63}Cu(n,\alpha)^{60}Co$	5.24 y	∿1 d	∿1.5	1	∿0.3 mb	∿ 1 mb [b]

[a] Computed using Eq.(3) from the text.

[b] Ref. 5.

[c] Ref. 9 (special techniques were used to measure the lowest-energy points for the ^{58}Ni reaction).

Table II

Neutron Sources : Energetics

1. Li + p

Reaction	Q-Value (MeV)	Threshold (MeV)
$^{7}Li + p \rightarrow n + {}^{7}Be$ (gnd. state)	-1.644	1.881
$^{7}Li + p \rightarrow n + {}^{7}Be^{*}$ (1st state)	-2.079	2.380
$^{7}Li + p \rightarrow n + {}^{7}Be^{**}$	-6.18	7.06
$^{7}Li + p \rightarrow n + {}^{3}He + {}^{4}He$	-3.23	3.68
$^{6}Li + p \rightarrow n + {}^{6}Be$	-5.07	5.92
$^{6}Li + p \rightarrow n + p + {}^{5}Li$	-5.67	6.62

2. D + d

Reaction	Q-Value (MeV)	Threshold (MeV)
$D + d \rightarrow n + {}^{3}He$	+3.268	0
$D + d \rightarrow n + p + D$	-2.225	4.45
$d + d \rightarrow 2n + 2p$	-4.45	8.90

3. T + p

Reaction	Q-Value (MeV)	Threshold (MeV)
$T + p \rightarrow n + {}^{3}He$	-0.765	1.020
$T + p \rightarrow n + p + D$	-6.258	8.342
$T + p \rightarrow 2n + 2p$	-8.483	11.31

4. T + d

Reaction	Q-Value (MeV)	Threshold (MeV)
$T + d \rightarrow n + {}^{4}He$	+17.639	0
$T + d \rightarrow 2n + {}^{3}He$	-2.990	4.98
$T + d \rightarrow 2n + p + D$	-4.653	7.75
$T + d \rightarrow 3n + 2p$	-10.708	17.84

Table III

Comparison of Several 100-keV
Thick Neutron-Source Targets

Reaction	Charged-Particle Energy (MeV)	Maximum Neutron Energy (MeV)	Target	Zero-Degree[a] Reaction Cross Section (mb/sr)	Target Atoms per cm^2	Relative[b] Figure of Merit (no dim)
$^7Li(p,n)^7Be$	2.3	0.6	Li-metal	150	6.7×10^{19}	1
$T(p,n)^3He$	3	2.3	T_2 Gas	120	2.2×10^{20}	2.7
$T(p,n)^3He$	3	2.3	Ti-T [c]	120	2.2×10^{19}	0.3
$D(d,n)^3He$	10	~13	D_2 Gas [d]	100	3.1×10^{20}	3.1

[a] Cross section at energy of maximum yield derived from Fig. 2.

[b] Computed by multiplying the target atoms per cm^2 times the maximum zero-degree differential cross section.

[c] Tritiated-titanium metal.

[d] Deuterated-metal targets are only useful for relatively low-energy deuterons because of competition from (d,n) reactions in metal targets.

Table IV

Estimated Uncertainties in Current Knowledge of the Fast-Fission Cross Sections for ^{235}U, ^{238}U and ^{237}Np

Reaction	Energy Range	Percent Uncertainty
$^{235}U(n,f)$[a]	200-400 keV	5
	All other energies in range 25 keV-20 MeV	3
$^{238}U(n,f)$[b]	< 2 MeV	10
	2 - 6 MeV	4
	6 - 15 MeV	6
	> 15 MeV	10
$^{237}Np(n,f)$[c]	0.51 - 1 MeV	10
	1 - 5.4 MeV	3
	5.4 - 14.1 MeV	10
	14.1	4
	> 14.1	10

[a] Values derived from the report of a working group on absolute fission cross sections (Ref. 34). These uncertainties are considerably smaller than the assigned uncertainties in the ENDF/B-IV Dosimetry File (Ref.6).

[b] Values derived from the report of a working group on fission cross section ratios (Ref.34).

[c] Ref. 6.

Table V

Estimates for Major Sources of
Error in Measurements
of Differential Dosimetry Cross Sections

1.	Neutron fluence determination	3 - 5%
2.	Gamma-ray detector calibration	2 - 3%
3.	Statistics	1 - 3%
4.	Gamma-ray absorption	< 1%
5.	Neutron absorption and multiple scattering	1%
6.	Secondary neutrons	< 1%
7.	Isotopic properties and decay data	Variable
	Total error [a]	>4 - 7%

[a] Partial errors combined in quadrature to yield the total error.

FIGURE CAPTIONS

Fig. 1. Probable useful ranges of neutron-source reactions commonly used for monoenergetic cross section measurements in the range E_n = 0 - 20 MeV.

Fig. 2. Zero-degree laboratory differential cross sections for neutron source reactions used for monoenergetic cross section measurements in the range E_n = 0 - 20 MeV.

Fig. 3. Apparatus used for ratio measurements of activation cross sections relative to uranium fission (Ref. 13).

Fig. 1

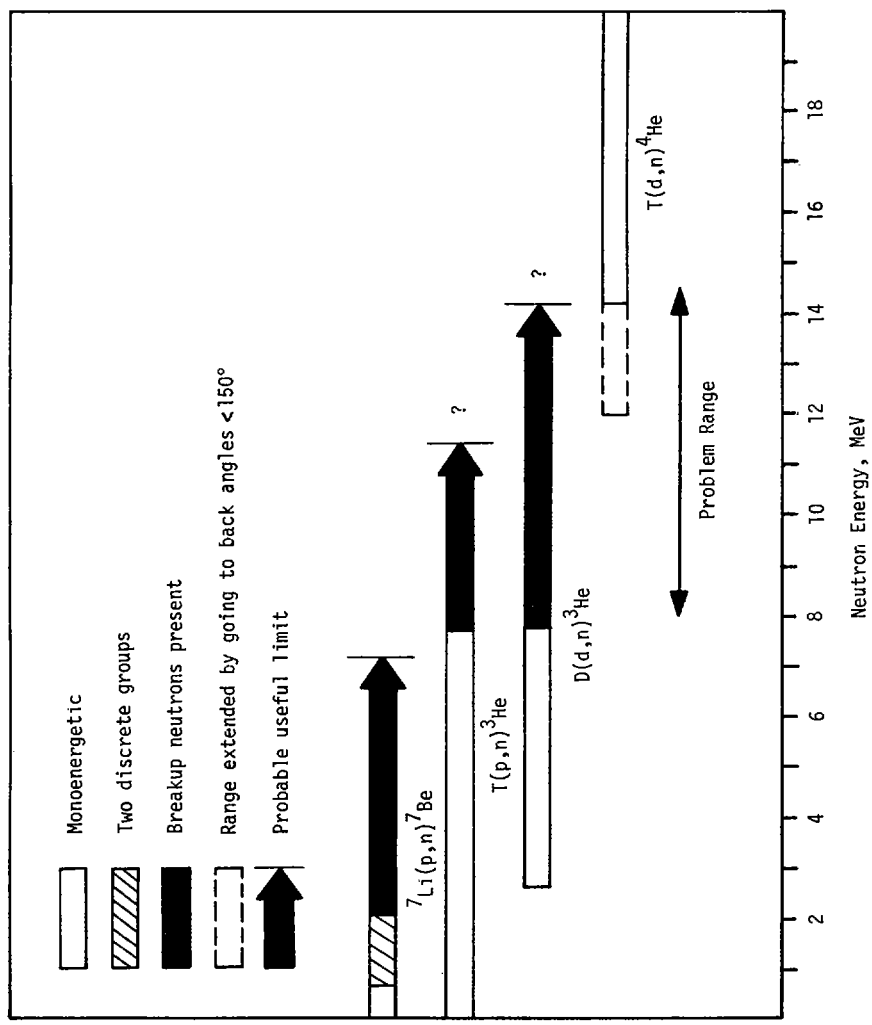
Monoenergetic
Two discrete groups
Breakup neutrons present
Range extended by going to back angles <150°
Probable useful limit
$^{7}Li(p,n)^{7}Be$
?
$T(p,n)^{3}He$
?
$D(d,n)^{3}He$
$T(d,n)^{4}He$
Problem Range
2
4
6
8
10
12
14
16
18
Neutron Energy, MeV

Fig. 2

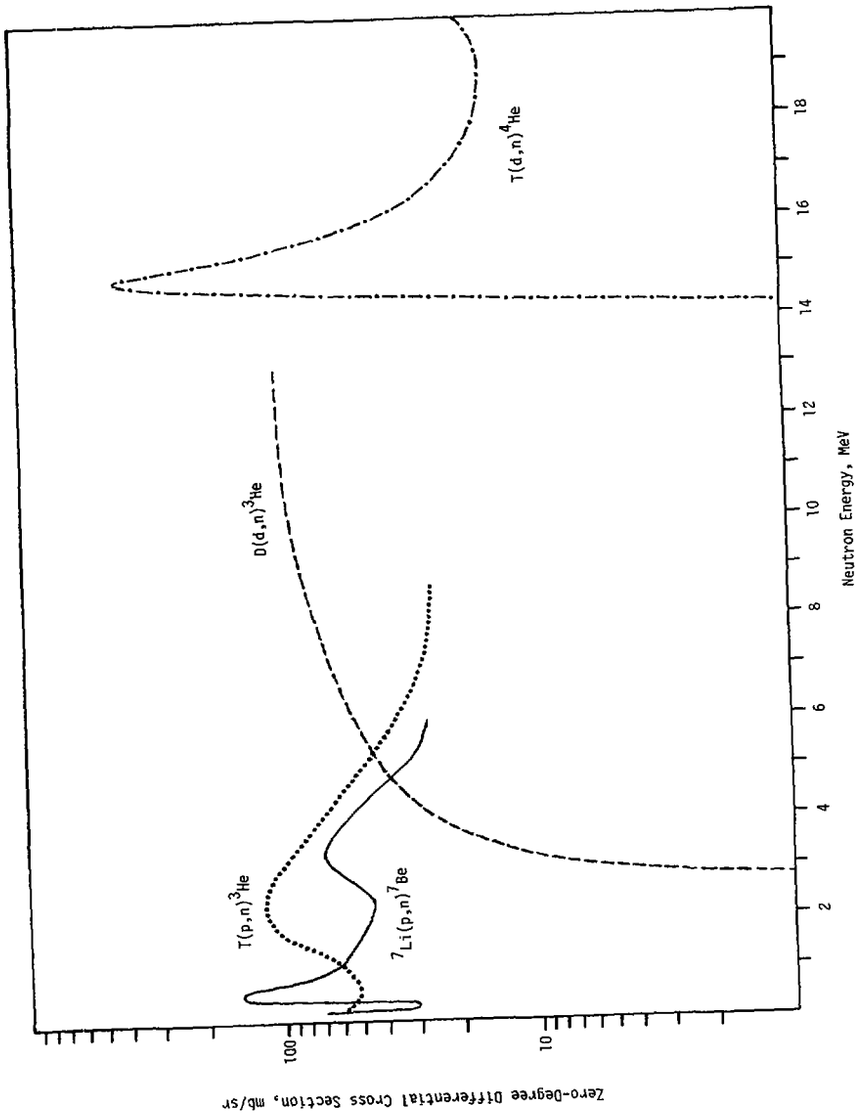
T(d,n)4He
D(d,n)3He
T(p,n)3He
7Li(p,n)7Be
Neutron Energy, MeV
Zero-Degree Differential Cross Section, mb/sr
100
10
2
4
6
8
10
12
14
16
18

Fig. 3

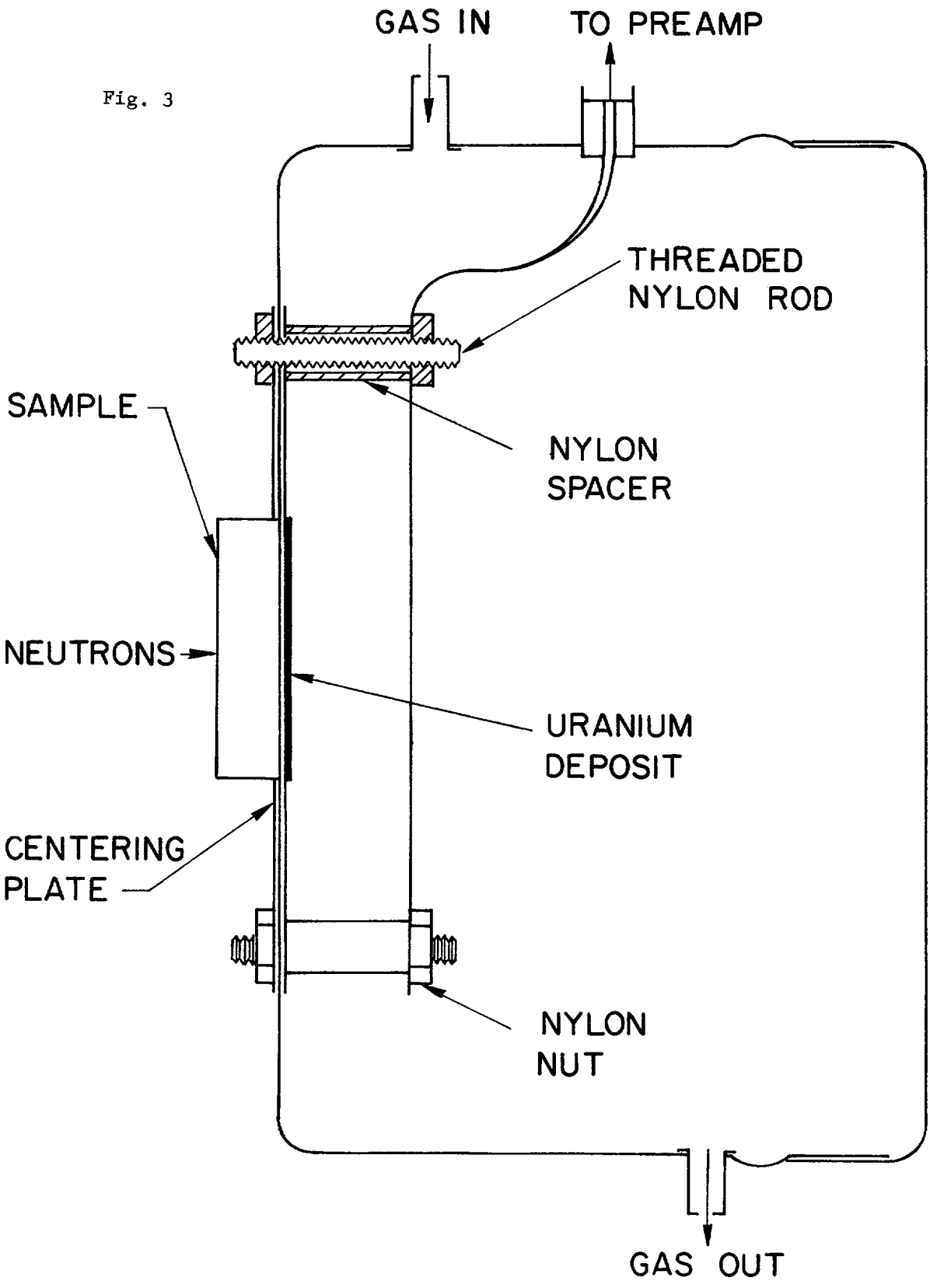
GAS IN
TO PREAMP
THREADED
NYLON ROD
SAMPLE
NYLON
SPACER
NEUTRONS
URANIUM
DEPOSIT
CENTERING
PLATE
NYLON
NUT
GAS OUT

IV.2. Comments on Excitation Functions of Threshold Reactions Used in Reactor Neutron Dosimetry.

M.F. Vlasov
Nuclear Data Section
IAEA, A-1011 Vienna.

Abstract:

A status of neutron cross sections for some reactions used in reactor dosimetry has been reported at the Lowell Conference [1]. Only some points related to this subject: i.e. the need for new measurements for some 'old' but important reactions, the 10-14 MeV energy gap problem, integral testing of high threshold reactions, long-term neutron fluence detectors, and new reactions for reactor dosimetry, will be discussed here.

No new measurements are available for some important 'old' reactions.

As example, two reactions may be considered: $^{31}P(n,p)^{31}Si$ and $^{32}S(n,p)^{32}P$. WRENDA 76/77* contains requests for measurements of both reactions with an accuracy of 5 % from 2.2 to 7 MeV and from 2.5 to 7.5 MeV respectively, and 10% above.

Both reactions are used for neutron spectrum unfolding by the activation technique; $^{32}S(n,p)^{32}P$ is also a standard for neutron flux measurements. The status of $^{31}P(n,p)^{31}Si$ cross section is presented in Figures 1 and 2. The detailed resonance structure of the excitation function above threshold is determined by very old relative measurements of Luscher 50, Ricamo 51, and Cuzzocrea 60. The first two are normalized to the absolute measurement of Metzger 48! As can be seen from the three available evaluations, a need exists for better establishment of the energy scale, especially near threshold. Large discrepancies in the cross section value above 6 MeV and a classical gap between 10-14 MeV, where no data are available, require new measurements in the whole energy range from threshold to 20 MeV. This need is also confirmed by serious discrepancies between integral and differential results: up to 10% for the energy response range of the reaction in χ_{25}** [1].

A similar situation, but with better integral-differential data agreement exists for $^{32}S(n,p)^{32}P$. This reaction is a component of practically every activation set used for neutron spectra unfolding, and the accurate knowledge of the excitation function in the energy range mentioned above is important. On the other hand the $^{32}S(n,p)^{32}P$ cross section above 4.8 MeV, where it varies smoothly with the energy, is often used as a reference for the measurement of other reactions [2]. However, only very old measurements of this cross section from threshold to 11 MeV are available: Klema 47, Luscher 50, Huerlimann 55, and Allen 57 (excluding a few points between 2.17 and 2.88 MeV by Rago 68).

---

* WRENDA: WORLD REQUEST LIST for Nuclear Data; IAEA publication WRENDA 76/77 is available on request from the IAEA Nuclear Data Section as report INDC(SEC)-55/URSF, Vienna, August 1976.

** χ_{25}: ^{235}U thermal neutron induced fission neutron spectrum.

Between 11 and 13 MeV, in the maximum of the excitation function, there are only 3 widely scattered results by Santry 63 (Fig. 3, 4). We agree to the following conclusion of the evaluators of this reaction for ENDF/B-IV Dosimetry File [3]: "The cross section is not satisfactorily well known to use it as a standard and additional measurements from threshold up to 20 MeV are required".

10 - 14 MeV energy gap: no data near threshold for reactions with high threshold.

The importance of high threshold reactions is much increased due to the radiation damage problem investigations for fast reactors and future fusion reactors. However, difficulties with neutron sources, which can provide monoenergetic neutrons in 10 - 14 MeV energy range make the progress in the measurement of the excitation functions of such reactions very slow. Two reactions are given as examples: $^{55}Mn(n,2n)^{54}Mn$ and $^{90}Zr(n,2n)^{89}Zr$. The present status of $^{55}Mn(n,2n)^{54}Mn$ is given in Fig. 5. The excitation function within the wide energy range from 13 to 18 + 20 MeV has been measured by Paulsen 65, Menlove 67 and Bormann 69; however, there are no measurements between threshold and ~13 MeV, where the request in WRENDA demands 5 % accuracy. Extrapolations based on theoretical considerations cannot provide such accuracy.

A similar situation exists with $^{90}Zr(n,2n)^{89}Zr$, see Fig. 6. It would be of great help if the laboratories, equipped with Tandem-Van de Graaff neutron generators could perform measurements in the 10 - 14 MeV energy range for some important reactions to meet requests in WRENDA.

Integral testing of high-threshold reactions.

The integral testing of cross sections for dosimetry reactions proved to be very important for the improvement of the evaluated cross section data files usually based on differential data obtained with monoenergetic neutrons only (ENDF/B Dosimetry File). The most recent and impressive example is the $^{48}Ti(n,p)^{48}Sc$ reaction. However, the testing of high threshold reactions in fundamental fission neutron spectra of ^{235}U and ^{252}Cf is difficult due to insufficient knowledge of the high energy tail of the spectra and very low intensity of neutrons in this energy range. The fission neutron spectra (^{252}Cf spontaneous and ^{235}U thermal neutron induced) have recently been evaluated at the National Bureau of Standards, USA, but only up to 8 MeV [4]; above this energy the uncertainty is ± 30%. The ^{235}U fission spectrum "SAND-2 adjusted" [5] obtained, using well known neutron cross sections and the SAND-2 technique, is much harder at higher energies than the NBS recommendation [Figures 9, 10]. The application of these two proposed ^{235}U spectra to the same high threshold reaction yields results (cross section averaged over the spectrum) which quite often differ by a factor of 2 while the uncertainty in the neutron cross section itself is only 15 - 20 % (example: $^{58}Ni(n,2n)^{57}Ni$ [1]).

Therefore the application of accelerator-based neutron fields for integral testing of neutron data should be encouraged: ^{9}Be (d,n) reaction on thick targets with time-of-flight technique for neutron spectrum determination [6], and $^{3}T(d,n)$ reaction with a spectrum determined by composition and geometry of the blanket surrounding the target, similar to that described in [7].

Long-term neutron fluence detectors.

The importance of the reliable fast neutron fluence detector for long-term irradiations required by radiation damage studies is well known. Two reactions are of special interest: $^{63}Cu(n,\alpha)^{60}Co$ and $^{93}Nb(n,n')^{93}Nb^{m}$. For the first reaction [Fig. 7] the excitation function is known in the whole energy range up to 20 MeV, but systematic disagreement exists between integral and differential data. Therefore it is important to confirm available differential data by new measurements. A few laboratories have agreed to perform them. The first results came from Prof. Vonach's Laboratory, Radiumforschungsinstitut, Vienna, see Fig. 7.

$^{93}Nb(n,n')^{93}Nb^{m}$, [Fig. 8], is in the focus of radiation dosimetry of materials now, because of its uniqueness. However, no direct measurement of this cross section with monoenergetic neutrons is available. Figure 8 is taken from our previous Review Report [8]. A solid line step function is the result of cross section unfolding in different reactor spectra, performed by Hegedüs 71, and point data are reconstructed from inelastic scattering γ-ray spectra using a known decay scheme. This second way looks quite promising and new measurements would be welcome.

New reactions.

The $^{199}Hg(n,n')^{199}Hg^{m}$ reaction is often used in the USSR. It has a rather low energy threshold ($\sim$ 500 keV), and a convenient half-life of $^{199}Hg^{m}$ equal to 43 min. The decay cascade γ-rays (158 and 375 keV) may be detected much easier than in the case of $^{103}Rh(n,n')$ or $^{93}Nb(n,n')$. $\sigma_{eff} = 480_{mb} \pm 11\%$ and $E_{eff} = 1.9$ MeV have been determined using the method described in [9]. The mercury activation detector is used together with ^{139}Ce calibration source (T 1/2 = 132.5 days). This reaction permits to measure integral neutron flux density above $\sim$1.9 MeV. At present there are practically no measurements of the excitation function.

REFERENCES

[1] M.F. Vlasov, A. Fabry and W.N. McElroy; Proceed. of the International Conference on the Interactions of Neutrons with Nuclei, Lowell, USA, July 1976, 2, p. 1187.

[2] D.C. Santry, and J.P. Butler, Can. J. of Physics, 52, 1421 (1974); and Can. J. of Physics, 54, 757 (1976).

[3] N.D. Dudey and R. Kennerly, "ENDF/B-IV Dosimetry File", edited by B.A. Magurno, April 1975, p. 34.

[4] J.A. Grundl, and C.M. Eisenhauer, NBS Special publication 425, 1, p.250 (1975).

[5] A. Fabry, Private communication to the IAEA Nuclear Data Section, 1976.

[6] L.R. Greenwood, R.R. Heinrich, N.D. Dudey, ASTM-EURATOM Symp. on Reactor Dosimetry, Petten 1975, EUR-5667 e/f, part II, 152 (1977).

[7] L. Kuijpers, "Experimental Model Studies for a Fusion Reactor Blanket", Thesis, 1976, and
P. Cloth, D. Filges, R. Herzing, L. Kuijpers and R. Hecker, Nucl. Instr. and Methods, 144, 215 (1977).

[8] M.F.Vlasov, C.L.Dunford, J.J.Schmidt, and H.D.Lemmel, INDC(NDS)-47/L,Oct.1972.

[9] E.I. Grigor'ev, S.Yu. Nozdrachev, R.D. Vasil'ev, and V.P. Yaryna, Proceed. of the First All-Union Meeting on Neutron Metrology, 1, p. 194, Moscow 1972, (in Russian).

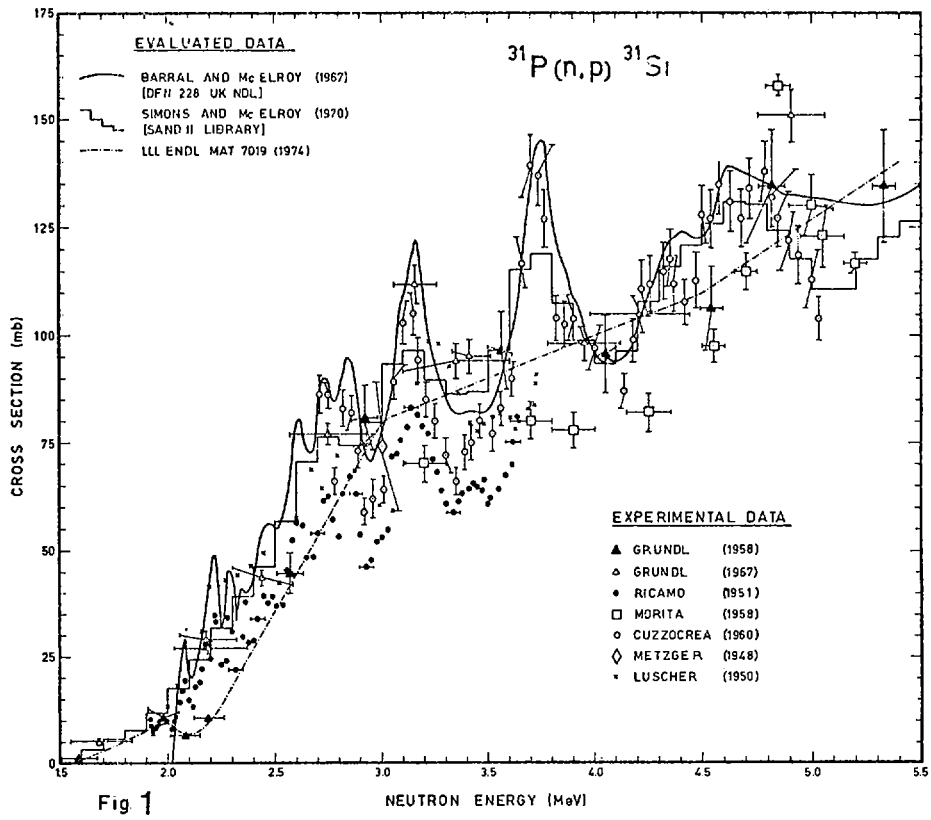
EVALUATED DATA
BARRAL AND Mc ELROY (1967) [DFN 228 UK NDL]
SIMONS AND Mc ELROY (1970) [SAND II LIBRARY]
LLL ENDL MAT 7019 (1974)
$^{31}P(n,p)^{31}Si$
EXPERIMENTAL DATA
GRUNDL (1958)
GRUNDL (1967)
RICAMO (1951)
MORITA (1958)
CUZZOCREA (1960)
METZGER (1948)
LUSCHER (1950)
CROSS SECTION (mb)
NEUTRON ENERGY (MeV)

Fig 1

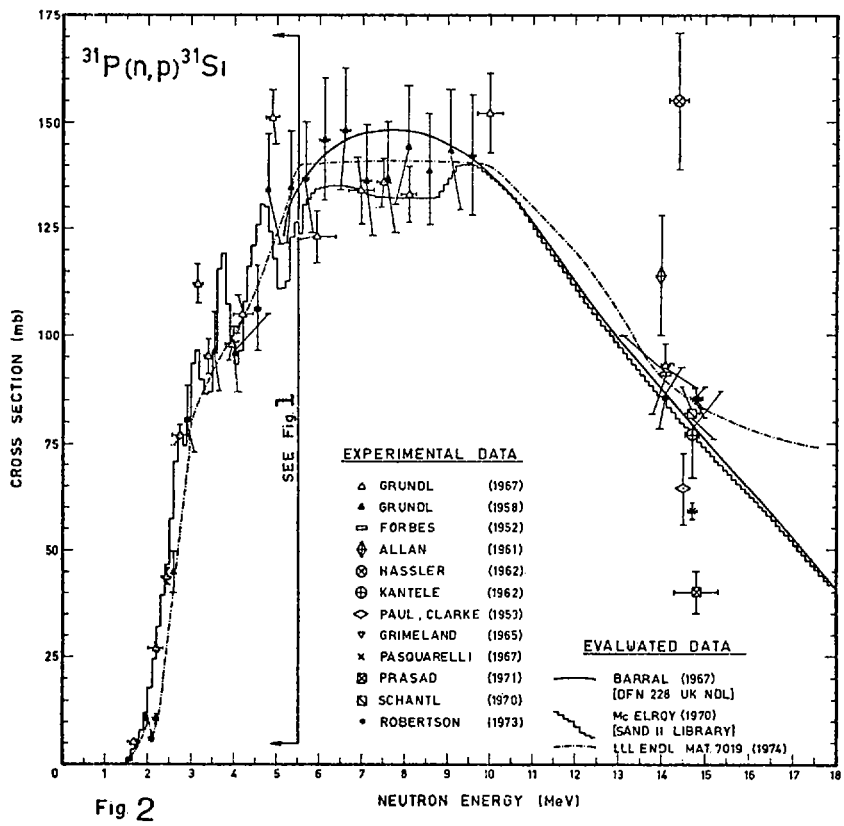
$^{31}P(n,p)^{31}Si$
SEE Fig. 1
EXPERIMENTAL DATA
GRUNDL (1967)
GRUNDL (1958)
FORBES (1952)
ALLAN (1951)
HASSLER (1962)
KANTELE (1962)
PAUL, CLARKE (1953)
GRIMELAND (1965)
PASQUARELLI (1967)
PRASAD (1971)
SCHANTL (1970)
ROBERTSON (1973)
EVALUATED DATA
BARRAL (1967) [DFN 228 UK NDL]
Mc ELROY (1970) [SAND II LIBRARY]
LLL ENDL MAT 7019 (1974)
CROSS SECTION (mb)
NEUTRON ENERGY (MeV)

Fig 2

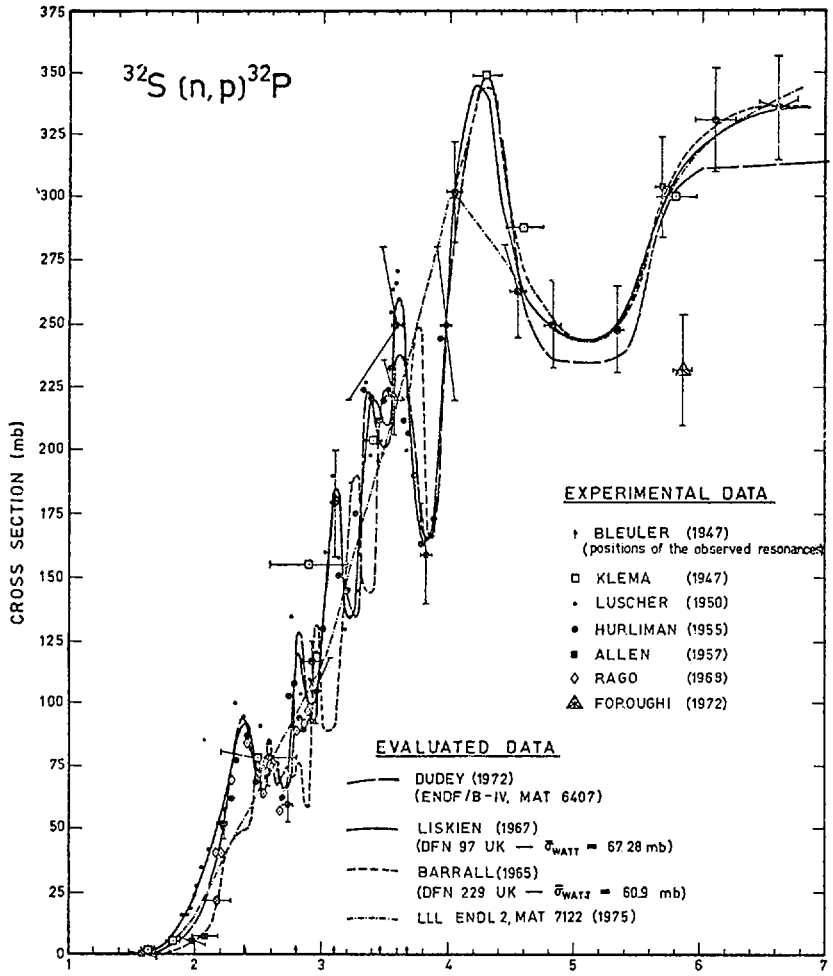
^{32}S (n, p) ^{32}P
CROSS SECTION (mb)
NEUTRON ENERGY (MeV)
EXPERIMENTAL DATA
BLEULER (1947)
(positions of the observed resonances)
KLEMA (1947)
LUSCHER (1950)
HURLIMAN (1955)
ALLEN (1957)
RAGO (1968)
FOROUGHI (1972)
EVALUATED DATA
DUDEY (1972)
(ENDF/B-IV, MAT 6407)
LISKIEN (1967)
(DFN 97 UK — $\bar{\sigma}_{WATT}$ = 67.28 mb)
BARRALL (1965)
(DFN 229 UK — $\bar{\sigma}_{WATT}$ = 60.9 mb)
LLL ENDL 2, MAT 7122 (1975)

Fig 3

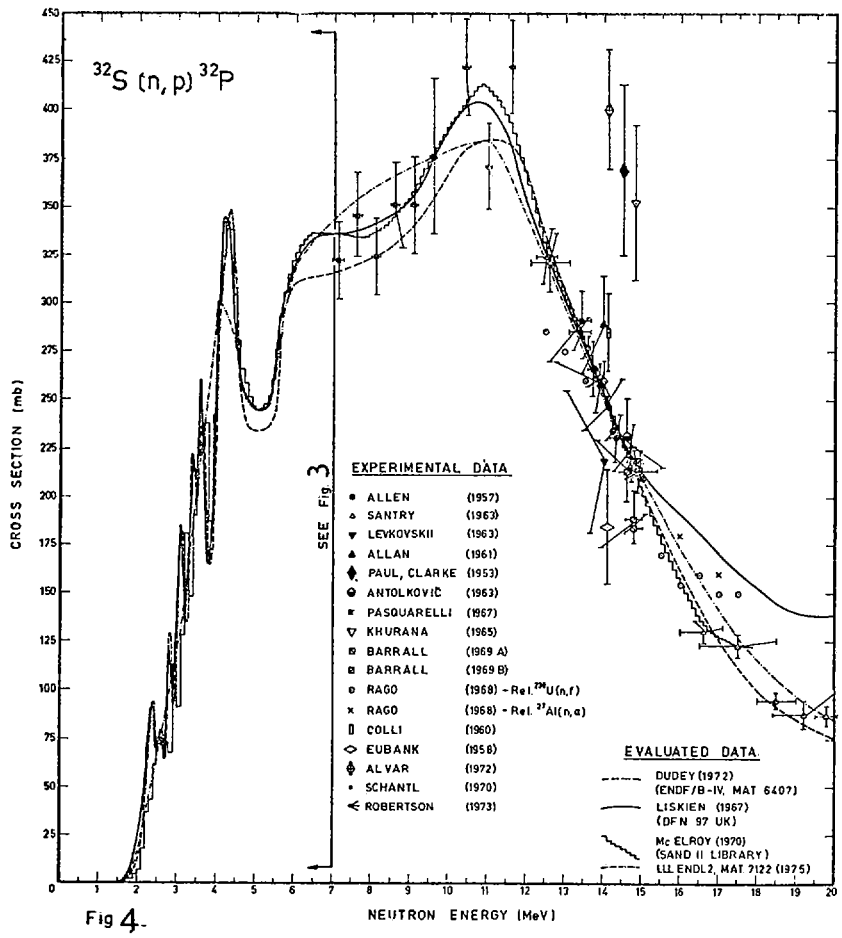
^{32}S (n, p) ^{32}P
CROSS SECTION (mb)
NEUTRON ENERGY (MeV)
SEE Fig 3
EXPERIMENTAL DATA
ALLEN (1957)
SANTRY (1963)
LEVKOVSKII (1963)
ALLAN (1961)
PAUL, CLARKE (1953)
ANTOLKOVIČ (1963)
PASQUARELLI (1967)
KHURANA (1965)
BARRALL (1969 A)
BARRALL (1969 B)
RAGO (1968) - Rel. $^{238}U(n,f)$
RAGO (1968) - Rel. $^{27}Al(n,\alpha)$
COLLI (1960)
EUBANK (1958)
ALVAR (1972)
SCHANTL (1970)
ROBERTSON (1973)
EVALUATED DATA
DUDEY (1972)
(ENDF/B-IV, MAT 6407)
LISKIEN (1967)
(DFN 97 UK)
Mc ELROY (1970)
(SAND II LIBRARY)
LLL ENDL2, MAT 7122 (1975)

Fig 4

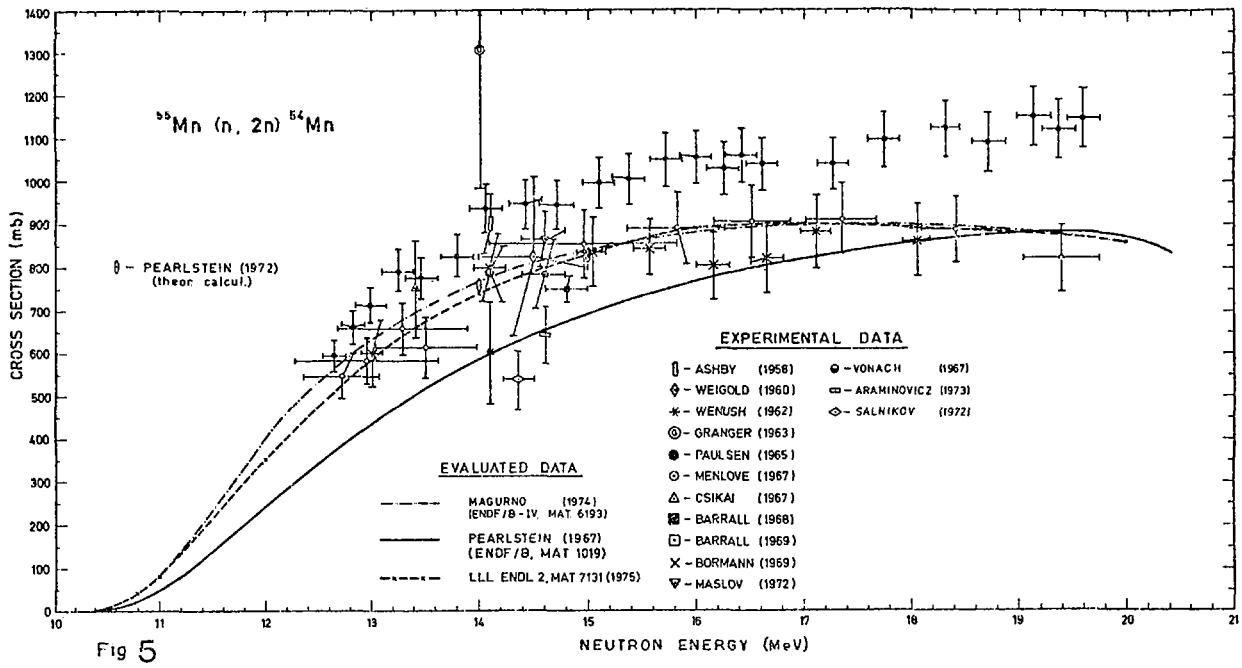
^{55}Mn (n, 2n) ^{54}Mn
θ – PEARLSTEIN (1972)
(theor. calcul.)
EVALUATED DATA
MAGURNO (1974)
(ENDF/B-IV, MAT 6193)
PEARLSTEIN (1967)
(ENDF/B, MAT 1019)
LLL ENDL 2, MAT 7131 (1975)
EXPERIMENTAL DATA
ASHBY (1958)
WEIGOLD (1960)
WENUSH (1962)
GRANGER (1963)
PAULSEN (1965)
MENLOVE (1967)
CSIKAI (1967)
BARRALL (1968)
BARRALL (1969)
BORMANN (1969)
MASLOV (1972)
VONACH (1967)
ARAMINOVICZ (1973)
SALNIKOV (1972)
CROSS SECTION (mb)
NEUTRON ENERGY (MeV)

Fig 5

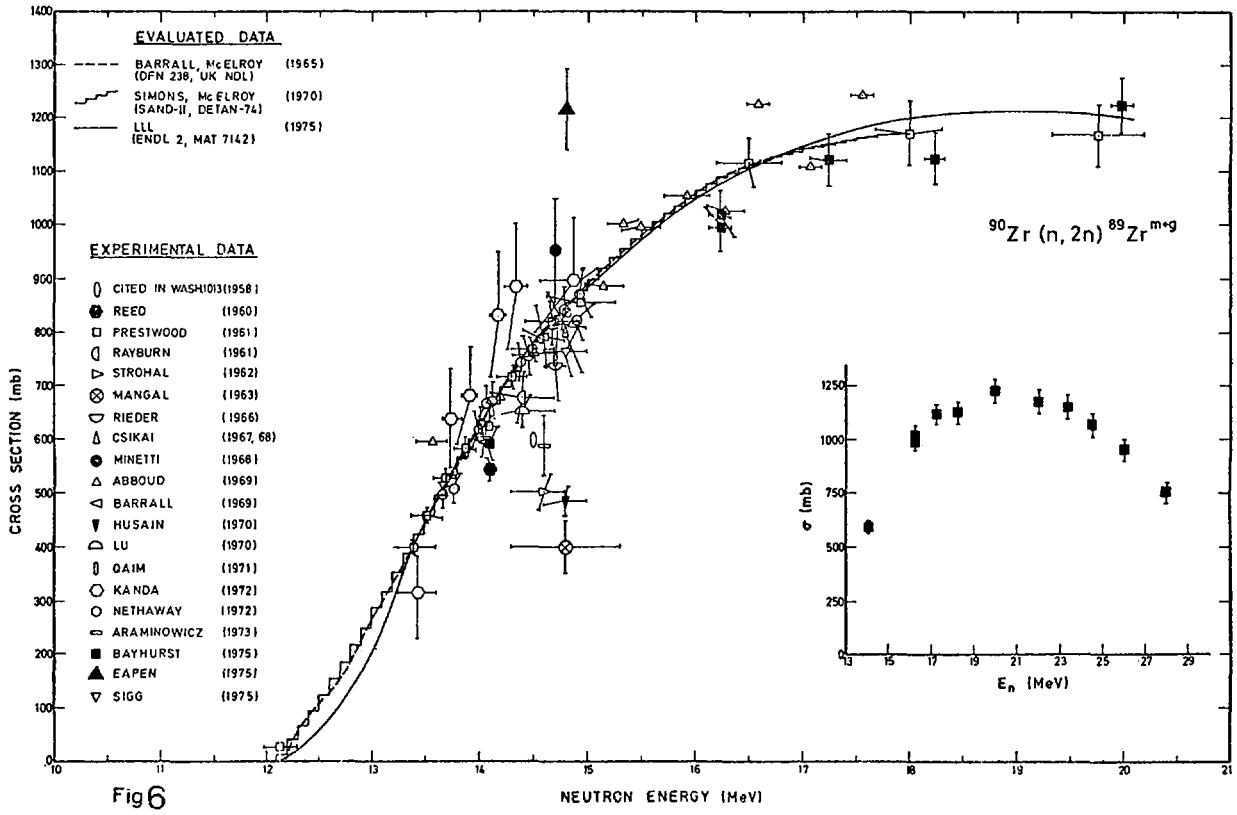
EVALUATED DATA
BARRALL, McELROY (1965)
(DFN 238, UK NDL)
SIMONS, McELROY (1970)
(SAND-II, DETAN-74)
LLL (1975)
(ENDL 2, MAT 7142)
EXPERIMENTAL DATA
CITED IN WASH1013 (1958)
REED (1960)
PRESTWOOD (1961)
RAYBURN (1961)
STROHAL (1962)
MANGAL (1963)
RIEDER (1966)
CSIKAI (1967, 68)
MINETTI (1968)
ABBOUD (1969)
BARRALL (1969)
HUSAIN (1970)
LU (1970)
QAIM (1971)
KANDA (1972)
NETHAWAY (1972)
ARAMINOWICZ (1973)
BAYHURST (1975)
EAPEN (1975)
SIGG (1975)
^{90}Zr (n, 2n) ^{89}Zr^{m+g}
σ (mb)
E_n (MeV)
CROSS SECTION (mb)
NEUTRON ENERGY (MeV)

Fig 6

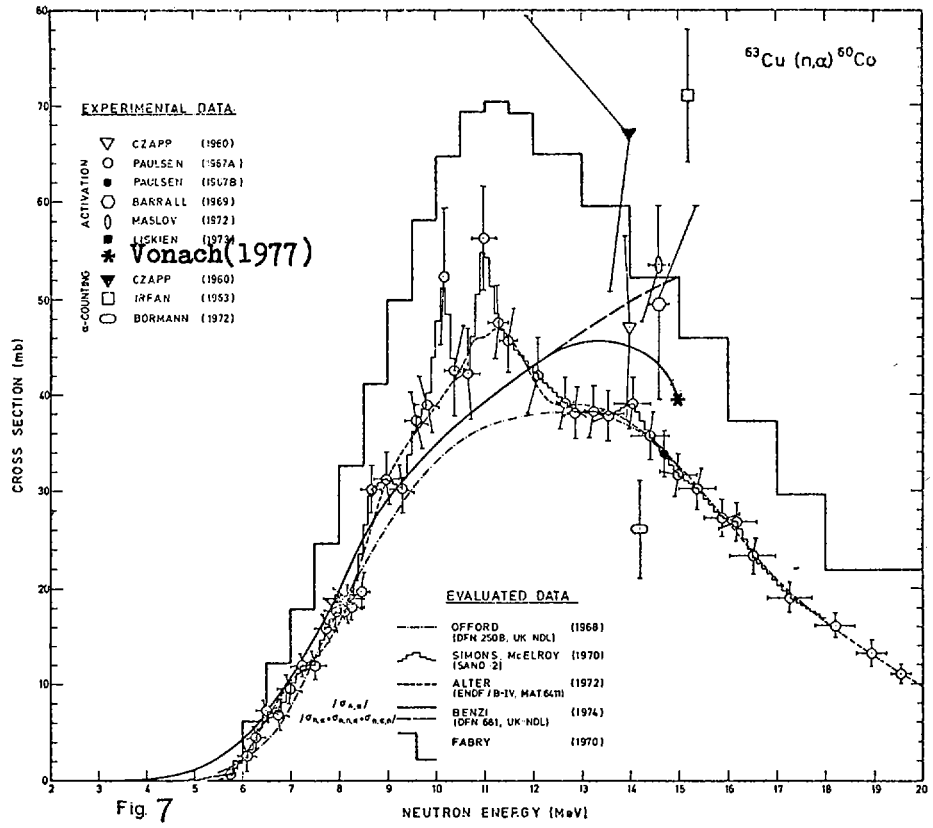
$^{63}Cu\ (n,\alpha)\ ^{60}Co$
EXPERIMENTAL DATA
ACTIVATION
CZAPP (1960)
PAULSEN (1967A)
PAULSEN (1967B)
BARRALL (1969)
MASLOV (1972)
LISKIEN (1973)
Vonach(1977)
α-COUNTING
CZAPP (1960)
IRFAN (1953)
BORMANN (1972)
EVALUATED DATA
OFFORD (1968)
(DFN 250B, UK NDL)
SIMONS, McELROY (1970)
(SANO 2)
ALTER (1972)
(ENDF/B-IV, MAT 6471)
BENZI (1974)
(DFN 681, UK-NDL)
FABRY (1970)
CROSS SECTION (mb)
NEUTRON ENERGY (MeV)

Fig. 7

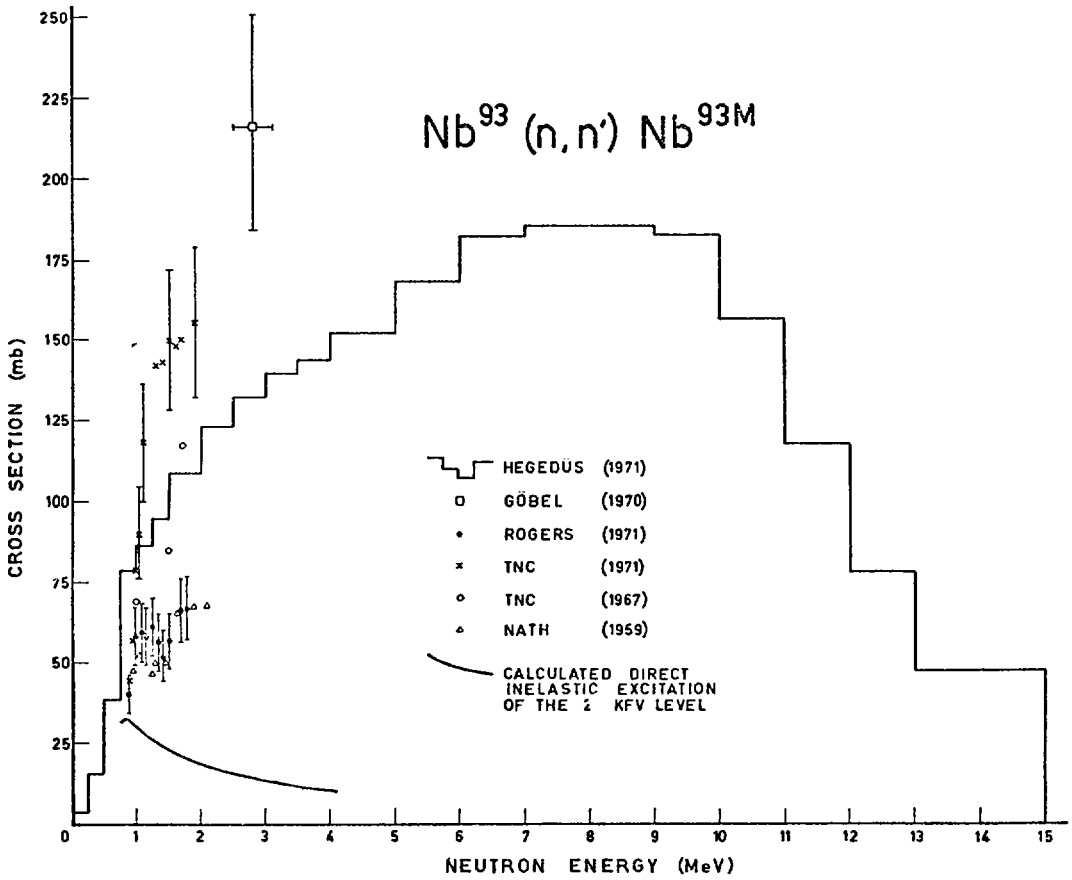
$Nb^{93}\ (n,n')\ Nb^{93M}$
HEGEDÜS (1971)
GÖBEL (1970)
ROGERS (1971)
TNC (1971)
TNC (1967)
NATH (1959)
CALCULATED DIRECT INELASTIC EXCITATION OF THE 2 KEV LEVEL
CROSS SECTION (mb)
NEUTRON ENERGY (MeV)

Fig. 8

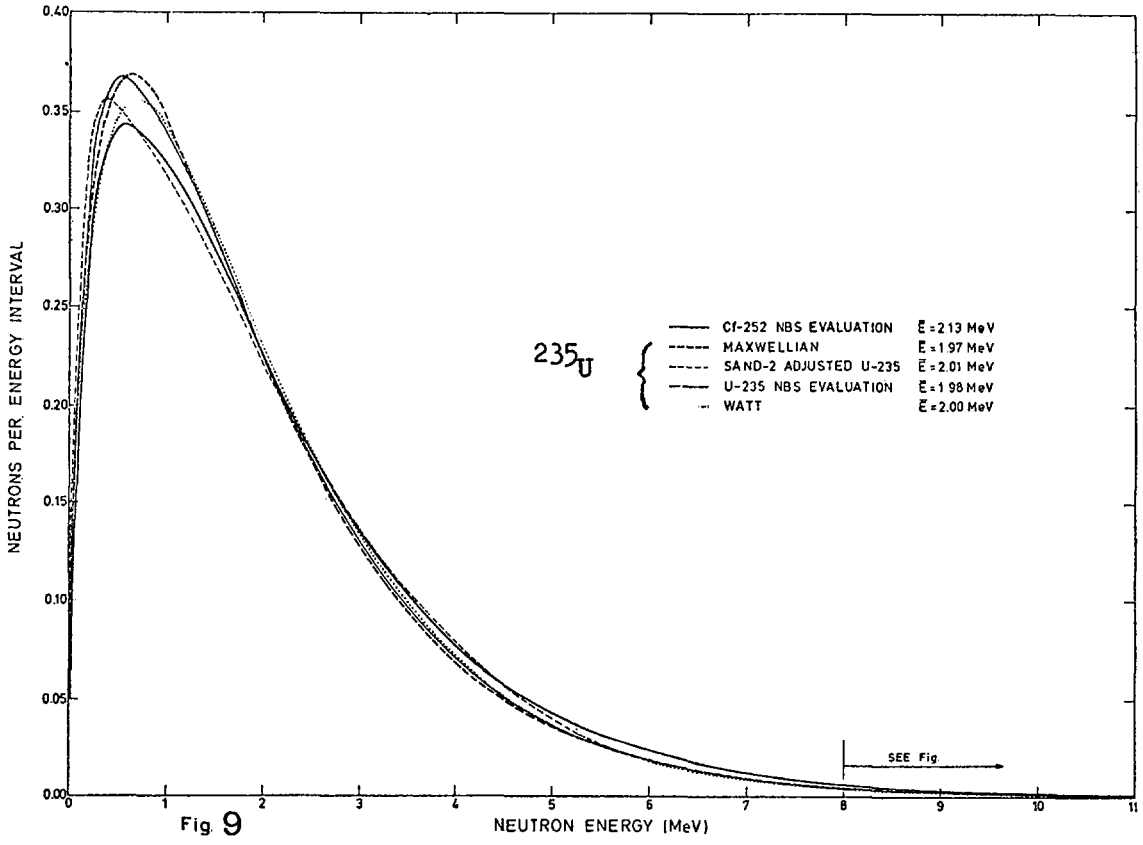
NEUTRONS PER ENERGY INTERVAL
NEUTRON ENERGY (MeV)
^{235}U
Cf-252 NBS EVALUATION Ē = 2.13 MeV
MAXWELLIAN Ē = 1.97 MeV
SAND-2 ADJUSTED U-235 Ē = 2.01 MeV
U-235 NBS EVALUATION Ē = 1.98 MeV
WATT Ē = 2.00 MeV
SEE Fig.

Fig. 9

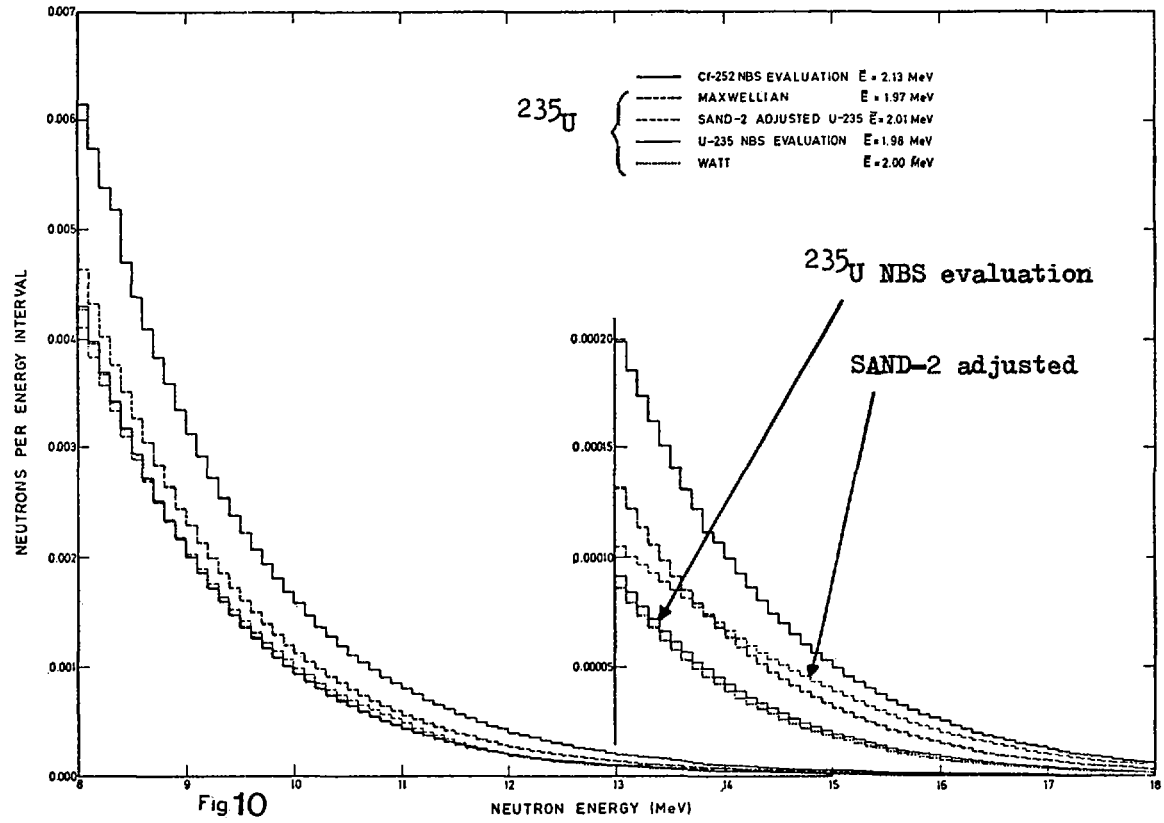
NEUTRONS PER ENERGY INTERVAL
NEUTRON ENERGY (MeV)
^{235}U
Cf-252 NBS EVALUATION Ē = 2.13 MeV
MAXWELLIAN Ē = 1.97 MeV
SAND-2 ADJUSTED U-235 Ē = 2.01 MeV
U-235 NBS EVALUATION Ē = 1.98 MeV
WATT Ē = 2.00 MeV
^{235}U NBS evaluation
SAND-2 adjusted

Fig. 10

IV.3. Status of some Activation Cross Sections for Reactor Neutron Dosimetry in the Range 13 - 15 MeV.

H. Vonach

Institut für Radiumforschung und Kernphysik, Vienna.

In this contribution the following aspects of the problem are to be discussed:

A) The accuracy obtainable at present in activation cross section measurement around 14 MeV neutron energy.

B) The present status of the activation cross sections in general and as specific examples the status of the following reactions: ^{27}Al (n,α), ^{56}Fe (n,p). ^{65}Cn (n,2n) ^{64}Cu.

C) What should be done to further improve the situation.

A) Accuracy of activation cross section measurements in the 13 - 15 MeV neutron range.

In the energy range 13 - 15 MeV conditions for accurate measurements of activation cross sections are especially favourable. Neutrons in this energy range can be produced by the T(d,n)^{4}He reaction at low bombarding energies with high intensity. This reaction has the further advantage that the absolute flux can be measured very accurately (to better 1 %) by means of the associate particle method that is by counting the ^{4}He recoils emitted into a definite solid angle /1-2/. In addition neutron emission is known to be isotropic in the c.m. system at the usual bombarding energies of some 100 keV /3-4/. Thus it is sufficient to determine the absolute neutron flux at one particular neutron energy (corresponding to one particular emission angle) and from this one can calculate accurately the flux

at all other energies corresponding to whole angular range according to the kinematics of the reaction /5/. Thus the situation can be summarized as follows: In the n-energy range 13 - 15 MeV it is possible to produce neutron fluences known to about 1 % with a relatively modest effort.

Concerning the second problem of cross section measurement the determination of the absolute activities formed by the various reactions is of course not different from that at other neutron energies apart from the fact that the high fluxes available allow the use of smaller samples which results in smaller problems with scattering, absorption and self-absorption corrections.

The problem of activity measurement has always been the simpler problem relative to the fluence measurement and so it is even here.

The standard methods developed for accurate absolute determinations of decay rates can be used. In some cases the most accurate method, the 4π β-γ coincidence method /6/ can be applied directly (e.g. for the ^{27}Al (n,α) ^{24}Na or ^{56}Fe (n,p) ^{56}Mn reactions) in other cases one can use NaJ scintillation detectors, the efficiency of which is determined as a function of γ-ray energy by means of 4π β-γ calibrated sources /7/, or as shown recently very accurate measurements of decay rates are possible if a large well type NaJ crystal is used and the investigated decay leads to emission of several γ-rays resulting in a detection efficiency close to unity /8-9/. (These conditions are fulfilled e.g. for all positron emitters, the reaction ^{48}Ti (n,p) ^{48}Sc, ^{27}Al (n,α) ^{24}Na, ^{63}Cu (n, α) ^{60}Co and others.) In this way it is possible to do absolute activity measurements with an overall accuracy in the range 0.5 - 1 % for most of the reactions important in reactor dosimetry.

This sounds considerably more optimistic than the figures quoted by D. Smith /10/ for the standard GeLi-detector technique. This technique, however, does not appear

to me to be the most favourable one for accurate measurements of decay rates. By using the mentioned NaJ crystals especially of the well type much higher efficiencies can be obtained with corresponding better counting statistics if integral counting above a low threshold is used.Moreover, such systems are considerably more stable and reproducible in time than GeLi detectors at present. The main advantage of the GeLi detector to discrminate against interfering activities from competing reactions within the sample itself is not needed in most cases, especially if the contributions from interfering activities are minimized by proper choice of initiating and waiting times. Of course, a check for radiochemical purity with a GeLi detector in addition to the main measurement with the NaJ crystal might be advisable in many cases.

Thus it appears to me that the present state of the art does allow measurements of activation cross sections for most of the dosimetry reactors with accuracies of 1 - 2 % at a 95 % coefficience level.

B) Present status of activation cross sections in the 13 -15 MeV region.

Actually the discussed accuracy has not been reached except for a very small number of cases.

In general, the situation is the following: A relatively large number of rather reliable measurements in the 5 - 10 % accuracy range have been performed, mainly by groups at Hamburg, Geel, Chalk River and various places in the US /11/ in the early sixties and cross sections accurate to about 5 % can be derived by evaluation of this body of data for most reactions.

A much better status has been achieved for the $^{27}Al(n,\alpha)^{24}Na$ reaction as shown in fig. 1. This figure shows all the absolute cross section determinations based on either the

associate particle method of the hydrogen or the fission standard which have been formed to date /12-24/ and in addition an excitation function derived by my coworkers and myself based on a precision cross section measurement at 14.43 MeV /2/ and a relative measurement based on the known angular dependence of the neutrons emitted in the DT-reaction /5/. As the figure shows our precision data are in good agreement with most of the other data, although there is some discrepancy ($\sim$ 4 %) with the most recent precision measurement of Robertson /13/. However, this measurement relies on the differential n-p scattering cross section at zero degree, which is much less well known than the total n-p cross section.

In addition several other precision measurements on the relative value of the $^{27}Al(n,\alpha)$ cross section exist, e.g. from Bormann et al /34/, Paulsen et al /23/ and most recently from Gardner et al /35/, which agree well within a few % as shown in fig. 2. Thus it appears to me that an evaluation of all the existing relative and absolute cross section data will give a result rather close to the curve drawn in fig. 1 with errors of about 1 - 1,5 % and thus this reaction at present seems to be the best choice for a secondary standard in the discussed energy region. There is only one problem left which is not quite solved and that is the question of cross section fluctuations. Earlier /36,37/ claims concerning the existence of cross section fluctuations in the 10 % range had shown to be in error by several careful measurements /9,34,38/. However, recent measurements of Gardner /35/ claim the existence of such fluctuations in the order of 1.5 %. To me the evidence still appears somewhat marginal. However +) if confirmed fluctuations of this amplitude and period would not be very detrimental for the further use of this reaction as secondary standard.

It should however be emphasized that cross-section fluctuations even this small can be completely avoided if a

+) even

reaction on some nuclides with A$\geq$ 50 is used and perhaps a secondary cross section standard of this kind should eventually replace the $^{27}Al(n,\alpha)$.

One possible candidate for this purpose is shown in fig. 3 the $^{56}Fe(n,p)$ reaction /9, 12-15, 17, 20, 22, 39-42/. Here the situation is still somewhat worse. There are no single measurements more accurate than 3 % and most measurements in the 5 - 10 % range, however data are in general (with some obvious exceptions) mutually consistent (again Robertson gives some trouble) and proper evaluation should give adopted values with errors in the two % range.

As the last case to be discussed in detail fig. 4 shows the very strange strange situation which exists for the ^{65}Cu (n,2n) reaction, which puzzles me for many years.

There are a large number of measurements from experienced experimenters /13-15, 19, 22-23, 27-28, 41 - 43/ all the 900 - 1000 mb range and there is my own precision measurement /9/ which is about 10 % below. When I first got such result in 1968 /5/ I was very unhappy and asked my collegues in Vienna to check this cross section. The check performed by Dr. Tagesen confirmed my value /45/ and thus I presented the result at the Washington Cross Section Conference. Five years later, Dr. Mannhart after improving the techniques further made another precision measurement /9/ which also confirmed within 1.5 % the earlier low value. In addition, such low values have also been found by Nagel /46/, a coworker of Prof. Aten at Amsterdam, who did rather careful measurements of the $^{65}Cu(n,2n)$ cross sections relative to the $^{56}Fe(n,p)$ value. At present I do not have any explanation for this discrepancy. Thus at present the situation can be summarized as follows: For a large fraction of cross sections important for reactor neutron dosimetry cross sections accurate to better 5 % can probably be derived from the existing data by careful evaluation for most of the others such evaluations will probably result in errors of 5 - 10 %.

C) Possibilities of improvement of the present state.

As discussed in part A the present state of the art definitely allows the goal of 5 % accuracy for all cross sections interesting for reactor neutron dosimetry to be achieved in the 13 - 15 MeV energy range and it appears to me that this needs only a relatively small effort. A possible approach might be the following.

1) Careful evaluation of the $^{27}Al(n,\alpha)^{24}Na$ data in order to establish this as a cross section standard. This could be done in two steps; at first calculate a weighted average of the form of the excitation function from the data given in fig. 2, then use this relative cross section curve to reduce all absolute measurements to one common excitation energy, e.g. 14.4 MeV, and derive a weighted mean of the absolute cross section for this reference energy.

2) New cross section measurements relative to the $^{27}Al(n,\alpha)$ reaction (which can be done very simply by the sandwich-technique) for those reactions, which at present do not yet fulfill the accuracy demands, whereby the enormous experience of the verious standardisation laboratories engaged in absolute activity measurements (NBS, PTB, NPL, IAEA and so on) should be utilized for the absolute activity measurements and the methods for the activity measurements should be chosen individually according to the specific decay schemes of the nuclides to be measured. Especially in the case of the $^{65}Cu(n,2n)$ reaction the existing discrepancies should be removed in this way, preferably by measurements of both the ^{24}Na and ^{64}Cu activities checked at different laboratories.

Literature:

1) P. Fieldhouse, E.R. Culliford and D.S. Mathev,
J. Nuclear Energy 21, (1967)131
2) H. Vonach, M. Hille, G. Stengl, W. Breunlich and E. Werner
Z. Physik 237, 155 (1970)
3) H. Liskien and A. Paulsen, Nuclear Data Tables A11 (1972) 602
4) G. Stengl Diplomarbeit München 1969
5) H. Vonach, W. Vonach, H. Münzer and P. Schrammel,
Proc. Conf. on Nuclear Cross Sections and Technology,
Washington, NBS Special Publ. 299 Vol 1, 885
6) L.B. Remsberg, Ann. Rev. Nucl. Sci. 17 (1967) 347
7) R. Vaninbrokx and G. Grosse,
Int. J. Appl. Rad. Isotopes 14 (1963) 503
8) W. Mannhart and H. Vonach,
Nucl. Instr. Meth. 136 (1976) 109
9) W. Mannhart and H. Vonach,
Z. Phys. A 272 (1975) 279
10) D.L. Smith
ANL/NDM 23 1976
11) A. Schett, K. Okomoto, L. Lesca and F.H. Fröhner, H. Liskien
and A. Paulsen, Compilation of Threshold Neutron Reactions
EANDC 95 "Ü" 1974
12) J.D. Hemingway, R.H. James, E.B.M. Martin, G.R. Martin,
Proc. Roy. Soc. A 292, 180 (1966)
13) J.C. Robertson, B.N. Andric, P. Kolkovski,
Journ. Nucl. En. 27 (1973) 139
14) Forbes, S.G.: Phys. Rev. 88, 1309 (1952)
15) E.B. Paul, R.L. Clarke,
Can. J. Phys. 31, 267 (1953)
16) I. Kumabe, E. Takekoshi, Y. Tsuneaka, H. Ogata,
Phys. Rev. 106, 155 (1957)
17) S. Yasumi, J.Phys. Soc. Japan 12, 443 (1957)
18) B.D. Kern, Nucl. Phys. 10, 226 (1959)
19) B.P. Bayhurst, R.J. Prestwood, J. Morg,
Nucl. Chem. 23, 173 (1961) + Phys. Rev. 121 (1961) 1438
20) F. Gabbard, B.D. Kern, Phys. Rev. 128, 1276 (1962)

21) P.M. Aron, S.S. Burgorkov, K.A. Petrzhah, A.V. Sorokina, Atomn. Energ. 16, 370 (1964)
22) G.C. Bonazzola, P. Broretto, E. Chiavassa, R. Spinoglio, A. Pasquarelli, Nucl. Phys. 51, 337 (1964)
23) A. Paulsen, H. Liskien, Nucl. Energy 19 (1965) 907
24) J. Seebeck, M. Bormann, Nucl. Phys. 68, 387 (1965)
25) J.P. Butler, D.C. Santry, Can. J. Phys. 41, (1963) 372
26) J.A. Grundl, R.L. Henkel, B.L. Perkins, Phys. Rev. 109 (1958) 425
27) R.C. Barral, M. Silbergeld, Nucl. Phys. A 138 (1969) 387
28) D. Crumpton, A.J. Cox, P.N. Cooper, P.E. Francois, S.E. Hunt, J. Inorg.Nucl. Chem. 31, 1 (1969)
29) P. Boschung St. Gagneux, P. Huber, E. Steiner, R. Wagner, Helv. Phys. Act. 42 (1968) 252
30) H.O. Menlove, K.I. Coop, H.A. Grench, Phys. Rev. 163 (1967) 1308
31) J.M.F. Jeronymo, G.S. Mani, J. Olkowski, A. Sadeghi and C.F. Williamson, Nucl. Phys. 47 (1963) 157
32) H.W. Schmitt, J. Halperin, Phys. Rev. 121 (1961) 827
33) R.C. Barall, J.A. Holmes, M. Silbergeld, AFWL-TR-68-134 (1969)
34) M. Bormann and I. Riehle, Z. Phys. 207 (1964) 77
35) M.A. Gardner and D.G. Gardner Nucl. Phys. A 265 (1976) 77
36) P. Cuzzocrea, E. Perillo, S. Notarrigo, Nuovo Cim. 54B, 53 (1968)
37) N. Cindro et al. Phys. Letters 6 (1963) 205
38) J.M. Ferguson and J.C. Albergotti, Nucl. Phys. A98 (1967) 65

39) H. Pollehn, H. Neuert, Z. Naturforschugg 16A, 227 (1961)
40) H. Liskien, A. Paulsen,
Journ. Nucl. En. 16 (1965) 467
41) D.C. Santry and J.P. Butler,
Can. Journ. Phys. 42 (1964) 1030
42) M. Bormann, B. Lammers,
Nucl. Phys. A 130, 195 (1969)
43) R. Mogharrab, H. Neuert,
Atomkernenergie 19, 107 (1972)
44) M. Bormann, S. Cierjacks, E. Fretwurst, K-J Giesecke, H. Neuert,
H. Pollehn, Z. Phys. 174 (1963) 1
45) S. Tagesen, private communication
46) W. Nagel, A.H.W. Aten,
Physica 31. 1091 (1965)

Figure Captions:

Fig. 1: Comparison of absolute cross section measurement for the $^{27}Al\ (n,\alpha)^{24}Na$ reaction.

Fig. 2: Comparison of different measurements of the relative cross sections for the $^{27}Al(n,\alpha)^{24}Na$ reaction in the 13 - 15 MeV range. All cross section curves are normalized to a value 117 mb /2/ at 14.4 MeV.

Fig. 3: Absolute cross section measurements for the $^{56}Fe(n,p)^{56}Mn$ reaction.

Fig. 4: Absolute cross section measurements for the $^{65}Cu(n,2n)^{64}Cu$ reaction.

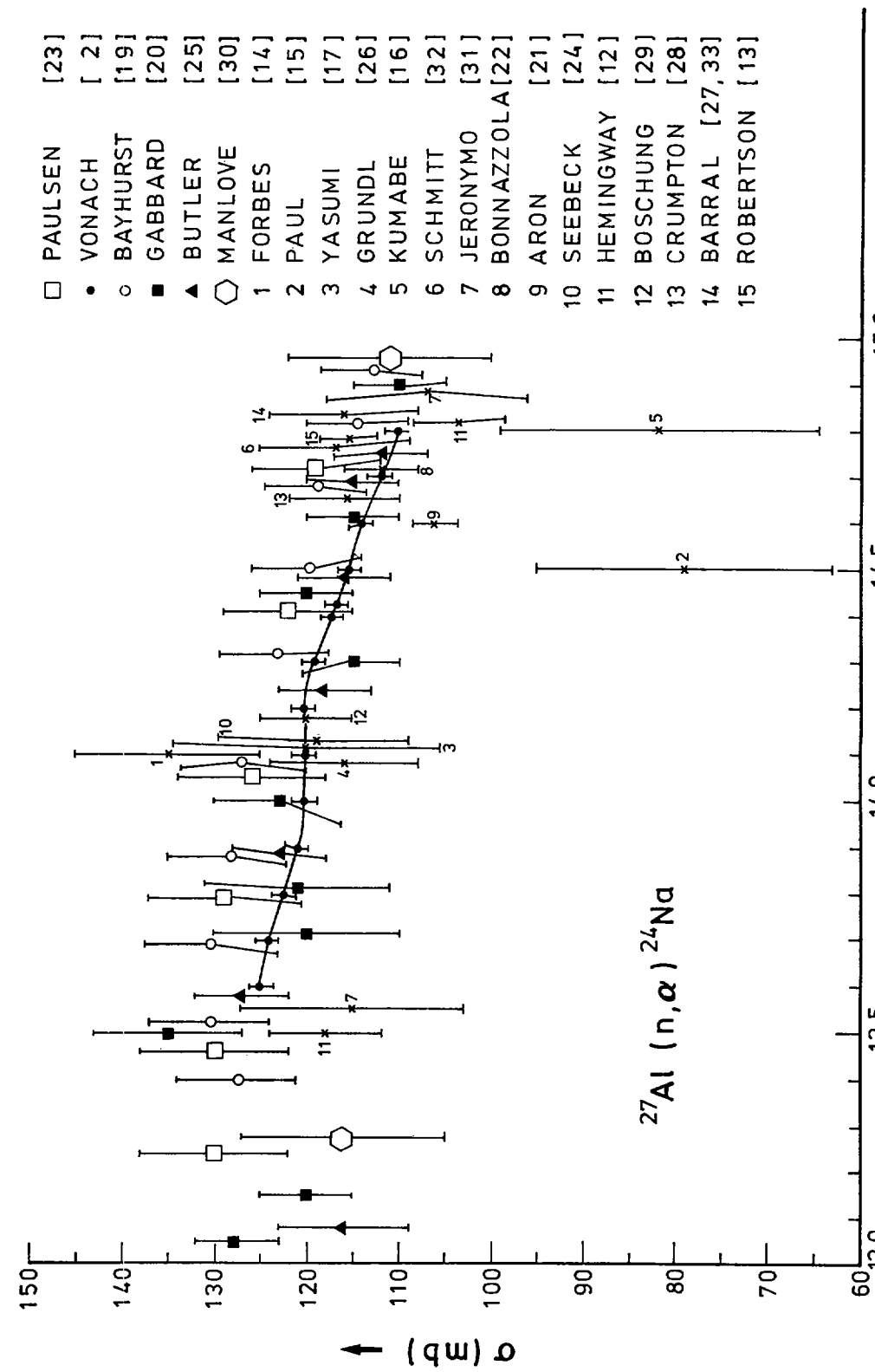
□ PAULSEN [23]
• VONACH [2]
○ BAYHURST [19]
■ GABBARD [20]
▲ BUTLER [25]
⬡ MANLOVE [30]
1 FORBES [14]
2 PAUL [15]
3 YASUMI [17]
4 GRUNDL [26]
5 KUMABE [16]
6 SCHMITT [32]
7 JERONYMO [31]
8 BONNAZZOLA [22]
9 ARON [21]
10 SEEBECK [24]
11 HEMINGWAY [12]
12 BOSCHUNG [29]
13 CRUMPTON [28]
14 BARRAL [27,33]
15 ROBERTSON [13]
$^{27}Al\ (n,\alpha)\ ^{24}Na$
σ (mb) ←
En (MeV) →
150
140
130
120
110
100
90
80
70
60
13.0
13.5
14.0
14.5
15.0

Fig.1

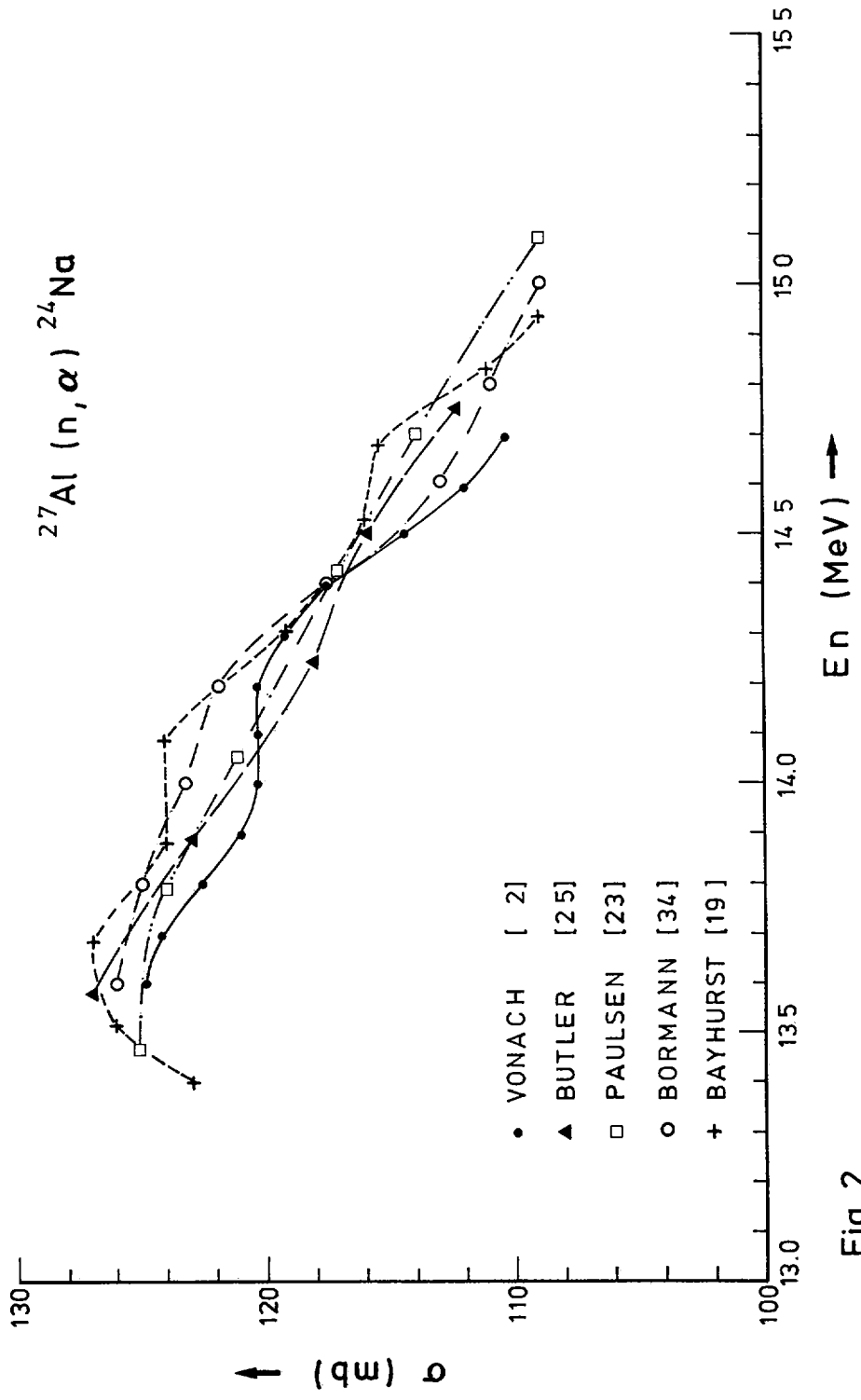
$^{27}Al\ (n,\alpha)\ ^{24}Na$
σ (mb)
En (MeV)
130
120
110
100
13.0
13.5
14.0
14.5
15.0
15.5
• VONACH [2]
▲ BUTLER [25]
□ PAULSEN [23]
o BORMANN [34]
+ BAYHURST [19]

Fig. 2

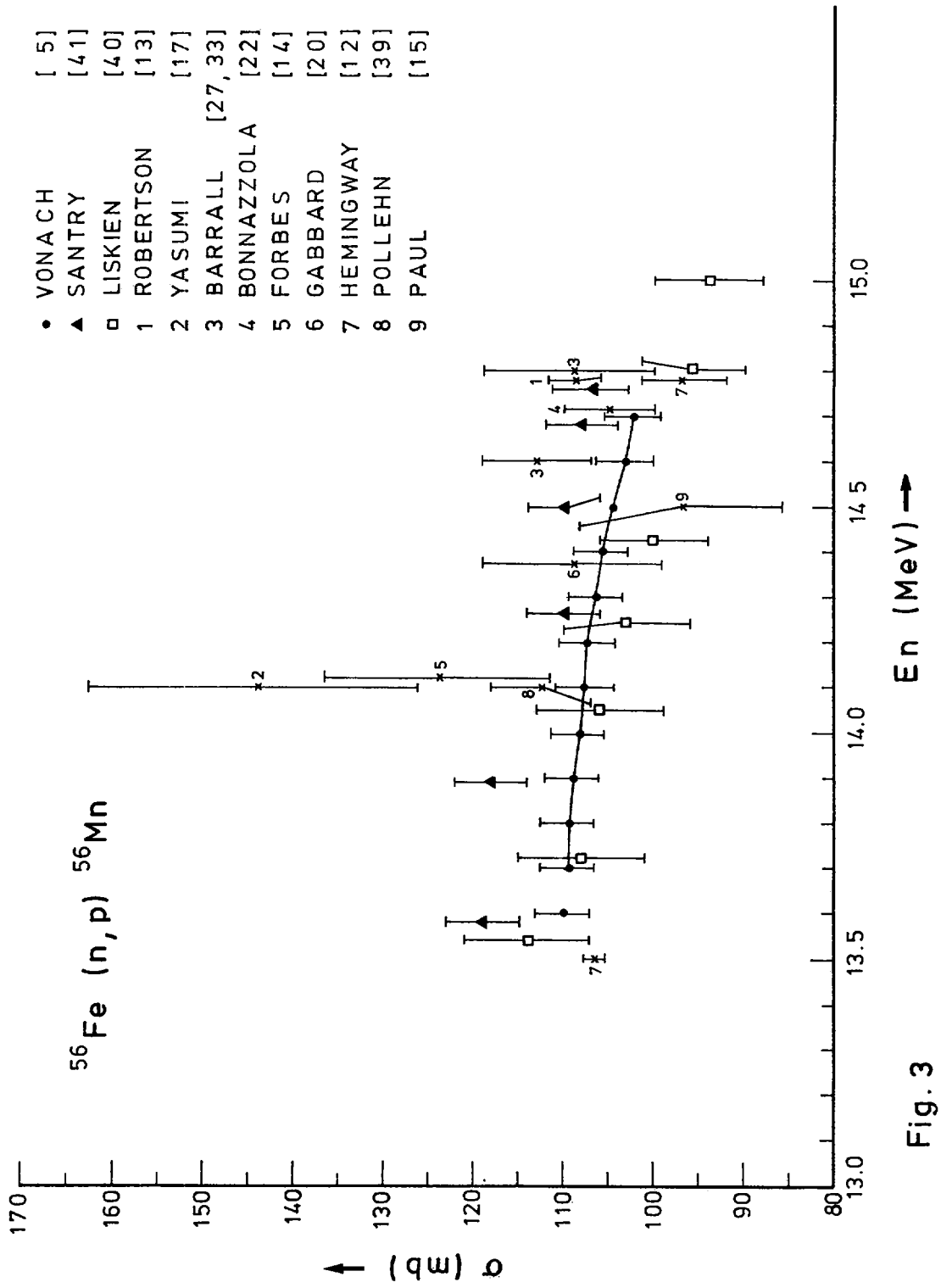
• VONACH [5]
▲ SANTRY [41]
□ LISKIEN [40]
1 ROBERTSON [13]
2 YASUMI [17]
3 BARRALL [27,33]
4 BONNAZZOLA [22]
5 FORBES [14]
6 GABBARD [20]
7 HEMINGWAY [12]
8 POLLEHN [39]
9 PAUL [15]
56Fe (n,p) 56Mn
σ (mb)
En (MeV)
170
160
150
140
130
120
110
100
90
80
13.0
13.5
14.0
14.5
15.0

Fig. 3

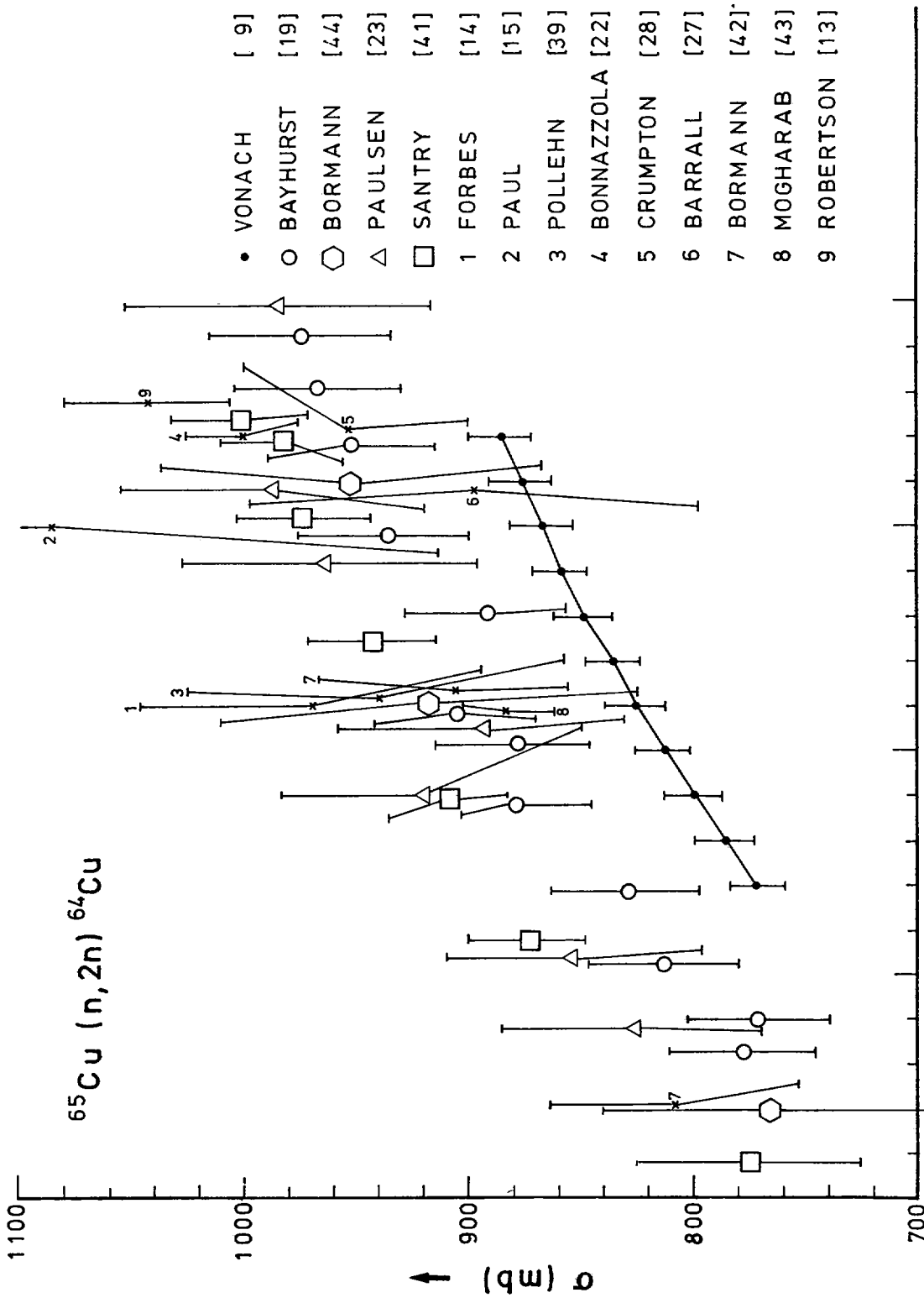
^{65}Cu (n, 2n) ^{64}Cu
σ (mb)
En (MeV)
1100
1000
900
800
700
13.0
13.5
14.0
14.5
15.0
• VONACH [9]
○ BAYHURST [19]
⬡ BORMANN [44]
△ PAULSEN [23]
□ SANTRY [41]
1 FORBES [14]
2 PAUL [15]
3 POLLEHN [39]
4 BONNAZZOLA [22]
5 CRUMPTON [28]
6 BARRALL [27]
7 BORMANN [42]
8 MOGHARAB [43]
9 ROBERTSON [13]

Fig. 4

IV.4. ENDF/B Dosimetry File for Version V*

B.A. Magurno
Brookhaven National Laboratory
Upton, New York

Abstract:

The Cross Section Evaluation Working Group (CSEWG) effort to supply differential energy dependent cross sections for the Inter-Laboratory LMFBR Reaction Rate Program (ILRR)[1] culminated with the preparation and distribution of the ENDF/B-IV dosimetry tape (tape 412).[2] The release of the above tape fulfilled the primary commitment of the 1972 Task Force.[3] The data library which evolved was tested in reference neutron fields and compared with experimental integral numbers. The first sets of results were presented at the 1973 winter meeting of the American Nuclear Society (ANS) in San Francisco[4] by Magurno and Ozer.[5]

Version V will include updates to the majority of isotopes in the dosimetry file. Table I is divided into three parts; part one shows reactions to be carried over; part two, the reactions to be updated; and part three, the reactions that remain unassigned (may be dropped). It is too soon to give a complete report on all reactions to be updated for version V, but all the work done at Brookhaven National Laboratory will be reported here. The status of all updated reactions can be seen in the Table.

* Research supported by the U.S. Energy Research and Development Administration.

A complete set of results including contributions from all laboratories involved in integral testing can be found in ENDF-230.[6] The above results pointed to apparent discrepancies that when solved could strengthen the program. Non-consistent use of standards, lack of cross section information in the energy region of excitation functions that includes thresholds, and different interpretations of reference spectra all contributed to the discrepancies.

Of all the materials listed in the Table the most important are the primary standards, since they effect both the differential cross sections and the spectra. Special effort has been placed on the inter-relations of these standards by CSEWG. The Normalization and Standards Subcommittee organized a task force[7] to obtain a consistent set of standards for use in all ENDF files. As a result of the evaluation of $^{6}Li(n,\alpha)$, $^{10}B(n,\alpha)$, $^{197}Au(n,\gamma)$, and $^{235}U(n,f)$, of Hale and Dodder,[8] Hale and Arthur,[9] Mughabghab[10] and Bhat[11] were adopted along with (n,p) of Stewart[12] (already accepted for ENDF/B-V). The two to be discussed here as standards are $^{235}U(n,f)$ and Au(n,γ).

The $^{235}U(n,f)$ cross section for Version V (preliminary to date) from 100 eV to 20 MeV was a two part evaluation by the Task Force. The first part, (100 eV - 200 keV), used input that indicated structure and the second part (200 keV - 20 MeV) was represented by a smooth curve and is a primary

ENDF/B standard. The results of this evaluation were presented by M. Bhat[8] at a recent NEANDC meeting. $\langle\sigma_f\rangle$ tabulated as a function of energy (in energy bins) to 200 keV and σ_f (E) 200 keV-20 MeV are presented in the above paper, along with the evaluation methods used. Since the paper by Bhat is available I will not go into detail but will show the resultant fission cross evaluation.

Fig. 1: 0-100 keV shows the data considered and the ENDF/B-IV curve.

Fig. 2: 0-100 keV is the $\langle\sigma_f\rangle$ for ENDF/B-V and an overlay of both shows the fit.

Fig. 3: 100-250 keV data considered and ENDF/B-IV curve.

Fig. 4: 100-250 keV $\langle\sigma_f\rangle$ for ENDF/B-V and again an overlay of both shows the fit.

Fig. 5: 0.1-1 MeV shows the comparison between ENDF/B-IV and ENDF/B-V. This lowering of the cross section (~5%) should help solve the spectral distortions in χ_{25} and χ_{82} described in a paper by Vlasov et al.[13]

Fig. 6,7: The cross sections from 1 to 20 MeV. The Version IV and Version V cross sections inter-weave but the changes should have little import for integral tests.

Because of observed structure in the capture cross section of Au below 200 keV and the lack of data above 3.5 MeV, the use of Au as a standard outside the energy range 200 keV-3.5 MeV is de-emphasized (excluding thermal). This evaluation differs from its predecessors in that the input data measured relative to a standard were renormalized to other approved primary standards to give a consistent set. A description of the evaluation, comparisons of ENDF/B-V vs. ENDF/B-IV evaluated curves and a comparison of the calculated fission spectrum average cross section vs. published experimental values are given in Appendix I, an informal report by S. F. Mughabghab.

While $^{10}B(n,\alpha)$ and $^{6}Li(n,\alpha)$ have been adopted as standards, the dosimetry requirements call for ^{10}B(n,total He) and ^{6}Li(n,total He). These are Los Alamos evaluations and are underway at the present time. There will be a description change in these files, i.e. MT=107 (ENDF description of (n,α)) will become MT=207 (n,total He). This nomenclature change is necessitated by the outcome of a special meeting of Normalization and Standards Subcommittee[14] chaired by L. Stewart at Los Alamos. Special catagories for ENDF files were discussed and three files, Dosimetry, Neutron Induced Gas Production, and Activation evolved. The minutes of this meeting were reported to and will be included in the Normalization and Standards Subcommittee report. The production and maintenance of these files was deemed an unnecessary burden

for the Normalization and Standards Subcommittee and a new subcommittee was formed; Special Applications File (SAFE) Subcommittee, The nucleus of this subcommittee was formed with B. Magurno (BNL) chairman and in charge of Dosimetry, L. Stewart (LASL) in charge of Neutron Induced Gas Production, R. Schenter (HEDL) in charge of Activation, and W. McElroy (HEDL) in charge of User Needs and Test Recommendations. In addition the radioactive decay file was transferred from the Fission Product Subcommittee to SAFE and will be in the charge of C. Reich (EG & G, Idaho, Inc.). As was the case in dosimetry, a reaction that appears in any or all of the special applications files and the General Purpose File must be consistent. An example of the above is Fe. The General Purpose Elemental File is being generated by P. Fu (ORNL). ^{54}Fe(n,p), ^{58}Fe(n,p) and ^{58}Fe(n,γ) are being evaluated by R. Schenter (HEDL); Fu and Schenter are cooperating to be sure that the partial reaction cross sections sum to the elemental reactions.

^{23}Na, ^{232}Th, ^{238}U, ^{237}Np, and ^{239}Pu will come directly from the General Purpose File.

Cobalt and manganese are being evaluated for the General Purpose File by S. F. Mughabghab. The (n,γ) and the (n,α) for cobalt and the (n,2n) for both isotopes will be added to the dosimetry file. The Co(n,α) is essentially the same as MAT 6199 by J. D. Jenkins in Version IV library. Co(n,γ) and (n,2n) are in process.

Fig. 8: shows a model calculation normalized to existing data and compared to the Version IV evaluation. The threshold area contains the upper limit of the Version V (n,2n) and indicates that fission spectrum average cross section will be equal to or slightly larger than 0.262 mb (the Version IV value of the cross section).

Fig. 9: The preliminary Mn(n,2n) curve Version IV compared to Version V The new curve in the threshold area is lower than the Version IV curve and joins the Version IV curve at 15 MeV. This will yield a fission spectrum average cross section of about 0.30 mb. The Version IV value was 0.37 while the reported experimental value of Fabry[15] was 0.25 mb.

The elemental evaluation of Ti for the General Purpose File is a joint effort by C. Philis of Bruyeres-le-Chatel and D. L. Smith and A. B. Smith of ANL. To construct the reaction cross section of elemental Ti they evaluated each of the isotopes separately.

Fig. 10: Since the work is not complete no graphs are available for publication. A comparison of several evaluations of the ^{46}Ti(n,p) is taken from Vlasov[13] for demonstration. The new data of Smith does not change the ENDF/B-IV fission spectrum average cross section (10.24 mb) significantly but an anticipated energy shift in the threshold will raise $\langle\sigma_f\rangle$ about 7½%.

Fig. 11: ^{47}Ti an exoergic reaction with an effective threshold at approximately 0.5 MeV. This graph shows several evaluations including ENDF/B-IV and experimental data. There are differences expected in the ANL evaluation but not in the threshold region and the ENDF/B-IV $\langle\sigma_f\rangle$ is not expected to change by more than a percent. The argument put forth by Vlasov[13] about β^- branching ratio (68.5% by ANL vs 73% recommended by Lederer) can only be settled by the authors of the ENDF/B-V evaluation.

Fig. 12: The graph shows a series of evaluations, none of which were accurate in threshold region. The dotted line going through the Smith data is approximately the same as the new ANL evaluation and the change in $\langle\sigma_f\rangle$ is about 55% bringing it into agreement with the integral number.

Nickel reaction cross sections, part of the nickel evaluation for the General Purpose File, are being evaluated at BNL under the auspices of M. Divadeenam. He is also supplying the isotopic reaction cross sections required by the dosimetry file and by extending the evaluations to 40 MeV is supplying the isotopic nickel reactions for the neutron-induced gas production file. However, for our purposes only up to 20 MeV will be considered. An extensive description of the $^{58}Ni(n,p)$, $^{58}Ni(n,2n)$ and $^{60}Ni(n,p)$ is reported by M. Divadeenam in Appendix II of this report. The fission spectrum average cross sections of the nickel isotopes are listed in Table II.

TABLE I

1. Reactions to be carried over to Version V.

Isotope/Reaction	MAT	LAB	Author	Comment
^{27}Al (n,p)	6156	LASL	P.G. Young & D.G. Foster	
^{27}Al (n,α)	6156	LASL	P.G. Young & D.G. Foster	
^{59}Co (n,α)	6199	BNL	J.D. Jenkins	
^{115}In (n,γ)	6416	HEDL	F. Schmittroth	
^{232}Th (n,f)	6296	B&W	W.A. Wittkopf	
^{232}Th (n,γ)	6296	B&W	W.A. Wittkopf	(> 50 keV)

2. Reactions to be updated for Version V.

Isotope/Reaction	MAT	LAB	Author	Comment
^{6}Li (n, TOTAL He)		LASL	Hale	
^{10}B (n, TOTAL He)		LASL	Hale	
^{23}Na (n,γ)		ORNL	Larson	
^{45}Sc (n,γ)		BNL	Magurno	(> 20 keV)
^{46}Ti (n,p)		BNL ANL	Magurno D.L. Smith	in conjunction with ANL-elemental evaluation
^{47}Ti (n,p)+(n,np)		As Above		As Above
^{48}Ti (n,p)+(n,np)		As Above		As Above
^{55}Mn (n, 2n)		BNL	Mughabghab	
^{54}Fe (n,p)		ORNL HEDL	Perey (Fu) Schenter (Mann)	in conjunction with elemental evaluation of iron
^{56}Fe (n,p)		As Above	As Above	
^{58}Fe (n,γ)		As Above	Perey (Fu) Schenter (Schmittroth)	
^{59}Co (n, 2n)		BNL	Mughabghab	
^{59}Co (n,γ)		BNL	Mughabghab	
^{58}Ni (n, 2n)		BNL	Divadeenam	in conjunction with elemental evaluation of Ni
^{58}Ni (n,p)		BNL	Divadeenam	

TABLE I (Cont'd)

Isotope/Reaction	MAT	LAB	Author	Comment
^{60}Ni (n,p)		BNL	Divadeenam	As Above
^{115}In (n,n')		HEDL	Schmittroth	
^{127}I (n, 2n)		Stanford	Sher	
^{197}Au (n,γ)		BNL & Task Force	Mughabghab	
^{232}Th (n,γ)		BNW	Leonard	(< 50 keV)
^{235}U (n,f)		BNL & Task Force	Bhat	
^{238}U (n,f)		ANL & Task Force	Pennington	
^{238}U (n,γ)		As Above	As Above	
^{237}Np (n,f)		HEDL	Mann	
		LASL	Stein	
^{239}Pu (n,f)		GE & Task Force	Kujawski	

3. Unassigned Reactions (may be dropped).

S^{32} (n,p)
Cu^{63} (n,γ)
Cu^{63} (n,α)
Cu^{65} (n, 2n)

Table II*

	A	Maxwellian T=1.29	Cranberg	Watt	Maxwellian T=1.321	Expt.
(np)	58	103.765	107.762	109.758	108.029	98.70±4.60[a]
	60	2.469	2.344	2.500	2.722	{1.9±5 / 2.3±.3}[b]
	61	3.699	3.772	3.899	3.934	
	62	0.040	0.0379	0.035	0.047	
	64	0.0028	0.0022	0.002	0.0034	
	Ni	71.55	74.25	75.65	74.53	67.8±2[c]
(np+npn'+....)	58	103.910	107.851	109.864	108.203	
	60	2.472	2.346	2.502	2.725	
	61	3.830	3.862	4.005	4.091	
	62	0.041	0.031	0.0356	0.049	
	64	0.0032	0.0022	0.0026	0.0038	
	Ni	71.66	74.31	75.69	74.66	
(nα+nα'n+nn'α)	58	6.072	6.036	6.315	6.549	6.06[d]
	60	1.155	1.137	1.194	1.251	1.12[d]
	61	1.909	1.925	1.962	1.977	1.83[d]
	62	0.105	0.094	0.102	0.119	0.097[d]
	64	0.069	0.048	0.056	0.083	0.108[d]
	Ni	4.473	4.441	4.652	4.827	4.76±.54[e] 4.7[f]

* All cross sections in mb.

a) Weighted average of exptl data KAPL-M-7291.

b) Liskien and Paulsen Nucleonic 8,(1966).

c) ENDF/III.

d) Weighted average of exptl data.

e) H. Farrar IV (unpublished); experimental error is ~5%.

f) Lippincott, Nuclear Cross Sections and Technology, 375 (1975).

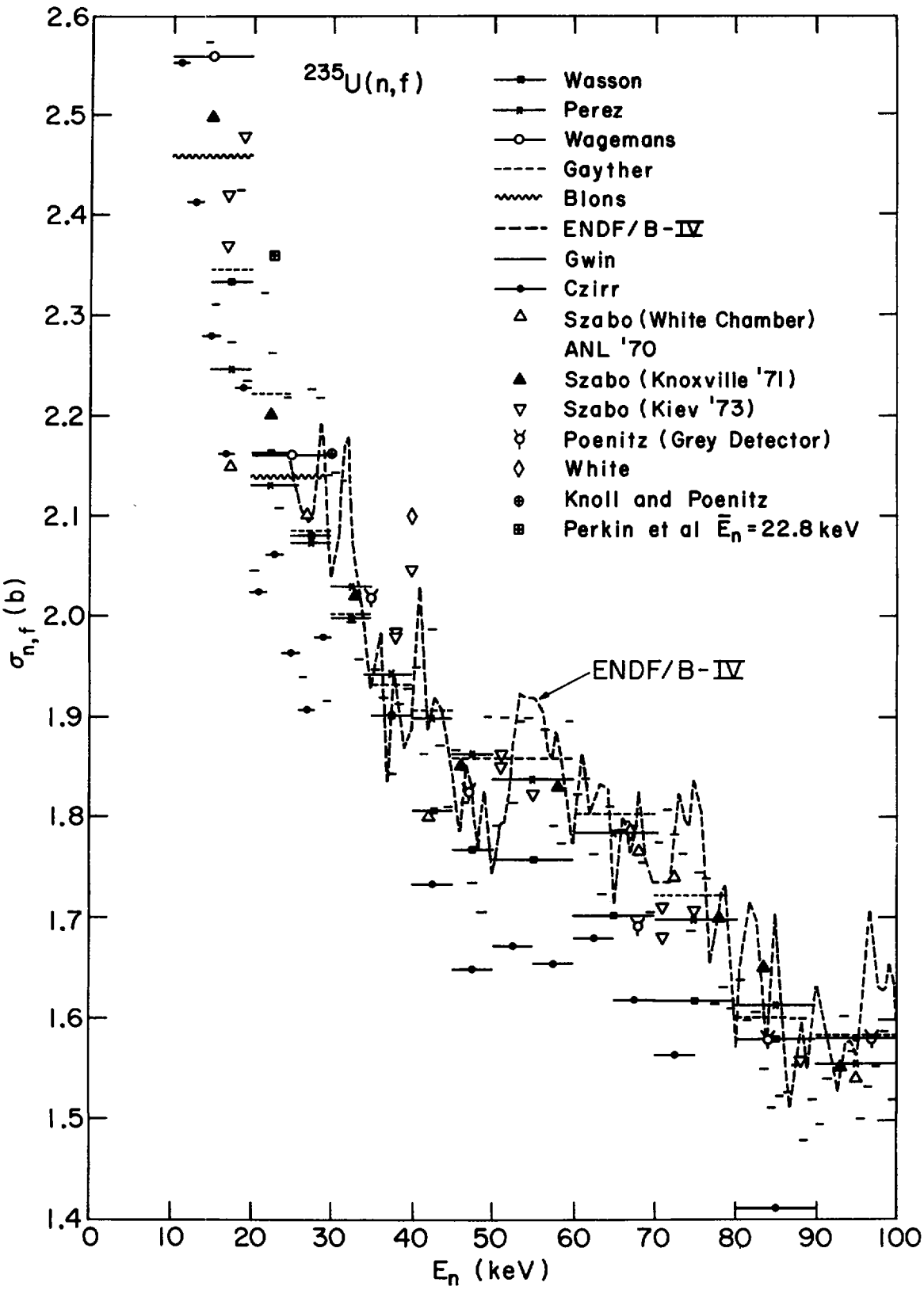

Fig. 1 ^{235}U(n,f) Data up to 100 keV

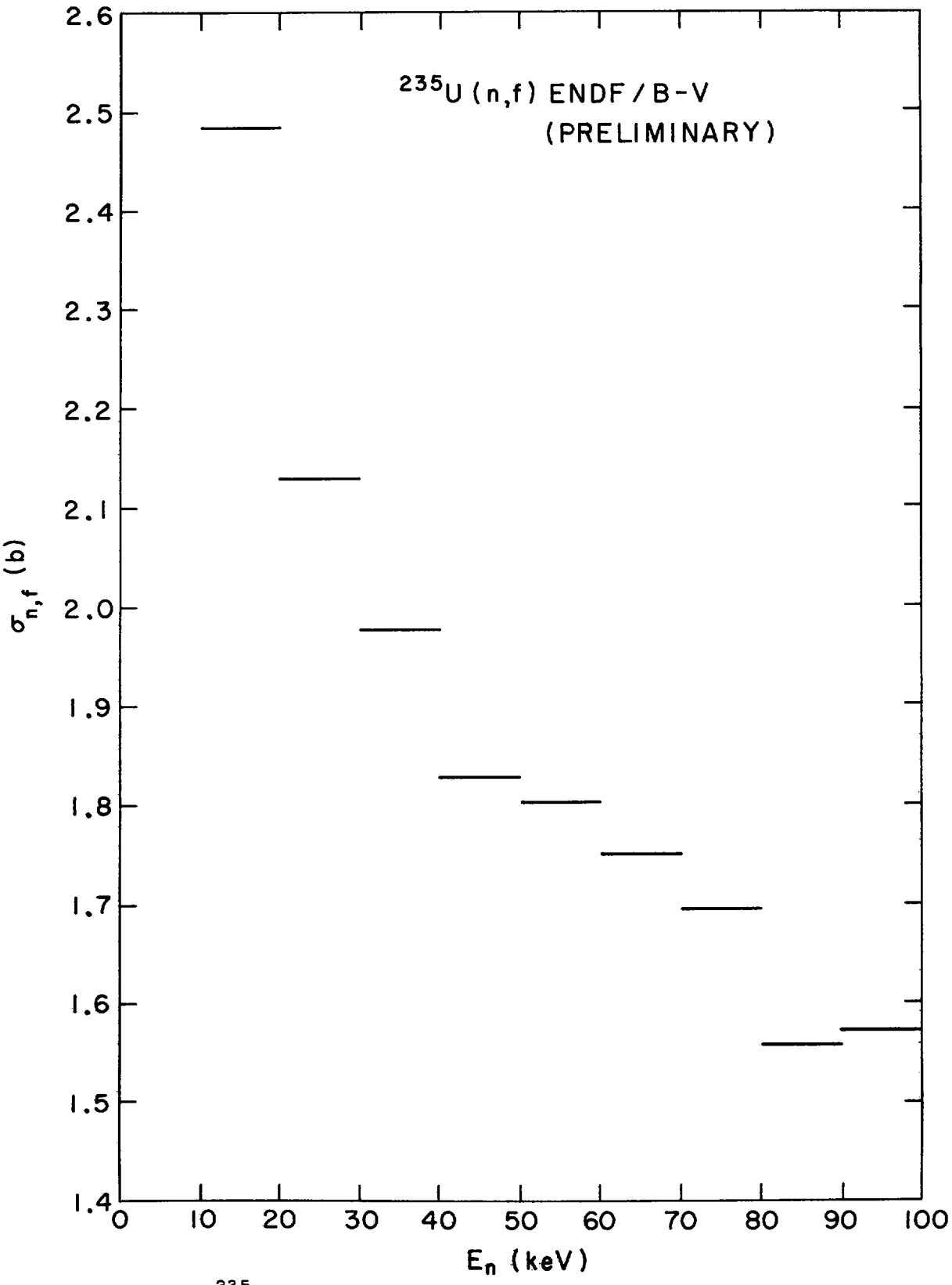

Fig. 2 ^{235}U(n,f) Evaluations up to 100 keV

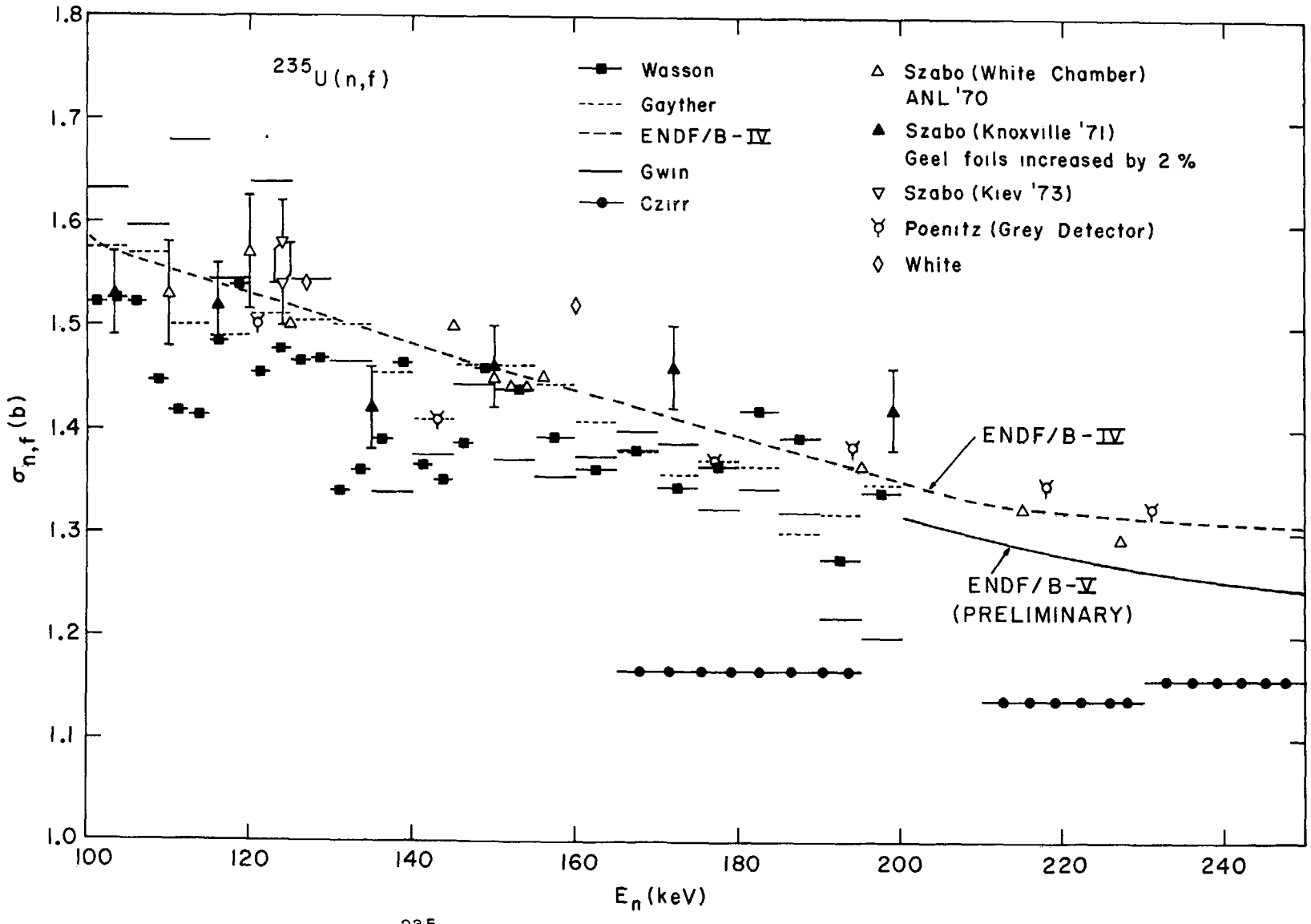

Fig. 3 $^{235}U(n,f)$ data 100 - 200 keV.

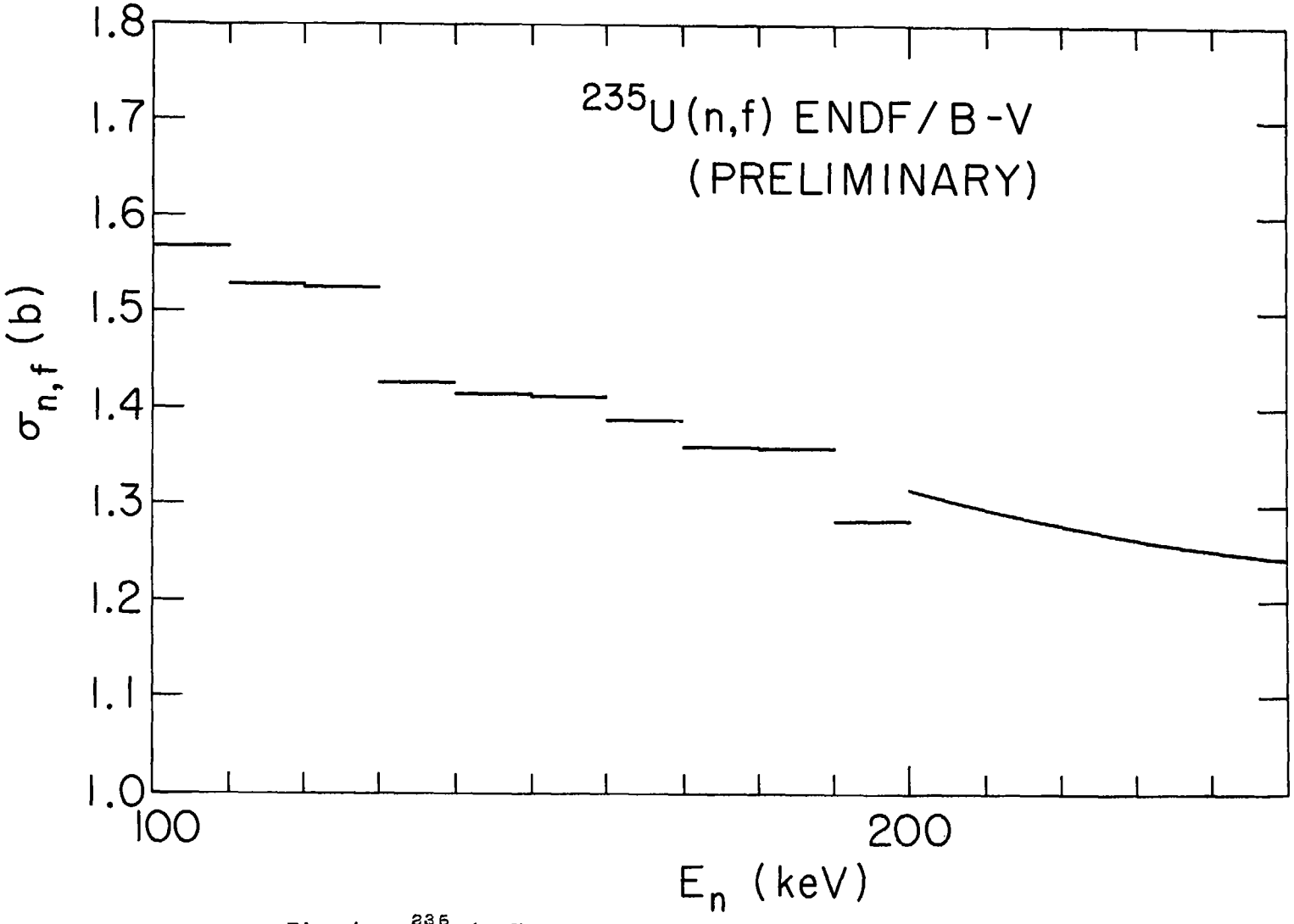

Fig. 4 ^{235}U(n,f) Evaluation 100 - 200 keV

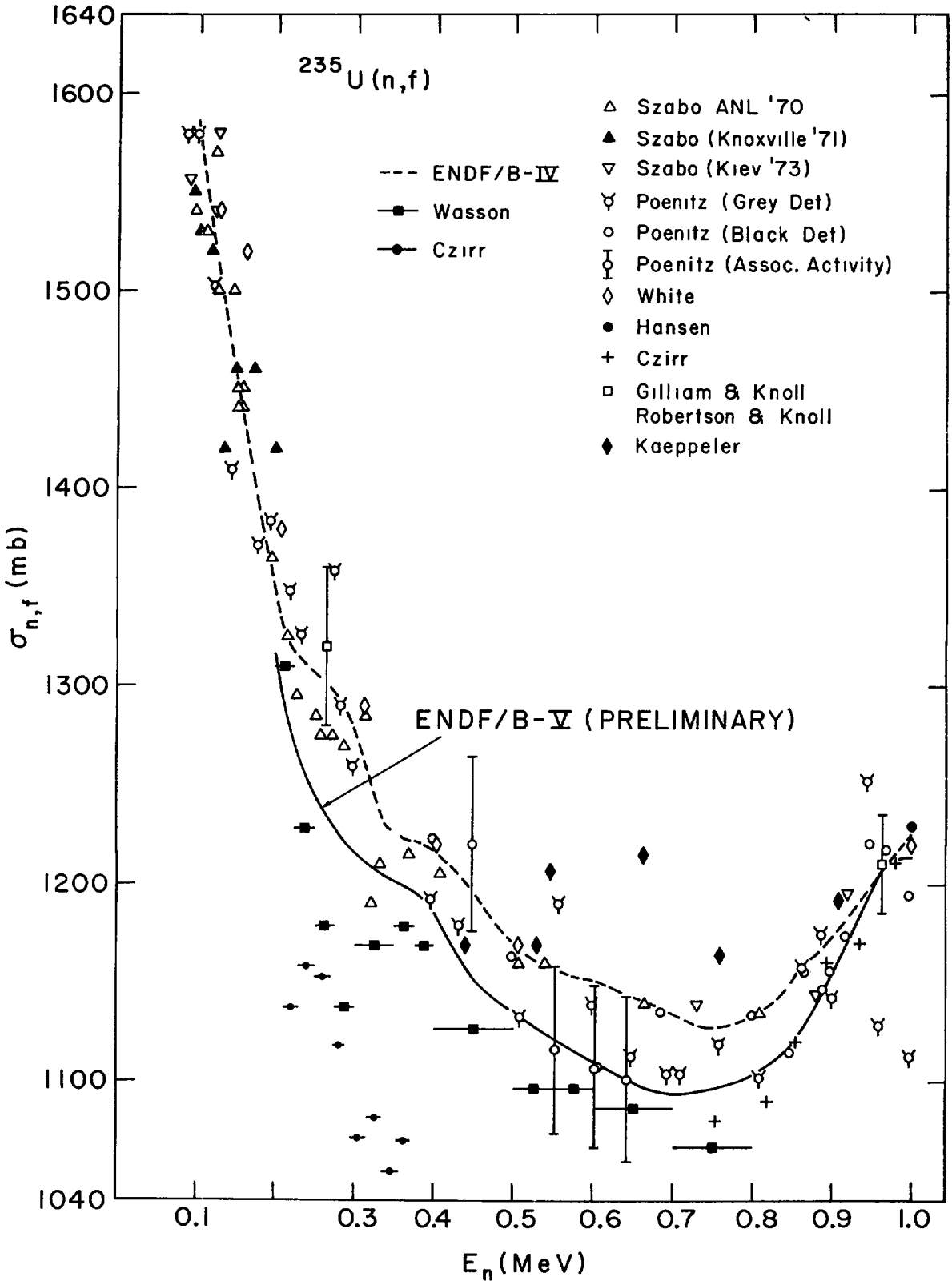

Fig. 5 ^{235}U(n,f) Data and Evaluation 0.1 - 1.0 MeV

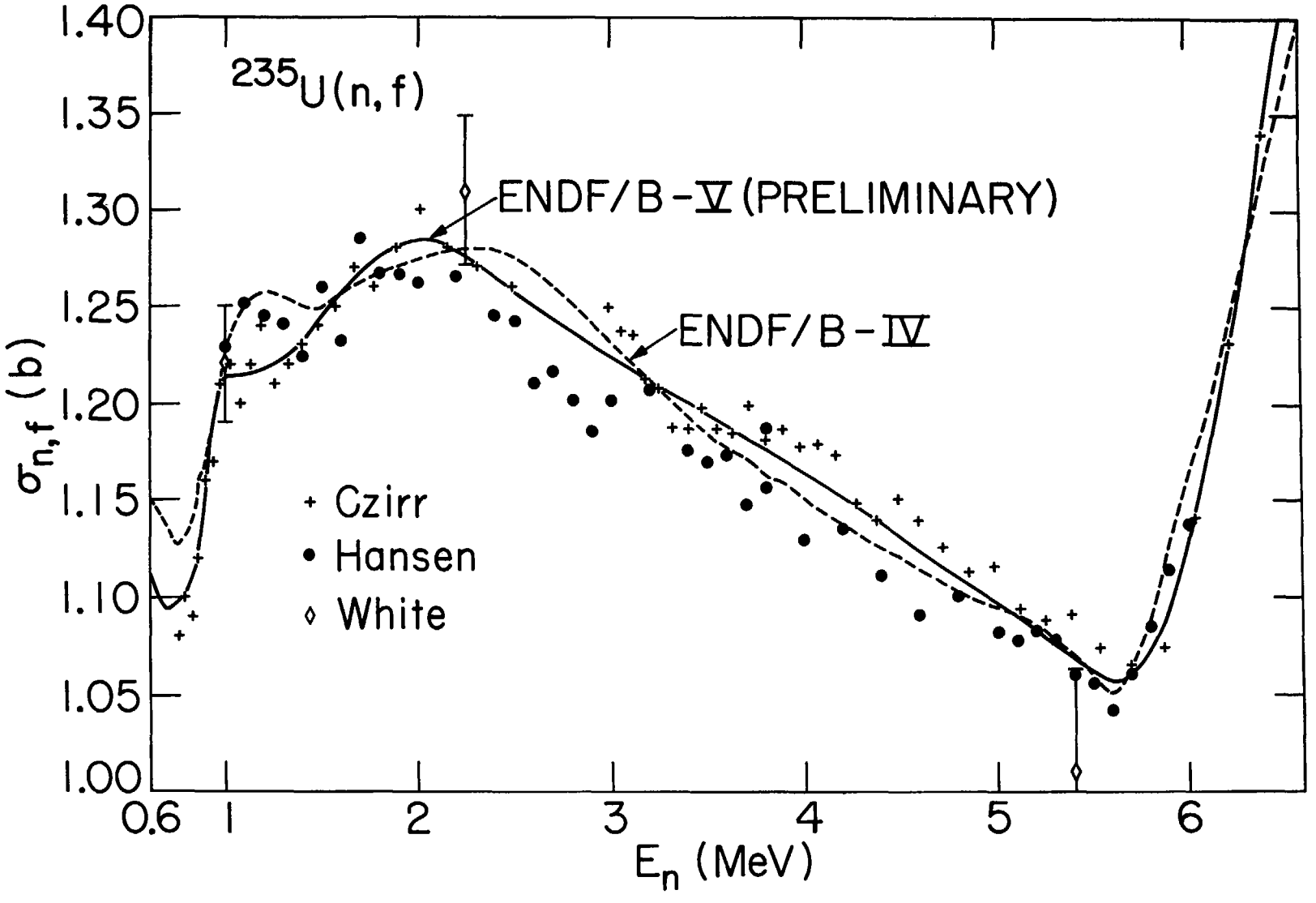

Fig. 6 ^{235}U(n,f) Data and Evaluation 0.6 - 6.6 MeV

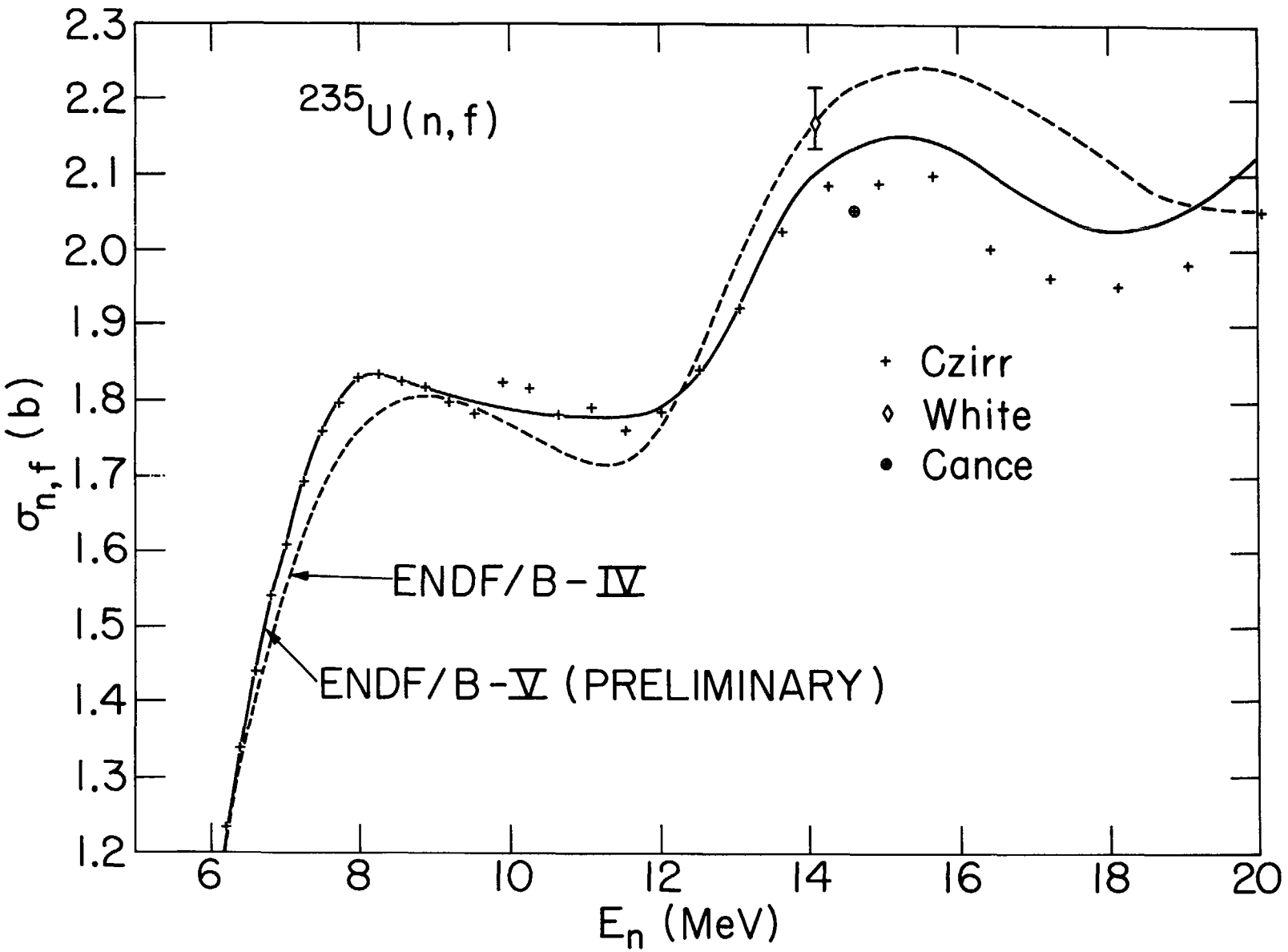

Fig. 7 $^{235}U(n,f)$ Data and Evaluation 5.0 - 20.0 MeV

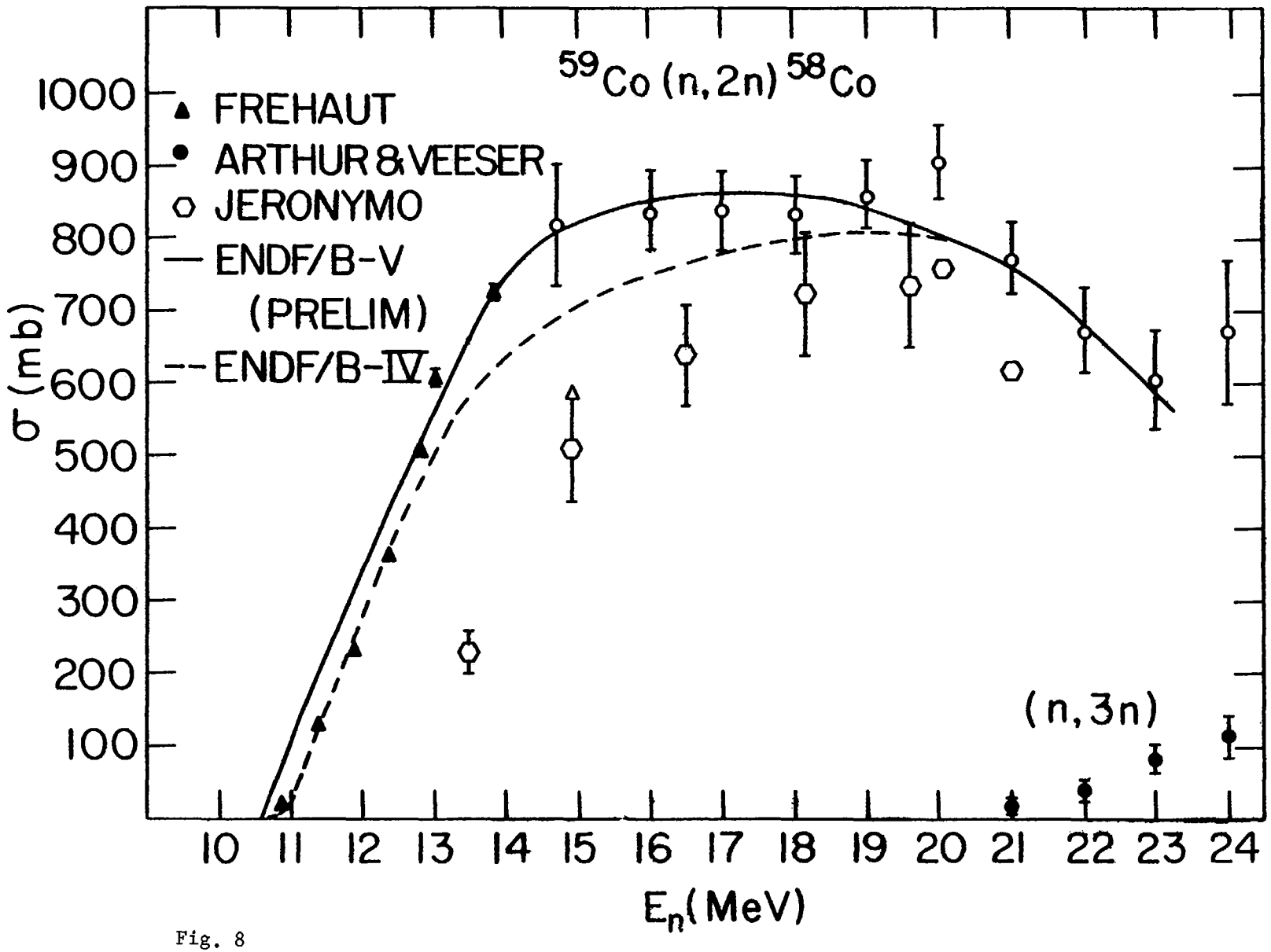
^{59}Co (n, 2n) ^{58}Co
FREHAUT
ARTHUR & VEESER
JERONYMO
ENDF/B-V
(PRELIM)
ENDF/B-IV
(n, 3n)
σ (mb)
E$_n$ (MeV)
1000
900
800
700
600
500
400
300
200
100
10
11
12
13
14
15
16
17
18
19
20
21
22
23
24

Fig. 8

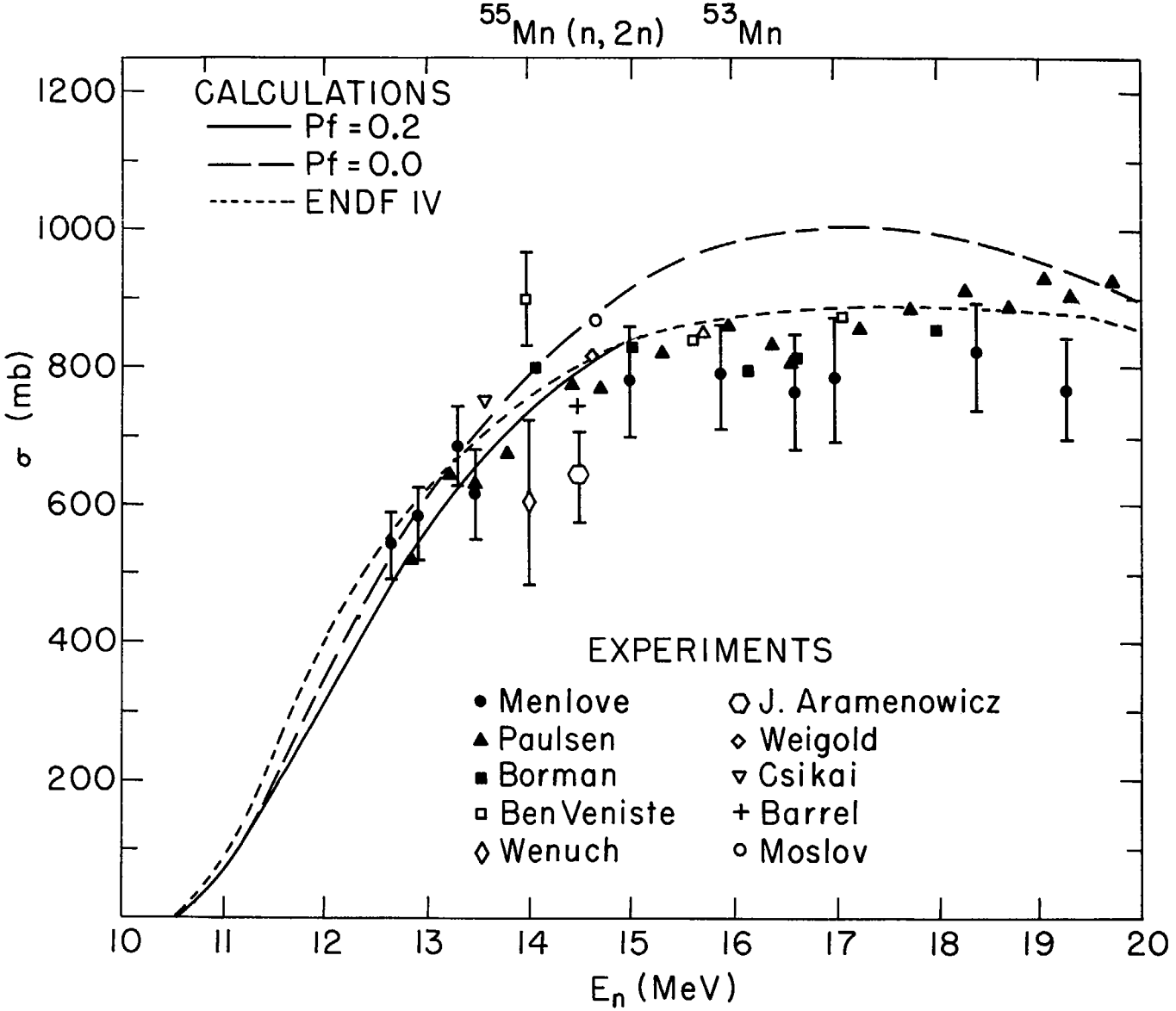
55Mn (n, 2n) 53Mn
CALCULATIONS
Pf = 0.2
Pf = 0.0
ENDF IV
EXPERIMENTS
Menlove
Paulsen
Borman
Ben Veniste
Wenuch
J. Aramenowicz
Weigold
Csikai
Barrel
Moslov
σ (mb)
En (MeV)
1200
1000
800
600
400
200
10
11
12
13
14
15
16
17
18
19
20

Fig. 9

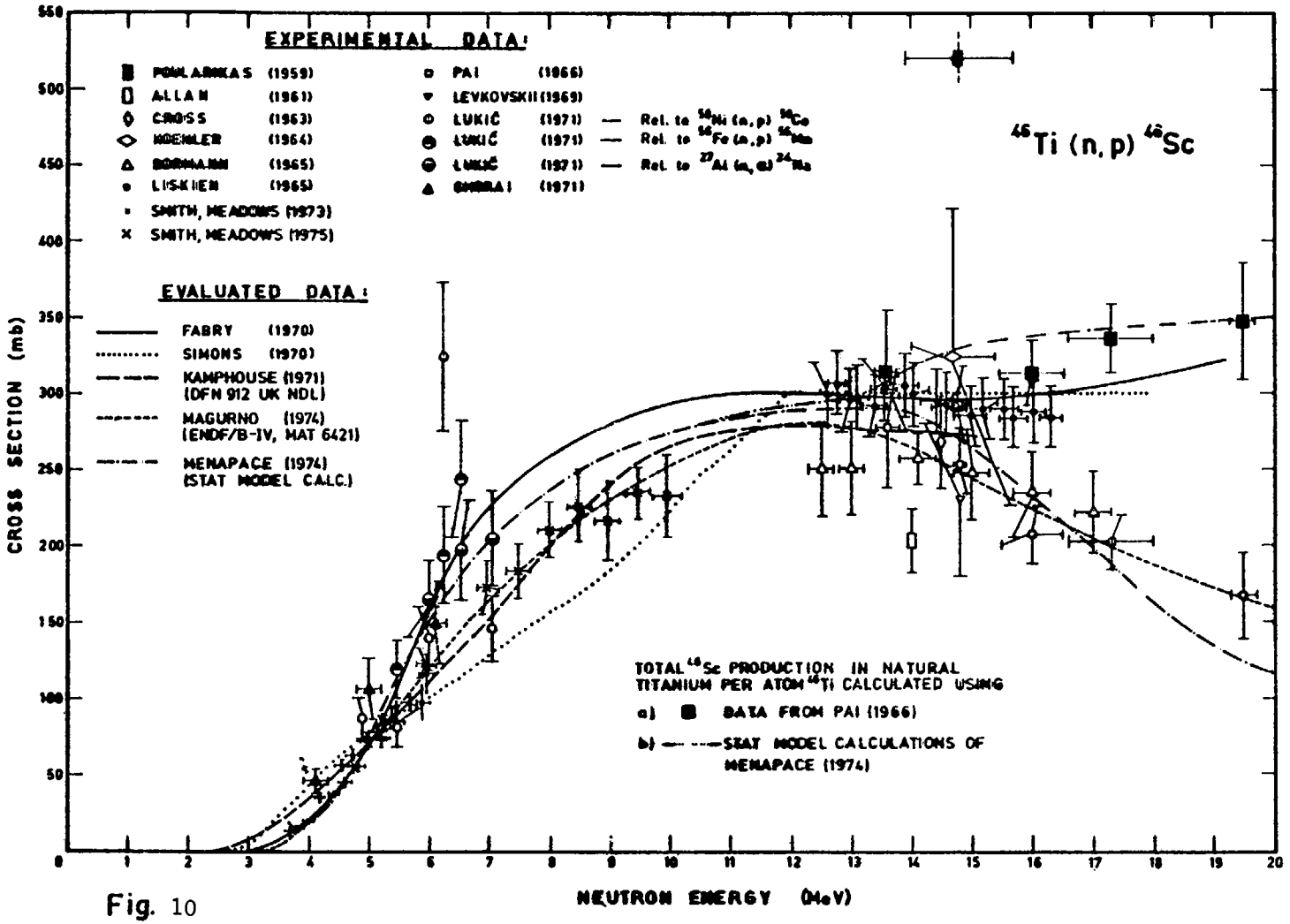
EXPERIMENTAL DATA:
POULARIKAS (1959)
ALLAN (1961)
CROSS (1963)
MOEHLER (1964)
BORMANN (1965)
LISKIEN (1965)
SMITH, MEADOWS (1973)
SMITH, MEADOWS (1975)
PAI (1966)
LEVKOVSKII (1969)
LUKIĆ (1971) — Rel. to ^{58}Ni (n,p) ^{58}Co
LUKIĆ (1971) — Rel. to ^{56}Fe (n,p) ^{56}Mn
LUKIĆ (1971) — Rel. to ^{27}Al (n,α) ^{24}Na
GHORAI (1971)
EVALUATED DATA:
FABRY (1970)
SIMONS (1970)
KAMPHOUSE (1971) (DFN 912 UK NDL)
MAGURNO (1974) (ENDF/B-IV, MAT 6421)
MENAPACE (1974) (STAT MODEL CALC.)
^{46}Ti (n, p) ^{46}Sc
TOTAL ^{46}Sc PRODUCTION IN NATURAL TITANIUM PER ATOM ^{46}Ti CALCULATED USING
a) DATA FROM PAI (1966)
b) STAT MODEL CALCULATIONS OF MENAPACE (1974)
CROSS SECTION (mb)
NEUTRON ENERGY (MeV)

Fig. 10

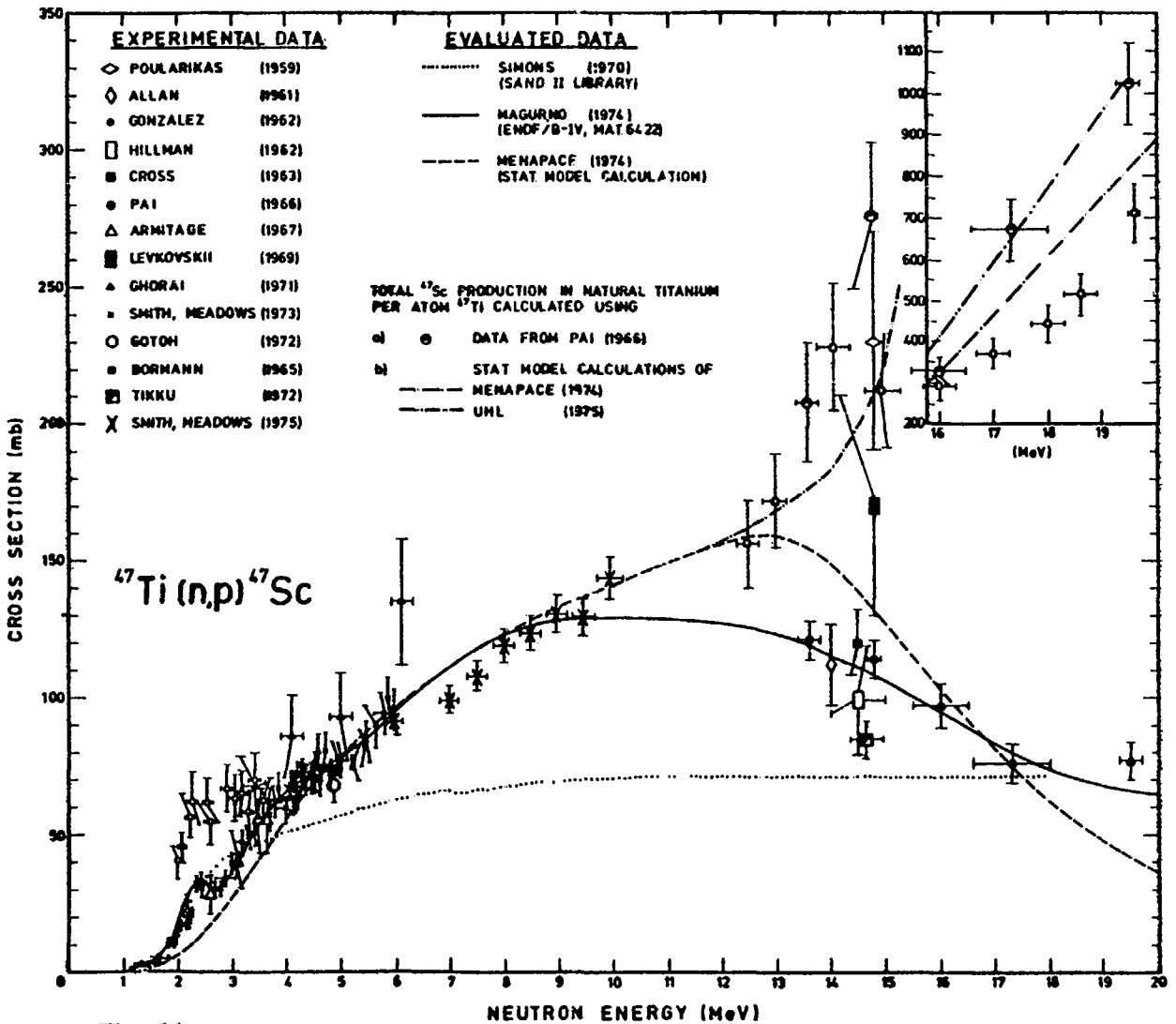
EXPERIMENTAL DATA
POULARIKAS (1959)
ALLAN (1961)
GONZALEZ (1962)
HILLMAN (1962)
CROSS (1963)
PAI (1966)
ARMITAGE (1967)
LEVKOVSKII (1969)
GHORAI (1971)
SMITH, MEADOWS (1973)
GOTOH (1972)
BORMANN (1965)
TIKKU (1972)
SMITH, MEADOWS (1975)
EVALUATED DATA
SIMONS (1970) (SAND II LIBRARY)
MAGURNO (1974) (ENDF/B-IV, MAT 6422)
MENAPACE (1974) (STAT. MODEL CALCULATION)
TOTAL 47Sc PRODUCTION IN NATURAL TITANIUM PER ATOM 47Ti CALCULATED USING
a) DATA FROM PAI (1966)
b) STAT MODEL CALCULATIONS OF
MENAPACE (1974)
UHL (1975)
47Ti (n,p) 47Sc
CROSS SECTION (mb)
NEUTRON ENERGY (MeV)
(MeV)

Fig. 11

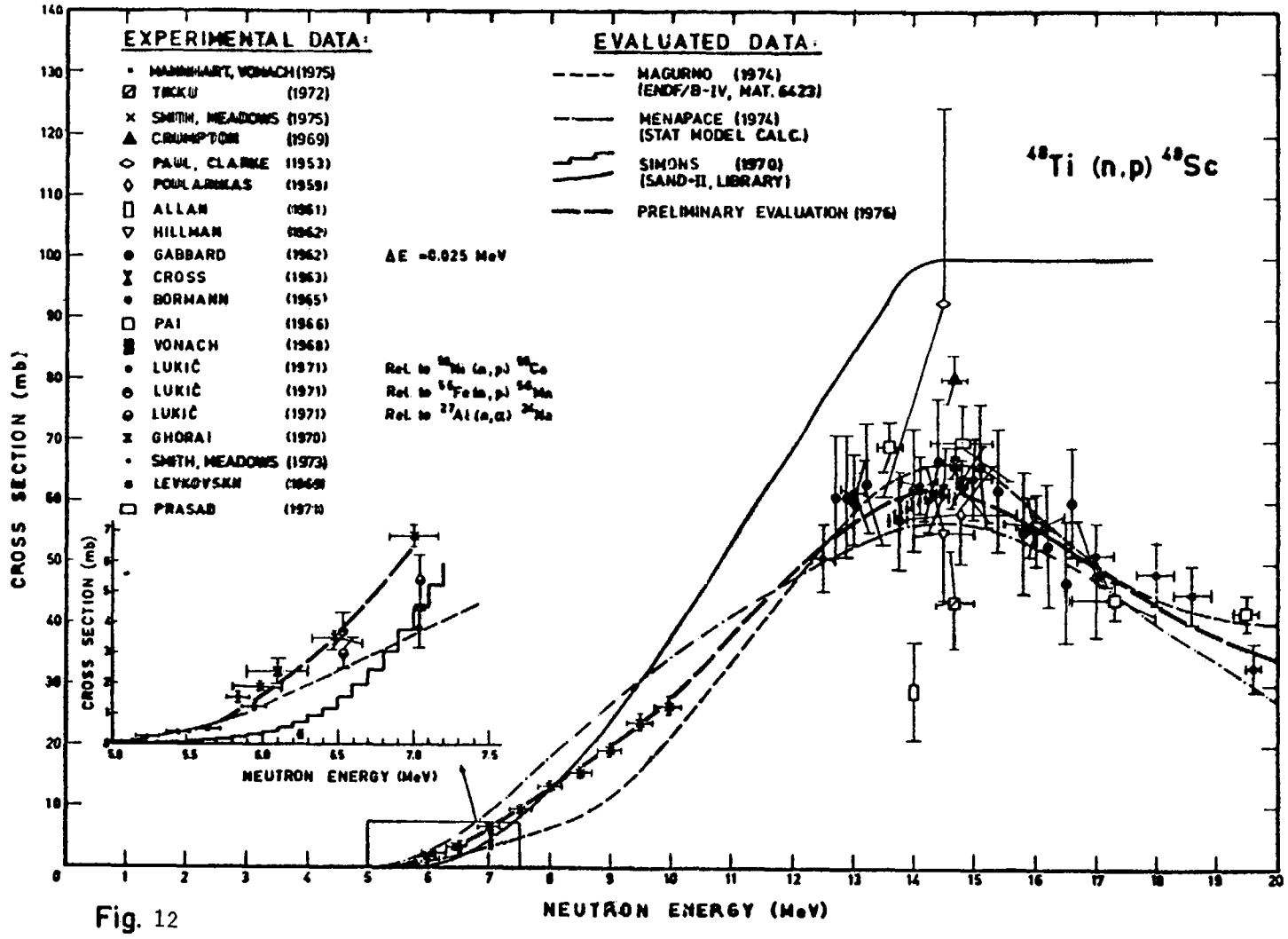
EXPERIMENTAL DATA:
EVALUATED DATA:
MAGURNO (1974)
(ENDF/B-IV, MAT. 6423)
MENAPACE (1974)
(STAT MODEL CALC.)
SIMONS (1970)
(SAND-II, LIBRARY)
PRELIMINARY EVALUATION (1976)
TICKU (1972)
SMITH, MEADOWS (1975)
PAUL, CLARKE (1953)
ALLAN (1961)
HILLMAN (1962)
GABBARD (1962)
CROSS (1963)
BORMANN (1965)
PAI (1966)
VONACH (1968)
LUKIČ (1971)
LUKIČ (1971)
LUKIČ (1971)
GHORAI (1970)
SMITH, MEADOWS (1973)
PRASAD (1971)
ΔE =0.025 MeV
^{48}Ti (n,p) ^{48}Sc
CROSS SECTION (mb)
NEUTRON ENERGY (MeV)

Fig. 12

REFERENCES

1. Interlaboratory LMFBR Reaction Rate (ILRR) program established by USAEC/RRD to develop a capability to accurately measure neutron reaction rates for LMFBR fuels and materials development programs.

2. ENDF/B-IV Dosimetry File; Tape 412 issued January 1975.

3. Dosimetry Task Force, organized by Normalization and Standards Subcommittee of CSEWG, held at Battelle-Northwest, March 1972.

4. Nuclear Technology 25 (2), 169-422, Feb. 1975.

5. Magurno and Ozer, Reference 4, pp 376-380.

6. Benchmark Testing of ENDF/B-IV ENDF-230 March 1976.

7. Proceedings of NEANDC/NEACRP Specialists Meeting on Fast Neutron Fission Cross Sections of U-233, U-235, U-238, and Pu-239 June 28-30 Argonne National Laboratory. Ed. W. Poenitz and A. B. Smith.

8. Hale and Dodder (LASL) Li-6 Evaluation submitted for ENDF/B-V.

9. Hale and Arthur (LASL) B-10 Evaluation submitted for ENDF/B-V.

10. S. F. Mughabghab (BNL) Au-197 Evaluation submitted for ENDF/B-V.

11. M. Bhat Reference 7 pp. 307-332

12. L. Stewart LA 4574 1971

13. M. Vlasov International Conference on Interactions of Neutrons with Nuclei Lowell, Mass. July 6-9, 1976

14. Special Meeting of CSEWG Standards Subcommittee, Los Alamos Scientific Laboratory, Aug. 3-5, 1976. Chaired by L. Stewart.

15. A. Fabry ASTM-Euratom Symposium on Reactor Dosimetry Developments and Standardization; Petten, Netherlands 1975.

EVALUATION OF THE CAPTURE CROSS SECTION OF ^{197}AU

S.F. Mughabghab

Brookhaven National Laboratory
Upton, L.I., N.Y. 11973

ABSTRACT

Evaluation of the capture cross section of ^{197}Au is described with emphasis on its use as a standard in the energy region 200-3500 keV where the cross section appears to vary smoothly with energy. In this energy region, the capture cross section is presented in graphical and tabular forms.

A INTRODUCTION

Because of its monoisotopic nature, its chemical purity, its large thermal neutron capture cross section and absorption resonance integral [1], and the simple decay scheme of the product nucleus formed by neutron capture, the capture cross section of gold has become one of the primary basic standards. For these reasons, and the fact that several recent measurements appeared in the literature and became available through private communications, it became evident and essential that a new evaluation of the capture cross section of gold is warranted. An additional reason is the requirement for a consistent set of primary standards on (n,p), ^{6}Li(n,α), ^{10}B(n,α) and ^{235}U(n,f) for ENDF/B-V. This evaluation was carried out in conjunction with the Standards and Normalization Subcommittee of CSEWG and its Task Force [a].

As indicated by the data of Macklin, et.al., [2] and Le Rigoleur, [3], substantial structure possibly attributable to doorway states, is observed in the gold capture cross section up to about 200 keV. Above this energy, the capture cross section seems to vary smoothly with energy. Because of this situation, and with the exception of the thermal energy region, the point-wise capture cross section of ^{197}Au is de-emphasized as a standard below 200 keV. In the present note, we primarily describe the ENDF/B-V evaluation of the gold capture cross section in the energy range from 200 keV-3500 keV and outline the procedures followed in the resonance region and high energy region (3.5 - 20.0 MeV).

[a] The Au Task Force Members are: B.R. Leonard, Jr., (BNW) (Chairman); M.R. Bhat, (BNL) A.D. Carlson (NBS), M.S. Moore (LASL) S.F. Mughabghab (BNL), R.W. Peelle (ORNL), W.P. Poenitz (ANL), L. Stewart (LASL).

Although the presently described gold capture cross section (200 - 3500 keV) has been approved by the Standards and Normalization Subcommittee of CSEWG, it should be considered preliminary until approved by CSEWG. This evaluation differs from its predecessor [4] in that the input data measured relative to a standard cross section, were renormalized to other approved primary standards to give a consistent set of standard cross sections. Because of the various inter-relations between the primary standard cross sections, (n,p) ^{6}Li(n,α), ^{10}B(n,α), ^{197}Au(n,γ), ^{235}U(n,f), an attempt was made by various evaluators to obtain a consistent set of standard cross sections. As a result, the evaluations of ^{6}Li(n,α), ^{10}B(n,α), and ^{235}U(n,f) cross sections by Hale and Dodder [5a], Hale and Arthur [5b] and Bhat [6] were adopted here. In addition, the evaluation of the (n,p) cross section carried out by Stewart, et.al., [7], (approved for ENDF/B-V), and which is essentially based on the analysis of Hopkins and Breit [8] was considered in this evaluation. For details of the ^{6}Li(n,α) and ^{10}B(n,α) cross section analysis in terms of R matrix analysis, the reader is referred to reference [9].

B ^{197}Au Capture Cross Section Between 200-3500 keV

The first step in this evaluation is to assemble the input data from the NNCSC data files, CSISRS (Cross Section Information Storage and Retrieval System) from the literature, and through private communications with the experimenters. A brief summary of the recent data since the last evaluation of gold capture cross section (1972 vintage) is shown in Table 1 which represents the leading author, adopted standard, relative to which gold capture cross sections is measured, the neutron energy range, method (activation or prompt γray measurement), monitor and sample detectors, and reported accuracy. The data can be found in references 2,3 and 10-27 or in the NNCSC data files, CSISRS. Data prior to 1972 can be found in reference 4. At first, the totality of the old and recent data were divided into two groups depending on whether the measurement is designated as absolute or relative. Subsequently, the relative gold capture cross sections were separated into four groups corresponding to one of the adopted standards (n,p), ^{6}Li(n,α), ^{10}B(n,α) or ^{235}U (n,f). In those cases where the ratio values were not reported by the authors, these were reconstructed whenever enough information was provided by the authors. As an example, the ^{6}Li(n,α) cross section adopted by Macklin, et.al., [2] in his flux measurements, was derived here from the reported prescription and the ratio values of the gold capture cross section to the ^{6}Li(n,α) cross section were obtained. Then various ratio values corresponding to each standard were plotted separately and were initially compared with the ratio values derived from ENDF/B-IV. Such a procedure is helpful in discerning any systematic trends in the data as may be indicated by high or low values or possible changes in the shape of the relative cross sections. Ratio values which deviated by more than two standard deviations from ENDF/B-IV or the average of the experimental values were rejected.

Figs 1 and 2 show the renormalized recent data in the energy ranges 100-1000 keV and 1.0-3.5 MeV respectively. For comparison ENDF/B-IV and ENDF/B-V (preliminary) evaluations are shown. At the abscissa, thresholds of the inelastic channels and their spins are indicated by vertical lines.

The following observations could be made regarding these data:

(1) data of Macklin, et.al., [2], Lindner, et.al., [10] and Le Rigoleur [3] are generally in very good agreement.

(2) as shown by Fort and Le Rigoleur [3] the activation and non-activation measurements are in reasonable agreement with each other particularly in the energy region 400 - 500 keV where the deviation is only about 2%.

(3) data of Paulsen, et.al., [12] Fricke, et.al., [23] and Barry, et.al., [24] measured relative to the (n,p) cross section are consistently high with respect to the ENDF/B-IV evaluation and with the data of Macklin, et.al., [2], Lindner, et.al., [10], Poenitz [11], and Fort and Le Rigoleur [3]. This may have to do with response of the hydrogen proportional counter.

(4) in the energy range 1000 - 3500 keV, the data of Paulsen, et.al., [12] appears to converge, particularly at the high energy end, with that of Poenitz [11] and Lindner, et.al., [10].

(5) the Robertson, et.al., [25] cross section value at 966 keV is about 12% high with respect to Poenitz [11], Lindner, et.al., [10] and ENDF/B-IV evaluation but somehow in agreement with the data point of Paulsen, et.al., [12]. Since it is believed that there is no structure in the gold capture cross section at this energy, the result of Robertson, et.al., [25] was down-graded.

(6) the apparent structure in Macklin, et.al.'s renormalized data at about 250 keV is partially due to a lack of a precise knowledge of the peak position of the resonance at about this energy.

(7) the data of Czirr and Stelts [17] is high when compared with other data, and with the ENDF/B-IV evaluation. It is to be noted that the data points at 319, 412, and 532 keV were withdrawn by the authors.

On the basis of these observations, it was decided to base the ENDF/B-V evaluation on the data sets of Macklin, et.al., [2] Fort and Le Rigoleur [3], Poenitz [11], and Lindner, et.al., [10] in the energy range 100 - 1000 keV. Above 1000 keV, the ENDF/B-IV evaluation is based on the Poenitz [11] and Lindner's, et.al.'s [10] data. The result of this is essentially to decrease the capture cross section of gold by not more than about 4%. This is about the magnitude of uncertainty of the gold capture cross section in this energy range. The ENDF/B-V capture cross section in the energy range 200 - 3500 keV is given in Table II. A detailed analysis of the variance-covariance estimates of the ^{197}Au capture cross section will be carried out.

C ^{197}Au Capture Cross Section in the Resolved and Unresolved Energy Regions.

Because of the presence of structure in the gold capture cross section, it was decided by the Standards and Normalization Subcommittee of CSEWG to extend the resolved energy region from 2.0 to 4.8 keV. Unfortunately, individual resonance parameters (Γ_n, Γ_γ, J, values) are not available as yet. The $g\Gamma_n\Gamma_\gamma/\Gamma$ values of Macklin, et.al., [2] are combined with renormalized $g\Gamma_n^2/\Gamma$ values of Hoffman, et.al., [28] to obtain J, Γ_n, Γ_γ values for the individual resonances.

A comparison of the $g\Gamma_n^2/\Gamma$ values of Hoffman, et.al., [28] with those derived from BNL 325, [1] shows that the values of these authors are under-estimated by about a factor of 3.5 for the strong resonances. As a result correction factors have been applied to the data [28] before combining them with those of Macklin, et.al., [2].

In the unresolved energy region, 5 - 200 keV, the point-wise cross section as supplied by Macklin, et.al., [2] will be adopted. In addition s- and p-wave and Yray strength functions which describe the capture cross section in this energy range will be specified.

D ^{197}Au Capture Cross Section in Energy Range 3.5-20 MeV

In this energy region, experimental data is sparse. These include the data of Johnsrud, et.al., [29] and Miskel, et.al., [30] both of which used the activation technique and measured the flux with a fission counter. Between 4 MeV and 20 MeV, only 14 MeV data by Drake, et.al., [20] and Schwerer, et.al., [21] are available, which indicate that the capture cross section of gold at 14 MeV is about 1mb. As a result, the ENDF/B-V evaluation between 3.5-20 MeV is based on COMNUC calculations which are normalized to a value of 14 mb at 4.8 MeV (renormalized Johnsrud, et.al., [29] data point), and 1mb at 14 MeV.

E Comparison With Integral Measurements

It is of interest to calculate the fission spectrum average of the capture cross section and compare it with experimental measurements. Absolute capture cross section measurements for ^{197}Au for ^{252}Cf spontaneous fission neutrons was carried out recently by Green [31] who reported a value of 79.9±2.9 mb. In addition, Fabry, et.al., [32] reported an integral cross section ratio measurements of ^{197}Au(n,Y) relative to ^{238}U(n,f) for a thermal-neutron induced ^{235}U fission neutron spectrum. Adopting a value of 295.4 mb for ^{238}U(n,f) fission spectrum average from the ENDF/B-IV dosimetry file [33], one obtains a value of 85 ± 4 mb for ^{198}Au(n,Y).

A Maxwellian fission spectrum of characteristic temperature T and represented by:

$$\Phi(E) = C\sqrt{E}\, e^{-\frac{E}{T}} \qquad (1)$$

was employed (C is a normalizing constant). Values for T of 1.32 MeV (ENDF/B-IV) and 1.39 MeV were used in the calculations for ^{235}U and ^{252}Cf fission spectra respectively.

The ^{235}U and ^{252}Cf fission spectrum averages of the ENDF/B-V gold capture cross section are calculated with aid of Eq 1, and are shown in Table III. The evaluated values are compared with experimental numbers [31, 32, 34].

F Comparison With ENDF/B-IV

Since the last evaluation of gold, two measurements of the thermal absorption cross section of Au at 2200 m/sec by Dilg, et.al., [35] and Steyerl, et.al., [36] were reported. Both of these authors used the transmission method in

their measurements and they reported σ_o = 98.68 ± 0.12 b and 99.3 ± 0.5 b for Au respectively. The recommended σ_o value in this evaluation will be the same as in its predecessor.

The resonance region in this evaluation will be extended to 4.9 keV to include the Macklin, et.al., [2] and Hoffman, et.al., [28] measurements. The unresolved region up to 200 keV will be represented by point-wise data of Macklin, et.al., [2] to describe the structure observed in the capture cross section. In addition, s-, p- wave neutron and γ ray strength functions will be specified. In the previous evaluation the unresolved region was described only by strength functions. Furthermore, data measured relative to the fission cross section of ^{235}U were disregarded in the previous evaluation in the energy region 100 - 1000 MeV. In the present evaluation such data were incorporated in the analysis. Between 300 - 3500 keV the present evaluation is 3 - 4% lower than ENDF/B-IV. Above 3.5 MeV, the present evaluation is based on model calculations and normalized to experimental values of 1 mb at 14 MeV and 14 mb at 4.8 MeV. In contrast, the ENDF/B-IV evaluation was based on ENDF-III which in turn was essentially based on the Vaughn and Grench [37] and Bogart [38] evaluations.

CONCLUSION

Gold capture cross section in the energy region 200 - 3500 keV is emphasized as a primary standard. The uncertainty in the evaluated curve is about 4%. The datum point of Robertson, et.al., [25] needs additional study and confirmation. In addition, the high data points of Paulsen, et.al., [12] measured relative to the (n,p) scattering cross section calls for further investigations. It is suggested perhaps the same authors carry simultaneous measurements relative to (n,p) and some other standard, or perhaps a study of the response of the hydrogen proportional counter is warranted.

Comparison of integral measurements with the present evaluation yields good agreements.

ACKNOWLEDGMENTS

I would like to acknowledge fruitful and critical discussions with B.R. Leonard, Jr., (BNW), M.R. Bhat (BNL), A.D. Carlson (NBS), M.S. Moore (LASL), R.W. Peelle (ORNL), W.P. Poenitz (ANL), and L. Stewart (LASL). This work was supported by the U.S. Energy Research and Development Administration.

REFERENCES

1. S.F. MUGHABGHAB and D.I. GARBER, BNL-325, Neutron Cross Sections, Vol. 1, 3rd edition (1973).

2. R.L. MACKLIN, J.HALPERIN, AND R.R. WINTERS, Phys. Rev/C, 11, 1270 (1975).

3. E. FORT and C. LE RIGOLEUR, NBS special publication 425, Vol. 2, 957 (1975) and private communication. This represents two data sets, one by FORT using the activation technique, other by LE RIGOLEUR using prompt γ rays.

4. S.F. MUGHABGHAB, A. PRINCE, M.D. GOLDBERG, M.R. BHAT, and S. PEARLSTEIN BNL 50439 (ENDF-215) 1974.

5. [a] G.M. HALE and D.C. DODDER, [b] G.M. HALE and E.D. ARTHUR, Los Alamos Scientific Laboratory, private communication. To be published.

6. M.R. BHAT, Brookhaven National Laboratory, private communication. To be published.

7. L. STEWART, R.J. LABAUVE, and P.G. YOUNG, "Evaluated Nuclear Data for Hydrogen in the ENDF/B-II Format" USAEC Rep. LA-4575, Los Alamos Scientific Laboratory (1971).

8. J.C. HOPKINS, and G. BREIT "The ^{1}H(n,n) ^{1}H Scattering Observables Required for High Precision Fast-Neutron Measurements" Nuclear Data A9, 137 (1971).

9. G.M. HALE, NBS special publication 425, Vol. 1, 302 (1975).

10. M. LINDNER, R.J. NAGLE, and J.H. LANDRUM, Nucl. Sci. Eng. 59, 381 (76) and private communication.

11. W.P. POENITZ, Nucl. Sci. Eng. 57, 300 (1975).

12. A. PAULSEN, R. WIDERA, and H. LISKIEN, Atomkernenergie, 26, 80 (1975).

13. K. RIMAWI and R.E. CHRIEN, NBS special publication 425, Vol. 2, 920 (1975).

14. V.S. SHORIN, V.N. KONONOV, and E.D. POLETAEV Yad. Fiz. 19, 5 (1975) A/N 40222.

15. N. YAMAMURO, T. DOI, T. HAYASE, Y. FUJTA, K. KATSUHEI, and R.C. BLOCK private communication.

16. C.L. LE RIGOLEUR, A. ARNAUD, and J. TASTE, CEA-N-1662, 1973.

17. J.B. CZIRR and M.L. STELTS, Nucl. Sci. and Eng. 52, 299 (73).

18. R. GWIN, E.G. SILVER, R.W. INGLE, and H. WEAVER, Nucl. Sci. Eng. 59, 79 (76).

19. K. SIDDAPA, M. SRIRAMACHANDRA MURTY, and J. RAMA RAO, Nuovo Cimento 18A. 218 (73).

20. D. DRAKE, I. BERGGUIST, and D.K. MC DANIELS Phys. Letters 36B, 557 (1971), private communications A/N 10193/5.

21. O. SCHWERER, M. WINKLER-ROHATSCH, H. WARHANCK, and G. WINKLER, Nucl., Phys. A264, 105 (1976).

22. LE RIGOLEUR CEA-N-1662 (1973).

23. M.P. FRICKE, W.M. LOPEZ, S.J. FRIESENHAHN, A.D. CARLSON, and D.G. COSTELLO, Proc. Nuclear Data for Reactors, Conference, Helsinki, Vol. 2, 281 (1970).

See also FRICKE, et.al., Neutron Cross Sections and Technology, Vol. 1, p252 (1971) Knoxville, Tennessee.

24. J.F. BARRY, J. Nucl. Energy 18, 491 (1964).

25. J.C. ROBERTSON, T.B. RYVES, E.J. AXTON, I. GOODIER, and A. WILLIAMS Jour. Nucl. Ener. 23, 205 (1969).

26. V.B. CHELNOKOV, V.A. TOLSTIKOV, YU. YA. STAVISSKY, A.A. BERGMEN, and A.E. SAMSONOV, INDC(CCP)-32/U 1973.

27. BAJKALOV, et.al., Kiev 75 (350-900 keV) from CINDA. Data unavailable yet.

28. M.M. HOFFMAN, G.J. BERZINS, W.M. SANDERS, L.J. BROWN, D.D. PHILLIPS, Neutron Cross Sections and Technology, Vol. 2, p868 (1971) Knoxville.

29. A.E. JOHNSRUD, M.G. SILBERT, and H.H. BARSHALL, Phys. Rev. 116, 927 (1959).

30. J.A. MISKEL, K.V. MARSH, M.LINDNER, and R.J. NAGLE, Phys. Rev. 128, 2717 (1962).

31. L. GREEN, Nucl. Sci. and Eng. 58, 361 (1975).

32. A. FABRY, J.A. GRUNDL and C. EISENHAUER, NBS special publication 425, Vol. 1, 254 (1975) Nuclear Cross Sections and Technology.

33. ENDF/B-IV Dosimetry File Edited by B.A. MAGURNO BNL-NCS-50446 (1975).

34. H. PAUW and A.H. W. ATEN, JR., Nucl. Energy 25, 457 (1971).

35. W. DILG, W. MANNHART, E. STEICHELE, and P.ARNOLD, Z. Physik 264, 427 (1973).

36. A. STEYERL and H. VONACH, Z. Physik 166 (1972).

37. F.J. VAUGH and H.A. GRENCH, Proc. Neutron Cross Sections and Technology Conference, p340 Knoxville, March (1971).

38. B. BOGART, Proc. Neutron Cross Sections and Technology Conference p486, Washingto (March 1966).

Table I Summary of Recent ^{197}Au Data

Author	Standard	Energy Range (keV)	Method	Monitor	Sample Detector	Error
Lindner	ENDF/B-IV ^{235}U	121-2730	activation	^{235}U fission counter	NaI ($4\pi\beta\gamma$)	0.4-2.9%[c]
Macklin	$^{6}Li(n,\alpha)$,[a] 4.9 eV Resonance of Au	2.75-550	prompt γ's	^{6}Li glass scintillator	Total energy detector	3%
Poenitz	absolute	400-3500	prompt γ's	"Black" and "Grey" neutron detector and ^{6}Li-glass detector	large liquid scintillator	10%
Paulsen	(n,p) Hopkins-Breit	200-3000	activation	recoil proportional counter recoil proton telescope counter	Ge-Li	4.4%
Le Rigoleur	^{10}B, ^{6}Li[b]	12.13-159.7	prompt γ's	$^{10}BNaI(T\ell)$, ^{6}Li		
Fort	^{10}B, ^{6}Li	119-503	activation	$^{10}BNaI(T\ell)$, ^{6}Li	β(prop-) γ(NaI)	4-9%
Gwin	^{10}B ENDF/B-III, 4.9 eV Resonance	10-50 keV	prompt γ's	$^{10}BF_3$ ionization chamber	liquid scintillator	
Shorin	^{10}B, 30 keV	5-80	prompt γ's	$^{10}B(n,\alpha\gamma)$ detector	liguid scintillator	~ 5%
Siddapa	$^{127}I(n,\gamma)$ ^{128}I	23±5(5b-Be Source)	activation	^{127}I	Na $I(T\ell)$	10%
Yamamuro	$^{10}B(n,\alpha_1\gamma)$ 5.200 Ag	24(Fe filter)	prompt γ's	$^{10}B(n,\alpha_1\gamma)$	C_6F_6 total energy detector	5%
Rimawi	$^{10}B(n,\alpha\gamma)$ ENDF/B-IV	24(Fe-filter)	prompt γ's	$^{10}B(n,\alpha_1\gamma)$	Ge-Li	2%
Schwerer	$^{27}Al(n,\alpha)$ ^{24}Na	14.6 MeV	activation	$^{27}Al(n,\alpha)$ ^{24}Na	Ge-Li	57%
Drake	$^{208}Pb(n,\gamma)$ ^{209}Pb	14 MeV	spectrum measurement	counter telescope	Na $I(T\ell)$	2.7%
Le Rigoleur	^{10}B NaI	75.25-542.5	prompt γ's	C_6F	C_6F_6 liquid scintillator	3.6-14%

[a] See Ref. [2] for details

[b] Details not specified by authors. See also Fort, et.al., Neutron Standard Reference Data, Proceedings of a Panel, Vienna, Nov. 1972 IAEA p239.

[c] Counting statistics

Table II

ENDF/B-V AU Capture Cross Section 200 - 3500 KeV

E_n(keV)	σ_γ(mb)	E_n(keV)	σ_γ(mb)
200	257.5	560	122.8
210	251.0	580	119.5
220	245.0	600	116.2
230	240.0	650	108.0
240	234.0	700	101.0
250	229.0	750	95.2
260	224.0	800	90.8
270	219.0	850	87.2
280	214.8	900	85.5
290	210.0	950	84.2
300	206.5	1000	83.0
310	201.0	1100	79.2
320	195.0	1200	76.0
330	191.0	1300	73.5
340	186.0	1400	72.0
350	180.5	1500	71.5
360	175.0	1550	71.0
370	171.0	1600	69.0
380	167.0	1700	65.0
390	163.0	1800	61.5
400	159.5	1900	57.8
410	156.0	2000	54.0
420	152.8	2100	50.0
430	150.0	2200	46.0
440	147.0	2300	43.0
450	144.8	2400	40.0
460	142.5	2500	37.5
470	140.2	2600	34.2
480	138.0	2700	32.0
490	136.0	2800	29.5
500	134.0	2900	27.5
520	130.0	3000	26.0
540	126.5	3500	20.5

Table III Comparison With Integral Measurements

Fission Spectrum	Experimental Values (mb)	Present Evaluation. (mb)	Reference
^{235}U(T=1.32 MeV)	84.8 ± 4.1	82.1	Fabry [32]
^{252}Cf(T=1.39 MeV)	79.9 ± 2.9	78.9	Green [31]
	95.5 ± 2.3		Pauw [34]

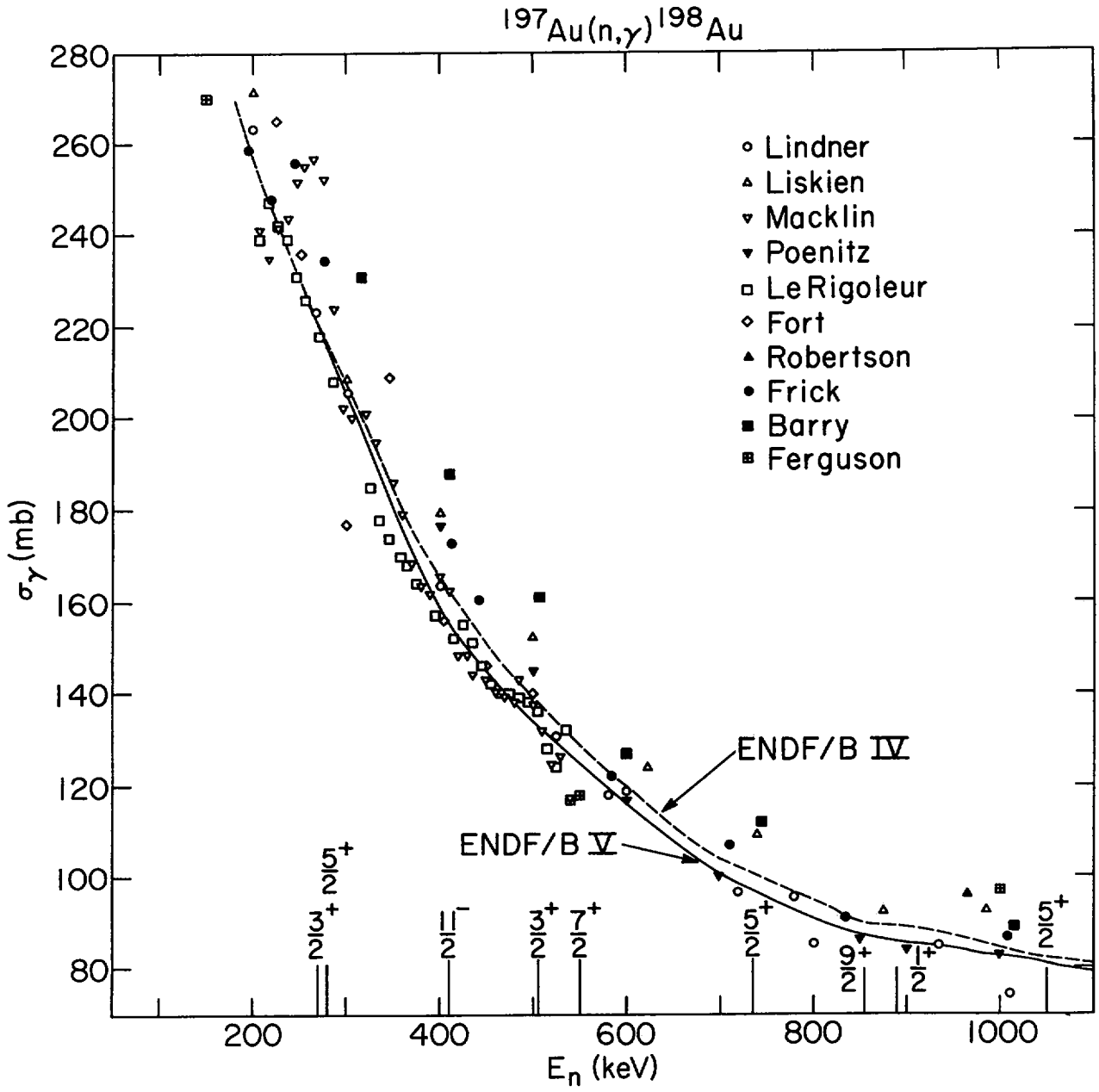

Figure I. Capture cross section of gold in the energy range 200-1000 keV. The vertical lines represent the thresholds for the inelastic channels.

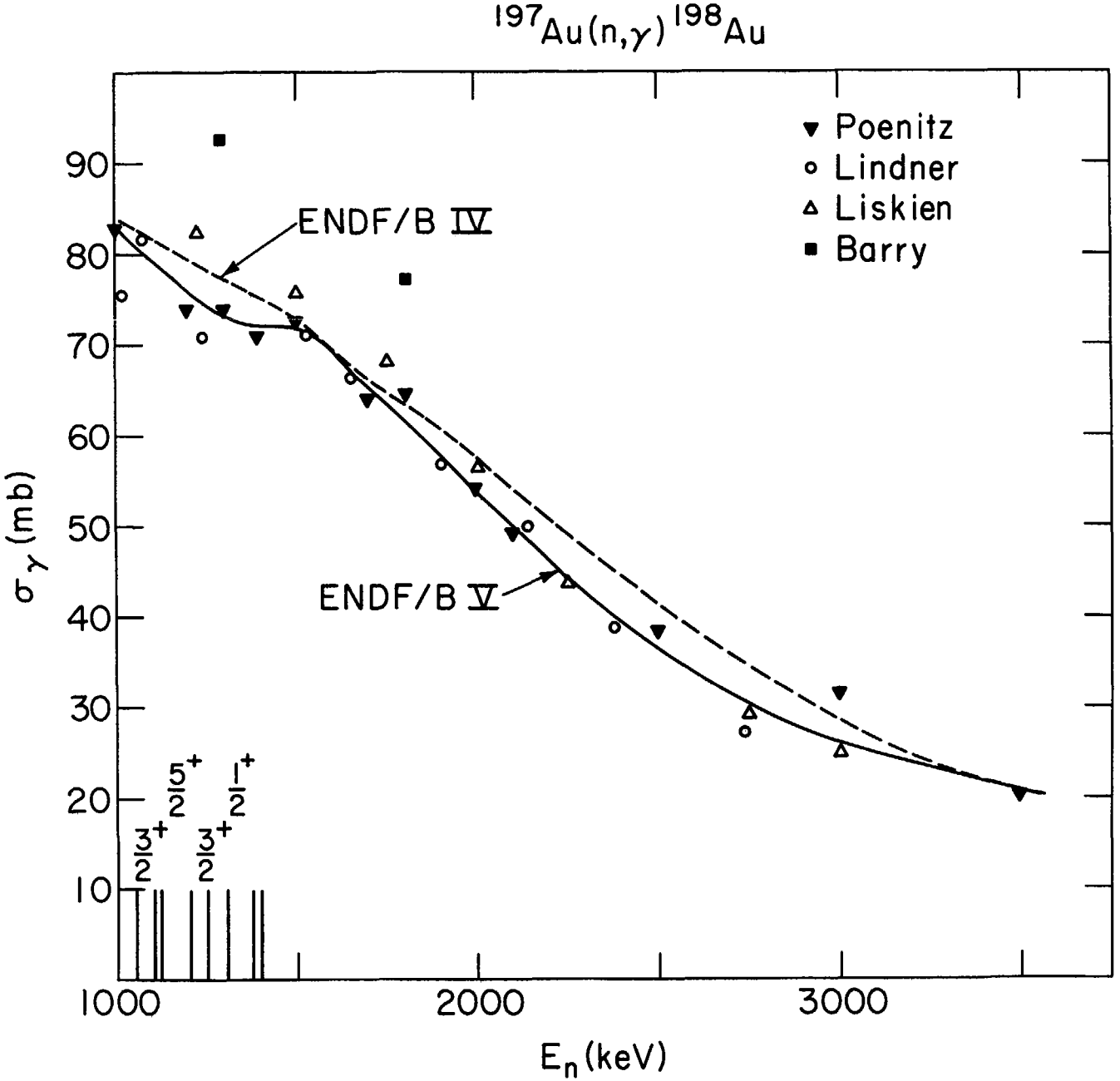

Figure II. Capture cross section of gold in the energy region 1.0 - 3.5 MeV.

APPENDIX II*

$^{58}Ni(n,p)^{\dagger}$, $^{58}Ni(n,2n)$ and $^{60}Ni(n,p)$ Evaluation for ENDF/B-V

M. Divadeenam

$^{58}Ni(n,p)$ reaction Q = .3947 MeV

The previous $^{58}Ni(n,p)$ evaluation was done by Schenter[1]. In the low energy region, his evaluation closely follows the experimentally measured values of Smith and Meadows[2], in that local fluctuations of the cross section are retained in the evaluated curve. In addition, the 6-13 MeV range had only four measured points. However, for the present evaluation, extended measurements by Smith and Meadows[3] are available.

The data on $^{58}Ni(n,p)$ cross section is extensive, and of reliable quality. This reaction is used in dosimetry applications, and also treated as a secondary standard for measuring other neutron induced reactions.

The most extensive sets of data on $^{58}Ni(n,p)$ reaction are:

1) Smith and Meadows[2,3]	0.44 - 10 MeV
2) Meadows and Whalen[4]	1.04 - 2.67 MeV
3) Barry, et.al.,[8]	1.6 MeV - 15 MeV
4) Paulsen and Widera[6]	1-2 and 12.7 - 16.4 MeV
5) Okumura[15]	13.4 - 15 MeV
6) Borman[9]	13 - 19.6 MeV

In addition, there are other measured data sets at few energy points ranging from 2 - 15 MeV.

For the purpose of evaluation, we have looked at the entire experimental data in detail in the following energy ranges:

0.4 - 1.0 MeV
1.0 - 2.0 MeV
2.0 - 4.0 MeV
4.0 - 6.0 MeV
6.0 - 10. MeV
10.0 - 12.7 MeV Gap - no data
12.7 - 15.0 MeV
15.0 - 20.0 MeV

* This Report is extracted from a Report on the evaluation of Nickel for the ENDF/B-V General Purpose File to be published. †For the sake of brevity all the figures referred to in the text are suppressed. Instead one figure (a) giving the entire energy range of evaluation is included.

0.4 - 1.0 MeV:

In this low energy region, only the data of Smith and Meadows[3] is available. There are some deviations from the expected[(1)] smooth energy dependence of the low energy (n,p) cross section. The 0.5 MeV and 1 MeV cross section values were determined from the simple prescription (given in Fermi's book) for exothermic neutron-induced and outgoing charge-particle reactions. Most of the experimental points at these low energies follow this prescription. Our evaluation vs Schenter's evaluation[1] is shown in fig. 1.

1.0 - 2.0 MeV

In this energy range, Smith-Meadows[3], Meadows-Whalen[4], Paulsen-Widera[6], Temperley[5] and Nakai[7] data are shown. Temperley points are too high compared to the general trend of the Smith-Meadows and Meadows-Whalen data. Furthermore, Natai's points have very large errors. Temperley's and Nakai's data were not considered in the evaluation.

As in figure 1, our evaluated curve is shown along with the ENDF/B-IV evaluation in fig. 2.

2.0 - 4.0 MeV

There are several data sets in this energy range. Smith-Meadows data covers most of the range Gonzalez's[20] points, and some of the Konijn's[9] points are high and a few of the latter ones are low beyond 3.5 MeV from the general trend of most of the data points, while Nakai's points are low. Some structure (fluctuation) is evident in the 2.5-4 MeV range especially around 3.0 MeV, and 3.25 MeV in the Smith-Meadows data. For the purpose of evaluation, it was decided to draw a smooth curve to indicate the increasing trend of the experimental points. Schenter's evaluation retained all of the details of local fluctuations. Our evaluated curve and Schenter's is shown for comparison in fig. 3.

4 - 6 MeV

Three data sets cover this energy range - there is some paucity of the data which suggests some fluctuations, however, a smooth curve indicating the increasing trend of the data is drawn as an evaluated curve. As in the other energy regions considered, the ENDF/B-IV evaluation retains most of observed structure in the evaluated curve (cf fig. 4).

6 - 10 MeV

As in the previous energy region, the curve data sets span this energy range Barry's points are higher than that of Smith-Meadows, where as Smith-Meadows has same point scatter. For the evaluation purpose a smooth curve (fig. 5) with a value of 600 mb at 8.5 MeV is suggested as the evaluated curve. Notice Schenter's curve is higher than the present evaluation.

10 - 12.7 MeV

Unfortunately no experimental data exists in this energy region.

12.7 - 15 MeV

From fig. (6) we note that there are plenty of experimentally measured σ_{np} cross sections in the 14-15 MeV range. Point scatter is very large in the measured cross sections. Decowski's points are way high - above the general trend of the other points in this energy region. Curve through most of the points in the 14-15 MeV range is drawn in this region. The choice to draw an evaluated curve is not unique.

15 - 20 MeV

Two data sets cover this energy range, that of Paulsen-Widera and Borman[9] extending only up to 18 MeV. A curve through mid-way between these two sets is drawn. This is justified as the ground that HF calculations with 0.3 pre-compound fraction predicts a similar trend.

Errors:

^{58}Ni(n,p)	errors
0 - 1 MeV	25%
1 - 2 MeV	10%
2 - 4 MeV	9%
4 - 6 MeV	5%
6 - 10 MeV	5%
10 - 12.7 MeV	- (10%)
12.7 - 15 MeV	15%
15 - 20 MeV	13%

References

1) R. Schenter, in ENDF/B-IV Dosimetry File, Edited by B. Magurno, BNL-NCS-50446 (19 5).

2) D.L. Smith and J.W. Meadows
Trans. Am. Nucl. Soc. 16, 1 (1973)
Nucl. Sc. and Eng.

3) D.L. Smith and J.W. Meadows, private communication to M.R. Bhat.
These authors measured ^{58}Ni(n,p) reaction cross section by activation method for neutron energies from near threshold to 10 MeV. The cross sections were determined relative to the ^{235}U and ^{238}U fission cross sections.

0.44 - 3-96 MeV	relative to	^{235}U(n,f)
4.008 - 5-87 MeV	relative to	^{238}U(n,f)
5.398 - 9-87 MeV	relative to	^{238}U(n,f)
2.854 - 3-994 MeV	relative to	^{235}U(n,f)
4.019 MeV	relative to	^{238}U(n,f)

neutrons from the ^{7}Li(p,n) were used for all the ranges given above except for the 5.398-9.87 MeV range measurements: D(d,n) reaction was used as a source for neutrons. The 2.854-3.994 MeV range measurements were measured with high resolution. The different data sets were normalized to the corresponding ^{235}U(n,f) and ^{238}U(n,f) version V standard cross sections.

4) J.W. Meadows and T.F. Whalen, Phys. Rev. 130,(1963).
Meadows and Whalen measured ^{58}Ni(n,p) ^{58}Co^{m,g} cross section ratios relative to ^{235}U(n,f) cross sections. Resolution varied from 100 keV at 1.04 MeV to 75 keV at 2.67 MeV. Overall error is of the order of 8% for all points above 1.14 MeV. All of the data points have been normalized to the ENDF/B-V ^{235}U(n,f) cross sections[9].

5) J.K. Temperley, Nucl. Sci. and Eng. 40, 331 (1970).
Temperley measured ^{58}Ni(n,p) cross section by activation method. The neutron flux was determined by associated particle counting. Overall error is of the order of 10%.

6) A. Paulsen and Widera, EANDC(E) 1504, 1972
These authors employed the activation technique to measure ^{58}Ni(n,p) cross sections in the 1-6 MeV and 12-17 MeV energy regions. Recoil proton telescope was used to determine the neutron fluency. The quoted errors (< 7%) reflect the total uncertainties in the cross sections.

7) K. Nakai, H. Grotoh and H. Amano, J. Phys. Soc. Japan, 17, 1215 (1962).
Nakai measured σ_{np} from 1.84 - 4.82 MeV neutron energy. No standard information is given in the cited paper. Total uncertainty is 15%. Other data sets in the measured energy region are much more reliable than these are.

References (Cont'd.)

8) J.F. Barry, J. Nucl. Energy Parts A/B, 16, 467 (1962).
The $^{58}Ni(n,p)$ cross sections with respect to the $^{235}U(n,f)$ cross sections were measured. The data set has been renormalized to the version V $^{235}U(n,f)$ cross sections. All errors add up to 10%.

9) J. Konijn and A. Lauber, Nucl. Phys. 48, 191 (1963).
Most of the cross sections are either too high or too low compared to the other data sets in the region of measurements. This data set is not considered in the evaluation.

10) J.J. Van Lueff, N.P. 24, 340 (1961)
σ_{np} at 3.3 MeV is very high compared to the rest, hence not used in the evaluation.

11) M. Borman, Z. Naturforsch, 21A, 988 (1966).
Activation technique was used to measure 13-19 MeV (n,p) cross sections with $^{63}Cu(n,2n)$ and $^{19}F(n,2n)$ reactions as standard cross sections at 14.1 MeV. All errors add up to 10%.

12) R.C. Barral, Nucl. Phys. A138, 387 (1969).
En=14.8 MeV, measured with respect to $^{27}A\ell(n,\alpha)$. Renormalized to the version IV $^{27}A\ell(n,\alpha)$ cross section.

13) G.N. Maslov, F. Nasyrov and Paslikin, YK-9-50 (1972).
E_n= 14.6 MeV, $^{65}Cu(n,2n)$ standard. The data point has been renormalized to ENDF IV value.

14) P. Decowski, et.al., Nucl. Phys. A112, 513 (1968).
σ_{np} was measured with respect to $^{65}Cu(n,2n)$ in the 12.6 - 17.8 MeV range. Prestwood and Bayhurst's (Phys. Rev. 121, 1438 (1961) ^{65}Cu (n,2n) at 14.5 MeV was used.

15) R.W. Fink, BAP 15, 1372 (19
E_n= 14.4 MeV, no standard information.

16) W. Cross, R.L. Clark, K. Morin, G. Slinn, N.M. Ahmed & K. Beg, AECL 1542 (1962), and BAP 7, 335 (1962).
E_n= 14.5 MeV, standard $^{27}A\ell(n,\alpha)$, Renormalized.

17) S. Okumura, Nucl. Phys. A93, 74 (1967).
Okumura measured $\sigma_{np}{}^{m}/\sigma_{np}$ for 13.4-15 MeV neutrons. Associated particle counting was done. Measurements are absolute and the errors < 5%.

18) J. Dresler, et.al., INR 1464, 12 (1973).
E_n= 14.6 MeV, with respect to $^{56}Fe(n,p)$. Renormalized.

19) I.L. Preiss and R.W. Fink, BAP 15, 1372 (19
E_n= 14.8 MeV. Measurements with respect to $^{65}Cu(n,2n)$ and $^{27}A\ell(n,\alpha)$. Cross section renormalized.

References (Cont'd.)

20) R.N. Glover and E. Weigold, Nucl. Phys. 29, 309 (1962).
Measurements with respect to $^{63}Cu(n,2n)$ and $^{65}Cu(n,2n)$ in the energy range of 13.8 - 14.9 MeV. Absolute measurements of the $^{63}Cu(n,2n)$ and $^{65}Cu(n,2n)$ were made. Renormalization of $^{58}Ni(n,p)$ to the ENDF/B-IV $^{65}Cu(n,2n)$ and were done.

21) J.D. Hemingway, JNE, 27, 241 (19
E_n = 14.7 MeV. Cross section measured with respect to $^{56}Fe(n,p)$ reaction. $^{58}Ni(n,p)$ cross section was renormalized to version IV $^{56}Fe(n,p)$ cross section.

22) L. Gonzales, et.al., Phys. Rev. 120, 1319 (1960).
$^{58}Ni(n,p)$ measured by activation method with respect to $^{31}P(n,p)$ from 2.22 to 3.55 MeV.

^{58}Ni(n,2n) Q = 12.415 MeV

Since the last evaluation of ^{58}Ni(n,2n) reaction only one set of new measurements were done by Bayhurst, et.al.[17] They used radio chemical method for measuring the cross section. ^{27}Al(n,α) reaction cross section was measured to determine the fluency. ^{58}Ni(n,2n) measured cross sections were renormalized to the ENDF-IV ^{27}Al(n,α) cross section.

There are extensive measurements (in addition to the one referred to above) on the ^{58}Ni(n,2n) cross section. Paulsen an Liskien and Borman, et.al., measured over a wide energy range. Details of their data and other data has been discussed by Bhat[18] in his evaluation.

We like to point out that some of the cross sections which required renormalization have been corrected for the ENDF-IV cross sections. The exception being that of Prestwood and Bayhurst who measured with respect to ^{238}U(n,f). The ^{238}U(n,f) cross sections are not listed in their paper for use in renormalization.

Paulsen and Liskien and Borman's data are in good agreement with each other below 16 MeV, they diverge above this energy with the Paulsen data being larger than the other set.

There are three other sets that extend up to 20 MeV: one by Prestwood and Bayhurst, the second by Bayhurst, et.al., and the third one by Jeronymo, et.al. These data agree with the general trend up to 14 MeV; above this energy they are very high. Particularly that Bayhurst, et.al., which are recent measurements from their paper it is not clear whether they had done any multiple scattering corrections, etc.

Jeronymo data (not shown in the figure) are too low to be considered for evaluation. Similarly Lu and Finks, Ross, et.al., and Csikai, et.al., measure around 14 MeV. All of these three measured cross sections are higher than the rest. They are not given any weight in the evaluation.

Glover and Weigold's measurement (not shown) follow the general trend of other data.

The evaluated curve (cf, fig. b) was drawn following the general trend of the Borman data at higher energies and lying in between Paulsen-Liskien and Borman data. Near the threshold HF calculated values were used to draw the curve. Essentially, the present evaluation is same as before, done by

Bhat, except near the threshold. Bibliography of the data used in the evaluation are given in the references.

One unreported measurements by Marcinkowski and collaborators confirms the trend of the evaluation at higher energy end. The data is still awaited from Marcinkowski.

E-range	Method	Renormalized	Standard	Reference
16.2 - 20	Radiochemical	yes	$^{27}Al(n,\alpha)$	Bayhurst
12.9 - 19.6	Activation	-	Absolute	Paulsen-Liskien
12.9 - 19.6	Activation	not required	Hydrogen	Borman
13.7 - 14.8	Activation	-	Absolute	Temperley
13.5 - 19.8	Radiochemical	measured $^{238}U(n,f)$ not available	$^{238}U(n,f)$	Prestwood Bayhurst
13.8 - 14.9	Activation	-	Absolute	Glover-Weigold

Errors:

$^{58}Ni(n,2n)$	Errors
12. - 14	10%
14. - 15	10%
15 - 17	7%
17 - 20	12%

References

1. A. Paulsen and H. Liskien Nuk 7, 117 (1965).
2. M. Bormann, F. Dreyer and V. Zielinski EANDC (E) 66, 42 (1966).
3. R.J. Prestwood and B.P. Bayhurst, Phys. Rev. 121, 1438 (1961).
4. J.M.F. Jeronymo, G.S. Marri, J. Olkowsky, A. Sadeghi and G.F. Williamson, Nucl. Phys. 47, 157 (1963).
5. Wen-deh Lu and R.W. Fink, Phys. Rev. C/4, 1173 (1971).
6. W.G. Cross, R.L. Clarke, K. Morin, G. Slinn, N.M. Ahmed and K. Beg, Bull. American Phys. Soc. Ser. II, 7, 335 (1962).
7. J. Csikai EANDC-50, 2 (1965), Conf on Study of Nuclear Structure with Neutrons, Antwerp, paper 102 (1965).
8. M.D. Goldberg, S.F. Mughabghab, B.A. Magurno and V.M. May, BNL-325, Second Ed. Supplement No. 2, II-A, (1966).
9. J.K. Temperley, Nucl. Sci. & Engineering 32, 195 (1968).
10. R.C. Barrall, M. Silbergeld and D.G. Gardner, Nucl. Phys. A138, 387 (1969).
11. R.C. Barrall, M. Silbergeld and D.G. Gardner SUPH-69-2 (1969).
12. R.C. Barrall, J.A. Holmes and M. Silbergeld AFWL-TR-68-134 (1969) CSISRS AN/SN-10022/14.
13. L.A. Rayburn, Phys. Rev. 122, 168 (1961).
14. I.L. Preiss and R.W. Fink, Nucl. Phys. 15, 326 (1960).
15. E.T. Bramlett and R.W. Fink, Phys. Rev. 131, 2649 (1963).
16. R.N. Glover and E. Weigold, Nucl. Phys. 29, 309 (1962).
17. B.P. Bayhurst, J.S. Gilmore, R.J. Prestwood, J.B. Wilhelmy, Nelson Jarmie, B.H. Erkkila and R.A. Hardekopf, Phy. Rev. 12, (1975).
18. M.R. Bhat, in ENDF/B-IV Dosimetry file, Edited by B. Magurno, BNL-NCS-50446 (1975).

^{60}Ni(n,p) Q = 2.0411 MeV

Extensive data for this reaction is measured by Paulsen and Liskien- the covered energy range is 6-19.6 MeV. In addition to this set of data, there are some spotty measurements around 14 MeV. Except Allan's the rest of the 14 MeV data is high compared to the general trend indicated by the Paulsen and Liskien data.

Bhat[1] has done the previous (ENDF/B-IV version) ^{60}Ni(n,p) evaluation. The present evaluation differs from that of Bhat's in two respects.

1) The low energy (< 6 MeV) part of the ^{60}Ni(n,p) cross section was extrapolated with the help of the HF predicted (n,p) cross section from threshold to 6 MeV neutron energy.

2) The dominant structure suggested by Paulsen-Liskien set is retained in the evaluated curve (fig. c). Justification for such a procedure is given below.

The data references are given at the end of the report.

To explain the Giant resonance phenomenon in ^{60}Ni compound nucleus (^{60}Ni+$\gamma\rightarrow$ n,$\gamma\rightarrow$ p) Ligensa and Greiner[14] have performed 1p-1h calculations for $J^{\pi} = 1^-$, T=1 states in ^{60}Ni. They predict five 1^- states between 16-22 MeV excitation in ^{60}Ni. In addition, they also calculated neutron and proton escape widths for these 1^- states to the corresponding ground and excited states. Giant dipole energy position is a slowly varying function of A. The ^{61}Ni "2p-1h" states could be constructed by coupling the ^{61}Ni ground state to the predicted ^{60}Ni 1^- states. The excitation energies in ^{61}Ni would be the same as those in ^{60}Ni. Now if we subtract the neutron binding energy from the ^{61}Ni "2p-1h" state energies, we get the "2p-1h" state energies with respect to neutron threshold. The "2p-1h" state energies ($J^{\pi}=\frac{1}{2}^+$---$5/2^+$) and their neutron, proton escape widths and the corresponding resonance strengths are shown in Table 1. Resonance Strengths are shown both for $\Gamma^{\downarrow} \sim 0$, and $\sim .5$ MeV. We would like to point out that all the numbers quoted in this table are taken from Ligensa and Greiners' paper.

A comparison of the resonance strengths shown in the previous table with the ^{60}Ni(n,p) experimental cross section data is shown in figure (d). The resonance strengths are shown as vertical bars. The cross hatched bar refer to the resonance strength when $\Gamma^{\downarrow} = .5$ MeV and the full height of the

bar corresponds to the situation when $\Gamma^{\downarrow} = 0$. The smooth curve through the experimental points is drawn merely to guide the eye. The sum of $\Gamma^{\uparrow}_{n}$ and $\Gamma^{\uparrow}_{p}$ are also shown in numbers adjacent to the resonance-strength bars. As can be seen, the agreement between theory and experiment is remarkable; both the relative strength and the energy position of the predicted 2p-1h doorways. Until the exact calculations for the ^{61}Ni 2p-1h doorways is performed this type of comparison should be considered as semi-quantitative type. We are planning to do the calculations. One might ask: why the intermediate structure is observed in ^{60}Ni(n,p) and not in ^{58}Ni(n,p)?

Two possible explanations are:

2) The peak cross section for ^{60}Ni(n,p) is only 160 mb whereas it is about 650 mb in the case of ^{58}Ni(n,p). It would be difficult to observe the intermediate structure in ^{58}Ni(n,p) with similar strength as observed in ^{60}Ni(n,p). i.e., the background cross section is too large for the fluctuations to be discernible as resonances.

3) ^{60}Ni ground state could be treated as the neutron sub-shell closed at $2p_{3/2}$. Whereas in the case of ^{58}Ni there are two particles (holes) above (in) $1f_{7/2}(2p_{3/2})$.

Errors:

^{60}Ni(n,p)

Range	Error
Thresh - 6 MeV	5%
6 - 8	11%
8 - 9.5	9%
9.5 - 1.0	9%
10.0 -12.5	9%
12.5 - 15	7%
15 - 20	8%

References

1) M.R. Bhat, in ENDF/B-IV Dosimetry File, Edited by B. Magurno, BNL-NCS-50446 (1975).
2) H. Liskien and A. Paulsen, Nucl. Phys. 63, 393 (1965).
3) H. Liskien and A. Paulsen, Nukleonik, 8, 315 (1966).
4) A. Paulsen, Nukleonik 10, 91 (1967).
5) A. Paulsen, Z. Physik 205, 226 (1967).
6) W.G. Cross, R.L. Clarke, K. Morin, G. Slinn, N.M. Ahmed and K. Beg, EANDC (Can)-16 (1963).
7) D.L. Allan, Nucl. Phys. 24, 274 (1961).
8) R.S. Storey, W. Jack, and A. Ward, Proc. Phys. Soc. 75, 526, (1960).
9) J.D. Hemingway, Jour. Nucl. Energy 27, 241 (1973).
10) V.N. Levkovskii, G.P. Vinitskaya, G.E. Kovilskaya and V.M. Stepanov, Sovt. Jour. Nucl. Phys. 10, 25 (1969).
11) I.L. Preiss and R.W. Fink, Nucl. Phys. 15, 326 (1960).
12) P.V. March and W.T. Morton, Phil. Mag. 3, 577 (1958).
13) D.L. Allan, Proc. Phys. Soc. A70, 195 (1957).
14) Ligensa and W. Greiner, Ann. of Physics 51,28 (1969).

^{60}Ni Giant Dipole Resonances

^{60}Ni	^{60}Ni + n	WIDTHS			RESONANCE STRENGTH		Dipole Strength
$\langle E_{p-h} \rangle$ (MeV)	E_n (MeV)	$\Gamma_{no}^{\uparrow}$ (MeV)	$\Sigma \Gamma_{ni}^{\uparrow}$ (MeV)	$\Sigma \Gamma_{pi}^{\uparrow}$ (MeV)	$\Gamma^{\downarrow} = 0$	$\Gamma^{\downarrow} = .5$ MeV	
16.35	8.53	.29	.36	.07	.110	.023	428
18.17	10.33	.29	.46	.14	.113	.034	185
19.17	11.35	.04	.42	.13	.017	.005	21
19.68	11.86	.21	.50	.28	.097	.036	92
21.02	13.20	.10	.75	.38	.036	.023	35

$$\text{Resonance Strength (at Resonance)} = \frac{\Gamma_{no}^{\uparrow}\,\Gamma_{p}^{\uparrow}}{(\Gamma^{\uparrow} + \Gamma^{\downarrow})^2}$$

$$\Gamma^{\uparrow} = \Gamma_n^{\uparrow} + \Gamma_p^{\uparrow}$$

$$\Gamma_n^{\uparrow} = \sum_i \Gamma_{ni} \qquad (i \rightarrow \text{ground and excited states})$$

$$\Gamma_p^{\uparrow} = \sum_i \Gamma_{pi}^{\uparrow}$$

$\Gamma_{no}^{\uparrow}$ = Ground State (or elastic escape width)

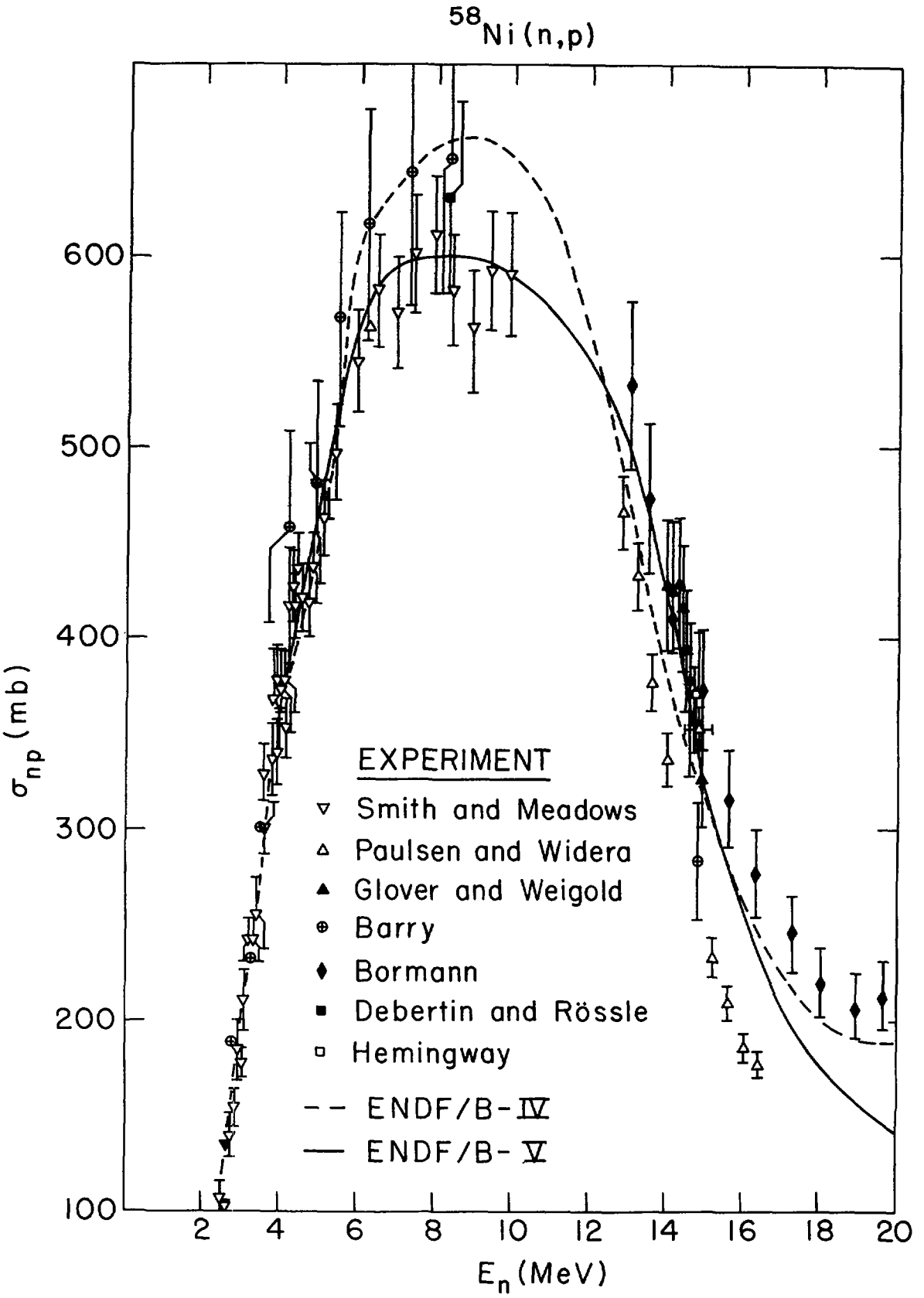

Fig. (a)

The ENDF/B-IV evaluated structure below 5 MeV is omitted to avoid cluttering the figure.

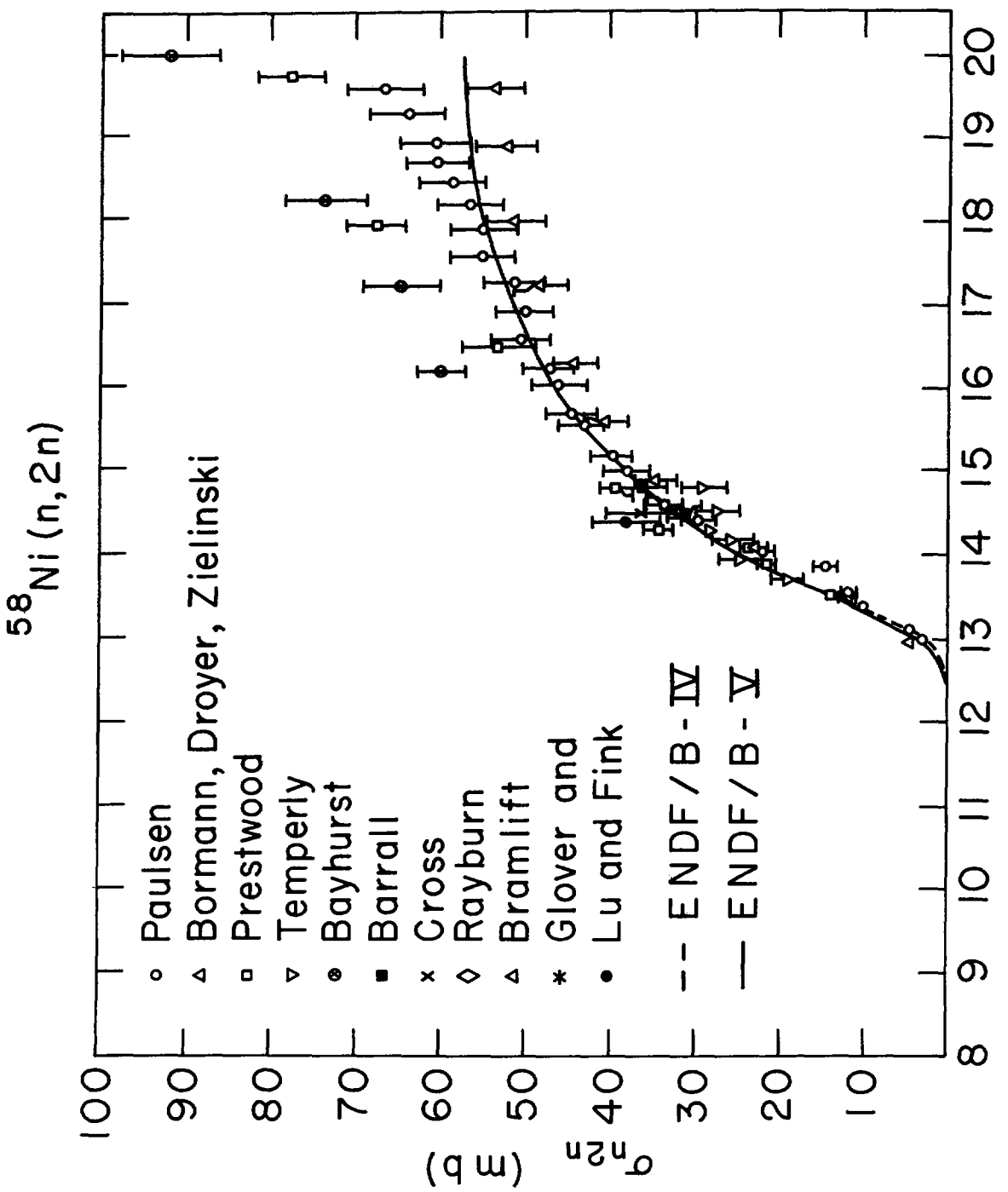
^{58}Ni (n,2n)
Paulsen
Bormann, Droyer, Zielinski
Prestwood
Temperly
Bayhurst
Barrall
Cross
Rayburn
Bramlift
Glover and
Lu and Fink
-- ENDF/B-IV
— ENDF/B-V
σ_{n2n} (mb)
E_n (MeV)
100
90
80
70
60
50
40
30
20
10
8
9
10
11
12
13
14
15
16
17
18
19
20

Fig. (b)

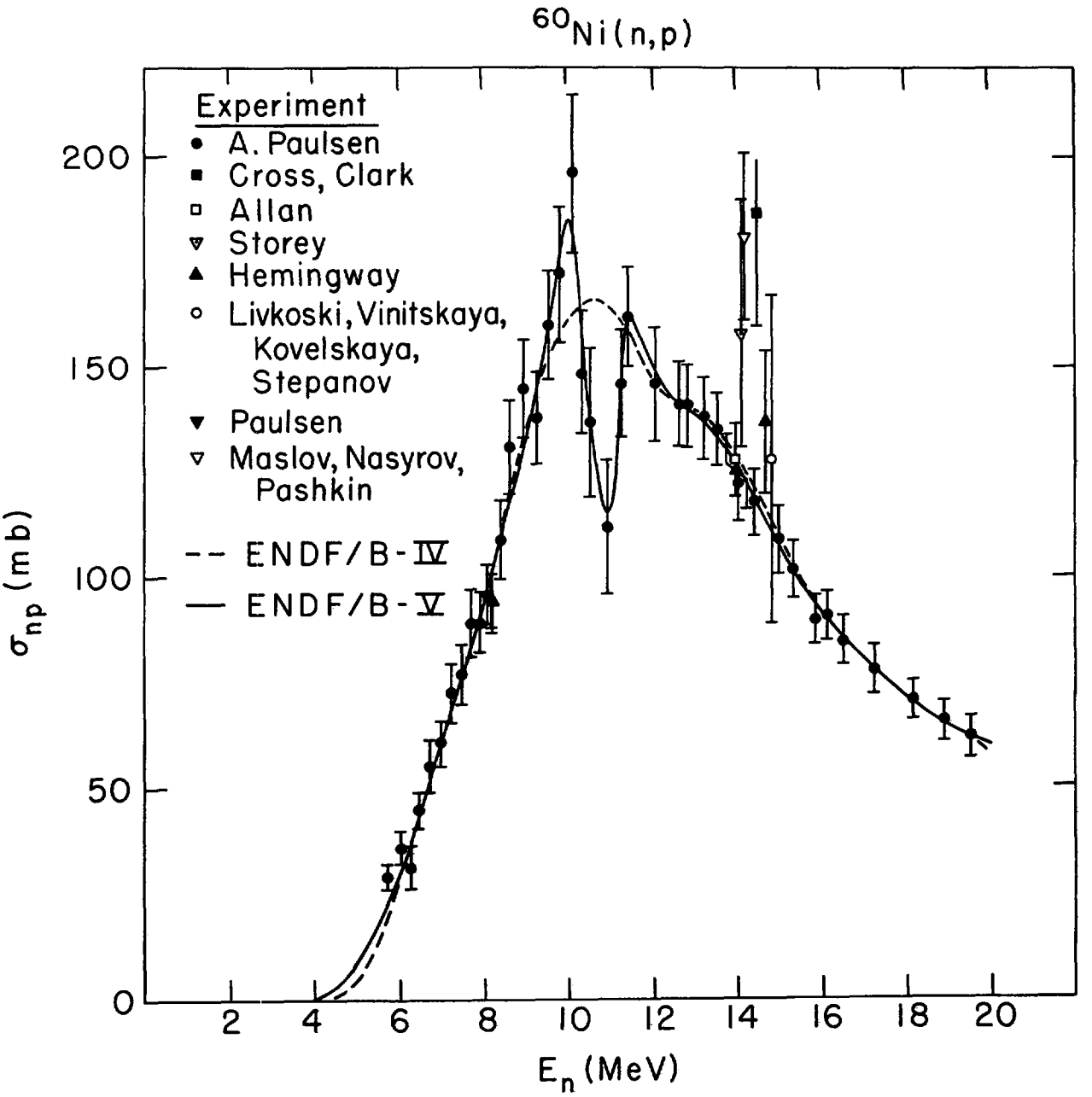
^{60}Ni(n,p)
Experiment
A. Paulsen
Cross, Clark
Allan
Storey
Hemingway
Livkoski, Vinitskaya, Kovelskaya, Stepanov
Paulsen
Maslov, Nasyrov, Pashkin
ENDF/B-IV
ENDF/B-V
σ_{np} (mb)
E_n (MeV)
0
50
100
150
200
2
4
6
8
10
12
14
16
18
20

Fig. (c)

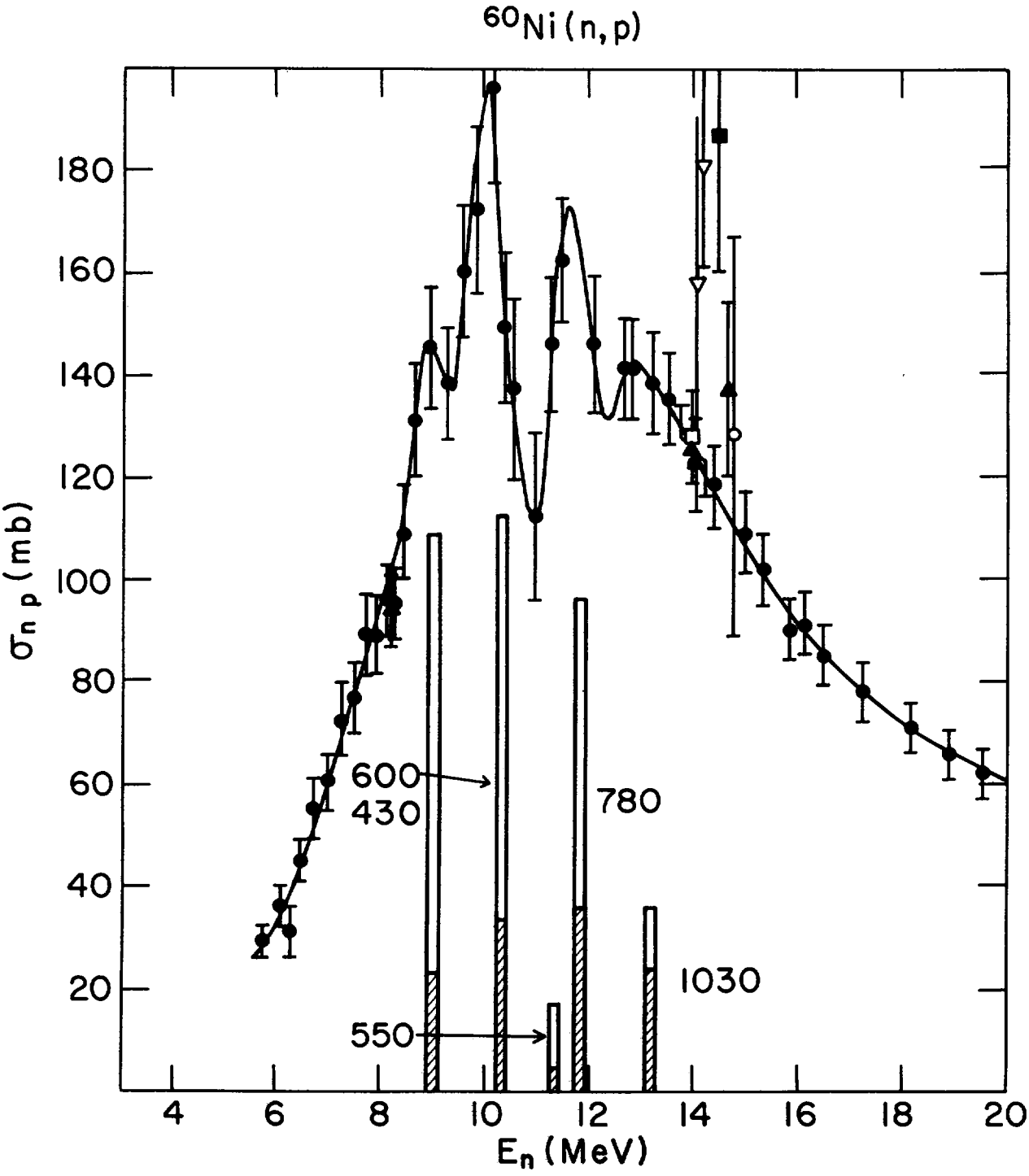
60Ni(n,p)
σn p (mb)
180
160
140
120
100
80
60
40
20
600
430
780
1030
550
4
6
8
10
12
14
16
18
20
En (MeV)

Fig. (d)

V. VALIDATION AND ADJUSTMENT OF DIFFERENTIAL CROSS SECTIONS ON THE BASIS OF INTEGRAL DATA

V.1. GENERAL PROPOSALS OF METHODOLOGY FOR CROSS-SECTION VALIDATION AND ADJUSTMENT

Prof. U. Farinelli

(Revised transcription of the oral presentation)

A year ago at a meeting in Paris on Shielding Benchmarks I was asked to review the same subject but concerning Benchmarks for Shielding instead of Dosimetry. Incidentally I think that some information which I collected then is of interest and it has been published in an OECD paper [1]. I started by recalling an Italian proverb that says that you should not sell the skin of the bear before you have killed the bear. This means that you should not discuss on how to use integral experiments before you have proven that you can make reliable and good integral experiments in benchmark spectra. Then I observed that bear hunters would not get around hunting bears if they did not have a market. So they must do some marketing before and we must assess whether there is a use for integral experiments in the dosimetry field as well as in the shielding field. In principle the possibilities opened to using the results of integral experiments are varied. One could just look at them and see if the results are consistent with those calculated with the cross sections one has available. If they are consistent he is happy and that is a validation. If they are not, if there are discrepancies between integral and differential information, then he may try different sets of cross sections and choose the best from the point of view of the integral experiment. Or he may go to some sort of adjustment which can be done in many ways. It can be some sort of empirical procedure, in a broad group structure, to force consistency according to some prescriptions, or it may be a rather sophisticated procedure. Probably the most sophisticated procedure which could be employed (and I will come back to it in a moment) is the one which is called consistent approach and in which the information which comes from nuclear models is taken into account and only those corrections which are consistent with the nuclear model calculations are introduced [2].

Three years ago we took some steps in order to define what use should be made of the integral experiments by defining two categories of dosimetry reactions [3]. Essentially the idea was that category I reactions should not be adjusted in the most common sense but it was essential that if discrepancies showed up they should be solved by a very detailed analysis of the differential evidence and in fact the idea was that the responsibility for looking at category I reactions should stay with the original evaluator who essentially takes into account the differential evidence and the nuclear models, while category II reactions were to be adjusted with respect to category I cross sections

by using the results of the integral experiments, but of course taking into account what was the evidence from differential measurements. In other words, in this case the responsibility for the changes in the cross sections should stay with the integral measurer rather than with the differential evaluator. This was the basic idea and I think we will have to come back to this to either confirm or modify this original statement. Now let's come to the adjustment procedure itself.

When one wants to derive from an integral measurement of a reaction rate some adjustment on the cross section of the detector, one should take into account a number of information. The first one is the sensitivity. Taking into account the sensitivity means applying corrections only in those energy ranges where a small change in the cross sections means an important change in the reaction rate and not changing the cross sections where it has no effect on the reaction rate. That means using the information where it is valuable. In the reaction rate measurement we are in the fortunate position that the calculation of the sensitivity is very simple because the sensitivity is simply the energy flux. So this is very simple to know and to use. The second information which we want to have in order to proceed to the adjustment is the uncertainty in the original cross section, of course as a function of energy. We want to correct cross sections where the uncertainty is large and not where the uncertainty is small; we don't want to correct good differential measurements, but we rather want to correct within the limit of uncertainties as much as possible, and especially where there are large uncertainties. But this is not enough. There is also an uncertainty in the spectrum. So we must know how much we can rely on the spectrum and we would not like to make corrections on the cross sections when the actual cause of the discrepancy may be in the spectrum rather than in the cross section. And then we have the uncertainty in the reaction rates: these measurements too are of course affected by an uncertainty and we don't want to force agreement by assuming that the reaction rate is measured exactly. There will always be a certain margin within which we should not force the agreement because of these uncertainties. Unfortunately this is not the end of the list. If it were so it would be comparatively easy! But then we also have to take into account, as we have seen, the correlations in uncertainties, and so we have correlations in cross section uncertainties which we have discussed to some length yesterday. Correlations in cross section uncertainties mean correlations at different energies of the same cross section; they also mean correlations between different cross sections if they were measured with respect to the same standard or by using methods which could be affected by the same systematical errors. In a way correlations on cross sections also include some information on the nuclear models. The fact that a certain curve is used by the evaluator to interpolate the measured points reflects some sort of a priori information that he may have either on the basis of his own judgement or on the basis of a nuclear model calculation.

And of course this kind of information, this kind of correlation should possibly be taken into account and preserved when adjusting the cross section. If this is an extremely difficult thing to do, the following is even more difficult, which is taking into account the correlations in the spectrum uncertainties. It is quite clear that we cannot just arbitrarily change the flux if we want to adjust taking into account the fact that the spectrum is not exactly known, we cannot adjust it randomly. It depends very much on how it was measured or calculated so that in principle we should also include this kind of information in a complete adjustment procedure. Finally the correlations in the uncertainties on reaction rate measurements: If we measure different reaction rates for different detectors we do it with a certain method which can be affected by some errors, for instance the sensitivity of the detector is calibrated as a function of energy and perhaps there is some systematic deviation which is probably a minor cause of concern with respect to the others but, if you want to put down a complete list, we should also consider that.

The message that I think is in these considerations, is that it is not so important to find what is the best code to do all this. I think we could find a code which performs all the corrections which we want according to a specified prescription on the quantities and uncertainties that I have mentioned; some linear programming code of some complexity could probably be used more or less effectively to correct cross sections while posing a certain minimization of a certain function within certain limits. This can be done more or less effectively but it is normal procedure. What is really at stake is the possibility of having the information which is needed in order to make such a correction. So while in line of principle it's very well to say we must take into account the uncertainty of the cross sections in a certain way, then in practice we have no idea of what the uncertainty of the cross section is, not to speak of the correlations as we have seen yesterday. I think that the main difficulty in adjustment procedures is really the input data rather than the code itself, the mathematical method in which to apply a certain prescription.

Finally I should like to point out just a few thoughts on a simpler ground. There is a lot of symmetry between flux and cross sections as we have seen. We are looking at reaction rates which are essentially products of fluxes and cross sections and there is good symmetry between the two, which I think has been enhanced by the decision to distinguish between different kinds of benchmarks, just in the same way as we have done for the cross sections. So, in a way we have category I and category II cross sections and we have standard spectra, reference spectra and controlled environments. Now, I think that one of the points that we should try to arrive at is that category I cross sections and standard spectra should have some more permanence than the others, that we do not change category I cross sections every second day; but we have some reference values that last for at least perhaps a couple of years so that we think we know what has been used in some reference calculations. And the same should be true for the spectra. We don't

want standard spectra to vary from one day to another so that you are really no longer in a position to know whether some cross sections are consistent or inconsistent with some integral measurements etc., while the category II cross sections and the other types of benchmarks can be varied with less concern and they should be more open to discussion. In other words, you could use measurements of category II detectors in standard spectra to correct the cross sections; you could use measurements of category I cross sections in reference or controlled environments to correct the spectrum. You could use measurements of category II detectors in reference and controlled environments to correct both cross sections and spectra. And you could use measurements of category I detectors in standard spectra to hope for the best.

Finally, one point which is becoming increasingly clear is that we should take into account the information on different cross section measurements in different spectra simultaneously in order to arrive at a better procedure.

REFERENCES

[1] Proceedings of the Specialists' Meeting on Sensitivity Studies and Shielding Benchmarks, OECD-NEA, Paris 1975.

[2] A. Gandini, M. Petilli and M. Salvatore, " Nuclear Data and Integral Measurements Correlation for Fast Reactors. Statistical Formulation and Analysis of Methods: the Consistent Approach", International Symposium on Physics of Fast Reactors, Vol. II, 612, Tokyo (1973).

[3] Proceedings of a Consultants' Meeting on Nuclear Data for Reactor Neutron Dosimetry held at Vienna, 10-12 September 1973; IAEA Nuclear Data Section, INDC(NDS)-56/6, Vienna (1973).

V.2. Foil Activation Detectors - Some Remarks on the Choice of Detectors, the Adjustment of Cross-Sections and the Unfolding of Flux Spectra.

A.K. McCracken, A. Packwood

AEE Winfrith

1 Introduction

Neutron spectroscopy, when applied in a favourable environment by an experienced experimenter, can yield without supporting calculations a wealth of spectral detail which can not be approached by the multiple foil analysis (MFA) method. There is nevertheless a well-known justification for using foil detectors in controlled experiments, when advanced spectroscopic techniques are available; in hostile environments only MFA methods are available and they therefore require validation and/or improvement by exposing them to comparison with other types of measurement and definitive calculation in tightly controlled test neutron spectra. All experiments raise the following questions in the mind of the interpreter:-

(i) Is the unfolding of the instrumental signal adequate in that all energy ranges are satisfactorily covered and, of considerable importance, can extrapolation from the position of measurement to other points of interest be made with confidence?

(ii) Have systematic errors associated with the absolute calibration of the instruments been minimised?

(iii) Can the knowledge of the energy-dependent response of the instruments be improved?

(iv) Have the best instruments been chosen for the purpose of this experiment, and can a limited number of instruments be chosen which will be of maximum use in all environments of current interest?

This paper considers in turn in the following sections the above problems and suggests some answers.

2 MFA Unfolding

Reviews of MFA unfolding methods currently in use are given by Zijp (1) and Stallmann (2) and comparisons of these methods have been presented by Fischer (3) and Dierckx (4). These methods differ in some respects but they have many features in common, and SAND II by McElroy (5) can be considered a typical, successful MFA code - it has enjoyed widespread use and the confidence of users, supplies its own cross-section library and has been the object of continuous refinement over several years. Like all methods it is dependent on the quality of the detector cross-sections used and Zijp (1) concludes that "the physical quality of the solution responses . . . . are mainly determined by the accuracy of the cross-section data and not by the mathematical quality of unfolding procedures". We may suppose from this that small returns are to be expected from work on the method of unfolding in comparison with the gains available from a similar effort displayed on the improvement of detector cross-sections. This supposition merits further examination and we may profitably consider the way in which SAND II and similar codes work.

(i) There is a requirement for a starting spectrum. This could be derived from a calculation (approximate if necessary) which encompasses the whole reactor, or from an intelligent guess of the spectral shape at the position of measurement.

(ii) An iterative procedure then pulls the starting spectrum towards the spectrum implied by the reaction-rates of the detectors. This spectral adjustment is only effective in energy regions where detectors carry significant spectral information; it is common to find little or no adjustment taking place between a few keV and a few hundred keV due to the lack of suitable activation detectors. If, therefore, considerable adjustment is required outside this 'dead' region an unrealistic spectral shape, with the likelihood of oscillations, can be produced; there are, moreover, many situations where the spectrum in the range 1 keV - 1 MeV is of great importance.

(iii) Sensible refinements to the starting spectrum can be made at the point of measurement - if considerable adjustment of the starting spectrum is required little confidence can be placed in the calculation at other points in a reactor.

We suggest that, in some situations at least, a more complicated and expensive method of unfolding could remove the difficulties listed above - the method will only work in a medium which can be successfully modelled for a method of calculation which has an adjoint capability. The modelling need not be exact nor need the method of calculation - all that is required is the ability to perform semi-realistic calculations in forward and adjoint mode and a perturbation code to analyse the effect of cross-section changes. Consider now a concrete example - the measurement of the reaction-rates of Rh^{103} (n,n') Rh^{103m} and of a tungsten sandwich detector with a near-singular response at 18.8 eV. Let a forward calculation be performed with ANISN, a transport code, to predict these reaction-rates, say Rc and Sc, whose measured values are Rm, Sm.

Using the respective detector cross-sections as sources the adjoint flux can be determined appropriate to each reaction-rate. These adjoint fluxes together with the forward fluxes already calculated can be supplied to a perturbation code such as SWANLAKE (5) which determines the sensitivity of a reaction-rate to changes in cross-sections used in the calculations. Thus,

$$\frac{\delta R_c}{R_c} \Big/ \frac{\delta x_i}{x_i} = U_i \; ; \quad \frac{\delta S_c}{S_c} \Big/ \frac{\delta x_i}{x_i} = W_i$$

are the sensitivities of respectively Rhodium and Tungsten calculated reaction-rates to an item X_i of data used in SWANLAKE.

Let y_j be $Rh(n,n')$ group cross-sections of standard deviation $\sigma(y_j)$

f be the singular response of the sandwich detector with standard deviation $\sigma(f)$

Φ be the original calculation of flux at the energy of the sandwich detector response.

ϕ_j be the original group flux calculated at the point of measurement.

It is now required to choose new values $R_c'(\delta\underline{x}, \delta\underline{y})$, $S_c'(\delta\underline{x}, \delta f)$ to minimise

$$Q = \frac{(R_c' - R_M)^2}{\sigma^2(R_M)} + \frac{(S_c' - S_M)^2}{\sigma^2(S_M)} + \sum_i \frac{(\delta x_i)^2}{\sigma^2(x_i)} + \sum_j \frac{(\delta y_j)^2}{\sigma^2(y_j)} + \frac{(\delta f)^2}{\sigma^2(f)}$$

$$= \frac{\left[R_c - R_M + R_c \sum U_i \frac{\delta x_i}{x_i} + \sum \phi_j \delta y_j\right]^2}{\sigma^2(R_M)} + \frac{\left[S_c - S_M + S_c \sum W_i \frac{\delta x_i}{x_i} + \Phi \delta f\right]^2}{\sigma^2(S_M)}$$

$$+ \sum \frac{(\delta x_i)^2}{\sigma^2(x_i)} + \sum \frac{(\delta y_j)^2}{\sigma^2(y_j)} + \frac{(\delta f)^2}{\sigma^2(f)}$$

Differentiating with respect to $\delta\underline{x}$, $\delta\underline{y}$ and δf and setting the differentials to zero gives a set of linear equations in $\delta\underline{x}$, $\delta\underline{y}$ and δf which are readily solved.

The best adjusted spectrum is now determined by carrying out a new forward ANISN calculation with revised data $\underline{x}' = \underline{x} + \delta\underline{x}$. The argument is clearly valid for any number and type of detectors and for any reasonable method of calculation. The disadvantages are obvious:-

(1) It can only be applied to measurements in positions which can be approximately modelled for calculation.

(2) It is clearly much more expensive in both human and computer time that a method like SAND II.

Despite this, there are special situations for which this method could have important advantages over other methods. A completely realistic calculation is carried out and modified, not by a partially arbitrary adjustment procedure, but by statistically credible perturbations of basic data. These perturbations produce a best fit to measured data at high and low energies. The high energy perturbations transmit their effects, as it were, by physically realistic processes across the energy range 1 keV - 1 MeV to low energies, and perturbations made in the 'dead' energy range will also contribute to the achievement of a good fit at low energies. In these circumstances there is every reason to expect an equally good unfolding at all energies spanned by the detectors. A second important gain is that by means of this perturbed calculation we have at once achieved good quality spectral predictions at positions other than the place of measurement thus, partially at least, solving the problem of extrapolating the results of measurements to another dose point. This method, programmed under the name FOILAK, is now being tested on measurements made in the Winfrith iron benchmark experiments (6).

3 Systematic and Random Errors in Detector Measurements

The programme RADAK (7) can be regarded as a tool which requires adjustment of detector responses to achieve maximum likelihood flux unfolding. An alternative view - one we adopt here - is that it processes data and in so doing produces a spectrum unfolding as a by-product.

Figure 1 shows schematically an arrangement of detectors used in the Winfrith iron benchmark experiment. Partitions 1 to 5 represent hydrogen filled proportional counters of various sensitivities, partitions 6, 7, 8 respectively the threshold detectors $S_{n,p}$, $In_{n,n'}$ and $Rh_{n,n'}$ and partition 9 an NE213 organic liquid scintillator. Separate unfoldings and simultaneous multi-position unfoldings with this arrangement of detectors have been carried out with RADAK at four penetration depths in this experiment.

The factors f which appear on the left-handside of Figure 1 are allowed to vary from their initial value of unity; they represent the systematic errors in the instrument calibrations - for example in the case of the hydrogen - filled counters the estimated number of hydrogen atoms present, and in the case of the activation detectors the uncertainty in the absolute calibration of the activation decay counters. Table 1 shows the final values of the f factors for the gas-filled counters after a multi-position unfolding.

Matrix Partition	Counter Filling (atm. at 15°C)			Adjusted f	σ(f)
	H_2	CH_4	A		
1	4.58	0.49	4.58	0.78	
2	9.63			1.00	
3	2.94			1.02	10%
4	0.94			1.00	
5	0.488			1.08	

Table 1 - Gas Counter Systematic Errors

The adjustment on counter 1 is remarkable; it confirmed in magnitude what the the experimenters had long suspected - that the H_2 pressure was about 1 atm less than was claimed. This demonstrates clearly that systematic errors in measurements can be removed to some extent by demanding single-valued flux solutions which give maximum likelihood predictions of the reaction-rates of all detectors. (No significant adjustments of the threshold detectors or NE213 calibrations was indicated in this exercise). The question of 'shape' adjustment now arises and we consider from here onwards only possible adjustments to the energy-dependent cross-sections of activation detectors paying particular attention to the Rh^{103} (n,n') Rh^{103m} reactions. Figure 2, taken from (8), shows the spectra of some standard neutron fields; the high-energy part of the spectrum measured in the Winfrith Fe Benchmark experiment at a penetration depth of

76.2 cm has been added to the original. The Fe spectrum is startlingly different from the others - (it is not greatly dissimilar to the spectrum leaking from the breeder of a fast reactor) - and it is quite clear that, for detectors with low threshold energies like Rh and In, almost the whole of the reactions will take place at energies very near the threshold where the activation cross-sections are relatively poorly known. In the TAPIRO spectrum, by contrast, such detectors would be largely insensitive to detector cross-sections in the energy region below the plateaux. This point is reinforced by Figure 3 which shows energy-dependent fractional contributions to the reaction-rate of Rh in three different spectra. The vertical line at 175 keV indicates the lowest-energy differential measurement of the Rh (n,n') reaction cross-section. At a PWR pressure vessel the threshold region is totally unimportant. At 100 cm of Fe and at the edge of a fast reactor core, however, the threshold region is very important - in both cases a significant fraction of the reaction-rate is caused by neutrons at energies where no measurements of the Rh cross-section exist. Even where measurements do exist considerable uncertainty must attach to cross-sections where they vary rapidly with energy. In energy regions of plateaux where many measurements exist and where the cross-section shape is rather well known the evaluators "best line" will be considerably more accurate than the accuracy claimed for single measurements.

From the foregoing one may conclude that worthwhile refinements of threshold cross-sections can only be achieved at energies near the threshold and, if this is to be achieved by means of integral measurements very hard spectra will be of limited use.

The multiple-position unfolding described earlier, and single position unfoldings were repeated with the refinement that individual group cross-sections of Rh were allowed to vary. A separate calculation was also carried out for three measurements made in a simulated fast reactor radial shield in ASPIS. The measurements were carried out at the front and rear of a 30 cm breeder containing Na, natural UO_2 and Fe, and at a depth of 60 cm into the sodium following this breeder. Again a multi-position simultaneous unfolding of these results was carried out with the individual group cross-sections of Rh being allowed to vary. Table 2 shows the group structure and three schemes of allotted standard deviations on the Rh group cross-sections.

GROUP	UPPER ENERGY keV	Standard Deviation %		
		A	B	C
18	52.5	500	100	100
19	59.5	405	81	87
20	67.4	328	65	76
21	76.4	266	53	67
22	86.5	215	43	58
23	90.0	174	35	51
24	111.1	141	28	44
25	125.9	114	23	39
26	142.6	93	19	34
27	161.6	75	15	29
28	183.2	61	12	26
29	207.5	49	10	23
30	235.2	40	8	19
31	266.5	32	6	17
32	302.0	26	5	15
32	342.2	21	4	13

Table 2

Energy Structure and Rh Error Allocation

Scheme A is very pessimistic and is not intended to be realistic. Schemes B and C are more reasonable with the former reducing to 1% in the plateau region and the latter, more realistically to 5% in this region. For all calculations the standard deviations on the calibration factors f were taken as 15% and 5% respectively for S and In; calculations with Rh used values of both 30% and 10%.

Table 3 shows the final adjusted values of the f factors for a variety of single and multiple unfoldings.

Position	s.d on Rh f	s.d on Rh Cross-Sections	Adjusted f Values		
			S	In	Rh
20 cm Fe	30%	Scheme A	1.06	0.97	0.97
50 cm Fe	30%	"	1.04	0.94	0.96
76 cm Fe	30%	"	1.00	1.00	1.03
101 cm Fe	30%	"	1.00	1.00	1.13
Multiple Fe	30%	"	1.08	0.95	0.96
Multiple Fe	30%	Scheme B	1.07	0.94	0.99
Multiple Fe	10%) 30%)	Scheme C	1.09	0.95	0.99
Multiple Breeder	10%	Scheme C	0.93	-	0.94

Table 3 - Systematic Errors in Counter Calibrations

It is fairly clear from the above numbers that there is no serious source of systematic error in the measured reaction-rates of the three detectors. If continuing experience confirms the numbers noted above one might consider altering the S and In calibrations by about 3% or 4%. Rh appears to be very well calibrated.

Table 4 shows for a few cases the implied adjustments to the Rh group cross-sections suggested by RADAK.

Group	Multiple Fe Rh f ± 30% Scheme B		Multiple Fe Rh f ± 30% Scheme C		Multiple Fe Rh f ± 10% Scheme C		Multiple Breeder Rh f±10% Scheme C	
	s.d	%	s.d	%	s.d	%	s.d	%
18	+. 04	+4.2	+. 04	3.7	+.04	3.6	+.02	1.8
19								
20	+. 06	3.9	+. 06	4.6	.06	4.5	.04	2.8
21								
22	+.095	4.1	+.112	6.5	.11	6.2	.04	2.6
23								
24	+.063	1.7	+. 09	4.9	.08	3.6	.05	2.1
25								
26	+.126	2.3	+.198	6.6	.19	6.4	.03	1.1
27								
28	+.071	0.9	+.126	3.3	.12	3.1	.03	0.7
29								
30	+.047	0.5	+.091	1.7	.09	1.6	.03	0.6
31								
32	+.056	0.3	+.127	1.9	.12	1.7	0.4	0.6
33								

Table 4 - Change in Rhodium Cross-Section near Threshold

The basic group cross-sections were taken from the UK Nuclear Data Library and were averaged over an E^{-1} spectrum below 0.8 MeV and over a fission-spectrum above this energy. There seems to be little desire on the part of RADAK to alter the evaluators shape or magnitude; very small fractional standard deviations and involved suggesting increases in the cross-section of only a few per cent below 175 KeV - the lowest energy of measurement. Our conclusion is that a useful comment can be passed on both systematic errors (involving calibration) and random cross-section errors by the type of analysis indicated above. It happens that we have investigated a detector which seems to be known well - it would be very interesting to carry out a similar investigation on Nb if irradiations could be arranged in markedly different and rather well-known spectra.

4 Choice of Detectors

The number of activation detectors available for use in a given spectrum is still rather large even after elimination on grounds of counting-rates, compatability etc. A simple selection procedure used by Zijp (9) in the STEK facility was to reject reactions whose calculated reation-rates differed markedly from those measured. There are good reasons for wishing to refine this procedure and to discover which detectors provide important information in a given situation. These reasons are:-

(i) Access and/or effort may limit the number of detectors which can be used; in this case we want the maximum of information for the minimum of effort.

(ii) It may be that the same few detectors provide important spectral information in most environments of current interest; these would then be the detectors where cross-section refinement would show most gain. Conversely major improvements in the accuracy of rather badly-known cross-sections could be of little value because of a relatively unimportant contribution to spectral information of the detectors. The spectral information contributed by a detector depends upon:-

(i) The other detectors used in the measurement.

(ii) The nature of the flux spectrum, and

(iii) The integral quantities it is required to estimate at the position of measurement.

Suppose we choose any m from n detectors. Let A be the matrix of their responses and let $\underline{\phi}$ be the best estimate of the flux spectrum; the measured detector reaction-rates are then calculated as $\underline{r} = A\underline{\phi}$. The response matrix can now be altered to A_i, taking into account both systematic and random errors after the manner of Section 2, and the reaction-rates to r_i based on assumed counting statistics. A_i and r_i could then be supplied to say SAND II with the starting guess $\underline{\phi}$ to provide a perturbed flux $\underline{\phi}$; and perturbed values of reaction-rates to be predicted:

$P_i = \underline{p}^T \underline{\phi}$, and $Q_i = \underline{q}^T \underline{\phi}$; where $\underline{p}$ and $\underline{q}$ are appropriate cross-sections. The procedure could be repeated say 50 times to give estimates of $\sigma^2(P)$, $\sigma^2(Q)$ and $\sigma^2(\phi)$ and the whole process repeated for each possible choice of m detectors; a league table could now be drawn up placing all possible choices of m detectors in order of merit for the environment chosen. A useful sophistication would be to repeat the whole exercise with m varying from 1 to n - 1. Picking the best choice of detectors for each value of m (ie those which gave the lowest variances) one could then plot variances as a function of the number of detectors used; it might be that the law of diminishing returns would be seen to set in after a smaller number of detectors than is normally considered desirable. An alternative approach is by means of the so-called condition number of the response matrix of the detectors. Thus one could use the well-known results:-

$$\frac{\|\delta\phi\|}{\|\phi\|} \leq C_A \frac{\|\delta r\|}{\|r\|} \quad \text{and} \quad \frac{\|\delta\phi\|}{\|\phi\|} \leq \frac{C_A \|\delta A\| / \|A\|}{1 - C_A \|\delta A\| \|A\|}$$

where the double lines represent the Euclidean norm of the enclosed quantities and the condition number $C_A = \|A\| \|A^{-1}\|$

Thus the smaller the condition number, the better is the set of detectors.

Neither of the above is suggested at this stage as the best approach to the problem of candidate selection, and both involve a considerable amount of effort and computer time. Nevertheless it is suggested that some such semi-rigorous approach to avoiding redundancy of information could repay the effort involved by reducing experimental time, particularly in the refinement of cross-section data for detectors which are of relatively small importance.

REFERENCES

(1) Zijp, W. L. Review of Activation Methods for the Determination of Neutron Flux Density Spectra. RMG Note 75/19, 1975.

(2) Stallmann, F. W. et al. Review of Unfolding Methods for Neutron Flux Dosimetry. Proc. First ASTM - Euratom Symposium on Reactor Dosimetry, Petten, September, 1975.

(3) Fischer, A. Internation Intercomparison of Neutron Spectra Evaluating Methods using Activation Detectors. Report JUL-1196, KFA Julich, 1975.

(4) Dierckx, R. Sanguist, V. Intercomparison of Neutron Spectra Evaluation Methods using Activation Detectors. Proc. First ASTM - Euratom Symposium on Reactor Dosimetry, Petten, 1975.

(5) Bartine, D . E. et al. SWANLAKE, A Computer Code Utilising ANISN Radiation Transport Calculations for Cross-Section Sensitivity Analysis. ORNL-TM-3809.

(6) McCracken, A. K. Grimstone, M. J. Preliminary Analysis of the Winfrith Iron Benchmark Experiment. Paper presented at the NEA/IAEA Meeting on Sensitivity Studies and Shielding Benchmarks, Paris, 1975.

(7) McCracken, A. K. The RADAK Unfolding Code. EACRP-L-102.

(8) Fabry, A. et al. Reactor Dosimetry Integral Reaction-Rate Data in LMFBR Benchmark and Standard Neutron Fields: Status, Accuracy and Implications. Presented at First ASTM-EURATOM Symposium on Reactor Dosimetry, Petten 1975.

(9) Zijp, W. L. et al. Neutron Spectra in the STEK facility determined with the SAND II Activation Technique. RCN-232, 1975.

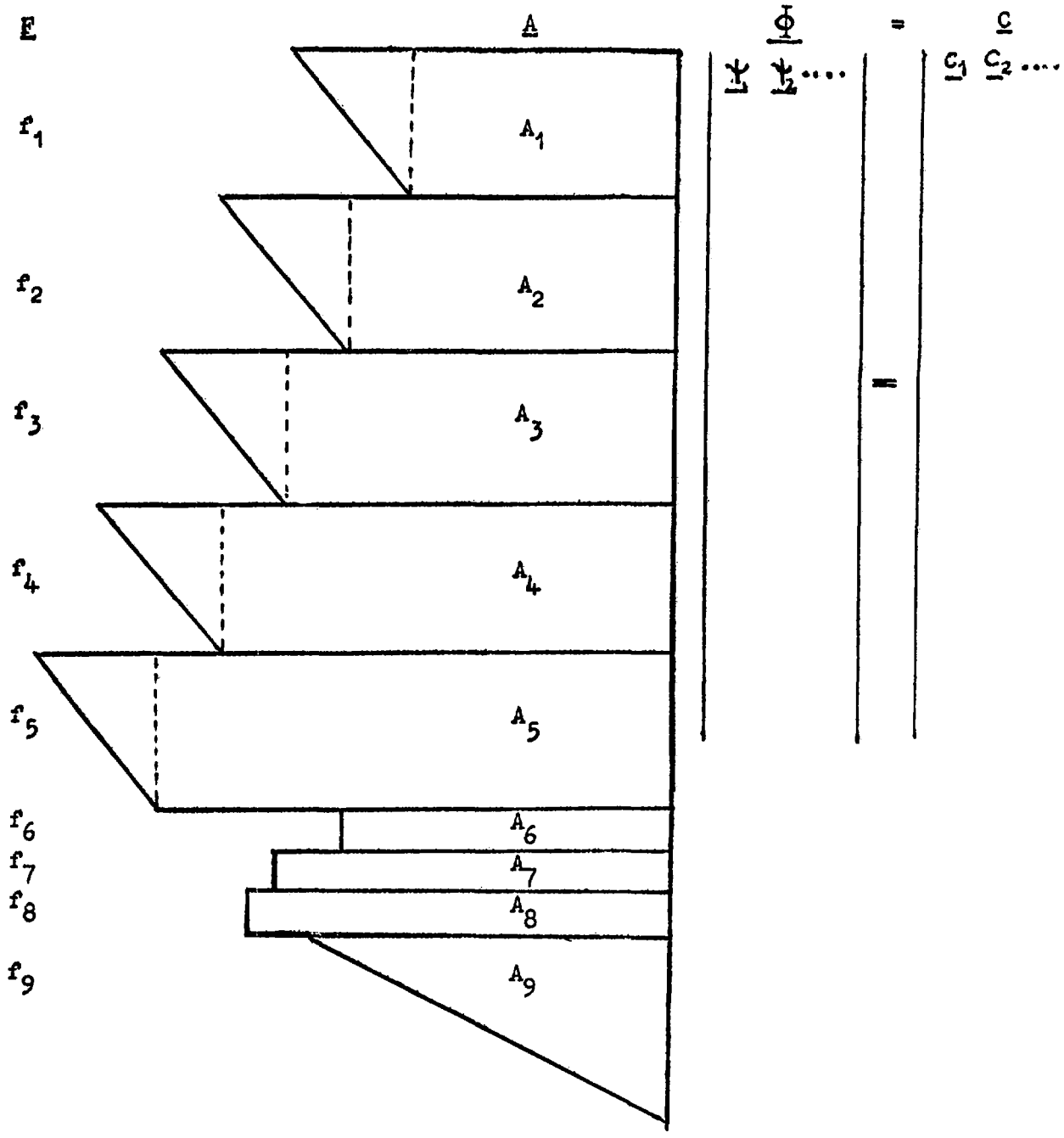

FIGURE 1: Scheme of Multi-Detector Unfolding

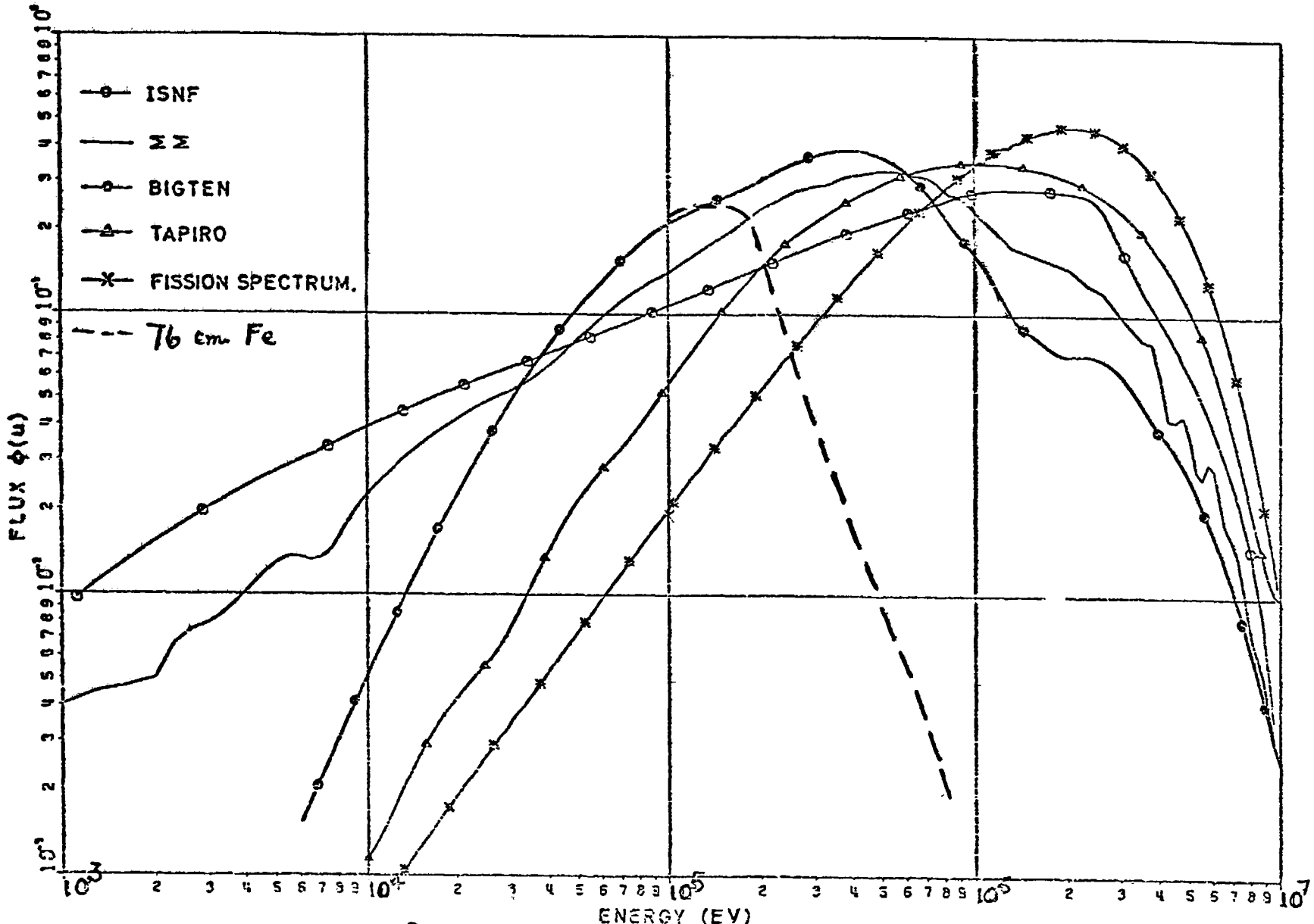

FIGURE 2 STANDARD NEUTRON SPECTRA

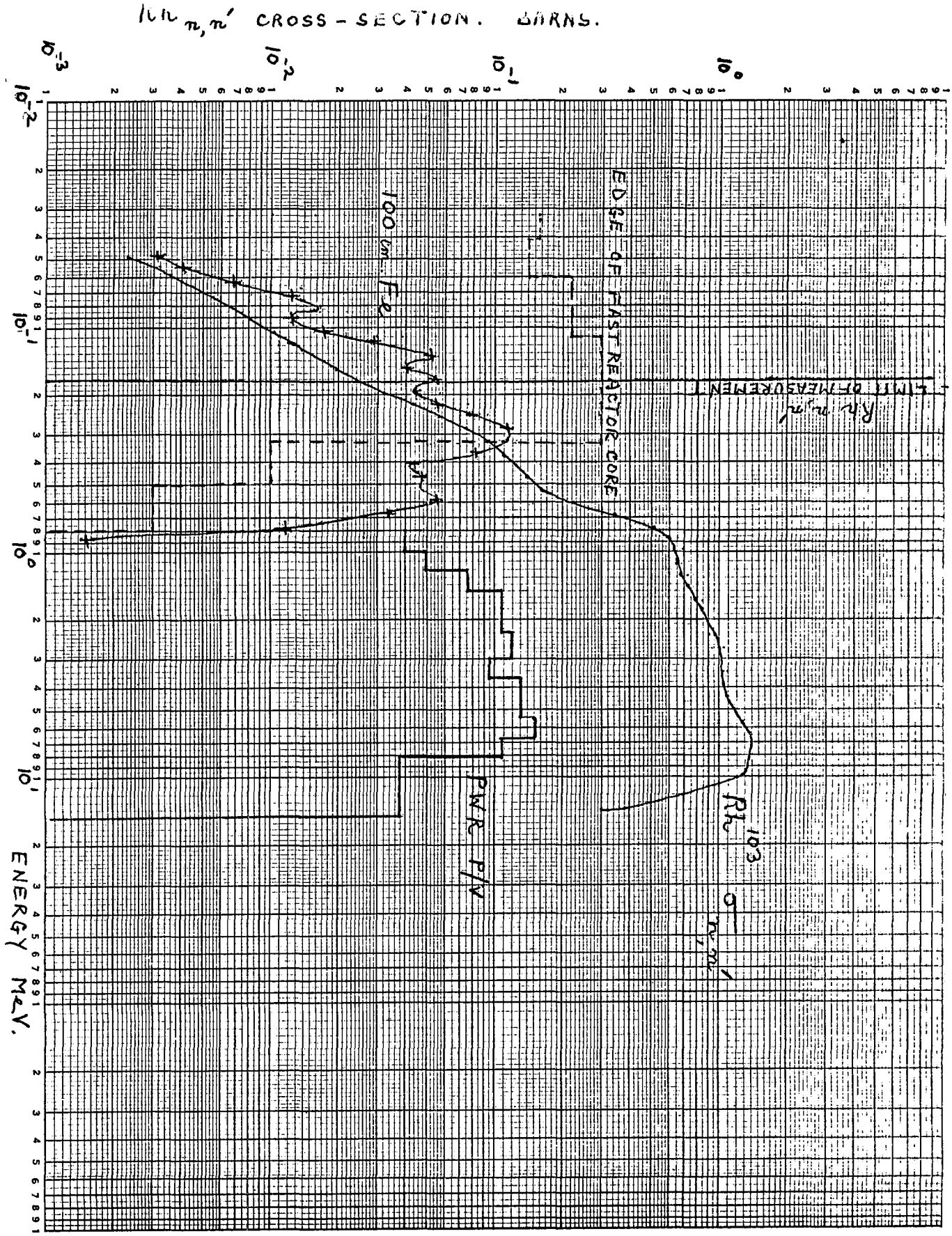

Relative Contribution to Reaction-Rate - Arbitrary Units

FIG 3 - ENERGY DEPENDENT CONTRIBUTION TO THE RHODIUM REACTION RATE